



ΕΘΝΙΚΟ ΜΕΤΣΟΒΙΟ ΠΟΛΥΤΕΧΝΕΙΟ
ΣΧΟΛΗ ΜΗΧΑΝΟΛΟΓΩΝ ΜΗΧΑΝΙΚΩΝ
ΤΟΜΕΑΣ ΘΕΡΜΟΤΗΤΑΣ
ΕΡΓΑΣΤΗΡΙΟ ΑΤΜΟΚΙΝΗΤΗΡΩΝ & ΛΕΒΗΤΩΝ

Διδακτορική Διατριβή

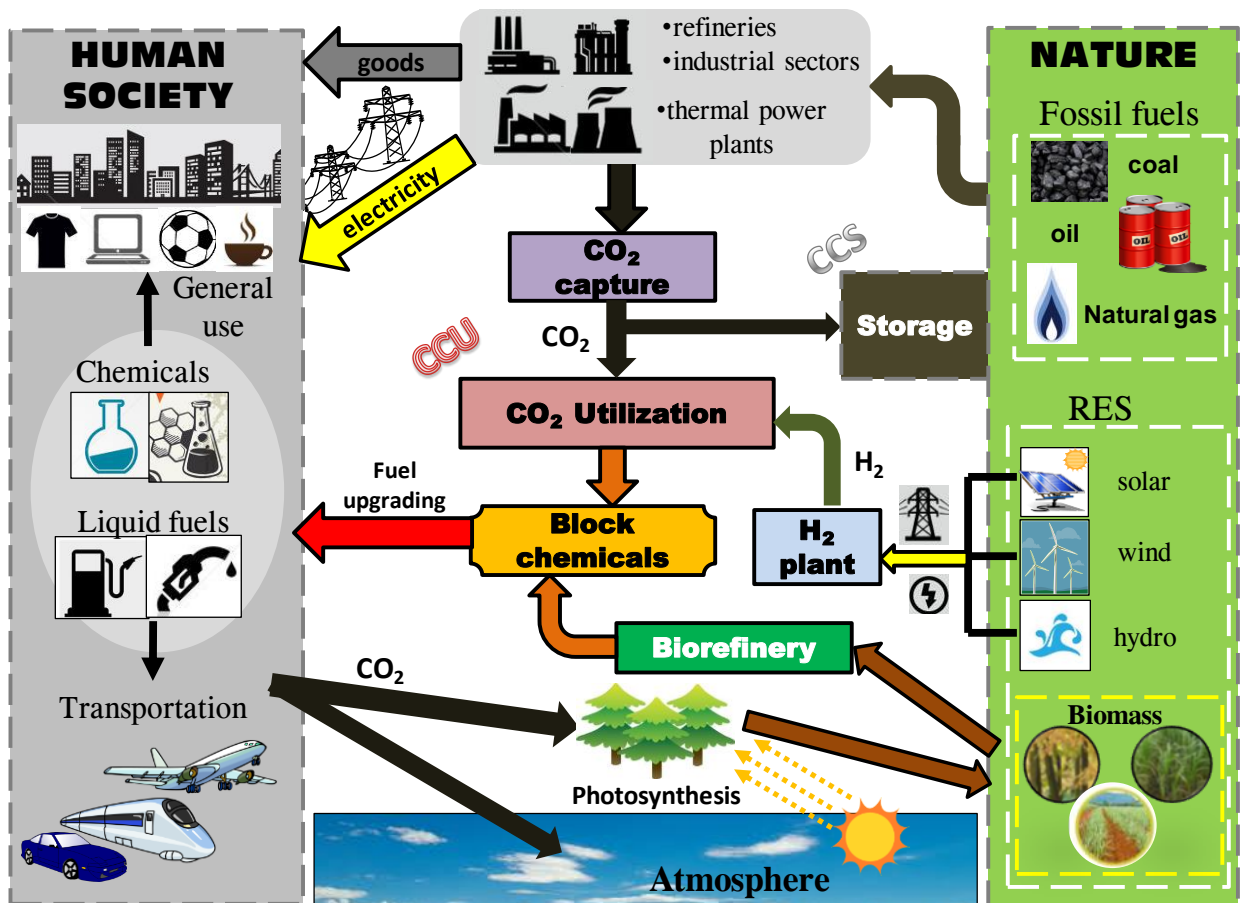
**ΟΛΟΚΛΗΡΩΜΕΝΟΣ ΣΧΕΔΙΑΣΜΟΣ ΠΡΟΗΓΜΕΝΩΝ
ΔΙΕΡΓΑΣΙΩΝ ΔΕΣΜΕΥΣΗΣ ΑΝΘΡΑΚΑ ΚΑΙ ΠΑΡΑΓΩΓΗΣ
ΕΝΑΛΛΑΚΤΙΚΩΝ ΚΑΥΣΙΜΩΝ ΑΠΟ CO₂ ΚΑΙ ΒΙΟΜΑΖΑ**

Κωνσταντίνος Α. Ατσόνιος
Διπλ. Μηχανολόγος Μηχανικός Ε.Μ.Π.

Επιβλέπων Καθηγητής: Εμμ. Κακαράς

Αθήνα, 2015

Στην οικογένειά μου



“Κάθε επιστήμη αρχίζει σαν φιλοσοφία και τελειώνει σαν τέχνη.”

Will Durant, 1885-1981, ιστορικός & φιλόσοφος

Ευχαριστίες

Η παρούσα διατριβή εκπονήθηκε στο Εργαστήριο Ατμοκινητήρων και Λεβήτων του Τμήματος Μηχανολόγων Μηχανικών του ΕΜΠ στα πλαίσια της ερευνητικής μου ενασχόλησης από τον Απρίλιο του 2010 έως τον Ιούλιο του 2015.

Πρώτα από όλα θα ήθελα να ευχαριστήσω τον καθηγητή Δρ. Εμμανουήλ Κακαρά για την ανάθεση της εν λόγω διατριβής, τη δυνατότητα που μου έδωσε να συνεργαστώ με ερευνητικές ομάδες του και λαμπρούς επιστήμονες και μηχανικούς του εσωτερικού και του εξωτερικού, στα πλαίσια της ερευνητικής μου δραστηριότητας και τη συνεχή υποστήριξη και εμπιστοσύνη που έδειξε στο πρόσωπό μου όλα αυτά τα χρόνια.

Παράλληλα, οφείλω ένα πολύ μεγάλο ευχαριστώ στο Δρ. Κυριάκο Πανόπουλο για την αδιάλειπτη και ουσιαστική επιστημονική καθοδήγησή του σε όλη τη διάρκεια της εκπόνησης της διατριβής. Με βοήθησε με τον καλύτερο τρόπο τόσο στην εμβάθυνσή μου στην Επιστήμη της μοντελοποίησης φυσικοχημικών διεργασιών όσο και στην ανάπτυξη κριτικής σκέψης γύρω από το αντικείμενο της επιστήμης των διεργασιών. Η συνεισφορά του ήταν καταλυτική ειδικά σε στιγμές που το «ένα βήμα παρακάτω» φαίνονταν ακατόρθωτο.

Στους συναδέλφους Χρήστο Χριστοδούλου και Εφηγιάννα Κουτσούμπα που ξεκινήσαμε μαζί την περιπέτεια που λέγεται διδακτορική διατριβή και μέσα από αυτή την συνοδοιπορία προέκυψε μια βαθιά φιλία τους οφείλω ένα μεγάλο ευχαριστώ για την συνεισφορά τους σε όποια στιγμή χρειάστηκα τη βοήθειά τους. Οι στιγμές που μοιραστήκαμε μαζί στο υπόγειο του κτηρίου Ο της Σχολής των Μηχανολόγων Μηχανικών θα μου μείνουν αξέχαστες.

Σε όλο το επιστημονικό, διοικητικό και τεχνικό προσωπικό του του παραρτήματος του ΕΚΕΤΑ/ΙΔΕΠ στην Αθήνα οφείλω ένα μεγάλο ευχαριστώ, που με βοήθησαν με κάθε δυνατό τρόπο και σε κάθε δυσκολία. Ιδιαίτερα, στους ερευνητές Δρ. Παναγιώτη Γραμμέλη και Δρ. Νίκο Νικολόπουλο καθώς και στο Δρ. Αριστείδη Νικολόπουλο αισθάνομαι υπόχρεος για την πολύπλευρη συμβολή τους και την εξαιρετική έως τώρα συνεργασία μας. Παράλληλα αισθάνομαι υπόχρεος στο προσωπικό του Εργαστηρίου Ατμοπαραγωγών και Λεβήτων και ιδιαίτερα, τον αναπληρωτή καθηγητή κ. Σωτήριο Καρέλλα καθώς και τους Δρ. Άγγελο Δουκέλη και Δρ. Αντώνη Κουμανάκο για την αгаστή συνεργασία και πολύτιμη βοήθειά τους, κυρίως στην αρχή της εκπόνησης της διατριβής.

Επίσης, θα ήθελα να ευχαριστήσω θερμά τους διπλωματικούς φοιτητές Χριστόφορο Τσακαλογιάννη, Κώστα Μπραϊμάκη, Μιχάλη Κουγιουμτζή και Ευαγγελία Παπαδήμου για την άψογη συνεργασία που είχαμε κατά τη διάρκεια της εκπόνησης των διπλωματικών τους εργασιών.

Ένα ευχαριστώ θέλω επίσης να απευθύνω στο Ευγενίδειο Ίδρυμα για την χορήγηση υποτροφίας κατά τη διάρκεια του δεύτερου έτους της διατριβής μου.

Ιδιαίτερες ευχαριστίες στη φίλη μου Αθηνά Γόντικα για την φιλολογική επιμέλεια και διόρθωση του ελληνικού κειμένου της διατριβής.

Τέλος, από τις ευχαριστίες δεν θα μπορούσαν να λείπουν η οικογένειά μου και οι φίλοι μου που με στήριξαν οικονομικά και ηθικά για να φτάσω μέχρι τέλους σε αυτό το δύσκολη μα συνάμα όμορφη προσπάθεια.

Ατσόνιος Κωνσταντίνος

Αθήνα, Οκτώβριος 2015

Σύμφωνα με απόφαση της Γενικής Συνέλευσης της Σχολής Μηχανολόγων Μηχανικών του ΕΜΠ στις (28/09/2015) η παρούσα Διατριβή γίνεται αποδεκτή στην Αγγλική γλώσσα. Έχει επιπλέον προστεθεί ελληνική περίληψη με έκταση ίση περίπου με τον ένα τρίτο της έκτασης του αγγλικού κειμένου.

Η έγκριση της Διδακτορική Διατριβής από τη Σχολή Μηχανολόγων Μηχανικών του Εθνικού Μετσόβιου Πολυτεχνείου δεν υποδηλώνει αποδοχή των γνωμών του συγγραφέα (Ν. 5343/ 1932, Άρθρο 202).

Επιβλέπων Καθηγητής

Δρ. Εμμ. Κακαράς
Καθηγητής ΕΜΠ

Τριμελής Συμβουλευτική Επιτροπή

Δρ. Κ. Πανόπουλος
Β' Ερευνητής ΕΚΕΤΑ

Δρ. Κ. Ρακόπουλος
Καθηγητής ΕΜΠ

Δρ. Εμμ. Κακαράς
Καθηγητής ΕΜΠ

Επταμελής Εξεταστική Επιτροπή

Δρ. Εμμ. Κακαράς
Καθηγητής ΕΜΠ

Δρ. Σ. Καρέλλας
Αναπληρωτής Καθηγητής ΕΜΠ

Δρ. Κ. Πανόπουλος
Ερευνητής Β' ΕΚΕΤΑ/ΙΔΕΠ

Δρ. Αγγ. Λεμονίδου
Καθηγήτρια ΑΠΘ

Δρ. Κ. Ρακόπουλος
Καθηγητής ΕΜΠ

Δρ. Αθ. Κωνσταντόπουλος
Καθηγητής ΑΠΘ

Δρ. Π. Γραμμέλης
Ερευνητής Β' ΕΚΕΤΑ/ΙΔΕΠ

Summary

Scope of this Thesis is the design, the process integration and the simulation of various advanced energy systems, the common feature of which is the absence or the minimization of GHG emissions. The main issues that are attempted to be addressed in this Thesis are related to the terms and frames of proper and feasible operation of innovative energy systems. Through the process modeling (Aspen PlusTM), numerous valuable conclusions are extracted related to the design and operation of the total systems and each of the sub-process that compose them. Moreover, the basic economic indexes that determine their economic feasibility of the under investigation concepts are estimated by means of the techno-economic analysis on them.

In the first chapter, the methodology followed for the selection of the energy systems that are investigated in this Thesis is explained. In first, a brief discussion is made concerning the prediction of the worldwide energy consumption and CO₂ emissions derived from the fossil fuel combustion. At a second level, the predominant strategic options for the drastic reduction of the anthropogenic GHG emissions are defined and presented: a) Carbon Capture and Storage (CCS), b) Carbon Capture and Utilization (CCU) and c) Biomass exploitation for advanced fuels and chemicals production. As far as the CCS is concerned, the analysis is distinguished by the fuel type (natural gas or coal) whereas regarding to the CCU, more attention is paid on the CO₂ conversion into alcohols (methanol and ethanol) through catalytic hydrogenation. Concerning the biomass utilization route, the investigation was focused on the biomass conversion into value added fuels and chemicals such higher alcohols and aviation biofuels.

The aim of the second chapter is to present a natural gas (NG) fired power plant where Pd membranes are employed for the CO₂ capture leading to a near zero GHG emissions energy system. According to this concept, natural gas is transformed into a H₂-rich fuel through the consecutive processes of autothermal reforming and water gas shift reaction. Pure hydrogen is recovered through Pd membranes and is led to be combusted in GT. The methodology that is adopted for the selection of the best design of the process in terms of system optimization is presented in detail for each section/unit. Next, a sensitivity analysis of several operating parameters is performed in order to determine the key parameters that maximize the plant efficiency and minimize the total required membrane area. Simulation results showed that the Pd membranes employed with NGCC with 90% CO₂ capture efficiency can reach a net efficiency equal to 50.82%, revealing it as the most efficient option for CO₂ capture in a NG fired system, as far as the net efficiency is concerned. From the economic analysis it is concluded that the investment cost, which is strongly influenced by the membrane area requirement, plays the most important role on the total plant cost. From this evaluation it is shown that the case with the optimum (i.e. minimum) membrane area can achieve a CO₂ avoidance cost 7.4% lower than the MDEA base case.

In the third chapter, the most important post combustion carbon capture technologies i.e. the amines scrubbing, and the Calcium looping, are investigated in order to compare their efficient application in large scale fossil fired power plants in comparison with oxyfuel combustion. The post combustion capture techniques differently affect the power plant: the amine system consumes steam for stripping (reboiler), whilst calcium sorbents regeneration process consumes fuel. On the other hand, oxyfuel technology has to suffer the power consumption penalties for the oxygen production from an Air Separation Unit. The comparative tool used is the exergetic analysis of the most significant processes employed in these schemes techniques. The carbonation/calcination process is the most energetically and exergetically efficient with the lowest exergy penalty (-9.0%, whereas in the amine and oxyfuel

case is -10.0% and -9.5% respectively), even though a considerable amount of exergy (22.3% of total exergy in fuel) is lost in the CaL unit. In the MEA case, 7.7% of the exergy input was calculated that is lost in the capture unit and 1.0% during CO₂ compression. In the oxy-combustion case, the ASU is the main unit where most of the exergy losses for CO₂ capture are observed (5.1% of the total exergy input in the system).

In the fourth chapter, various design and operating aspects are investigated for the valorization of industrially captured CO₂ towards methanol production and the circumstances under of which this concept can be economically viable. Cost breakdown in various Power-to-Fuel concepts confirm that hydrogen cost is the most crucial factor. Several power delivery options for hydrogen production through electrolysis are compared for their economics. The use of cheap electricity in conjunction with adequate time coverage throughout the annum is of high importance for lowering the overall H₂ production costs. Also, a Power-to-Fuel system integrated with a coal fired power plant can be an interesting option for excess power transformation when the electricity sell is not profitable. The economic analysis on the H₂ production scheme revealed that each of the three main parameters for the determination of the H₂ cost (electrolyzer capital cost, electricity cost and storage cost) can play the key role in the feasibility of the plant depending on the concept each time. A considerable effort is needed in order the CO₂ derived fuels to reach a competitive level in the global market.

The fifth chapter is dedicated to the investigation of various design aspects for the valorization of industrially captured CO₂ towards methanol and/or ethanol. In the framework of the CO₂ conversion unit, two novel concepts are examined aiming to the improvement of the process performance, one for methanol and another for ethanol production. For the methanol case ($\text{CO}_2 + 3\text{H}_2 \rightarrow \text{CH}_3\text{OH} + \text{H}_2\text{O}$), a new scheme of employing a membrane reactor with high selectivity either in methanol permeation (organophilic) or in water permeation (hydrophilic) is explored via process simulation. The methanol extraction has a beneficial effect on the methanol yield and requires a more compact sized reactor. In ethanol case ($2\text{CO}_2 + 6\text{H}_2 \rightarrow \text{C}_2\text{H}_5\text{OH} + 3\text{H}_2\text{O}$), a new process configuration through the intermediate DME (di-methyl ether) synthesis is presented and compared to the conventional method based on CO₂ conversion to CO in a reverse water gas shift (rWGS) reactor followed by the mixed alcohol synthesis reactor. The novel synthesis route via DME has a higher efficiency (total energy efficiency: 70.3% on LHV basis whereas the corresponding efficiency of the conventional scheme is 63.2%) because of lower heat and power demands for its effective operation. From the economic analysis, it is shown that the novel ethanol plant results to lower ethanol production cost than the conventional one through the rWGS by 18% but the high cost for H₂ production through water electrolysis keeps it far for competitive levels.

In the framework of the biomass utilization, the sixth chapter is related with the synthesis of Higher Alcohols (i.e. ethanol, plus C₃-C₄) from biomass gasification. These compounds could be used directly as fuel or fuel additives or as important intermediates for the chemical industry. A comparison is performed between the different process configurations. All steps and important unit operations are modeled and presented with the aim to correctly evaluate the peripheral energy requirements and conclude with the overall thermodynamic limitations of the processes. The differentiation between black liquor and solid biomass gasification, the type of catalyst employed, and the effect of the recycling scheme adopted for the reutilization of unconverted syngas are evaluated. The design has to cope with the limited yields and poor selectivity of catalysts developed so far. The gas cleaning is different depending on the different requirements of the catalysts as far as H₂S purity. The process simulation results reveal that the CO hydrogenation to higher alcohols is favoured by high pressure, temperature around 325 °C and high reactor residence times. A biorefinery using modified Fisher – Tropsch (FT) catalysts (MoS₂) prevail over modified MeOH catalyst (Cu-Zn based) for HA production. The efficiency of HA production in HHV terms can reach up to 25%.

In the seventh chapter, the conceptual process design for the production of branched paraffins with high carbon number is presented, based on the upgrading of alcohols synthesized from biomass-derived syngas and the economic evaluation and comparison with the Fischer-Tropsch (FT) process and biochemical pathways. Two routes, one based on n-butanol and another on isobutanol upgrading, are described and modeled. The flow sheeting results reveal high performance for both process configurations, resulting in an aviation fuel yield $0.172\text{kg/kg}_{\text{feedstock}}$ and a thermal efficiency of 40.5% in the case of employing a modified Methanol catalyst for the mixed alcohols synthesis (MAS). Such alternative pathways offer higher efficiencies compared to FT synthesis because specific products such as C_{12+} branched paraffins for jet fuel applications are achieved with higher selectivity in the conversion processes. The water balance at the whole process reveals that the annual demands for fresh water from a 190MW_{th} biorefinery plant are 641000m^3 , emerging the water management as an important issue with considerable environmental impacts. Simulations of the overall process show a rather high biomass carbon to product utilization ratio (up to 30%) leading to relative low CO_2 emissions. The economic evaluation reveals that the minimum jet fuel selling price in a FT plant (1.24 €/l jet fuel) is lower than the corresponding price in a MAS plant (1.49 €/l and 1.28 €/l for cases with different catalysts). The biochemical route based on Acetone-Butanol-Ethanol fermentation is considered as the most economically desirable option (0.82 €/l). Moreover, the option of selling organic compounds, which are produced intermediately (i.e. light and heavy olefins, C_4 alcohol isomers) via the alcohols' upgrading processes was proved promising enough for the feasibility of such biorefineries plants.

Σύνοψη

Ο σκοπός αυτής της διατριβής είναι η ανάπτυξη και η βελτιστοποίηση προηγμένων ενεργειακών συστημάτων που έχουν ως κοινό χαρακτηριστικό τις ελαχιστοποιημένες –αν όχι μηδενικές– εκπομπές διοξειδίου του άνθρακα (CO_2). Τα βασικά ζητήματα που τίθενται προς διερεύνηση αφορούν το πλαίσιο και τις συνθήκες για την σωστή και αποδοτική λειτουργία νέων ενεργειακών συστημάτων που δεν έχουν έως τώρα μελετηθεί. Πολλά και χρήσιμα συμπεράσματα προκύπτουν από την μοντελοποίηση αυτών των συστημάτων σε Aspen Plus™ καθώς και από την οικονομοτεχνική ανάλυση. Αυτά σχετίζονται με το σχεδιασμό, τη λειτουργία όχι μόνο των συστημάτων συνολικά αλλά και των επιμέρους διεργασιών που τα αποτελούν και με την οικονομική βιωσιμότητα αυτών.

Στο πρώτο κεφάλαιο εξηγείται το πλαίσιο και οι θεματικές περιοχές που εντάσσονται τα ενεργειακά συστήματα που μελετώνται στην εν λόγω διατριβή. Αρχικά γίνεται μια σύντομη παρουσίαση σχετικά με τις ενεργειακές καταναλώσεις παγκοσμίως και τις εκπομπές CO_2 που προέρχονται από την εκμετάλλευση ορυκτών καυσίμων. Σε δεύτερο επίπεδο παρατίθενται οι κυρίαρχες στρατηγικές για τη δραστηκή μείωση των εκπομπών αυτών: α) Δέσμευση CO_2 και αποθήκευση, β) Δέσμευση CO_2 και επαναξιοποίηση και γ) αξιοποίηση βιομάζας για την παραγωγή προηγμένων καυσίμων και υλικών. Σχετικά με την πρώτη επιλογή, η ανάλυση γίνεται για θερμικούς σταθμούς με διαφορετικό τύπο καυσίμου (φυσικό αέριο ή στερεός άνθρακας), ενώ σχετικά με τη δεύτερη επιλογή περισσότερη έμφαση δίνεται στη μετατροπή του CO_2 σε αλκοόλες (μεθανόλη και αιθανόλη) μέσω καταλυτικής υδρογόνωσης. Όσον αφορά την περίπτωση της αξιοποίησης της βιομάζας αυτή επικεντρώθηκε στη μετατροπή αυτής σε ανώτερης ποιότητας καύσιμα και χημικές ενώσεις, όπως ανώτερες αλκοόλες και αεροπορικά βιοκαύσιμα.

Ο σκοπός του δεύτερου κεφαλαίου είναι η διερεύνηση της εφαρμογής της τεχνολογίας μεμβρανών παλλαδίου (Pd) για τη δέσμευση CO_2 από συνδυασμένο κύκλο φυσικού αερίου σε μια λειτουργία με ελαχιστοποιημένες εκπομπές αερίων του θερμοκηπίου. Σύμφωνα με την υπό εξέταση διεργασία, το φυσικό αέριο μετατρέπεται σε ένα αέριο καύσιμο πλούσιο σε υδρογόνο μέσω διαδοχικών θερμοχημικών διεργασιών. Το υδρογόνο αυτό διαχωρίζεται από το CO_2 στις μεμβράνες και οδηγείται προς καύση στον αεριοστρόβιλο. Μεταξύ των στόχων είναι ο προσδιορισμός του βέλτιστου σχεδιασμού και ο καθορισμός των παραμέτρων λειτουργίας για μέγιστη απόδοση, σε συνδυασμό με χαμηλό κόστος ηλεκτροπαραγωγής. Τα αποτελέσματα των προσομοιώσεων έδειξαν ότι η διάταξη που προτείνεται μπορεί να φτάσει το 50.82% καθαρή απόδοση με ταυτόχρονη απόδοση δέσμευσης CO_2 ίση με 90%, καθιστώντας την υπό εξέταση τεχνολογία ως την πιο αποδοτική επιλογή για δέσμευση CO_2 από ενεργειακά συστήματα φυσικού αερίου. Από την οικονομική ανάλυση προκύπτει ότι το κόστος των μεμβρανών, που εξαρτάται κατά πολύ από την επιφάνειά τους, παίζει σημαντικό ρόλο στην όλη επένδυση. Στην οικονομικά βέλτιστη περίπτωση, το κόστος αποφυγής CO_2 μπορεί δυνητικά να γίνει 7.4% μικρότερο από αυτό της περίπτωσης αμινών με MDEA.

Στο τρίτο κεφάλαιο εξετάζονται οι πιο σημαντικές τεχνολογίες δέσμευσης CO_2 δηλαδή έκπλυση με αμίνες, κύκλος ασβεστίου και καύση με καθαρό οξυγόνο, υπό το πρίσμα της αποδοτικότητάς τους και τη δυνατότητα βελτίωσής τους κατά την εφαρμογή τους σε λιθανθρακικό θερμοηλεκτρικό σταθμό. Οι μετά καύσης δέσμευσης τεχνολογίες επιδρούν διαφορετικά στη λειτουργία του σταθμού: οι αμίνες καταναλώνουν ατμό για την αναγέννηση του διαλύτη, ενώ για την αναγέννηση των στερεών ασβεστίου καταναλώνεται καύσιμο. Από την άλλη μεριά, η τεχνολογία καθαρού οξυγόνου έχει να κάνει με υψηλές καταναλώσεις στη μονάδα διαχωρισμού του αέρα για την παραγωγή του καθαρού οξυγόνου. Ως εργαλείο σύγκρισης αυτών των τεχνολογιών επιλέχθηκε η εξεργειακή ανάλυση. Στην περίπτωση των αμινών (MEA), 7.7% της συνολικής εξέργειας που εισέρχεται στο σταθμό καταστρέφεται στη μονάδα

δέσμευσης και 1.0% κατά τη συμπίεση του διοξειδίου του άνθρακα. Αν και ένα σημαντικό ποσό εξέργειας (22.3% της συνολικής στο καύσιμο) χάνεται στη μονάδα κύκλου του ασβεστίου, η εν λόγω διεργασία είναι η πιο αποδοτική τόσο από ενεργειακής όσο και εξεργειακής πλευράς με τη μικρότερη ποινή εξέργειας (-9.0%). Στην περίπτωση της καθαρής καύσης με οξυγόνο, η παραγωγή οξυγόνου στη μονάδα διαχωρισμού του αέρα είναι η διεργασία με τις περισσότερες εξεργειακές απώλειες (647.8 kJ/kgCO₂).

Ο σκοπός του τέταρτου κεφαλαίου είναι η διερεύνηση διαφόρων στοιχείων και παραμέτρων για την επαναξιοποίηση του δεσμευόμενου CO₂ προς παραγωγή μεθανόλης σε μεγάλης κλίμακας εφαρμογές. Τα στοιχεία αυτά σχετίζονται με την πηγή παραγωγής ενέργειας που απαιτείται κυρίως για την παραγωγή υδρογόνου, την τεχνολογία δέσμευσης διοξειδίου του άνθρακα και τη διαχείριση (μεταφορά και αποθήκευση) των αέριων αντιδρώντων (H₂ και CO₂). Η ανάλυση κόστους σε διάφορες περιπτώσεις συστημάτων παραγωγής καυσίμων από ενέργεια επιβεβαιώνουν ότι το κόστος υδρογόνου είναι ο πιο κρίσιμος παράγοντας. Διάφορες επιλογές για τη μεταφορά ηλεκτρικής ενέργειας για την παραγωγή του υδρογόνου μελετώνται και συγκρίνονται όσον αφορά την οικονομική τους βιωσιμότητα. Η χρήση φτηνής ηλεκτρικής ενέργειας σε συνδυασμό με το μεγάλο συντελεστή χρησιμοποίησης είναι απαραίτητα για την μείωση του κόστους παραγωγής του υδρογόνου. Επίσης, η σύνδεση τέτοιων συστημάτων με λιθανθρακικό σταθμό παραγωγής ενέργειας είναι μια ενδιαφέρουσα ιδέα για την εκμετάλλευση της περίσσειας ηλεκτρικής ενέργειας όταν η πώλησή της στο δίκτυο δεν καθίσταται συμφέρουσα. Κάθε μια από τις παραμέτρους για τον καθορισμό του κόστους του υδρογόνου (κόστος κεφαλαίου του ηλεκτρολύτη, κόστος ηλεκτρισμού και κόστος αποθήκευσης του υδρογόνου) μπορεί να παίζει καθοριστικό ρόλο στη βιωσιμότητα κάθε σχεδίου αναλόγως το σχέδιο κάθε φορά. Πάντως, μεγάλη προσπάθεια θα πρέπει να καταβληθεί έτσι ώστε τα καύσιμα που προέρχονται από την επαναξιοποίηση του CO₂ να φτάσουν ένα ανταγωνιστικό επίπεδο στην αγορά.

Το πέμπτο κεφάλαιο αφορά την διερεύνηση διαφόρων στοιχείων σχεδιασμού για την αποδοτικότερη μετατροπή του διοξειδίου του άνθρακα σε υψηλής αξίας καύσιμα. Δυο καινοτόμες διεργασίες παρουσιάζονται για τη βελτίωση της παραγωγής αλκοολών, ένα για μεθανόλη και ένα για αιθανόλη. Στην περίπτωση της μεθανόλης ($\text{CO}_2 + 3\text{H}_2 \rightarrow \text{CH}_3\text{OH} + \text{H}_2\text{O}$) παρουσιάζεται ένα νέο σχήμα βασισμένο σε καταλυτικούς αντιδραστήρες με μεμβράνες με υψηλή διαπερατότητα είτε από μεθανόλη (οργανόφιλες) ή από νερό (υδρόφιλες). Η απομάκρυνση μεθανόλης στην πρώτη περίπτωση έχει ευεργετική επίδραση στην παραγωγικότητα της μεθανόλης, μειώνοντας τον απαιτούμενο όγκο του αντιδραστήρα. Στην δεύτερη περίπτωση ($2\text{CO}_2 + 6\text{H}_2 \rightarrow \text{C}_2\text{H}_5\text{OH} + 3\text{H}_2\text{O}$), παρουσιάζεται για πρώτη φορά μια νέα διάταξη για την παραγωγή της αιθανόλης μέσω ενδιάμεσης παραγωγής DME. Συγκρινόμενο με τον συμβατικό τρόπο παραγωγής μέσω της αντίστροφης αντίδρασης μετατόπισης ($\text{CO}_2 + \text{H}_2 \rightarrow \text{CO} + \text{H}_2\text{O} \rightarrow \text{C}_2\text{H}_5\text{OH}$) προκύπτει ότι το προτεινόμενο σχήμα έχει υψηλότερη απόδοση λόγω των χαμηλότερων θερμικών και ενεργειακών απαιτήσεων. Η οικονομική ανάλυση οδηγεί στο συμπέρασμα ότι το κόστος παραγωγής στο πρωτότυπο σχήμα είναι χαμηλότερο κατά 18% από αυτό που βασίζεται στην αντίστροφη αντίδραση μετατόπισης.

Στο πλαίσιο της διερεύνησης τρόπων αξιοποίησης της βιομάζας, το έκτο κεφάλαιο σχετίζεται με την σύνθεση ανώτερων αλκοολών (αιθανόλη, προπανόλη κτλ) μέσω θερμοχημικών διεργασιών (αεριοποίηση βιομάζας). Αυτές οι ενώσεις μπορούν να χρησιμοποιηθούν είτε απευθείας ως καύσιμα ή προσθετικά καυσίμων ή σαν βάση για την σύνθεση άλλων χημικών ουσιών. Παρουσιάζονται και συγκρίνονται δυο διαφορετικές διατάξεις διεργασιών, καθώς και κάθε υποσύστημα και διεργασία που τις συνθέτουν. Η μοντελοποίηση αυτών έχει σκοπό να προσδιοριστούν όλες οι θερμικές και ενεργειακές απαιτήσεις ενός τέτοιου συστήματος, καθώς και να καθοριστούν τα όρια που τίθενται από θερμοδυναμικής πλευράς στη λειτουργία κάθε διεργασίας. Εξετάζεται η επίδραση του τύπου της πρώτης ύλης βιομάζας που χρησιμοποιείται στο σχεδιασμό και τη λειτουργία όλου του συστήματος,

καθώς και η ανακυκλοφορία και επαναχρησιμοποίηση των αερίων που δεν αντέδρασαν στον αντιδραστήρα σύνθεσης. Οι χαμηλές επιδόσεις των σύγχρονων καταλυτών τέτοιου τύπου (χαμηλή μετατροπή CO και μικρή επιλεκτικότητα σε ανώτερες αλκοόλες) δρουν σαν ανασταλτικός παράγοντας στη λειτουργία του σταθμού και αυτό λαμβάνεται υπόψη στο σχεδιασμό και στον καθορισμό των παραμέτρων λειτουργίας. Το αέριο σύνθεσης και τα αέρια που πρέπει να απομακρυνθούν από αυτό (κυρίως πίσσες, σωματίδια, H_2S και CO_2) καθορίζεται από τον τύπο της πρώτης ύλης και αυτό με τη σειρά του καθορίζει το σύστημα καθαρισμού που θα επιλεγεί. Οι προσομοιώσεις έδειξαν ότι η υδρογόνωση του μονοξειδίου του άνθρακα ευνοείται σε υψηλή πίεση, θερμοκρασία γύρω στους 325 °C και σε μεγάλους χρόνους παραμονής στον αντιδραστήρα. Αυτό επιτρέπει τη μείωση της παροχής των ανακυκλοφορούντων αερίων, γεγονός που οδηγεί στη σημαντική μείωση των ενεργειακών καταναλώσεων τόσο για τη συμπίεση αυτών όσο και για τη λειτουργία του αναμορφωτήρα. Το βιοδιυλιστήριο που χρησιμοποιεί τροποποιημένο καταλύτη Fischer-Tropsch υπερέχει έναντι αυτού με τροποποιημένο καταλύτη για σύνθεση μεθανόλης στην παραγωγή ανώτερων αλκοολών. Η απόδοση στην παραγωγή αυτών των ενώσεων σε βάση Ανώτερης Θερμογόνου Ικανότητας μπορεί να φτάσει έως το 25%.

Τέλος, στο έβδομο κεφάλαιο, παρουσιάζονται δυο πρωτότυποι τρόποι παραγωγής διακλαδισμένων παραφινών βασισμένοι στην αναβάθμιση αλκοολών, που προέρχονται από το ενεργειακό σύστημα που παρουσιάστηκε στο προηγούμενο κεφάλαιο. Η ανάλυση περιλαμβάνει την οικονομική αξιολόγηση και σύγκριση αυτών των θερμοχημικών συστημάτων με ανάλογα συστήματα Fischer-Tropsch ή βιοδιυλιστήρια που βασίζονται σε βιοχημικές διεργασίες. Ο ένας τρόπος παραγωγής βασίζεται στην αναβάθμιση N-βουτανόλης ενώ ο άλλος στην ισοβουτανόλης. Τα αποτελέσματα των προσομοιώσεων έδειξαν υψηλές επιδόσεις και στα δυο συστήματα, υπολογίζοντας παραγωγικότητα καυσίμου τζετ έως και 0.172kg/kg_{feedstock} και 40.5% θερμικό βαθμό απόδοσης στην περίπτωση που εφαρμόζεται η δεύτερη θερμοχημική διαδρομή παραγωγής. Το ισοζύγιο νερού σε όλο το βιοδιυλιστήριο δυναμικότητας 190 MW_{th} έδειξε ετήσιες ανάγκες φρέσκου ύδατος 641000 m³, αναδεικνύοντας τη διαχείριση του νερού ως ένα μείζον περιβαλλοντικό ζήτημα για τέτοια προηγμένα συστήματα. Η αξιοποίηση του άνθρακα που εμπεριέχεται στην αρχική βιομάζα είναι σχετικά υψηλή (30%), οδηγώντας σε χαμηλές εκπομπές CO₂. Από την οικονομική αξιολόγηση προέκυψε ότι η ελάχιστη τιμή πώλησης καυσίμου τζετ σε ένα σύστημα Fischer-Tropsch (1.24 €/l jet fuel) είναι ελαφρώς χαμηλότερη από τα προτεινόμενα θερμοχημικά συστήματα (1.49 €/l και 1.28 €/l για τις δυο περιπτώσεις με τους διαφορετικούς καταλύτες), αλλά το σύστημα που βασίζεται στη βιοχημική διεργασία της ζύμωσης Ακετόνης-Βουτανόλης-Αιθανόλης είναι η οικονομικά πιο επιθυμητή επιλογή (0.82 €/l). Επιπλέον, η περίπτωση του να πωλούνται οι οργανικές ενώσεις που παράγονται ενδιάμεσα στη συνολική διεργασία (ελαφρές και βαρείς ολεφίνες και ισομερή C4 αλκοολών) αποδεικνύεται ως πολλά υποσχόμενη για τη βιωσιμότητα τέτοιων σταθμών αξιοποίησης βιομάζας.

Preface

My name is Konstantinos Atsonios and I studied Mechanical Engineering in the National Technical University of Athens (NTUA) during the period 2004-2010. Currently, I am a PhD candidate of NTUA. My major field of expertise is the modeling of conventional advanced processes mainly in the energy sector.

My diploma thesis in NTUA was undertaken in collaboration with CERTH (Centre for Research & Technology Hellas) and focused on the numerical investigation of Circulating Fluidized Beds (CFBs). The main scope was the implementation of the arithmetic results from the formulation of an Energy Minimization Multi – Scale (EMMS) analysis in a CFD code and the performance of 3D simulations of the isothermal flow of a 1.2 MW_{th} CFBC unit. The EMMS model is used for the better estimation of drag coefficient between the co-existing phases in a CFB riser. Two papers in an international scientific journal (Chemical Engineering Science) and one in an international conference (Efficient and clean coal technologies conference) were published in the frame of this diploma thesis.

In 2010, I started working as a research mechanical engineer in both the Laboratory of Steam Boilers and Thermal Plants (LSBTP) in NTUA and the Centre for Research and Technology Hellas / Institute of Solid Fuels Technology and Applications (CERTH/ISFTA), in parallel. More especially, I was involved in two EU funded for CO₂ capture and storage (CCS) with Palladium membrane CACHET-II project), (EU-7FP Contract no.: 241342, <http://www.cachet2.eu>) and with calcium looping process (CAL-Mod, contract: RFCS-CT-2010-0013, <http://cal-mod.eu-projects.de/>). Part of my research work on these projects was used for the writing of the 2nd and 3rd chapters of this PhD Thesis.

Seeking for a more sustainable option for the future energy systems, since the CCS concept will be in force as soon as the fossil fuel deposits are depleted, I started turning my interest into the biorefinery concept. In 2011 and in collaboration with a diploma thesis student, the process units that compose a thermochemical biorefinery plant such the gasification and the gas cleaning unit were started to be developed. The system integration of a biorefinery plant that is based on the thermochemical conversion of higher alcohol synthesis was completed in early 2013. Afterwards, and inspired by the research work that was undertaken in the frame of the EU funded project EURO BIOREF (contract: FP7-ENERGY-241718), two novel thermochemical routes for aviation fuel production from alcohols were developed in Aspen PlusTM and simulated. The upgrading unit for aviation fuels production was coupled with the alcohol plant that was examined in the previous study. In collaboration with a diploma thesis student, the economic evaluation of biomass-to-aviation fuel schemes was accomplished.

Since the last years, the “Power to Fuel” was emerged and considered as the main alternative route of the CCS concept for the feasible management of the captured CO₂, I also included two studies on this field in this Thesis. The first one is an attempt to identify the terms and conditions for viable operation of the “Power to Fuel” concept. The second one was a new idea for a more effective ethanol production via CO₂ hydrogenation.

In short, this Thesis consists of the investigation of advanced energy systems that belong to the main categories/options for GHG emissions minimization. At different stages of this work, results were published in journals and conferences. A list of publications, that are relevant with this thesis, is given below:

Book Chapters

1. K. Atsonios, K.D. Panopoulos, A. Doukelis, A. Koumanakos, E. Kakaras. Introduction to palladium membrane technology. In: Doukelis A, Panopoulos K, Koumanakos A and Kakaras E, (eds.). Palladium Membrane Technology for Hydrogen Production, Carbon Capture and Other Applications. Woodhead Publishing, 2015, p. 1-21.
2. K. Atsonios, A. Koumanakos, K.D. Panopoulos, A. Doukelis, E. Kakaras. Using palladium membranes for carbon capture in natural gas combined cycle (NGCC) power plants: process integration and techno-economics. In: Doukelis A, Panopoulos K, Koumanakos A and Kakaras E, (eds.). Palladium Membrane Technology for Hydrogen Production, Carbon Capture and Other Applications. Woodhead Publishing, 2015, p. 247-85.
3. K. Atsonios, K.D. Panopoulos, A. Doukelis, E. Kakaras. Review of palladium membrane use in biorefinery operations. In: Doukelis A, Panopoulos K, Koumanakos A and Kakaras E, (eds.). Palladium Membrane Technology for Hydrogen Production, Carbon Capture and Other Applications. Woodhead Publishing, 2015, p. 345-68.

International Journals

1. K. Atsonios, K.D. Panopoulos, A. Doukelis, A. Koumanakos, Em. Kakaras. Exergy analysis of a hydrogen fired combined cycle with natural gas reforming and membrane assisted shift reactors for CO₂ capture. Energy Conversion and Management, Volume 60, August 2012, Pages 196-203.
2. K. Atsonios, K.D. Panopoulos, A. Doukelis, A. Koumanakos, Em. Kakaras. Cryogenic Method for H₂ and CH₄ recovery from a rich CO₂ stream in pre-combustion CCS schemes. Energy 53, pp. 106-113.
3. K. Atsonios, K.D. Panopoulos, A. Doukelis, A. Koumanakos, J. Morud, Em. Kakaras. Natural gas upgrading through hydrogen selective membranes: Application in Carbon Free Combined Cycles. Energy Procedia, 37 (2013) 914-923.
4. E.-I. Koytsoumpa, K. Atsonios, K. D. Panopoulos, S. Karellas, E. Kakaras, J. Karl. Comparison of acid gas removal processes in coal-derived SNG production. Applied Thermal Engineering 74 (2015) 128-135.
5. I. Vorrias, K. Atsonios, A. Nikolopoulos, N. Nikolopoulos, P. Grammelis, Em. Kakaras, Calcium Looping for CO₂ capture from a lignite fired power plant, Fuel 113 (2013) 826–836
6. K. Atsonios, Ch. Christodoulou, E.-I. Koytsoumpa, K.D. Panopoulos, Em. Kakaras. Plant design aspects of catalytic bio-syngas conversion to higher alcohols. Journal of Biomass & Bioenergy 53 (2013) 54-64.
7. K. Atsonios, M.-A. Kougioumtzis, K.D. Panopoulos, E. Kakaras. Alternative thermochemical routes for aviation biofuels via alcohols synthesis: Process modeling, techno-economic assessment and comparison. Applied Energy 138 (2015) 346–366
8. K. Atsonios, P. Grammelis, S.K. Antiohos, N. Nikolopoulos, E. Kakaras, Integration of calcium looping technology in existing cement plant for CO₂ capture: Process modeling and technical considerations, Fuel, 153 (2015) 210-223.
9. K. Atsonios, M. Zeneli, A. Nikolopoulos, N. Nikolopoulos, P. Grammelis, E. Kakaras, Calcium looping process simulation based on an advanced thermodynamic model combined with CFD analysis, Fuel, 153 (2015) 370–381.
10. K. Atsonios, K. D. Panopoulos, E. Kakaras. Thermocatalytic CO₂ hydrogenation for methanol and ethanol production: process improvements. International Journal of Hydrogen Energy 2016 (doi: 10.1016/j.ijhydene.2015.12.001)

11. K. Atsonios, K. D. Panopoulos, E. Kakaras. Investigation of technical and economical aspects for methanol production through CO₂ hydrogenation. International Journal of Hydrogen Energy 2016 (paper accepted)
12. K. Atsonios, K. D. Panopoulos, P. Grammelidis, E. Kakaras. Exergetic comparison of CO₂ capture techniques from solid fossil fuel power plants (submitted to International Journal of Greenhouse Gas Control – under 2nd review)

Conferences and workshops

1. A. Nikolopoulos, K. Atsonios, I. Vorrias, N. Nikolopoulos P. Grammelidis, Em. Kakaras, “Numerical Tools for the Simulation of the Calcium Looping Process for CO₂ Capture”, Proceedings of 37th International Technical Conference on Clean Coal & Fuel Systems June 3 to 7, 2012, Sheraton Sand Key Clearwater, Florida, USA
2. A. Nikolopoulos, K. Atsonios, N. Nikolopoulos, P. Grammelidis, Em. Kakaras, “An advanced thermodynamic model for the simulation of the Calcium looping process coupled with CFD model”, 2nd International Conference on Chemical Looping as "A Concept for Efficient and Clean Use of Fossil Resources", 26 to 28 September 2012 at Maritim Conference Hotel in Darmstadt, Germany.
3. K. Atsonios, I. Vorrias, A. Nikolopoulos, N. Nikolopoulos, P. Grammelidis, Em. Kakaras, Calcium looping for CO₂ capture from a lignite fired power plant, Proceedings of the 9th European Conference on Coal Research & its Applications (ECCRIA 9) September 10-12, 2012, University of Nottingham.
4. K. Atsonios, M. Zeneli, A. Nikolopoulos, N. Nikolopoulos, P. Grammelidis, E. Kakaras. “Calcium looping process simulation based on an advanced thermodynamic model integrated with CFD analysis”, 6th International Conference on Clean Coal Technologies 12-16 May 2013, Thessaloniki, Greece.
5. K. Atsonios, K. D. Panopoulos, A. Doukelis, A. Koumanakos, E. Kakaras. Cryogenic Method for H₂ and CH₄ recovery from a rich CO₂ stream in pre-combustion CCS schemes. Proceedings of 25th ECOS Conference June 26 to 29, 2012, Perugia, Italy
6. K. A. Atsonios, K. D. Panopoulos, A. F. Doukelis, A. K. Koumanakos, J. Morud, E. Kakaras. Natural gas upgrading through hydrogen selective membranes: Application in Carbon Free Combined Cycles. Proceedings of the International Conference on Greenhouse Gas Technologies (GHGT-11), 18th-22nd November 2012, Kyoto, Japan
7. K. Atsonios, K. D. Panopoulos, A. Doukelis, A. Koumanakos, E. Kakaras, Exergy Analysis of a Hydrogen Fired combined cycle with Natural Gas reforming and membrane assisted shift reactors for CO₂ capture, in ECOS in Novi Sad, July 2011.
8. E.-I. Koytsoumpa, K. Atsonios, K. D. Panopoulos, S. Karellas, E. Kakaras. Comparison of acid gas removal processes in coal-derived SNG production. 6th International Conference on Clean Coal Technologies 12-16 May 2013, Thessaloniki, Greece
9. K. Atsonios, K. D. Panopoulos, A. Doukelis, A. Koumanakos, E. Kakaras. Techno economic comparison of CO₂ capture technologies employed with natural gas derived GTCC. Proceedings of the ASME Turbo Expo 2013 July 3-7, 2013, San Antonio, Texas, USA
10. K. Atsonios, K.D. Panopoulos, P. Grammelidis, S. Karellas and E. Kakaras. Exergetic comparison of CO₂ capture techniques from solid fossil fuel power plants. Proceedings of ECOS. Turku, Finland 2014.

11. K. D. Panopoulos, K. Atsonios and M.-A. Kougiumtzis. Biomass Gasification into a Multilevel Integrated Biorefinery – EuroBioRef. 4th International Symposium on Gasification and its applications Vienna, Austria 2014.
12. K. Atsonios, P. Grammelis, S. K. Antiohos, N. Nikolopoulos and E Kakaras. Integration of calcium looping technology in existing cement plant for CO₂ capture: process modeling and technical considerations. 10th European Conference on Coal Research & its Applications (ECCRIA 10). Hull, England 2014.
13. K. Atsonios, K.D. Panopoulos, E. Kakaras. Process modeling and economic analysis of ethanol synthesis via CO₂ hydrogenation. Proceedings of ECOS. Pau, France 2015.
14. D.S. Kourkoumpas, E. Papadimou, K. Atsonios, S. Karellas, P. Grammelis and E. Kakaras. Power to fuel concept: process analysis and economic evaluation. Proceedings of ECOS. Pau, France 2015.

Table of Contents

Summary	xix
Σύνοψη.....	xxiii
Preface	xxvii
Table of Contents.....	1
1. Introduction	13
1.1 <i>Necessity for a low-carbon energy</i>	13
1.2 <i>Strategies for a low carbon energy.....</i>	14
1.2.1 CO ₂ capture and storage.....	16
1.2.2 CO ₂ capture and utilization	21
1.2.3 Biomass usage for fossil fuels substitution	23
1.3 <i>Scope of this PhD thesis.....</i>	25
1.4 <i>Process modeling: general definitions, methodology, contribution.....</i>	26
2. Using palladium membranes for carbon capture in natural gas combined cycle power plants: Process integration and techno-economics.....	29
2.1 <i>Introduction</i>	29
2.2 <i>NGCC case without capture</i>	31
2.3 <i>Design of key components for the optimum operation of the power plant.....</i>	34
2.3.1 Air separation unit.....	34
2.3.2 Gas heated reformer – autothermal reforming reactor (GHR-ATR).....	35
2.3.3 Design of water gas shift reactors (WGS) and membrane separators (MSs)	37
2.4 <i>Purification, compression and recirculation</i>	39
2.4.1 Off-gases recirculation of the catalytic oxy-combustion at the ATR.....	42
2.5 <i>Determining optimum operating parameters.....</i>	43
2.5.1 Steam to carbon ratio (S/C) at the ATR	43
2.5.2 Hydrogen recovery factor	44
2.5.3 ATR temperature.....	44
2.5.4 Carbon Capture Rate (CCR)	44
2.5.5 Membrane pressure	46
2.6 <i>Optimized case study</i>	49
2.7 <i>Comparison with other CO₂ capture techniques</i>	53
a. Chemical absorption options.....	54
b. Physical absorption options	57
c. Cryogenics	58
d. CO ₂ selective membranes	58

e. O ₂ /CO ₂ cycle.....	58
Results – thermodynamic performance	58
2.8 <i>Economic evaluation</i>	61
2.8.1 Specific investment costs	61
2.8.2 Cost of electricity and cost of CO ₂ avoided.....	62
2.8.3 Effect of membrane area reduction on COE and cost of CO ₂ avoided	64
2.9 <i>Conclusions</i>	65
3. Exergetic comparison of CO₂ capture techniques from solid fossil fuel power plants	67
3.1 <i>Introduction</i>	67
3.2 <i>Model description</i>	69
3.2.1 MEA Scrubbing	70
3.2.2 Calcium Looping Process	70
3.2.3 Oxyfuel	72
3.2.4 CO ₂ purification and compression	73
3.3 <i>Exergy analysis – Methodology</i>	76
3.4 <i>Results and Discussion</i>	78
3.5 <i>Conclusions</i>	85
4. Techno-economic aspects for methanol production systems based on CO₂ hydrogenation	87
4.1 <i>Introduction</i>	87
4.2 <i>Process description</i>	88
4.3 <i>Methanol synthesis from CO₂</i>	89
4.4 <i>Pure CO₂ from coal derived flue gas</i>	91
4.5 <i>Hydrogen production</i>	91
4.6 <i>Concluding remarks</i>	100
5. Process improvements on energy systems based on thermocatalytic CO₂ hydrogenation for methanol and ethanol production	103
5.1 <i>Introduction</i>	103
5.2 <i>Process Description</i>	104
5.2.1 Feedstock gases.....	104
5.2.2 Methanol synthesis from CO ₂	105
5.2.3 Ethanol synthesis from CO ₂	108
5.3 <i>Cost analysis</i>	112
5.4 <i>Results and discussion</i>	113
5.4.1 Process simulation results	113
5.4.2 Economic analysis.....	117
5.5 <i>Conclusions and further considerations</i>	119
6. Plant design aspects of catalytic biosyngas conversion to higher alcohols.....	121

6.1	<i>Introduction</i>	121
6.2	<i>Process description</i>	122
6.2.1	Air separation unit	123
6.2.2	Gasification	123
6.2.3	Gas Cleaning	124
6.2.4	Alcohol synthesis unit	125
6.2.5	Alcohol separation and recovery	125
6.2.6	Steam production and power generation unit	126
6.3	<i>Methodology and model description</i>	126
6.3.1	ASPEN Plus™ modeling configuration	126
6.3.2	Modeling of the Mixed Alcohol Reactor (MAR)	128
6.4	<i>Results and discussion</i>	130
6.4.1	Comparison of the performance of two different catalyst types	130
6.4.2	Sensitivity analysis	132
6.5	<i>Conclusions</i>	134
7.	Alternative thermochemical routes for aviation biofuels via alcohols synthesis: process modeling, techno-economic assessment and comparison	135
7.1	<i>Introduction</i>	135
7.2	<i>Biomass-to-jet fuel potential pathways</i>	137
7.2.1	Syngas production from lignocellulosic biomass	139
7.2.2	Mixed Alcohols Synthesis and Fuel Upgrading	140
7.3	<i>Process modeling</i>	143
7.3.1	Paraffins from mixed alcohols with modified FT (case 1)	145
7.3.2	Paraffins from mixed alcohols with modified Methanol (case 2)	146
7.4	<i>Cost analysis methodology</i>	148
7.5	<i>Results and Discussion</i>	150
7.5.1	Mass and Energy Balance calculations	151
7.5.2	Effect of self-power production for the coverage of the electrical demands	156
7.5.3	Investigation of the recycling gas returning route & the effect of gasification temperature	157
7.5.4	Investigation of potential CO ₂ utilization	158
7.5.5	Comparison with Fischer-Tropsch Synthesis process	159
7.6	<i>Economic Evaluation</i>	160
7.6.1	Thermochemical Cases 10kg/s biomass input (or 864 t/day)	160
7.6.2	Effect of Plant capacity	163
7.6.3	Comparison with Biochemical Pathways	164
7.6.4	Sensitivity analysis	166
7.6.5	Investigation of setting the intermediate organic compounds as the final products	167
7.7	<i>Further discussion and Conclusions</i>	168

8. Conclusions – Future work.....	171
8.1 Main Conclusions	171
I. Carbon Capture and Storage.....	171
II. Carbon Capture and Utilization.....	172
III. Biomass utilization for advanced fuels/chemicals production	173
8.2 Innovative aspects.....	174
8.3 Future study	174
Annex	177
A. Supplementary Data related to cost equipment estimation in Chapter 7.....	178
Εκτεταμένη Περίληψη της Διδακτορικής Διατριβής στην Ελληνική Γλώσσα	189
1. Εισαγωγή	191
1.1 Η αναγκαιότητα για μετακίνηση προς ένα ενεργειακό σύστημα με χαμηλές εκπομπές άνθρακα.....	191
1.2 Στρατηγικές για ένα ενεργειακό σύστημα με χαμηλές εκπομπές άνθρακα	192
1.2.1 Δέσμευση και Αποθήκευση CO ₂	193
1.2.2 Δέσμευση CO ₂ και επαναχρησιμοποίηση	193
1.2.3 Χρήση βιομάζας προς αντικατάσταση των ορυκτών καυσίμων	194
1.3 Σκοπός της Διδακτορικής Διατριβής.....	194
2. Εφαρμογή μεμβρανών παλλαδίου για δέσμευση και αποθήκευση CO₂ σε σταθμό συνδυασμένου κύκλου: Ολοκληρωμένος σχεδιασμός και τεχνοοικονομική ανάλυση	197
2.1 Εισαγωγή.....	197
2.2 Σταθμός αναφοράς.....	198
2.3 Σχεδιασμός της διάταξης του συστήματος για βέλτιστη λειτουργία.....	198
2.4 Καθορισμός των λειτουργικών παραμέτρων για βέλτιστη απόδοση	198
2.5 Σύγκριση με άλλες τεχνικές δέσμευσης CO ₂	201
2.6 Οικονομική αξιολόγηση.....	201
2.6.1 Κόστος ηλεκτροπαραγωγής και κόστος αποφυγής εκπομπών CO ₂	203
2.6.2 Επίδραση της μείωσης της επιφάνειας μεμβρανών στο κόστος ηλεκτροπαραγωγής και στο κόστος αποφυγής εκπομπών CO ₂	204
2.7 Συμπεράσματα.....	205
3. Εξεργειακή ανάλυση και σύγκριση τεχνικών δέσμευσης CO₂ σε λιθανθρακικό θερμοηλεκτρικό σταθμό	207
3.1 Εισαγωγή.....	207
3.2 Περιγραφή μοντέλου.....	207
3.2.1 Έκπλυση με αμίνες (MEA) Scrubbing.....	208
3.2.2 Διεργασία Κύκλου Ασβεστίου.....	208
3.2.3 Καύση με καθαρό οξυγόνο	209
3.2.4 Καθαρισμός CO ₂ και συμπίεση	209
3.3 Εξεργειακή ανάλυση	209

3.4	Αποτελέσματα.....	209
3.5	Συμπεράσματα.....	212
4.	Οικονομοτεχνική διερεύνηση για την παραγωγή μεθανόλης μέσω υδρογόνωσης CO₂.....	213
4.1	Εισαγωγή.....	213
4.2	Περιγραφή της συνολικής διεργασίας παραγωγής μεθανόλης από CO ₂	213
4.3	Καθαρό ρεύμα CO ₂ από καυσαέρια που προέρχονται από ορυκτά καύσιμα	214
4.4	Παραγωγή υδρογόνου.....	214
4.5	Συμπεράσματα - παρατηρήσεις.....	217
5.	Αναβαθμισμένες διεργασίες σε ενεργειακά συστήματα βασισμένα στην καταλυτική υδρογόνωση CO₂ προς παραγωγή μεθανόλης και αιθανόλης	219
5.1	Εισαγωγή.....	219
5.2	Περιγραφή των εξεταζόμενων διεργασιών.....	219
5.2.1	Σύνθεση μεθανόλης από CO ₂	219
5.2.2	Σύνθεση αιθανόλης από CO ₂	221
5.3	Αποτελέσματα.....	222
5.3.1	Αποτελέσματα προσομοιώσεων.....	222
5.3.2	Οικονομική ανάλυση	223
5.4	Συμπεράσματα.....	224
6.	Σχεδιασμός και μοντελοποίηση βιοδυλιστηρίου για τη καταλυτική μετατροπή αερίου σύνθεσης σε ανώτερες αλκοόλες	225
6.1	Εισαγωγή.....	225
6.2	Περιγραφή του βιοδυλιστηρίου.....	225
6.3	Μεθοδολογία μοντελοποίησης και περιγραφή του μοντέλου	226
6.4	Αποτελέσματα.....	227
6.4.1	Σύγκριση της αποδοτικότητας των δυο διαφορετικών καταλυτών	227
6.4.2	Ανάλυση ευαισθησίας.....	228
6.5	Συμπεράσματα.....	229
7.	Εναλλακτικές θερμοχημικές τεχνικές για τη σύνθεση αεροπορικών βιοκαυσίμων μέσω αλκοολών: μοντελοποίηση και σχεδιασμός διεργασιών, οικονομοτεχνική αξιολόγηση και σύγκριση	231
7.1	Εισαγωγή.....	231
7.2	Περιγραφή των πρωτότυπων θερμοχημικών διεργασιών.....	231
7.2.1	Σύνθεση αλκοολών και αναβάθμιση καυσίμου	232
7.3	Περιγραφή της μοντελοποίησης των υπό εξέταση διεργασιών	233
7.3.1	Παραφίνες από μίγμα αλκοολών με τροποποιημένο FT καταλύτη (περίπτωση 1).....	234
7.3.2	Παραφίνες από μίγμα αλκοολών με τροποποιημένο καταλύτη μεθανόλης (περίπτωση 2)	234
7.4	Ανάλυση κόστους.....	235
7.5	Αποτελέσματα.....	236
7.5.1	Ισοζύγιο μάζας και ενέργειας.....	236

7.5.2	Επίδραση της κάλυψης των ηλεκτρικών απαιτήσεων από αυτόνομη παραγωγή.....	237
7.5.3	Ανακυκλοφορία αερίων στον αεριοποιητή αντί για αναμόρφωση.....	238
7.5.4	Διερεύνηση της πιθανής αξιοποίησης του CO ₂	238
7.5.5	Σύγκριση με τη διεργασία σύνθεσης κατά Fischer-Tropsch.....	238
7.6	Οικονομική Αξιολόγηση.....	239
7.6.1	Θερμοχημικά σενάρια με εισαγωγή βιομάζας 10kg/s (ή 864 t/ημέρα).....	239
7.6.2	Επίδραση της δυναμικότητας της μονάδας.....	241
7.6.3	Σύγκριση με τις αντίστοιχες Βιοχημικές διαδρομές.....	241
7.6.4	Ανάλυση ευαισθησίας.....	242
7.6.5	Ορίζοντας τις ενδιάμεσες οργανικές ενώσεις ως τελικά προϊόντα.....	242
7.7	Συμπεράσματα.....	243
8.	Συμπεράσματα – προτάσεις για μελλοντική εργασία.....	245
8.1	Καινοτόμα στοιχεία.....	245
8.2	Βασικά συμπεράσματα.....	245
	I. Δέσμευση και Αποθήκευση Διοξειδίου του Άνθρακα	245
	II. Δέσμευση CO ₂ και επαναχρησιμοποίηση	246
	III. Αξιοποίηση βιομάζας για την παραγωγή αναβαθμισμένων καυσίμων/χημικών	247
8.3	Μελλοντική εργασία	248
	References.....	249

Nomenclature

Symbol	Units	Explanation
A_i		pre-exponential factor (reaction kinetics)
b	kJ/kg	specific exergy index
C_f	%	capacity factor
C_i	M€	equipment cost of each component
C_o	M€	reference erected cost
E	kW	exergy
E_a	J/mol	activation energy
E_{carb}	-	carbonation efficiency
f	-	Scale factor
F_R	kmol/kmol	Ca solids looping ratio
F_0	kmol/kmol	make-up (fresh limestone) ratio
h	kJ/kg	enthalpy
I	kW	irreversibility
J_{H_2}	mol/(m ² s)	hydrogen flux
k_i		driving force factors (reaction kinetics)
K_i		adsorption factors (reaction kinetics)
m	kg/s	mass flow rate
MW	kg/kmol	molecular weight
N	kmol/s	molar flow rate
p	bar or MPa	pressure
P	kW	electricity power output
p_{H_2}	Pa	hydrogen partial pressure
q_{H_2}	mol/(msPa ⁿ)	hydrogen permeability
Q	kW	heat stream
Q_{H_2}	mol/(m ² sPa ⁿ)	hydrogen permeance
R	8.314 J/molK	gas constant
r_i	kmol/s·kg _{cat}	reaction rate
s	kJ/kg	entropy
S_o	-	reference size
S/C	-	steam to carbon ratio
S/CO	-	steam to CO ratio
$SPECCA$	MJ _{LHV} /kgCO ₂	Specific Energy Consumption for CO ₂ Avoided
T	°C or K	temperature
x	-	molar fraction
X	-	average conversion of solids in the carbonator/calciner
W	kW	work power

Greek Symbol	Units	Explanation
γ	-	mass fraction
δ	m	membrane thickness
ε	kJ/mol	standard chemical exergy
$\varepsilon_{o,i}$	kJ/mol	chemical exergy
η	%	efficiency
λ	-	O ₂ /O _{2st} ratio

Subscripts and superscripts	Explanation
ave	maximum average
calc	calcination
carb	carbonation
ch	chemical
e	electrical
ex	exergy
f	fuel
feed	feed side in membrane
FG	flue gas
m	material
o	reference state
perm	permeate side in membrane
pre	pre-reforming
REF	reference
ph	physical
th	thermal
tot	total
ut	utilization

Acronyms	Explanation
ABE	Acetone-Butanol-Ethanol process
AEP	Average Electricity Price (€/MWh _e)
AGR	Acid Gas Removal
AMP	2-Amino-2-Methylpropanol
ASU	Air Separation Unit
ATJ	Alcohol to Jet fuel
ATR	Autothermal Reformer
BL	Black Liquor
BMC	Bed Material Cooler
BMH	Bed Material Heater

CaL	Calcium Looping
CAPEX	Capital Expenditure (M€)
CC	CO ₂ capture unit
CCR	Carbon Capture Rate
CCS	Carbon Capture and Storage
CCU	Carbon Capture and Utilization
CDS	Clean Dark Spread (€/MWh _e)
CFB	Circulating Fluidized Bed
CFD	Computational Fluid Dynamics
CHP	Cogeneration Heat and Power
CLC	Chemical Looping Cycle
CLOU	Chemical Looping Oxygen Uncoupling
COE	Cost of Electricity (€/MWh _e)
COT	Combustor Outlet Temperature (°C)
CRI	Carbon Recycling International
CtL	Coal to Liquid
CUU	Carbon (CO ₂) Utilization Unit
DCAC	Direct Contact Air Cooler
DCFRROR	Discounted Cash Flow Rate of Return
DDB	Double-Declining-Balance
DEA	Diethanolamine
EBTF	European Benchmark Task Force
EC	Evaporative Cooler
EGR	Enhanced Gas Recovery
EIA	Energy Information Administration
ENRTL	Electrolyte Non Random Two Liquid
EOR	Enhanced Oil Recovery
EU	European Union
FCI	Fixed Capital Investment
FT(S)	Fischer-Tropsch (Synthesis)
GHG	Greenhouse Gas
GHR	Gas Heated Reformer
GHSV	Gas Hourly Space Velocity ($l_{\text{gas}}/l_{\text{cat}}\cdot\text{h}$)
GT	Gas Turbine
GTCC	Gas Turbine Combined Cycle
GtL	Gas to Liquid
HA	Higher Alcohols
HAS	Higher Alcohol Synthesis
HC	Hydrocarbons

HHV	High Heating Value
HP	High Pressure (bar)
HPC	High-Pressure Column
HRF	Hydrogen Recovery Factor
HRSG	Heat Recovery Steam Generator
HSMR	Hydrogen Separation Membrane Reactors
HT	High Temperature
H2P	Hydrogen Plant
IC	Indirect Costs
ICE	Internal combustion engine
IEA	International Energy Agency
IPCC	International Panel on Climate Change
IP	Intermediate Pressure (bar)
LH	Langmuir-Hinshelwood (kinetic model)
LHV	Lower Heating Value (kJ/kg)
LNG	Liquefied Natural Gas
LP	Low Pressure (bar)
LT	Low Temperature
LPC	Low-Pressure Column
LPG	Liquefied petroleum gas
LUVO	Luftvorwärmer (Air pre-heater in German)
MACRS	Modified Accelerated Cost Recovery System
MAO	Methylaluminoxane
MAR	Mixed Alcohols Reactor
MDEA	Methyl diethanolamine
MEA	Monoethanolamine
MES	Microbial Electrosynthesis System
MFSP	Minimum Fuel Selling Price
modFT	modified Fischer Tropsch synthesis catalyst
modMeOH	modified methanol synthesis catalyst
MR	Membrane Reactor
MS	Membrane Separator
MSW	Municipal Solid Waste
NG	Natural Gas
NGCC	Natural Gas Combined Cycle
NMP	Normal Methyl Pyrrolidone
NREL	National Renewable Energy Laboratory (U.S.)
NRTL	Non Random Two Liquid (property method)
OECD	Organization for Economic Co-operation and Development

O&M	Operating and Maintenance
OPEX	Operating Expenditure (M€)
PCU	Purification and Compression Unit
PR	Pre Heater
PSA	Pressure Swing Adsorption
PtF	Power to Fuel
PtG	Power to Gas
PV	photovoltaics
RDF	Refuse Derived Fuel
RES	Renewable Energy Sources
RH	Reheater
SET Plan	Strategic Energy Technology Plan
SH	Super Heater
SNG	Substitute Natural Gas
ST	Steam Turbine
TCI	Total Capital Investment
TDIC	Total Direct and Indirect Costs
TEC	Total Equipment Costs
TEG	Triethylene-glycol
TIC	Total Installed Cost
TIT	Turbine Inlet Temperature (°C)
TPC	Total Plant Costs
TPEC	Total Purchased Equipment Cost
TRL	Technology Readiness Level
USAF	U.S. Air Force
WC	Working Capital
WGS	Water Gas Shift

1. Introduction

1.1 Necessity for a low-carbon energy

From the dawn of the Industrial Revolution, Energy is considered as one of the most important goods for the maintenance of the developed and developing communities. Thousands of wars have been declared and millions of people have been sacrificed in the name of the conquest or the defense of power sources. The contemporary human civilization owns a lot at the power sources obtained by the inner of the Earth; the fossil fuels (coal, oil and natural gas). Especially the last 100 years, the oil price has strong correlation with the geopolitical situation mainly around the Mid East (**Figure 1**).

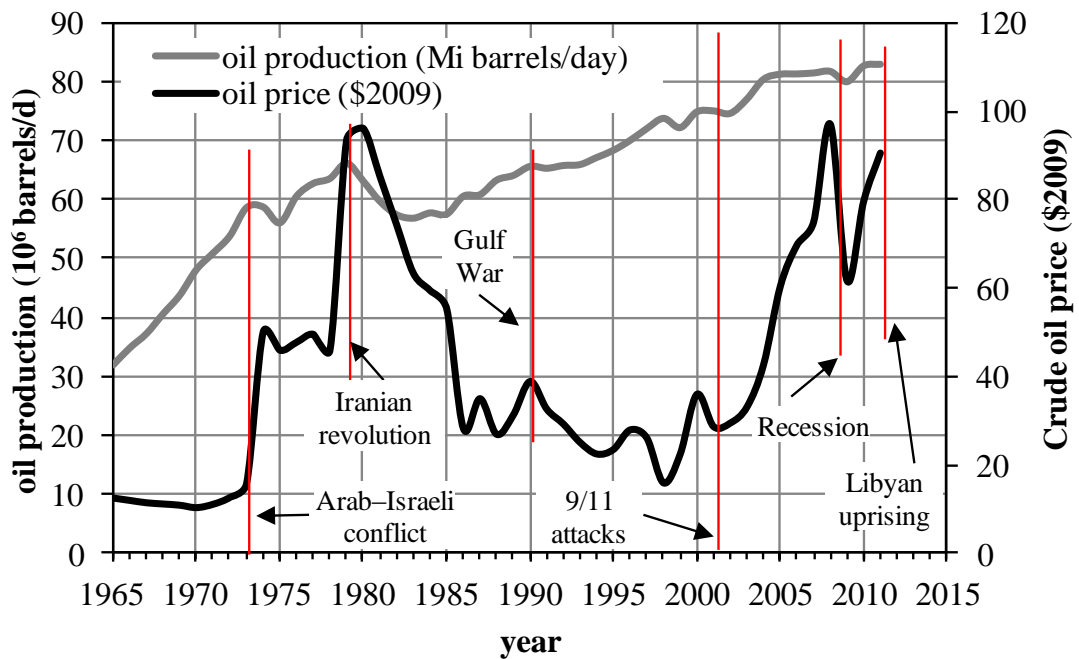


Figure 1. Temporal evolution of crude oil price and world production the last 50 years [1, 2]

The continuous increase in global energy demand is considered as one of the major concerns that should be seriously addressed in short term. According to the predictions of the U.S. Energy Information Administration (EIA), all the fuel types will be exploited with an increasing rate, the total energy consumptions are expected to increase by 10% in 2040 (**Figure 2**).

However, the worldwide power production cannot rely on fossil fuels forever. Two are the main reasons for this: The first is the fact that fossil fuel reserves beneath the surface of Earth are not infinite. According to Shafiee and Topal prediction model, coal reserves are available up to 2112, and will be the only fossil fuel remaining after 2042 [3].

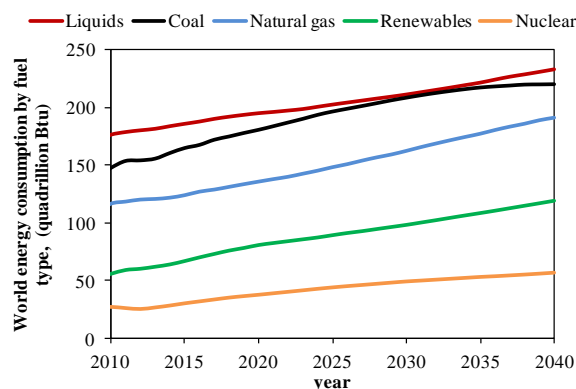


Figure 2. Global energy consumptions by fuel type – prediction [4]

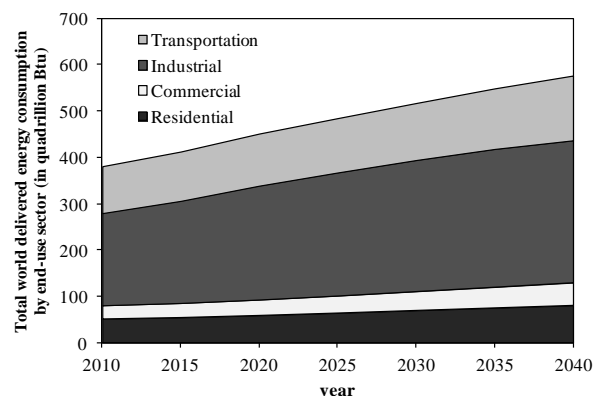


Figure 3. Global energy consumptions by end-use sector– prediction [4]

The second one is the environmental impacts of fossil fuel combustion, which have been proved that are a lot. Due to human activities, CO₂ emissions has increased by 3.9% with respect to the natural carbon cycle [5] and the CO₂ concentration is 385ppm, 30% more than in two centuries ago. A great controversy that has been blown up the last years whether the anthropogenic derived CO₂ emissions is the main cause of the so called “Greenhouse Gas Effect” [6]. According to the International Panel on Climate Change (IPCC), if severe measurements are not taken, the CO₂ concentration in atmosphere may be up to 570 ppm by 2100, causing a rise in the mean global temperature of around 1.9 °C, with irretrievable effects on the life on Earth [7].

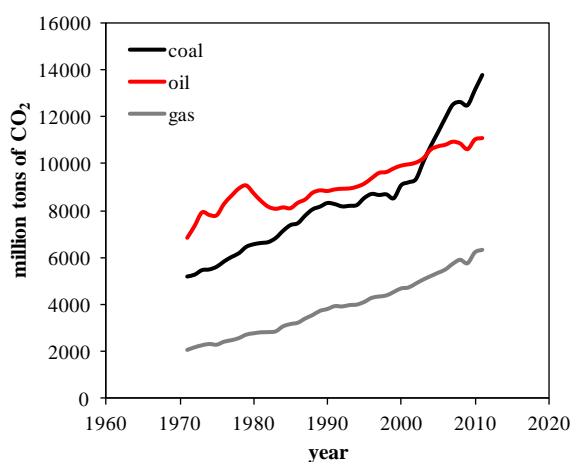


Figure 4. Global Carbon dioxide emissions from major fuel sources since 1970 (data from [8])

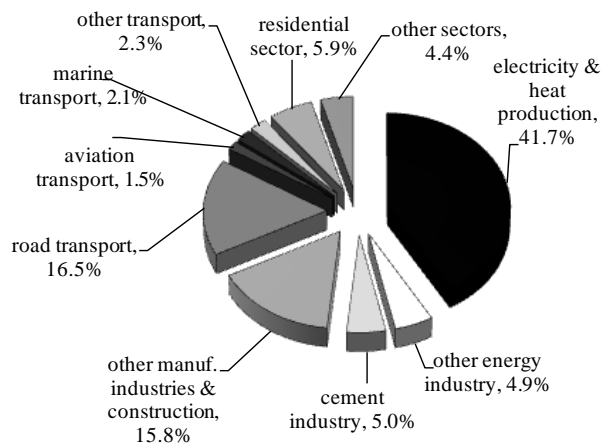


Figure 5. Carbon dioxide emissions by sector in 2011 (data from [8])

1.2 Strategies for a low carbon energy

In this light, EU has put in high priority the development of affordable, cost-effective and resource-efficient technology solutions, towards a decarbonised energy system in a sustainable way. In parallel, EU aims to secure energy supply and to complete the energy internal market in line with the objectives of the Strategic Energy Technology Plan (SET-Plan) and of the related energy legislation (notably the Renewable Energy and CCS Directives) and energy policies designed to deliver the targets: According to them, the GHG emissions in EU should be reduced 20% below 1990 levels by 2020, and a further reduction to 80-95% is intended by 2050. Furthermore, RES should cover 20% of the final energy

consumption in 2020 [9, 10]. More specifically in the transport sector, a reduction of at least 60% of GHGs by 2050 with respect to 1990 is required, while by 2030 the goal for transport will be to reduce GHG emissions to around 20% below their 2008 level [11].

Although the increment of the share of the Renewable Energy Sources (RES) on the energy mixture is considered as a viable option that has strong contribution to the drastic reduction of GHG emissions, there are some bottlenecks that prevent the predominance of RES in the global energy map. Firstly, the RES electricity cost is in general terms higher than the cost of electricity derived from conventional power plants, thermal or nuclear. As it is extracted from **Figure 6**, the increase of RES contribution to the energy mixture leads to increase in the electricity price. Secondly, the electricity grid cannot rely on RES exclusively due to the stochastic feature of the renewable power production (mainly for solar and wind power) and the extreme load fluctuations that require a highly flexible system for an efficient operation. In order to secure the stability of the energy supply to the grid, and taking into account that any energy storage technique is currently economically unfeasible, fuel thermal plants have the lion's share on the electricity production worldwide.

Furthermore, the contemporary societies are not prepared for a no-carbon economy: Apart from power consumption, carbon is an indispensable compound for an enormous range of applications and uses (materials, plastics, clothes, steel), which is primarily derived from fossil fuel sources. Hence, on the one hand, carbon use should be drastically mitigated, on the other hand, our everyday life cannot become independent of the petroleum and coal derived goods and products within a very short period.

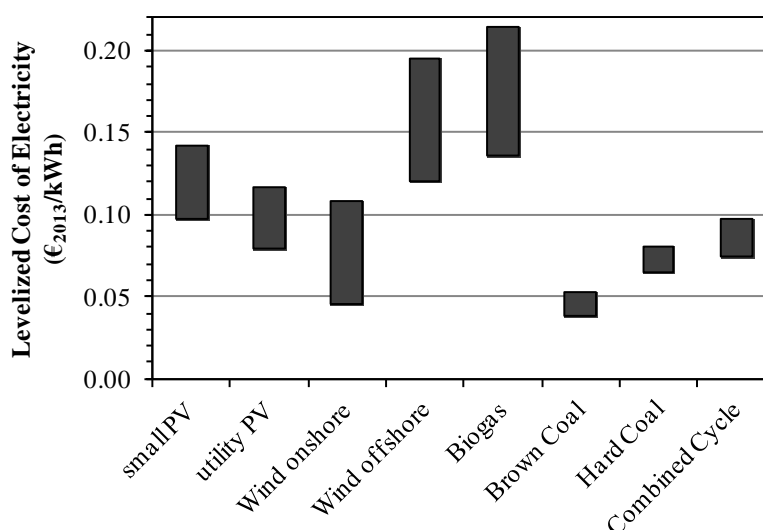


Figure 6. LCOE of renewable energy technologies and conventional power plants at locations in Germany in 2013 (data from [12])

Among the Clean Coal Technologies that are related to the GHG emissions reduction is the adoption of methodologies that increase the power plant efficiency such as advanced supercritical steam cycle, novel materials, improved steam turbines etc. Also, the use of pre-drying technologies in low coal rank cases may lead to an efficiency increase of 4 to 6 percentage points [13-15]. Even though all these options are already commercially available, they have limited influence on the radical reduction of CO₂ emissions.

The three main strategies for drastic mitigation of GHG emissions from anthropogenic sources are the Carbon Capture and Storage (CCS) concept, the Carbon Capture and Utilization (CCU) concept and the biomass based technologies for fossil fuel substitution.

1.2.1 CO₂ capture and storage

According to the Blue Map Scenario of the International Energy Agency (IEA), Carbon Capture and Storage is expected to play the most significant role in the endeavor to meet the 2°C target contributing with 8.2 Gt of the total CO₂ emission cap (14 Gt) [16]. The main options available for storage of CO₂, in a scale sufficiently high to have an impact as a greenhouse gas mitigation option are:

- Storage in the oceans
- Storage in geological formations (deep aquifers, depleted gas and oil reservoirs or deep coal seams, mineral sequestration, etc)
- Enhanced oil and gas recovery (EOR and EGR)

Table 1 summarizes the large scale CO₂ capture projects that are in operation or are scheduled to start worldwide as they are published in the Global CCS Institute web site [17]. In more than half, are captured CO₂ is used for EOR. 35% of them are located in United States and 25% in Asia. 22 out of 54 projects are employed in Power Production sector and 13 of them in Natural Gas processing plants. In most of these cases (60%), a pre-combustion capture option has been selected.

Mitsubishi Heavy Industries, Ltd. (MHI) holds the world leading in large scale post-combustion CO₂ capture units with 11 commercial plants in operation so far [18]. The world largest CO₂ capture and compression plant is expected to start operation in Texas in late 2016, where 4766t/d will be separated and sequestered from flue gases derived from coal fired boiler with 90% capture efficiency.

As stated above, power sector is responsible for the majority of the CO₂ emissions worldwide and therefore, the most of studies, projects and roadmaps in the field of CCS are focused on application in fossil fuel power plants. Generally, the methodology for carbon capture is correlated with the type of fossil fuel (gas/liquid or solid) that is employed in the plant.

Table 1. Status of current large scale CCS projects worldwide ¹ [17]

a/a	Project name	status	Country	CO ₂ capture capacity (Mtpa)	Operation date	Industry/ sector	Capture type	Transport type	Primary storage type
1	Val Verde Natural Gas Plants	Operate	U.S.A.	1.3	1972	NG	Pre-combustion	Pipeline	EOR
2	Enid Fertilizer CO ₂ -EOR	Operate	U.S.A.	0.7	1982	Fertiliser	Industrial separation	Pipeline	EOR
3	Shute Creek Gas Processing Facility	Operate	U.S.A.	7.0	1986	NG	Pre-combustion	Pipeline	EOR
4	Sleipner CO ₂ Storage	Operate	Norway	0.9	1996	NG	Pre-combustion	direct injection	storage - offshore
5	Great Plains Synfuel Plant & Weyburn-Midale	Operate	Canada	3.0	2000	SNG	Pre-combustion	Pipeline	EOR
6	In Salah CO ₂ Storage	Operate	Algeria	0	2004	NG	Pre-combustion	Pipeline	storage - onshore
7	Snøhvit CO ₂ Storage Project	Operate	Norway	0.7	2008	NG	Pre-combustion	Pipeline	storage - offshore
8	Century Plant	Operate	U.S.A.	8.4	2010	NG	Pre-combustion	Pipeline	EOR
9	Air Products Steam Methane Reformer	Operate	U.S.A.	1.0	2013	Hydrogen	Industrial separation	Pipeline	EOR
10	Coffeyville Gasification Plant	Operate	U.S.A.	1.0	2013	Fertiliser	Industrial separation	Pipeline	EOR
11	Lost Cabin Gas Plant	Operate	U.S.A.	0.9	2013	NG	Pre-combustion	Pipeline	EOR
12	Petrobras Lula Oil Field CCS Project	Operate	Brazil	0.7	2013	NG	Pre-combustion	direct injection	EOR
13	Boundary Dam Integrated CCS Demonstration	Operate	Canada	1.0	2014	Power	Post-combustion	Pipeline	EOR
14	Alberta Carbon Trunk Line with Agrium CO ₂ Stream	Execute	Canada	0.3-0.6	2015	Fertiliser	Industrial separation	Pipeline	EOR
15	Illinois Industrial CCS	Execute	U.S.A.	1.0	2015	Chemical	Industrial separation	Pipeline	storage - onshore
16	Quest	Execute	Canada	1.08	2015	Hydrogen	Industrial separation	Pipeline	storage - onshore
17	Uthmaniyah CO ₂ EOR Demonstration	Execute	S. Arabia	0.8	2015	NG	Pre-combustion	Pipeline	EOR
18	Gorgon Carbon Dioxide Injection	Execute	Australia	3.4-4.0	2016	NG	Pre-combustion	Pipeline	storage - onshore
19	Kemper County Energy Facility	Execute	U.S.A.	3.0	2016	Power	Pre-combustion	Pipeline	EOR
20	Abu Dhabi CCS	Execute	U.A.E.	0.8	2016	Iron & steel	Industrial separation	Pipeline	EOR
21	Petra Nova Carbon Capture	Execute	U.S.A.	1.4	2016	Power	Post-combustion	Pipeline	EOR
22	Sinopec Qilu Petrochemical CCS	Define	China	0.5	2016	Chemical	Pre-combustion	Pipeline	EOR
23	Yanchang Integrated CCS Demonstration	Define	China	0.46	2016	Chemical	Pre-combustion	Pipeline	EOR
24	Alberta Carbon Trunk Line with North West Sturgeon Refinery CO ₂ Stream	Execute	Canada	1.2-1.4	2017	Oil refining	Pre-combustion	Pipeline	EOR
25	FutureGen 2.0	Define	U.S.A.	1.1	2017	Power	Oxy-fuel	Pipeline	storage - onshore
26	Rotterdam Opslag en Afvang Demonstratieproject	Define	Netherlands	1.1	2017	Power	Post-combustion	Pipeline	storage - offshore
27	Sinopec Shengli Power Plant CCS	Define	China	1.0	2017	Power	Post-combustion	Pipeline	EOR
28	Sargas Texas Point Comfort	Define	U.S.A.	0.8	2017	Power	Post-combustion	Pipeline	EOR

Chapter 1

29	Medicine Bow Coal-to-Liquids Facility	Define	U.S.A.	2.5	2018	CTL	Pre-combustion	Pipeline	EOR
30	Spectra Energy's Fort Nelson CCS	Define	Canada	2.2	2018	NG	Pre-combustion	Pipeline	storage - onshore
31	Korea-CCS 1	Evaluate	Korea	1.0	2018	Power	Post-combustion	Shipping	storage - offshore
32	Quintana South Heart	Evaluate	U.S.A.	2.1	2018	Power	Pre-combustion	Pipeline	EOR
33	China Resources Power Integrated CCS Demonstration	Identify	China	1.0	2018	Power	Post-combustion	Pipeline	storage - offshore
34	Don Valley Power	Define	U.K.	5.0	2019	Power	Pre-combustion	Pipeline	storage - offshore
35	Hydrogen Energy California	Define	U.S.A.	2.7	2019	Power	Pre-combustion	Pipeline	EOR
36	Texas Clean Energy	Define	U.S.A.	2.7	2019	Power	Pre-combustion	Pipeline	EOR
37	Peterhead CCS	Define	U.K.	1.0	2019	Power	Post-combustion	Pipeline	storage - offshore
38	Bow City Power	Evaluate	Canada	1.0	2019	Power	Post-combustion	Pipeline	EOR
39	Indiana Gasification	Evaluate	U.S.A.	5.5	2019	SNG	Pre-combustion	Pipeline	EOR
40	Mississippi Gasification	Evaluate	U.S.A.	4.0	2019	Chemical	Pre-combustion	Pipeline	EOR
41	Dongguan Taiyangzhou IGCC with CCS	Identify	China	1.0 - 1.2	2019	Power	Pre-combustion	Shipping	storage - offshore
42	Huaneng GreenGen IGCC	Evaluate	China	2.0	2020	Power	Pre-combustion	Pipeline	under review
43	Korea-CCS 2	Evaluate	Korea	1.0	2020	Power	Pre-combustion	Shipping	storage - offshore
44	Shenhua Ordos CTL Project (Phase 2)	Evaluate	China	1.0	2020	CTL	Pre-combustion	Pipeline	storage - onshore
45	South West Hub	Evaluate	Australia	2.5	2020	Fertiliser	Industrial separation	Pipeline	storage - onshore
46	Shanxi International Energy Group CCUS	Identify	China	2.0	2020	Power	Oxy-fuel	Pipeline	not specified
47	Shenhua / Dow Chemicals Yulin Coal to Chemicals	Identify	China	2.0-3.0	2020	Chemical	Industrial separation	Pipeline	storage - onshore
48	Shenhua Ningxia CTL	Identify	China	2.0	2020	CTL	Pre-combustion	Pipeline	Not Specified
49	Caledonia Clean Energy	Evaluate	U.K.	3.8	2022	Power	Pre-combustion	Pipeline	storage - offshore
50	PetroChina Jilin Oil Field EOR (Ph. 2)	Define	China	0.8	2016-17	NG	Pre-combustion	Pipeline	EOR
51	Riley Ridge Gas Plant	Evaluate	U.S.A.	2.5	2018-2020	NG	Pre-combustion	Pipeline	EOR
52	C.GEN North Killingholme Power	Evaluate	U.K.	2.5	2019	Power	Pre-combustion	Pipeline	Not specified
53	White Rose CCS	Define	U.K.	2.0	2019-20	Power	Oxy-fuel	Pipeline	storage - offshore
54	CarbonNet	Evaluate	Australia	1.0-5.0	2020's	Under evaluation		Pipeline	storage - offshore

¹ explanatory notes: a) storage – onshore/offshore: dedicated geological storage – onshore/offshore deep saline formations, b) EOR: Enhanced Oil Recovery, c) CTL: Coal to Liquids, d) SNG: Synthetic Natural Gas

An overview of the available options for CO₂ separation from a gas stream (flue gas or synthesis gas) is presented in **Figure 7**. Apart from the CO₂ storage in order to mitigate the global GHG emissions, the CO₂ removal from a gaseous stream is a known process in gas processing industry that is performed for various other purposes, too: a) in gas purification (e.g. in a hydrogen plant), b) in syngas cleaning section in a Gas to Liquid Plant before the Fischer-Tropsch process, c) in case that the pure CO₂ stream is the final product in a chemical industry, etc. Therefore, the investigation of CO₂ separation has a multiple interest in terms of environmental protection and industrial processes optimization.

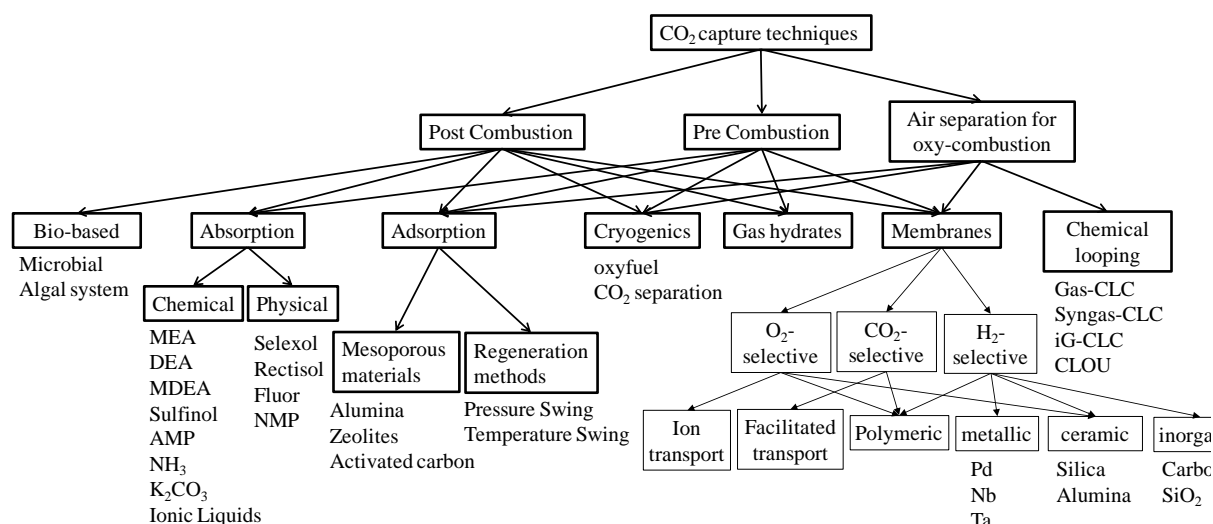


Figure 7. Process and various options for pre-combustion carbon capture

a) CO₂ capture from Natural Gas fired power plants

In CEASAR project, the most representative capture technologies for NG-fired power plants was investigated and evaluated for the case of a state-of-the art combined cycle power plant. According to it, chemical absorption is considered as the most preferable techniques for such application. the MEA scrubbing for post-combustion option and MDEA for pre-combustion option [19].

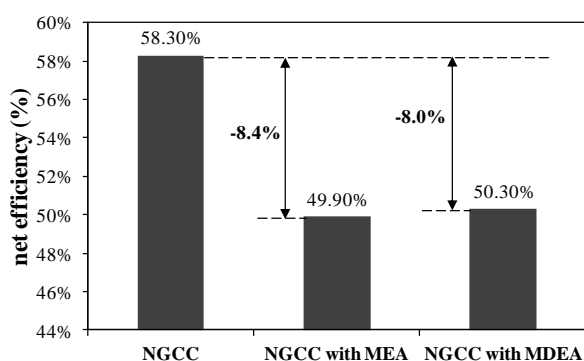


Figure 8. Net efficiency of MEA/MDEA for CO₂ capture in NGCC

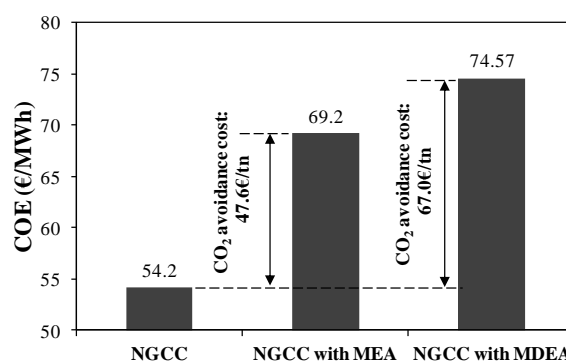


Figure 9. Cost of Electricity and CO₂ avoidance cost of MEA/MDEA for CO₂ capture in NGCC plant

Even though the post combustion capture has lower estimated COE (**Figure 9**), pre-combustion CO₂ capture offers the unique opportunity to co-produce H₂ and power. In a future low carbon economy, H₂ may be one of the most efficient energy vectors, with possible application to fuel cells in the transport

or power sector. The interest for further development of the pre-combustion options is also illustrated by the several commercial scale plants that are designed for pre-combustion capture (see **Table 1**).

Among the various pre-combustion techniques, palladium (Pd) or Pd-alloys membranes technology is considered as a promising option. Palladium membranes were first developed for pure hydrogen production in the early 1950's and their development has been spurred by the desire to produce ultra pure H_2 for applications such as fuel cells. Palladium membranes have demonstrated its superiority to other H_2 -selective membranes due to its ability to be permeable to hydrogen over a range of temperatures and its high selectivity resulting in the production of hydrogen of the highest purity. Palladium membranes have previously only been applied in niche markets [14]. Although it is an already known application mainly for ultra-pure hydrogen production and other processes [20], the use of a Pd membrane reactor (MR) or membrane separator (MS) for H_2/CO_2 separation has not been investigated so far in an advanced energy system such a NG fired power plant.

b) CO_2 capture from coal fired power plants

The issue of capturing CO_2 from coal fired power plants has been extensively investigated the last years. Especially, three PhDs in the Laboratory of Steam Boilers and Thermal Plants were dedicated to CO_2 capture techniques in coal/lignite fired power plants, using both post-combustion, oxy-fuel [21, 22] and pre-combustion [23] options.

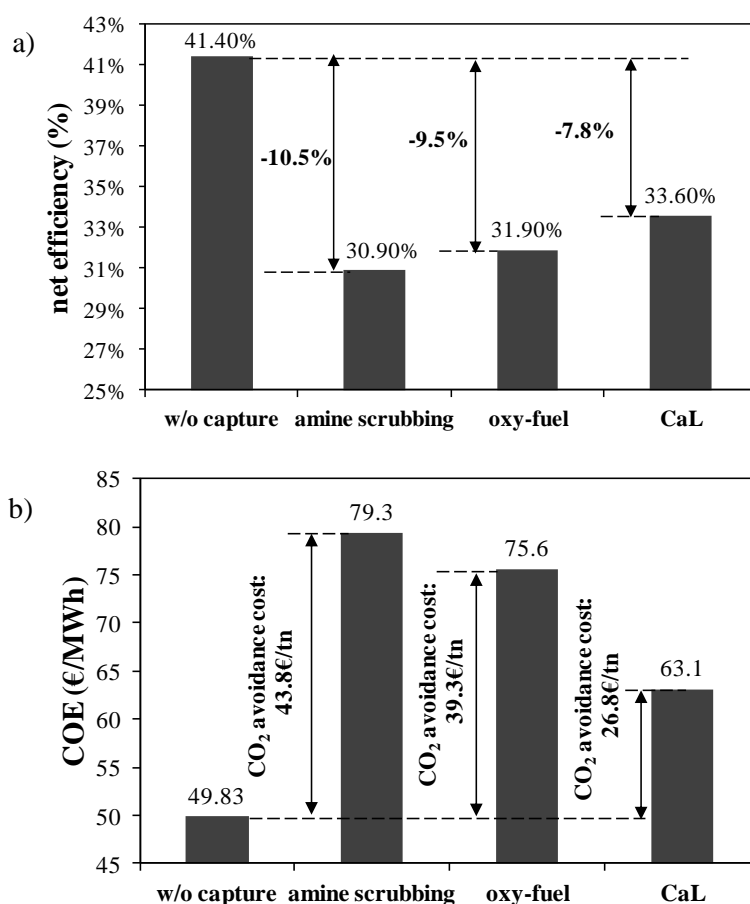


Figure 10. a) Net efficiency and b) Cost of Electricity and CO_2 avoidance cost of three CO_2 capture techniques employed in coal fired power plant [24, 25]

Among the most competitive capture technologies for possible implication in a coal fired power plant in future are the amine scrubbing (e.g. MEA solvent), the oxyfuel (or O_2/CO_2 cycle) and the Calcium Looping process (CaL). Based on data from the International Energy Agency [24] and the EU funded CAL-MOD project [25], the CaL technology presents better characteristics in terms of net efficiency (**Figure 10a**) and cost of electricity/ CO_2 avoidance cost (**Figure 10b**).

It is admitted that special effort is dedicated to minimize the energy penalty in all the capture techniques, in the framework of numerous studies worldwide. There is room enough for technology improvements that will beneficiate the plant performance and the concept feasibility. Nevertheless, the enhancement of such three technologies is fundamentally limited by the thermodynamics. The proper tool for the evaluation and estimation of such thermodynamic constrains is exergy analysis.

Another issue that is not taken into account in most of the theoretical studies is the quality of the final CO_2 stream in terms of the impurities. Although the gas stream that is derived from a capture unit is in high CO_2 concentration, it is not allowed to be transferred and stored unless the concentration of the species except CO_2 fulfils certain specifications owed to H&S (explosion avoidance), technical reasons (mainly corrosion), [26-28] and increase in storage capacity [29]. Hence an intensive gas treatment before compression is compulsory in the most of the capture cases.

1.2.2 CO_2 capture and utilization

The alternative concept for the management of captured CO_2 is the utilization of it in various purposes, namely as ‘the CO_2 capture and utilization (CCU) concept’. The majority of CO_2 use in industry is for urea production, which accounts for more than half of the global annual usage [30]. Alternatively, CO_2 is utilized also physically in various applications such as refrigerant medium, in fire extinguishers and in the petroleum and NG industry for Enhanced Oil Recovery (EOR) and Enhanced Gas Recovery (EGR), respectively [31, 32]. Even though CO_2 is a thermodynamically and kinetically stable molecule, various ways have been developed, mainly based on the fact that the central carbon of the CO_2 molecule is electrophilic and can be easily attacked by nucleophiles [33]. The methods for CO_2 transformation can be sorted in six categories [30, 34]: chemical reduction (i.e. Boudouard), electrochemical reduction [35], photochemical reduction (i.e. artificial photosynthesis), thermochemical conversion (i.e. dry reforming and hydrogenation), biological (i.e. photosynthesis, anaerobic conversion) and inorganic transformation [36]. **Figure 11** shows the potential pathways for CO_2 transformation into valuable products.

Up to now, only 0.5% of the total anthropogenic CO_2 emissions are used in industrial applications, which is translated into 24 Gt CO_2 per year [38]. In order the CCU concept to have effective impact on the drastic reduction of the CO_2 emissions, the quantities of end-products derived from CO_2 transformation should cover the market demand. The selection of the final products should be correlated to global demands and consumptions of them.

The CO_2 hydrogenation towards methane production (also known as Sabatier reaction) has extensively investigated since 1910 and the substitute natural gas (SNG) was the first CCU based energy carrier that was examined. The most significant advantages of the Power to Gas (PtG) concept against other energy storage techniques are a) the high storage capacity compared to H_2 , b) the high energy density ($\sim 40 \text{ MJ/m}^3$) and c) the existing infrastructure for distribution in the NG grid and utilization in domestic, power and industrial sectors.

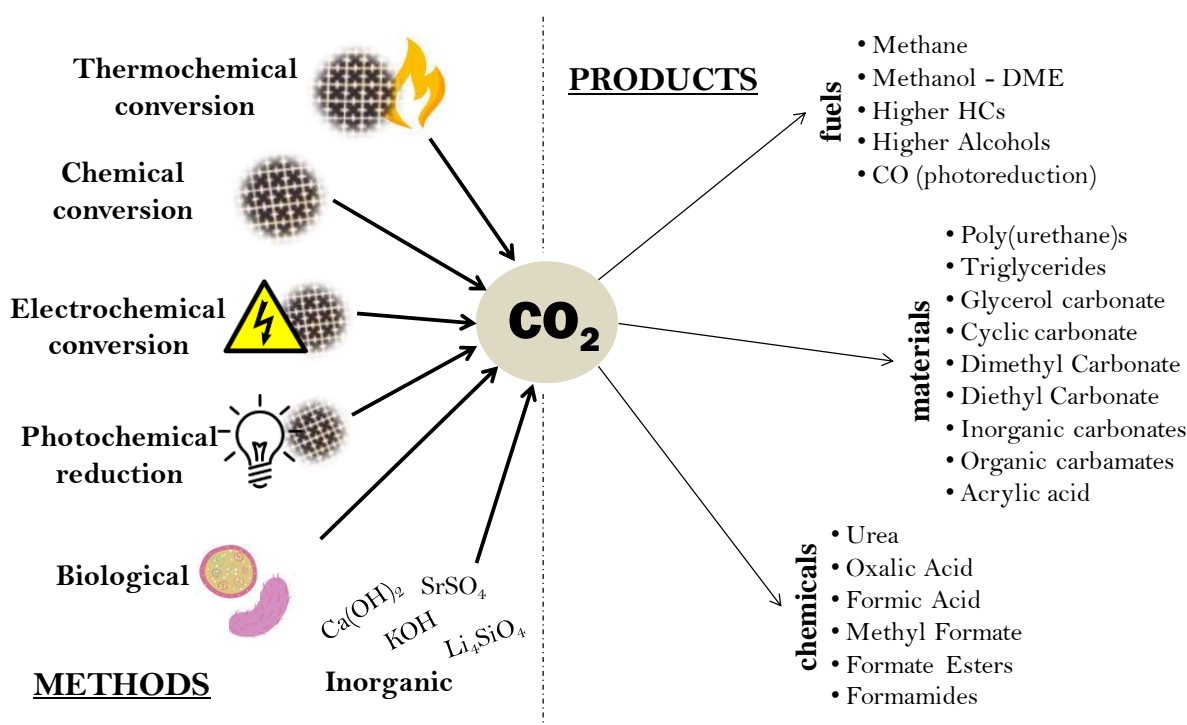


Figure 11. CO₂ fixation options [30, 34, 37]

However, this is an eight-electron process with significant kinetic limitations, which thus requires specific operating conditions (high pressure and temperature) in presence of catalyst in order to achieve acceptable rates and selectivities [39, 40]. The great disadvantage of the PtG concept is the high production cost of SNG which may be 5 to 6 times than current market prices [41]. This last fact mainly turned the interest towards the production of advanced liquid fuels such methanol.

Methanol is considered as one of the most valuable chemicals with a series of uses in various sectors (power, transport, steel, chemical industry) either as fuel or as block for the synthesis of other chemicals (dimethyl ether, formaldehyde, methyl tert-butyl ether, acetic acid, gasoline, etc). Moreover, since methanol has the lowest production cost to market price ratio among the fuels that can be potentially produced from CO₂, it is the most representative product of the so called “Power-to-Fuel” (PtF) concept. In Iceland, a demonstration plant with capacity 4,000 tons of renewable methanol per year is operating since 2011 and a larger plant with capacity 40,000 t/y is planned to be constructed by Carbon Recycling International (CRI)[42]. In Canada, Blue Fuel Energy will built a methanol plant with capacity 400,000 t/y, powered by renewable electricity [43].

The “Power to Fuel” concept has been linked with the production of fuel mainly used for transportation. Transportation sector has a considerable share on the total energy use worldwide (~18%), the vast majority is derived from liquid fuels usage [44]. The remarkable development of China and India induces the considerable increase in energy demand in the transportation sector the next decades (Figure 12). This matter is inextricably connected with the global warming crisis, and the inevitable depletion of the fossil based energy sources (energy shortage crisis). Thus, the reduction of CO₂ footprint in the transportation sector should focus on the origin of the carbon or the adoption of renewable sources (biofuels).

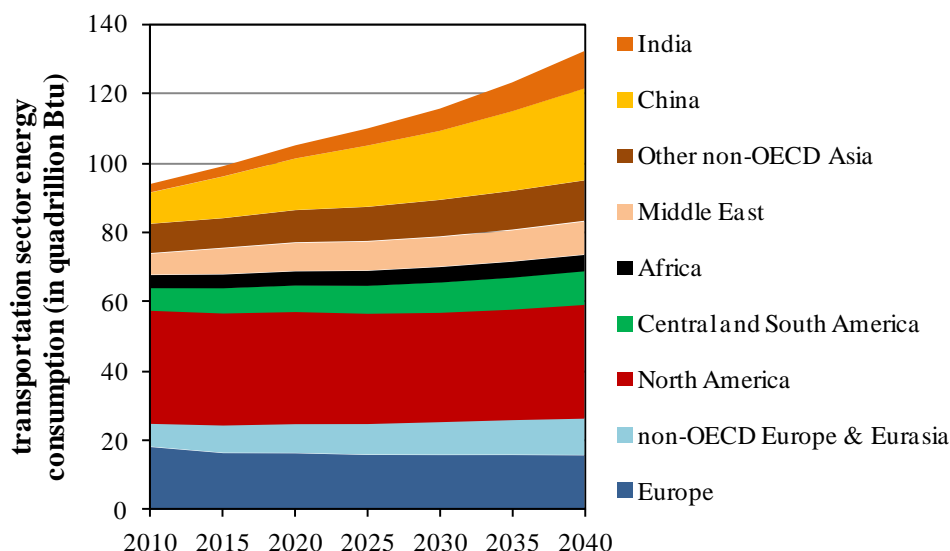


Figure 12. Energy consumption in the transportation section by region in the period 2010-2040, (data from [4])

1.2.3 Biomass usage for fossil fuels substitution

As quoted above, the contemporary civilization is tightly bonded with the petroleum based economy; even if the problem of power production and supply is totally solved by the use of renewable and sustainable energy sources, we cannot imagine our lives without the petroleum based materials and products such as plastics, clothes, chemicals, etc.

Bio-based energy (bioenergy) is expected to play a crucial role in the achievement of the targets for GHG emissions mitigation contributing to more than half the European renewable energy in 2020 and covering about 11% of the total energy consumption in Europe. However, several actions are still required to promote the development of alternative fuels and advanced biofuels from lignocellulose and other non-food feedstocks, putting them into commercialization and securing their sustainability [11].

The term biorefinery is referred to an energy system that uses as feedstock biomass to convert it into valuable fuels, heat & power or chemicals. **Figure 13** illustrates the potential pathways in a biorefinery plant. The four criteria for the classification of a biorefinery plant are: a) the kind of feedstock, b) the platform that is used for the biomass transformation (C6 sugars, syngas, oils, bio-oil, biogas, lignin, etc.), c) the kind of process for the final products accomplishment (thermal, chemical or biological) and d) the final products and their application: energy products (fuel, heat and power) or material products (chemicals).

Some of the chemical compounds that are widely produced in most of the biorefinery systems are the higher alcohols (C2+) and especially ethanol (or bioethanol), which is considered as the most widespread renewable fuel accounting 23430 million gallons in 2013 globally [28]. Only 5% of the global ethanol is petroleum derived (synthetic) [27, 29]. In commercial scale, bioethanol is produced through biochemical conversion (hydrolysis and fermentation) of lignocellulosic or sugar/starch feedstocks. USA and Brazil are the world leading countries in bioethanol production [30] mainly from grains (corn) and sugar, respectively.

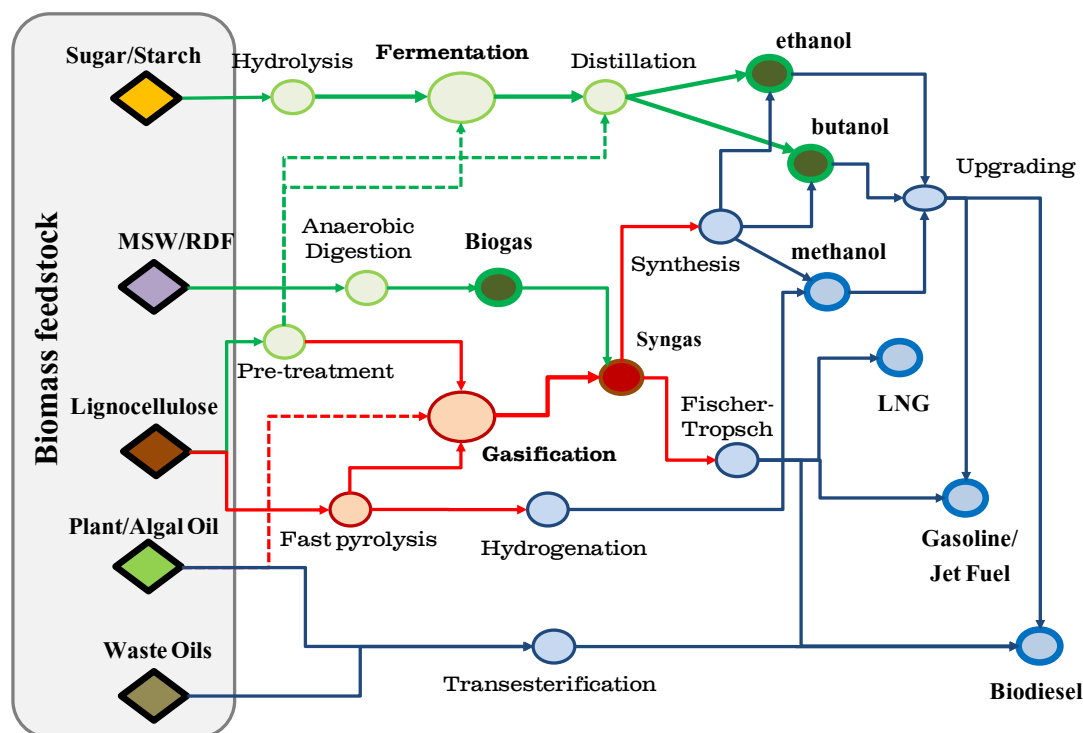


Figure 13. The multiple synthetic conversion routes of major biofuels produced from first and second-generation biomass feedstock

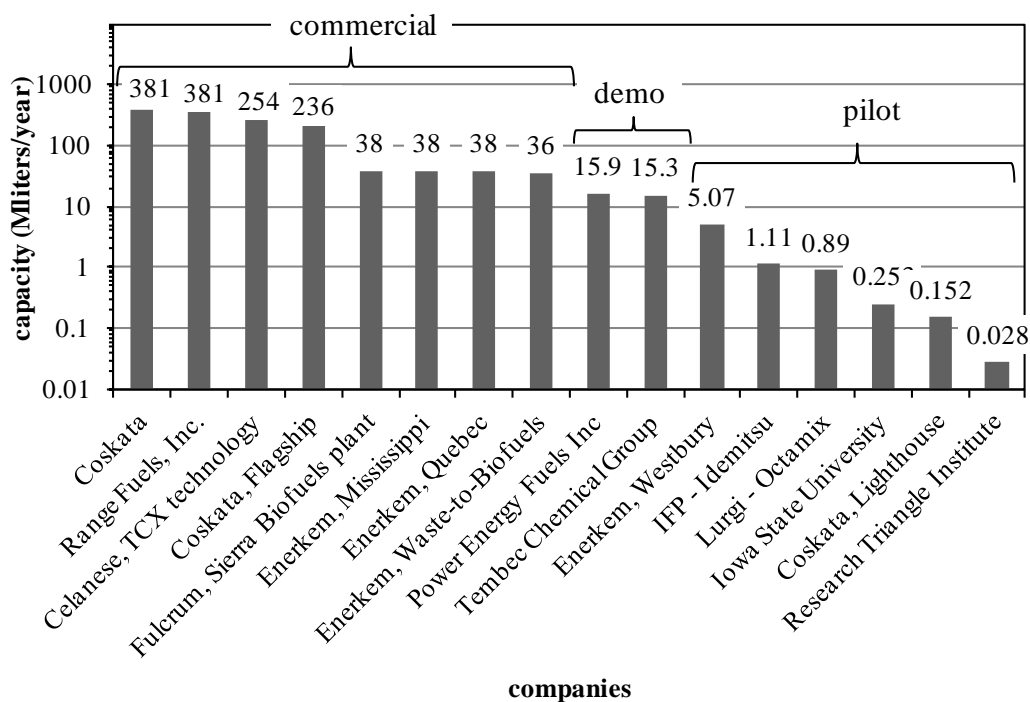


Figure 14. Current status of Higher Alcohols Synthesis using thermochemical technologies [45]

The plants that are dedicated to higher alcohols (HA) production in commercial, demo and pilot scale via thermochemical methods are presented in **Figure 14** with their corresponding capacity in millions liters per year.

Even though the selectivity rates through biochemical processes are very high, only the cellulosic part of the biomass can be transformed into ethanol, resulting to rather low carbon utilization rates (~25%). The alternative method for biomass to higher alcohol synthesis (HAS), where the biomass carbon utilization is potentially higher, is the thermochemical pathway. This route has very strong similarities with the coal to liquid (CtL) and gas to liquid (GtL) concepts, since the produced syngas is converted into C₂+ alcohols under high temperature and pressures (240-420°C, 40-260 bars) over specific catalyst (Cu-Co, Cu-Zn, Rh- and MoS₂). The basic steps of a thermochemical biorefinery based on biomass basification are shown in **Figure 15**. The principal weakness for commercial application in industrial level is the high methane and methanol selectivities. Very few studies have focused on the improvement of the process as far as the selectivity into alcohols with large carbon number is concerned.



Figure 15. Fundamental steps of a thermochemically based biorefinery system

1.3 Scope of this PhD thesis

The scope of this Thesis is the development, the design and the modeling of advanced energy systems and processes that are oriented to the significant reduction of the GHG emissions and especially the CO₂ emissions. The methodology for process integration and design of novel systems that are based on low TRL (Technology Readiness Level) is presented in detail: Most of the case studies use data obtained from lab or bench scale tests for the design of systems in full scale. In the first section of the Introduction, it is explained why it is important to move to a low carbon energy era, while in the second section the roadmap for the accomplishment of this transition. Hence, three parts are determined for the investigation of such energy systems, the Carbon Capture and Storage, the Carbon Capture and Utilization and the bio-based advanced fuels and chemicals production. These options are presented justifying why are considered as the most attractive and promising.

The first part is dedicated to the process integration of power production systems with CCS. More specifically, the implementation of the Pd Membrane Technology in gas fired power plant and the exergy analysis of the most competitive capture techniques in a coal fired power plant are studied. On the one hand, the identification of the design specifications and the operating conditions is addressed for the optimum performance of the plant, in terms of efficiency and electricity cost. On the other hand, in the second analysis of the first part, the calculation of the exergy losses in each process can answer to identify the best kind of energy to be spent for CO₂ capture in a coal power plant: low quality heat through steam (amine scrubbing), high quality heat through fuel combustion (CaL process) or electrical power (oxyfuel combustion). Special attention is paid for the CO₂ stream quality in accordance to specific regulations for the compression, transport and storage.

The second part relates to the evolution of the second strategic option for the management of the capture CO₂, the transformation into valuable chemicals and fuels. More specific, in the case of the methanol production from CO₂ and the need for further investigation in order to be an economically competitive concept, several techno-economic aspects and parametric analyses are investigated. The main goal of the fourth chapter is the determination of the boundary conditions that make it as a profitable option. In the second chapter of this part, two novel process schemes of CO₂ hydrogenation

with advanced characteristics are presented towards the enhancement of methanol and ethanol production. The main goal in this analysis is to develop new process concepts that can yield the desired products with lower losses and power/heat consumptions.

The third part deals with the development, design, process integration, optimization and techno-economic analysis of a thermochemical biorefinery that employs higher alcohols as chemical blocks. In the first chapter, a detailed description of the bio-based higher alcohols production process through thermochemical route is performed and the modelling methodology that is followed in each step. In addition, the influence of various parameters on the plant operation is investigated in terms of the maximization of the final products yields in conjunction with the minimization of the thermal and power consumptions. In the second chapter, a further investigation in this bio-based concept is made focusing on the mixed alcohols upgrading towards the synthesis of added value fuels mainly for aviation use. More specifically, two novel schemes are presented in detail, one based on ethanol and another based on isobutanol. These systems are thoroughly examined from the energy and economic point of view, comparing with the corresponding biochemical schemes.

The Thesis focuses on several advanced and novel energy systems, while the main goals that are set are summarized below:

- Design and process integration of new energy systems and identification of the parameters for the best operation
- Comprehension of the operation principles of various new processes and the impact of these parameters on the plant performance
- Identification and suggestion the direction of research for the improvement of the advanced technologies and processes that are examined in this Thesis
- Cost estimation, CAPEX and OPEX calculation and sensitivity analysis in order these systems to be an economically attractive option
- Comparison with existing and corresponding technologies for the definition of the most promising techniques for further investigation in larger scale
- Determination of the roadmap of the future research activities for further improvement of these energy systems and processes

1.4 Process modeling: general definitions, methodology, contribution

The most appropriate way to assess the potential commercialization and erection of advanced systems is by means of the techniques of the Chemical Process Modeling in conjunction with the Cost Engineering disciplinary. The basic advantage of the Thermodynamic Tools in contrast to other numerical approaches such CFD analysis is that, in general terms, the calculated results can be yielded very fast with negligible computational cost, enabling the performance of several runs, test cases, parametric investigations in steady or unsteady conditions (depending on the software used), in off-design loads. These analyses lead to valuable conclusions about a) the effective operation of the plant in terms of efficiency and the main design data, b) the size and the main dimension of the most significant components, c) the potential modifications for the plant improvement (if any) and d) capital and operational cost.

The simulation tool that was mainly used in this Thesis is ASPEN PlusTM. The main features of this process simulation software are summarized below:

- Component databank that consists of thermophysical properties, reaction kinetics, enthalpy and transport properties.
- Equipment database for the simulation of basic operating principles providing mass and energy balance and the main operation features, depending the unit block.
- Sophisticated thermodynamic model solver that is served for the calculation of thermodynamic interactions such as vapour-liquid equilibria, properties of each stream, the operation of complex units such columns, etc. Mathematical solver that solves the equations that are used to simulate the process operations.
- Inter-connection with Excel and FORTRAN that enables the user to simulate more processes that do not exist in the default options such user defined operation unit, reaction kinetics, etc.
- Main flowsheet program – Controls and keeps track of the flowsheet calculations. This part of the software interacts with the data banks and solvers and controls the order of calculation. This part usually has a graphical user interface.

2. Using palladium membranes for carbon capture in natural gas combined cycle power plants: Process integration and techno-economics

2.1 Introduction

The enhancement of innovative technologies for Carbon Capture and Storage (CCS) is an important option for the drastic reduction of greenhouse gas emissions. In this way, thermal plants can remain as the predominant energy source while causing fewer environmental impacts, since it seems renewable sources will be unable to replace them completely in the foreseeable future. The three commonly proposed options for CO₂ removal and storage in thermal plants are:

- post-combustion capture, mostly used as a retrofitting option for existing plants, where the flue gases from fossil fuel combustion are treated to clean them of CO₂ before the stack [46-48].
- oxy-fuel combustion, where the oxidant is pure oxygen (almost 99% purity or higher) that is produced in an Air Separation Unit (ASU) [49].
- pre-combustion capture, where fossil fuel (i.e. coal and natural gas) is transformed to synthesis gas (or syngas, composed mostly from H₂, CO, CO₂ and H₂O) before it enters the combustion chamber. Thus, carbon is separated before the power island. The carbon sequestration options are independent of the initial fuel type (gas or solid) since the produced syngas is able to attain the desired conditions (temperature, pressure, composition) for the carbon-capture process. The gas-conditioning step can include processes like shift, quench, gas cleaning and cooling.

Several studies have investigated pre-combustion capture modelling for natural gas thermal plants in recent years, employing various separation technologies. Most case studies employ chemical absorption for CO₂ separation from synthetic gas, with an air-blown ATR reactor [50-54]. There are also simulations that adopt other approaches, like physical absorption [55] and hydrogen separation membrane reactors (HSMR), where various other reactions are also carried out, such as reforming [56] and water gas shift [57]. Useful information can be derived from the review by Scholes et al. [58] concerning carbon sequestration with membranes. CO₂-selective membranes have limited application in power plants with carbon capture [59] and therefore there is no further discussion in this area.

Each type of membrane is based on a different operating principle. For instance, hydrogen separation with metallic membranes, where the predominant material is Pd, can occur owing to the dissociative chemisorption of H₂ [60]. **Figure 16** shows a schematic depiction of a Pd membrane separator with the basic terms and the H₂ permeation mechanism. A *membrane* is a thin sheet of natural or synthetic material that is permeable to substances in solution. Consequently, a membrane is a physical barrier between two compartments; the *feed side*, containing the mixture (*feed*) that consists of the compound that needs to be recovered and the *permeate side*, where the permeating specie is retrieved. The driving force for H₂ permeation is the difference in hydrogen partial pressure between the two sides, Δp_{H_2} . The hydrogen flux J_{H_2} (mol/(m²s)) at steady state is expressed by Sievert's law:

$$J_{H_2} = Q_{H_2} \left[p_{H_2, feed}^n - p_{H_2, perm}^n \right] \quad (\text{Eq. 1})$$

where $p_{H_2, feed}^n$, $p_{H_2, perm}^n$ are the hydrogen partial pressure in the feed and permeate side respectively and Q_{H_2} (mol/(m²sPaⁿ)) is the hydrogen permeance which can be represented by the Arrhenius equation:

$$Q_{H_2} = \frac{q_{H_2}}{\delta} e^{-\left[\frac{E_a}{RT} - \frac{E_a}{RT_{REF}}\right]} \quad (\text{Eq. 2})$$

where q_{H_2} is the hydrogen permeability (mol/(msPaⁿ)), δ is the membrane thickness (m), E_a is the activation energy (J/mol), R is the gas constant (8.314 J/molK) and T is the operating temperature (K). The exponent n expresses the exponential correlation of partial pressure with the permeation. A typical value of n is 0.5. Maintaining a high driving force ($p_{H_2,feed}^n - p_{H_2,perm}^n$) at elevated rates along the length of the membrane is achieved by the application of the *sweep gas*. Another feature of a membrane is *selectivity*, which expresses the ability to permit only hydrogen to permeate through the membrane. An operating condition that is a function of the applied feed flow rate, concentration and available membrane area is the *Hydrogen Recovery Factor (HRF)*. It is defined as the ratio of hydrogen permeated to the maximum amount of hydrogen that can be recovered or derived from the feed gas and the stoichiometrically maximum amount of produced H₂ from reactions obtained in the feed side:

$$HRF = \frac{m_{H_2,permeate}}{m_{H_2,feed} + m_{H_2,max}^{produced}} \quad (\text{Eq. 3})$$

This parameter and the permeability determine the required membrane area for a certain separation, which is the most important factor affecting the cost of the whole equipment.

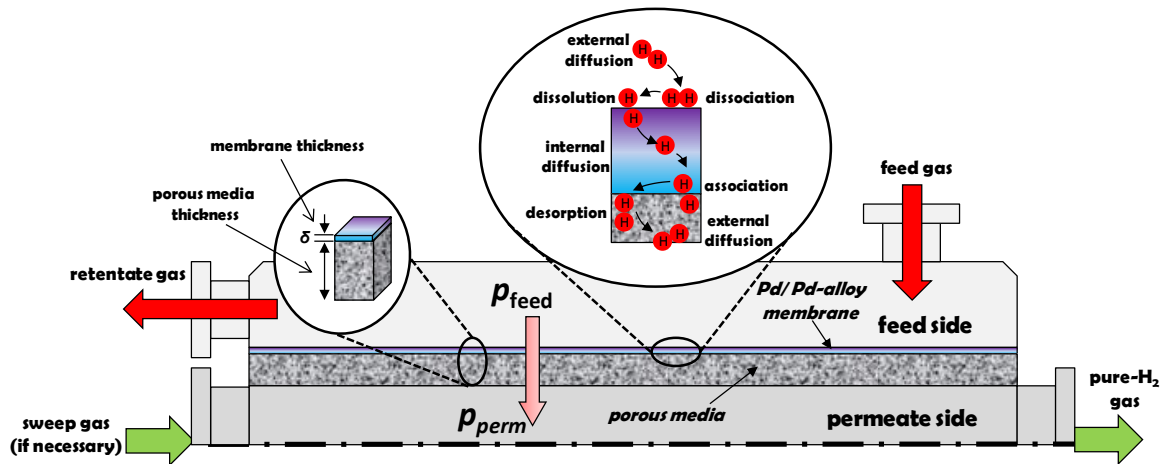


Figure 16. Hydrogen permeation through Pd membranes: general definitions and mechanism

On the other hand, porous inorganic membranes, mostly made from silica [61] and zeolites [62] or alumina [63] are correlated with molecular diffusion of H₂ [64]. Polymeric membranes (non-porous) combine solution and diffusion mechanisms [65]. Although the main disadvantage of membranes with Pd-alloys is the high cost of the material, they offer perfect hydrogen permeability and selectivity, contributing to the achievement of zero CO₂ emissions [58] [66]. Nevertheless, considerable efforts are being made to improve membrane characteristics, lowering membrane cost by reducing the required membrane area [47, 58, 67].

In this chapter, Pd membrane implementation for CO₂ capture in a natural-gas-fired power plant is investigated. After a brief description of the process, the rest of the chapter is separated into two parts: a thermodynamic and an economic analysis. In the thermodynamic analysis, the methodology for the process optimization is investigated concerning the optimum design of the system and the suitable operating parameters. In the second part, a cost analysis and calculation of the cost of electricity and CO₂ avoided is presented for the six selected cases. Additionally, the effect of membrane area on the economic feasibility of the system is investigated.

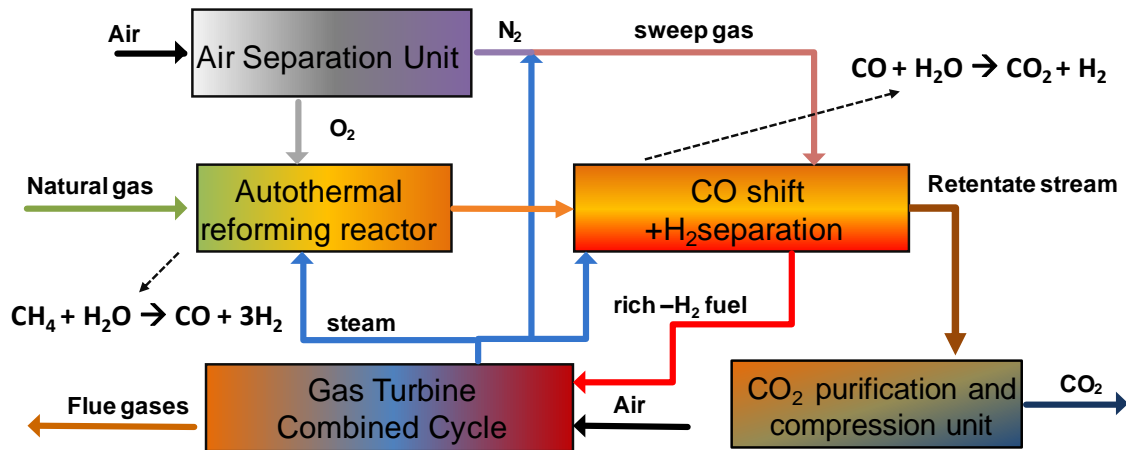


Figure 17. Process flowsheet diagram of the total power system

The outline of the system is presented in **Figure 17**. An H_2 -rich fuel is produced from natural gas reforming in an Autothermal Reformer (ATR), and CO is further shifted in the water gas shift reactor (WGS). The autothermal conditions are met using a rich oxygen stream (95% purity) produced in an air separation unit (ASU). The maximization of hydrogen production and purification is performed in the two-stage water gas shift membrane separation unit, where H_2 production further increases and H_2 is separated from the rest of the syngas. The nitrogen stream that is produced from the ASU is utilized as sweep gas, increasing the hydrogen recovery driving force in the membranes. The H_2 -fuel mixture is fed to the power plant island, which consists of a gas turbine combined with a heat recovery steam generator (HRSG). The rest of the syngas enters the purification and compression unit, where the rich CO_2 is purified, compressed and sent for storage under supercritical conditions.

2.2 NGCC case without capture

The selected reference NGCC for electricity production without carbon capture is based on two large-scale identical gas turbines (GT), “F class”, each equipped with a heat recovery steam generator (HRSG), and one steam turbine. The plant layout is shown in **Figure 18**. Each HRSG is of triple pressure with single reheat type. Before feeding the gas turbine combustor, natural gas is preheated up to 160°C by means of saturated water extracted from the intermediate pressure (IP) drum, increasing the overall plant efficiency. The water after the fuel preheating is returned to the point after the condensates pump. The fuel flow rate to the gas turbine combustor is set to keep the same Turbine Inlet Temperature (TIT) of the case without natural gas preheating, which is 1360°C . The GT exhaust temperature is 604°C .

Apparatuses and systems that produce or consume energy, power should be modeled with high accuracy in order to yield quite representing results as the energy balance is concerned. For instance, the majority of power generated in a NGCC comes from the Gas Turbine (GT). Especially in case that the energy system is modeled with ASPEN PlusTM, a commercial turbomachinery has strong differences with a simple C-B-T approach (only a compressor a burner and a turbine). Not only does the produced power deviates from the real value but outlet stream mass and enthalpy are also far from the expected values, affecting the corresponding results of the steam cycle, too.

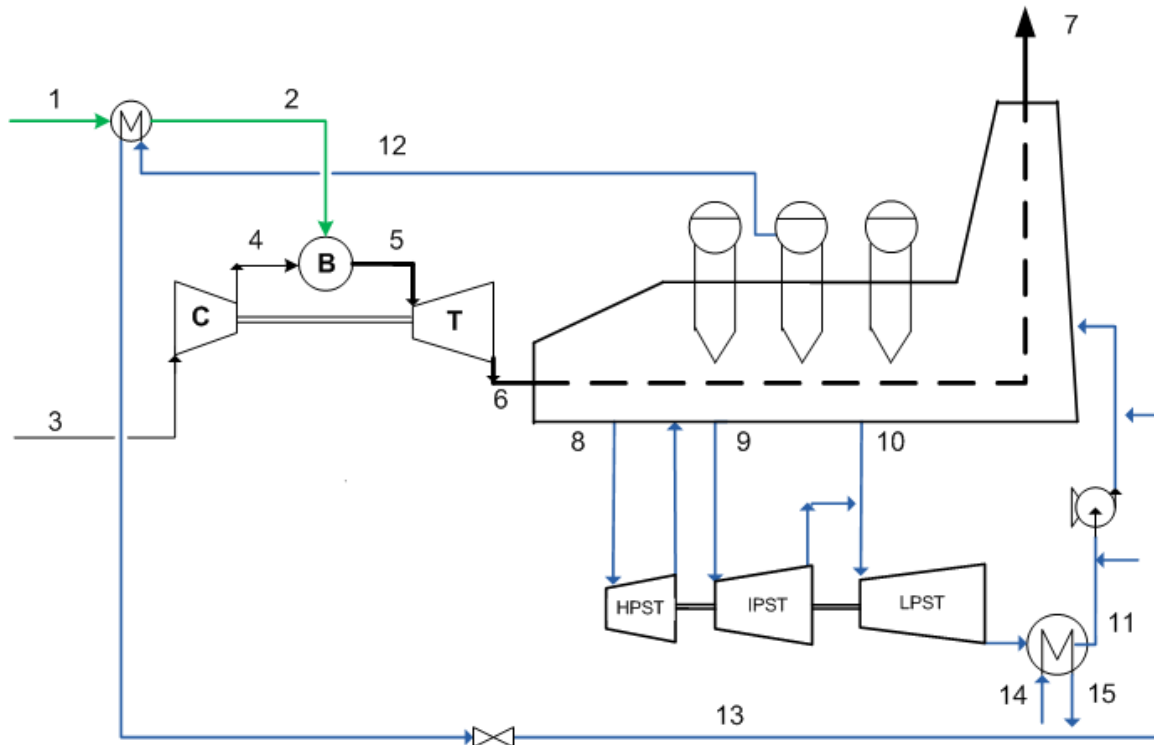


Figure 18. Reference Natural Gas Fired Combined Cycle Power Plant

The power island consists of two Gas Turbines (GTs) each with a Heat Recovery Steam Generator (HRSG) and one Steam Turbine (ST), so called ‘2-2-1 scheme’. This 2-2-1 arrangement is quite popular among utilities, since it adds operational flexibility as required by competitive electricity market. Each GT has a net power of 275.7 MW_e and the ST a net power of 279.3 MW_e (without steam extractions). The power island provides the other parts of the plant with electrical power and steam where required.

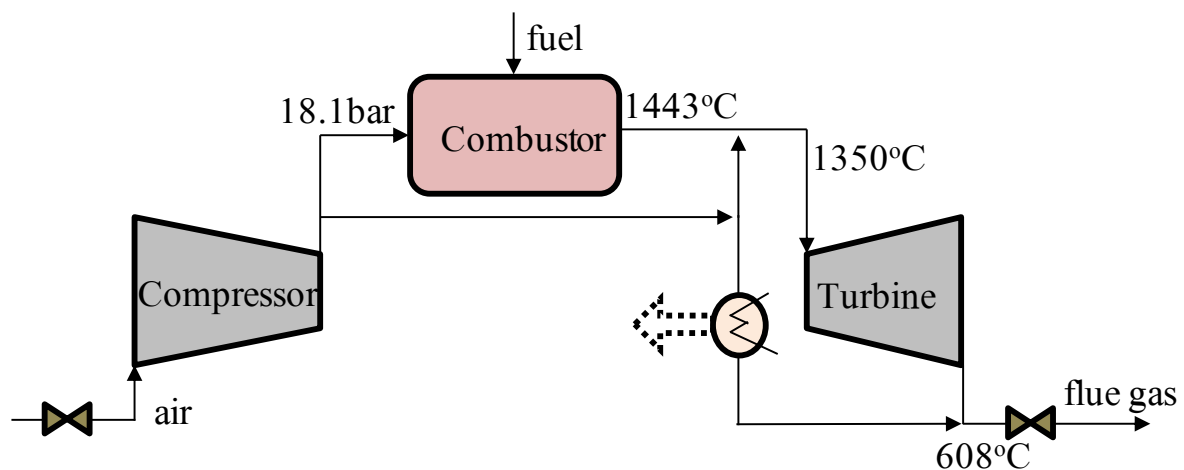


Figure 19. Gas Turbine scheme

As far as the GT is concerned, special effort is paid for the modeling of a real turbo-machinery engine using generic tools of the ASPEN PlusTM taking into account the EBTF (European Benchmark Task Force) specifications [19]. While the characteristics of a GT designed for firing a H₂-rich fuel may

be somewhat different from NG, it is assumed in this study that they are similar. The combustor outlet temperature (COT) is at 1443°C and the outgoing flue gases are mixed and cooled with a fraction of the compressed air, so that the turbine inlet temperature (TIT) is 1355°C . A part of the compressed air is by-passed for the cooling of the turbine blades (see **Figure 19**). The amount of air required for blade cooling is not calculated in detail in this work but is determined from the EBTF specification for the Turbine outlet temperature (TOT) which is set to 608°C . The validation of this approach has been based on the GateCycle[®] built-in libraries for GT modeling at commercial scale.

Regarding the steam cycle, it is designed so as to maximize the heat recovery from the flue gases (triple pressure with single reheat). The operating parameters of the power island are summarized in the following **Table 2**.

Table 2. Power island specifications

Natural Gas LHV	46502 kJ/kg
GT pressure ratio	18.1
Turbine Inlet Temperature	1355°C
Flue gas HRSG outlet temperature	69°C
Compressor η_p	90.85 %
Turbine η_{is}	93.65 %
Inlet filters/exhaust pressure drop	0.01 bar
HP/IP/LP ST η_{is}	92/94/88 %
Generator efficiency	98.5 %
Mechanical efficiency	99.6 %
Steam cycle pressures:	
HP/IP/LP evaporation	130/35/5 bar
Condenser	0.048 bar
Deaerator	5.0 bar
Pinch point at evaporators	10°C
Heat exchangers Δp_{loss}	3 % $p_{initial}$

The basic simulation results for the reference NGCC power plant are shown in **Table 3**, while the main thermodynamic data of the streams are provided in **Table 4**.

Table 3. Overall power balances for NGCC power plant without CO_2 capture

Gas turbine net output, MWe	275.7×2
Steam turbine gross output, MWe	285.0
Total steam cycle auxiliary consumption, MWe	5.7
Net power output, MWe	830.7
Fuel input (LHV base), MWth	712.4×2
Gross LHV efficiency, %	58.7
Net LHV efficiency, %	58.3
Specific CO_2 emissions, kg/MWh	354.3

Table 4. Stream flows, conditions and compositions of NGCC reference plant (see **Figure 18**)¹

Stream no	mass flow kg/s	T °C	p bar	h kJ/kg	H ₂	CO	Composition % v/v, wet				
					CO ₂	N ₂	O ₂	Ar	H ₂ O		
1	15.32	15.0	22.57	-1.14	NG, See EBTF document [19]						
2	15.32	160.0	22.12	326.04							
3	649.98	15.0	1.01	-0.56	-	-	0.03	77.30	20.74	0.92	1.01
4	649.98	426.2	18.10		-	-	0.03	77.30	20.74	0.92	1.01
5	665.30	1355.0	17.56		-	-	3.97	74.39	12.39	0.89	8.36
6	665.30	607.6	1.04	656.07	-	-	3.97	74.39	12.39	0.89	8.36
7	665.30	88.2	1.01	76.36	-	-	3.97	74.39	12.39	0.89	8.36
8	70.71	559.5	120.92	3503.5	-	-	-	-	-	-	100.0
9	93.39	561.0	22.97	3599.8	-	-	-	-	-	-	100.0
10	11.18	234.6	5.09	2927.8	-	-	-	-	-	-	100.0
11	104.58	32.1	0.05	134.23	-	-	-	-	-	-	100.0
12	5.65	230.8	28.42	993.43	-	-	-	-	-	-	100.0
13	5.65	25.0	28.02	107.01	-	-	-	-	-	-	100.0
14	5167.1	18.2	1.01	76.05	-	-	-	-	-	-	100.0
15	5167.1	29.2	2.03	122.16	-	-	-	-	-	-	100.0

¹ mass flows refers to 1 GT and 1 HRSG, while power balances shown in **Table 3** to a configuration with 2GT and 2HRSG and 1 steam turbine

2.3 Design of key components for the optimum operation of the power plant

The operation of each unit of the novel power plant configuration has been investigated in detail in order to reach the most efficient overall performance, taking into account the minimum cost per ton of CO₂ avoided.

2.3.1 Air separation unit

Two streams are produced by the ASU by the cryogenic method: rich O₂ and pure N₂. The process flowsheet is displayed in **Figure 20**. Firstly, half of the required air (1) is compressed in four stages (2), employing inter-cooling at 28°C in order to reduce the compressors' power consumption. The rest of the air (3) is extracted from the GT compressor and mixed before air pre-cooling and purification. Air is dehydrated and cleaned before its introduction into the main heat exchanger (7). Air is cooled in two stages in the direct contact air cooler (DCAC). Consequently, molecular sieves completely remove any remaining water and any other impurities. The clean air stream enters the main heat exchanger at a temperature of 20°C (7) and exits at a temperature near the dew point (8b).

The oxygen and nitrogen separation is achieved in two distillation columns at different operating pressures. Since products should be at elevated pressures, the oxygen stream is firstly pumped at a high pressure and is evaporated afterwards in the main heat exchanger. In order to refrigerate the air stream efficiently, part of the air (7a) is compressed up to 30 bar, so that the required refrigeration load for liquefaction is lower. The first column operates at high pressures (HPC – high-pressure column), where both air streams come into contact with the liquid nitrogen stream, which is condensed at the top of the column. The outlet streams are liquid air (9) with high concentration in O₂ (almost 40%) and a nitrogen-rich gaseous stream (10) with relatively high purity. In the second column (LPC – low-pressure column), the separation is completed. The produced streams are a liquefied oxygen stream (11) and a highly pure (>99.5%) nitrogen stream (12) in gaseous phase at the top of the LPC. Both columns consist of 30 stages and their outlet flow rates are modified so that the produced streams have the desirable

composition and purity. Both product streams, O_2 (liquid) and N_2 (gas), are pumped and compressed (16) to 52 and 25 bar, respectively. To increase the reforming and post-combustion efficiency, the oxygen stream is preheated up to 130°C before utilization (13).

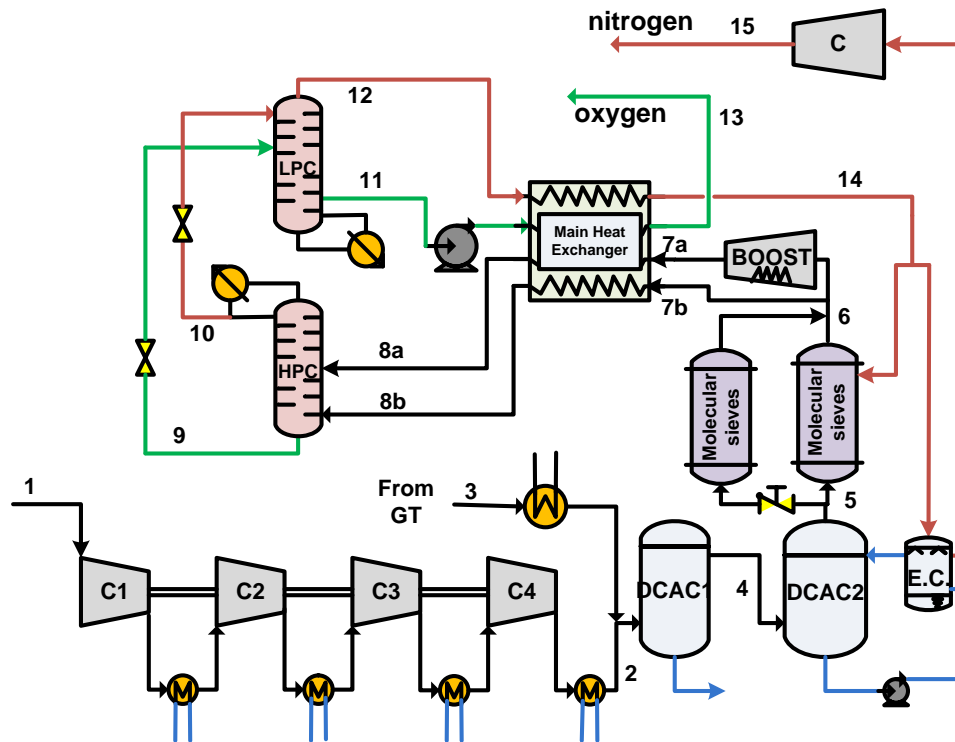


Figure 20. Air Separation Unit layout

The basic characteristics of the ASU system are presented in **Table 5**.

Table 5. ASU main specifications

O_2 recovery efficiency	%	99.1%
N_2 recovery efficiency	%	99.7%
Oxygen purity	% v/v	95.0%
Nitrogen purity	% v/v	99.6%
Specific O_2 production @50bar	kWh/tn O_2	218.08
Specific N_2 production @25bar	kWh/tn N_2	187.33

2.3.2 Gas heated reformer – autothermal reforming reactor (GHR-ATR)

Before the reforming process, the natural gas is pre-heated. Theoretically, the hotter the fuel, the less the heat demand for the hot reformate gas to sustain the autothermal condition, if the pre-reforming temperature is assumed to be constant. The temperature is increased to 120°C by means of the hot compressed air extracted from the GT compressor to the ASU. Nevertheless, these two streams are subject to self-ignition if coupled into a heat exchanger. Therefore, an intermediate heat transfer medium (e.g. water) is included. Additionally, the CO_2 purification system delivers a hot condensed water stream which mixes with the natural gas through injection. This reduces the required steam from the steam cycle. Finally, natural gas is preheated up to 360°C using the hot sweep gas before it enters

the membrane separator (MS). In the high-pressure reformer reactor, GHR-ATR, the natural gas (NG) hydrocarbons are reformed to CO and H₂ (**Figure 21**).

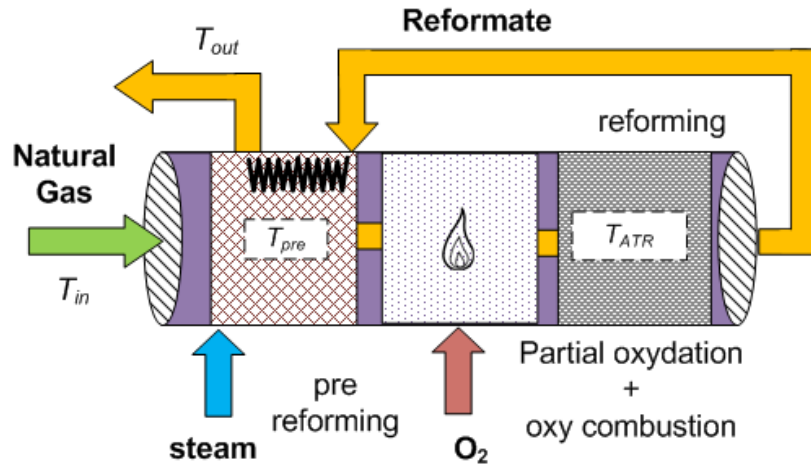
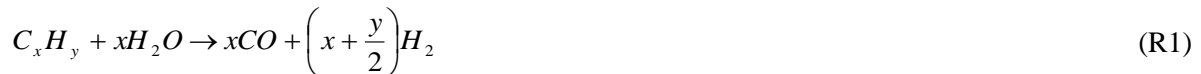
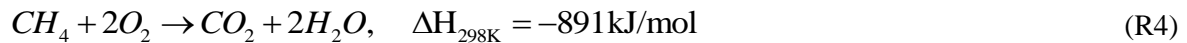
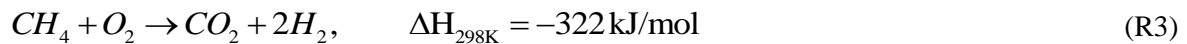


Figure 21. Scheme of the autothermal reforming reactor (ATR)

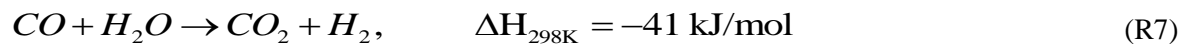
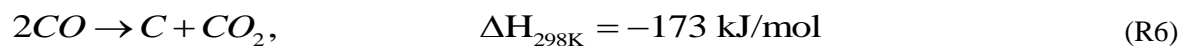
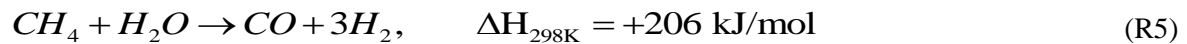
This conversion is conducted in two consequential steps: in the first step, the NG stream is mixed with steam and undergoes pre-reforming in a gas-heated reformer (GHR). In the pre-reformer, hydrocarbons with more than one carbon in their molecular chain mainly participate in the reforming reaction ($T=700^{\circ}\text{C}$):



Subsequently, part of the mixture reacts with oxygen from the oxidizing agent via catalysts in order to reach the desirable reforming temperature. In reality, apart from partial oxidation (R2), there is also carbon dioxide yield according to the exothermic reactions (R3) and (R4).



The main part of the process is conducted in a third step, where natural gas is reformed in the presence of catalysts. Typical materials used for autothermal reforming catalysts are the same as those used for methane reforming and partial oxidation, mostly nickel-based [68-70]. Reaction (R5), for steam reforming of methane, is strongly endothermic.



As the presence of catalysts achieves an outlet condition practically in chemical equilibrium, the ATR process can be easily modelled with a Gibbs reactor in ASPEN PlusTM, which predicts an outlet mixture with the least Gibbs energy [71]. Under these conditions, the reverse Boudouard reaction (R 6) and the water gas shift (R 7) are also taken into account for calculation of equilibrium. This part of syngas production is of high importance because it affects the efficiency of the other components of the hydrogen plant. It should be noted that any NG quantity that is not reformed cannot be utilized in any other process that enhances hydrogen production. A further issue is the way it is removed from the

retentate stream leading to CO₂ purification before compression and storage. There are three basic parameters that define an autothermal reaction: temperature, pressure and steam-to-carbon ratio (S/C, the amount of steam to total carbon in hydrocarbons of NG). As shown in the following figures (**Figure 22** and **Figure 23**), higher S/C ratio and temperature increase the oxygen demand but reduce the rate of unconverted hydrocarbons after the process.

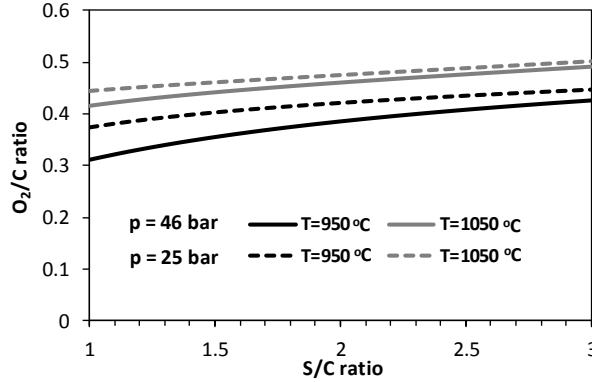


Figure 22. Oxygen demand at the ATR parametrically with temperature and pressure

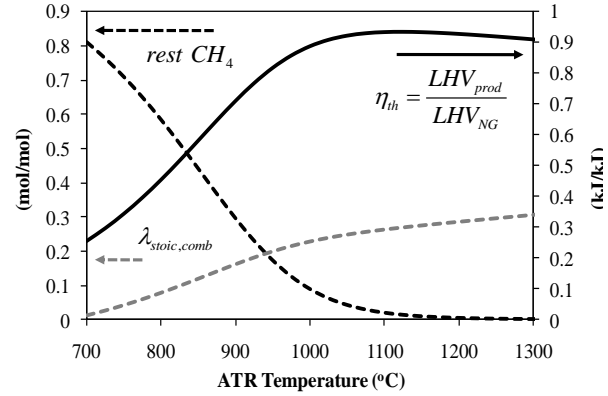


Figure 23. Effect of ATR temperature on autothermal reforming process ($p=50.9$ bar, $S/C=1.5$)

Regardless of the type of hydrogen plant investigated, the foremost objective is to maximize the CO yield and the secondary objective is to produce H₂. These goals correlate with the Chatelier's principle in WGS, which suggests that the equilibrium of shift reaction (R7) will favour the maximum hydrogen production only if the reactant concentrations are as great as possible in the reaction zone.

2.3.3 Design of water gas shift reactors (WGS) and membrane separators (MSs)

The configuration of WGS reactors with non-integrated MS is presented in **Figure 24**.

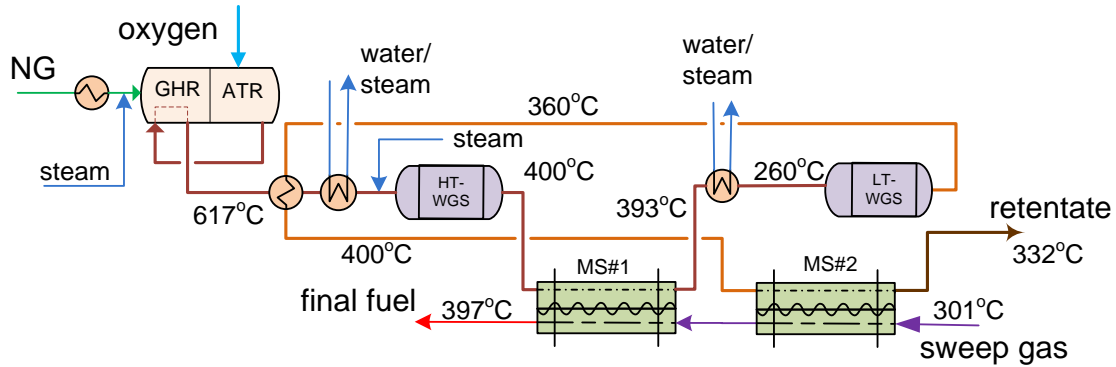
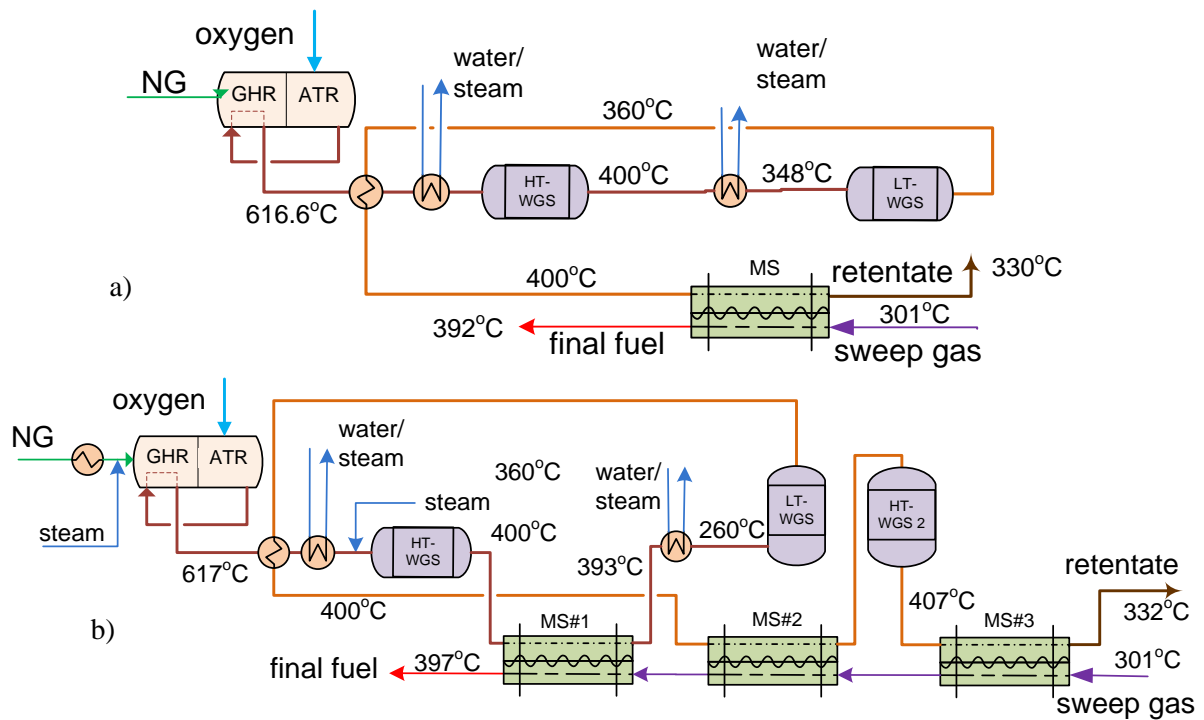


Figure 24. Hydrogen production unit scheme with two separation stages

On the one hand, low WGS temperature favours CO shift, but the demand for $T_{syngas} \rightarrow 400^\circ\text{C}$ for high H₂ fluxes through the membranes increases the complexity and equipment cost of the unit. The WGS reaction process is performed at two stages, i.e. at high temperature (400°C) and at lower temperature (360°C) in order to achieve high CO conversion rates, which directly correlate to the hydrogen recovery factor (HRF). The syngas is cooled down before each WGS reactor (at 272 °C) so that the reactors operate adiabatically. The stream outlet temperatures from the membrane separators (MSs) are calculated with the simulation tool presented in [72] for the rigorous modelling of H₂ separation through membranes.

a) Investigation of the H_2 separation stages in the membranes**Figure 25.** H_2 plant with a) one stage and b) three stages of hydrogen separation

In order to define the number of H_2 separation stages, two more cases, with one and three membrane separators, are investigated. In the first case, the CO shift is performed at the same temperatures before the H_2 separation. The one-reactor case is illustrated in **Figure 25a**. The composition of feed gas and permeate gas for the three membrane stages is shown in **Table 6**.

Table 6. Gas composition of the streams at the 3-stages membrane case (Case I)

molar fraction	H_2	CO	H_2O	CO_2	CH_4	N_2+Ar
MS# 1 feed inlet	0.569	0.043	0.202	0.172	0.006	0.007
MS# 1 feed outlet	0.377	0.062	0.292	0.249	0.009	0.011
MS# 2 feed inlet	0.413	0.027	0.257	0.284	0.019	0.000
MS# 2 feed outlet	0.203	0.037	0.348	0.386	0.026	0.012
MS# 3 feed inlet	0.216	0.025	0.336	0.396	0.026	0.000
Retentate	0.101	0.029	0.385	0.454	0.030	0.000
Final fuel	0.499	0	0.004	0	0	0.497
MS# 1 perm inlet	0.302	0	0.005	0	0	0.692
MS# 2 perm inlet	0.107	0	0.007	0	0	0.887
MS# 3 perm inlet	0	0	0.007	0	0	0.993

The selection of two stages of H_2 separation through membranes is justified in **Figure 26**. It is clear from that for a certain hydrogen recovery factor, the plant efficiency for all the cases is almost the same – as expected, because the final fuel composition is the same and the amount of heat that is recovered from the steam cycle is also approximately the same. Furthermore, the CO conversion at the WGS reactors is performed at an equal rate in all cases. However, the required membrane area is the critical factor for the selection of the number of hydrogen separation stages: in the single-MS case, the required membrane area is the largest, and in the two- and three-MS cases the corresponding total membrane

area does not differ considerably. However, the introduction of the third WGS reactor increases the equipment cost, despite the fact that the membrane area is reduced by around 1.5%. Thus, the selected number of stages is two.

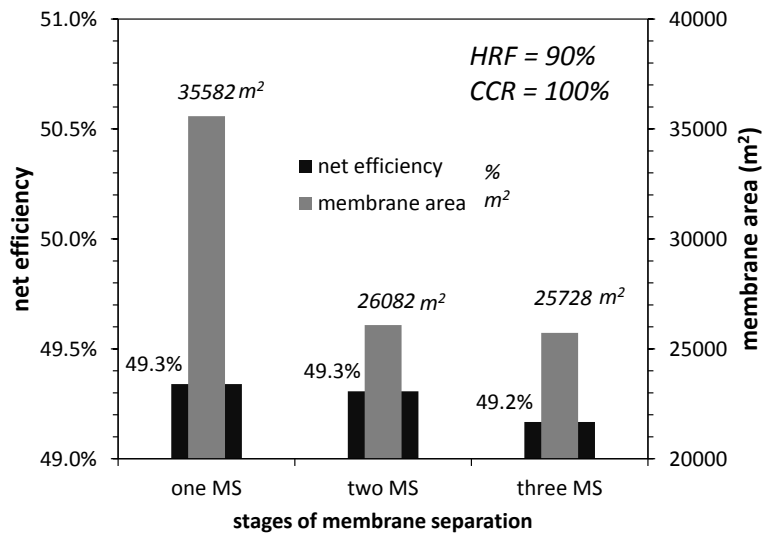


Figure 26. Comparison of one-stage, two-stage and three-stage membrane separation

b) Investigation of the H_2 separation rate at the membranes

In order to determine the optimum operating conditions at the membranes, i.e. the rate of separation at the two reactors that correlates with the corresponding membrane area, a sensitivity analysis is performed. According to **Figure 27**, the rate of H_2 separation at the first membrane, which determines the difference of hydrogen partial pressure at the rear end of the first membrane, affects the CO conversion rate at the LT-WGS and the Δp_{H_2} at the second membrane. From **Figure 27**, the best value of Δp_{H_2} at the outlet of the first membrane is around 9 bar.

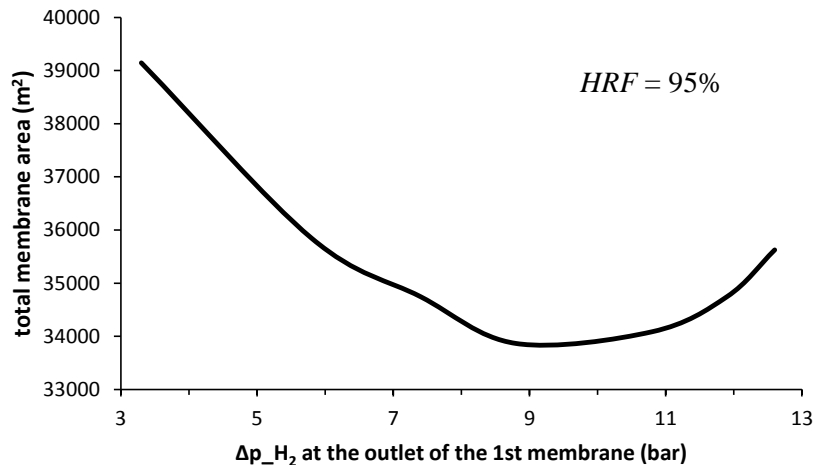


Figure 27. Effect of Δp_{H_2} at the outlet of the 1st membrane separator on total membrane area (Case I)

2.4 Purification, compression and recirculation

Special attention should be paid to the design and optimization of the Purification and Compression Unit (PCU). Unlike other pre-combustion CO_2 capture technologies, the retentate stream after H_2 -selective membrane separation does not contain pure CO_2 , and a purification process must be included before CO_2 compression and storage. It is clear that apart from CO_2 the retentate stream contains H_2O , unreformed CH_4 and other hydrocarbons, plus unconverted CO and H_2 that did not permeate the

membranes. Regarding oxygen stream purity, N_2 and Ar are expected, too. Two options are investigated here: oxy-combustion of the remaining combustibles and cryogenic separation.

- The first concept suggests the elimination of the remaining combustibles like CH_4 , H_2 and CO with pure O_2 , derived from the ASU (**Figure 28a**). The combustion is performed under catalytic conditions under near-stoichiometric conditions so as to minimize the excess oxygen at the final CO_2 stream. In this concept, the use of an expander before combustion is investigated. Adding an expander has a triple positive effect. Firstly, the mixture is separated more easily at lower pressures. Secondly, the manufacturing cost of units such as the evaporator is significantly lower if they operate at lower pressures. Thirdly, the CO_2 -rich mass flow rate that is compressed is less than the corresponding retentate stream that is expanded, contributing positively to the total power balance.

- The second concept suggests the recovery of the combustibles in cryogenic conditions. The sensitivity analysis is focused in the CO_2 stream purification and compression block based on two separation methods: (a) flash separator, and (b) distillation column.

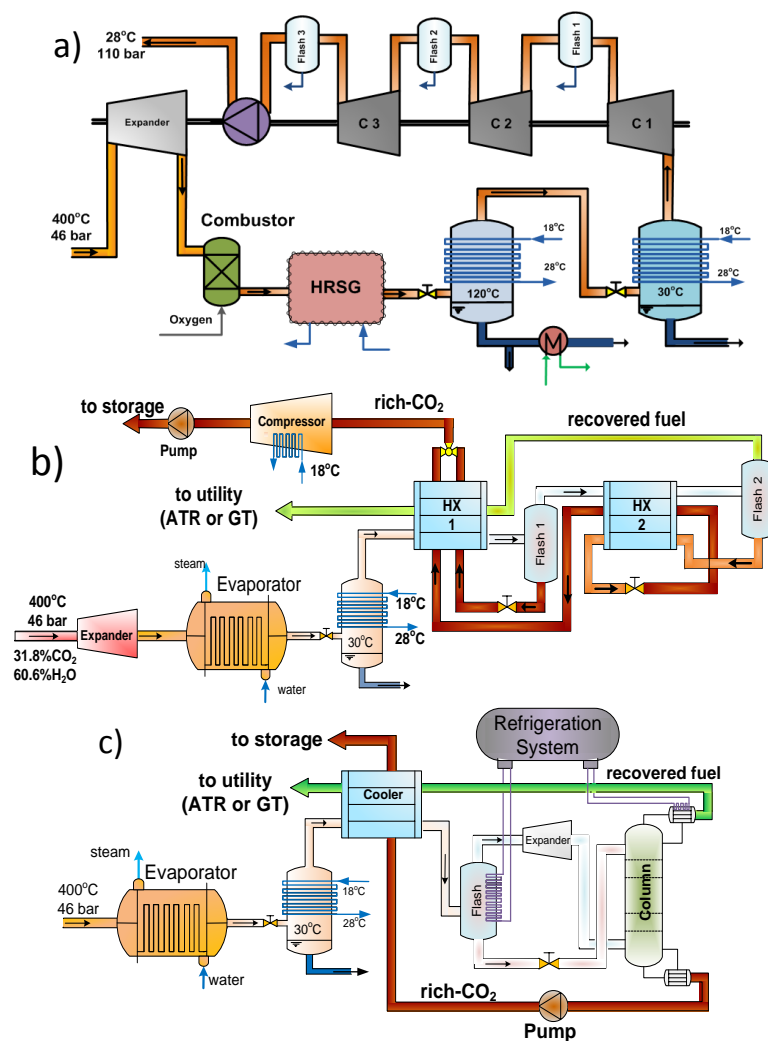


Figure 28. Purification schemes a) oxy-combustion, and cryogenic separation with b) flash separators and c) distillation column

Combustibles recovery mainly involves a distillation column, a heat exchanger, a flash separator (**Figure 28b**) and an external refrigeration system (**Figure 28c**). After passing through the heat exchanger, the inlet stream is partly condensed and is separated at the flash separator. The liquid stream

is further cooled by means of the Joule-Thomson effect, while the gas stream is cooled through expansion. Both streams enter the distillation column to make combustibles separation more effective. The cooling loads for the column's condenser are obtained from an external refrigerant and are dependent on the desirable rate of carbon capture efficiency. The corresponding heat in the reboiler can be obtained by the refrigerant inter-cooling while it is compressed. The distillation column outlet streams can be used to assist the cooling of the retentate stream after water removal (reducing energy consumption).

The refrigeration system comprises a two-stage compressor in order to provide cooling loads at two different temperatures: at -20°C for the retentate stream cooling and at around -65°C (depending on the recovery rate, which determines the dew point of the outlet gas stream) to fulfil the condenser duties at the distillation column. The most suitable cooling medium employed in the modelling is R1150 (ethylene - C_2H_4). Assuming that the temperature approach of all heat exchangers is 3°C , the pressure levels for the evaporation are 2.26 and 23.47 bar, and for condensing 27 bar. Finally, the compressor's polytropic efficiency is assumed to be equal to 0.82. Since the present cooling medium cannot reject its heat directly into the ambient air while it is condensed, a secondary auxiliary cooling cycle is required. The cooling medium in this refrigerant cycle is the commercial R134a and the coefficient of performance *COP* of this cycle is assumed to be 3.59.

Table 7. Outlet streams from PCU for the three purification methods

separation method		flash separator		distillation column		post combustor
stream		rich CO_2	recovered combustibles	rich CO_2	recovered combustibles	rich CO_2
$T (^{\circ}\text{C})$		18.0	-29.2	18.0	16.7	18.0
p (bar)		110.0	25.0	110.0	25.0	110.0
m (kg/s)		2x49.96	2x2.21	2x49.66	2x2.52	2x46.70
% mole fraction	CO_2	96.28	18.65	99.77	7.74	96.59
	CO	0.01	0.23	0.00	0.26	0.00
	H_2	0.62	47.95	0.00	43.50	0.00
	CH_4	1.80	16.20	0.04	26.25	0.00
	N_2	0.40	8.68	0.00	10.03	1.38
	Ar	0.75	8.29	0.01	12.22	1.89
	H_2O	0.14	0.00	0.18	0.00	0.13

The characteristics of the outlet streams from the PCU for the three purification methods are depicted in **Table 7**, whereas the results of the four cases are compared in **Figure 29** and **Table 8**. For a certain carbon capture rate ($\text{CCR}=90\%$), the best CO_2 purification option is oxy-combustion without an expander. It seems that the heat utilization of the hot gases after the oxy-burner stage contributes more effectively to the plant performance than the retentate stream expansion after the membrane section.

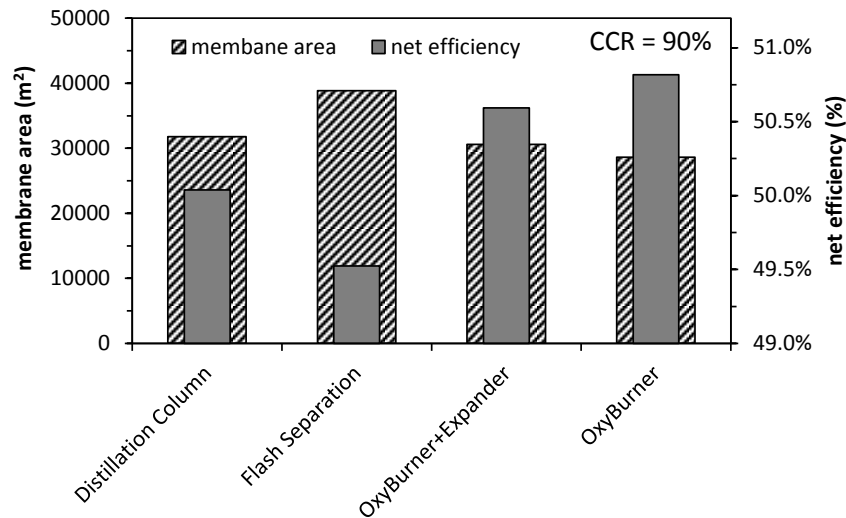


Figure 29. Net efficiency and total membrane area of the four under investigation cases

Table 8. Energy balance of the four cases based on different purification schemes

case number	I	III	V	VI
purification scheme	oxy-combustion w/o expander	oxy-combustion with expander	distillation column	flash separation
CO ₂ avoided (%)	90%	90%	90%	90%
GT net power (MWe)	667.94	667.91	695.77	698.30
ST gross power (MWe)	350.73	336.23	274.83	275.77
Steam cycle auxiliaries (MWe)	-8.19	-7.89	-7.07	-7.11
ASU consumption (MWe)	-33.97	-34.00	-28.35	-29.60
N ₂ compression (MWe)	-61.32	-60.78	-50.76	-50.78
CO ₂ purification & compression (MWe)	-4.69	5.08	-14.61	-11.98
Net electric power (MWe)	910.50	906.55	869.81	874.60
Thermal power input LHV (MW _{th})	1791.71	1791.82	1738.25	1766.05
Net electric efficiency LHV (%)	50.82%	50.59%	50.04%	49.52%
Efficiency penalty (%)	7.5%	7.7%	8.3%	8.8%
CO ₂ specific emissions (g/kWh)	42.16	42.73	43.29	43.60
SPECCA* (MJ _{LHV} /kgCO ₂)	2.91	3.02	3.28	3.52

* SPECCA (Specific Energy Consumption for CO₂ Avoided) is the additional fuel energy (in MJ, referred to LHV) required to avoid one kg of CO₂

2.4.1 Off-gases recirculation of the catalytic oxy-combustion at the ATR

As stated above, the gas stream that exits the post-combustor consists mainly of CO₂ and H₂O at high temperature. Partial recirculation of this stream back to the ATR has multiple positive effects, such as i) less steam extraction from the steam cycle, and ii) less oxygen demand for keeping autothermal conditions in the ATR, since the inlet temperature of the mixture of NG with retentate increases. On the other hand, the complexity of the unit increases, and consequently so does the operational cost of the system. According to **Figure 30**, the recirculation of the retentate stream has a small beneficial effect on efficiency (maximum 0.30% increase). The maximum plant performance is achieved for a split fraction around 50%; however, since most of the units and pipelines would greatly increase in size in this case, it must be concluded that this should not be adapted to the process.

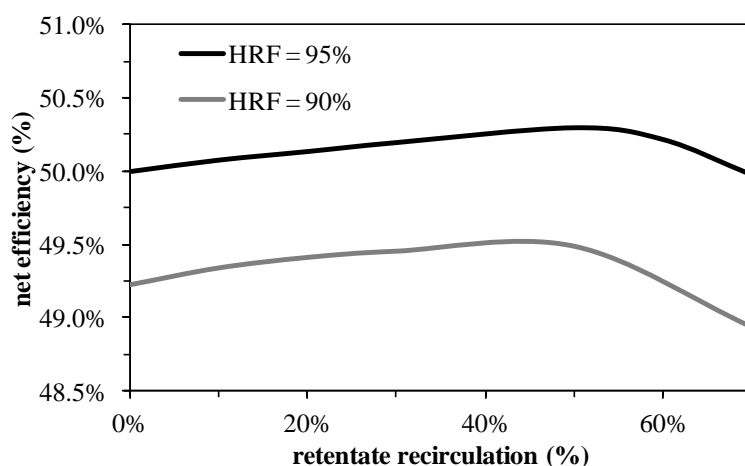


Figure 30. Effect of recirculation of fraction of retentate stream on plant efficiency

2.5 Determining optimum operating parameters

Having determined the configuration of the energy system that is being studied, the best values for the operating parameters are investigated.

2.5.1 Steam to carbon ratio (S/C) at the ATR

The effect of both the S/C ratio and the HRF on the net efficiency is illustrated in **Figure 31**. It is concluded that the steam to CO ratio (S/CO) limitation in the WGS for the avoidance of coke formation on catalysts ($S/CO \geq 2.0$) plays a considerable role in the determination of the optimum value of the S/C ratio in the ATR. For both cases, for an S/C ratio less than 1.7, additional steam is required to be extracted from the steam cycle and mixed with the syngas before the WGS reaction. Were it not for this limitation, the best value of the S/C ratio would be smaller. The S/C value chosen is thus 1.7.

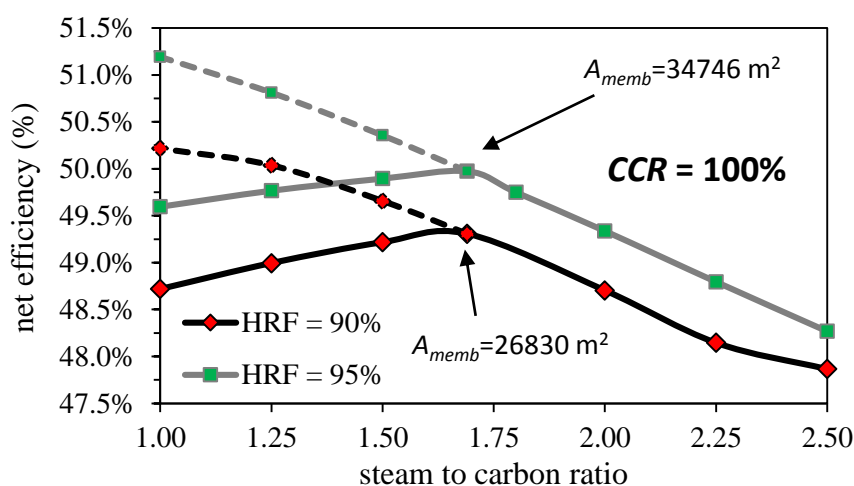


Figure 31. S/C ratio effect for two HRF cases (with dash lines is the hypothetical trend of efficiency in case of no restriction for S/CO ratio at the WGS)

2.5.2 Hydrogen recovery factor

According to the above graph (**Figure 31**) the rate of hydrogen separation plays an important role not only in plant efficiency but also in the total required membrane area. It is clear that the greater the HRF the more hydrogen enters the GT instead of the oxy-combustor, and consequently the more effectively the system operates. On the other hand, high HRF values require a greater membrane area, which has a negative effect on the investment cost.

2.5.3 ATR temperature

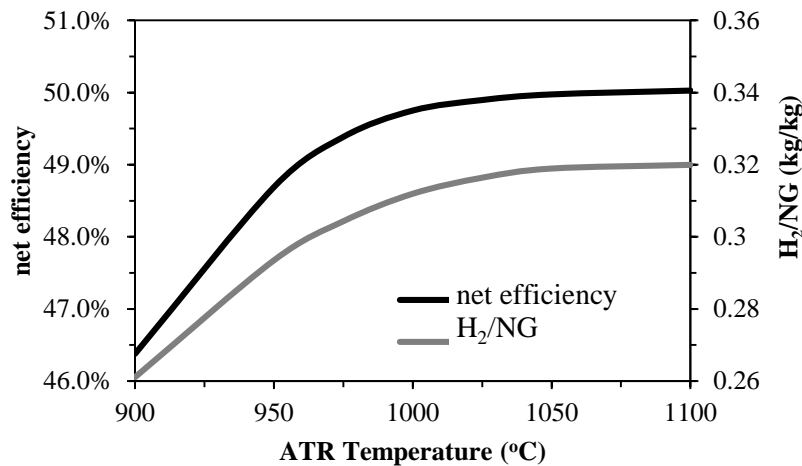


Figure 32. Effect of temperature at the ATR on the plant performance and H₂ productivity

As seen above, a comparatively low temperature in the ATR deteriorates the heat quality of the produced syngas. The same trend is observed for plant efficiency and the specific hydrogen production (**Figure 32**). Even though the heat input of the unreformed hydrocarbons and other combustibles is transferred to the steam cycle through oxy-combustion, the net efficiency drops dramatically for temperatures below 1000°C. The temperature that is set for the case study is therefore 1050°C.

2.5.4 Carbon Capture Rate (CCR)

One of the major advantages of Pd-membranes technology is the absence of carbon in the permeate stream, which allows us to adjust the rate of CO₂ avoided by splitting off a portion of the inlet NG directly to the GT. This benefits the efficiency of the plant and reduces the total membrane area required. There are two possible positions for the introduction of the natural gas to the fuel: (a) in the sweep gas phase before entrance to the membrane separator (MS#2) and (b) after the membrane separation and before entrance to the GT, taking into account that the hydrogen molar fraction on the permeate side cannot be greater than 50%.

As shown in **Figure 33**, lowering the carbon capture rates leads to higher net efficiency and lower membrane area. Furthermore, the introduction of the natural gas before the membrane separation reduces the demand for steam extraction in order to reach the desired H₂ concentration in the final fuel. This has a beneficial effect on plant efficiency. However, the increase in the mass transfer rate of the

hydrogen on the permeate side due to the presence of the hydrocarbons deteriorates the H_2 permeation, resulting in an increase of the membrane area by 7%.

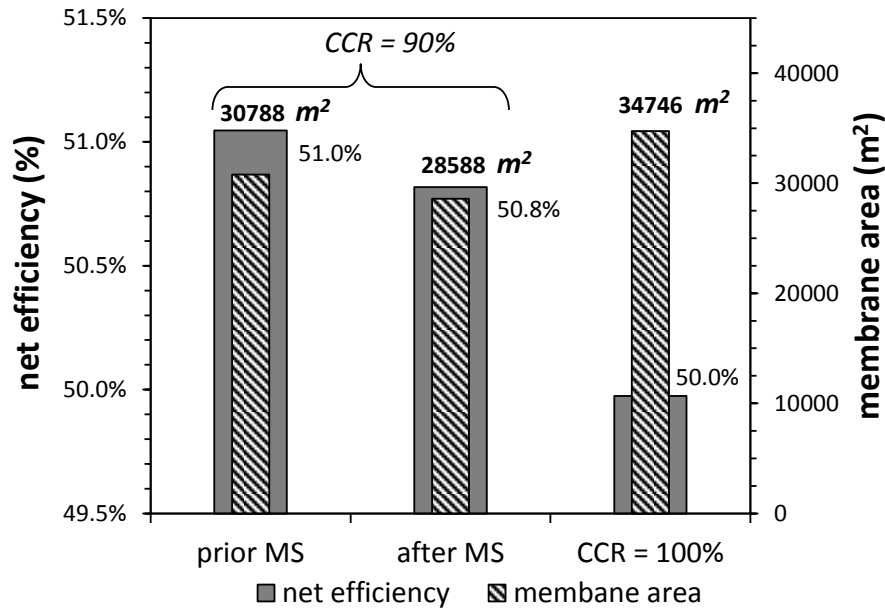


Figure 33. Effect of CCR and the introduction of NG (prior or after the Membrane Separators) in case of $CCR \neq 100\%$ ($HRF = 95\%$)

Hence, in $CCR \neq 100\%$ cases it is favourable to introduce the natural gas after the membrane separators. The cases with different CCR are compared in **Table 9**.

Table 9. Energy balance of the cases under investigation based on different capture rate and use or not of expander

purification scheme	oxy-combustion w/o expander		oxy-combustion with expander	
	II	I	IV	III
case number	II	I	IV	III
CO ₂ avoided (%)	100%	90%	100%	90%
GT net power (MW _e)	682.19	667.94	682.12	667.91
ST gross power (MW _e)	358.45	350.73	342.15	336.23
Steam cycle auxiliaries (MW _e)	-8.53	-8.19	-8.19	-7.89
ASU consumption (MW _e)	-38.52	-33.97	-38.59	-34.00
N ₂ compression (MW _e)	-69.54	-61.32	-68.99	-60.78
CO ₂ purification & compression (MW _e)	-5.34	-4.69	5.79	5.08
Net electric power (MW _e)	918.71	910.50	914.29	906.55
Thermal power input LHV (MW _{th})	1838.38	1791.71	1838.59	1791.82
Net electric efficiency LHV (%)	50.00%	50.82%	49.73%	50.59%
Efficiency penalty (%)	8.3%	7.5%	8.6%	7.7%
CO ₂ specific emissions (g/kWh)	2.15	42.16	2.16	42.73
SPECCA (MJ _{LHV} /kgCO ₂)	2.92	2.91	3.02	3.02

2.5.5 Membrane pressure

Feed gas pressure

The operating pressure on the feed side of the membrane separator (MS) determines the operational pressure of the whole H₂ production plant. In the present study, the feed gas pressure is set at 46 bar. A sensitivity analysis is performed in order to investigate the pressure effect on the total efficiency of the plant and on the required total membrane area (**Figure 34**).

It is clear that a high operating pressure on the feed side of the membrane allows a significant reduction of the total required membrane area, but the net efficiency of the plant deteriorates. This is due to the fact that the hydrogen partial pressure difference on both sides plays a very important role in hydrogen flux. As can be seen from **Figure 34**, an increase in the operating pressure on the feed side of the membranes from 46 to 55 bar contributes to a reduction of the membrane area by 22%. On the other hand, the cost of the other components in the hydrogen production unit (e.g. ATR, WGS and combustor) is expected to increase – but there are no available data on this.

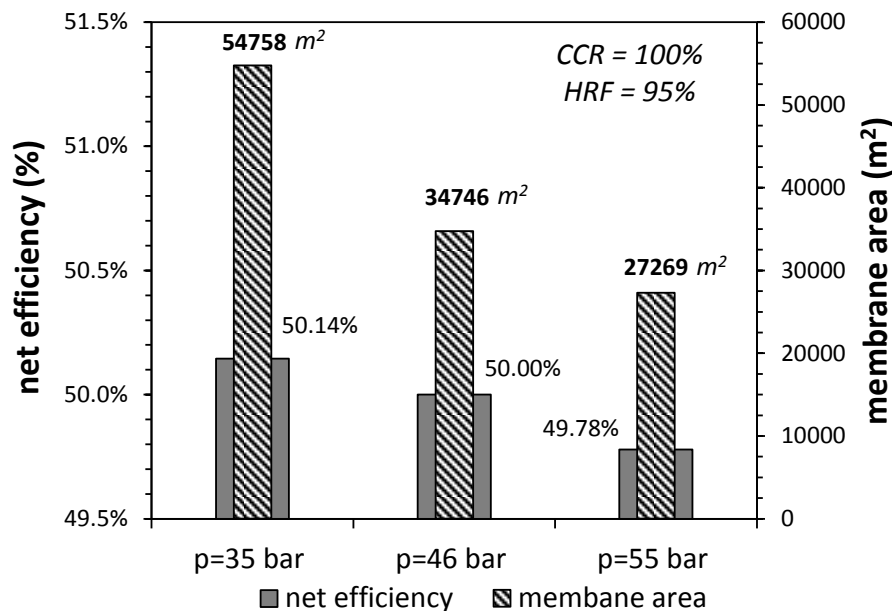


Figure 34. Effect of the feed gas pressure in the membranes

Sweep gas pressure

Another way to enhance the H₂ flux through the membranes is to reduce the hydrogen partial pressure at the permeate side. For lowering the sweep gas pressure below 25 bar, an extra compressor is required downstream of the MS#2, so that the fuel enters the GT combustion chamber at an appropriate pressure (**Figure 35**). Contrary to the previous case, when the volume of the gas is doubled, the compression duty is considerably greater. In this section, cases where $p_{\text{perm}} < 25 \text{ bar}$ are examined. For the hydrogen plant system to be operational, several modifications should be made, which are illustrated in the following figure. Where the fuel temperature after the C2 stage is greater than 500°C, inter-cooling is required.

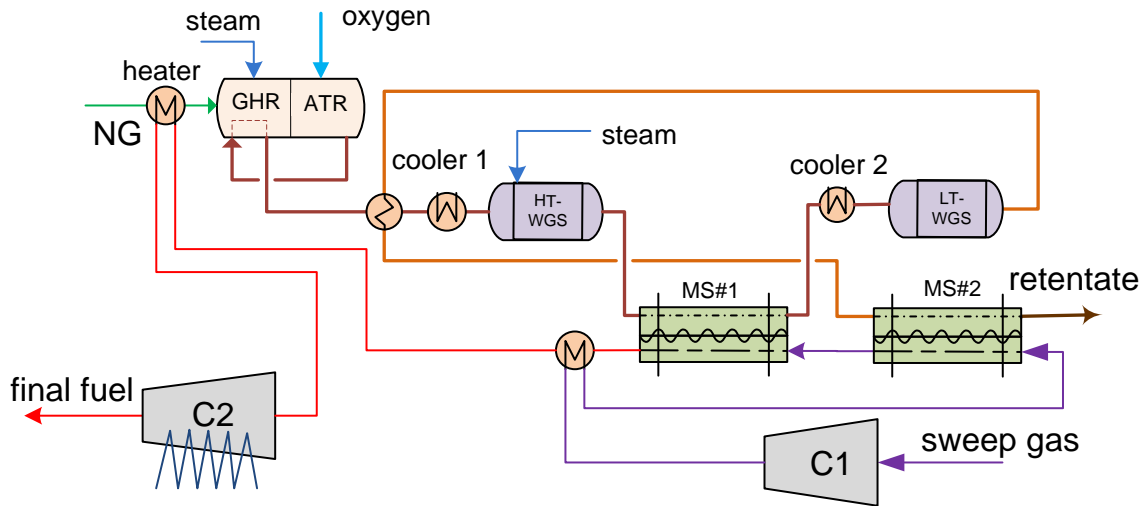


Figure 35. H₂ plant in case of $p_{perm} < 25$ bar

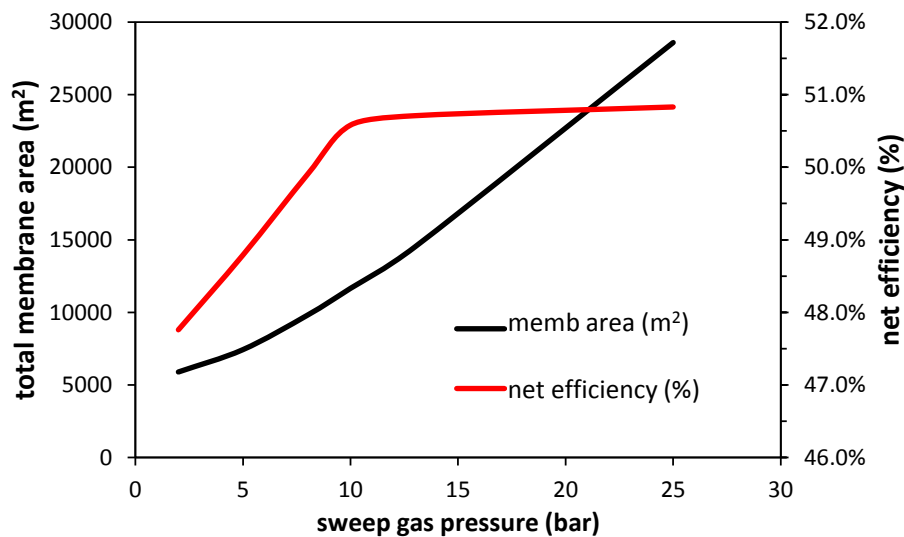


Figure 36. Effect of pressure at the permeate side (CCR=90%, HRF=95%)

Figure 36 shows the efficiency of the system drops considerably when p_{perm} is less than 10 bar. This is due to the lower fuel inlet temperature at the GT combustor. Since the m_{air}/m_{fuel} ratio is relatively high (around 7.0) the fuel inlet temperature plays a considerable role in the GT efficiency. For $p_{perm} \geq 10$ bar, the energy penalty due to fuel consumption after the membrane stage is balanced by the increased fuel inlet temperature; thus, the net efficiency drops only slightly. On the other hand, the required membrane area is reduced dramatically (up to 75% reduction of the membrane area), which has a positive effect on the equipment cost of the plant. Another configuration is also investigated here: the membrane separation takes place at two different permeate pressures. Only a part of the sweep gas is compressed up to 25 bar and used in two coupled counter-current membrane separators; the rest of the sweep gas is employed at lower pressures in a third membrane module (MS#3). The layout of the hydrogen plant is shown in **Figure 37**.

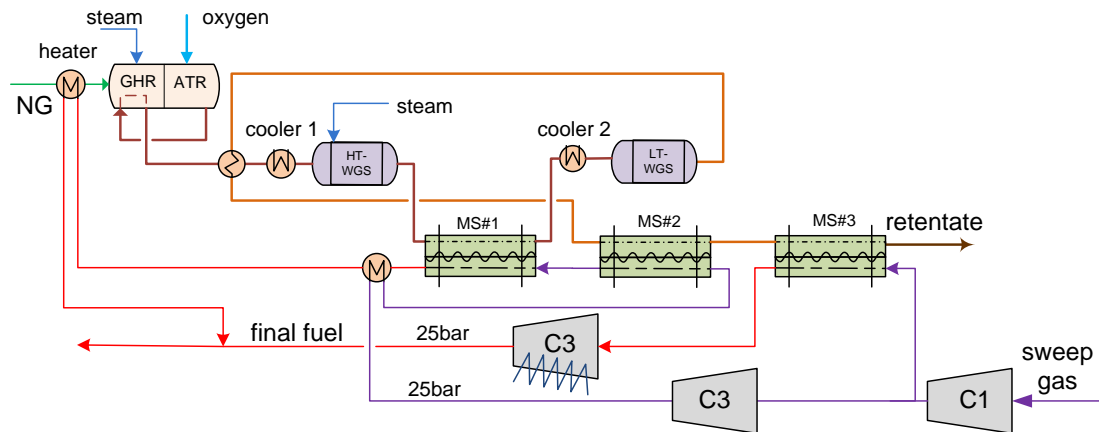


Figure 37. H₂ plant for two permeate pressures

This configuration is investigated for MS#3 permeate pressure of 5 and 10 bar; the basic results are summarized in **Figure 38**. For a greater proportion of permeated hydrogen at MS#3, the required membrane area is reduced, while net efficiency drops due to higher power consumption for the fuel compression at C3. However, the best case proves to be where the permeate side is at 10 bar at each membrane separator: here, the efficiency remains above $\eta_{net} > 50\%$ and the total membrane area is lowered significantly (69.4% reduction of the membrane area compared to $p_{perm} = 25$ bar). The *HRFs* of MS#1 and MS#2 and 37.2% and 89.2%; the total *HRF* is equal to 95%.

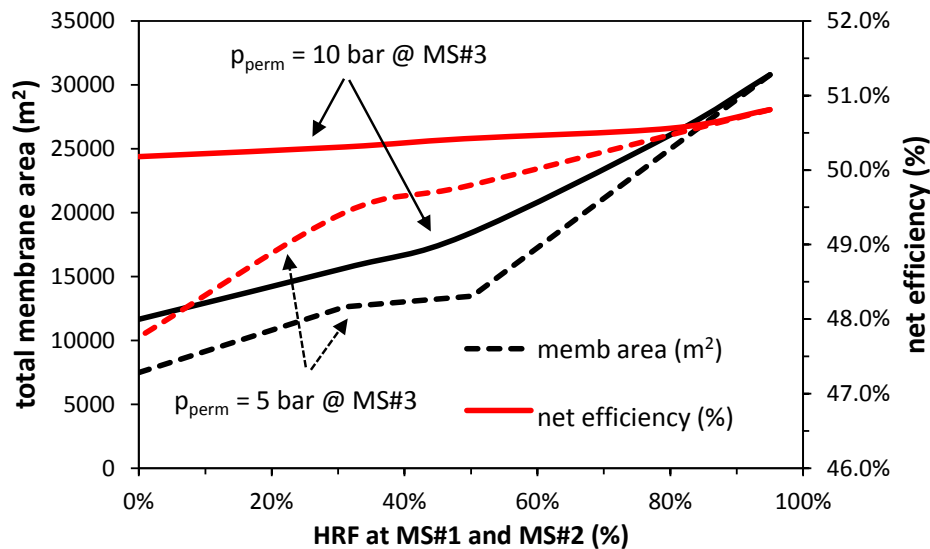


Figure 38. Sensitivity analysis of the combination of membranes with different permeate pressure ($HRF_{total} = 95\%$)

An alternative option for the use of the fuel stream from MS#3 is to fire it in the HRSG (i.e., the afterburning option as suggested for the IGCC case by partner PTM). In the IGCC case, the turbine exhaust temperature (front temperature on the gas side of the HRSG) is lower than that of the NGCC (without any additional firing, 597°C for the IGCC compared to 608°C for the NGCC). This means that post-firing fuel brings larger benefit for the IGCC case than for the NGCC case. Furthermore, by firing combustibles at a point after the gas turbine, only the steam cycle efficiency is involved. Steam cycle efficiencies are much closer to the ~45% total efficiency of the IGCC compared to the natural gas

combined cycle of above 50% efficiency. Therefore, moving towards a larger steam cycle in the NGCC is much more detrimental to overall efficiency, i.e. in terms of increased running costs.

2.6 Optimized case study

Following process selection and sensitivity analyses in sections 2.3 and 2.4, Case I emerges as the optimum case as far as plant performance is concerned, since it shows the greatest net efficiency. The schematic configuration of the base case is depicted in **Figure 39**. The process parameters for Case I are summarized in **Table 10**. The energy balance of the plant is presented in **Table 13**, while the basic characteristics of the streams relevant to the process flow sheet of **Figure 39** are presented in **Table 11**.

Table 10. Process parameters for Cases I and VII

CASE		I	VII
purification scheme		oxy-combustion w/o expander	
S/C ratio at the ATR	mole/mole		1.7
NG temperature before ATR	°C		360
Pre-reforming Temperature	°C		700
ATR Temperature	°C		1050
HRF at MS#1	%		37.2
HRF at MS#2	%		89.2
HRF total	%		95.0
HT-WGS Temperature	°C		400
LT-WGS Temperature	°C		360
Sweep gas inlet temperature	°C		303
Oxygen purity	%		95.0
Δp_{H_2} at the outlet of 1st membrane	bar		9.0
pressure at the feed side	bar	45	55
pressure at the permeate side	bar	25	10
total membrane area	m ²	28588	9412

According to the previous sensitivity analyses, membrane pressure on both sides plays a significant role in the reduction of the required membrane area. The optimum case for the minimization of the required membrane area in conjunction with a net efficiency higher than 50% is Case VII. In this case, the total required membrane area is 9412 m². The MS#1 has an area equal to 2x836 m² contributing to hydrogen separation where $HRF=37.1\%$. The MS#2 has a total surface area of 2x3870 m², contributing to hydrogen recovery up to $HRF=95\%$. All the investigations to find the best combination of high efficiency and low membrane area were performed keeping the design parameters of the membrane constant (outer diameter d_o , inner diameter d_i , length L).

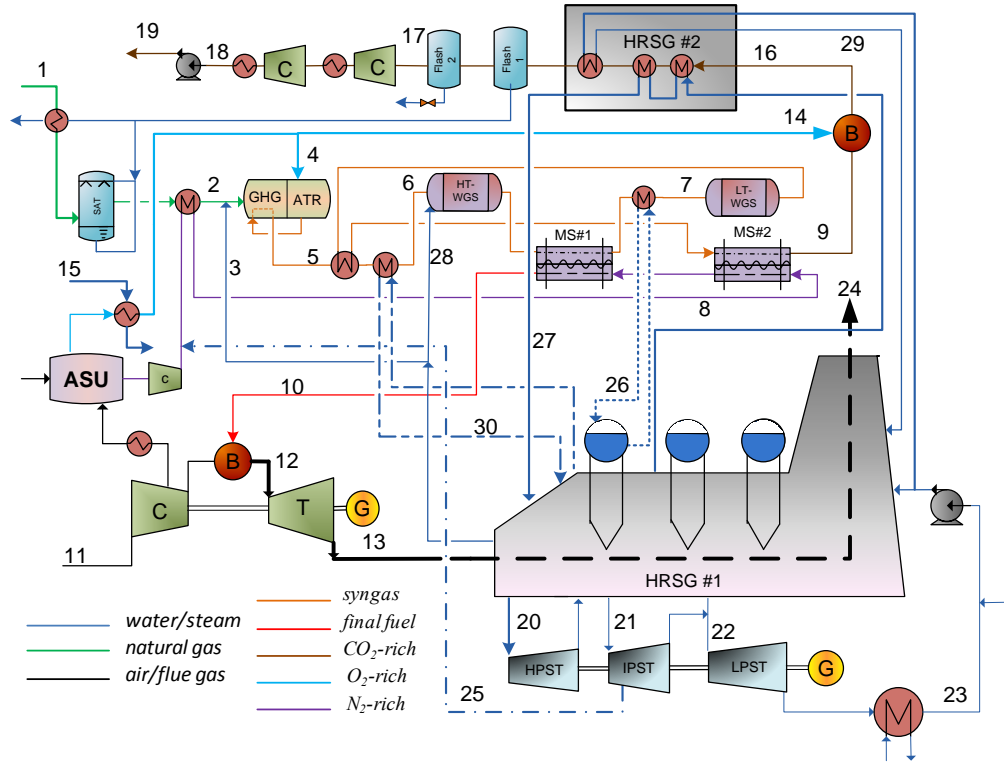


Figure 39. Process Flow Diagram for case I

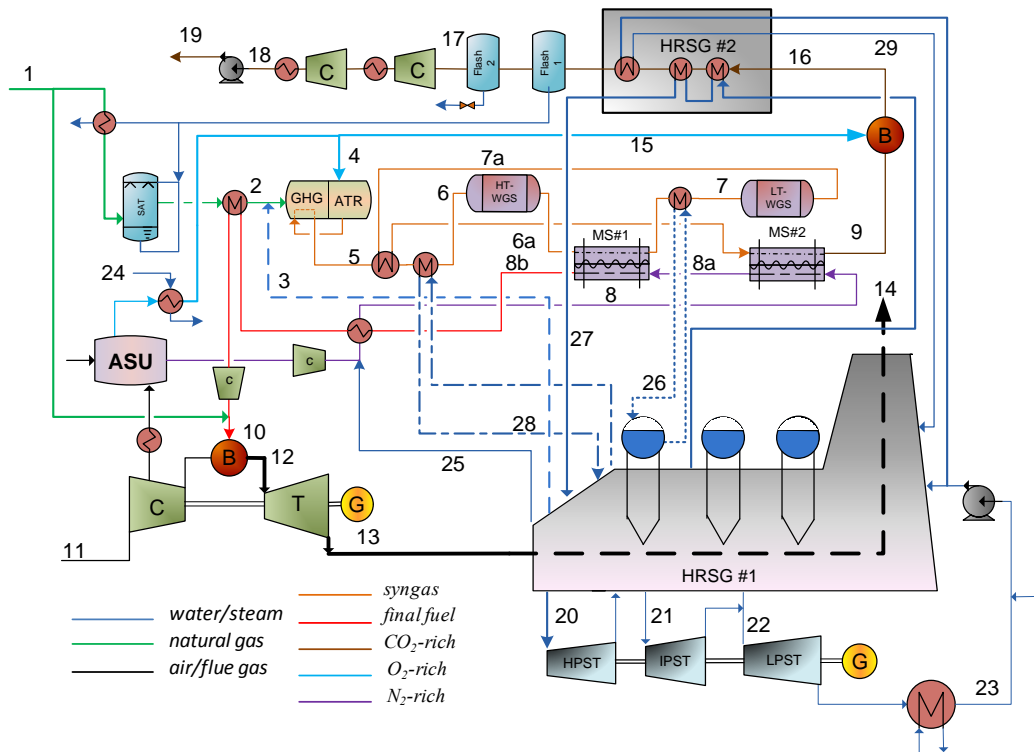


Figure 40. Process Flow Diagram for Case VII

Table 11. Main streams characteristics for case I (see Figure 39)

a/a	Total Flow kmol/s	Total Flow kg/s	T °C	p bar	molar composition (%)								
					H ₂ O	CO ₂	H ₂	N ₂	O ₂	Ar	CO	CH ₄	C _x H _y
1	2.19	39.53	10.0	70.00	0.00	2.00	0.00	0.89	0.00	0.00	0.00	89.00	8.00
2	2.33	41.95	360.0	50.51	5.77	1.88	0.00	0.84	0.00	0.00	0.00	83.86	7.54
3	3.81	68.67	433.2	50.50	100	0.00	0.00	0.00	0.00	0.00	0.00	0.00	0.00
4	1.21	38.95	130.0	50.50	0.00	0.14	0.00	1.29	95.00	3.57	0.00	0.00	0.00
5	10.74	149.57	626.8	49.00	31.72	5.67	45.38	0.33	0.00	0.40	15.89	0.61	0.00
6	10.75	149.70	272.0	49.00	31.77	5.66	45.35	0.33	0.00	0.40	15.88	0.61	0.00
6a	10.75	149.70	400.0	48.00	20.21	17.22	56.91	0.33	0.00	0.40	4.32	0.61	0.00
7	5.56	139.25	299.0	47.50	39.03	33.27	16.78	0.63	0.00	0.78	8.35	1.17	0.00
7a	5.56	139.25	385.6	47.00	36.61	56.10	46.47	0.63	0.00	0.78	2.93	0.00	0.00
8	6.24	167.64	302.4	25.00	11.71	0.00	0.00	87.86	0.26	0.17	0.00	0.00	0.17
8a	8.75	173.93	386.0	24.00	7.17	0.00	36.61	56.10	0.00	0.12	0.00	0.00	0.00
9	4.46	137.03	331.8	46.00	40.42	49.75	4.45	0.79	0.00	0.97	2.16	1.46	0.97
10	12.51	180.31	397.3	23.10	6.10	0.00	50.00	43.82	0.00	0.08	0.00	0.00	0.08
11	45.05	1300.0	15.0	1.01	1.01	0.03	0.00	77.30	20.74	0.92	0.00	0.00	0.92
12	47.38	1276.7	1355.0	17.56	15.62	0.02	0.00	73.47	9.94	0.76	0.00	0.00	0.76
13	50.99	1380.7	607.5	1.04	14.59	0.02	0.00	73.74	10.70	0.77	0.00	0.00	0.77
14	0.29	9.44	131.8	50.50	0.00	0.14	0.00	1.29	95.00	3.57	0.00	0.00	3.57
15	0.52	9.39	1500.0	5.00	100	0.00	0.00	0.00	0.00	0.00	0.00	0.00	0.00
16	4.61	146.47	911.8	41.00	46.29	51.69	0.00	0.84	0.01	1.16	0.00	0.00	1.16
17	2.47	107.92	28.0	40.50	0.12	96.13	0.00	1.57	0.01	2.17	0.00	0.00	2.17
18	2.47	107.92	25.0	78.30	0.11	96.13	0.00	1.57	0.01	2.17	0.00	0.00	2.17
19	2.47	107.92	28.0	110.00	0.11	96.13	0.00	1.57	0.01	2.17	0.00	0.00	2.17
20	14.48	260.79	559.5	110.34	100	0.00	0.00	0.00	0.00	0.00	0.00	0.00	0.00
21	12.95	233.26	560.5	26.45	100	0.00	0.00	0.00	0.00	0.00	0.00	0.00	0.00
22	13.68	246.47	308.7	4.85	100	0.00	0.00	0.00	0.00	0.00	0.00	0.00	0.00
23	13.68	246.47	26.0	0.05	100	0.00	0.00	0.00	0.00	0.00	0.00	0.00	0.00
24	50.99	1380.8	68.3	1.01	14.59	0.02	0.00	73.74	10.70	0.77	0.00	0.00	0.77
25	3.69	66.51	335.0	130.00	100	0.00	0.00	0.00	0.00	0.00	0.00	0.00	0.00
26	0.62	11.24	245.0	35.00	100	0.00	0.00	0.00	0.00	0.00	0.00	0.00	0.00
27	2.92	52.62	560.0	118.65	100	0.00	0.00	0.00	0.00	0.00	0.00	0.00	0.00
28	0.69	12.44	559.0	25.00	100	0.00	0.00	0.00	0.00	0.00	0.00	0.00	0.00
29	0.42	7.48	61.8	5.15	100	0.00	0.00	0.00	0.00	0.00	0.00	0.00	0.00
30	0.01	0.13	433.2	50.90	100	0.00	0.00	0.00	0.00	0.00	0.00	0.00	0.00

Table 12. Main streams characteristics for Case VII (see Figure 40)

a/a	mass flow kmol/s	molar flow kg/s	T °C	p bar	molar composition (%)								
					H ₂ O	CO ₂	H ₂	N ₂	O ₂	Ar	CO	CH ₄	C _x H _y
1	2.10	37.91	10.0	70.0	0.00	2.00	0.00	0.89	0.00	0.00	0.00	89.00	8.00
2	2.01	36.19	360.0	59.5	5.73	1.89	0.00	0.84	0.00	0.00	0.00	83.90	7.54
3	3.29	59.27	433.2	59.5	100.0	0.00	0.00	0.00	0.00	0.00	0.00	0.00	0.00
4	1.03	33.32	130.0	59.5	0.00	0.14	0.00	1.29	95.00	3.57	0.00	0.00	0.00
5	9.23	128.78	624.6	58.0	31.89	5.68	45.12	0.33	0.00	0.40	15.76	0.82	0.00
6	9.23	128.78	272.0	57.0	31.77	5.66	45.35	0.33	0.00	0.40	15.88	0.61	0.00
6a	9.23	128.78	400.0	56.5	20.40	17.17	56.61	0.33	0.00	0.40	4.27	0.82	0.00
7	7.15	124.39	301.1	56.5	26.34	22.24	43.91	0.63	0.00	0.77	8.20	1.57	0.00
7a	7.15	124.39	360.0	56.0	23.71	24.86	46.54	0.63	0.00	0.77	2.89	1.57	0.00
8	5.32	144.98	380.0	10.0	8.18	0.00	0.00	91.37	0.27	0.18	0.00	0.00	0.18
8a	6.27	146.87	383.1	10.0	6.95	0.00	15.03	77.64	0.23	0.15	0.00	0.00	0.15
8b	10.68	155.80	334.0	10.0	4.35	0.00	50.00	45.56	0.00	0.09	0.00	0.00	0.09
9	3.86	117.96	400.0	55.0	40.66	49.12	4.40	0.78	0.00	0.96	2.12	1.96	0.96
10	10.89	159.59	469.5	23.0	4.27	0.04	49.03	44.70	0.00	0.09	0.00	1.72	0.24
11	45.05	1300.0	15.0	1.0	1.01	0.03	0.00	77.30	20.74	0.92	0.00	0.00	0.92
12	46.69	1269.3	1355.0	17.6	14.18	0.51	0.00	74.00	10.33	0.78	0.00	0.00	0.78
13	50.23	1371.6	607.5	1.0	13.25	0.48	0.00	74.24	11.07	0.79	0.00	0.00	0.79
14	50.23	1371.6	68.3	1.0	13.25	0.48	0.00	74.32	11.16	0.79	0.00	0.00	0.79
15	0.29	9.42	132.1	59.5	0.00	0.14	0.00	1.29	95.00	3.57	0.00	0.00	3.57
16	4.03	127.38	1031.3	50.0	46.96	51.02	0.00	0.84	0.01	1.18	0.00	0.00	1.18
17	2.13	93.15	28.0	49.5	0.11	96.06	0.00	1.59	0.02	2.22	0.00	0.00	2.22
18	2.13	93.15	25.0	78.3	0.11	96.06	0.00	1.59	0.02	2.22	0.00	0.00	2.22
19	2.13	93.15	34.0	110.0	0.11	96.06	0.00	1.59	0.02	2.22	0.00	0.00	2.22
20	14.07	253.55	559.5	110.3	100.0	0.00	0.00	0.00	0.00	0.00	0.00	0.00	0.00
21	12.91	232.50	560.5	26.5	100.0	0.00	0.00	0.00	0.00	0.00	0.00	0.00	0.00
22	13.94	251.17	307.6	4.9	100.0	0.00	0.00	0.00	0.00	0.00	0.00	0.00	0.00
23	13.94	251.17	26.0	0.0	100.0	0.00	0.00	0.00	0.00	0.00	0.00	0.00	0.00
24	0.47	8.41	150.5	5.0	100.0	0.00	0.00	0.00	0.00	0.00	0.00	0.00	0.00
25	0.40	7.29	414.7	10.0	100.0	0.00	0.00	0.00	0.00	0.00	0.00	0.00	0.00
26	0.57	10.28	245.0	35.0	100.0	0.00	0.00	0.00	0.00	0.00	0.00	0.00	0.00
27	2.81	50.67	560.0	118.6	100.0	0.00	0.00	0.00	0.00	0.00	0.00	0.00	0.00
28	3.15	56.69	335.0	130.0	100.0	0.00	0.00	0.00	0.00	0.00	0.00	0.00	0.00
29	0.15	2.64	61.8	5.2	100.0	0.00	0.00	0.00	0.00	0.00	0.00	0.00	0.00

The basic characteristics of the streams relevant to the process flow sheet for Case VII, the optimum case, are presented in **Table 12**. The process flowsheet for Case VII is depicted in **Figure 40**, while the process parameters are summarized in **Table 10** and the corresponding energy balance is depicted in **Table 13**:

Table 13. Energy balance

CASE	I	VII
CO ₂ avoided (%)	90%	90%
GT net power (MWe)	667.94	661.72
ST gross power (MWe)	350.73	362.25
Steam cycle auxiliaries (MWe)	-8.19	-8.37
ASU consumption (MWe)	-33.97	-34.25
N ₂ compression (MWe)	-61.32	-96.56
CO ₂ purification & compression (MWe)	-4.69	-3.27
Net electric power (MWe)	910.50	881.52
Thermal power input LHV (MW _{th})	1791.71	1762.76
Net electric efficiency LHV (%)	50.82%	50.01%
Efficiency penalty (%)	7.5%	8.3%
CO ₂ specific emissions (g/kWh)	42.16	42.16
SPECCA (MJ _{LHV} /kgCO ₂)	2.91	3.28

By increasing membrane-tube diameter and keeping the outer gas flow envelope constant, the cross-section of the permeate side is increased and the corresponding cross-section of the feed side is reduced. This could positively affect the H₂ mass transfer on the radial axis on both sides, which increases the H₂ flux. For instance, an increase of membrane-tube diameter by 30% would result in a total membrane area of 7890 m² (16.2% reduction).

2.7 Comparison with other CO₂ capture techniques

In order to evaluate and compare the Pd membrane technology with other CO₂ capture techniques in terms of plant efficiency, the thermodynamic analysis of other known options is performed and discussed in this section. Each of these units is modelled in ASPEN PlusTM: in all cases an issue of utmost importance is choosing the right set of physical properties model, including the set of reactions. These options for the processes modelled are presented in **Table 14**.

Table 14. Property methods selection for process modeling

Unit	Property method
CO ₂ removal with Selexol process	PC-SAFT
CO ₂ removal with Rectisol process	RK-Soave
CO ₂ removal with MEA/MDEA/K ₂ CO ₃ process	NRTL with electrolytes

a. Chemical absorption options

In CO₂ capture by chemical absorption, separation from the syngas is performed bringing a MEA aqueous solvent into contact with CO₂ in an absorber column, where the following reaction occurs:

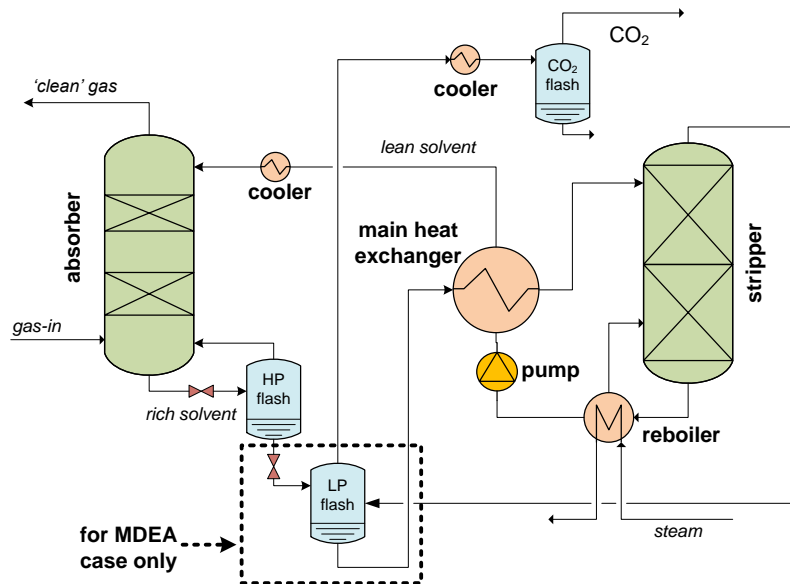
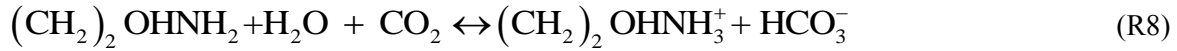


Figure 41. Typical design of chemical absorption systems

The gas outlet of the first flash separation (HP flash) contains light gases (CO & H₂ for pre-combustion case and N₂, O₂ for the post combustion case) and is returned back to the absorber to increase the overall recovery at the ‘clean’ gas stream. The release of CO₂ carried in the solvent occurs in the stripper unit that operates at elevated temperatures, allowing the reverse reaction (1) to take place. The MEA solvent is thus regenerated and reused. The required heat for solvent regeneration is provided by steam extracted from the steam cycle. The gaseous outlet of the stripper mainly consists of CO₂ and steam, and these two components are separated by condensation at ambient temperature.

Post-combustion CO₂ capture consists of CO₂ absorption by chemical absorption with MEA. The power block parameters are kept the same as in the reference case. It has been assumed that the capture rate is 90%. The pressure in the absorption column is set to 1.1 bar with a booster fan upstream, in order to account for pressure drops and keep the GT exhaust pressure equal to the reference NGCC without carbon capture. The absorption temperature is set to about 50°C, so a cooler is required after the HRSG. The CO₂ captured by MEA in the absorption column is released in the stripper, where heat is required for the reboiler. This heat is supplied by steam extracted from the steam turbine, de-superheated with water. Stripper pressure at the bottom of the column is set at 1.8 bar and the reboiler temperature is 119°C. The CO₂ released in the stripper column is compressed according to the EBTF requirements[19], with three compression stages (4.35 bar, 18.65 bar and 80 bar) with intermediate cooling to 28°C and one pumping stage after the 80 bar compressor raising the pressure to 110 bar.

The nominal net output decreases because i) of the steam required for amine regeneration and ii) of the additional auxiliary power consumption (amine circulation pumps, fans overcoming the gas pressure

losses, additional cooling water pumps, CO₂ compressors). The amount of energy for regeneration is assumed equal to 3.95 GJ/tonneCO₂ with steam at a pressure of ca 4.2 bar. Under these assumptions, the predicted net electric efficiency penalty is of about 8.6 percentage points. The plant layout is shown in **Figure 42**.

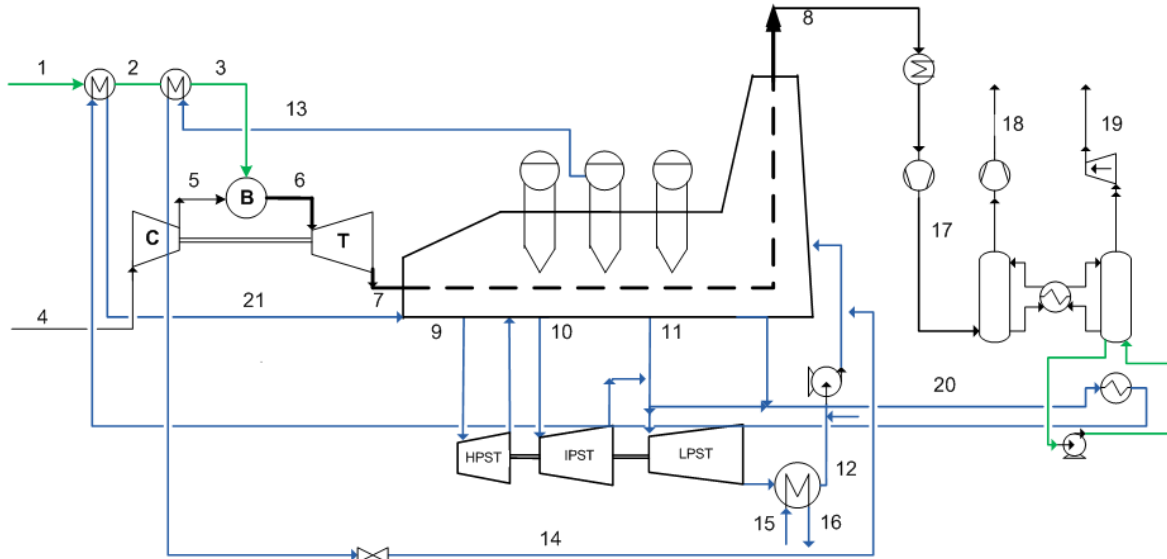
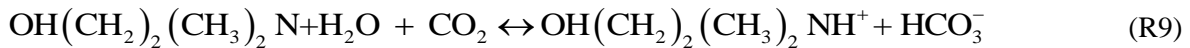


Figure 42. Natural Gas Combined Cycle with post-combustion Carbon Capture employing MEA

In the MDEA case, the solvent regeneration is performed partially with pressure throttling and the rest of it with thermal stripping at ambient pressure. Therefore, the corresponding specific heat for solvent desorption is considerably lower than that of the MEA process [54, 73]. The principle of CO₂ capture with MDEA is similar to the MEA process:



The MDEA process is suitable for pressurized systems since it has a better performance at high CO₂ partial pressures [74]. The main components of the NGCC power plant with pre-combustion MDEA-based technology are:

- A GHR-ATR that converts a steam-methane mixture into hydrogen into two consequential steps: a pre-reforming gas heated reformer (GHR) and a more conventional air blown auto-thermal reformer (ATR). In order to avoid catalyst poisoning from sulphur components present in the natural gas, a desulphurization section is required in front of the reformer. The NG is humidified in a saturator and preheated inside a heat exchanger with HP saturated water from the HP drum, before it mixes with steam and enters the pre-reformer. The operating pressure of the GHR-ATR is 30 bar. Reforming is conducted at 950°C with a S/C ratio of 1.5 and the additional required heat is obtained using air as oxidant which is extracted from the GT compressor. Heat from the syngas is integrated in the steam cycle by producing HP superheated steam.
- Two water-gas shift reactors (WGS) that convert the CO within the syngas produced by the ATR into CO₂ and H₂. The first WGS is a high temperature reactor allowing a fast conversion (smaller catalysts volumes). The water-gas shift reaction is exothermic with the exit temperature rising to 400 °C and the heat released in the reaction is recovered by superheating HP and LP saturated steam inside a heat exchanger. The second WGS reactor operates at lower equilibrium temperatures

(around 224°C), where the reaction is promoted and enhances a further CO conversion. After the LT WGS follows a heat exchanger heating up water for syngas saturation.

- A CO₂ separation unit (carried out with MDEA technology) to capture CO₂ from the syngas exiting the WGS in order to produce a decarbonised fuel (H₂ and N₂ with some traces of CH₄, CO and H₂O remaining from the previous reactions) which is then fed in the combined cycle. The operating pressure of the CO₂ absorber is around 24 bar. The specific energy consumption for the process is 1 ca. MJ/kg_{CO2} and the required heat is provided by means of steam extraction from the LP ST. The syngas output stream has high hydrogen content (58% vol) and is moisturized and preheated before entering the combustor. A small fraction of the syngas is mixed with the natural gas feed and the mixture is directed to the desulphurization unit.
- Two saturators: the first saturator humidifies and heats the NG before the pre-reformer reactor; this reduces the amount of steam bled from the turbine in order to reach the desired Steam-to-Carbon ratio (S/C ratio). The second saturator humidifies the syngas before the combustor inlet lowering the flame temperature with benefits on NO_x formation.
- The power block parameters are kept the same as in the reference case. This includes the Turbine Inlet Temperature (TIT); this represents a change from current hydrogen fired turbine manufacturer's recommendations. However, this type of advancement may be expected as demand for hydrogen fired gas turbines increases.
- The CO₂ stream compression train is according to the EBTF requirements, with three compression stages (4.35 bar, 18.65 bar and 80 bar) with intermediate cooling to 28°C and one pumping stage after the 80 bar compressor raising the pressure to 110 bar.

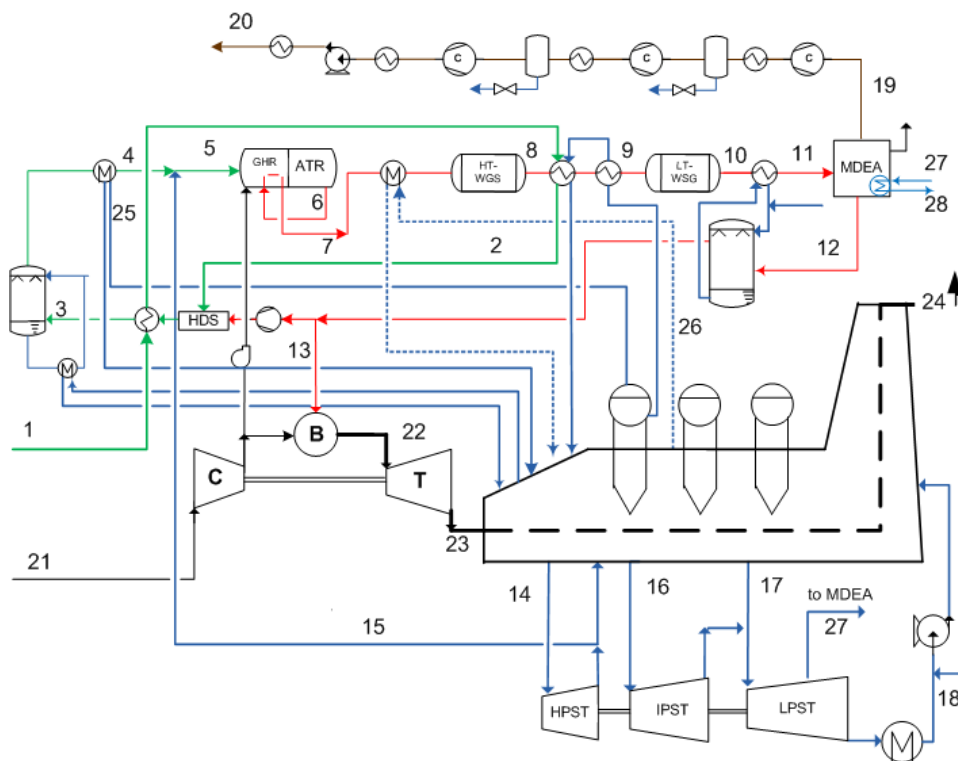


Figure 43. Natural Gas Combined Cycle with pre-combustion Carbon Capture employing MDEA

The plant layout is shown in **Figure 43**. The same configuration is adopted for all the pre-combustion options (physical absorption, hot potassium, cryogenics, CO₂-selective MS etc.).

The hot potassium technology for CO₂ capture is conducted in same configuration with the amine scrubbing one. For the hot potassium (K₂CO₃) process modeling, the equilibrium modelling of chemical solvents in ASPEN Plus™ is based on Electrolyte NRTL (ENRTL) model, while the Redlich-Kwong-Soave (RK-SOAVE) equation-of-state is employed for vapor phase prediction. In 35% w/w K₂CO₃ solvent is considered (boiling point of the solvent: 115 °C, operating pressure: 20 bar) [75]. The temperature dependent equilibrium constants of the CO₂ and H₂S reactions were introduced to the model according to [76].

b. Physical absorption options

Concerning the capture technology based on physical absorption, the CO₂ separation is also performed through a contacting gas/solution absorption column. Since the process operates at high pressures, the solvent regeneration can be achieved only with stages pressure throttling. The energy duties for these technological options include power consumption for solvent pumping and cooling provided from a refrigeration system. The CO₂ removal from syngas through physical absorption is achieved with the increased solubility rates of CO₂ in certain water solutions, such as Selexol® (a blend of dimethyl ethers of polyethylene glycol) and Rectisol® (methanol) at low temperatures [77, 78].

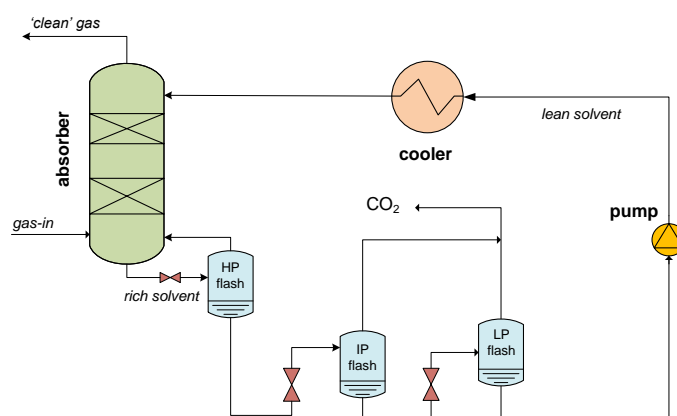


Figure 44. Typical design of physical absorption systems

The process scheme of a typical physical absorption unit that is assumed for CO₂ capture is presented in **Figure 44** and the process parameters are summarized in the following **Table 15**:

Table 15. CO₂ capture Plant specifications

chemical absorption	MEA	MDEA	K ₂ CO ₃
absorber stages	8	8	6
lean solvent %w/w	40	40	
lean solvent temperature, °C	40	40	
stripper stages	4	4	6
specific heat at reboiler, MJ _{th} /kg _{CO2}	4.17	1.92	
specific power consumptions, MJ _e /kg _{CO2}			
physical absorption	Rectisol™	Selexol™	
lean solvent %w/w	98.0	90.0	
lean solvent temperature, °C	-20	0	
HP/IP/LP flash pressure, bar	5/1.01/0.16	5.5/1.01/0.18	
specific power consumptions, MJ _e /kg _{CO2}	0.24	0.36	

c. Cryogenics

The technique of CO₂ separation under cryogenic conditions (-54.5°C) is examined for both the pre and post combustion options. The PCU scheme and operation parameters in both cases that are adopted are based on flash separator and are presented in **Section 2.4**. In the post-combustion case, the PCU operation does not affect the operation of the reference plant, but for the use of electricity for the coverage of the power demands (compression duties). As mentioned above, in the pre-combustion case, the system configuration is the same with the plant layout that is presented for the MDEA case.

d. CO₂ selective membranes

The core idea of the Pd membrane concept is the hydrogen separation from a H₂/CO₂ mixture composing a pure fuel stream for the GT. The opposite idea is the permeated stream to be the pure CO₂ stream that is sent for compression and storage by means a CO₂ selective membrane separation unit. To increase the CO₂ permeability, extracted steam from the ST is used as sweep gas. Huang et al. proved experimentally that using membrane with the facilitated transport mechanism and using steam as the sweep gas, high CO₂ recovery (>95%) and selectivity rates (98%) can be achieved [79]. For the CO₂-selective membrane, a simplified approach is adopted, assuming 100% selectivity and 90% CO₂ recovery factor. The pressure in the permeate side is set at 11.5 bar. The permeate stream is cooled down to 30°C and enter the TEG unit for effective H₂O/CO₂ separation according to the EBTF guidelines. The pure CO₂ stream undergoes compression to 110 bar. The process configuration of the H₂ plant is the same with the MDEA case (see **Figure 43**)

e. O₂/CO₂ cycle

In this case, the Air Separation Unit that is considered for the pure oxygen production is similar to the proposed ASU in **Section 2.3.1**. In this case, since the oxygen is provided at the GT in gaseous form in atmospheric pressure, the air booster is omitted. The ASU produces oxygen with 95% v/v purity with specific consumptions 230.0 kWh/tn_{O₂}. The oxidizing medium that enters the GT also consists of recycling rich-CO₂ stream with oxygen concentration 23%. The GT operation parameters are the same with the air-fired case. The flue gases that exit the boiler undergo intensive purification in order to produce a pure CO₂ stream suitable for transport and storage. The PCU configuration that is adopted is based on flash separator and is presented in **Section 2.4**.

Results – thermodynamic performance

Table 16 summarizes the main results from the process simulation for various CO₂ techniques in NG fired power plant, in terms of plant performance, i.e. energy balance and specific CO₂ emissions. It is clear that the CO₂ capture scheme based on Pd membrane separators has the best performance in terms of net efficiency (or energy penalty) and SPECCA index. In this case, the major energy penalty is for O₂ production and N₂ compression, while the energy duty for CO₂ compression is negligible due to the high operating pressure. On the other hand, in the case of the capture technology with amines, steam extraction for solvent regeneration deteriorates the ST gross efficiency. The high energy penalty for CO₂ compression for the physical solvent cases is due to the low CO₂ separation pressure from the solvents.

As it is also stated in the Introduction [19], the amine scrubbing technique using MDEA in a pre-combustion scheme has higher net efficiency than the MEA scrubbing in post-combustion option, owed to lower specific regeneration heat. The comparison of the MDEA case with the two physical absorption cases reveals that chemical absorption solvents have a greater loading capacity at relative low partial

pressures than the SelexolTM/RectisolTM processes. It should be mentioned that the CO₂ concentration in a syngas stream derived from natural gas reforming, is two or three times smaller than for a syngas derived from biomass or coal gasification.

The use of cryogenic techniques for post-combustion capture has the worst performance, contrary to the pre-combustion option, where the net efficiency is relatively high. In this case, the highest power consumptions are observed in the CO₂ Compression Unit, due to the fact that the purified CO₂ stream exit the Purification Unit with pressure below the atmospheric.

Finally, the oxy-combustion scheme is a less competitive option for NG-fired power plants due to high consumptions mainly in the ASU and the Purification and Compression Unit.

Table 16. CO₂ capture (CCR=90%) in NGCC with various CO₂ capture techniques - main results

CO ₂ capture scheme	no CO ₂ capture	post-combustion		pre-combustion							oxy-fuel
		MEA	cryogenics	MDEA	Selexol™	Rectisol™	K ₂ CO ₃	cryogenics	CO ₂ selective MS	Pd- MS	
GT net power, % MWe/LHV	38.70	38.70	38.66	35.92	35.15	35.59	36.06	35.47	34.57	37.28	32.96
ST gross power, % MWe/LHV	20.00	14.72	20.44	17.96	19.14	19.36	13.41	19.38	16.92	19.58	25.35
steam cycle auxiliaries, % MWe/LHV	-0.40	-0.34	-0.41	-0.44	-0.49	-0.50	-0.40	-0.50	-0.46	-0.46	-0.40
ASU + N ₂ compression, % MWe/LHV	-	-	-	-	-	-	-	-	-0.83	-5.32	-6.43
CO ₂ capture unit, % MWe/LHV	-	-1.53	-15.90	-1.20	-2.68	-2.09	-0.87	-1.10	-	-	-0.66
CO ₂ compression, % MWe/LHV	-	-1.85	-6.01	-1.87	-3.20	-2.98	-1.41	-3.23	-0.81	-0.26	-0.95
Net electric power, % MWe/LHV	58.30	49.71	36.78	50.37	47.93	49.38	46.79	50.02	49.39	50.82	49.88
Efficiency penalty, %	-	8.6	21.52	7.93	10.37	8.92	11.51	8.28	8.91	7.48	8.42
CO ₂ avoided, %	-	88.3	83.30	88.40	90.00	89.80	60.73	89.47	92.16	89.5	90.60
CO ₂ specific emissions, g/kWh	354.3	41.6	56.0	41.0	42.6	42.5	179.8	43.4	32.7	42.2	25.4
SPECCA, MJ_{LHV}/kgCO₂	-	3.41	12.11	3.10	4.29	3.58	8.70	3.29	3.46	2.91	3.17

2.8 Economic evaluation

This section presents an economic assessment of the membrane cases discussed in the previous sections from a thermodynamic point of view. This analysis can indicate the optimal membrane operating conditions and configurations in terms of economic viability. To this end, specific investment costs will be firstly presented and discussed, while the cost of electricity and CO₂ avoided will be considered afterwards. The assumptions and methodology for the economic analysis are consistent with the EBTF common framework. The examined cases are benchmarked against the MDEA pre-combustion carbon capture technology.

2.8.1 Specific investment costs

The calculated specific investment costs for membrane application in NGCC with different CCR are presented in **Table 17**. In this calculation, the cost of the membrane module is assumed to be equal to 5.4 k€/m². Total Capital Requirement is determined from Total Plant Costs (TPC), which are estimated from Total Equipment Costs (TEC), adding installation costs (68% of TEC), indirect costs (14% of total direct cost) and contingencies and owner costs (15% of TPC). The calculated membrane surface area is large, resulting in economic penalties. The examined cases are:

- oxy-combustor for the CO₂ stream remaining combustibles (feed-side pressure: 46 bar, permeate-side pressure: 25 bar) – Cases I and II
- oxy-combustor and expander (feed-side pressure: 46 bar, permeate-side pressure: 25 bar) – Cases III and IV
- distillation column for the separation of the combustibles (feed-side pressure: 46 bar, permeate-side pressure: 25 bar) – Case V
- flash separation of the combustibles (feed-side pressure: 46 bar, permeate-side pressure: 25 bar) – Case VI
- oxy-combustor for the CO₂ stream remaining combustibles (feed-side pressure: 55 bar, permeate-side pressure: 10 bar) – Case VII

Table 17. Plant costs and specific investment cost for the different cases and different CCR

	Oxy-combustion w/o expander (feed / permeate side: 45/25bar)		oxy-combustion with expander		distillation column	flash separation	Oxy-combustion w/o expander (feed / permeate side: 55/10 bar)
	Case I	Case II	Case III	Case IV	Case V	Case VI	Case VII
CCR (%)	90%	100%	90%	100%	90%	90%	90%
Membrane cost (M€)	108.6	132.0	116.2	129.5	120.7	147.6	35.8
Total Equipment Cost (M€)	563.2	607.7	584.8	625.8	589.4	591.4	482.8
Total plant cost (M€)	1078.6	1163.8	1120.1	1198.5	1128.9	1132.7	924.7
Specific costs (€/kW _{net})	1362.3	1456.8	1436.5	1524.9	1492.5	1489.3	1206.4

Table 17 illustrates that the specific investment costs for oxy-combustion without expander are the lowest (among the cases with membrane feed-side pressure of 46 bar and permeate-side pressure of 25 bar). Membrane costs represent a significant part of the total equipment costs between 108.6 and 147.6

M€, with the total equipment cost lying in the range 563.2–625.8 M€. Most of the cost of the reactor is related to membrane manufacturing and layer deposition (which is not affected by the membrane) as well as manifolding (which is assumed to be independent from the feed pressure). However, when the membrane feed-side pressure is increased up to 55 bar and the permeate-side pressure is reduced down to 10 bar (Case VII), the membrane costs and consequently the total equipment costs are reduced significantly. The CCR significantly affects the membrane cost, since the greater the CCR the greater the membrane area requirements. The second most expensive component is the GT (see Table 18).

Table 18. Total Plant Costs (M€) and Specific Investment Cost for the different cases and different CCR

	Case VII	Case II	Case I	Case IV	Case III	Case V	Case VI
CCR (%)	90	90	100	90	100	90	90
GT generator and auxiliaries	104.77	105.06	105.73	105.06	105.73	106.35	106.47
HRSG, ducting and stack	53.54	54.06	55.27	51.28	52.92	51.31	50.71
HRSG 2 (GHR ATR)	6.72	6.90	7.54	4.26	7.54	4.93	4.97
HRSG 3 (WGS)	2.38	2.37	2.59	3.35	2.59	2.47	3.15
HRSG 4 (post combustion)	8.67	5.50	9.54	4.65	8.35	6.46	4.31
ST generator and auxiliaries	50.17	49.10	49.82	46.76	47.26	41.70	41.79
Cooling water system and BOP	63.23	62.12	63.21	61.08	62.11	51.72	54.19
CO ₂ compressors and condensers	4.81	6.14	6.73	17.90	19.55		15.56
Distillation column						43.12	
GHR ATR	54.43	55.02	60.07	55.02	60.07	57.86	58.48
WGS HT+LT	14.61	14.77	16.13	14.77	16.12	15.53	15.70
N ₂ compressor	14.67	21.77	23.69	21.64	23.55	19.19	19.39
ASU	67.51	69.93	73.36	69.91	76.31	61.26	61.90
Expander				11.20	12.23	4.99	4.11
Heat exchangers	1.58	1.78	1.94	1.78	1.91	1.85	2.52
Membrane separators	35.77	108.63	132.03	116.16	129.53	120.67	147.58
Fuel compressor							0.59
H ₂ compressor	22.07						
Total Equipment Costs	482.84	563.18	607.65	584.83	625.77	589.41	591.42
Total Installation Costs	328.33	382.96	413.20	397.69	425.52	400.80	402.17
Total Direct Plant Costs	811.17	946.14	1020.86	982.52	1051.29	990.22	993.59
Indirect Costs	113.56	132.46	142.92	137.55	147.18	138.63	139.10
Total Plant Costs	924.73	1078.60	1163.78	1120.08	1198.47	1128.85	1132.69
Contingency	92.47	107.86	116.38	112.01	119.85	112.88	113.27
Owner's costs	46.24	53.93	58.19	56.00	59.92	56.44	56.63
Total Capital Requirement	1063.44	1240.39	1338.34	1288.09	1378.24	1298.17	1302.60
Net Power Output (MW)	881.52	910.50	918.71	896.71	903.83	869.81	874.63
Specific Cost (Euros/kW)	1206.37	1362.32	1456.76	1436.45	1524.89	1492.49	1489.32

2.8.2 Cost of electricity and cost of CO₂ avoided

The cost analysis of the examined cases on a yearly basis is illustrated in Table 12.12, while in Table 12.13 the cost analysis per MWh_{el}, the cost of electricity (COE), and the CO₂ avoidance cost are presented. The economic viability of the application of the Pd-membrane-based CO₂ capture technology in NGCC systems is examined on the basis of the break-even electricity-selling-price method. The comparison of the examined cases in terms of cost of electricity and CO₂ avoidance cost demonstrates that the CO₂ avoidance cost and the COE are strongly dependent on membrane cost, which potentially represents a

significant part of the total capital requirement of the installation if there are high membrane area requirements. The fuel costs and the investment costs represent the most important part of the cost per MWh. Given that membranes have to be replaced every five years, membrane cost reduction or flux increase is fundamental to reduce the cost of consumables and render the technology more competitive. The CCR-100% cases result in reduced energy efficiencies and increased COE compared to the respective CCR-90% cases. However, the cost of CO₂ avoided is lower.

Table 19. Cost analysis on yearly basis

	Oxy burner w/o expander, feed/permeate side: 55/10 bar	Distillation column - CCR 90%	Flash separation - CCR 90%	Oxy Burner CCR 90%	Oxy Burner CCR 100%	OxyBurner +expander CCR 90%	OxyBurner +expander CCR 100%
	Case VII	Case V	Case VI	Case I	Case II	Case III	Case IV
Net Electric efficiency (%)	50.01	50.04	49.52	50.82	49.97	50.06	49.17
Electric efficiency (%)	50.01	50.04	49.52	50.82	47.97	50.06	49.17
Fuel cost (M€/y)	309.36	305.06	309.94	314.45	322.64	314.39	322.59
PAI (M€/y)	32.12	37.22	37.32	35.97	38.09	37.00	38.96
Maintenance (M€/y)	18.49	22.58	22.65	21.57	23.28	22.40	23.97
Consumables, (M€/y)	9.73	17.24	20.32	17.25	19.87	17.78	19.40

Table 20. Cost analysis per MWh_{el}

Electricity cost components	Oxy Burner w/o expander, feed/permeate side: 55/10 bar	Distillation column – CCR 90%	Flash separation - CCR 90%	Oxy Burner CCR 90%	Oxy Burner CCR 100%	Oxy Burner + expander CCR 90%	Oxy Burner + expander CCR 100%
	Case VII	Case V	Case VI	Case I	Case II	Case III	Case IV
Investment cost, (€/MWh)	16.78	20.76	20.72	18.95	20.27	19.98	21.21
Fixed O&M costs, (€/MWh)	7.82	9.36	9.34	8.61	9.1	9.02	9.48
Consumables, (€/MWh)	1.48	2.68	3.15	2.56	2.93	2.68	2.90
Fuel costs, (€/MWh)	46.79	46.76	47.25	46.05	46.82	46.75	47.59
COE, (€/MWh)	72.87	79.56	80.46	76.17	79.12	78.43	81.18
Cost of CO ₂ avoided, (€/t _{CO2})	62.05	83.57	86.48	72.49	72.55	79.91	78.41

The cost of electricity as a function of membrane cost for the cases under investigation is shown in **Figure 45**, while **Figure 46** illustrates the cost of CO₂ avoided. It can be seen that the Pd-membrane-based concept with oxy combustion (Case I), which is the optimum choice for the CO₂ stream purification in terms of energy efficiency vs. the MDEA pre-combustion CO₂ capture technology, can achieve reduced cost of CO₂ avoided, given that the membrane cost does not exceed the threshold of c. 4.5 k€/m², which could be regarded as a target cost for early-stage application of the technology. From the figures below, it is evident that when the membrane feed pressure is increased up to 55 bar, while the permeate-side pressure is reduced down to 10 bar, the costs of electricity and CO₂ avoided are significantly lower than the MDEA base case, even when the membrane cost is assumed to be 5.8 k€/m². In this case, a CO₂ avoidance cost 7.4% smaller than the MDEA base case is achieved.

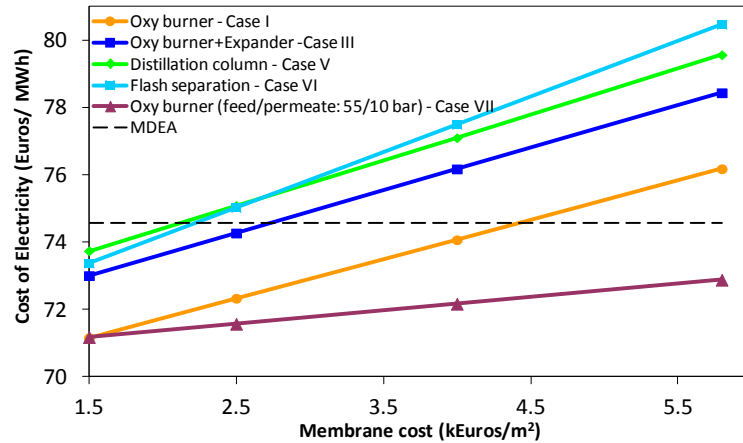


Figure 45. COE as a function of membrane cost

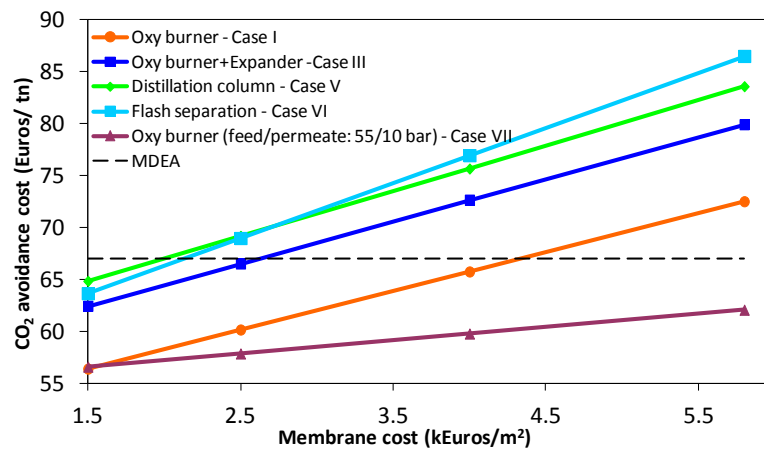


Figure 46. Cost of CO₂ avoided as a function of membrane cost

2.8.3 Effect of membrane area reduction on COE and cost of CO₂ avoided

The CO₂ avoidance cost and the COE for the optimum case, i.e. where there is oxy-combustion w/o expander, can be further reduced when different membrane characteristics are taken into consideration (Table 21). The following cases are examined: (i) membranes with double permeance compared to the original case, and (ii) membranes with the support layer thickness reduced by half compared to the original case. In these cases the membrane area requirements are reduced by 14% and 26%, respectively.

Table 21. Plant costs for different membrane characteristics

CCR (%)	Original case	Double permeance	Reduced support layer thickness
Membrane (M€)	108.6	93.1	80.7
Total Equipment Cost (M€)	563.2	547.7	535.3
Total plant cost (M€)	1078.6	1048.9	1025.1
Specific costs (€/kW _{net})	1362.3	1324.8	1294.7

As expected from the thermodynamic results and investment cost assessment, the lowest cost of electricity and CO₂ avoided is achieved when the membrane surface area is minimized (see **Figure 47** and **Figure 48**). This is because membrane costs take up a significant share of the overall plant costs. Membranes also lead to higher total plant costs, as they affect investment and fixed costs. This is because membrane lifetime is assumed to be only five years.

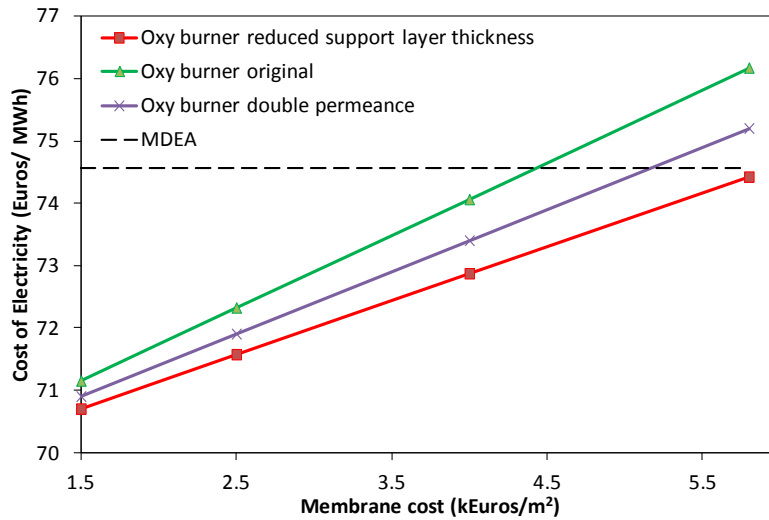


Figure 47. COE as a function of membrane cost

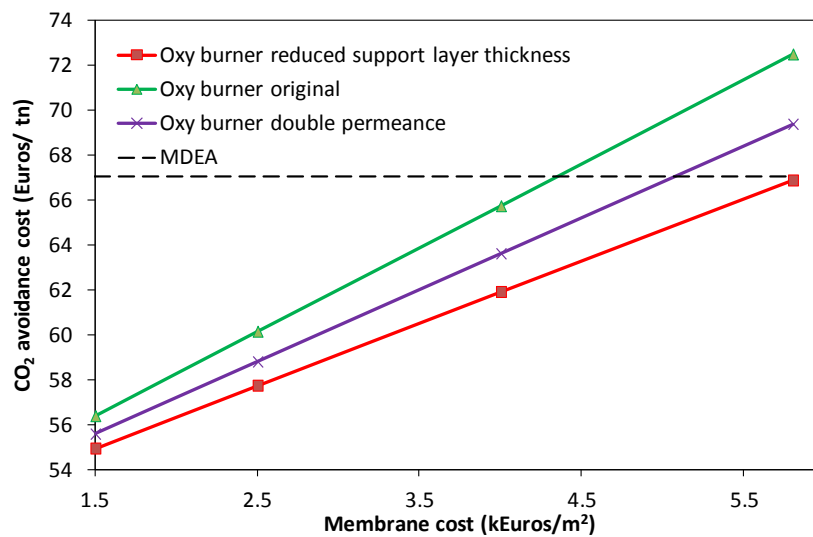


Figure 48. Cost of CO₂ avoided as a function of membrane cost

2.9 Conclusions

Through rigorous process simulation and sensitivity analyses, it can be concluded that an NGCC-CCS plant integrated with Pd membranes can achieve a net energy efficiency of 50.3% at a carbon capture rate close to 100%, or a net energy efficiency of 51.10% at a reduced capture rate of 90% (the same, for example, as the NGCC-CCS base case using MDEA). The latter can be achieved by downsizing the hydrogen block and mixing the fuel gas stream with natural gas. The economic evaluation reveals that the optimum membrane case can achieve a CO₂ avoidance cost 7.4% lower than the MDEA base case. The

economic evaluation also reveals that the most important part of the cost per MWh, where improvements are possible, is the investment cost, which is strongly affected by the required membrane area and associated costs. Thus, in order to render this technology competitive, it is of utmost importance to focus on the reduction of these costs. To understand the potential of membrane area reduction, a sensitivity analysis of H_2 flux against various membrane parameters has been performed. The study has highlighted that mass transfer resistance on the feed side and across the ceramic support layer is the most significant limiting factor on the overall H_2 flux across pure Pd membranes. This indicates that future R&D activity in Pd membranes needs to devote more effort to membrane modules and support designs in order to reduce mass transfer resistance and unleash a higher H_2 flux for Pd membranes. Membrane material research will remain essential, but for natural gas application it will be more driven by the stability and robustness of the Pd material than H_2 permeability.

3. Exergetic comparison of CO₂ capture techniques from solid fossil fuel power plants

3.1 Introduction

The development of carbon capture from gases produced in thermal process like combustion in the form of CO₂ and its storage in appropriate geological formations is one of the most promising options for Greenhouse Gas (GHG) effect reduction. The greatest interest for Carbon Capture and Storage (CCS) implementation is found on the power production sector, and more specifically, on coal-fired thermal plants which account for most of the anthropogenic CO₂ emitted worldwide [8]. Post-combustion capture options are considered the most mature of the options for CO₂ separation, i.e. its separation and capture from flue gases. The other important technology is oxy-combustion, i.e. the replacement of air with pure oxygen stream as the oxidizing medium.

Among the post-combustion CO₂ capture techniques, the most mature technology that is most likely to become commercially available in large scale is chemical absorption by mean of amine solution such MEA (monoethanolamine)[80]. The CO₂ separation from the flue gas is performed in the absorber column where an amine aqueous solvent reacts with the CO₂. The release of CO₂ and simultaneously the solvent regeneration is conducted in a stripper, at elevated temperatures where the reverse reaction takes place. The required heat for the solvent regeneration is obtained through steam extracted from the power plant's steam cycle. The rich-CO₂ stream is easily purified by water condensation and is compressed with inter-stage cooling (Figure 49).

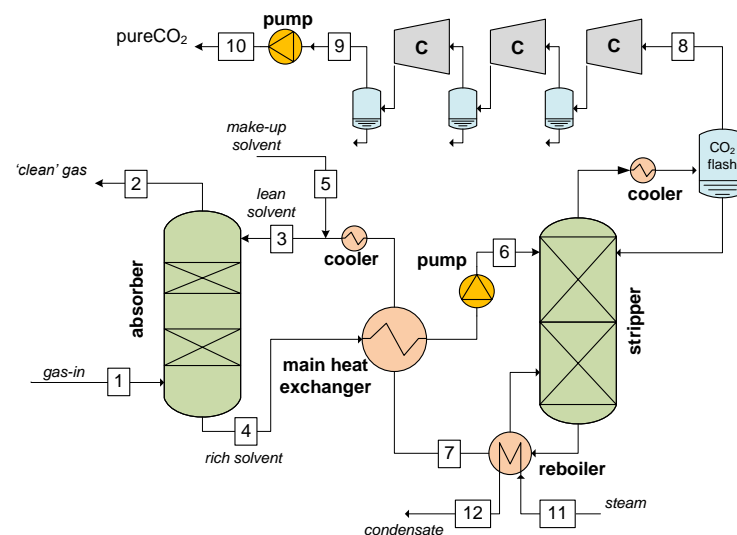


Figure 49. amine scrubbing configuration

Another promising technology is the calcium looping (CaL) [81]. The main principle of this process is the continuous calcium sorbents recirculation between a carbonator and calciner reactor. In the carbonator, CO₂ from flue gas is captured by reacting with solid lime (CaO) to form limestone (CaCO₃). The sorbent's regeneration and CO₂ release is performed with a calcination process. Due to the endothermic nature of the calcination reaction, the simultaneous fuel combustion in the reactor (calciner) is required. To achieve high CO₂ concentrations in the out-coming gas, pure O₂ stream is used. The great

amounts of excess heat from the process is recovered and utilized for electricity generation. Previous studies have shown that the CaL process can achieve the lowest energy penalty compared to other capture techniques like chemical absorption [82] and oxyfuel [33]. The process flowsheet diagram is depicted in **Figure 50**.

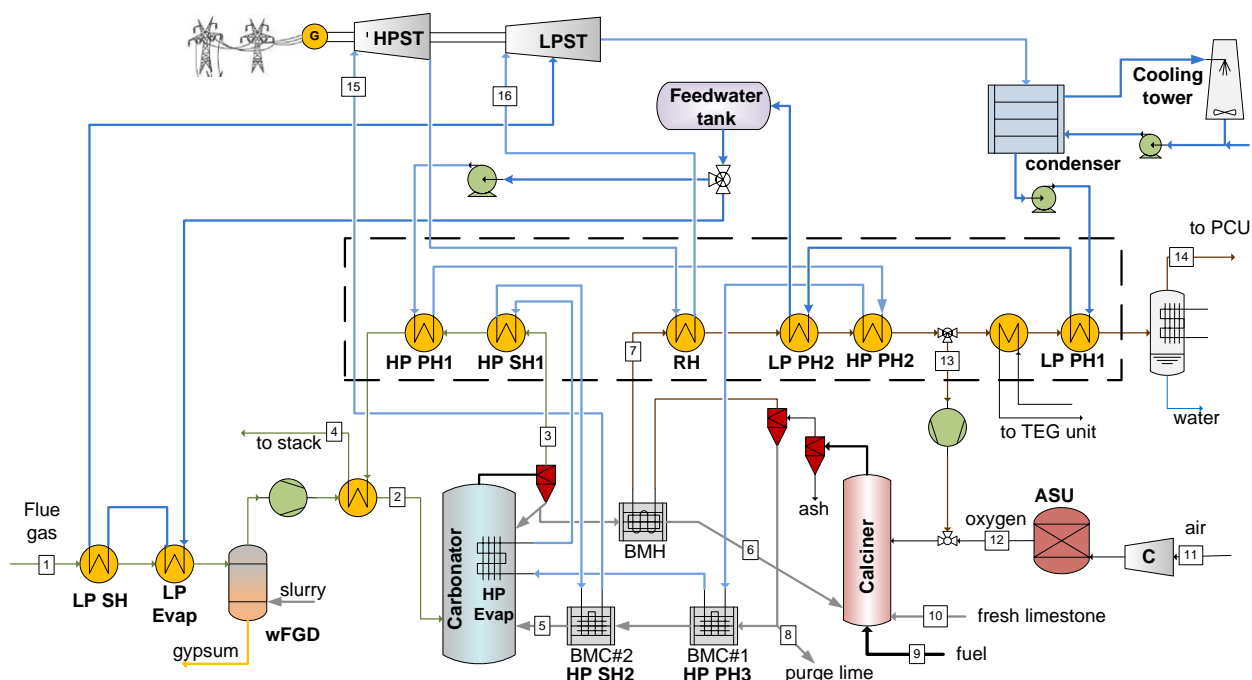


Figure 50. CaL process flowsheet

Finally, the third pathway studied here is based on the so called oxy-combustion - O_2/CO_2 combustion. Using oxygen in CO_2 instead of air as oxidizing agent, the produced flue gas is composed of CO_2 and H_2O which are easily separable through cooling and water condensation. In order to regulate the combustion temperature through thermal mass introduction that would otherwise be air's N_2 , portion of the flue gases is recirculated and mixed with the pure oxygen stream prior to combustion. The technology that is adopted for large quantities of pure O_2 (95% v/v) is through cryogenic distillation in Air Separation Unit (ASU) (**Figure 51**).

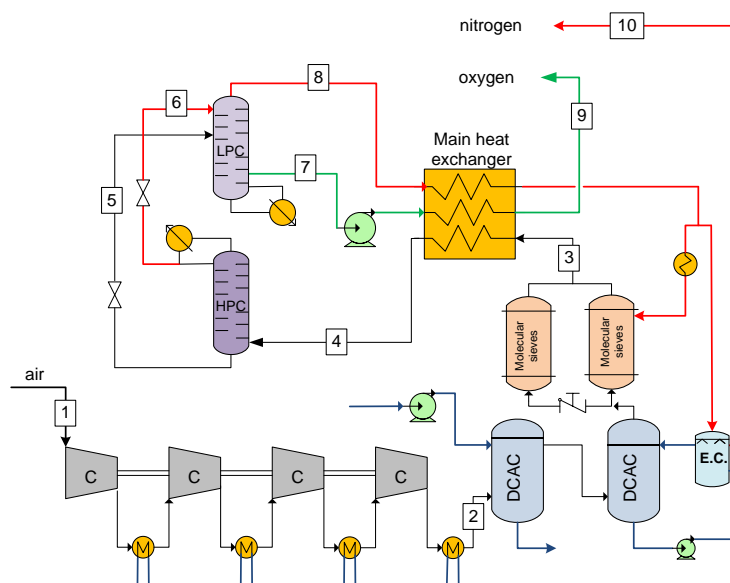


Figure 51. Air Separation Unit configuration for pure O₂ production

Exergy analysis of CCS schemes is already presented by other researchers with valuable results for understanding each process limitations. Amrollahi et al. revealed for the amine scrubbing process that the greatest amount of exergy is mainly lost in the CO₂ absorption process and in the solvent regeneration unit [83]. Through exergy analysis in calcium looping process [84, 85] it is revealed that a large amount of exergy dissipation is observed during calcination. In the oxy-fired power plants, exergy based studies were focused on the improvement of sub processes performance comprising the power plant. For example in [86, 87], it is revealed that a great part of exergy losses occur in the Air Separation Unit and the CO₂ purification Unit respectively Xiong et al. [88] showed that an oxy-fired combustion boiler has lower exergy penalty than the corresponding air-fired. They also estimated that an overall 4.08% exergy penalty in the oxy-combustion case without taking into account the CO₂ compression. Exergetic analysis has also been performed for other CCS technologies such as a pre-combustion scheme including H₂ selective membranes and cryogenic separations [89, 90].

The main scope of this study is to perform the exergy analysis of the three capture technologies and to calculate the irreversibilities in each process indicating which of them operate with the most effective way in principle, based on the second law of thermodynamics. Firstly a certain coal-fired power plant is assumed, retrofitted with these three capture techniques. Through this analysis, the determination of the limitations for further improvement of these is addressed. The second law analysis a very useful tool is an approach that can lead to more objective conclusions. The main question that is addressed to be answer in this study is the following: “*What kind of energy is best to be spent for CO₂ capture in a coal PP, low quality heat through steam (MEA), high quality heat through fuel combustion (CaL) or electrical power (oxyfuel)?*”

3.2 Model description

The process simulations are performed with ASPEN PlusTM. The process modelling of the selected reference case is not presented in detail since the plant performance optimization at the main boiler is beyond the scope of the paper. The reference case is assumed to be a modern pulverised coal fired atmospheric steam boiler, supercritical with single reheat and air preheater with hot flue gas (LUVVO). The feedwater preheating before it enters the boiler is also taken into account by using extracted steam from both high and low pressure steam turbine. The net electrical power output is defined at 300.0 MWe and the corresponding gross 310.9 MWe. The fuel properties and the main specifications for the reference plant operation are summarized in **Table 22**.

Table 22. Reference plant key parameters

Fuel properties		Operating parameters	
C (% d.b.)	69.8	air equivalence ratio	1.25
H (% d.b.)	3.9	HP steam (°C/bar)	600/240
O (% d.b.)	7.2	CRH steam (°C/bar)	370/65
N (% d.b.)	1.7	HRH steam (°C/bar)	600/60
S (% d.b.)	0.4	steam turbine isentropic efficiency HP/IP/LP (%)	92/94/88
ash (% d.b.)	17.0	condenser pressure (bar)	0.050
moisture (w/w %)	7.8	feedwater preheating temperature (high/low pressure °C)	125/240
LHV (kJ/kg a.r.)	25460	fuel gas temperature before LUVVO (°C)	325
		air temperature after LUVVO (°C)	300

3.2.1 MEA Scrubbing

In CO₂ capture by chemical absorption with amines, separation from the flue gas is performed bringing a MEA aqueous solvent into contact with CO₂ in an atmospheric absorber column, where the following reaction occurs:



The required heat for solvent regeneration is obtained from low pressure steam condensation (i.e. 5 bar), which is extracted from the turbine. The property method that is selected for such a model case is NRTL with electrolytes, as it is in the ASPEN PlusTM library [91]. The make-up MEA for amine compensation due to degradation is determined according to the Strube & Manfrida's study [92] (see Table 26). The main characteristics of the basic streams for the amine scrubbing case are shown in Table 23.

Table 23. Streams characteristics of amine scrubbing case (for stream numbering see Figure 49)

stream	m (kg/s)	T (°C)	p (bar)	molar composition (%)					
				H ₂ O	CO ₂	N ₂	O ₂	Ar	MEA
1	346.7	50.0	1	7.0	14.6	74.2	3.3	0.9	0.0
2	284.0	55.2	1	10.4	1.6	83.3	3.7	0.9	0.0
3	2108.9	40.1	1	80.4	6.8	0.0	0.0	0.9	12.7
4	2171.6	58.7	1	80.6	13.4	0.0	0.0	0.0	6.0
5	24.6	25.0	1	99.8	0.0	0.0	0.0	0.0	0.2
6	2170.8	95.3	1.3	80.6	13.4	0.0	0.0	0.0	6.0
7	2084.3	110.6	1.1	80.4	6.8	0.0	0.0	0.9	12.7
8	67.8	29.5	1	1.9	97.8	0.2	0.0	0.0	0.0
9	67.3	25.0	60	0.3	99.4	0.2	0.0	0.0	0.0
10	67.3	24.9	110	0.3	99.4	0.2	0.0	0.0	0.0
11	93.3	248.6	5.0	100.0	0.0	0.0	0.0	0.0	0.0
12	93.3	120.6	4.6	100.0	0.0	0.0	0.0	0.0	0.0

3.2.2 Calcium Looping Process

The methodology for the carbonation process simulation is mainly based on the model introduced by Charitos et al. [93], slightly modified in order to take into account the presence of sulphated part of sorbents. The basic equations for the estimation of the carbonation efficiency (E_{carb}), the carbonate ratio (X_{carb}), the reaction rate (RR_{carb}), the fraction of active particles for carbonation reaction (f_{act}) and the CO₂ fraction at the clean gas ($y_{CO_2,out}$) are presented below:

$$E_{carb} = 1 - \frac{y_{CO_2,out}}{y_{CO_2,in}} = \min\left(E_{eq}, (\phi \cdot f_{act} \cdot RR_{carb} \cdot \tau)\right) \quad (\text{Eq. 4})$$

$$E_{eq} = 1 - \frac{y_{CO_2,eq}}{y_{CO_2,in}} = 1 - \frac{4.137 \cdot 10^7}{y_{CO_2,in}} \exp\left(-\frac{20474}{T[K]}\right) \quad (\text{Eq. 5})$$

$$\tau = \frac{N_{Ca,inv}}{F_{CO_2,in}} \quad (\text{Eq. 6})$$

$$f_{act} = 1 - \exp\left(-\frac{t^*}{N_{Ca,inv}/F_{Ca,in}}\right) = 1 - \exp\left(-\frac{X_{max} - X_{calc} - X_{sulf}}{\phi \cdot RR_{carb} N_{Ca,inv}} F_{Ca,in}\right) \quad (\text{Eq. 7})$$

$$RR_{carb} = k_c \cdot X_{max} \cdot \left(\overline{y_{CO_2}} - y_{CO_2,eq}\right) \quad (\text{Eq. 8})$$

where, $\phi=1$, $k_c=0.26 \text{ s}^{-1}$ [93]. The carbonate conversion is calculated via the following expression:

$$X_{carb} = \frac{F_{CO_2,in}}{F_{Ca,in}} E_{carb} + X_{calc} \quad (\text{Eq. 9})$$

The estimation of maximum CO_2 carrying capacity (X_{max}) as a function of the looping ratio (F_R) and the fresh limestone ratio (F_0) was according to the approach developed by Hawthorne et al. [94]. According to this, the maximum fraction of CaO available to form CaCO_3 after the N^{th} cycle for a random particle is estimated from the following empirical equation:

$$X_N = \frac{1}{(1 - X_r)^{-1} + kN} + X_r \quad (\text{Eq. 10})$$

where $k=0.52$ and $X_r=0.0863$ (residual capacity) are constants depending on the type of sorbent. The average total carrying capacity X_{max} is based on the population balance and is given by the following equation:

$$X_{max} = \sum_{N=1}^{\infty} \frac{F_0}{F_R} \left(1 - \frac{F_0}{F_R}\right)^{N-1} \cdot X_N \quad (\text{Eq. 11})$$

Figure 52 presents the dependence of X_{max} by the variation of the fresh limestone ratio (F_0) and looping ratio (F_R). Increase of fresh limestone enhances the maximum carrying capacity, whilst high looping ratios have the opposite effect.

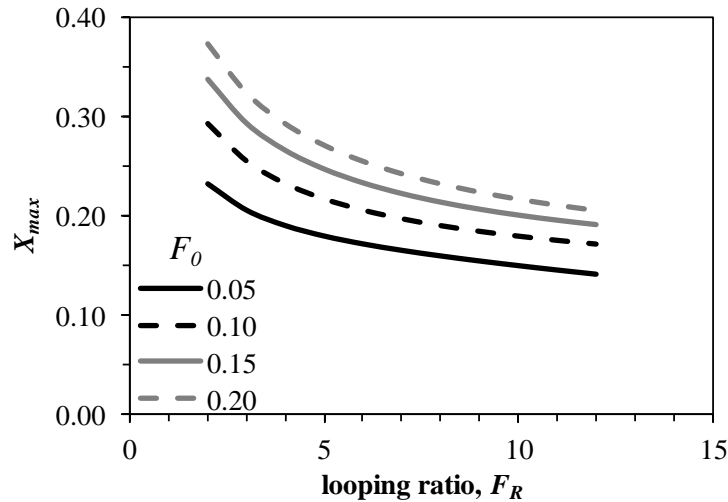


Figure 52. Influence of operating conditions (F_R , F_0) on X_{max}

The algorithm for the calculation of the carbonation reaction rate based on the aforementioned methodology was developed using a FORTRAN house-built code, interconnected with the carbonator model in ASPEN PlusTM (as a continuous stirred reactor). The calciner modeling was based on chemical equilibrium, which predicts total carbonate conversion under the specified conditions in the calciner

reactor. The main operation parameters of the CaL system are summarized in **Table 26**. The characteristics of the basic streams of the CaL base case are shown in **Table 24**.

Table 24. Streams characteristics of CaL unit (for stream numbering see **Figure 50**)

stream	m	T	p	molar composition (%)								
				H ₂ O	CO ₂	N ₂	O ₂	Ar	CaO	CaCO ₃	CaSO ₄	SiO ₂
	(kg/s)	(°C)	(bar)									
1	346.1	164.0	1	7.0	14.6	74.2	3.3	0.9	0.0	0.0	0.0	0.0
2	346.1	330.0	1	7.0	14.6	74.2	3.3	0.9	0.0	0.0	0.0	0.0
3	280.5	649.9	1	8.0	2.0	85.2	3.8	1.0	0.0	0.0	0.0	0.0
4	280.5	90.0	1	8.0	2.0	85.2	3.8	1.0	0.0	0.0	0.0	0.0
5	672.6	899.5	1	0.0	0.0	0.0	0.0	0.0	99.3	0.0	0.6	0.1
6	738.2	700.0	1	0.0	0.0	0.0	0.0	0.0	86.7	12.6	0.6	0.1
7	257.9	763.0	1	15.8	78.7	1.1	2.7	1.6	0.0	0.0	0.0	0.0
8	10.1	898.5	1	0.0	0.0	0.0	0.0	0.0	99.2	0.0	0.6	0.2
9	26.6	25.0	1	coal analysis – see Table 22								
10	16.4	25.1	1	0.0	0.0	0.0	0.0	0.0	0.0	91.9	0.0	8.1
11	246.6	15.0	1	1.0	0.0	77.3	20.7	0.9	0.0	0.0	0.0	0.0
12	58.7	29.6	1	1.5	95.0	3.5	0.0	0.0	0.0	0.0	0.0	0.0
13	104.9	260.3	1	15.8	78.7	1.1	2.7	1.6	0.0	0.0	0.0	0.0
14	143.5	28.0	1	2.8	91.0	1.3	3.2	1.9	0.0	0.0	0.0	0.0
15	256.1	600.1	260	100	0.0	0.0	0.0	0.0	0.0	0.0	0.0	0.0
16	177.1	600.0	38	100	0.0	0.0	0.0	0.0	0.0	0.0	0.0	0.0

3.2.3 Oxyfuel

Pure oxygen production is performed based on a cryogenic method applied in the ASU. The separation of oxygen from air is based on the different dew point of oxygen and nitrogen, preferably at high pressures. The split of these two compounds is accomplished in two distillation columns, one high and one low pressure. The outlet stream from the latter are in low temperature and are used as the cooling medium for air refrigeration in a heat exchanger. The process parameters specification are adjusted in order to achieve 95% pure oxygen stream and >99% purity in the nitrogen one.

Table 25. Streams characteristics of ASU for the oxyfuel case (for stream numbering see **Figure 51**)

stream	m	T	p	molar composition (%)			
				H ₂ O	N ₂	O ₂	Ar
	(kg/s)	(°C)	(bar)				
1	278.7	15.0	1.0	1.0	77.3	20.7	0.9
2	278.0	28.0	4.7	0.6	77.6	20.8	0.9
3	276.8	20.0	4.5	0.0	78.1	21.0	0.9
4	276.8	-177.2	4.4	0.0	78.1	21.0	0.9
5	191.1	-187.0	1.9	0.0	67.8	30.8	1.4
6	85.7	-189.6	1.9	0.0	100	0.0	0.0
7	65.5	-182.7	1.1	0.0	1.5	95.0	3.5
8	211.3	-189.8	1.9	0.0	98.8	1.0	0.2
9	65.5	15.0	1.3	0.0	1.5	95.0	3.5
10	211.9	9.5	1.9	0.4	98.4	1.0	0.2

Due to the fact that the fuel combustion is performed with oxygen excess, which cannot be easily removed from the rich-CO₂ gas stream - contrary to the water content, which is removed through condensation after cooling - a cryogenic separation unit is required. The process parameters of all the CO₂ capture cases are summarized in **Table 26**. The characteristics of the basic streams of the ASU regarding the oxyfuel case are shown in **Table 25**.

Table 26. CO₂ capture Plant specifications and modelling assumptions

chemical absorption with MEA	
absorber / stripper stages	8 / 4
lean solvent w/w	40 %
lean solvent temperature	40 °C
Make-up MEA	$1.2 \cdot 10^{-4}$ kg/kg _{lean solvent}
specific heat at reboiler	3.58 MJ _{th} /kg _{CO2}
Calcium Looping process	
carbonation / calcination Temperature	650 / 900 °C
looping ratio, F_R	8.2 (mol/mol)
make-up ratio, F_0	0.05 (mol/mol)
maximum sorbents conversion, X_{max}	0.1624
solids inventory at the carbonator	415000 kg
pressure drop in the carbonator	150 mbar
carbonator reactor volume	4685 m ³
BMH – solids temperature outlet	700 °C
specific oxygen production	220 kWh/ton O ₂
O ₂ concentration in rich-O ₂ stream	95.0%
O ₂ concentration in oxidizing medium	40.0%
oxygen concentration at the calciner outlet	6% v/v
O₂/CO₂ cycle	
O ₂ concentration in rich-O ₂ stream	95.0%
O ₂ concentration in oxidizing medium	30.0%
specific power consumption in ASU	220 kWh/tnO ₂
pressure ratio at ASU compressor	4.8

3.2.4 CO₂ purification and compression

Even though the gas stream that is produced in the oxy-fired reactor (combustor or calciner) is in high CO₂ concentration, it is not allowed to be transferred and stored unless gas purification takes place. The problem of O₂ tracking in the rich-CO₂ stream is observed for any oxy-fired case, regardless of the process under investigation. From experimental and numerical studies on both Pulverized Coal (PC) [49, 95] and Circulating Fluidized Bed (CFB) [96-99] oxy-fired boilers, the specified oxygen to fuel equivalence ratio (λ) is specified between 1.1-1.2 and the corresponding O₂ concentration at the flue gas exit is around to 1.5% or even higher. On the contrary, very few experimental studies on oxy-calcination have been performed using coal so far and the reported oxygen excess at the exit of the reactor is reported to be more than 5% to ensure high fuel combustion efficiencies [100, 101]. Hence, like in oxy-fuel cases [102-104] the implementation of CO₂ purification unit for the removal of oxygen and other inert gases is essential for the CaL technology, too. Primarily for H&S (explosion avoidance), technical reasons (mainly corrosion), [26-28] and increase in storage capacity[29] the limitations for condensable and non-condensable components are rather strict, making the gas treatment before compression compulsory.

For the case of CO₂ stream derived from the oxy-calcliner, according to the limitations shown in **Table 27**, H₂O and O₂ are the species that require intensive removal in order to meet the abovementioned specifications. Inert gases (Ar, N₂) are present in the CO₂ stream but their concentration is under 4%. Regarding the NO_x, there is not a justified conclusion about the impact of calcination reaction on the rate of their formation in the oxy-calcliner. However, the NO_x emissions are expected to be low and around 100 ppm [49, 105]. Similarly for the SO_x production, there is not clear view. In this study it is assumed that S originating from the fuel totally reacts with CaO sorbents forming CaSO₄.

Table 27. Indicative CO₂ stream specifications for transportation, EOR and geological storage (adopted by [27])

component	transportation	EOR	geological storage
CO ₂	>95%	>95%	>90%
H ₂ O	<50 ppmv	<50 ppmv	<500 ppmv
H ₂ S	<10-200 ppmv	<50 ppmv	<1.5%
O ₂	<10 ppmv	<10 ppmv	<4%
Ar	<4%	<4%	<4%
N ₂	<4%	<4%	<4%
H ₂	<4%	<4%	<4%
CO	0.2%	<4%	<4%
CH ₄	<5%	<4%	<4%
NO _x	<100 ppmv	<50 ppmv	<200 ppmv
SO _x	<100 ppmv	<50 ppmv	<200 ppmv

The specified excess air in the calciner plays the most important role on the concentration of the non-condensable components in the rich-CO₂ stream. The water content depends on the moisture and hydrogen content of the fuel used in the calciner. **Figure 53** shows the gas species concentration in the CO₂ stream in comparison with the corresponding limitations for the application of the pure CO₂ in Enhanced Oil Recovery (EOR) processes [26, 27]. According to **Figure 53**, the nitrogen and argon concentration are below the threshold, however extensive removal for water and oxygen is required, regardless of the oxygen ratio. Additionally, current combustion technologies in fluidized bed boilers can insure high combustion efficiency rates with low excess oxygen ranging from 1.05 to 1.20 [105]. As it is illustrated in **Figure 53**, an oxygen removal unit is inevitable.

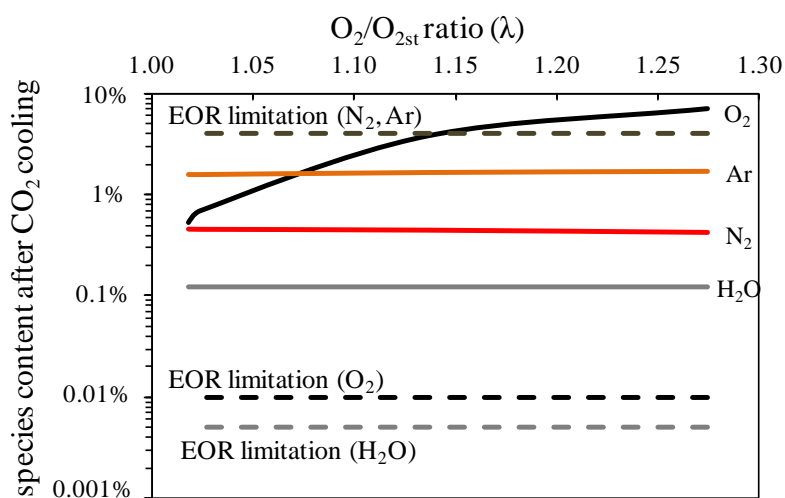


Figure 53. Effect of excess air on gas species content in the CO₂ stream after gas cooling and comparison with the specified limitations

The process flow diagram of the Purification and Compression Unit (PCU) is depicted in **Figure 54**. The O_2/CO_2 separation is based on the Joule-Thomson effect, like in the ASU operation: At first, rich- CO_2 stream is compressed up to 10.5 bar through a three-stage compression train with inter-cooling. Then, it enters the absorber for water removal. The solvent used is triethylene-glycol (TEG) in 99.95% wt. at 40°C. The rich-solvent is throttled at 1.3 bar and heated up to 195°C for the solvent regeneration in a stripper. This heat is obtained from the lean solvent that is cooled and pumped before re-entering the absorber. The reboiler heat at the stripper is taken from the rich- CO_2 stream (see **Figure 54**).

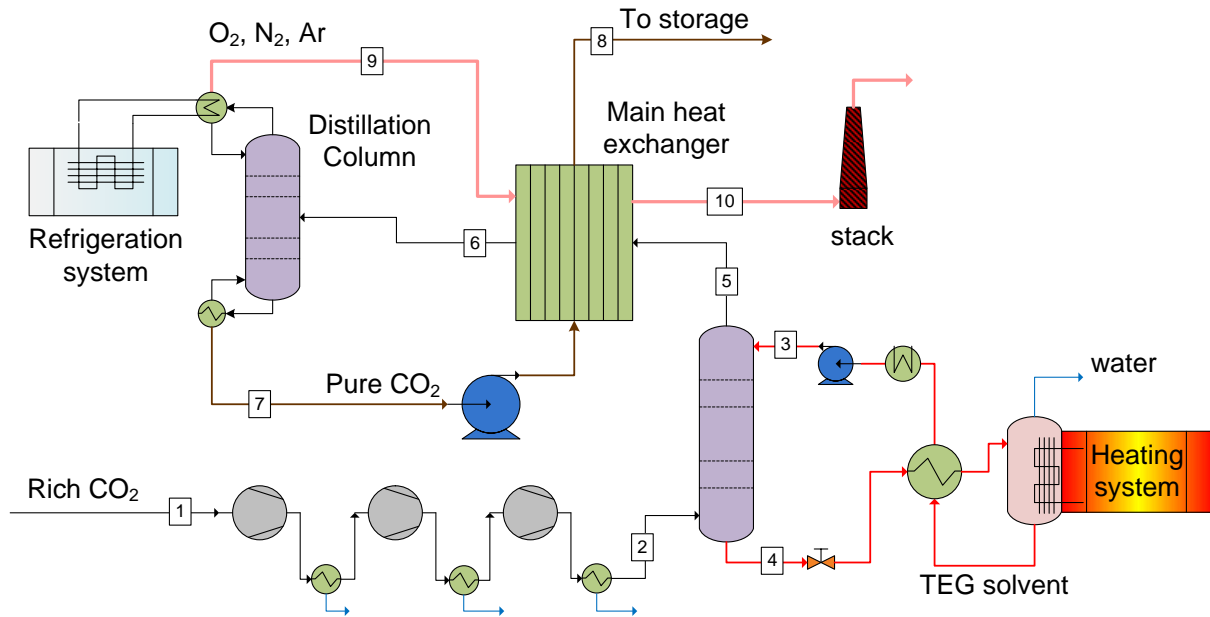


Figure 54. Process flowsheet of the Purification and Compression unit consisting of H_2O and non-condensable gas removal

Table 28a. Streams characteristics of PCU for the CaL case (for stream numbering see Figure 54)

stream	m (kg/s)	T (°C)	p (bar)	vapor fraction	molar composition (%)					
					H_2O	CO_2	N_2	O_2	Ar	TEG
1	161.8	300.0	1.01	1	15.8	76.2	0.4	6.1	1.5	0.0
2	150.1	5.0	10.5	1	0.1	90.4	0.5	7.2	1.8	0.0
3	50.6	40.0	15.0	0	0.4	0.0	0.0	0.0	0.0	99.6
4	53.8	12.6	10.3	0	0.7	17.7	0.0	0.1	0.0	81.5
5	146.8	40.5	10.3	1	$2 \cdot 10^{-2}$	90.2	0.5	7.4	1.9	0.0
6	146.8	-42.1	10.3	0.90	$2 \cdot 10^{-2}$	90.2	0.5	7.4	1.9	0.0
7	128.9	-41.2	9.5	0	$3 \cdot 10^{-2}$	100	0.0	$1 \cdot 10^{-3}$	$8 \cdot 10^{-5}$	0.0
8	128.9	15.0	110	0	$3 \cdot 10^{-2}$	100	0.0	$1 \cdot 10^{-3}$	$8 \cdot 10^{-5}$	0.0
9	17.9	-69.5	9.5	1	0.0	31.6	3.4	51.8	13.1	0.0
10	17.9	15.0	9.5	1	0.0	31.6	3.4	51.8	13.1	0.0

Table 28b. Streams characteristics of PCU for the oxyfuel case (for stream numbering see Figure 54)

stream	m (kg/s)	T (°C)	p (bar)	vapor fraction	molar composition (%)					
					H ₂ O	CO ₂	N ₂	O ₂	Ar	TEG
1	78.2	28.0	1.013	1	2.7	87.2	1.6	5.6	2.8	0.0
2	77.3	5.0	10.5	1	0.1	89.7	1.6	5.8	2.9	0.0
3	32.4	40.0	15	0	0.4	0.0	0.0	0.0	0.0	99.6
4	34.2	18.7	10.3	0	0.6	15.6	0.0	0.1	0.0	83.7
5	75.5	40.0	10.3	1	2·10 ⁻²	89.5	1.6	5.9	3.0	0.0
6	75.5	-42.4	10.3	0.91	2·10 ⁻²	89.5	1.6	5.9	3.0	0.0
7	62.4	-41.2	9.5	0	3·10 ⁻²	100	0.0	1·10 ⁻³	1·10 ⁻⁴	0.0
8	62.4	15.0	110	0	3·10 ⁻²	100	0.0	1·10 ⁻³	1·10 ⁻⁴	0.0
9	13.2	-61.3	9.5	1	5·10 ⁻⁸	46.0	8.4	30.3	15.3	0.0
10	13.2	15.0	9.5	1	5·10 ⁻⁸	46.0	8.4	30.3	15.3	0.0

Table 29. Process parameters for the PCU

Compression train	
pressure outlet	10.5 bar
intercooling stages	1.8, 3.4 and 5.5 bar
isentropic efficiency	75%
Dewatering Unit	
solvent	triethylene-glycol (99.95% wt.)
solvent loading	17.1 kmol TEG/kmol H ₂ O removed
number of stages of the absorber / stripper	6 / 3
regeneration temperature of the solvent	295
specific heat of regeneration	237.6 kJ/t TEG
Cryogenic Unit for light gases (mainly O ₂) removal	
hot stream temperature after the Heat Exchanger	-42.1 °C
number of stages of the distillation column	20
COP of the Refrigeration System	1.06
pure CO ₂ final pressure	110 bar

The CO₂ purification through the removal of the light gases (mainly O₂) is accomplished cryogenically, in a distillation column, taking advantage from the different boiling point of CO₂ from the other species. The cooling loads for the proper operation of the cryogenic system are obtained by an external Refrigeration System. The main parameters for the PCU are summarized in **Table 29**.

3.3 Exergy analysis – Methodology

For the gaseous/liquid material streams, the total exergy amount E_m (kW) is defined as the sum of the physical ε_{ph} and chemical ε_{ch} (kJ/kmol) part:

$$E_m = N \cdot (\varepsilon_{ph} + \varepsilon_{ch}) \quad (\text{Eq. 12})$$

where N is the molar flow in kmol/s. The physical and chemical exergy are defined:

$$\begin{aligned}\varepsilon_{ph} &= (h - h_o) - T_o (s - s_o) \\ \varepsilon_{ch, gas} &= \sum x_i \varepsilon_{o,i} + RT_o \sum x_i \ln x_i\end{aligned}\quad (\text{Eq. 13})$$

The specific chemical exergy $\varepsilon_{o,i}$ and the molecular weight of the components that are taken into consideration for the exergy analysis of the three capture technologies are presented in **Table 30**.

Table 30. Chemical exergy and the molecular weight of various components

component	$\varepsilon_{o,i}$ (kJ/mol)	MW (kg/kmol)
H ₂ O (l)	0.88	18.02
H ₂ O (g)	9.47	18.02
CO ₂	19.61	44.01
N ₂	0.72	28.02
O ₂	3.97	32.00
Ar	11.69	39.95
CaO	110.20	56.08
CaCO ₃	1.00	100.09
CaSO ₄	8.20	136.14
SiO ₂	1.90	60.09
MEA	1534	61.08

For the calculation of the fuel chemical exergy (the corresponding physical exergy is assumed equal to zero), the following equation is adopted based on the Lower Heating Value and the Ultimate (elemental) analysis [106]:

$$E_{ch,f} = \dot{m}_f LHV_f \left(1.0437 + 0.1896 \frac{\gamma_H}{\gamma_C} + 0.0617 \frac{\gamma_O}{\gamma_C} + 0.0428 \frac{\gamma_N}{\gamma_C} \right) \quad (\text{Eq. 14})$$

To calculate the chemical exergy of MEA in liquid phase, the group contribution method was adopted [107]. According to this method, when the chemical constitution of the substance is known, the contribution of simple chemical groups in chemical exergy can be considered. Monoethanolamine (MEA) with known molecular formula (C₂H₇NO) has the following group constituents with the corresponding chemical exergy: -CH₂- (651.46 kJ/mol), -OH- (-51.34 kJ/mol) and -NH₂ (284.34 kJ/mol). Hence, the MEA chemical exergy was calculated at 1534 kJ/mol. This approach can also be found in similar studies in the literature [83, 108]. In order to calculate the exergy losses I_{total} in each process, the exergy balance around the CO₂ separation and compression unit is required.

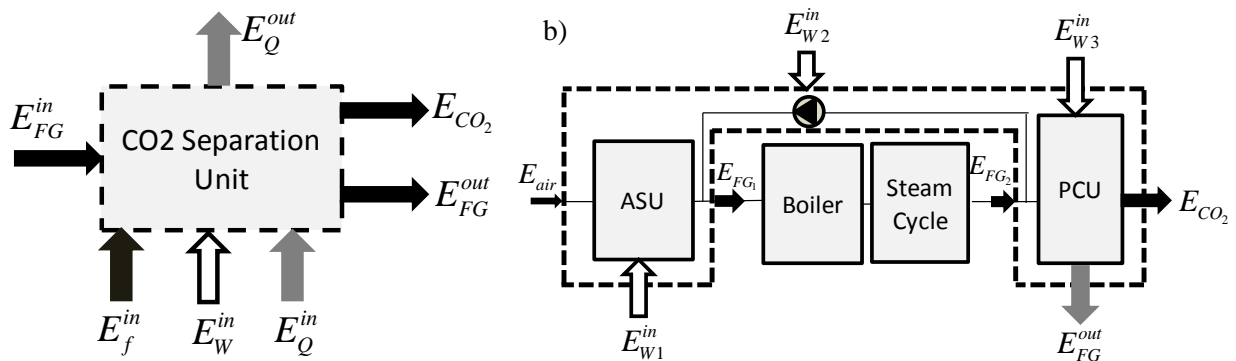


Figure 55. Exergy balance around the CO₂ capture unit for a) the post-combustion techniques and b) the oxyfuel techniques

The exergy balance at each CO₂ capture process according to the exergy streams shown in **Figure 55** is summarized in the following equation.

$$E_{FG}^{in} + E_{air}^{in} + E_f^{in} + E_W^{in} + E_Q^{in} = E_{FG}^{out} + E_{CO_2}^{out} + E_Q^{out} + I_{total} \quad (\text{Eq. 15})$$

The main goal of this study is to identify the amount of exergy needed and destroyed for CO₂ capture in an existing coal fired power plant. For the post combustion options (amine scrubbing and calcium looping), the required intervention is the installation of the capture plant before the stack of flue gases and the exergy balance that should be calculated is shown in **Figure 55a**. In the oxy-fuel case, the exergy balance is defined somehow differently. The operation of this capture mode requires the installation of the ASU, the PCU and the flue gas recirculation (**Figure 55b**). Hence, the exergy balance of the oxyfuel case for the abovementioned purpose includes these main processes.

Four indexes are introduced for the exergetic comparison of the capture technologies. The first one is the specific required exergy, $b_{ex_required}$:

$$b_{ex_required} = \frac{E_f^{in} + E_W^{in} + E_Q^{in}}{CO_2 \text{ captured}} \text{ [kJ/kg]} \quad \text{Eq. (16)}$$

This index expresses the amount of exergy in kJ that is required either as heat, power or chemical exergy, in order 1kg CO₂ to be separated from flue gas and captured. The amount of exergy in kJ that is spent by the form of heat, power or chemical exergy in order to capture 1 kg CO₂ is represented by the following index:

$$b_{ex_spent} = \frac{I_{total}}{CO_2 \text{ captured}} \text{ [kJ/kg]} \quad \text{Eq. (17)}$$

The total irreversibility I_{total} is calculated from the equation (**Eq. 15**). Additionally, the exergy utilization efficiency (η_{ex_ut}) is introduced and expresses the fraction of the total exergy than enters the capture and purification and compression unit that is not destroyed in the form of irreversibilities:

$$\eta_{ex_ut} = 1 - \frac{I_{total}}{E_{FG}^{in} + E_{air}^{in} + E_f^{in} + E_W^{in} + E_Q^{in}} \quad \text{Eq. (18)}$$

Finally, the overall exergy efficiency of the whole plant (η_{ex_tot}) is defined as the net power generation ($P_{tot,net}$) to the fuel exergy input (E_{fuel}):

$$\eta_{ex_tot} = \frac{P_{tot,net}}{E_{fuel}} \cdot 100\% \quad \text{Eq. (19)}$$

3.4 Results and Discussion

Simulations at the reference power plant reveal an overall thermal net efficiency equal to 39.2% on a LHV basis. The specific fuel consumption is calculated at 360.6 kg/MWh_e, whereas the specific CO₂ emissions are 851.7 kg/MWh_e. The overall exergy efficiency was calculated equal to 36.9%. A detailed description of exergy flows in this case is seen in **Figure 56**. Half of the fuel exergy is dissipated in the boiler, during the conversion of chemical energy to heat, for the steam generation and reheating process. The hot flue gases contain 3.2% of the total fuel exergy at the boiler exit, after the air preheater (LUVU). Around 10.4% of exergy is dissipated at the rest steam cycle (expansion, condensation and preheating).

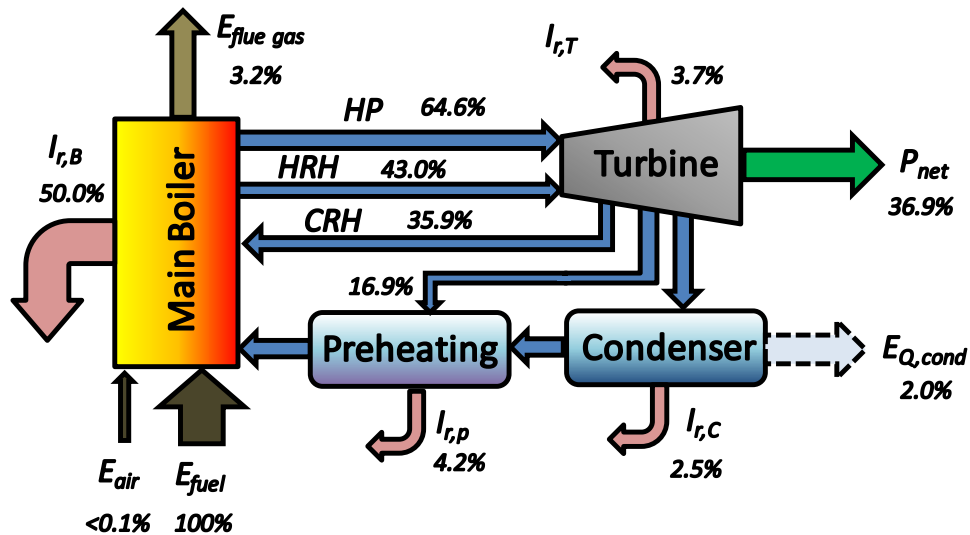


Figure 56. Exergy flow at the reference power plant without CO₂ capture

Figure 57 shows the exergy flow at the amine scrubbing case. A considerable amount of exergy in the form of low enthalpy heat is required for the solvent regeneration while 11% of the produced power electricity is used for the power requirements of the compression step (totally 8.8% of the exergy input is lost in MEA capture and CO₂ compression processes). Due to the reduced amount of steam expanded in the turbine, the exergy losses in Turbine and Condenser & Preheater are lower, in comparison to the reference case (Figure 56).

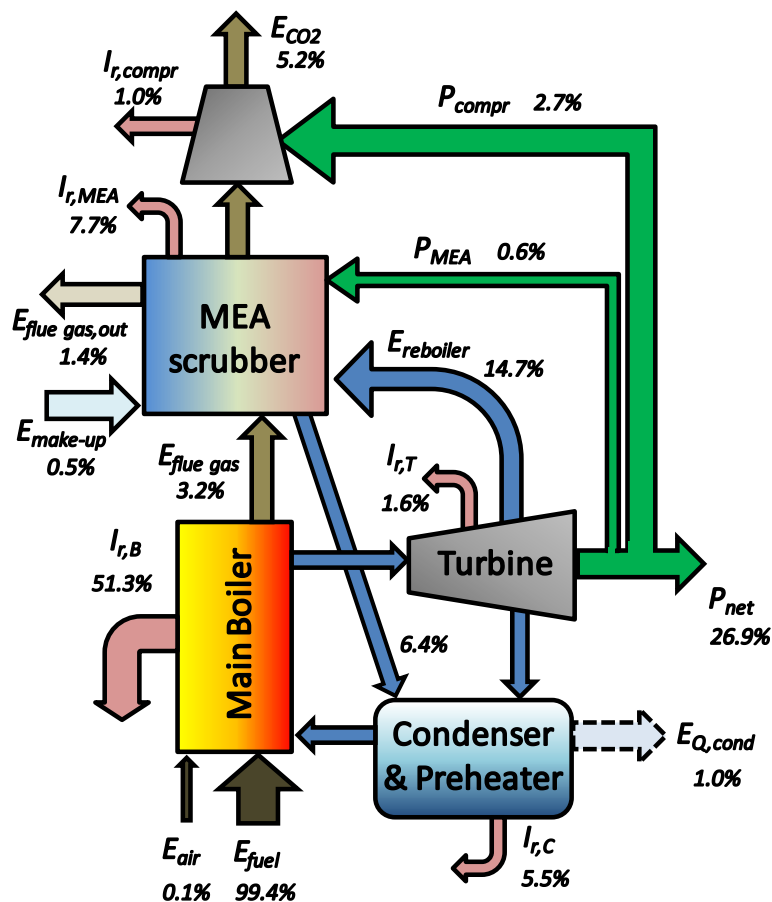


Figure 57. Exergy flow at the MEA post-combustion capture case

A more detailed analysis on the exergy dissipation in the amine capture unit follows in **Table 31**. Solvent regeneration has the highest exergy losses in the capture process followed by the CO₂ separation in the absorber. The exergy losses in the CO₂ purification process that takes place during CO₂ cooling are 77.4 kJ/kgCO₂ or 0.9% of I_{tot} . It is underlined that this parameter refers only to the cooling of gaseous stream after the stripper, where the rich-CO₂ stream is cooled and water is removed through condensation. Only 1.0% of the total irreversibilities are observed during the increase of pure CO₂ pressure using the typical compression train with inter-stage coolers. If the CO₂ compression was conducted in one stage up to 60 bar without intercooling, the irreversibilities in this unit would be 33.2% higher. It should be pointed out that E_{fuel} is not the sole exergy that enters the plant: 0.08% of the total exergy input comes from the combustion air and 0.49% from the amine solvent make-up. Nevertheless, the discussion about the exergy dissipation is made on the basis of the E_{fuel} in all the examined cases.

Table 31. Irreversibility (% total exergy losses in the plant and in kJ per kg CO₂ separated) by unit sections for the CO₂ capture and compression plant for amine scrubbing case (40 wt. % MEA, 10 wt. % CO₂)

process	I/I_{tot} (%)	I (kJ/kgCO ₂)
Flue Gas blower	0.1%	13.1
Flue Gas cooling	0.1%	6.8
CO ₂ absorption	3.8%	315.9
solvent regeneration	7.1%	595.2
rich/lean heat exchanger	0.3%	21.2
CO ₂ cooling	0.9%	77.4

The influence of the solvent composition on the plant performance in terms of energetic and exergetic performance is also investigated in this study. As it is seen in **Table 32**, high MEA/CO₂ ratio in the lean solvent promotes the effectiveness of the process (compare the 1st and 3rd cases with the 2nd and 4th ones). This is illustrated by the less reboiler duty and the exergy losses in the amine unit in the first case, where the MEA/CO₂ mass ratio is equal to 4. Additionally, low MEA concentrations leads to less efficient capture system, comparing the 1st with the 3rd case.

Table 32. Effect of lean solvent composition on the plant and capture unit performance

a/a	lean solvent composition (% wt.)	reboiler duty, Q_{reb} (kJ/kgCO ₂)	lean solvent exergy, E_{solv} (kJ/kgCO ₂)	Amine Unit exergy losses, I_{MEA} (kJ/kgCO ₂)	net energy efficiency (%)	net exergy efficiency (%)
1	40 wt. % MEA, 10 wt. % CO ₂	3583	316646	971.6	28.8	26.1
2	30 wt. % MEA, 10 wt. % CO ₂	5977	880093	1692.5	24.8	23.3
3	30 wt. % MEA, 7.5 wt. % CO ₂	4002	254560	1037.9	27.9	25.6
4	25 wt. % MEA, 8 wt. % CO ₂	5217	517391	1460.8	25.6	24.0

In the CaL case, the exergy flow is quite different (**Figure 58**).

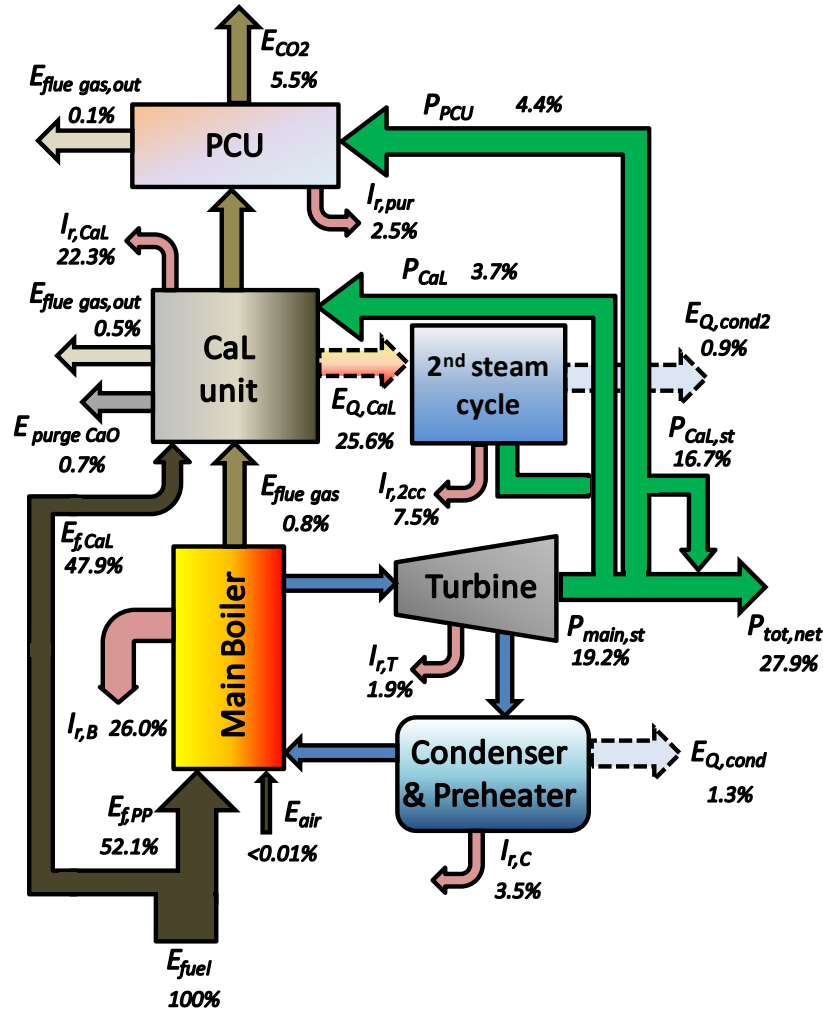


Figure 58. Exergy flow at the CaL post-combustion capture case

The required exergy for the operation of the calcium sorbents cycle is inserted in the unit mainly in the form of chemical (fuel) and work (ASU and boosters) power. Almost half (47.9%) of the initial fuel input is used for the carbonate sorbents regeneration in the calciner, while more than half of which is transformed into useful heat for steam generation in the secondary steam cycle (25.6%). The amount of fuel (E_{fuel}) compared to the case of MEA is about 92% more because of the requirement to cover the calciner heat duty demands. Moreover, 22.2% of the total gross power produced is consumed for the proper operation of the compressors in the ASU, the CaL Unit and the PCU. It is observed that Ca looping process induces significantly more exergy losses (22.3% of total E_{fuel}) than MEA (7.7%) due to the fact that fuel combustion, which occurs in the calciner, has by definition a large amount of irreversibility. More specifically, from the total 22.3% of exergy losses in the CaL, 2.1% comes from the carbonation process where CO_2 capture takes place, 2.7% in the ASU, and 16.3% in the calciner unit. Less significant losses in the CaL unit are the losses in the solid heat exchangers (0.5% of total E_{fuel}).

Furthermore, the exergy of the spent (purge) CaO solids that exit the loop due to the introduction of fresh material represents the 0.7% of the total exergy losses of the system. Keeping in mind that the utilization of heat from the cooling of this solid stream is not technically feasible, the exergy regain from such heat recovery is not considered. On the other hand, 25.6% of the total exergy is recovered as high enthalpy heat at the CaL unit and is utilized for steam generation and subsequently for power production.

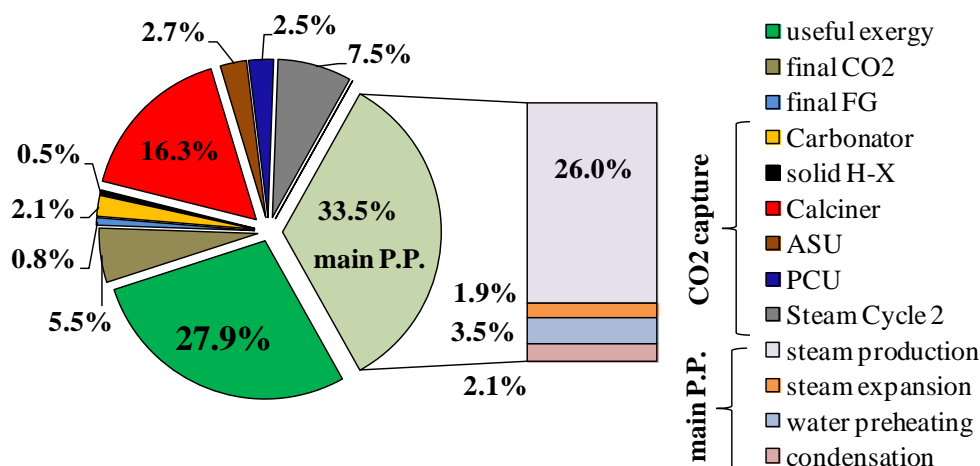


Figure 59. Percentage contribution of the exergy losses (irreversibility) in each process in CaL case

Figure 59 presents the percentage contribution of the dissipated exergy in all the process steps of the CaL case. The calcination process accounts for most of the losses mainly due to the simultaneous combustion in the reactor for direct heating. It is noteworthy that 5.5% of the exergy is remained at the “final product CO₂” –apart from electricity- that can be sent for storage or further application (i.e. EOR, CO₂ fixation, etc.). The exergy content of the make-up limestone is significantly low compared to the exergy input ($5 \times 10^{-3} \%$) and thus it is neglected.

A sensitivity analysis is performed in CaL case in order to investigate the effect of some parameters on exergy losses reduction. Among the most important operational parameters are the quality of the supplementary fuel that is used in the calciner and the limestone make-up ratio, F_0 . A sensitivity analysis (**Table 33**) reveals that the overall plant operates more effectively –in energetic and exergetic point of view- when the minimum make-up ratio for certain CO₂ capture in the carbonator is required. Nevertheless, the similar values of the $\eta_{ex,ut}$ of the two cases with different F_0 reveal that the CaL performance is not considerably affected by the make-up ratio. Low F_0 value induces lower X_{max} and thus, high looping ratio is needed for certain CO₂ capture. Hence, the $b_{ex,required}$ is high, the $b_{ex,spent}$ and $\eta_{ex,ut}$ indexes are higher. The way that the two cases have different overall plant efficiency (energy and exergy) is explained below.

Table 33. Sensitivity analysis on the CaL process case (90% overall capture efficiency)

case	“base case”	“high F_0 case”	“high S” case
fresh limestone ratio, F_0 (mol/mol)	0.05	0.10	0.20
fuel used in the calciner	coal	coal	petcoke
CaO looping ratio, F_R (mol/mol)	8.20	4.47	16.78
maximum capacity, X_{max} (mol/mol)	0.1624	0.2254	0.1887
SPECCA (MJ/kgCO ₂)	4.05	4.49	4.68
$b_{ex,required}$ (kJ/kgCO ₂)	6892.8	6241.1	10461.2
$b_{ex,spent}$ (kJ/kgCO ₂)	3073.5	2815.3	4909.6
$\eta_{ex,ut}$ (%)	56.7%	56.4%	54.0%
$\eta_{ex,tot}$ (%)	27.9%	27.3%	27.4%

The comparison of the results derived from the “base case” with the “high S” case highlight that the properties of the supplementary fuel plays important role in the CaL performance. Specifically, for the petcoke case, where S is 4.65%, high make-up ratios are required in order to achieve 90% capture efficiency in the carbonator [109]. Taking into account that the effective removal of sulfur from the loop

cannot be realized with mechanical or other separation methods, calcium sulfate (CaSO_4) tends to accumulate in the solid loop. Having increased X_{sulf} values at the loop, the X_{max} deteriorates, leading to higher F_R , inevitably. This fact has negative impact on both the plant efficiency and the CaL performance, suggesting low sulfur fuels for the sorbent regeneration in the calciner. Furthermore, high S content in the spent lime makes it inappropriate for utilization in cement manufacture by substitution of raw materials for clinker production [109].

In an ideal case, when high the sorbents have high X_{max} value and thus low looping ratio is required, the $b_{\text{ex,required}}$ and the $b_{\text{ex,spent}}$ do not drop up to the corresponding levels of MEA and oxy-combustion cases. These high rates are mainly attributed to the increased temperature levels at which both carbonation and calcination take place. Taking into account that 650/900 °C have been proven as the most suitable temperatures for carbonation and calcination respectively, little modifications can be done in this certain process configuration for exergy losses reduction by changing the operational temperatures. Another option should be the adoption of new advanced sorbents with higher carrying capacity and ability of CO_2 absorption/desorption at lower temperatures. For instance, regarding the improvement of X_{max} parameter, sorbent treatment methods such as steam regeneration and thermal pre-treatment have been investigated and proposed [110]. However, even though this would be a thermodynamically appropriate suggestion, several issues in terms of technical and economic feasibility of the technology should be addressed.

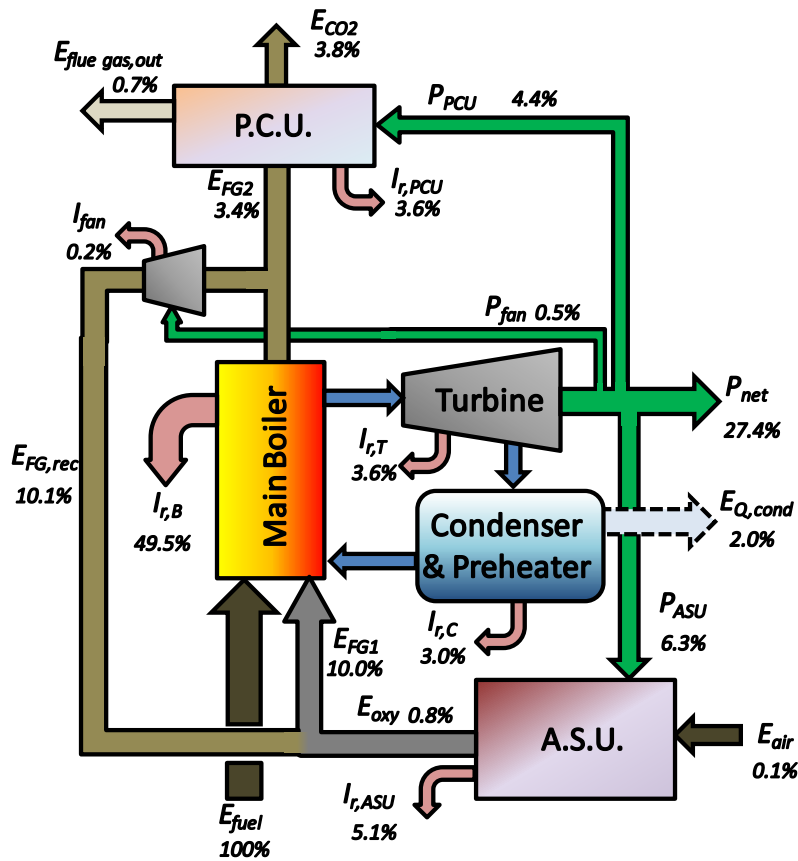


Figure 60. Exergy flow at the oxy-combustion capture case

In the oxy-combustion case (see Figure 60), considerable power fractions are consumed for the compressors required for the CO_2 capture, i.e. the cryogenic air separation in the ASU, the cryogenic CO_2 purification and compression. Most of power is consumed at the ASU for pure oxygen production. During the flue gas cooling water is removed in liquid form, the exergy of which is negligible (0.01%). Although

the pressure ratio in the Purification and Compression Unit is higher, the energy requirements for rich CO₂ stream compression are lower than in the ASU case. Although 70% of the flue gas recirculates in order to reduce O₂ concentration at the oxidizing medium from 95% after the ASU to 30% before the boiler, the energy duties for fan operation are 0.6% of the total *LHV* input and 0.2% the corresponding exergy losses. In other words, if the boiler can afford pure oxygen without mixing with flue gases as the oxidizing medium, this would have a marginal positive impact of 0.6% in terms of exergy efficiency. . It is noteworthy that flue gases at the boiler exit (FG2) contain 3.4% of the fuel exergy whereas the corresponding value of flue gases at the boiler inlet (FG1, oxidizing medium) is 10.0%. This relative high value in the oxidizing medium is attributed to fact that CO₂ has higher specific chemical exergy ($\varepsilon_{0,i}$) than N₂ (see **Table 30**), which is the corresponding inert gas in the reference case, where air is used for combustion.

It is seen from the exergy analysis in all the examined cases that at least 8.7% of the exergy is destroyed for CO₂ purification and compression is inevitable for any capture scheme that is implemented on atmospheric thermal plants: Part of this exergy is in the form of power for CO₂ compression and purification, whereas another part is the total exergy of the final streams (final CO₂ stream and clean flue gases) that cannot be further utilized. **Table 34** shows the basic energy and exergy balance results of the three investigated CO₂ capture schemes. It should be underlined that the purpose of this study is not to present the best option for CO₂ capture after the comparison of the optimized cases of them but to indicate the potential of each technology improvements with respect to exergy losses reduction. Based on the ASPEN PlusTM simulations, it is concluded that CaL technology is slightly the most efficient option for carbon capture from existing coal power plant. The overall capture efficiency is defined as:

$$\text{carbon capture efficiency (\%)} = \frac{\text{kg of C captured}}{\text{kg of total C in the plant}} \quad \text{Eq. (20)}$$

For the better evaluation of the energy systems in terms of energy efficiency, SPECCA (Specific Energy Consumption for CO₂ Avoided) is introduced. This index expresses the additional fuel heat energy in MJ that is required to avoid 1 kg of CO₂. The SPECCA values indicate that the CaL case uses the least fuel energy for CO₂ capture:

$$\text{SPECCA} = 3600 \cdot \frac{1/\eta - 1/\eta_{ref}}{E_{ref} - E} \left(\text{MJ}_{JHV} / \text{kg}_{CO_2} \right) \quad \text{Eq. (21)}$$

Table 34. Energy and exergy balance

	Reference without capture	amine scrubbing	CaL	Oxy-fuel
overall capture efficiency (%)	-	90.0	90.0	90.0
net electric efficiency (%)	39.2	28.8	29.4	29.1
energy penalty (%)	-	-10.4	-9.8	-10.1
exergy penalty (%)	-	-10.0	-9.0	-9.5
specific CO ₂ emissions (kg _{CO2} /MWh)	851.7	116.2	119.8	115.3
SPECCA index (MJ _{LHV} /kg _{CO2})	-	4.54	4.05	4.36
$b_{ex, required}$ (kJ/kg _{CO2})	-	2366.6	6892.8	1345.1
$b_{ex, spent}$ (kJ/kg _{CO2})	-	1113.5	3073.5	1565.7
$\eta_{ex, ut}$ (%)	-	59.8	56.7	48.6
$\eta_{ex, tot}$ (%)	36.9	26.9	27.9	27.4

The specific exergy requirements for the proper operation of the Calcium looping process are by far the highest ones. Around 86% of this is chemical exergy in the form of fuel in the calciner and the rest 14% accounts for power consumed in the ASU's compressors and the refrigeration system operation. Similarly, the total specific irreversibility in this technology is almost three times higher than the others. Besides, the exergy utilization, which is illustrated from the $\eta_{ex,ut}$ index, is lower than the corresponding value in the post-combustion case (59.8%) but higher than the corresponding of the oxy-combustion case (48.6%). Hence, the rest of exergy that is not used or lost for CO₂ capture at the carbonation-calcination cycle can be effectively recovered for further power production. This heat is high enthalpy valued and is transformed in a Rankine cycle into work power with high efficiency.

Table 35 explains why the CaL technology has the highest efficiency despite it has the highest specific exergy losses in capture unit. **Table 35** groups the irreversibilities for each technology, depending on the process type. The I_i are expressed as kJ per CO₂ captured. Ca looping reactors for CO₂ capture and release have by far higher specific losses. On the other hand, the contribution of ASU is 2 times less in the CaL case, in comparison to the oxyfuel case. Additionally, due to the nature of the CaL process, almost half of the fuel input is not combusted in the boiler, where the specific exergy losses are higher. The fact that the autothermal oxy-calciner is more efficient by exergy point of view than the boiler (air or oxy fired) is the main reason why the total plant has the lowest irreversibilities when the CaL technology is employed for CO₂ capture. The CO₂ compression with inter-stage cooling has lower exergy losses than the CO₂ purification based on the cryogenic separation and its compression in liquid form. The difference between the CaL and oxy-fuel technology is attributed to the fact that the O₂ concentration in the rich-CO₂ gas is higher in the latter case.

Table 35. Contribution of each process to the total exergy penalty for each capture technology

I_i (kJ/kgCO ₂) for each process	capture technology		
	amine scrubbing	CaL	Oxyfuel
main power plant	7424.0	3151.0	7110.0
CO ₂ separation from flue gas	315.9	235.4	179.1
sorbent/solvent regeneration	661.3	1977.8	-
CO ₂ purification & compression	135.2	303.5	453.6
O ₂ production in ASU	-	322.5	647.8
total irreversibilities	8523.8	7711.3	8236.9

3.5 Conclusions

In this chapter, the energetic and exergetic comparison of three competitive technologies for CO₂ capture at an existing coal fired power plant was presented. Calcium Looping (CaL) process was proven the best option for CO₂ capture among the others, in terms of overall energy and exergy efficiency. In other words, it seems that the answer to the question raised in the introduction is high quality heat through fuel combustion. In the MEA case, 7.7% of the exergy input was calculated to be lost in the capture unit and 1.0% during CO₂ compression. High MEA/CO₂ ratios and high MEA concentrations in the lean solvent promote the effectiveness of the process. Although a considerable amount of exergy (22.3% of total E_{fuel}) is lost in the CaL unit, the carbonation/calcination process is the most energetically and exergetically efficient with the lowest exergy penalty (-9.0%). From the sensitivity analysis in the CaL case, it was concluded that low F_0 ratios have little beneficial contribution to the exergy losses reduction. Sulfur content in the supplementary fuel has negative impact on both the plant efficiency and the CaL performance. Only lowering the operating temperatures at the two reactors would induce to the technology

lower irreversibilities. This is not technically possible presently in the present being, according to the existing Ca sorbents. In the oxy-combustion case, the ASU is the main unit where most of the exergy losses ($647.8 \text{ kJ/kg}_{\text{CO}_2}$) for CO_2 capture are observed. A potential development of O_2 selective membranes or other technology with minimum or zero power consumptions would help to save more than 9% of the total exergy input.

4. Techno-economic aspects for methanol production systems based on CO₂ hydrogenation

4.1 Introduction

The control of the Greenhouse Gas (GHG) emissions is one of the most challenging environmental issues that should be faced in the 21st century. The increase of CO₂ concentration from 280 ppm at the beginning of the Industrial Revolution to 370 ppm up-to-date is proved that a great part of it comes from anthropogenic factors and has disastrous effects on the global weather, the climate, and the average temperature [6, 44]. According to IEA Blue Map Scenario for reducing CO₂ emissions, the Carbon Capture and Storage (CCS) is considered among the major measurements that should be addressed in large scale worldwide [31, 44]. However, several obstacles such as high capital and operational cost, the several social and technical issues that should be addressed for the CO₂ safe storage in conjunction to the low carbon pricing policy, hinder the adoption of this option for CO₂ footprint mitigation.

A more feasible option to mitigate CO₂ emissions is to transform it into valuable compounds, like fuel organic and inorganic chemicals, namely as ‘the CO₂ capture and utilization (CCU) concept’. The majority of CO₂ use in industry is for urea production, which accounts for more than half of the global annual usage [30]. Alternatively, CO₂ is utilized also physically in various applications such as refrigerant medium, in fire extinguishers and in the petroleum and NG industry for Enhanced Oil Recovery (EOR) and Enhanced Gas Recovery (EGR), respectively [31, 32]. Even though CO₂ is a thermodynamically and kinetically stable molecule, various ways have been developed for CO₂ reduction, mainly based on the fact that the central carbon of the CO₂ molecule is electrophilic and can be easily attacked by nucleophiles [33]. The methods for CO₂ transformation can be sorted in six categories [30, 34]: chemical reduction (i.e. Boudouard), electrochemical reduction [35], photochemical reduction (i.e. artificial photosynthesis), thermochemical conversion (i.e. dry reforming and hydrogenation), biological (i.e. photosynthesis, anaerobic conversion)[36] and inorganic transformation. This study focuses on synthesis of methanol from CO₂ through catalytic hydrogenation. Hence, the main feedstock apart from CO₂ that is required is pure hydrogen.

Since the H₂/CO₂ ratio for CO₂ hydrogenation towards hydrocarbons synthesis should be four (4) for methane and three (3) for methanol synthesis, the required amounts of hydrogen are very large. There are three routes for non-fossil derived hydrogen production: water electrolysis, biomass conversion and solar conversion [33, 111]. Electrolysis is based on the water splitting into H₂ and O₂, the energy for this reaction is given in the form of electricity derived from Renewable Energy Source (RES) i.e. photovoltaic panels (PV), wind farms hydropower and geothermal plants. The second category consists of thermochemical (i.e. gasification, pyrolysis) or biochemical conversion of biomass, the intermediate products of which process are properly converted into rich H₂ fuel. Through solar conversion, either via thermolysis or photolysis, heat or photons are respectively used for hydrogen synthesis [112, 113]. Biomass gasification and separation of H₂ from the produced product gas is not commercially available at large scales while thermolysis and photolysis processes are just beginning to be explored for their potential use by research projects in the EU [114, 115]. In the present study, the hydrogen is considered to be derived from electrolysis, since this is the most mature and well-established technology even in industrial scale [116] and also it is not relied on carbon-contained source like biomass.

Several electricity sources have been proposed in the literature, including cheap grid electricity [117], surplus electricity from power plants [118, 119], renewable electricity [120, 121], etc. In the case of RES one of the major issues that should be addressed is the stochastic nature of the renewable power production and the extreme load fluctuations that require a highly flexible system for an efficient operation. Besides, the CCU unit cannot operate with maintain high performances under these variable throughputs conditions as it incorporates, according to the existing technology, since components such unit operations that have lower efficiencies at part load, such as compressors, steam production cycle and the CO₂ capture system itself. A technical solution to this issue is the intermediate storage of the produced H₂ in order to secure the constant hydrogen delivery to the CCU unit with the negative effect of the increase in the investment cost.

The scope of this study is the investigation of various aspects for the valorization of CO₂ towards the production of liquid fuel (methanol), in large scale applications. These aspects are related to the power source for the hydrogen production through electrolysis (grid electricity, renewable energy source), the CO₂ capture scheme (selection of the proper capture technique) and the input gas (H₂ and CO₂) transportation options (pipeline, truck or trailer). The assessment is made in terms of minimization of methanol production cost by performing the economic evaluation, determining the boundary conditions and the next steps that should be done so that the proposed concept can be profitable.

4.2 Process description

The concept for liquid fuel (methanol) synthesis through CO₂ hydrogenation is shown in **Figure 61**. The pure CO₂ stream is fossil derived and comes from separation and purification from combustion gases of a power plant or other intensive carbon emission industry (e.g. cement plant, steel industry).

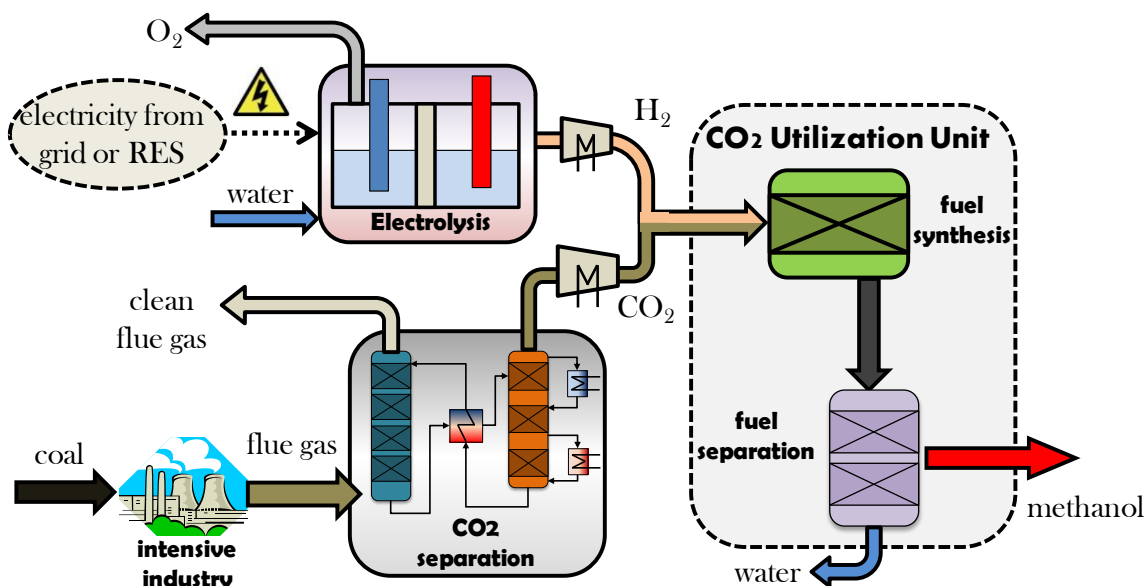


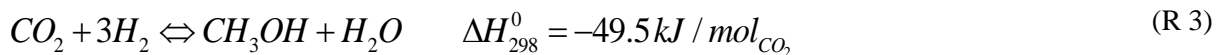
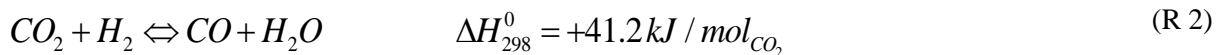
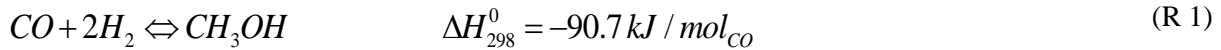
Figure 61. Conceptual design of the proposed methanol production from CO₂

The concept that is presented in this study is not based on a total utilization of the produced CO₂ from fossil fuel combustion (power plant or intensive industry). In case that the total amount of the CO₂ captured from the flue gases of a typical 300 MW_e coal fired power plant undergoes to hydrogenation, the required power duty for water electrolysis is estimated at 1.77GW_e which is technically infeasible and economically unprofitable.

Several studies dedicated to the techno-economic investigation of this concept can be found in the literature [117, 119, 122-127]. Among the major conclusions that are extracted from them is that the hydrogen production cost is most significant factor that affects the economics of this methanol-from-CO₂ concept.

4.3 Methanol synthesis from CO₂

Concerning the CO₂ fixation step towards the production of valuable chemicals, the catalytic hydrogenation for methanol is examined. Methanol is formed from CO₂ hydrogenation under three-phase conditions [128]:



The adopted methodology for the methanol synthesis is kinetically based and the equations for the estimation of the kinetic rates of the above mentioned reactions are based on [128].

The process flow diagram of a typical methanol synthesis unit from CO₂ is shown in **Figure 62**. The unit consists of the methanol synthesis, gas separation and product purification. The inlet gas is heated up to a temperature level so that the reactor operates adiabatically under the specified temperature. The required heat for crude methanol heating and separation is obtained from the gas outlet cooling. In order to achieve high purity levels in the methanol product (>99.2%), the liquid stream after the first flash separator is throttled down to some kPa below the atmospheric pressure, following the same approach with the Rectisol™ process. A small portion (1%) of the recycling gas is extracted as purge gas in order to avoid by-products accumulation such as hydrocarbons, inert gas etc.

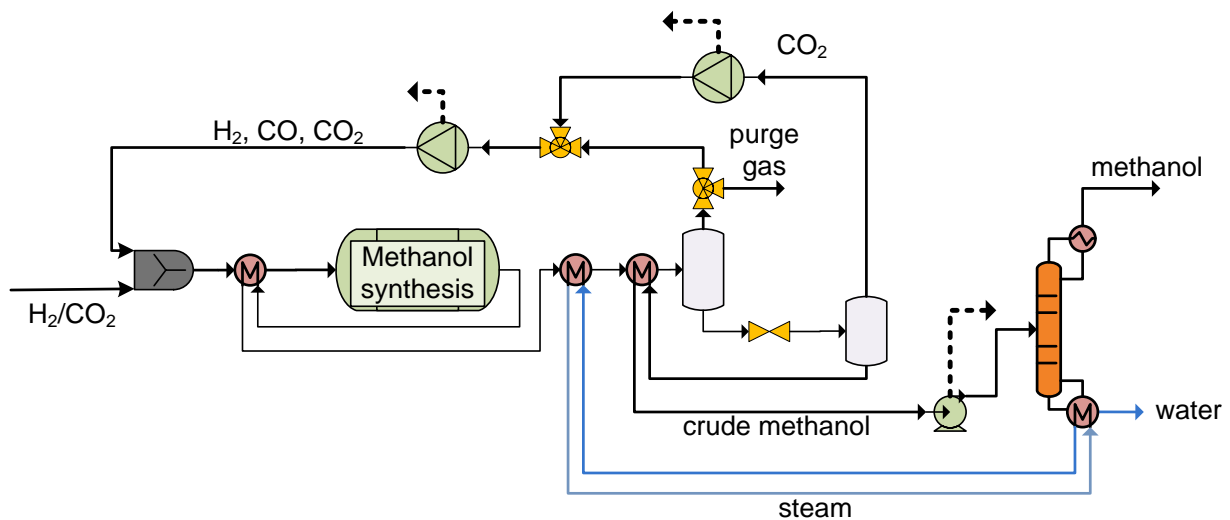


Figure 62. Process flowsheet of the CO₂ to MeOH concept

Table 36 presents the main specifications of the process modeling design of the methanol production unit. The methanol plant capacity is determined by the hydrogen capacity in each case examined. This process model is served for the calculation of the scaling parameters that are required for the total equipment cost estimation (see **Table 37**). The process modeling is necessary at this stage in order to make the energy balance calculations and to determine parameters such as the rejected heat duty and the power

consumptions in the compressors and the blowers, which are not easily calculated otherwise. For simplicity reasons these operating parameters are constant regardless of the plant size. The methodology for the development of the process design for the methanol synthesis and purification is inspired mainly from [122]. The reactor modeling is based on the kinetic model developed in [128].

Table 36: Key Process specifications for the conventional MeOH synthesis from CO₂

H ₂ /CO ₂ ratio	3.0
inlet gas preheating temperature	168 °C
MeOH reactor temperature/pressure	250°C/65bar
flash separator #1 temperature/pressure	30.0°C/64.5 bar
flash separator #2 temperature/pressure	24.5°C/0.2 bar
crude methanol preheating	85°C
distillation column, number of stages	60
distillation column, inlet pressure	1.3bar
final product composition (% v/v)	99.3%CH ₃ OH, 0.1%H ₂ O, 0.6%CO ₂

Regarding the economic evaluation, the methodology for the calculation of the equipment cost of each component in the CUU and the assumptions for Capex and Opex estimation are following.

The Total Capital Investment (TCI) estimation is performed according to Peters & Timmerhaus methodology [129] and is based on a series of intermediate cost types, the first of which is the Total Purchased Equipment cost (TPEC) for each case. The equipment cost of each component is estimated based on similar equipment costs from the literature according to the following equation:

$$C_i = C_0 \cdot \left(\frac{S_i}{S_0} \right)^f \quad (\text{Eq. 22})$$

Table 37. Equipment cost estimation for the methanol production unit

Equipment List	Scaling parameter	Reference erected cost, C_o (M€)	Reference size S_o	Scale factor f	installation factor n	Ref year	Ref.
methanol reactor	feed gas (kg/h)	7.69	87.5	0.6	2.1	2006	[126]
heat exchanger	heat duty (MW _{th})	39.26	355	1	1.49	2007	[130]
distillation unit	MeOH flow rate (t/h)	16.58	6.75	0.7	1.52	2006	[126]
compressor	power (MW _e)	12.08	10	0.67	1.72	2006	[131]
cooling system	Q rejected (MW _{th})	49.600	470	0.67	1.49	2007	[132]
booster	power (MW _e)	14.770	47.61	0.67	2.47	2011	[133, 134]
wastewater treatment	kg/hr water input	20.353	393100	1.05	2.47	2010	[135]
flash tank	gas feed (kg/s)	installation cost (in M€) = $2.47 \cdot 983.2 \cdot 10^{-6} \cdot (\text{feed gas in kg/s})^{0.8}$				2000	[136]

Furthermore, having the Total Purchased Equipment Cost (TPEC) estimated, the next step is the Total Installed Cost (TIC) calculation. This is accomplished by multiplying each equipment cost with an installation factor n , specified for each component (see **Table 37**). The parameters for the operational cost calculation such as O&M and insurance are considered as a portion of the Fixed Capital Investment (FCI).

The assumptions that are made for the economic evaluation of the methanol plant are summarized in **Table 38**.

Table 38. Economic assumptions

exchange rate	0.755 €/€
discount rate	10%
recovery period	25 years
Capital Recovery Factor	0.11
year basis	2012
Operating and Maintenance (O&M)	5% FCI
Insurance	2% FCI

4.4 Pure CO₂ from coal derived flue gas

The Carbon Capture and Storage concept has attracted a lot of attention the past decade. A great development has been gained on each of the main CO₂ separation techniques, even though no concept has reached to a commercial level yet. Among the several CO₂ caption options, amine scrubbing (MEA) and oxyfuel technology are considered the most competitive and ready to apply technologies for the first generation of applications in industrial scale. The post-combustion chemical absorption technique with amine scrubbing is the most mature technology with higher Technology Readiness Level and has already been tested and implemented in large scale applications [137]. Therefore, the amine scrubbing is selected as the CO₂ capture technology for this study.

The cost for CO₂ capture with the amine scrubbing post-combustion technology is set at 43.8 €/tn_{CO₂}[24]. The delivered CO₂ stream bares the same specification with storage specification: oxygen should absent from the pure CO₂ stream to avoid ignition after reaction with the H₂ in the reactor. The specific heat demands for amine regeneration are 4.17 MJ_{th}/kg_{CO₂} and the electric power consumption 0.021 kWh/kg_{CO₂} [138].

The second parameter that composes the cost of CO₂ is the transportation cost. The location of the CO₂ capture unit with respect to the CO₂ utilization unit influences the cost for CO₂ delivery. In case that the two units are in the same place, the cost of CO₂ equals to the cost for CO₂ separation (CO₂ delivery cost is zero). Otherwise, a specific cost 9.23 €/tn for CO₂ transportation is assumed based on [139] when a pipeline network is applied. From the same study [139], it is concluded that the specific cost for CO₂ storage in liquid form 4.46 to 13.86 €/tn CO₂. Hence, in the present study, the total cost for CO₂ transport and constant when the CO₂ is conducted far away from the CO₂ capture plant is set 20 €/tn following the assumption made by Barbato et al. in [127].

4.5 Hydrogen production

In water electrolysis, water is split into O₂ and H₂ by means of electrical power. This option for H₂ production has the lowest efficiency (35-42%) and the highest H₂ production cost (for large scale 20-25 \$/GJ_{H₂}) among the other technological options. However, currently it is considered as the best option among the other RES based technologies for sustainable and clean hydrogen production in large scale [140, 141]. There are three main electrolysis options (alkaline electrolysis, polymer electrolyte membranes and high-temperature electrolysis). Alkaline (KOH) electrolysis is the best available since it is quite mature up to large scale H₂ production [142]. Moreover, it has been tested successfully for discontinuous operation, and its load can be altered easily by adapting the current density [121]. Therefore, KOH electrolysis is selected as the most suitable technique for the examined concept in this study.

The water electrolysis process is not modeled in detail in this study. For the analysis, the basic aspects that affect the techno-economic evaluation are only taken into account: It is assumed that highly pure ($>99.9\%$) H_2 and O_2 gaseous streams are produced in the electrolyzer, the operating conditions of which are $80\text{ }^\circ\text{C}/30\text{ bar}$, which are typical for large scale commercial alkaline electrolyzers [121, 143, 144]. The specific power consumption is set 4.34 kWh/Nm^3 based on [121]. Assuming that the rest of power demands in the electrolysis unit is 10% of the consumptions for water electrolysis and hydrogen production [143], the overall electrical consumptions are $55.56\text{ kWh/kg}_{H_2}$.

Figure 63 shows a schematic depiction of a H_2 production plant with water electrolysis. Apart from the electrolyzer which is the main component, the balance-of-plant also consists of several items: the rectifier, the control system, the water purification, and the water and alkaline tank. The process water is purified in the demineralizer before it enters the electrolyzer removing minerals and other impurities that may hurt the electrolyzer. As the electrolysis type that is selected is alkaline, a KOH tank is required in order to feed the electrolyzer with the electrolyte solution. The rectifier is served for the transformation of the alternating current (AC) to direct current (DC). The cooling water system is used for both the maintenance of the electrolysis temperature at a constant level and the cooling of the product gas streams before compression and storage. Furthermore, the produced oxygen that is in high purity is considered as product and therefore, the oxygen liquefaction and storage is taken into account.

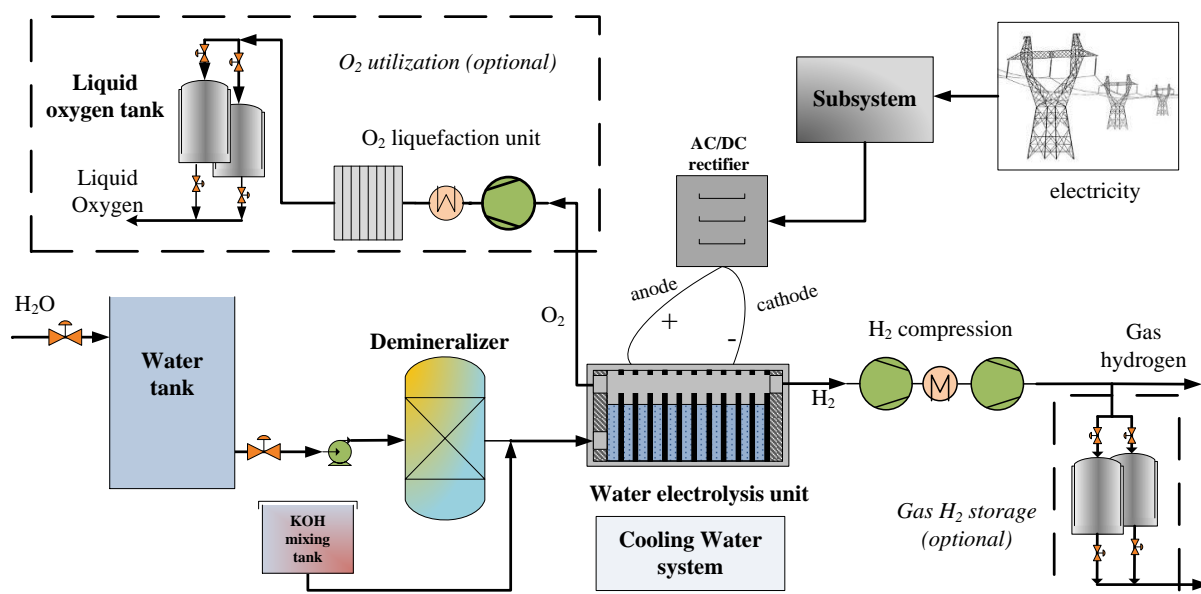


Figure 63. Conceptual process diagram of the water electrolysis plant

Provided that water electrolysis is an energy demanding process, special effort is paid in this study in order to determine the scheme with the lowest specific hydrogen production cost. **Table 39** summarizes the key parameters of a selected number of studies based on hydrogen production. The definition of the index capacity factor (C_f) is the fraction of the actual operation to the designed operation (i.e. if the electrolyzer operates at full load at 24/7 mode).

Table 39 illustrates the considerable discrepancy in the estimated hydrogen production costs even amongst studies with similar parameters. Furthermore special note has to be made to avoid wrong assumptions such as the use of renewable electricity from a “network” of wind farms in 24/7 mode or the use of a dam for hydrogen production with a capacity factor more than 50-60%. In the following paragraphs, the aspects of some of the cases studies are discussed and evaluated in respect to the source of power for H_2 production.

Table 39. Key parameters production costs of various hydrogen production plants

Power source	Electricity Price (€/kWh)	Capacity Factor, C_f (%)	H ₂ Plant Capacity	H ₂ production cost (€/kg)	Year	Reference
grid	0.004-0.047	98.6%	22 MWe	2.29-3.75	1985	[145]
grid	0.0543	90.0%	150,000 kg/day	4.113	2002	[144]
grid	0.0560	100.0%	3.3 MWe	3.270	2011	[121]
grid	0.0427	85.0%	1,500 kg/day	4.695	2005	[146]
grid	0.0427	88.0%	1,500 kg/day	3.989	2009	[143]
grid	0.0233	70.0%	0.14 MWe	1.994	1996	[147]
grid	0.0475	97.0%	1,500 kg/day	3.989	2013	[148]
grid	0.0483	86.0%	50,000 kg/day	3.973	2013	[148]
RES	0.016	91.3%	100, 500 MWe	1.590	2003	[117]
wind	0.0427	97.0%	>50,000 kg/day	3.492	2005	[146]
wind	0.0349	98.0%	>50,000 kg/day	2.328	2009	[143]
wind	0.0520	44.0%	50,000 kg/day	2.910	2011	[149]
solar PV	0.047-0.064	27.1%	592,000 kg/day	4.291-5.028	2008	[150]
hydropower	0.0104	87.7%	225,000 kg/day	1.558	2013	[127]

a) Large scale electrolyzer with electricity from grid

This first scenario is based on central H₂ production with electricity from the grid feeding an electrolysis process (large scale) with a capacity of 140 MW_e or equivalent to the production of 60.5 t_{H2}/day. Because of the size of the H₂ system, a central hydrogen production plant is considered with high capacity factor (90.0%). However, since the CCU plant is considered to have an 85% availability factor, the overall analysis is made with the latter value. The methodology for the cost estimation of the electrolytic hydrogen production plant is adopted from the Production Case Studies carried out from the Department of Energy H2A Analysis and more specifically from the study on “*Current Central Hydrogen Production from Grid Electrolysis version 3.0*” [151]. According to this, the capital cost of a Central hydrogen production plant with similar design capacity to the case that is currently investigated (67,200 kg/d) was estimated \$69,775,218 or 784.0 €/kg/d (2010 basis).

Table 40 shows the different costs of a water electrolysis hydrogen production depending on the country. It is pointed out that the only varying parameter is the purchased electricity price from the national grid of each country. The architecture of the total Power-to-Fuel scheme plays a very crucial role in the economic feasibility and implementation of the concept. In other words, the location of each major unit operation (H₂ plant, CO₂ capture and Carbon Utilization) is located determines the total cost.

Table 40. Regional difference in the electricity price and its impact on the H₂ economy

	Unit	U.S.A.	E.U.	Japan
Electricity price (industrial 2013)	€/kWh	0.050	0.126	0.099
Electrolyzer Cost	€/kg _{H2}	0.762	0.762	0.762
H ₂ Compression & Storage Cost	€/kg _{H2}	0.043	0.043	0.043
Electricity Cost	€/kg _{H2}	2.804	7.066	5.530
H ₂ production cost	€/kg _{H2}	3.609	7.871	6.334

According to several studies [144, 152-154], the specific cost for hydrogen transport varies with the different scenario and the methodology for handling and transportation. For instance, transporting hydrogen in liquid form has very low cost (0.1-0.2 €/kg) but hydrogen liquefaction is a capital (800 €/kg/day) and energy (10-13 kWh/kg) intensive process [144]. Hence, it is suitable only for very long distance transmissions. On the other hand, the hydrogen handling in gaseous form has a specific capital cost equal to 2000 €/kW_e for compression with corresponding energy consumption 0.5-2 kWh/kg and 1.63€/kg for transport via tube trailers and 0.2-0.6 M€/km via pipeline.

Table 41 presents the most suitable option for various cases of hydrogen transport, depending on size and transmission distance according to the study of Yang and Ogden [153]. It is concluded that for a large scale H₂ plant, the optimal way for H₂ transmission is through pipelines, regardless of the distance. Beyond this, according to the study of Tzimas et al. [152], the concept of centralized system that employs pipeline network for hydrogen delivery is expected to developed in the future.

Table 41. Comparative assessment for the best option for H₂ transport [153]

a/a	size plant		transmission distance		preferable option for H ₂ delivery	transmission cost estimation (€/kg)
	small	big	short	long		
1	X		X		gas tube trailer	0.60
2	X			X	liquid tanker truck	1.36
3		X	X		gas pipeline	0.23
4		X		X	gas pipeline	0.53

For the evaluation of the whole “Power to Fuel” concept and the cost breakdown estimation, the determination of the location of the subsystems each other (CCU general configuration) needs to be defined. **Table 42** presents various schemes with different configuration. The first three schemes are related to the main concept that is discussed in this section. It is concluded that, in terms of feedstock gas cost, hydrogen production scheme is preferable to be near to the unit that is consumed, i.e. the methanol plant. Thus, the first scenario is selected for the economic evaluation of the total concept with the same main assumptions (energy source: grid electricity, electricity price: 0.05 €/kWh). As it is revealed from the methanol plant cost breakdown in **Figure 64**, the hydrogen production has the lion’s share on the methanol production cost. The terms and conditions for the minimization of the electrolyzer and electricity cost in order the technology to be more competitive is not part of this study.

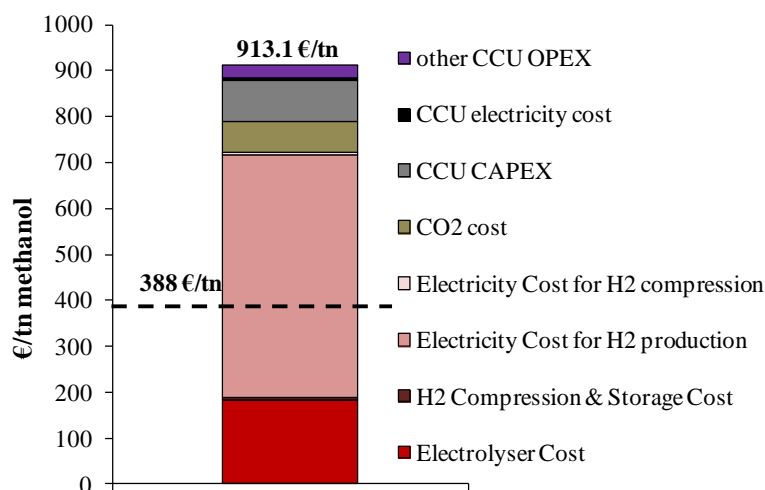


Figure 64. Power to Methanol cost breakdown

In the previous analysis, the market of oxygen is not taken into account. Oxygen is a valuable product that has numerous applications in various sectors such as the iron and steel industry, and the medical sector [155]. Given that oxygen that is produced through electrolysis is in high purity, it has the potential to fulfill the requirements for the implementation in every use (oxidizing agent or medical product). In this case, the compression, cooling and liquefaction of the produced oxygen and the corresponding power consumptions and operational costs are included. The specific power consumption for O₂ liquefaction is set 0.3711 kWh/kg_{O₂}. Because of the high quality in terms of purity, the oxygen selling price is set at 87.4 €/tn, based on [156]. The introduction of the oxygen liquefaction and compression unit causes 14.9% increase in the total capital cost and the corresponding total operational cost drops by 1.3% in the whole Power-to-Methanol system. As a consequence, the methanol production cost drops at 859.2 €/tn (10.1% decrease). It is seen that the oxygen marketing has a beneficial effect on the mitigation methanol production cost and should be taken into consideration.

b) Large scale electrolysis, plant using electricity from thermal power plant

Seeking for low electricity price for hydrogen production, a concept that has been recently emerged is the use of the “Power to Methanol” system as an energy storage option for the stabilization of the electricity system. In other words, in countries where the RES has a great share on the energy mix such in Germany, there is the need for the flexible operation of the thermal power plants, due to the stochastic behavior of the electricity production of the RES and the fluctuations in the energy demand. The conditions and under which the use of excess power can be profitable are examined in this section.

The analysis is carried out based on data provided from the European Energy Exchange regarding the fluctuation of the electricity price in Germany in 2014 (see **Figure 65a**) [157]. According to this, the average electricity price (AEP) for this year is 32.2 €/MWh. The economic evaluation is based on the term “clean dark spread”, (CDS), which is defined as:

$$CDS = AEP - COE \text{ [€/MWh]} \quad (\text{Eq. 23})$$

where the Cost of Electricity (COE) is determined by the sum of the fuel cost, the cost from CO₂ emissions and other costs. For simplicity reasons, several assumptions are made for the accomplishment of the economic evaluation of this case. The first is that the electricity pricing is the same for the whole examined period (see **Figure 65a**) and is not affected by the introduction or not of the power plant to the energy system. The electricity cost and the earnings from its selling to the system are exclusively determined by the (Eq. 23).

The power plant that is used from this analysis is considered as a lignite fired thermal plant with a typical capacity of 300 MWe and a net efficiency of 36%, a typical value for German lignite power plants according to RWE [158]. As a starting point, the fuel cost is assumed as 2.0 €/GJ_{th}, the specific CO₂ emissions 0.971 tn_{CO₂}/MWh, the CO₂ emissions tax 7.2 €/tn_{CO₂} and the other operational costs are 2.0 €/MWh. Based on these assumptions, the COE is calculated at 29.0 €/MWh and hence, the average CDS = 3.3 €/MWh. As it seen in **Figure 65b**, 27% of the year, the electricity production is not profitable to be sold to the energy system. Considering an availability factor of the plant 85% and making the arbitrary assumption that it operates only at full load, the annual incomes from selling the electricity is 7.4 M€.

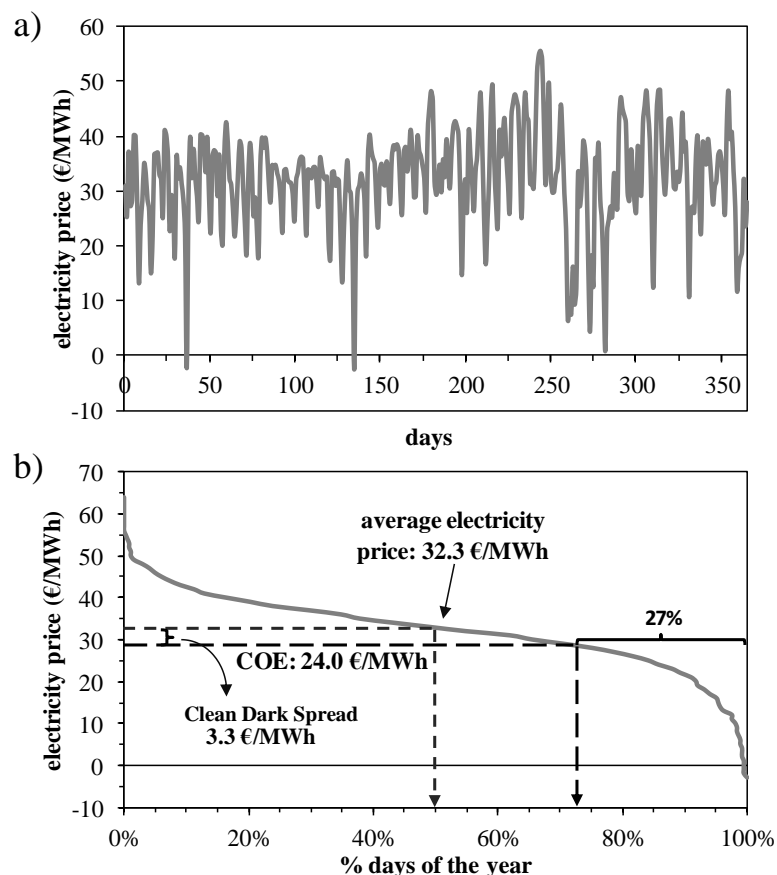


Figure 65. a) average daily electricity price and b) cumulated electricity price in 2014 in Germany

The H_2 plant capacity is the same with the power plant 300 MWe but the specifications for the economic evaluation the same with the previous scenario so that the comparison between the two cases to be made on equal terms. At a first analysis, the H_2 plant operates for 2203 h, when the average COE is higher than the electricity price. Taking also into account the 85% capacity factor of the power plant, the corresponding capacity factor is calculated at 25.2%. The electrolyzer specific capital cost, according to the previous analysis, is 582.92 k€/MW_{th} and the electrolyzer efficiency is 50.0 kWh/kg_{H₂}. Similarly, the methanol unit has the same specific capital and operational cost with the previous case: 42.05€/tn and 38.02 €/tn of methanol, respectively.

The decision for operating or not the “Power-to-Fuel” (PtF) system by the power plant operator is not taken suddenly or unexpectedly but it is programmed from the previous day, when the pricing of the electricity cost is determined by the electricity trading market. In this light and since the power to fuel plant operates in stable load, no storage units for H_2 and CO_2 are required.

The cost breakdown of the base case of this CCU concept that is studied is presented in **Figure 66**. Contrary to the previous case where the electricity is supplied from the grid, the electrolyzer unit capital cost is the most significant factor for the determination of the minimum selling process of the methanol in this case. This is attributed to the lower hours that the PtF system operates and the electricity cost for hydrogen production is a bit lower.

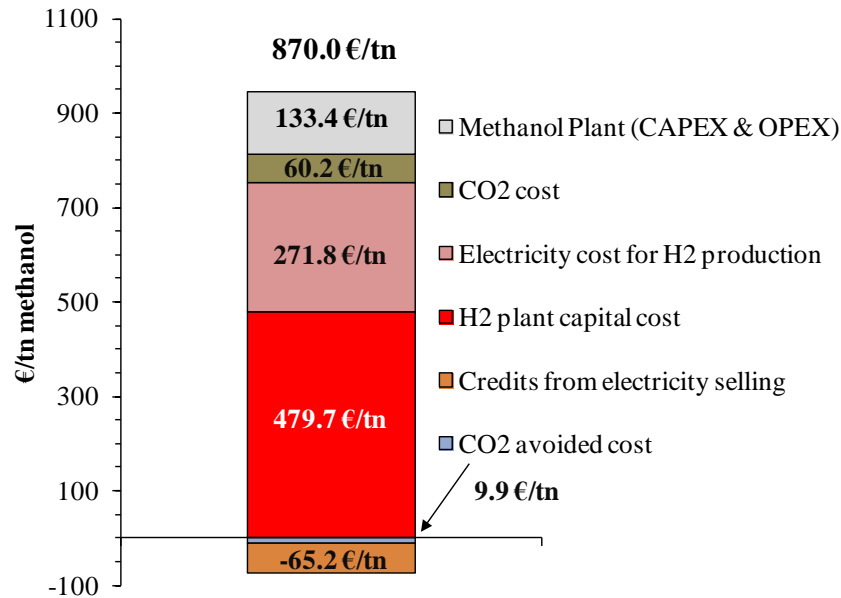


Figure 66. Methanol production cost break down (use excess electricity from lignite power plant)

A sensitivity analysis of the change of several important parameters by $\pm 20\%$ is performed. **Figure 67** presents how the minimum methanol selling price is affected.

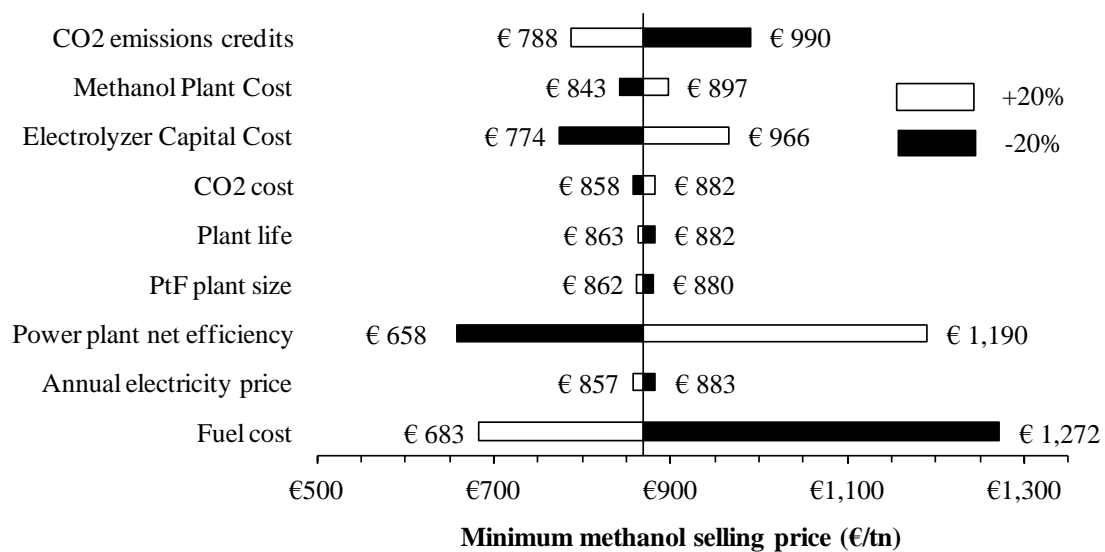


Figure 67. Using Power from Coal plant for Methanol Synthesis - Sensitivity analysis (the white bars are when an increase of 20% of each parameter is considered whereas the black bars for 20% decrease)

It is seen that the fuel cost and power plant performance have the greatest impact on the methanol price. Lower fuel price and power plant net efficiency increase the capacity factor of the PtF plant as the COE increases. Additionally, the reduction on the electrolyzer cost has a considerable effect on the methanol price minimization. Furthermore, the increase in CO₂ tax rate that is expected the next years beneficiates the feasibility of this concept.

It should be pointed out that in each case, only the under investigation parameter was changed, without affecting any other one. In most of these cases, this assumption is reasonable. For instance, changing the

COE by changing the net efficiency or the fuel cost, the annual average electricity price is not expected to be affected in a large country with high national power load like Germany. On the other hand, any change in the CO₂ emission credits will affect the electricity price, but this aspect is not easily determined because several factors related to energy policy and political issues should be taken into account, and therefore this correlation is neglected.

c) Decentralized H₂ production in small scale Electrolysis plants using electricity from grid

In the case of a decentralized H₂ plants with smaller capacity than the corresponding in the previous case (central production), the hydrogen compression, storage and transport parts (C/S/T) should be taken into account. According to the discussion above, for small plant size and relative short distances between the H₂ plants and the central CUU, the most appropriate option for hydrogen handling and transport is the transport of compressed H₂ with gas tube trailers. In the case of providing electricity from grid, thanks to the 100% availability of power, the storage capacity is not large and therefore the installation cost of a H₂ storage unit is not taken into account. The capital cost of the unit was calculated based on the H₂A analysis methodology for small forecourt plants with grid electrolysis in 2010 values.

Table 42. Summary of the several H₂/CO₂ production schemes (energy source: grid electricity, electricity price: 0.05 €/kWh)

case	Hydrogen Plant capacity	CCU configuration ¹	inlet gas production & delivery cost (€/kg _{H₂-CO₂})
1	140 MW _e	H2P-CC-CUU in the same location	3.003
2	140 MW _e	H2P away from CC-CUU	3.337
3	140 MW _e	CC away from H2P-CUU	3.005
4	1 MW _e	H2P away from CC-CUU	3.982
5	9.4 MW _e	H2P away from CC-CUU	4.560

¹ H2P: hydrogen plant, CC: CO₂ capture unit, CUU: CO₂ utilization unit

d) Decentralized H₂ production in small scale Electrolysis plants interconnected with RES (wind farm)

Contrary to the previous scenario, if electricity available is intermittent then a hydrogen buffering system to secure the continuous flow rate to the fuel synthesis plant is required. Hence, the H₂ compression storage and distribution components are also included in the investment cost analysis. In case that the H₂ plant is near to the CUU, the third part (i.e. hydrogen transport) is not taken into account.

For the investigation of this case, data of European Energy Exchange [157] obtained from [146] is used regarding a wind farm in Germany. This data is referred to the fluctuation of electricity price and the corresponding power feed-in per day (see **Figure 68a-b**).

It should be underlined that, on the one hand, the electrolyzer should be highly flexible and have an effective operation at even far from the design point in order to be capable to catch up with the great fluctuations of the power output of the wind plant. On the other hand, the methanation unit is not technically proven that can be operate with flexibility under conditions with great variables in the feed rate, since it consists of several equipment and complex heating & cooling network systems that perform effectively mainly in the design point. Hence, the hydrogen storage is necessary in order to secure the H₂ feeding with constant flow rate.

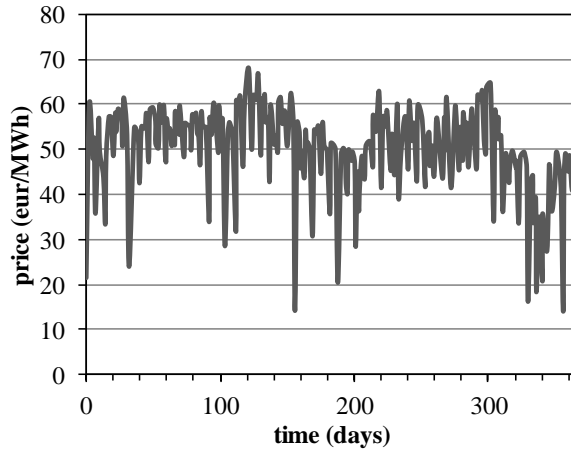


Figure 68a. Electricity price along one year period [146]

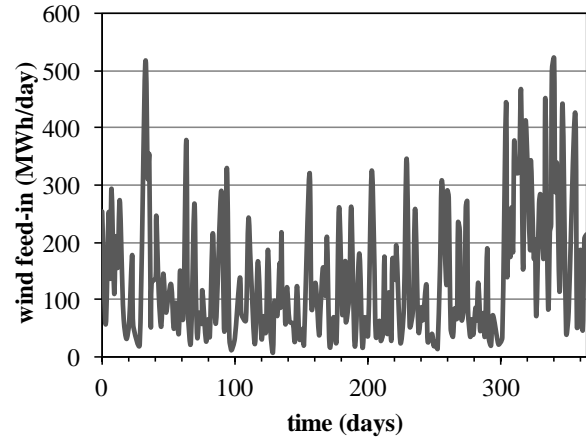


Figure 68b. Hourly wind in-feed along one year period [146]

The demand for a constant hydrogen flow rate to the CO₂ Utilization Unit is the main input for the determination of the hydrogen storage capacity. For each case, the hydrogen output flow rate is the mean value of the annual hydrogen production. On the other hand the tank should be big enough in order to can host all the quantity of the produced hydrogen anytime. The hydrogen production curve is calculated based on the data from only one year presented in **Figure 68a-b**, assuming to be representative for the whole plant life. The specific cost for the H₂ storage is set at 400 €/kg [144].

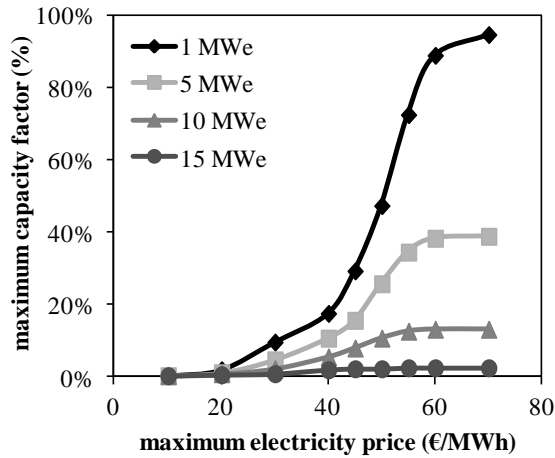


Figure 69a. Dependence of the maximum capacity factor of the electrolyzer on the maximum purchased electricity price

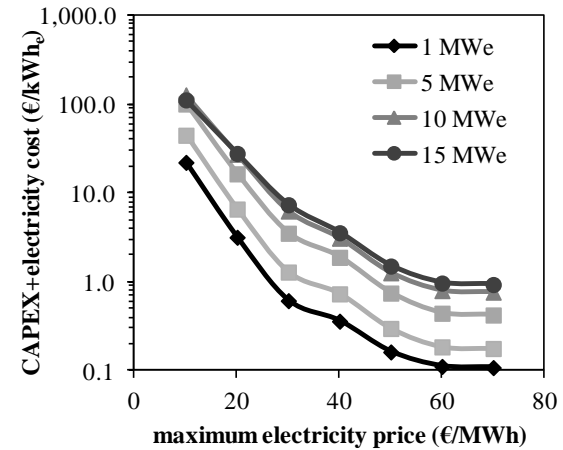


Figure 69b. Dependence of the capital cost and electricity cost with the maximum purchased electricity price

Figure 69a shows how much electrolyzer operation time is required for different plant sizes versus the maximum price allowed for the electricity purchased. It is clear that the option for cheap electricity in this case leads to low hydrogen productivity, a fact that has negative effect on the production cost regardless of the plant size, as it is shown in **Figure 69b**.

Figure 70 summarizes the H₂ production cost breakdown for electrolyzers with different sizes. It is clear that the cost for hydrogen storage plays the most significant role in the hydrogen production cost when the constant hydrogen flow rate is considered as a necessary condition. Moreover, it is proven that the maximization capacity factor of the unit, which is achieved with small size units, is a more important

parameter compared to the maximization of the utilization of the available electricity produced at the RES plant.

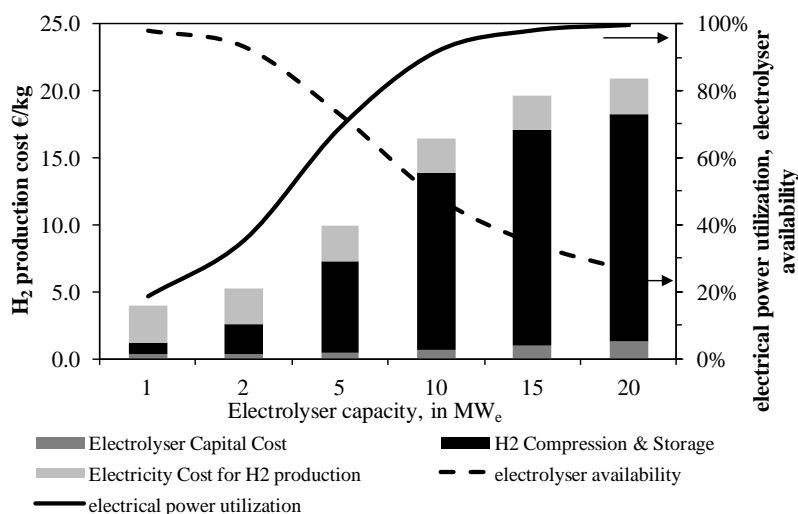


Figure 70. Sensitivity analysis on Electrolysis plant capacity (decentralized H₂ plant using electricity from RES)

4.6 Concluding remarks

Each of the three main parameters for the determination of the H₂ cost (electrolyzer capital cost, electricity cost and storage cost) play a key role in the feasibility of the scheme. When the capacity factor of the hydrogen plant is maximum (supply of grid electricity in large scale application) the minimum methanol cost is determined by the electricity cost. When cheap electricity is used in large scale application but with less operating time, the electrolyzer capital cost is the most important factor. Finally, when RES electricity is used in an autonomous H₂ plant, away from the methanol plant, the dominant factor is the H₂ management in terms of storage issue. The concept of central electrolysis using grid electricity preferably in the same site with the CO₂ capture and utilization units is the most appropriate in terms of H₂ production cost and consequently, the methanol production cost.

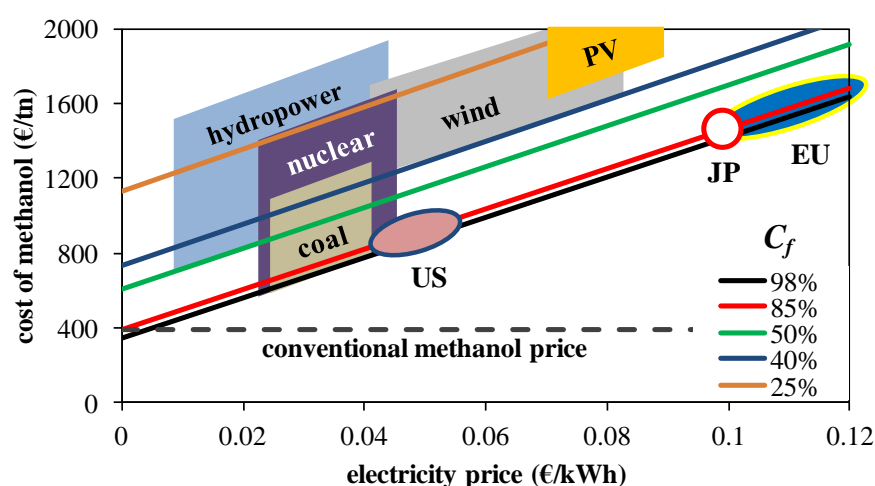


Figure 71. Influence of electricity price and capacity factor (C_f) on the methanol production cost. (US, JP, EU stands for the electricity grid provided in USA, Japan and EU-28, respectively)

Figure 71 illustrates the impact of the electricity price and the capacity factor (C_f) on the feasibility prospects of a Power to Methanol concept. Additionally, based on the typical ranges of cost of electricity and the operating hours for various power sectors [12, 159], the impact of the electricity provider to the hydrogen plant on the methanol production cost is also depicted. The maximization of the plant operation hours is of the most important requirements, since in case of low capacity factors, the methanol production cost becomes extremely high even in the case of low expensive or zero electricity cost. For this reason, concepts based on renewable hydrogen with high electricity cost and low capacity factor are not economically viable and thus are not suggested for the time being. It is concluded that the use of cheap electricity derived from thermal plants (coal or nuclear) under a regular basis has the potential to produce methanol from CO_2 with high prospects of competitiveness. Similarly, in case that electricity is provided from the grid, the region in which the concept is examined plays considerable role, because electricity pricing is a matter of policy of each state/country.

This study is an attempt to identify the aspects for the operation of a methanol production plant, based on CO_2 utilization. Several cases and sensitivity analyses were investigated in order to identify the influence of various design and operational parameters on the process, in terms of system efficiency and economic feasibility. The current status of the “Power-to-Fuel” (PtF) concept is not economically attractive under any conditions studied here. The production cost of methanol from CO_2 is about 2.5 times higher than the corresponding conventional prices. A considerable effort is needed in order the CO_2 derived fuels to reach a competitive level in the global market. This study aimed to define the barriers that should overcome in order to become feasible providing charting of electricity source per case, charting of gas storage and Capex /Opex estimation and cost breakdown. More specifically, the key parameters that strongly affect the viability of the PtF concept are the following:

- *electricity cost.* The electrical consumptions that are required in order to produce hydrogen from water and then to transform CO_2 into organic compounds with high energy content is the most significant factor that influences the power to fuel economic feasibility. In terms of efficiency enhancement, the state-of-the art electrolysis reaches the maximum achievable value (~70%), which is thermodynamically limited. Consequently, only the use of cheap electricity on regular basis (high capacity factor) can contribute to the minimization of the share of the electricity cost on the methanol/ethanol production cost.
- *system configuration.* It is revealed in this study that the hydrogen production is preferable to be near to the methanol plant, avoiding high logistics costs for delivery and storage of H_2 . On the other hand, the location of the CO_2 capture unit has small influence on the inlet gas production and delivery cost.
- *oxygen utilization.* The oxygen that is produced in the H_2 plant is in high quality and can be used in numerous applications in industrial, medical and other sectors. Selling the produced O_2 with a very competitive price, the methanol production cost reduces at least 10%.
- *Capex reduction.* The investment cost has a 30% share on the methanol production cost. The 2/3 of this is the alkaline electrolyzer cost. So, a new electrolyzer design with lower cost would reduce considerably the minimum selling price of the produced alcohol in order the investment to be profitable. A revolutionary and alternative route of CO_2 reduction to value added chemical synthesis is the technology based on microbial electrosynthesis system (MES) where microorganisms are used in order to convert the direct electric current into chemical energy such as ethanol, directly from water and CO_2 . On the one hand, this route is expected to have reduced investment cost as the water-to-ethanol process is conducted in only one step. On the other hand, since this is a relative new concept, it has not been implemented in large scale yet so that a complete economic assessment and comparison to be accomplished.

5. Process improvements on energy systems based on thermocatalytic CO₂ hydrogenation for methanol and ethanol production

5.1 Introduction

An option for the drastic mitigation of CO₂ emissions, alternative to the Carbon Capture and Storage concept, is to transform it into valuable compounds, like fuel and chemicals, namely as ‘the CO₂ capture and utilization (CCU) concept’. The majority of CO₂ use in industry is for urea production, which accounts for more than half of the global annual usage [30]. Alternatively, CO₂ is utilized also physically in various applications such as refrigerant medium, in fire extinguishers and in the petroleum and NG industry for Enhanced Oil Recovery (EOR) and Enhanced Gas Recovery (EGR), respectively [31, 32].

In order the CCU concept to have effective impact on the drastic reduction of the CO₂ emissions, the quantities of end-products derived from CO₂ transformation should cover the market demand. The selection of the final products should be correlated to global demands and consumptions of them. Thus, this study focuses on synthesis of alcohols that can be used as alternative fuels in the transportation sector. The method for CO₂ transformation that is examined in this study is the catalytic hydrogenation, which is considered the most mature and old technology in this field.

There are three routes for non-fossil derived hydrogen production: water electrolysis, biomass conversion and solar conversion [33, 111]. In the present study, the hydrogen is considered to be derived from electrolysis, since this is the most mature and well-established technology even in industrial scale [116] and also it is not relied on carbon-contained source like biomass. Electrolysis is based on the water splitting into H₂ and O₂, the energy for this reaction is given in the form of electricity derived from Renewable Energy Source (RES) i.e. photovoltaic panels (PV), wind farms hydropower and geothermal plants. Since the H₂/CO₂ ratio for CO₂ hydrogenation towards hydrocarbons synthesis should be four (4) for methane and three (3) for methanol synthesis, the required amounts of hydrogen are very large.

Apart from methanol, ethanol is gaining the interest the last decades not only as an alternative fuel [160, 161] but also a valuable chemical block for numerous products synthesis [39]. In order the CCU concept to become the most appropriate option for CO₂ mitigation in a global scale, the synthesis of several chemical products should be included in a generalized road map. Ethanol is considered as a perfect additive into petrol, contributing to the increase of octane number and the reduction of CO and PM emissions. Furthermore, ethanol has an important advantage over methanol for application as transportation fuel because it is less toxic and dangerous, permitting higher blending ratios with conventional gasoline [80, 162]. However, the alternative ethanol fuel is bio-based and is mainly produced from sugar/starch crops through fermentation. On the other hand, few studies [117, 163, 164] that have investigated the technical and economical prospects for CO₂ derived ethanol synthesis.

The scope of this study is the investigation of new process schemes for the valorization of CO₂ towards the production of methanol and ethanol. In the methanol case, the use of membrane catalytic reactor for the fuel synthesis is examined whereas in the ethanol case, a novel concept is presented that based on the use of DME as intermediate product. The produced alcohols (methanol, ethanol and DME) can be used either as transportation fuels or as the basis for the synthesis of other chemicals. The ASPEN PlusTM process specifications and the modeling approach of the fuel synthesis unit are described in the following paragraphs in detail. The comparison with the conventional technologies (traditional methanol reactor in

the first case and the ethanol synthesis based on the reverse water gas shift (rWGS) reaction in the second one) is made in terms of efficiency by performing the thermodynamic analysis and in terms of economic feasibility.

5.2 Process Description

The concept for transportation fuels through CO₂ hydrogenation is shown in **Figure 72**. Carbon dioxide is separated and purified from the flue gas of a power intensive industry such as power sector or cement plant. The required hydrogen for the CO₂ hydrogenation is derived from water electrolysis that is accomplished with electricity derived either from renewable energy sources or from the grid. The process configuration for the CO₂ transformation into fuels and the final product separation and purification depends on the product type (methanol or ethanol). Since the CO₂ hydrogenation is accomplished in high pressure (>40 bar) both the inlet gases should be compressed before they are delivered to the CO₂ Utilization Unit (CUU).

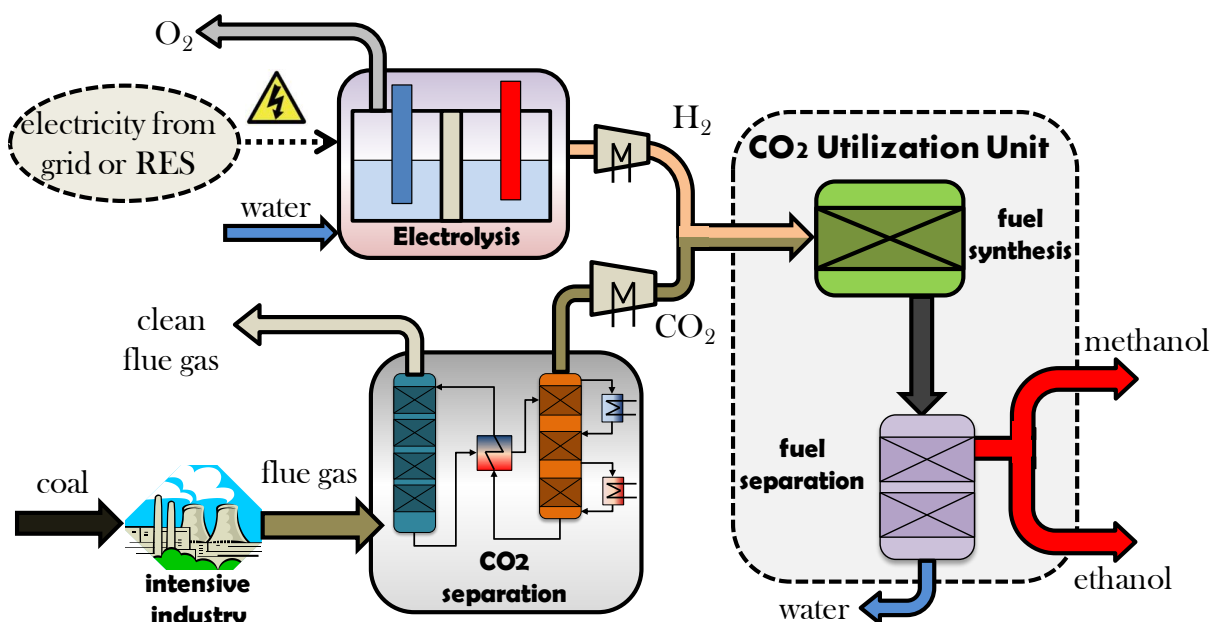


Figure 72. Conceptual design of the proposed avionics production from CO₂

5.2.1 Feedstock gases

The input gases that are required for the alternative ethanol synthesis are carbon dioxide (CO₂) and hydrogen (H₂).

Pure CO₂ separated from combustion gases of a power plant or other intensive carbon emission industry (e.g. cement plant) is considered as the source for the required CO₂. A great development has been gained on each of the main CO₂ separation techniques, even though no concept has reached to a commercial level yet. Among the several CO₂ caption options, amine scrubbing (MEA), Calcium Looping (CaL) and oxyfuel technology are considered the most competitive and ready to apply technologies for the first generation of applications in industrial scale. The chemical absorption technique with amine scrubbing is the most mature technology with the highest Technology Readiness Level and has already been tested and implemented in large scale applications [165]. Therefore, it is selected for this study as the

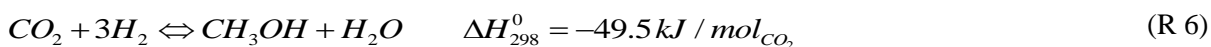
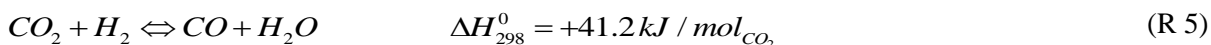
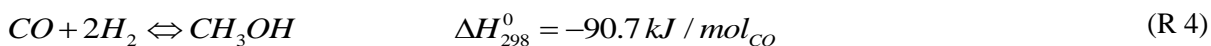
CO₂ capture technology. For the process analysis the specific heat demands for amine regeneration are set 4.17 MJ_{th}/kg_{CO2} and the electric power consumption 0.021 kWh/kg_{CO2} [138].

The water electrolysis is the selected method for pure H₂ production. In this process, water is split into O₂ and H₂ by means of electrical power. This option has the lowest efficiency (35-42%) and the highest H₂ production cost (for large scale 20-25 \$/GJ_{H2}) among the other technological options. However, it is considered as the best option for sustainable and non- fossil fuels oriented hydrogen production [140, 141]. Alkaline (KOH) electrolysis is the best available since it is quite mature up to large scale H₂ production [142]. Moreover, it has been tested successfully for discontinuous operation, and its load can be altered easily by adapting the current density [121]. Therefore, KOH electrolysis is selected as the most suitable technique for the examined concept in this study. Similar to the CO₂ capture, the water electrolysis process is not modeled in detail in this study. The basic aspects that affect the techno-economic evaluation are only taken into account: It is assumed that highly pure (>99.9%) H₂ and O₂ gaseous streams are produced in the electrolyzer, the operating conditions of which are 80 °C/30 bar, which are typical for large scale commercial alkaline electrolyzers [121, 143, 144]. The specific power consumption is set 4.34 kWh/Nm³ based on [121]. Assuming that the rest of power demands in the electrolysis unit is 10% of the consumptions for water electrolysis and hydrogen production [143], the overall electrical consumptions are 55.56 kWh/kg_{H2}.

5.2.2 Methanol synthesis from CO₂

Concerning the CO₂ fixation step towards the production of valuable chemicals, the catalytic hydrogenation for methanol and ethanol synthesis is examined. The scope of this analysis is to present novel process configurations for the production of these alcohols and to investigate how these schemes can improve the whole plant performance.

In this section, two different reactors types are presented, examining their influence on the process performance, in terms of mass flow rates and energy efficiency: The first is a tubular catalytic reactor, which is the traditional reactor scheme for methanol synthesis and is used in numerous commercial applications, and the second one is a zeolite membrane reactor. Methanol is formed from CO₂ hydrogenation under three-phase conditions [128]:



a) Methanol synthesis from catalytic CO₂ hydrogenation

The process flow diagram of a typical methanol synthesis unit from CO₂ is shown in **Figure 73**. The unit consists of the methanol synthesis, gas separation and product purification. The inlet gas is heated up to a temperature level so that the reactor operates adiabatically under the specified temperature. The required thermal energy for crude methanol heating up and distillation separation is recovered from the outlet stream after the methanol synthesis reactor. In order to achieve high purity levels of the methanol product (>99.2%), the liquid stream is throttled down to some Pa below the atmospheric pressure after the first flash separator, following the same approach with the RectisolTM process [166]. A small portion (1% v/v of the total stream) of the recycling gas is extracted as purge gas in order to avoid by-products accumulation such as hydrocarbons, inert gas etc.

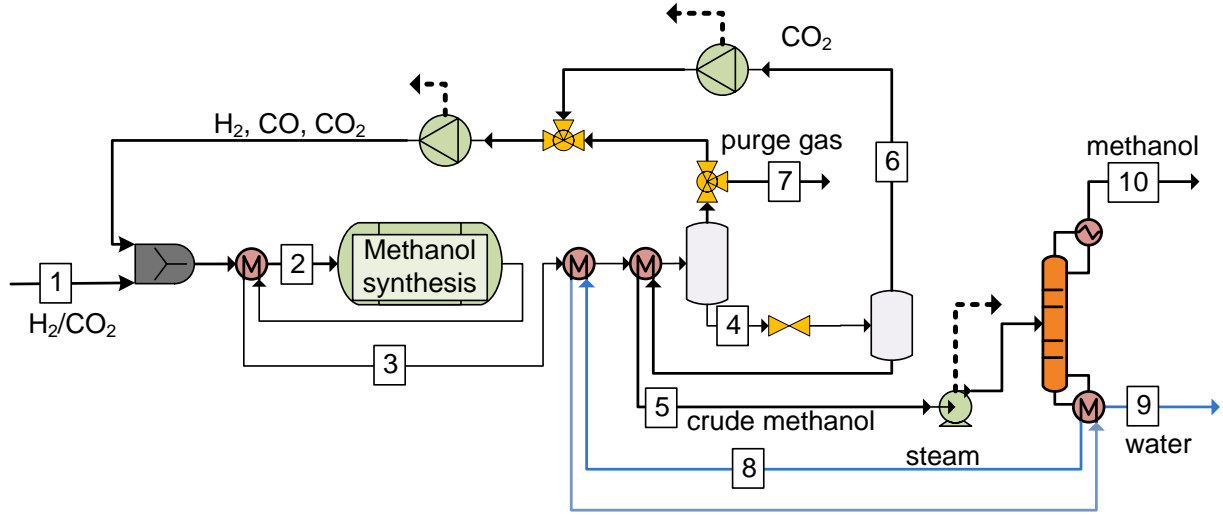


Figure 73. Process flowsheet of the CO₂ to MeOH concept

Table 43: Key Process specifications for the conventional MeOH synthesis from CO₂

H ₂ /CO ₂ ratio	3.0
Inlet gas preheating temperature	168 °C
MeOH reactor temperature/pressure	250°C/65bar
Flash separator #1 temperature/pressure	30.0°C/64.5 bar
Flash separator #2 temperature/pressure	24.5°C/0.2 bar
Crude methanol preheating	85°C
Distillation column, number of stages	60
Distillation column, inlet pressure	1.3bar
Final product composition (% v/v)	99.3% CH ₃ OH, 0.1% H ₂ O, 0.6% CO ₂

The key process specifications for the methanol plant are shown in **Table 43** and the parameters of the kinetic model in **Table 44**. The reaction rate r_i (kmol/kg_{cat}/s) expressions for the reactions (**R 4**), (**R 5**) and (**R 6**) are respectively:

$$r_1 = \frac{k_1 K_{CO} \left(p_{CO} p_{H_2}^{3/2} - \frac{P_{CH_3OH}}{K_{eq,1} \sqrt{p_{H_2}}} \right)}{\left(1 + K_{CO} p_{CO} + K_{CO_2} p_{CO_2} \right) \left(p_{H_2}^{1/2} + K_{H_2O} / K_{H_2}^{1/2} \cdot p_{H_2O} \right)} \quad (\text{Eq. 24})$$

$$r_1 = \frac{k_2 K_{CO_2} \left(p_{CO_2} p_{H_2} - \frac{P_{H_2O} p_{CO}}{K_{eq,2}} \right)}{\left(1 + K_{CO} p_{CO} + K_{CO_2} p_{CO_2} \right) \left(p_{H_2}^{1/2} + K_{H_2O} / K_{H_2}^{1/2} \cdot p_{H_2O} \right)} \quad (\text{Eq. 25})$$

$$r_1 = \frac{k_3 K_{CO_2} \left(p_{CO_2} p_{H_2}^{3/2} - \frac{P_{CH_3OH} p_{H_2O}}{p_{H_2}^{3/2} K_{eq,2}} \right)}{\left(1 + K_{CO} p_{CO} + K_{CO_2} p_{CO_2} \right) \left(p_{H_2}^{1/2} + K_{H_2O} / K_{H_2}^{1/2} \cdot p_{H_2O} \right)} \quad (\text{Eq. 26})$$

The output capacity of the methanol plant is set at 120 million liters annually, 2.5 times greater than the corresponding production capacity that the Carbon Recycling International (CRI) considers as a

standard commercial plant [167]. The main characteristics of the basic streams of this concept are summarized in **Table 45**.

Table 44. Kinetic rate calculation for MeOH synthesis [128]

parameter ¹	reaction (R 4)	reaction (R 5)	reaction (R 6)
exponential factor k_i	$k_1 = 2.69 \cdot 10^7 \exp\left(\frac{-10.99 \cdot 10^4}{RT}\right)$	$k_2 = 7.31 \cdot 10^8 \exp\left(\frac{-12.34 \cdot 10^4}{RT}\right)$	$k_3 = 4.36 \cdot 10^2 \exp\left(\frac{-6.52 \cdot 10^4}{RT}\right)$
equilibrium constant $\ln K_{eq,i}$	$\log_{10} K_{eq,1} = \frac{5139}{T} - 12.621$	$\log_{10} K_{eq,2} = -\frac{2073}{T} + 2.029$	$\log_{10} K_{eq,3} = \frac{3066}{T} - 14.650$
K_{CO_2}		$K_{CO_2} = 1.02 \cdot 10^{-7} \exp\left(\frac{6.74 \cdot 10^4}{RT}\right)$	
K_{CO}		$K_{CO} = 7.99 \cdot 10^{-7} \exp\left(\frac{5.81 \cdot 10^4}{RT}\right)$	
$K_{H_2O}/K_{H_2}^{1/2}$		$K_{H_2O}/K_{H_2}^{1/2} = 4.13 \cdot 10^{-11} \exp\left(\frac{-10.45 \cdot 10^4}{RT}\right)$	

¹ partial pressure p_i in bar, temperature T in K and $R=8.314$ J/molK

Table 45. Stream characteristics for the conventional CO₂ to MeOH concept

stream	m (kg/s)	T (°C)	p (bar)	molar composition (%)				
				CO ₂	H ₂	H ₂ O	CO	CH ₃ OH
1	5.8	20.5	60	25.0	75.0	0.0	0.0	0.0
2	20.4	138.5	60	18.8	79.0	0.1	1.6	0.6
3	20.4	158.4	60	14.5	69.3	6.9	1.8	7.5
4	7.9	50.0	59.4	16.0	0.0	41.5	0.2	42.3
5	5.8	24.2	0.2	0.3	0.0	49.9	0.0	49.9
6	1.9	50.0	12	95.2	0.0	0.6	1.3	2.9
7	12.5	50.0	59.4	14.3	82.9	0.1	2.1	0.6
8	1.6	111.4	1.5	0.0	0.0	100.0	0.0	0.0
9	2.1	99.7	1.1	0.0	0.0	98.5	0.0	1.5
10	3.7	48.1	1.1	0.6	0.0	0.1	0.0	99.3

b) Methanol synthesis through membrane reactor

The use of membranes technology for separation of the produced vapours along the reactor (either the methanol or the water) is investigated. This concept has been examined in several studies in the past [168-173]. Here the focus is primarily on the integration of such membrane reactors with the overall carbon utilization system. For this the process design takes into account the light gas recirculation.

Figure 74 depicts a sketch of the membrane reactor concept. For the modeling of the membrane reactor in ASPEN PlusTM, a series of equilibrium reactors are considered with the intermediate interpolation of split separators. The split fraction of the vapours (only water and methanol) that are assumed to permeate the membrane is specified by the determined separation factor. The separation factor of a component i (SF_i) is defined by the following equation:

$$SF_i = \frac{F_i^{permeate}}{F_i^{permeate} + F_i^{retentate}} \quad (\text{Eq. 27})$$

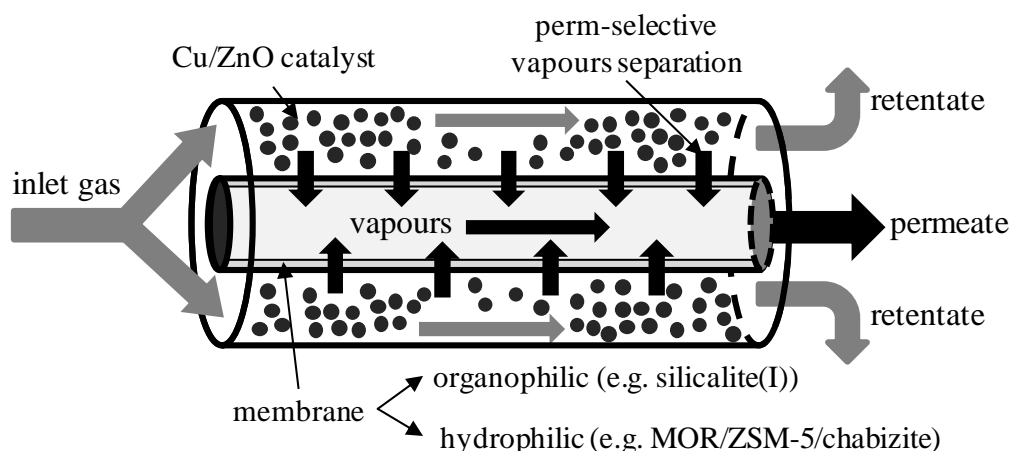


Figure 74. Sketch of the membrane methanol reactor

5.2.3 Ethanol synthesis from CO₂

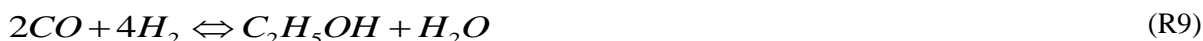
As quoted in the introduction, a central plan for CO₂ fixation towards to the drastic mitigation of GHG emissions should not rely on methanol production, exclusively, but it should include the production of other valuable chemical products. One of them is ethanol. In this section, two schemes for ethanol synthesis are presented, the first is the “traditional” route based on the reverse water gas shift reaction and the second scheme –the “novel” one - is based on the intermediate synthesis of DME.

a) Ethanol synthesis based on reverse WGS (rWGS)

The direct reaction of ethanol synthesis through CO₂ hydrogenation is the reverse reforming:



In practice, the direct ethanol synthesis suffers from very low selectivity to C₂₊ alcohols and low conversion rates at even high pressures [163, 164, 174]. Hence the thermochemical route that is adopted is in two steps through reverse water gas shift (rWGS) followed by the CO hydrogenation:



However, the effective CO₂ conversion into CO is achieved in high temperatures (in 575°C, a CO₂ conversion around 48% can be achieved) due to the endothermic nature of the rWGS, increasing the demands for a high temperature heat source, which is achieved through the combustion of a portion of the recycling gas (tail gas), as it shown in **Figure 75**. After the rWGS reactor, the produced H₂O is removed through condensation after gas cooling at 30°C. The gas is compressed at 80bar and introduced to the Mixed Alcohol Synthesis (MAS) reactor, where CO is catalytically hydrogenated at 325°C. The methodology for a modified FT catalyst MAS reactor and the process configuration for alcohols separation have already been described in previous studies [175, 176].

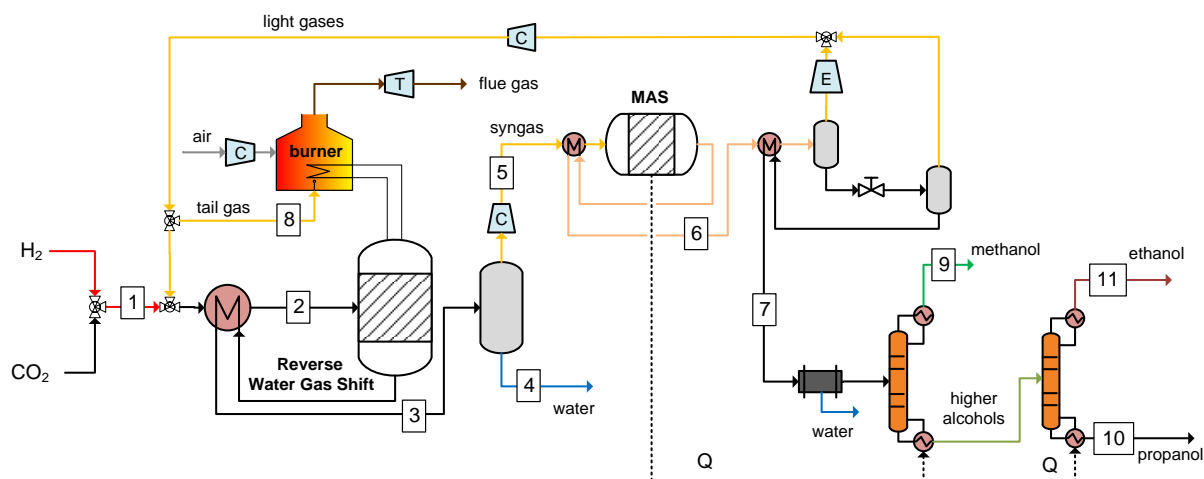


Figure 75. Process flowsheet of the rWGS-MAS concept

The main characteristics of the basic streams of this concept are summarized in **Table 46**.

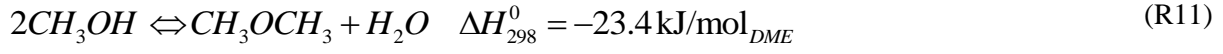
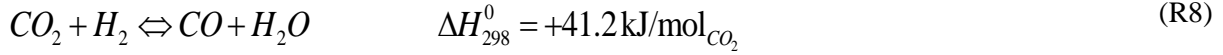
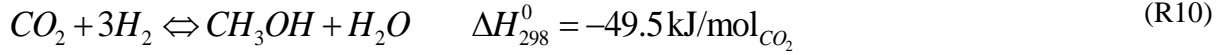
Table 46. Stream characteristics for the conventional CO₂ to EtOH concept based on rWGS

stream	<i>m</i> (kg/s)	<i>T</i> (°C)	<i>p</i> (bar)	molar composition (%)						
				H ₂ O	CO ₂	H ₂	CO	CH ₃ OH	C ₂ H ₅ OH	C ₃ H ₇ OH
1	5.8	50.0	25.0	0.0	25.1	74.9	0.0	0.0	0.0	0.0
2	26.6	487.8	25.0	0.0	12.1	70.8	17.0	0.1	0.1	0.0
3	26.6	120.0	25.0	5.8	6.3	65.0	22.8	0.1	0.1	0.0
4	2.7	102.1	4.1	98.5	0.1	0.0	0.0	0.6	0.7	0.0
5	24.2	115.2	80.0	0.2	6.7	68.9	24.2	0.0	0.0	0.0
6	24.2	211.9	80.0	0.9	8.6	67.1	20.5	1.0	1.9	0.0
7	24.2	211.9	80.0	1.0	9.2	66.9	20.0	1.0	1.6	0.3
8	2.7	126.1	4.1	26.5	0.9	0.0	0.0	22.6	41.1	8.9
9	0.4	28.9	0.2	0.0	4.6	0.0	0.0	94.4	0.9	0.0
10	1.2	43.3	0.2	0.0	0.0	0.0	0.0	0.3	99.7	0.0
11	0.3	30.0	0.2	0.0	0.0	0.0	0.0	0.0	0.0	100

b) Ethanol synthesis from DME

The novel thermochemical route for ethanol synthesis from CO₂ through DME that is proposed in this study consists of a series of two reaction stages.

The first stage is the DME synthesis from CO₂ and H₂. Even though the conventional method for commercial DME synthesis from syngas (including both CO and CO₂) is in two steps 1) methanol synthesis and 2) methanol dehydration, it have been shown that the one-step process based on bifunctional catalysts is more thermodynamically and economically favorable [124, 177-179]. The main reactions that take place in the DME synthesis reactor are (R10), (R8) and (R11). The first and the third are catalyzed by a methanol synthesis catalyst such as Cu/ZnO/Al₂O₃, while the second reaction by an acidic catalyst such HZSM-5 [179].



This process is kinetically rate depended and conducts in the range of 220–300 °C and 30–60 bar. The methodology for the kinetic rate calculation is adopted from the study of Lu et al. [179] and the parameters are summarized in **Table 47** while the expressions for the kinetic rates (r_i , kmol/kg_{cat}/s) calculation of the reactions R10, R8 and R11 respectively are the following:

$$r_1 = k_1 \frac{p_{CO_2} p_{H_2} \left(1 - \frac{1}{K_{eq,1}} \frac{p_{H_2O} p_{CH_3OH}}{p_{CO_2} p_{H_2}^3} \right)}{\left(1 + K_{CO_2} p_{CO_2} + K_{CO} p_{CO} + \sqrt{K_{H_2} p_{H_2}} \right)^3} \quad (Eq. 28)$$

$$r_2 = k_2 \left(\frac{p_{CH_3OH}^2}{p_{H_2O}} - \frac{p_{DME}}{K_{eq,2}} \right) \quad (Eq. 29)$$

$$r_3 = k_3 \frac{p_{H_2O} - \frac{1}{K_{eq,3}} \frac{p_{CO_2} p_{H_2}}{p_{CO}}}{1 + K_{CO_2} p_{CO_2} + K_{CO} p_{CO} + \sqrt{K_{H_2} p_{H_2}}} \quad (Eq. 30)$$

Table 47. Kinetic rate calculation for DME synthesis [179]

parameter ¹	reaction (R10)	reaction (R8)	reaction (R11)
exponential factor k_i	$k_1 = 35.45 \exp\left(\frac{-1.7069 \cdot 10^4}{RT}\right)$	$k_2 = 8.2894 \cdot 10^4 \exp\left(\frac{-5.2940 \cdot 10^4}{RT}\right)$	$k_3 = 7.3976 \cdot 10^4 \exp\left(\frac{-2.0436 \cdot 10^4}{RT}\right)$
equilibrium constant $\ln K_{eq,i}$	$\ln K_{eq,1} = \frac{4213}{T} - 5.752 \ln T - 1.707 \cdot 10^{-3} T$ $+ 2.682 \cdot 10^{-6} T^2 - 7.232 \cdot 10^{-10} T^3 + 17.6$	$\ln K_{eq,2} = \frac{4019}{T} - 3.707 \ln T - 2.783 \cdot 10^{-3} T$ $+ 3.8 \cdot 10^{-7} T^2 - 6.561 \cdot 10^{-4} T^{-3} - 26.64$	$\ln K_{eq,3} = \frac{2167}{T} - 0.5194 \log T - 1.037 \cdot 10^{-3} T$ $- 2.331 \cdot 10^{-7} T^2 - 1.2777$
K_{CO_2}		$K_{CO_2} = 1.02 \cdot 10^{-7} \exp\left(\frac{6.7400 \cdot 10^4}{RT}\right)$	
K_{CO}		$K_{CO} = 7.99 \cdot 10^{-7} \exp\left(\frac{5.8100 \cdot 10^4}{RT}\right)$	
K_{H_2}		$K_{H_2} = 0.249 \exp\left(\frac{3.4394 \cdot 10^4}{RT}\right)$	

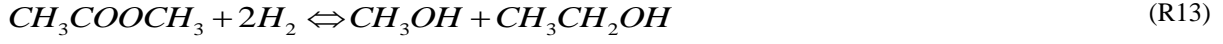
¹ partial pressure p_i in bar, temperature T in K and $R=8.314$ J/molK

The second stage of the proposed concept for alcohols synthesis is the DME transformation into C₂H₅OH. The alcohols (methanol and ethanol) production from methyl ether is conducted in two

consecutive steps [40, 180, 181]. The first is the DME carbonylation where methyl acetate (MA) is formed in the presence of H-Mordenite (H-MOR) zeolite:



The next one is the produced ester hydrogenation over the Cu/ZnO catalyst.



The reaction process is accomplished in a dual bed reactor sequentially, at 15 bar and 220 °C. Apart from the produced alcohols and the unconverted DME and MA, CO₂ and ethyl acetate (EA) are also found in the reactor exit [40, 180]. After the products separation, DME, MA and EA reenter to the reactor, whereas the CH₃OH and CO₂ are sent at the DME synthesis unit. The process configuration for the ethanol separation and purification is similar to the conventional CO₂ to ethanol plant.

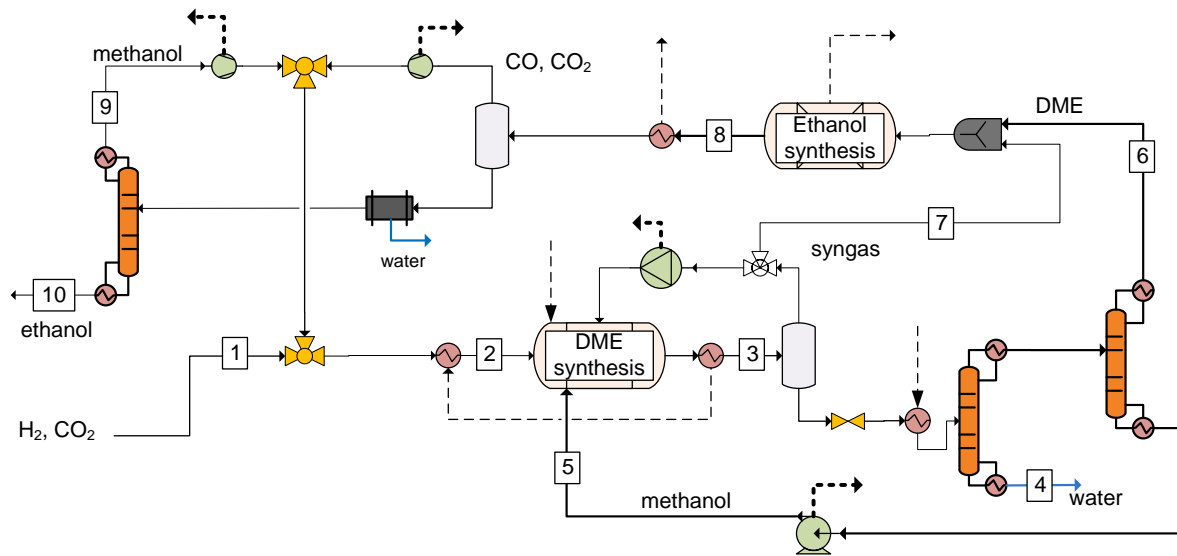


Figure 76. Process configuration of the CO₂ to Ethanol plant through DME

The main characteristics of the basic streams of this concept are summarized in the following Table.

Table 48. Stream characteristics for the conventional CO₂ to EtOH concept based on DME synthesis

stream	<i>m</i> (kg/s)	<i>T</i> (°C)	<i>p</i> (bar)	molar composition (%)						
				CO ₂	H ₂	H ₂ O	CO	CH ₃ OH	C ₂ H ₅ OH	DME
1	5.8	52.9	50	25.0	75.0	0.0	0.0	0.0	0.0	0.0
2	18.0	189.9	50	10.4	78.4	0.2	6.2	3.9	0.0	0.9
3	18.0	155.5	50	4.8	70.7	9.8	9.6	0.8	0.0	4.3
4	3.0	131.3	2.8	0.0	0.0	100.0	0.0	0.0	0.0	0.0
5	0.5	54.4	50	0.1	0.0	18.8	0.0	78.4	0.0	2.7
6	3.1	-25.8	1.1	23.0	0.0	0.0	6.7	0.2	0.0	70.1
7	4.0	28.1	15	4.6	82.8	0.0	10.9	0.0	0.0	1.7
8	7.1	220.0	15	7.0	65.1	1.4	2.2	12.2	12.1	0.0
9	2.0	64.7	1.1	7.1	0.0	0.0	0.3	92.3	0.3	0.0
10	2.7	80.4	1.1	0.0	0.0	0.0	0.0	0.1	99.9	0.0

5.3 Cost analysis

The Total Capital Investment (TCI) estimation is performed according to Peters & Timmerhaus methodology [129] and is based on a series of intermediate cost types, the first of which is the Total Purchased Equipment cost (TPEC) for each case. The equipment cost of each component is estimated based on similar equipment costs from the literature according to the following equation:

$$C_i = C_0 \cdot \left(\frac{S_i}{S_o} \right)^f \quad (\text{Eq. 31})$$

Furthermore, having the Total Purchased Equipment Cost (TPEC) estimated, the next step is the Total Installed Cost (TIC) calculation. This is accomplished by multiplying each equipment cost with an installation factor n , specified for each component (see **Table 49** and **Table 50**).

Table 49. Equipment cost estimation

Equipment List	Scaling parameter	Reference erected cost, C_o (M€)	Reference size, S_o	Scale factor, f	install factor, n	Ref. year	Ref.
methanol reactor	feed gas (kg/h)	7.69	87.5	0.6	2.1	2006	[126]
rWGS reactor	feed gas (t/h)	0.4720	210	0.8	2.47	2010	[182]
DME reactor	kmol/s feed gas	15.855	2.91	0.65	1.52	2007	[183]
ethanol reactor ¹	feed gas (lb/h)	49.600	729095	0.65	2.47	2005	[184]
heat exchanger	heat duty (MW _{th})	39.26	355	1	1.49	2007	[130]
distillation unit	MeOH flow rate (t/h)	16.58	6.75	0.7	1.52	2006	[126]
compressor	power (MW _e)	12.08	10	0.67	1.72	2006	[131]
cooling system	Q rejected (MW _{th})	49.600	470	0.67	1.49	2007	[132]
booster	power (MW _e)	14.770	47.61	0.67	2.47	2011	[133, 134]
alcohols separation	liquid feed (kg/s)	7.207	8.836	0.67	2.47	2005	[185]
wastewater treatment	kg/hr water input	20.353	393100	1.05	2.47	2010	[135]
gas turbine	power output (MW _e)	73.2	266	0.75	1.27	2007	[183]
flash tank	gas feed (kg/s)	installation cost (in M€) = $2.47 \cdot 983.2 \cdot 10^{-6} \cdot (\text{feed gas in kg/s})^{0.8}$				2000	[136]
boiler	boiler capacity (lb/hr)	online equipment cost estimation					[186]

¹ the same methodology for both ethanol reactors is followed.

The parameters for the operational cost calculation such as O&M and insurance are considered as a portion of the Fixed Capital Investment (FCI).

Table 50. Economic assumptions

exchange rate	0.755 €/€
discount rate	10%
recovery period	25 years
Capital Recovery Factor	0.11
year basis	2012
Operating and Maintenance (O&M)	5% FCI
Insurance	2% FCI

One of the most important aspects of the economic analysis is the determination of the H₂ cost. The selection of the power supplier for the electrolysis operation, the hydrogen management prior utilization,

the electrolysis technology are decisive parameters for the estimation of the hydrogen production and delivery cost [121, 127, 144]. However, since the detailed estimation of the hydrogen production cost is out of the scope of this study, it is assumed equal to 3.0€/kg.

Similar to the previous study, the cost for CO₂ capture with the amine scrubbing port-combustion technology is set at 43.8 €/tn_{CO₂}. The delivered CO₂ stream bares the same specification with storage specification [19]: oxygen should absent from the pure CO₂ stream to avoid ignition after reaction with the H₂ in the reactor. The specific heat demands for amine regeneration are 4.17 MJ_{th}/kg_{CO₂} and the electric power consumption 0.021 kWh/kg_{CO₂} [138].

5.4 Results and discussion

In this section the results derived from the process simulations and the economic evaluation of the two main systems (methanol and ethanol production) are presented and discussed.

5.4.1 Process simulation results

For the evaluation of the productivity rate of each component (CH₃OH and CO), the yield parameter is introduced, which is the product of the CO₂ conversion per pass with the selectivity of the specified component.

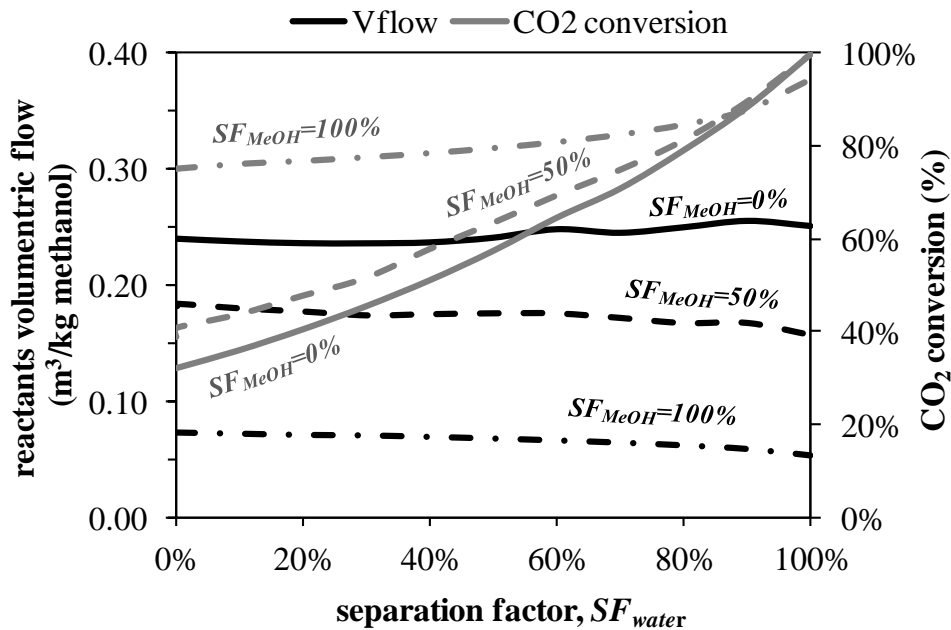


Figure 77. Volumetric flow inlet and CO₂ conversion as a function of the separation factors SF_{water} and SF_{MeOH}

An evaluation of the effect of water and methanol separation factor on the process in terms of performance is shown in **Figure 77**. The beneficial effect on the process performance with the increase of SF_{MeOH} is also illustrated by the decrease of the actual volumetric flow of the gas stream that enters the reactor. The volume flow rate of the reactant gas is depended on the methanol yield and the rate of the recycling gas. It is clear that the reactor size is determined by the gas inlet flow rate. Even though the design configuration of the membrane reactor is more complex than the traditional one, the basic dimensions of the former are expected to be up to 50% smaller, an aspect which could lead to reduced equipment cost.

The CO₂ conversion increases under hydrophilic or organophilic conditions. However, water removal from the reaction side has practically negligible influence on the inlet gas volumetric flow, a fact that is attributed to the increase in CO yield with the increase of water separation factor, SF_{water} , as it is depicted in **Figure 78**. In this case, water removal favors the increase of CO yield according because of the water gas shift reaction. The methanol yield, on the other hand, benefits by both water and CH₃OH permeation.

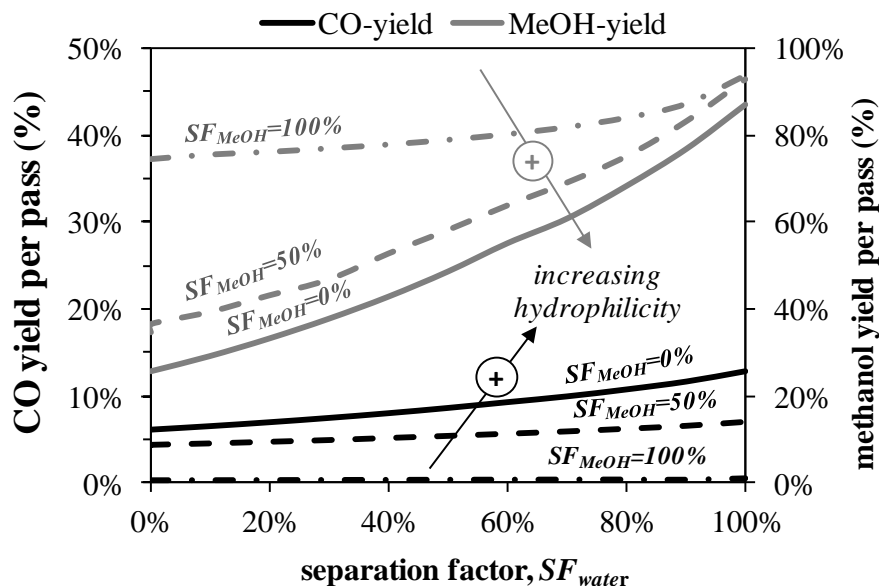


Figure 78. CO and CH₃OH yield as a function of the separation factors SF_{water} and SF_{MeOH}

The main results the CO₂ to Methanol schemes assuming 50% removal efficiency for both reactor types are shown in **Table 51**. In order to assess the performance of each CO₂ Utilization Unit, the CUU efficiency is introduced and defined as:

$$\eta_{CUU} = \frac{\dot{m}_{CH_3OH} \cdot LHV_{CH_3OH}}{\dot{m}_{H_2,inlet} \cdot LHV_{H_2} + \sum P_{cons}} \quad (\text{Eq. 32})$$

Table 51. Main results the CO₂ to Methanol schemes

	traditional reactor	hydrophilic membrane reactor	organophilic membrane reactor
methanol/water selectivity (mol/mol)	-	3	1/3
methanol removal ratio, SF_{H_2O}	-	18.1%	50.0%
water removal ratio, SF_{CH_3OH}	-	50.0%	16.7%
methanol selectivity (%)	80.7%	83.4%	88.4%
CO ₂ conversion (%)	31.9%	42.1%	39.7%
methanol yield per pass (%)	25.7%	35.1%	35.1%
recycling ratio (kmol/kmol)	3.16	2.09	1.99
inlet gas actual volume flow rate (m ³ /s)	2.751	1.440	1.396
methanol annual production (tn/y)	98343	98415	98390
methanol purity (%)	99.3%	99.5%	99.4%
total heat requirements (MW _{th})	9.64	9.14	9.05
rejected heat (MW _{th})	14.60	12.44	14.15
total power requirements (MW _e)	0.46	0.33	0.26
CUU efficiency (%) LHV basis)	85.7%	85.9%	85.9%

The methanol yield increases by 26% through the use of membrane reactor as a result of the increase in both CO_2 conversion rate and methanol selectivity. As a consequence, the recycling ratio (defined as the molar flow rate of the recycling gas to the feed gas) drops by 30% allowing the decrease of the reactor size (lower gas volume flow rate). This also slightly decreases heat and power demands. The CUU efficiency is not improved significantly but it is high in all cases.

The energy balance of the overall Power-to-Methanol concept is illustrated at the Sankey diagrams for both schemes (traditional concept and membrane reactor) in **Figure 79**. The equilibrium limitations in the traditional reactor leads to the recycling of a large amount of unconverted gas, its enthalpy of heat is 3.6 times greater than the feed H_2/CO_2 gas. The electrical demands in the electrolyzer unit dominate the overall requirements: up to 97% of the total electricity demands are for the hydrogen production. In terms of exergy, the exergy input by means of electricity in the H_2 unit is 90%, including thermal energy demands for the amine regeneration in the CO_2 capture unit. The calculated total exergy efficiency in the conventional scheme is 52.7%, whereas in the novel scheme with the membrane reactor is 53.7%.

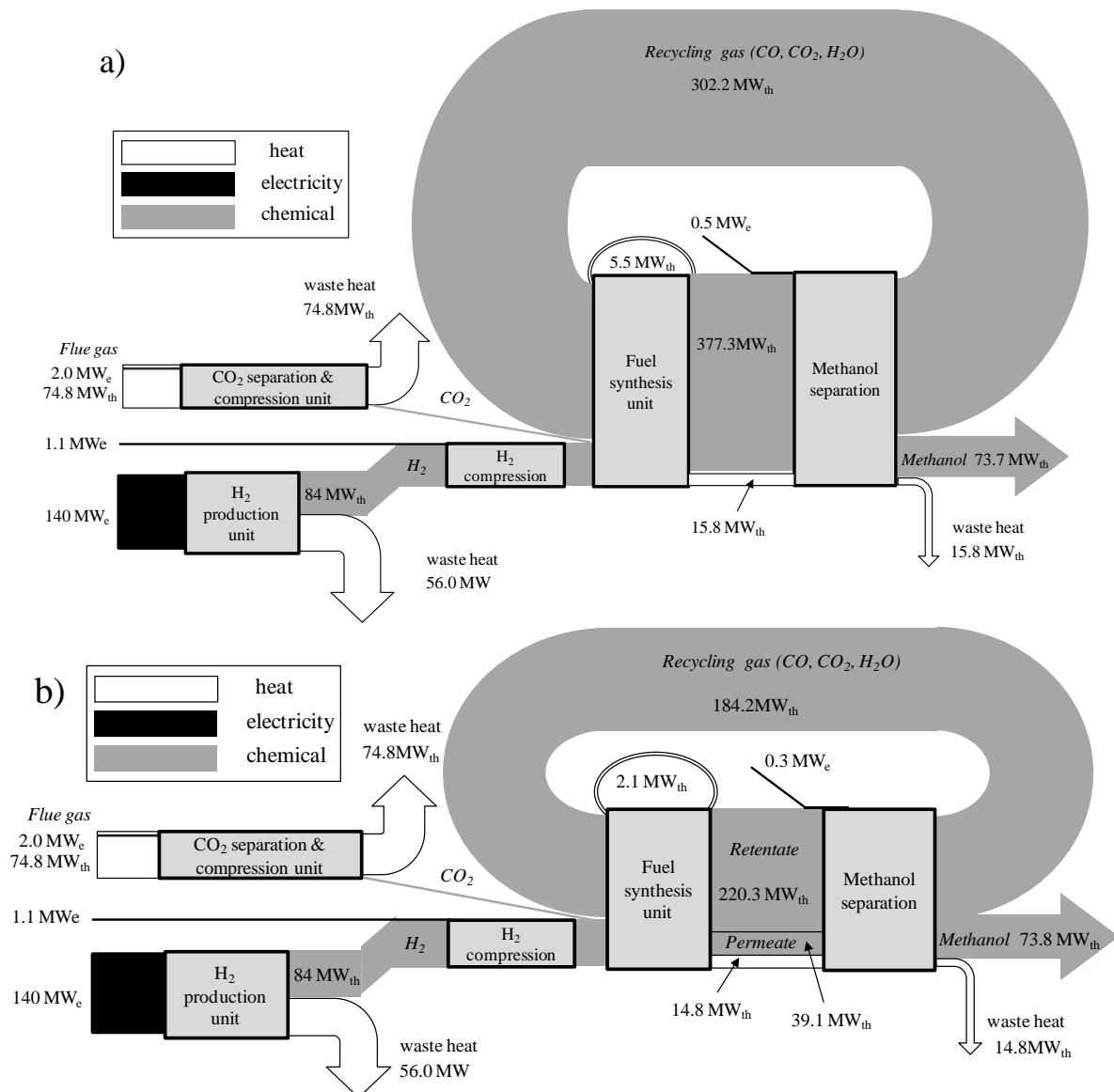


Figure 79. Energy flow diagram of the CCU process using a) traditional methanol synthesis reactor and b) membrane reactor for methanol synthesis (50% SF_{MeOH} and 16.7% SF_{water})

The energy flow at the two ethanol plants is illustrated by the corresponding energy flow diagrams in **Figure 80**. The heat streams in the DME scheme (**Figure 80b**) that are used for the coverage of the heat demands in various process come from the useful heat that is produced in the burner.

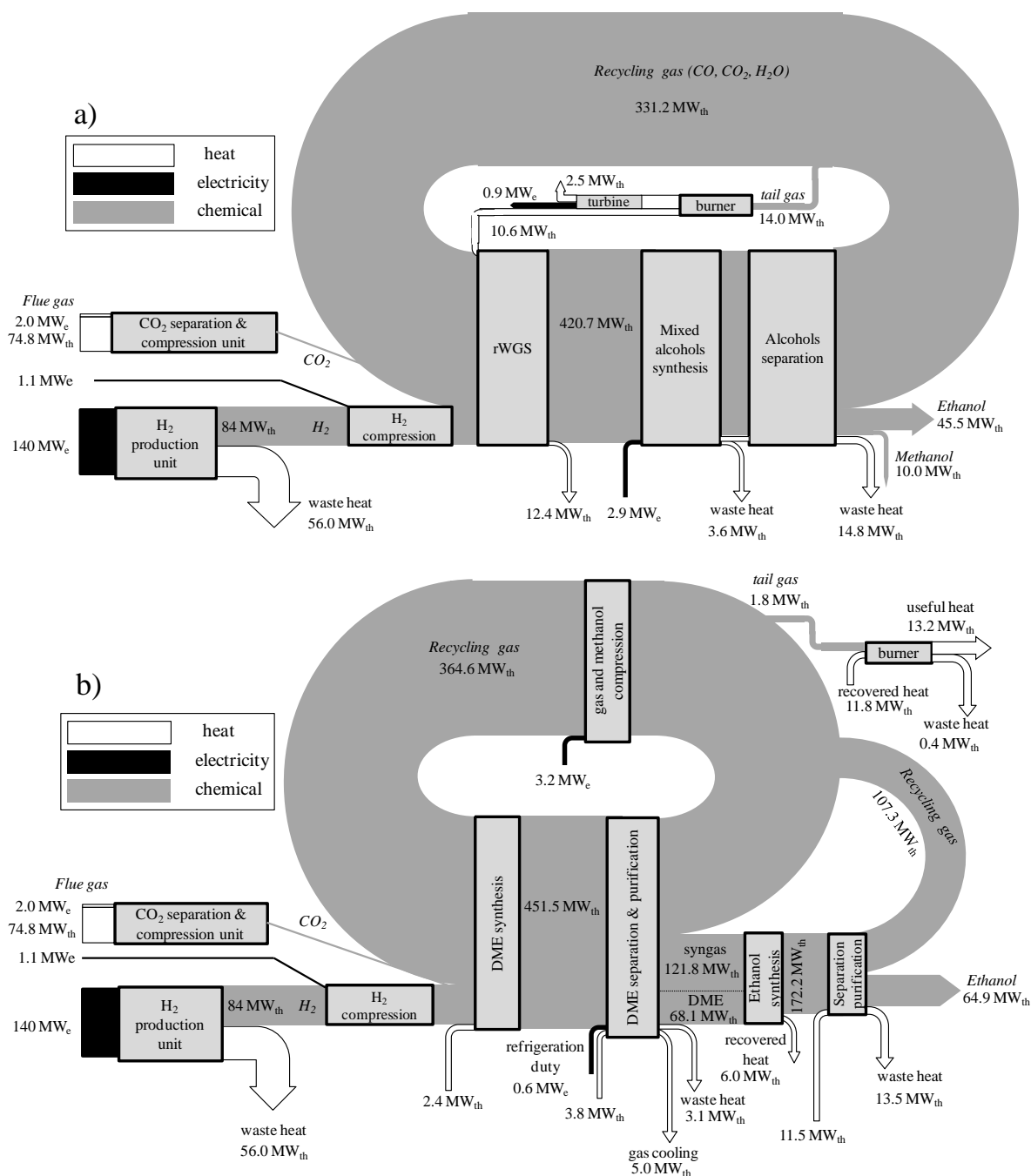


Figure 80. Energy flow diagram of the CO₂ to Ethanol Plant through a) reverse Water Gas Shift and b) DME synthesis

The main mass and energy balance simulation results are shown in **Table 52**. The DME annual production refers to the DME that is produced at the first reactor and undergoes to transformation into ethanol into the second reactor. Since the DME stream is purified, it could be considered as the final product in case that the ethanol is not the desired product. Due to the nature of the MAS catalyst, high selectivity rates for the ethanol and higher alcohols synthesis cannot be achieved. In this light, methanol

is considered as by-product. Alternatively, methanol can be reformed in high temperature under oxy conditions and reenter the mixed alcohol reactor, resulting to 100% selectivity in C2+ alcohols [175]. However, this option is not adopted in this analysis. On the other hand, the produced methanol in the ethanol synthesis reactor can be separated and returned to the first reactor for DME synthesis. Similar to the ethanol cases, large amounts of heat is required for products separation in both processes. Most of the heat requirements are covered by the cooling of the hot gases exiting the reactors. Even though the demands for heat along the whole process in the first scheme are more, the flow rate of the tail gas that is combusted is greater, due to the strong endothermic nature of the reverse water gas shift reaction. On the contrary, only 0.5% of the recycling gas at the DME reactor is extracted in order to be burnt. As a result, the carbon utilization in the second case is much greater than the “conventional” way.

Regarding the performance of the two process schemes, the Ethanol plant based on DME has greater CUU thermal efficiency (i.e. the chemical products heat input to the total energy input). This is mainly attributed to the milder reactions that take place along the process resulting to lower heat demands, despite the higher power consumptions due to gas recycling and compression. The total exergy efficiency for the both systems is 41.9% for the first case (rWGS) and 49.3% for the second one (DME based). It is clear that the synthesis of higher alcohols has smaller performance in comparison to the methanol case as it is illustrated by the comparison of the corresponding exergy efficiencies.

Table 52. Main simulation results from the Power-to-Ethanol cases

	EtOH from rWGS	EtOH from DME
DME annual production	-	72036
ethanol annual production (t/y)	32777	61983
methanol annual production (t/y)	12357	-
propanol annual production (t/y)	10079	-
CO ₂ conversion (%)	49.5	56.5
CO ₂ utilization (%)	68.7 (81.1) ¹	98.0
total heat requirements (MW _{th})	13.78	13.18
tail gas heating value (MW _{th})	14.03	1.82
rejected heat (MW _{th})	27.38	21.81
total power requirements (MW _e)	2.05	4.18
CUU efficiency (% LHV basis)	63.2	70.3

¹ the value in the parenthesis refers to the carbon in both methanol and higher alcohols

5.4.2 Economic analysis

Regarding the economic evaluation of the methanol production, it is performed and presented only for the conventional case. The plant cost breakdown in **Figure 81**, shows that the hydrogen production dominates the methanol production costs. The terms and conditions for the minimization of the electrolyzer and electricity cost in order the technology to be more competitive is not part of this study. The improvements on process performance and the reduction of the production cost by means of advanced techniques such as the membrane reactors are analysed and discussed.

In the previous analysis, the market of oxygen is not taken into account. Oxygen is a valuable product that has numerous applications in various sectors such as the iron and steel industry, and the medical sector [155]. Given that oxygen that is produced through electrolysis is in high purity, it has the potential to fulfill the requirements for the implementation in every use (oxidizing agent or medical product). The compression, cooling and liquefaction of the produced oxygen and the corresponding power consumptions

and operational costs are estimated and included in this study. The specific power consumptions for O₂ liquefaction is set 0.3711 kWh/kgO₂. Because of the high quality in terms of purity, the oxygen selling price is set at 87.4 €/tn, based on [156]. The introduction of the oxygen liquefaction and compression unit causes 14.9% increase in the total capital cost and the corresponding total operational cost drops by 1.3% in the whole Power-to-Methanol system. As a consequence, the methanol production cost drops at 859.2 €/tn (10.1% decrease). It is seen that the oxygen marketing has a beneficial effect on the mitigation methanol production cost and should be taken into consideration.

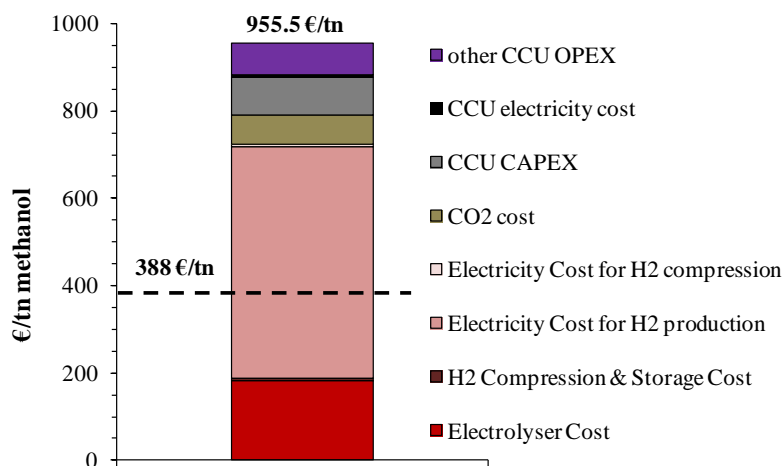


Figure 81. Power to Methanol cost breakdown

As far as the economic analysis for the ethanol case is concerned, **Figure 82** presents the ethanol cost breakdown for the two cases. The oxygen utilization is not taken into account in this analysis. The same qualitative conclusions with the methanol case are extracted: The hydrogen production cost, and more specifically the electricity for H₂ production is the most important parameters that influence the ethanol production cost. On the other hand, similar to the methanol case, the other component for the ethanol synthesis (CO₂) has a small contribution (only 6.6 to 7.0%) to the economic scale of the investment as the specific cost of the delivered CO₂ stream is 108 €/tn of ethanol (rWGS based) and 139.2 €/tn of ethanol (DME based). The specific cost of the CUU (both the capital and operational part) for the rWGS based and DME based scheme is 376.1 and 389.2 €/tn of ethanol, respectively.

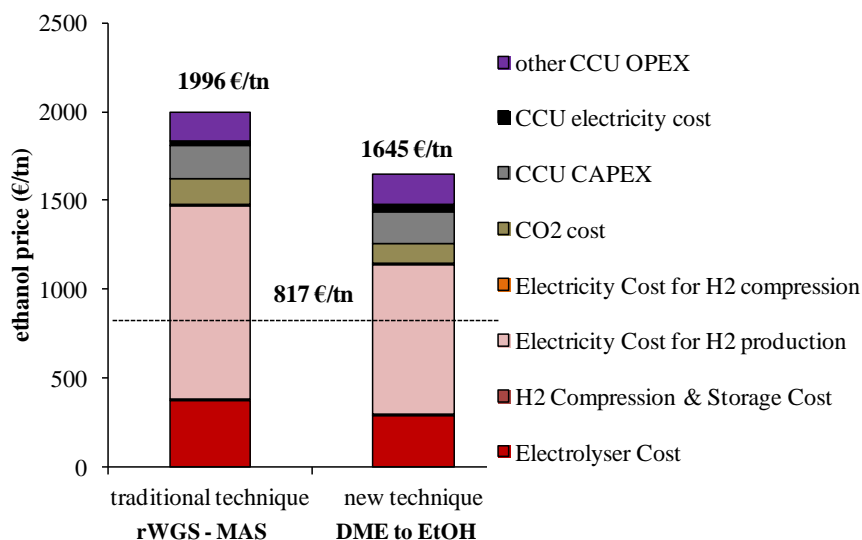


Figure 82. Ethanol production cost breakdown for the two CO₂-to-Ethanol schemes

Comparing the two process schemes, the proposed scheme for ethanol production via DME synthesis has lower production cost than the rWGS based scheme. The estimated production cost in the former scheme is 2.01 times greater than the current ethanol price whereas in the later scheme it is 2.44.

In case that the produced oxygen can be considered as a by-product and is sold, the minimum ethanol price in the rWGS case is 1.27 €/l whereas in the DME based case is 1.11 €/l. Taking into account that the cost of cellulosic ethanol, which is derived from lignocellulosic biomass fermentation is currently around to 0.70 €/l, more effort should be paid in order the CO₂ based options for alternative ethanol production can compete the bio-based routes.

5.5 Conclusions and further considerations

This study focuses on the improvement of the CO₂ conversion to value added fuels. Two new concepts are introduced one for methanol and another ethanol and are compared with the conventional schemes in terms of system efficiency and economic feasibility. In the methanol case, the adoption of membrane reactor for methanol synthesis has no effect on the methanol plant thermal efficiency but increases the methanol yield. This fact induces the reduction of the recycling gas flow rate, leading to reduced reactor dimensions and consequently, to lower investment cost.

In the ethanol case, the novel scheme through DME that is presented in this study has higher thermal efficiency because of lower heating demands, and thus, the ethanol production cost is lower than this of the rWGS case. The economic analysis reveals that using the novel DME-based ethanol plant that is proposed in this study, 18% reduction on the ethanol production cost is achieved. However, a considerable effort is needed in order the CO₂ derived fuels to reach a competitive level in the global market.

6. Plant design aspects of catalytic biosyngas conversion to higher alcohols

6.1 Introduction

Coal, lignite, oil and natural gas have been used over 100 years both in the power and chemicals production industry and have been the prime energy sources of the global economy. Important issues such as climate change, reduced fossil fuel resources, coupled with increased prices lead to efforts to supplement fossil fuels consumption by renewable biomass resources, which are abundant and unexploited. The realignment of the chemical industry from a petrochemical refining based to a biorefinery based has attracted a lot of attention and the feasibility of this concept has become a national goal of many countries [187].

Bioethanol is the most common 1st generation biofuel, currently being produced from the fermentation of sugars i.e. using edible biomass as feedstock. Gasification of biomass to synthesis gas (H_2/CO), followed by catalytic conversion of syngas, could produce significant amounts of ethanol, plus higher alcohols that could be used as additives into transportation fuels without competing with the food sector. The latter is a second generation biofuel approach and is regarded by many as a way to reduce the amount of carbon dioxide released into the atmosphere by replacing part of fossil and thus higher CO_2 footprint energy sources [188-191]. Except from the production of methanol and ethanol, and Fischer-Tropsch liquids' potential uses in automotive sector [192], extensive research efforts have been focused in the production of Higher Alcohols (HA: C_2 – C_4 alcohols), and in the development of active and selective catalysts [193-196]. The resulting alcohols mixture could be used directly as fuel, as fuel additives for octane or cetane enhancement, as oxygenate fuel additives for environmental reasons, and as intermediates to form other fuel components as well as for the production of solvents or other chemical sub-processes in the chemical industry. HA gained ground against other bioliquids, because they have a wide range of uses as final products or as key intermediate components for the chemical industry. The most common HA alcohol is ethanol (CH_3CH_2OH). Apart from being a fuel already produced by 1st generation biofuel routes, it has major industrial uses such as its conversion by oxidation into acetaldehyde (CH_3CHO). It is also used in the preparation of various derivatives, such as ethyl chloride, in plastics production etc. As a fuel, it is suitable for internal combustion engines (ICE) [192]. The next HA is propanol, and its principal use is in the production of acetone, which is used extensively as a solvent and as starting compound in the manufacture of numerous other organic compounds. Butanol is claimed to have good qualities for direct replacement of gasoline [197]. Even higher HAs are produced in large quantities and they have a wide range derivatives used in the production of resins, paints, polyester fibres and other applications [198, 199].

The biorefinery concept focuses on replacing the resources currently used (mainly natural gas) to transform biological raw materials into industrially useful intermediates up to end products. The production of HA in a biorefinery application could involve two different pathways: the first one is the biochemical conversion of biomass derived sugars through alcoholic fermentation (adopted in Brazil and the United States). The second route is via thermochemical conversion of biomass which offers a more effective means for the recovery of the energy content of biomass in a direct way and shorter times. Important thermochemical processes used for the production of highly energetic gaseous fuel are: (a) pyrolysis achieved in the absence of oxidant and (b) gasification, i.e. the thermal decomposition and

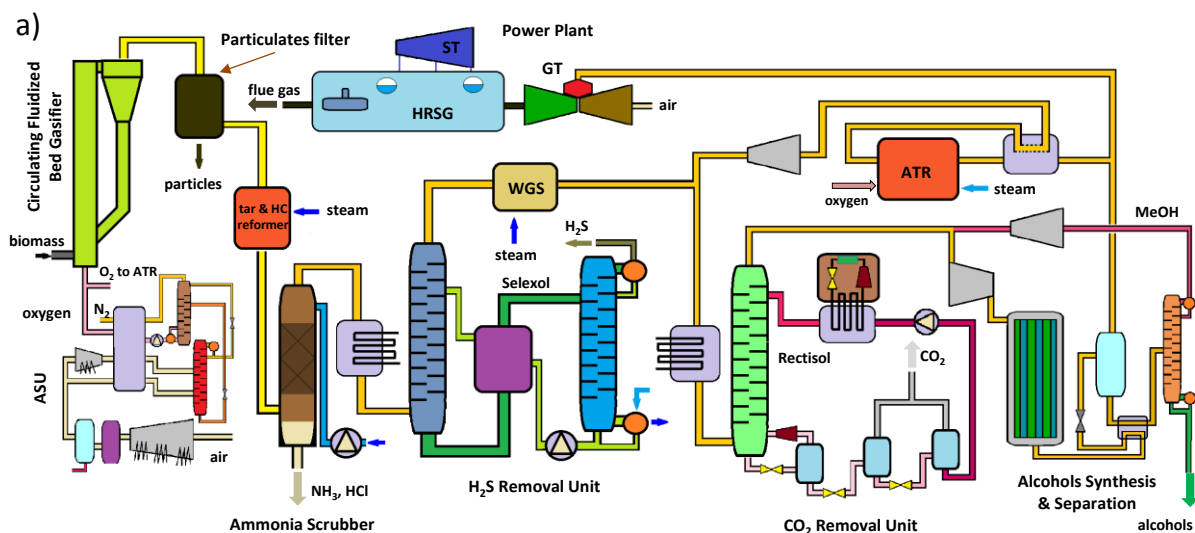
reaction of biomass occurring with the help of an oxidant such as pure oxygen or air (autothermal process) or steam (allothermal) to yield a combustible gas rich in carbon monoxide and hydrogen [193-196].

In this chapter, an energetically self-supported biorefinery section is designed for two different feedstocks: i.e. woody biomass and the pulp and paper industry by-product: black liquor. The latter is one of the largest concentrated biomass sources available in regions with many large pulp and paper industry units (i.e. northern Europe etc). Since the pulp industry has already tackled the logistics of handling huge amounts of wood it is more likely that their by-product is used apart from producing energy in recovery boilers, for the production of biofuels. Nevertheless, the production of syngas from solid biomass is a primary future target in case of the absence of an existing relevant industry. In all cases a biorefinery has to function without any requirements for energy above the levels its primary feedstock can cover. This study describes in detail the entire sub processes and simulation methodologies in Aspenplus™ process simulation tool. A detailed bibliographical search is performed into works employing this software for the evaluation of biorefinery operations based on syngas [200-203].

The modelled sections are the gasification (both black liquor and solid biomass), the oxygen production, the gas cleaning and removal of acid gas components and finally the production of HA (in two different cases fashions depending on the catalyst employed). The envisaged process could well function from sizes of 100 to 400 MW thermal input of biomass [204], with the first being the basis for the calculations.

6.2 Process description

A simplified flow diagram for the process is shown in **Figure 83**. Both wood based circulating fluidized bed gasification and black liquor gasification are shown in cases (a) and (b). All major processing steps for the conversion of wood or black liquor to syngas via oxygen gasification are apparent: the air separation unit, the gas-cleaning system and the catalytic synthesis of HA. Each process area in the scheme is described below.



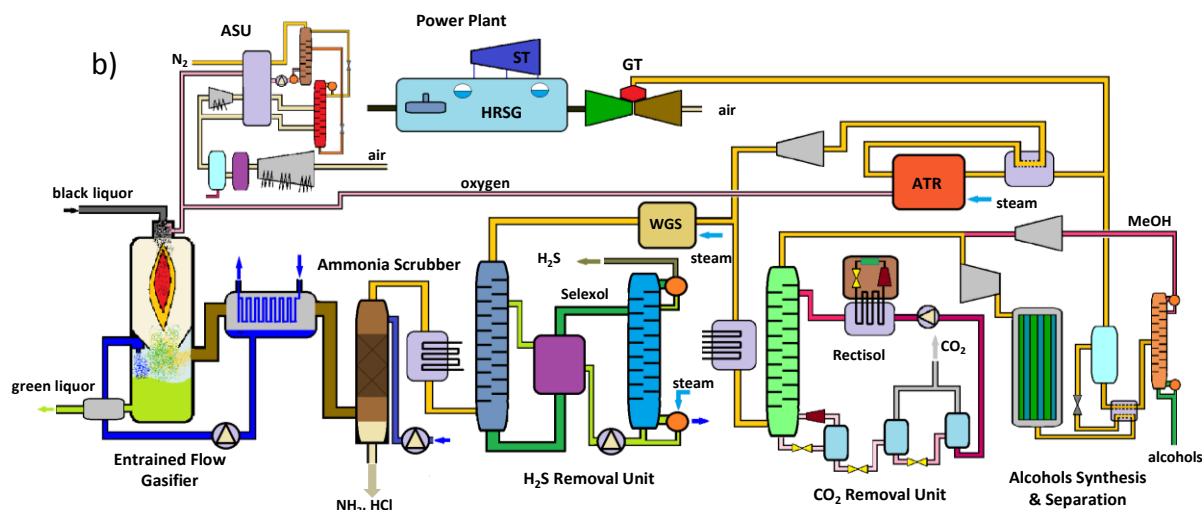


Figure 83. Process flow diagrams of different biorefinery systems derived from a) woody biomass and b) black liquor

6.2.1 Air separation unit

A cryogenic separation unit is required in order to produce a highly pure oxygen stream. Cryogenic distillation separates oxygen from air by liquefying at low temperatures. Ambient air is compressed in three stages via a compressor with inter-cooling and further cooled with chilled water. Residual water vapour, carbon dioxide, and atmospheric contaminants are removed in molecular sieve adsorbers. The cooling of air to cryogenic temperatures is achieved by heat exchanger and the required cooling loads derive from the already cold product streams. Such a configuration can reach to an oxygen purity of up to 98% [205]. For further oxygen purification, an extra column for argon separation would be required.

6.2.2 Gasification

Over the past decades many different gasifier types have been developed. Nevertheless for the sizes of a biorefinery operation i.e. well over 30 MW thermal input, only two technologies have the maturity to be considered for current or near future application. A circulating Fluidized bed (CFB) gasifier is recommended for solid fuels with diverse textures and moisture levels. If the biomass is in the form of liquid (such as in black liquor) or solid without serious problems and energetic requirements for its partitioning down to fine particles (<1mm), then an entrained flow system can also be considered.

Gasifying woody biomass in circulating fluidized beds and black liquor in entrained flow gasifiers has many differences in operating conditions, quality of produced gas etc. The typical chemical analyses of both fuels adopted are presented in **Table 53**. Primarily, the gasification temperature in a CFB is below 1000 °C compared to entrained flow reactors that surpass this (up to 1200 °C) [199, 206]. In most of cases, the entrained flow reactors are designed in order to operate with a specific fuel. The raw product gas from an entrained flow reactor has a lesser load of particulates (unconverted char) as well as tars due to its usual higher operating temperature as it is common that these systems operate in ash melting regimes. Both systems can operate at elevated pressures but black liquor gasification is technically easier to accomplish (pressurized feeding or liquids is easier). Therefore such a system can deliver gas more easily at closer to the operating pressures required for HA synthesis. Black liquor product gas yields high H₂S

concentrations. This sulphur is recovered either by employing a downstream Claus process or by absorption in the green liquor from where and it can be returned to the pulp mill [204].

Table 53. Biomass fuel properties used in the modeling.

	Ultimate Analysis (dry mass basis)		Proximate analysis (mass basis)		
	wood	black liquor		wood	black liquor
C	48.75	31.3	moisture	5.10	24.8
H	6.54	3.4	fixed carbon	9.38	12.6
O	44.10	37.3	volatiles	85.22	21.6
S	0.24	5.6	ash	0.30	41.0
N	0.05	0.1			
Na	-	22.4			
<i>HHV</i> (MJ kg ⁻¹)				18.88	12.57

6.2.3 Gas Cleaning

The basic product gas impurities are: particulates (inert material, fly ash, unconverted carbon called char), tars (condensable heavy hydrocarbons with molecular weight higher than benzene), sulphur species (mainly H₂S, COS and mercaptanes), halogen species (HCl, alkali chlorides), nitrogen species (NH₃, HCN), alkali species, as well as volatile metal traces [207]. For most of the catalytic systems, these have to be removed to a certain extent by gas cleaning technologies. A certain amount of tars and alkali species are removed in filtration systems downstream the gasifier together with the particle matter, whereas water and oil scrubbers or thermal cracking catalysts in cold and hot gas cleaning processes can be added for further elimination of these impurities. The desulphurization step is essential in the process as sulfur causes poisoning and limits the life duration of the catalysts used in the production of Higher Alcohols. According to [208], hydrogen sulfide (H₂S), carbonyl sulfide (COS), and mercaptans are reported to have a tolerance concentration level lower than 1 cm³ m⁻³ for both Cu-Zn and MoS₂ catalysts cases, while in [209] the MoS₂ catalysts are reported to have a less strict tolerance of 50 -100 cm³ m⁻³ is reported. The most commonly used cold desulfurization methods are chemical absorption in alkaline-water solution or in alkanolamines or physical solvents (RectisolTM, SelexolTM) whereas in hot methods catalytic conversion and solid sorption are used [210]. Black liquor-fired entrained flow gasifier produces much more sulphur species compared to the wood derived product gas in CFB. The sulfur contained in BL is mainly converted to hydrogen sulfide (H₂S) while some reacts with sodium carried in the fuel for the formation of green liquor. A comparison of H₂S levels for the two gasification systems is shown in the results sections. Although, H₂S can be retrofitted to the green liquor for the conversion to white liquor and further efficient use in the pulp's industry digester, the present work focuses only in the removal of H₂S. SelexolTM and RectisolTM are the mostly known processes for the removal of both H₂S and CO₂ involving di-methyl-ethers of polyethylene glycol and refrigerated methanol respectively. The operating pressure of SelexolTM process is lower than that of RectisolTM, usually 0.2 – 1.4 MPa. SelexolTM has greater selectivity ratio (H₂S to CO₂) than RectisolTM and therefore is selected for sulfur removal. After the solvents regeneration, the hydrogen sulfide can be directed to either a Claus unit for conversion to elemental sulfur or in the case of black-liquor to cover sulfur needs for the conversion to white liquor. Better ratios of absorbed H₂S to CO₂ are achieved with lower temperatures. In the RectisolTM process, which has comparably less energy consumptions than the SelexolTM, the solvent is cold methanol at approximately -60 to -75 °C, which

dissolves the acid gases from the feed gas at relatively high pressure, usually 2.5 – 6.0 MPa. The rich solvent containing the acid gases is then depressurised to release and recover the captured species. The Rectisol™ process can operate selectively to recover the remaining carbon dioxide.

6.2.4 Alcohol synthesis unit

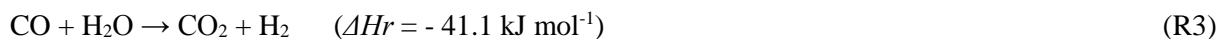
The HA synthesis is performed after the gas is compressed at relatively elevated pressures (8.0 MPa) and depicts higher selectivity at around 325 °C. The mechanism for HA synthesis involves a complex set of reactions with multiple pathways, leading to a variety of products that are impacted by kinetic and thermodynamic constraints [211]. Depending on the process conditions and catalysts used, the most abundant products are typically mixed alcohols (C₂-C₄), methanol, hydrocarbons and CO₂. Linear alcohols are produced in a stepwise fashion involving the synthesis of methanol followed by its successive upgrade to ethanol, propanol, butanol, etc. [212]. Therefore, the HA catalyst should have methanol synthesis activity because methanol can be considered a recurrent C₁ reactant. Both branched and straight chain alcohols can be synthesised with but the present analysis does not go into that detail. In the present conceptual design, two different types of catalysts for HA synthesis, were selected: the modified methanol synthesis catalysts [213], the modified FT (alkalized MoS₂ catalysts) [214]. The general HA synthesis reaction mechanism has the following overall stoichiometry, with n typically ranging from 1 to 8 [215-217]:



In addition, apart from the desirable products (higher alcohols) and methanol that are formed, alkanes and carbon dioxide are also produced, according to the following reaction:



The shift reaction is apparent in all cases:



6.2.5 Alcohol separation and recovery

The last stage of the alcohols production is the recovery unit. The configuration of this unit depends on the definition of “desirable final products”. In other words, the number of higher alcohol products that are required defines the number of separation columns. In all cases, light gases like hydrocarbons, H₂O, CO₂ and unconverted H₂ and CO are considered undesirable and are removed after cooling at a first high pressure flash separator stage. In this case study, the “desired final products” are assumed to be the mixture of the higher alcohols rather than individual compound stream of ethanol, propanol and butanol, so only one column is used for the alcohol mixture recovery. The flow diagram of the HA recovery unit is demonstrated at the **Figure 84**.

Due to low conversion rates of CO, it is very important to recover light gases such H₂ and CO for reuse. Moreover, other gas components such light hydrocarbons (HC) and CO₂ should be removed before mixing with the main syngas stream. In the case studied, an autothermal oxygen driven steam reformer is considered to produce more H₂ and CO from HCs. The light gases from the top of the first flash separator are split into two streams that are both throttled down to a lower pressure (2.6 MPa). One is led to the reforming step and the other to the gas turbine (GT) for power and steam generation in a small combined

cycle. The size of the power is determined by matching its output with the heat and power demands of the overall process.

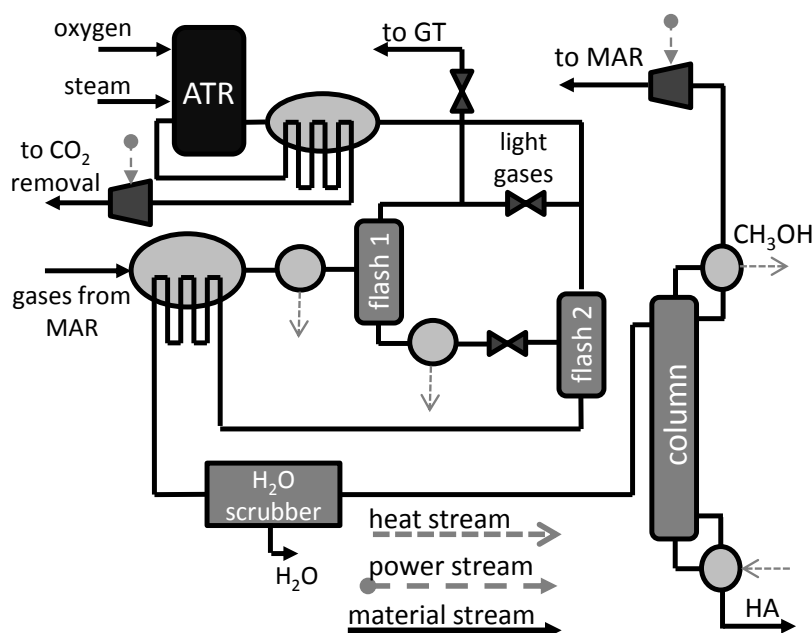


Figure 84. Flow diagram of the Mixed Alcohol separation unit.

6.2.6 Steam production and power generation unit

In order to meet the power and steam demands of the process, a steam cycle combined with gas turbine exists. A portion of the unconverted gases from the alcohol synthesis is led to the gas turbine to be combusted. The turbine exhaust gases provide heat for steam generation through a heat recovery steam generator (HRSG). Additional heat recovery for increase of steam generation is performed through product gas conditioning and cooling. Part of the produced steam is used at the WGS reactor and the Autothermal Reformer, as heating source in the reboilers of the strippers (at H_2S removal unit and alcohol separation unit).

6.3 Methodology and model description

6.3.1 ASPEN Plus™ modeling configuration

Both solid biomass and black liquor gasification modeling is mainly based on chemical equilibrium by means of minimization of free Gibbs energy. The woody biomass modeling is based on an equilibrium model corrected for the methane content of the syngas based on a previous work [207]. In the case of black liquor the prediction of the gaseous products needs to be accomplished together with an evaluation for the liquid (smelt) products: therefore the task is performed using two separated Gibbs reactors (RGIBBS) for the two phases. The adoption of two distinct equilibrium calculations is due to the fact that an overall mass Gibbs minimization would fail to reproduce significant Na_2S quantities which affect both gaseous and smelt compositions. The fate of elements between the two RGIBBSs is based on the ultimate/proximate analysis and on relevant studies [218, 219]. The reason is that the smelt is formed possibly near the wall, at the post flame region [77]. Both woody biomass and black-liquor elemental composition is reported in

Table 1. Special effort is paid for black liquor enthalpy estimation, since it cannot be treated as a typical non-conventional material in Aspenplus™ because its ash content influences the chemical equilibrium and is not considered as inert. The separation of syngas from the smelt is conducted at the quencher that is simulated as a flash separator, assuming phase equilibrium. The black liquor model closely predicts the syngas produced (**Table 54**) [215], but most importantly is a tool to predict the energy balance around the gasifier and its oxygen requirements.

Table 54. Comparison of prediction syngas composition with the corresponding experimental values from [215].

$\lambda = 0.40$	Experimental	this model
	mol fraction %	
H ₂	35.80	36.72
CO ₂	34.10	31.86
CO	25.50	26.06
CH ₄	2.70	2.70
H ₂ S	1.90	1.86
LHV (kJ kg ⁻¹)	7531	7964

The property method that is used at each unit of the biorefinery is shown in **Table 55**, whereas the input parameters of the whole biorefinery are summarized in **Table 56**. The selection of the suitable property method for each process unit was based mainly on the relevant to similar process design efforts works [77, 203, 220].

Table 55. Selection of physical property methods for process modeling.

Unit	Property method
Gasifier	IDEAL (Ideal gas law) [221]
H ₂ S removal (Selexol)	PC-SAFT (Perturbed-Chain Statistical Associating Fluid Theory equation of state) [92]
CO ₂ removal (Rectisol)	RK-SOAVE (Redlich-Kwong-Soave equation of state) [221]
Alcohol synthesis & separation	NRTL (Non-Random Two-Liquid activity coefficient model) [203]
Combined Cycle	RK-SOAVE (Redlich-Kwong-Soave equation of state) [222]

Gas cleaning from H₂S and CO₂ takes place in absorbers assuming phase equilibrium at each of their stages. The most important aspect is to define the appropriate thermo-physical properties and equation of state in order to simulate the phenomenon of physical absorption and acid gas removal with high accuracy. In the CO₂ removal unit, CO₂ is sequestered at two stages in flash separators after throttling the lean solvent. By using this configuration, the second column for stripping the Rectisol™ solvent is not needed. This unit requires power consumption for pumping and externally cooling the rich solvent before its introduction into the absorber.

Table 56. Assumptions for the process parameters (based on [89, 185, 203, 217, 223])

Air Separation	
Oxygen purity, y_{O_2}	97.0
Compressor polytropic efficiency η_{pol}	82.0
Gasification unit	
Equivalence ratio, ER	0.40 for BL & 0.30 for wood
Gasifier temperature, T_{gas}	950 °C for BL & 800 °C for wood
Gasifier pressure, p_{gas}	2.7 MPa
Syngas temperature after cooling, T_{syn}	120 °C for BL & 200 °C for wood
Syngas conditioning and acid gas removal unit	
Target H ₂ /CO	2.0
H ₂ S content in the clean syngas, $y_{H_2S, clean}$	10 ⁻⁶ vol
CO ₂ capture rate, CCR	99.0
H ₂ S absorber stages	10
CO ₂ absorber stages	10
H ₂ S stripper stages	3
Rich solution: Selexol solvent / H ₂ O (w/w %)	90.0
Rich solution: Rectisol solvent H ₂ O (w/w %)	98.0
Autothermal reforming temperature, T_{ATR}	950°C
HC conversion at the ATR	99.0
Alcohol synthesis unit	
Synthesis temperature, T_{alc}	325°C
Synthesis pressure, p_{alc}	8.0 MPa
Compressors polytropic efficiency, η_{pol}	80.0
Gas Hourly Space Velocity, GHSV	2000 h ⁻¹
Higher alcohol recovery unit	
Separation column stages	70
Pressure outlet of the column, p_{col}	2.6 MPa
% Methanol recovery	99.6
% HA recovery	99.9
Power island	
Turbine Inlet Temperature, TIT	1350 °C
GT Compressor & Turbine polytropic $\eta_{p,C}$ & $\eta_{p,T}$	90.9% & 93.6%
Combustor pressure, p_{comb}	1.8 MPa
Evaporators pinch point	10 °C
Superheated steam	500 °C & 15 MPa
Reheated steam	500 °C & 3 MPa
Steam turbine isentropic efficiency, η_{st}	84 (HP), 82 (LP)
Condenser pressure	5·10 ⁻³ MPa

6.3.2 Modeling of the Mixed Alcohol Reactor (MAR)

In this study, the mixed alcohols synthesis is investigated for two different types of catalysts based on the corresponding kinetic expressions obtained from the literature. For a rigorous investigation of the catalytic process, a Plug Flow Reactor (RPLUG) in conjunction with an equilibrium reactor (REQUIL) is used. The RPLUG simulates the alcohol production in the MAR according to the kinetic rates of the reactions while the REQUIL follows the former in order to estimate the CO₂ that is yielded from the water gas shift reaction. As far as the HAS with MoS₂ catalyst type is concerned, and according to the Langmuir-Hinshelwood (LH) model, the reaction rate is expressed by the following equation, based on mass of the catalyst and the partial pressure of the components that take part in the reaction:

$$r_i = \frac{\overbrace{A_i \cdot \exp\left(-\frac{E_i}{R}\left(\frac{1}{T} - \frac{1}{T_o}\right)\right)}^{\text{kinetic factor}} \left[\overbrace{k_1 \prod_{i=1}^N p_i^{a_i} - k_2 \prod_{j=1}^N p_j^{\beta_j}}^{\text{driving force}} \right]}{\underbrace{\left[\sum_{i=1}^M K_i \left(\prod_{j=1}^N p_j^{a_j} \right) \right]^m}_{\text{adsorption}}} \quad (\text{Eq. 33})$$

The production rates of methanol, ethanol, propanol and methane are evaluated according to the kinetic model that is presented in [224]. Concerning the HAS over a modified methanol catalyst (Cs-doped Cu-Zn composite catalyst) the corresponding kinetic rates are obtained from the experimental study of Kulawska and Skrzypek [214]. In this study, the following power law expression is proposed:

$$r_i = A_i \cdot \exp\left(-\frac{E_i}{RT}\right) p_{H_2}^{n_i} \quad (\text{Eq. 34})$$

However, in this study, the hydrocarbons formation is not taken into account, even though it is expected, according to similar studies [216, 225, 226]. The methane selectivity is assumed to an average value of 5% obtained from [216, 225, 226]. The expressions of the kinetic rates of the reactions that take place in the MAR and the parameters values are presented in **Table 57** and **Table 58a** and b respectively.

Table 57. Reactions and their corresponding rates according to the Gunturu model [213].

Reactions	LH kinetic rate expressions
$\text{CO} + 2\text{H}_2 \rightleftharpoons \text{CH}_3\text{OH} \quad \Delta H_r = -92 \text{ kJ mol}^{-1}$	$r_{\text{CH}_3\text{OH}}^{\text{gross}} = \frac{A_m \cdot \exp\left(-\frac{E_m}{R}\left(\frac{1}{T} - \frac{1}{T_o}\right)\right) [k_1 \cdot p_{\text{CO}} \cdot p_{\text{H}_2}^2 - k_2 \cdot p_{\text{CH}_3\text{OH}}]}{[1 + K_1 \cdot p_{\text{CO}} + K_2 \cdot p_{\text{H}_2}^2 + K_3 \cdot p_{\text{CH}_3\text{OH}}]^3} \quad (\text{Eq. 35})$
$\text{CH}_3\text{OH} + \text{CO} + 2\text{H}_2 \rightleftharpoons \text{C}_2\text{H}_5\text{OH} + \text{H}_2\text{O} \quad \Delta H_r = -165.1 \text{ kJ mol}^{-1}$	$r_{\text{C}_2\text{H}_5\text{OH}}^{\text{gross}} = \frac{A_e \cdot \exp\left(-\frac{E_e}{R}\left(\frac{1}{T} - \frac{1}{T_o}\right)\right) [k_1 \cdot p_{\text{CH}_3\text{OH}}]}{1 + K_1 \cdot p_{\text{CH}_3\text{OH}}} \quad (\text{Eq. 36})$
$\text{C}_2\text{H}_5\text{OH} + \text{CO} + 2\text{H}_2 \rightleftharpoons \text{C}_3\text{H}_7\text{OH} + \text{H}_2\text{O} \quad \Delta H_r = -432.2 \text{ kJ mol}^{-1}$	$r_{\text{C}_3\text{H}_7\text{OH}}^{\text{gross}} = \frac{A_p \cdot \exp\left(-\frac{E_p}{R}\left(\frac{1}{T} - \frac{1}{T_o}\right)\right) [k_1 \cdot p_{\text{C}_2\text{H}_5\text{OH}}]}{1 + K_1 \cdot p_{\text{C}_2\text{H}_5\text{OH}}} \quad (\text{Eq. 37})$
$\text{CH}_3\text{OH} + \text{H}_2 \rightleftharpoons \text{CH}_4 + \text{H}_2\text{O} \quad \Delta H_r = -265.2 \text{ kJ mol}^{-1}$	$r_{\text{HC}}^{\text{gross}} = \frac{A_h \cdot \exp\left(-\frac{E_h}{R}\left(\frac{1}{T} - \frac{1}{T_o}\right)\right) [k_1 \cdot p_{\text{CH}_3\text{OH}}]}{1 + K_1 \cdot p_{\text{CH}_3\text{OH}}} \quad (\text{Eq. 38})$

Table 58a Parameters for LH kinetic model setup for alcohol synthesis for MoS₂ catalyst [224]

i	pre-exponential factor	activation energy ¹	driving force factors		adsorption factors		
	A (kmol s ⁻¹ kg ⁻¹)	E (kJ mol ⁻¹)	k ₁	k ₂	K ₁	K ₂	K ₃
CH ₃ OH	4.062·10 ⁻⁶	143.472	1.396·10 ⁻¹⁹	1.087·10 ⁻²⁰	3.870·10 ⁻¹⁵	3.562·10 ⁻⁷	1.235·10 ⁻⁵
C ₂ H ₅ OH	8.477·10 ⁻⁷	24.986	1.237·10 ⁻⁵	0	9.111·10 ⁻⁶	0	0
C ₃ H ₇ OH	5.966·10 ⁻⁸	89.333	9.869·10 ⁻⁵	0	6.006·10 ⁻⁵	0	0
CH ₄	2.607·10 ⁻⁶	95.416	1.237·10 ⁻⁵	0	1.542·10 ⁻⁵	0	0

¹ T_o=598K

Table 52b: Parameters for kinetic model setup for alcohol synthesis for Cu-Zn catalyst [214]

i	pre-exponential factor	activation energy	exponent
	A (mol h ⁻¹ g ⁻¹ MPa ⁿ)	E (kJ mol ⁻¹)	n
CH ₃ OH	59.4	72.19	2.0
C ₂ H ₅ OH	268.0	81.45	1.5
C ₃ H ₇ OH	48.3	78.10	1.5

6.4 Results and discussion

6.4.1 Comparison of the performance of two different catalyst types

The stream results of the wood gasification system up to the MAR (mixed alcohol reactor) for both catalyst types are summarized in **Table 59a** and b. Both cases have similar pressures and temperature profiles. Cu-Zn catalyst has a much higher requirement for recycling of methanol and unreacted gas. This results in slightly higher temperatures of that case after mixing with the unreacted MeOH stream. The corresponding mass flows (here indicated as ratios over raw biomass processed) result higher for the case of Cu-Zn based catalysts.

Table 59a: Stream results of the syngas along its conditioning prior to MoS₂ catalyst.

	m	T	p	H ₂ O	CO ₂	H ₂	CO	CH ₄	Ar	CH ₃ OH	H ₂ S
stream after:	kg _{syngas} /kg _{wood}	°C	bar	mol fraction %							
Gasifier/quench	1.310	200.0	27.00	13.79	17.88	28.08	33.54	6.50	0.06	0.00	0.11
H ₂ S removal	0.683	110.0	25.96	0.08	1.36	40.99	48.38	9.07	0.07	0.00	50·10 ⁻⁴
WGS	0.730	300.0	25.96	0.19	7.07	44.36	39.72	8.54	0.07	0.00	49·10 ⁻⁴
mixing with recycling gas	4.274	369.4	25.96	13.16	4.55	52.05	26.04	2.61	1.50	0.00	8·10 ⁻⁴
CO ₂ removal	2.911	-20.0	24.94	0.00	0.06	63.33	31.63	3.06	1.79	0.03	0.00
mixing with recycling MeOH	2.937	-16.2	24.94	0.00	0.08	63.14	31.53	3.05	1.78	0.30	0.00
gas to GT (tail gas)	0.138	41.0	25.00	0.06	5.09	60.56	24.54	7.23	2.06	0.12	0.00

Table 53b: Stream results of the syngas along its conditioning prior to Cu-Zn catalyst.

	m	T	p	H ₂ O	CO ₂	H ₂	CO	CH ₄	Ar	CH ₃ OH	H ₂ S
stream after:	kg _{syngas} /kg _{wood}	°C	bar	mol fraction %							
Gasifier/quench	1.310	200.0	27	13.79	17.88	28.08	33.54	6.50	0.06	0.00	0.11
H ₂ S removal	0.683	110.0	25.96	0.08	1.36	40.99	48.38	9.07	0.07	0.00	10 ⁻⁴
WGS	0.709	300.0	25.96	0.11	4.72	42.99	43.31	8.76	0.07	0.00	0.97·10 ⁻⁴
mixing with recycling gas	5.423	333.9	25.96	8.79	2.90	55.77	27.83	4.00	0.66	0.00	0.10·10 ⁻⁴
CO ₂ removal	4.174	-20.0	24.94	0.00	0.03	63.35	31.48	4.34	0.73	0.03	0.00
mixing with recycling MeOH	4.480	17.5	24.94	0.00	0.04	61.78	30.70	4.23	0.71	2.50	0.00
gas to GT	0.246	51.6	25.00	0.00	0.61	62.65	30.30	4.65	0.75	0.94	0.00

In the case of MoS₂ catalyst applied to wood derived gas (“case A₁”), the CO and H₂ conversion rates are calculated at 32.8% and 17.2%, respectively. On the other hand, the conversion rates when applying the modified methanol catalyst on wood derived syngas (“case B₁”) are 7.7% and 5.2%. This means that the MoS₂ based catalysts are far better in achieving greater productivities of ethanol and propanol per kg wood processed (**Table 60**). Cu-Zn catalysts still sustain their attributes towards MeOH production which increases drastically the requirements for gas recirculation. The reactor size at least triples compared to an ideal case of a single-pass reactor. The requirements of the system for steam and power determine the portion of the tail gas that is diverted to the power island. In case A₁, this portion is 16.2% whereas in case B₁ is 32.2%.

Table 60. Specific flow rates of products and other basic streams of the biorefinery.

catalyst type	MoS ₂	Cu-Zn
Mass yields per kg _{wood}	g of alcohol	
Ethanol	89.45	39.64
Propanol	39.02	20.30
Specific steam demand per kg _{wood} for:	kg _{steam}	
WGS	0.023	0.027
Reforming	0.274	0.602
H ₂ S reboiler	0.005	0.019
Specific O ₂ demand per kg _{wood} for	kg of O ₂	
gasification	0.653	0.653
reforming	0.254	0.251

Table 61 shows the results of specific energy consumptions for those two cases. Most power is consumed at the Air Separation Unit for the production of pressurized pure oxygen stream, which is primarily used for the gasification and at the compressors for recycling of the unreacted syngas and recovered methanol at the main syngas stream. This is attributed to the low pressure of HAS recovery unit, as the pressure ratio of the compression is quite high (around 8.0). On the other hand, power consumptions for syngas compression is lower not only because of the lower pressure ratio (3.2) but also because of the low inlet temperatures of the gases coming out of the CO₂ removal unit.

The H₂S removal unit has both high power and heat consumptions, for the solvent pumping and its total regeneration at the stripper, respectively. This is the major disadvantage of the SelexolTM process for acid gas removal but the reasons for its selection were described above. MoS₂ based catalyst might be able to sustain H₂S to few ppm higher, provided the WGS catalysts employed is “sour type”.

Table 61 Biorefinery sub-units specific power consumptions.

	MoS ₂ catalyst		Cu-Zn catalyst	
	kJ/g _{HA}	% HHV biomass input	kJ/g _{HA}	% HHV biomass input
ASU	5.6	3.62	18.5	5.88
syngas compression	7.4	4.85	27.6	8.75
recycling compression	0.6	0.37	3.0	0.94
H ₂ S removal	0.1	0.52	1.6	0.52
CO ₂ removal	1.9	1.29	5.9	1.86
Total consumptions	15.6	10.17	56.6	17.96

As it is very likely that HA production from biosyngas might be first applied to black liquor gasification, these cases are also presented in **Table 62**, comparatively to the wood based gasification. The product gas heating value from wood gasification is greater than the corresponding of black liquor gasification. This is mainly due to the high ash content of black liquor that remains as liquid after the gasification in order to form the green liquor (reused in the pulping process). Although the H₂S removal from BL syngas has larger energy and heat demands than the wood based gasification, the impact on total power consumptions is not considerable.

Table 62. Comparing the energy balances of black liquor vs. wood biomass gasification.

feedstock type	wood	black liquor
	% HHV feedstock input	
Raw syngas HHV	74.0	60.7
Conditioned syngas HHV	63.6	52.6
ASU power consumptions	3.62	4.76
AGR power consumptions	1.33	2.02
Total power consumptions	10.2	10.4
Higher Alcohols HHV	21.0	14.2

Black liquor gasification has already found applications in MeOH production [204]. Assuming MeOH as a useful product that can be co-produced with higher alcohols widens the useful products list. This also reduces the power consumption attributed to methanol recirculation. **Table 63** summarizes the black liquor towards mixed alcohol productivity including the cases of methanol as a product (cases C and D based on MoS₂ and Cu-Zn catalyst respectively).

Table 63 Effect of methanol recirculation on plant performance (black liquor case).

case	catalyst type	MeOH recirculation	CO conversion	H ₂ conversion	HA production (g kg ⁻¹ of BL)	MeOH production (g kg ⁻¹ of BL)
A ₂	MoS ₂	yes	21.89	11.50	27.03	-
B ₂	Cu-Zn	yes	5.3	3.6	13.84	-
C	MoS ₂	no	21.51	11.71	24.78	7.32
D	Cu-Zn	no	5.4	3.6	7.75	4.21

6.4.2 Sensitivity analysis

In this section, sensitivity analyses of several operating parameters of the MAR are performed.

a) GHSV (gas hourly space velocity)

Figure 85 reveals the effect of the Gas Hourly Space Velocity (GHSV): lower values lead to higher production and selectivity rates by allowing the further completion of desired reactions. The flow rates of recycled gases are reduced together with power consumption.

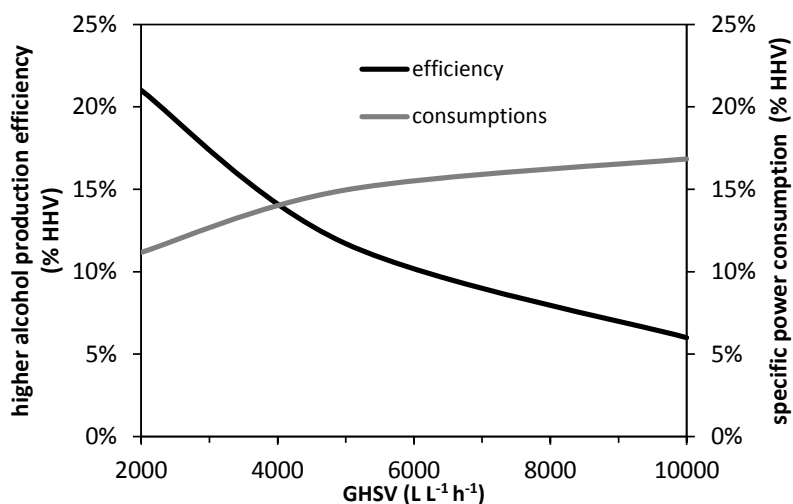


Figure 85. Effect of GHSV in the reactor on the system performance ($H_2/CO = 2$, MoS_2 catalyst at $T=325\text{ }^{\circ}C$ and $p=8.0\text{ MPa}$)

b) Synthesis Pressure and temperature

Figure 86a shows the positive effect of increased pressures on the synthesis process. For operating pressures up to 12.5 MPa the alcohols productivity increases dramatically and the power consumptions for recycling are lowered. However, it should be noted that as the operating pressure elevates, the capital cost increases too. **Figure 86b** shows clearly why 325 $^{\circ}C$ is considered the optimum temperature for HA synthesis [227, 228].

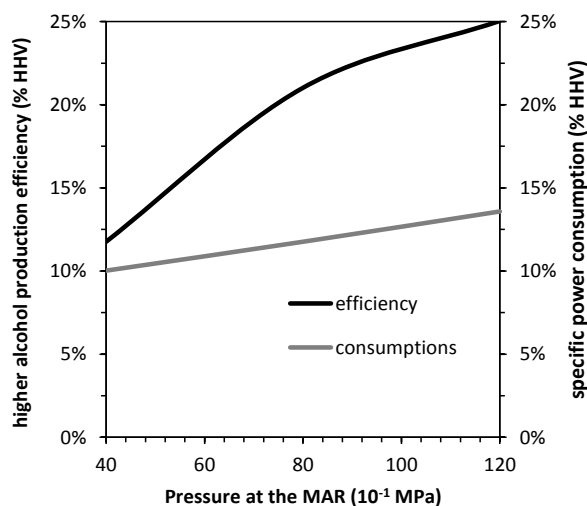


Figure 86a. Pressure effect on the alcohols productivity and the specific power consumption ($H_2/CO = 2$, MoS_2 catalyst at $T=325\text{ }^{\circ}C$)

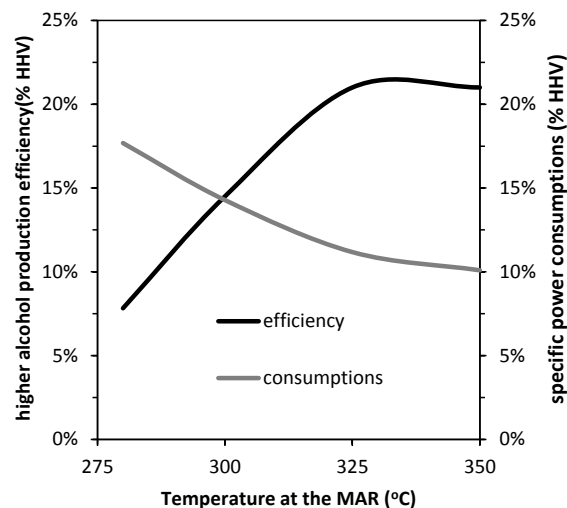


Figure 86b. Temperature effect on the alcohols productivity and the specific power consumption ($H_2/CO = 2$, MoS_2 catalyst at $p=8.0\text{ MPa}$)

c) The effect of H_2 to CO ratio

Running a Gibbs free energy minimization equilibrium calculation for a H_2/CO ratio of 2.0, and including the potential evolution of solid carbon in the clearly defined form of graphite $C_{(s)}$, at $T = 325\text{ }^{\circ}C$ and $p = 8\text{ MPa}$ it is apparent that carbon atoms could be lost (thermodynamically predicted at a rate of

26%). This means that the catalyst system would suffer in long term operation with deposited carbon. **Figure 87** shows that if higher than the usually adopted H_2/CO ratios were to be selected, the WGS reaction would have to be pushed by more H_2O and resulting into loss of CO towards CO_2 . Therefore, a special care has to be given to the H_2/CO to be high enough to avoid any carbon deposition on the catalysts but also maintain loss of carbon into the form of CO_2 low.

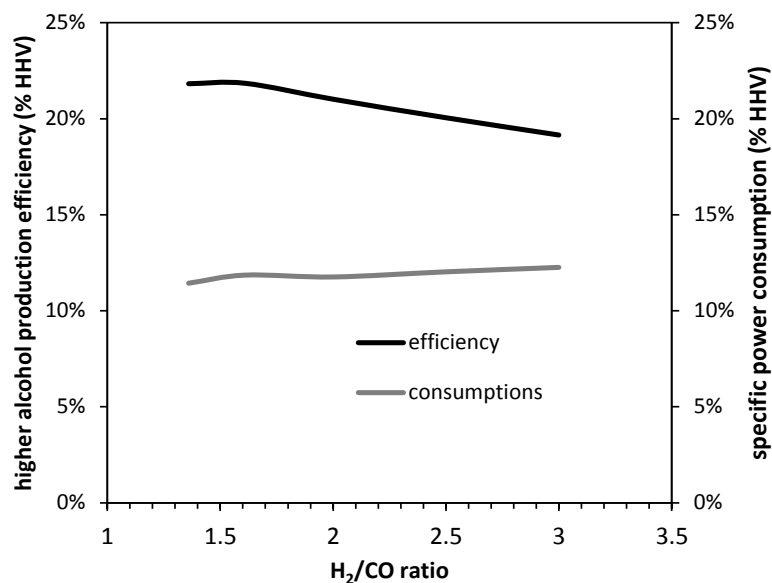


Figure 87. H_2 to CO ratio effect on efficiency and specific power consumption.

6.5 Conclusions

A process modeling of an integrated biorefinery for higher alcohols production based on black liquor gasification was set up in AspenplusTM. Modeling of two different catalysts types (Cu-Zn based) and (MoS₂ based) were integrated. The resulting systems were analysed for their energetic efficiency and the losses occurring in the major unit operations for both cases of using either woody biomass or black liquor. The results revealed that the MoS₂ based catalysts are far better as far as productivity and efficiency compared to modified Cu-Zn catalysts that produce a lot of MeOH that requires separation recirculation. If this MeOH is a useful product then system efficiencies could be slightly improved. Operating pressure has a positive effect on higher alcohols productivity. Technically black liquor gasification can be accomplished more easily at higher pressures but high pressures also lead to elevated methane content in the product gas, which needs to be reformed. Co-produced hydrocarbons have a detrimental effect on efficiency since the energetic penalties of their separation, oxygen driven autothermal reforming and recycling are great. These penalties are mainly associated with the Air Separation Unit and the compression power required for unconverted gas recycling.

7. Alternative thermochemical routes for aviation biofuels via alcohols synthesis: process modeling, techno-economic assessment and comparison

7.1 Introduction

In 2012, the worldwide flights produced 698 million tons of CO₂, making aviation fuels responsible for 12% of CO₂ emissions from all transport sources [229] with U.S. accounting for 40% of them [230]. In 2010, the world jet fuel consumption was calculated to nearly 5,220 barrels per day [231]. Forecasts predict that by 2020 the global aviation emissions will be 70% higher than in 2005 and by 2050 they will further grow by 300-700% [232]. Apart from the significant increase in Greenhouse Gas emissions, other factors like high dependency of aviation fuels on fossil fuels and great uncertainty on oil prices have turned the attention on alternative sources of aviation fuels. Only 2% of global transportation fuels are based on biofuels derived from biomass [233]. It is reported [124] that in 2012, the most energy consumptive sector was the transportation sector, demanding 27 quadrillion BTU of energy. EIA's report forecasts, for 2040, a world production of liquid fuels from biomass up to 2.5 Mbpd (million barrels per day). In addition to this, by the year 2050, it is forecasted that biofuels will contribute to bringing down the dependency of the transportation sector on oil products to 29% [234]. Another example that highlights the important role of biofuels is that of Asia. Asia, the world's largest emitter of carbon dioxide, which is forecasted to be the world's highest fuel consumer by 2030, has already turn its attention to the production and development of biofuels [235]. Stemming from these facts, the concept of blending biomass-derived aviation fuels, which have less contribution to carbon emissions than pure fossil based fuels became attractive and has been considered as a hopeful "environmental challenge" [236].

The two main types of aviation fuels are gasoline (avgas) and jet fuel (kerosene) (C8-C16) [237]. They are composed mainly of paraffins and cycloparaffins and smaller amounts of aromatics and olefins along with some additives specified by each category of aviation fuel [238]. Due to the special conditions during flight there are strict guidelines for the aviation fuel properties concerning its melting point, viscosity, non freezing or cloudiness phenomena at low temperatures, etc [239]. At atmospheric conditions both gasoline and kerosene are in liquid form. Owing to the lower carbon chain number in gasoline mixtures, it is more volatile than jet fuel (boiling points: 40-200°C and 150-300°C respectively). The characteristics of each aviation fuel type are strictly specified due to the extreme conditions under which combustion takes place. Avgas is used in internal combustion engines that can operate up to a limited altitude ceiling (<6000 m) and therefore is used in reciprocating engines like small aircrafts and light helicopters. This constraint has led to the predominance of jet engines in the air transport sector (more than 98% of the total aviation fuel consumed is jet fuel [240]). Concerning jet fuels, there is a greater variety in categories which are separated based on the military (e.g. JP4 and JP8) and commercial (e.g., Jet A1 and Jet B) use, since each service has its own operational requirements.

The main conventional method for aviation fuels production is through refining of crude oil. The main processes of upgrading crude oil to fuels are fractional distillation, hydrotreating and hydrocracking. Refining may include one or a mix of these processes depending on the specifications needed for the aviation fuel. Another method is through Fischer Tropsch Synthesis (FTS) where the feedstock (coal, natural gas or biomass) is firstly converted into a H₂/CO gas mixture (syngas) via gasification, following by the hydrocarbons synthesis mainly of long chain paraffins, olefins, alcohols and aldehydes. Depending

on the catalyst used, the operating temperature and pressure of the FTS reaction and the H_2/CO ratio of syngas, the carbon number of the fuel product can be oriented, thus meeting the requirements for aviation fuels [241]. However, FTS process using as feedstock coal or gas (Coal-to-Liquids, Gas-to Liquids concepts) has some drawbacks: Apart from the high cost of the process and the uncertainty on gas prices, there is an issue about CO_2 emissions as they are higher than refining crude oil [242]. Biomass, being a renewable source, offers the potential production of alternative fuels that have a smaller CO_2 emissions footprint compared with the fossil based fuels. This is the main drive that attracts policies and correspondingly industries to do business in this sector [243]. Yet, not only need the biomass derived fuels for the aviation sector to have the same specification with the conventional jet fuel types, but they also should be compatible with the typical jet fuel engines because of the aircrafts long lifetime [241]. C.J. Chuck & J. Donnelly [244] have examined the compatibility of several bio-derived fuels with Jet fuel and their potential for blending with the conventional aviation fuel.

Currently, there are companies that have adopted the FT process. Sasol, a South African company, produces and distributes aviation fuel, made from coal via Fischer Tropsch [245]. Another company, Syntroleum, produce jet fuel from FT process using natural gas as feedstock [246]. Both companies have turned their attention to producing jet fuel derived from biomass. U.S. Air Force (USAF), which is the leading user of aviation fuels worldwide, has embraced these methods and started co-operating with these companies by using a 50:50 blend of synthetic fuel and conventional kerosene [242, 247].

Along with the biomass derived fuels trend, another method for producing aviation fuels is conducted by Gevo [248]. During that process, biomass feedstock is firstly fermented to iso-butanol followed by dehydration to olefins, oligomerization and hydrogenation, resulting to iso-paraffinic kerosene, a blendstock for jet fuel with C12-C16 hydrocarbons. This final product can be blended up to 50:50 ratio with petroleum-derived jet fuel and has a low freezing point ($-80^\circ C$) suitable for aviation use. Last but not least, Byogy Renewables Inc. currently produces jet fuel from biochemically-derived ethanol. Ethanol after being dehydrated, it is converted into long chain hydrocarbons via catalytic synthesis that are continuously fractionated into jet fuel and gasoline. Apart from ethanol, Byogy's technology can effectively process either propanol or butanol. The produced jet fuel can be used even as a fully substitute for oil-derived jet fuel or used at any blend ratio with conventional jet fuel [249].


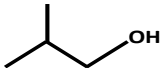
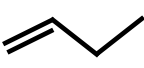
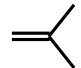
In this study, the techno-economic evaluation of various thermochemical pathways for branched paraffins production from biomass that are aimed at aviation fuel substitution is performed. Unlike the majority of similar assessments, this study pays attention to the fuel upgrading section, resulting to the desired final product (here, the long chain hydrocarbons as aviation fuel substitution). Among the under investigation cases, the conventional FTS route as well as novel thermochemical routes through Mixed Alcohol Synthesis (MAS) are involved. According to the latter, branched paraffins that can be used as kerosene substitute, are formed from butanol isomers after certain fuel upgrading procedure. The fuel upgrading methodology after mixed alcohol synthesis depends on the catalyst that is used, since different butanol isomers are formed (see next section). The main economic parameters that are related to the total capital and operational investment are estimated based on data provided from process simulation of the examined cases and on the literature for the cost estimation of each component. Besides, the biochemical options for bio-butanol production through bio-ethanol and the acetone-butanol-ethanol process (ABE) are also investigated and evaluated in comparison with the corresponding thermochemical options.

7.2 Biomass-to-jet fuel potential pathways

In order to convert biomass into aviation fuels, there are numerous pathways and processes to do so. In **Figure 88**, some of these pathways are indicated. There are several engineering research efforts on the development of alternative pathways to avionic jet fuel components [241] such as the production of lower alcohols (C1-C3) as block chemicals derived from thermochemistry [175, 194, 203, 250] or fermentation [251-254], followed by increasing the alcohols' carbon chain length by means of Guerbet reactions [255] or by dehydration to olefins that then undergo oligomerization [256]. For instance, in Gevo's technology isobutanol is used as block chemical [248], whereas in Byogy process, ethanol is the basis for long chain paraffins production [249]. In both cases, the (valuable) intermediate chemicals that are produced (olefins, higher alcohols and paraffins) along the processes can be retrieved, purified and considered as final products. Another, more direct, approach is the pyrolysis and upgrading of the pyrolytic oil (bio-oil) [257-259] which still requires basic development and will not be examined in this work. In addition, biofuels can also be produced from algae [260, 261], from animal residue [262] or from CO₂ with water and solar energy (Solar to petrol-S2P) [263]. Continuously, jet fuel can be also produced by catalytic conversion of biomass hydrolysate in aqueous phase [39]. Furthermore, there are even more routes that can lead to branched paraffins though they are not adopted because of high cost levels, and lack of technological establishment.

One of the important block alcohols mentioned before is butanol. As a biofuel for internal combustion engines, it has the potential to replace ethanol [233, 264]. Although it blends well with gasoline it cannot be successfully mixed in jet fuel without further upgrading to compounds with longer carbon chains. The carbon atoms structure in the butanol molecule can be either linear (1- and 2-butanol) or branched (tert- and iso-butanol), the properties of which such as boiling temperature and melting point are different (see **Table 64**). Consequently, the corresponding olefins that are produced via alcohol dehydration differ from each other. In this study, the aviation fuel (jet fuel and gasoline) production by means of syngas towards mixed alcohol synthesis is examined. The alcohols mixture, by gas phase Guerbet, leads to the C₄ block alcohols that undergo dehydration towards C₄ olefins, which through oligomerization and hydrogenation are transformed to desired branched paraffins that can blend well with fossil derived jet fuels.

Table 64. Main properties of main butanol and butylene isomers

butanol/butene isomers	n-butanol	isobutanol	1-butene	isobutylene
organic group	alcohols		olefins	
molecular weight (kg/kmol)	74.12	74.12	56.11	56.11
molecular structure				
boiling temperature (°C)	117.7	108	-6.47	-6.9
melting point (°C)	-89.8	-101.9	-185.3	-140.3
autoignition temperature (°C)	343	415	385	465
flash point (°C)	35	28	flammable	flammable
density at 20°C (kg/m ³)	809.8	801.8	2370	588
viscosity at 25°C (mPas)	2.54	4.31	7.76	7.36
standard heat of combustion (kJ/mol)	2670	2670	2717	2526

One of the purposes of this paper is the techno-economic evaluation of converting biomass to aviation fuels according to five process options/pathways, which are enclosed in frameworks with dotted line in **Figure 88**. Two of the three thermochemical pathways to aviation fuels are thoroughly investigated in terms of performance and cost analysis and are compared with the third thermochemical option, the FTS route, and with two cases on biochemical pathway. In the case of thermochemical routes, a detailed costing

methodology is presented, taking into account all the process steps that are involved in syngas production and conditioning, fuel synthesis and upgrading. On the other hand, in the biochemical pathways, the economic data for the part of the plant that is related with the alcohols synthesis (ethanol and butanol) was obtained from the literature and only the equipment costs in the fuel upgrading unit (alcohol to jet fuel) were calculated in detail. This study focuses on the technological choices for renewable bio based fuels production for airborne applications. Since these are bound to biomass feedstock choices, the appropriate feedstock for each technological route is considered.

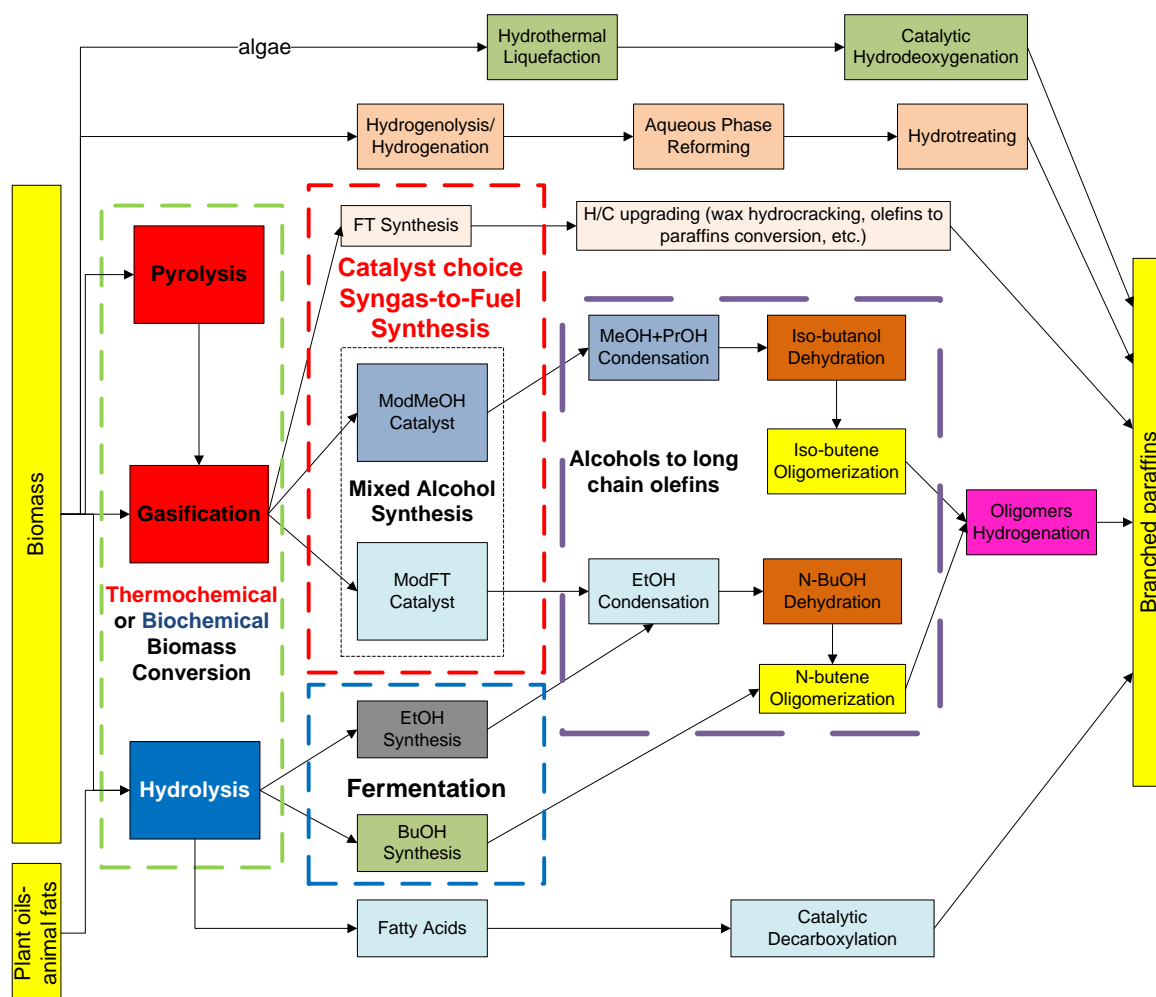


Figure 88. Biomass-to-branched paraffins pathways

Figure 89 presents schematically the process steps for the liquid aviation fuel production from biomass based on Alcohols to Jet fuel (ATJ) concept. The complex organic structures of lignocellulosic biomass are thermally transformed into simple compounds by mean of gasification. After a multi-step procedure, the syngas composed of CO and H₂ is used for synthesis of a mixture of light alcohols [175, 265]. The aviation fuels can be produced from these alcohols after they have been upgraded. The organic compounds that do not participate in the branched paraffins synthesis have to be reformed back into syngas and their carbon atoms to be reused. Such a biorefinery concept is able to cover its own heat and power requirements (self-sustained). Thus, part of the recirculating light gas (tail gas) is utilized in a Cogeneration Heat and Power (CHP) in order to meet steam, heat and power requirements of the overall process. The majority of the analyses of such biorefinery concepts are examined for large scale applications with feedstock thermal input ranging from 150 to 500 MW_{th} [266-272]. According to the NREL study, the

product cost (\$/kg) sharply increases for small plant capacities [273]. Furthermore, a typical value for the capital cost scaling factor of a biorefinery has been estimated at 0.7[274], implying the advantage of plants with larger capacity in terms of economic feasibility against the smaller ones. On the other hand, for higher capacities, issues like biomass availability and logistics costs emerge and therefore biorefinery concepts with larger scale are avoided for investigation. In this light and, in order the results to be easily compared to the corresponding studies in the literature, the selected feedstock thermal input of the examined plant is 190 MW_{th}.

7.2.1 Syngas production from lignocellulosic biomass

The biomass source assumed in this work is wood that can be easily gasified to produce syngas. This part of the bio-refinery process has already been described in previous study [175].

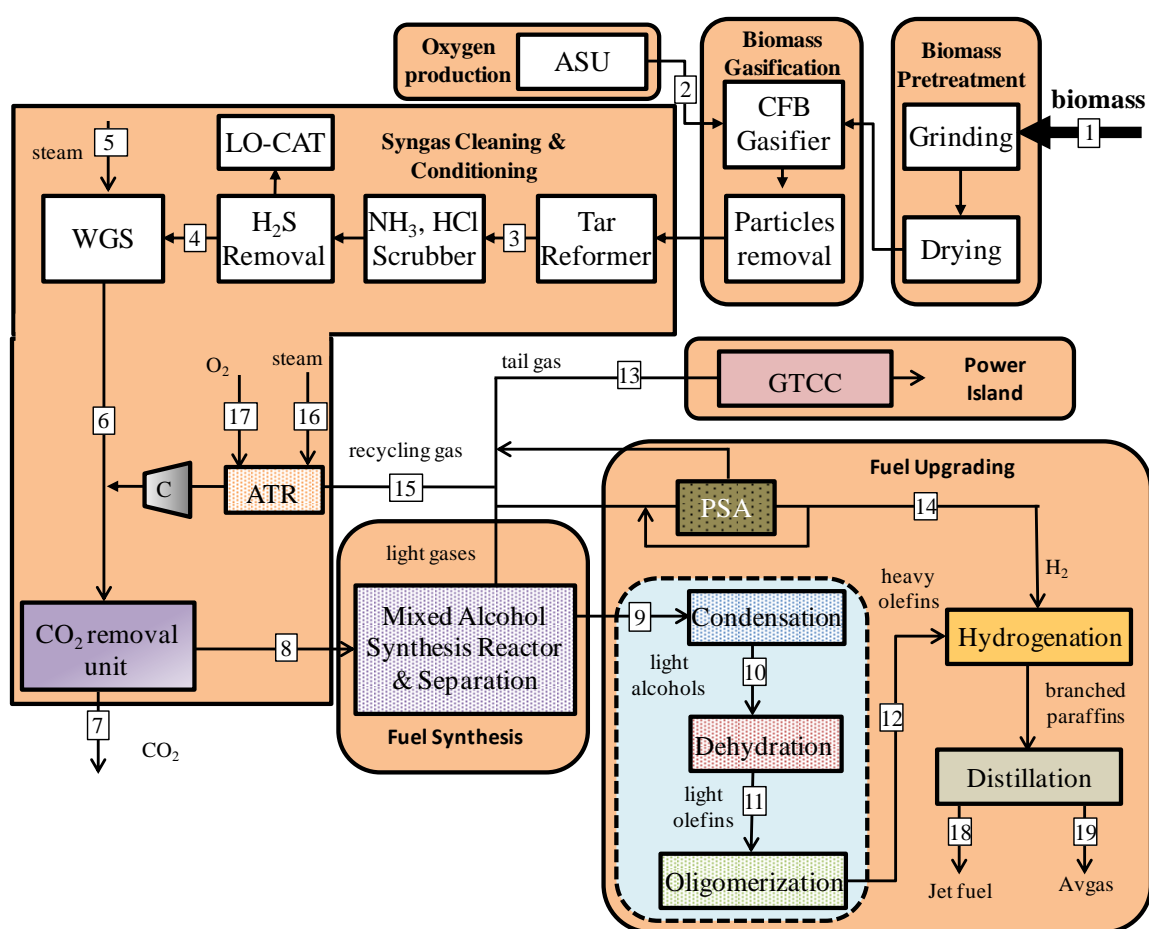


Figure 89. Conceptual process overview of branched paraffins production from mixed alcohols

Figure 89. depicts the process steps for syngas production at the pressurized oxy-blown gasifier, the gas cleaning including the NH_3 , HCl , H_2S and CO_2 and the syngas conditioning in the Water Gas Shift (WGS) reactor, so that to meet the desired H_2/CO ratio at the synthesis unit. This assessment study does not discuss at length the selection of each technology/method for syngas production, gas cleaning and conditioning but to present two novel AJF concepts and to compare each other and with FTS route and biochemical pathways. For that reason, this part of the thermochemical systems is common. The selection of the Rectisol process among the others options (Selexol, amines) was based on the following advantages a) high selectivity towards sour components, which results to an acid stream with high purity, b)

commercially available in large scale (>100 MW) applications by Lurgi and c) comparing to chemical AGR methods, such as amine, Rectisol is more suitable for CO₂ removal with high partial pressures [77]. The rate of S removal from syngas is determined by the specifications of the catalysts employed for fuel synthesis. The H₂S removal requirement for MAS reactor catalysts is 1ppmv [211, 275]. The same specification for H₂S removal is also adopted in the FTS analysis. As far as the CO₂ separation from the syngas, this has multiple beneficial effects since does not take part to the fuel synthesis: a) increase of H₂ and CO partial pressure, which enhances the conversion rate, b) decrease of syngas compression duty and c) reduction of the size of the Fuel Synthesis Unit. The typical CO₂ removal rate that is specified in the vast majority of the similar thermochemical cases is 90%, and is adopted in this study, too.

7.2.2 Mixed Alcohols Synthesis and Fuel Upgrading

A general scheme of the proposed process for paraffins production from syngas, through mixed alcohols upgrading, is shown in **Figure 89**. The clean syngas (6) is separated from CO₂ (7). The CO₂ removal technology that is adopted in this study is the RectisolTM process, the ASPEN PlusTM modeling of which has been also described in previous studies [175, 276]. The outlet streams from the Mixed Alcohol Synthesis (MAS) reactor and separation Unit are: the light gases that consist of the unconverted syngas, some CO₂ and light hydrocarbons and the produced higher alcohols (9). Part of the light gases stream (15) undergoes autothermal reforming (ATR) with the addition of water steam (16) and oxygen (17) in order to convert the hydrocarbons into CO and H₂. The reformat product is then recompressed and mixed with the original inlet syngas. Another part of the light gases is diverted to the Pressure Swing Adsorption process (PSA) for the production of pure H₂ (14) which is required for the branched paraffins production. The rest of the stream and the tail gas of the PSA process consists the fuel gas (13) that is sent to a GT combustor and used in a combined cycle for heat and power production to cover the energy requirements of the integrated plant. The produced alcohols (9) undergo a condensation reaction to enhance C₄₊ alcohols (10) followed by dehydration, in order to be transformed into the corresponding light olefins (11). The increment of carbon chain is performed in the next process step where the C₄⁺ oligomers synthesis (12) takes place. Finally, via hydrogenation process, branched paraffins are produced, which are essential for the jet fuel (18) and avgas (19) blending.

a) Mixed Alcohols Synthesis

The synthesis of mixed alcohol is conducted under high pressure (>40 bar) and at temperature 250-320 °C in presence of catalyst that favors the reactions of alcohol synthesis:



Apart from this reaction, water gas shift reaction and alkane synthesis reactions also take place due to the formation of H₂O from the alcohols synthesis reactions:



The higher alcohol synthesis mechanism involves a complex set of reactions leading to a mixture of products, the composition of which is determined by kinetic and thermodynamic constraints, the process conditions and catalyst type. The most abundant products are low carbon chain alcohols (C₂-C₄), methanol, hydrocarbons and CO₂. There are several types of mixed alcohol catalysts with a great variety on alloy composition and the promoters [226] which are classified into two main categories, *modified Fischer-Tropsch synthesis* (Fe, Ni, Co, Mo, Rh based) and *modified Methanol synthesis* (K, Zn, Cr, Cu based)

catalysts [160]. In the framework of this study, two catalysts from each group are selected from the literature and are investigated. Needless to say, they have performed differently as far as CO conversion and alcohol selectivity affecting the overall process configuration.

The procedure for branched paraffins formation is strongly dependent on the mixed alcohols composition after the synthesis reactor. The process pathways from the two under investigation cases are described in detail below.

b) Alcohols condensation (Guerbet reactions)

The main alcohol product from a MAS reactor with modified FT catalyst is ethanol, taking also into account the fact that the produced methanol reenters the reactor for the formation of higher alcohols. The first step of fuel upgrading is the ethanol condensation for higher alcohols formation. In this case, catalysts that promote the ethanol condensation for butanol synthesis should be used [186]. Typical catalysts that enhance ethanol upgrading to butanol are alkali earth metal oxides and modified MgO [277]. Dowson et al. [278] observed very good ethanol conversion and high n-butanol selectivity by using RuCl₂ catalyst.



In case of modified methanol catalyst implementation, the produced methanol is reacted with ethanol and propanol giving isobutanol [198, 279] in Pd or Cu based catalyst in the presence of sodium methoxide (CH₃ONa) as base [280]. To model it, basing on the experimental results of Carlini et al. [279] the following reactions are assumed to take place consecutively:



c) Alcohols dehydration

In alcohols dehydration, oxygen is removed in the form of H₂O, forming a double bond between the carbons that are connected with the OH⁻ and H⁺ that are removed:



Several relevant studies have proved that catalysts such as alumina, Ru, Amberlyst acidic resins and ZSM-5 zeolites have an efficient effect on alcohols dehydration under high pressure [281]. Macarova et al. [282] suggested a two-step mechanism for n-butanol dehydration; the reaction proceeds via fast ether formation (dibutyl ether - C₈H₁₈O) and subsequent slower decomposition of ether. From this perspective, higher temperatures are required in order to get high olefin selectivity. The same conclusion is drawn from the study of Lee et al. [283], where dehydration is dominant over the ether formation (alcohol dehydrogenation) at T > 250 °C. Concerning the products selectivity, from the same study it is concluded that the butene product is dependent on the butanol isomer that undergoes dehydration.

d) Olefins oligomerization

In this step, the increase of carbon atoms chain number is performed:



The way that is chosen, is the combination of unsaturated molecules (i.e. alkenes) to the formation of the corresponding oligomers (dimers, trimers and even, tetramers). The reaction takes place in liquid phase, inside stirred reactors, in presence of special catalyst that promotes oligomers formation against other reactions such as cracking, dehydrogenation, polymerization etc.

Ethylene is the most commonly used light olefin for oligomerization and polymerization as it is illustrated by the numerous relevant studies and by the industrial interest in polyethylene plastic material, owed to the several industrial applications that it has. However, high selectivity on C₂-C₈ oligomers against C₁₀₊ oligomers [284-286] makes this route inappropriate for high production rates of hydrocarbons required for jet fuel blends.

n-Butene attracts the interest of many studies for further upgrading such as oligomerization, mainly on the grounds that this C₄ isomer mainly is derived from biochemical processes through fermentation. Recently, Coelho et al. [287] investigated the influence of process parameters in 1-butene oligomerization with HZSM-5 revealing the existence of secondary reactions such as cracking after a certain temperature increase (200°C) that deteriorate the oligomers selectivity (mainly C₈). High pressure and short contact time favor the heavier products formation. The coke formation observed in a wide temperature range contributed to catalyst deactivation by either poisoning the acid sites or by blocking the pores. Simultaneous complete n-butene conversions with high selectivity on C₈ and C₁₂₊ oligomers are noted in Kolombos' patent [256] where gallium catalyst is used. Very promising results are remarked in the study of Lavrenov and Duplyakin [288] where over 85% conversion and 90% selectivity is observed after an oligomerization of butene mixture over borate-Containing alumina catalyst at 150°C/80 bar. One of the most promising yields of 1-butene oligomerization, revealing highly efficient batch catalytic methodology is the recent invention of Wright et al. [239] using Cp₂ZrCl₂ dissolved in methylaluminoxane (MAO) solution.

Similarly, isobutene oligomerization has been extensively studied not only for oligomers production purposes but as a separation method of isobutene from n-butenes in a C₄ refinery cut [289]. Amberlyst-15, a cationic ion-exchange resin, is frequently used as the catalytic medium for isobutene oligomerization thank to its very good performance related to high conversion rates (over 90%) and very good selectivity on dimers (diisobutylene), trimers (triisobutylene) and tetramers (tetraisobutylene) [289-291]. Alternatively, zeolites are also implemented presenting very good performance [292] but rapid deactivation has been observed [291, 293].

e) Oligomers Hydrogenation

In order to produce an organic mixture that will be treated as transportation fuel, the alkenes transformation into paraffins (alkanes) with the addition of H₂ is required. Several studies have reported the effective accomplishment of these reactions type in the presence of Pd alloys catalysts [294, 295] in relative high pressure (>20 bar), at 200 - 350 °C [296].



Figure 90 depicts how the carbon chain growth is realized and the mass distribution of organic compounds along the fuel upgrading process beginning from the two MAS catalyst types.

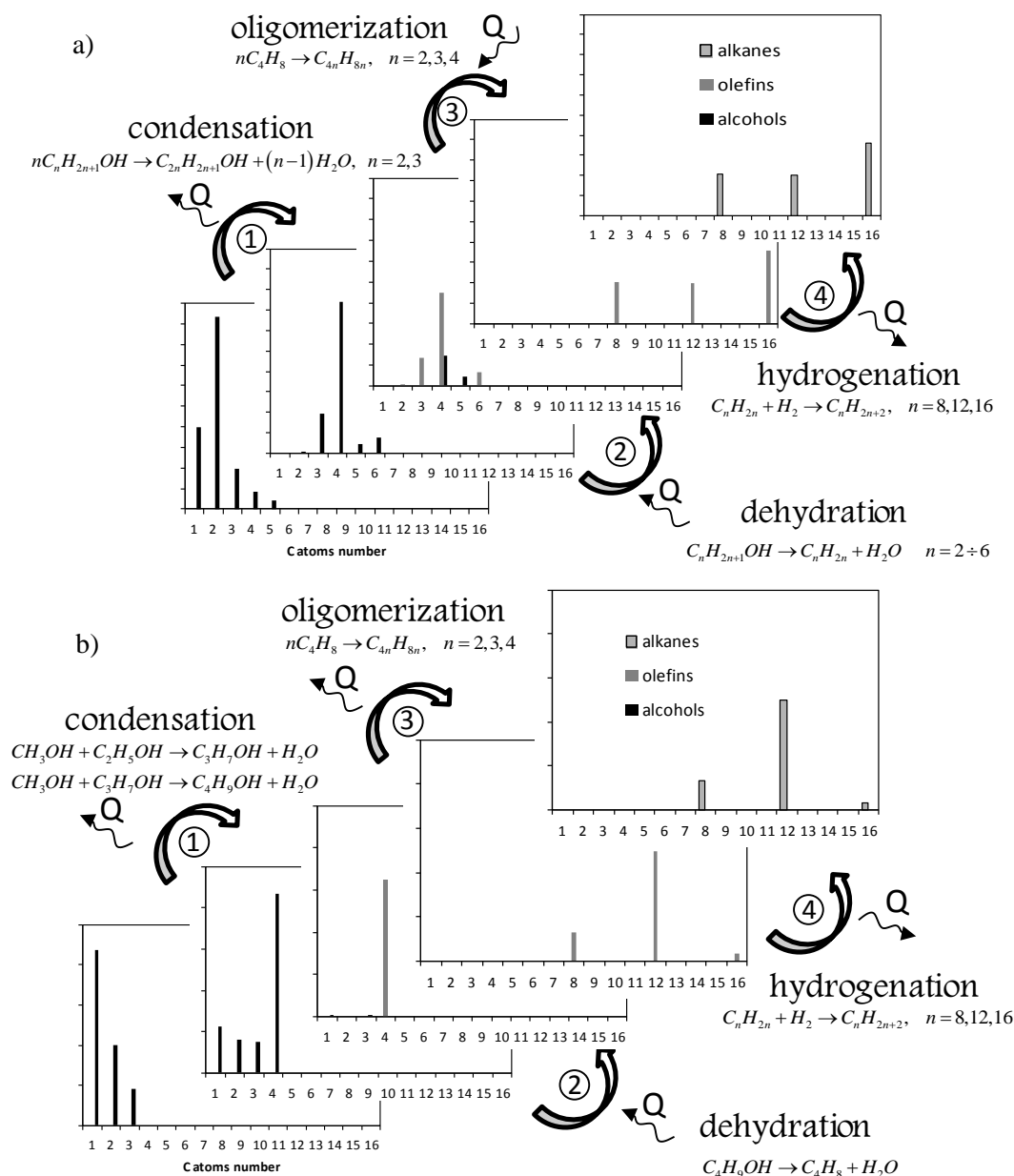


Figure 90. Mass distribution of organic compounds along the fuel upgrading process for mixed alcohols derived from a) modFT catalyst synthesis and b) modMeOH catalyst synthesis (for each process the main reactions and exothermic/endothermic nature are depicted)

7.3 Process modeling

The process modeling and simulation is performed with ASPENPlusTM. Based on generally approved methodologies and on data extracted from experimental studies in small scale or patents, the model of a large scale biorefinery plant with 190MW_{th} thermal capacity is developed, enabling the effective calculation of the mass and energy balance in each unit and the whole process, too. The selection of the suitable property method is of high importance and depends on the type of process and the kind of streams (phase, composition) that take place in each case. For the part of syngas production and conditioning, the RK-SOAVE property method is selected, whereas for the fuel synthesis and upgrading part the NRTL [175]. In the last part, the main factor that determines the most suitable property method is the accurate

vapor-liquid equilibrium calculation especially for the effective separation and upgrading of the produced hydrocarbons.

Two main case studies are examined in detail. In the first one (**case 1**), the alcohol synthesis is performed with modified FT (*MAS modFT*) catalyst while in the second one (**case 2**), the catalyst used is modified Methanol (*MAS modMeOH*). In both cases, the syngas comes from woody biomass gasification in oxygen blown pressurized gasifier, followed by the same gas cleaning and conditioning methodology.

The bio-refinery part that relates with the syngas production, cleaning and conditioning is common for both cases. A detailed description of model setup for this section can be found in previous study [276]. The method that is chosen for the acid gases removal is the Rectisol™ process for both H₂S and CO₂. In **Table 65**, the basic key parameters for the process modeling related to syngas production, gas cleaning, the ASU, the Autothermal reformer and the Power Island are summarized.

Table 65. Process specifications for syngas production, cleaning and conditioning section of the plant

Gasification plant	
fuel analysis (ultimate analysis on a dry basis, moisture content, heating value)	48.75% C, 6.54% H, 44.10% O, 0.24% S, 0.05% N, 5.10% moisture, 18.9 MJ/kg <i>LHV</i> (wet basis)
temperature/pressure/equivalence ratio	1000 °C/ 27 bar/ 0.3
Syngas temperature after cooling	200 °C
Air Separation Unit	
Oxygen purity	97.0%
high/low distillation columns pressure	4.9/1.2 bar
high/low distillation columns stages	30
air compressor polytropic efficiency	82.0%
Gas Cleaning Unit	
H ₂ S content in the clean syngas	1 ppm
absorbers stages (both for H ₂ S and CO ₂ removal)	10
H ₂ S stripper stages	3
CO ₂ separation efficiency	99.0%
Rich solution: Rectisol solvent H ₂ O (w/w%)	98.0%
Rectisol temperature inlet in H ₂ S/CO ₂ absorber	-40/-20 °C
refrigeration unit cooling medium	R134a
refrigeration unit <i>COP</i>	1.85
Autothermal Reformer	
temperature/pressure	950 °C/4.5 bar
steam to HC ratio	3.0
Power Island	
Turbine Inlet / Outlet Temperature	1350 / 608 °C
GT Compressor/Turbine polytropic	90.9% / 93.6%
GT pressure ratio	18.0
gas-liquid/gas-gas heat exchangers pinch point	10 / 25 °C
Superheated steam	500 °C / 150 bar
Reheated steam	500 °C / 30 bar
high/low pressure steam turbine isentropic efficiency	84% / 82%
Condenser pressure	0.05 bar

As far as the alcohol synthesis is concerned, the process parameters and the MAS reactor performance are summarized in **Table 66**. The catalyst from the study of Aden et al. [297], as referenced in the work of Zhu et al. [298], is the modified FT catalyst. More detailed description of the catalyst performance and

the methodology for yields calculation can be found in the study of Zhu et al. [298]. In this analysis, the carbon selectivity and conversion rate from the methanol reaction in the reactor is examined. As a result, it was possible to obtain useful data for modeling the methanol re-circulation, after it is recovered from the rest alcohols. These catalyst types promote the formation of higher alcohols, mainly ethanol. On the other hand, the modified methanol catalysts (Fe-Cu, Cu-Zn base) result to high selectivity in methanol [265, 299, 300] regardless the promotions employed.

Table 66. Process specifications for mixed alcohols production with two difference catalyst types

Case	1	2
reference study	Aden et al. 2005 [297]	Kulawska and Skrzypek 2001 [214]
catalyst	K/Co/MoS ₂ (modified FT)	Cs– doped Cu/Zn (modified MeOH)
temperature (°C)	298.8	320.0
pressure (bar)	137.9	90.0 bar
H ₂ /CO ratio (mol/mol)	1.2	2.0
CO conversion (%)	38.0	31.0
Methanol conversion (%)	71.5	-
C selectivity (% mol)	from CO	from Methanol
CO ₂	34.21%	-
CH ₄	11.84%	-
C ₂ H ₆	1.32%	-
C _n H _{2n+2} , n>5	-	-
Methanol	10.79%	-
Ethanol	30.00%	81.12%
Propanol	7.89%	9.79%
Butanol	2.63%	6.29%
Pentanol	1.32%	2.80%

7.3.1 Paraffins from mixed alcohols with modified FT (case 1)

The process flowsheet of the fuel upgrading in this case, including the reactors, separators (columns, flash separators and decanters), heat exchangers and stream recirculation, is presented in **Figure 91**. After the alcohols synthesis and separation of the light gases, ethanol product is isolated and sent for condensation. The recovered methanol is recycled and resent to the MAR, whilst the higher alcohols are mixed with produced n-butanol. The ethanol self-condensation approach is based on the experimental findings from the study of Dowson et al. [278]. For the set of the specifications of the dehydration process it is securely assumed that all the alcohols are totally converted into the corresponding alkenes [301, 302]. The higher alcohols separation in this stage is necessary in order to avoid accumulation at the next stage (i.e. Guerbet Reaction unit) during ethanol recirculation. For the same reason, water produced from the Guerbet reaction is removed by means of a water decanter. The Guerbet reactor and the Dehydration reactor, since both the reactants and the products are in gaseous phase, resemble to the MAR; they are considered as plug flow reactors filled with catalyst (fixed bed). On the other hand, the Oligomerization and the Hydrogenation reactors are regarded as continuous stirred reactors and the catalysts are diluted in the liquid phase. Since the latter reactors have batch operation, the number of batch reactors for each case is determined by the residence time of each reaction.

The hydrogen from the hydrogenation process is recovered from the unconverted syngas by means of the Pressure Adsorption Process (PSA). The required flow rate of hydrogen is equal to the amount of olefins that should be hydrogenated. The hydrogen concentration in the inlet stream at the PSA must be at least 70% v/v. Hence, a recycle is incorporated to meet the minimum H₂ concentration level. The

continuous operation of the PSA process is secured by the usage of two separate beds, where adsorption and desorption take place alternately [303, 304]. The hydrogenation reaction is assumed to take place in 30 bar and 250°C. Experiments in pressure higher than 20 bar showed very high olefins conversion rates (>90%) and very good alkanes selectivity (near to 100%) [296, 305].

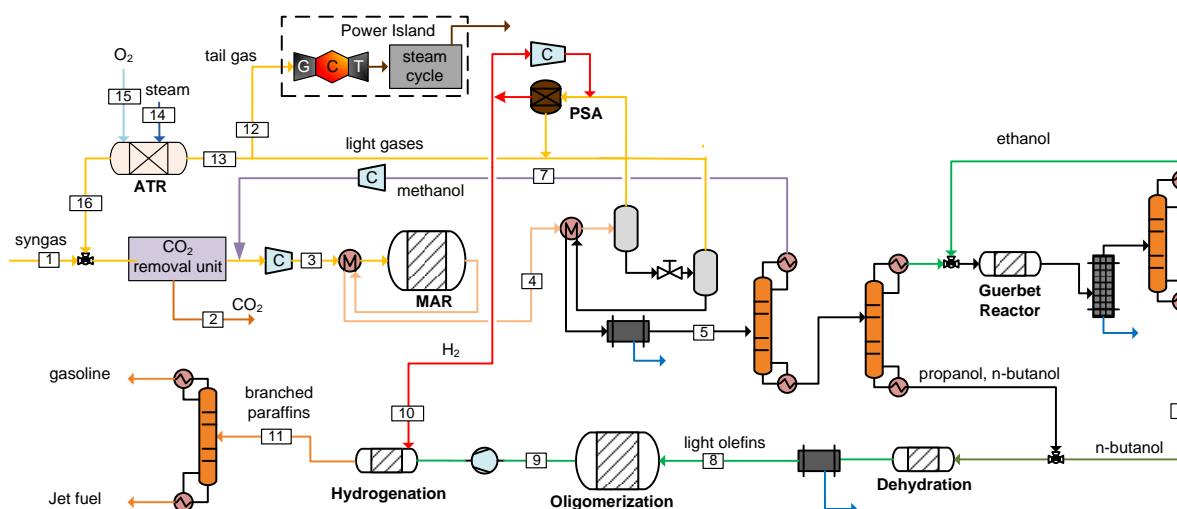


Figure 91. Process flowsheet of the paraffins production unit from mixed alcohols for modified FT catalyst

7.3.2 Paraffins from mixed alcohols with modified Methanol (case 2)

This concept has strong similarities to the Gevo's process for jet fuel production [306] based on isobutanol [305]. The fuel upgrading process flowsheet of this case, including all the main components such as reactors, separators, heat exchangers etc. is presented in **Figure 92**. After the Mixed Alcohol Synthesis and the light gas separation, the liquid alcohol mixture undergoes condensation for isobutanol transformation. After the condensation reactor, two consequent columns follow for methanol/isobutanol/ $C_{2-3}OH$ separation. The unreacted C_{2-3} alcohols return to the reactor whereas the recovered methanol is sent for reforming. The ethanol conversion by (**R 17**) is assumed equal to 71.2%, while the propanol conversion at (**R 18**) is set 82.0%, including the amount of propanol produced by the (**R 17**). These conversion rates were adopted by Carlini et al. [279]. According to Carlini et al. [198, 279] the selectivity to butanol was about 100%, so no other by-products are considered in this case. Afterwards, the isobutanol undergoes dehydration for the corresponding alkene formation (isobutene), in presence of alumina. From [281] it is confirmed that high isobutylene conversion and high selectivity to isobutylene can be achieved with no significant impurity effects. The carbon chain growth is performed in the next reactor where olefins oligomerization takes place. The produces dimers, trimers and tetramers are converted into branched paraffins by means of hydrogenation.

Table 67 summarizes the process specifications and assumptions that are considered on the present process modeling for both cases. The catalyst type is not taken into account on the ASPENPlus™ modeling but it is quoted for reasons of completeness. Adopting the experience from NREL’s group previous analyses [185, 195], all the distillation columns are assumed to have 70 stages with a pressure drop equal to 0.5bar and separation efficiency up to 99%. The reactors in the fuel synthesis and upgrading unit are modeled with stoichiometric reactors, the conversion rate of each reaction is determined by the selectivity yield and the reactants conversion rate (**Table 67**).

The successful performance of the two final process steps (oligomerization and hydrogenation) is decisive for the correct final product formulation. There exist patents describing these two final steps for both cases [239, 305] assuring the compatibility of the produced paraffins to jet fuel through the verification of the physical properties via certain standards. Hence, the use of the produced branched paraffins from the proposed concepts as fuel blends in jet engines can be considered valid.

7.4 Cost analysis methodology

After having determined the processes and operational data for each examined case, a cost analysis for a “next” plant is performed in order to evaluate the economical feasibility of each case. Thus, the Capex and Opex for each case are estimated. The methodology for the Total Capital Investment (TCI) is based on a series of intermediate cost types, the first of which is the Total Purchased Equipment cost (TPEC) for each case. The cost of each equipment is estimated either based on similar equipment costs from the literature or based on Peters & Timmerhaus [129] methodologies. In the first case, the similar equipment costs obtained from the literature are scaled up to this study’s operational data and streams, according to the six-tenths factor rule:

$$\text{Cost of equipment new} = (\text{cost of equipment reference}) * (X)^f \quad (\text{Eq. 39})$$

where X is the ratio of the capacity of the new equipment to the capacity of the reference equipment, raised to a scaling factor f given from reference. For some novel equipment that is not found in the literature, such as the dehydration and condensation reactors, a rough economical assumption is adopted. Since the reactants/products are apparent in those plug-flow reactors in gaseous form, the design configuration of them are considered to be similar with the mixed alcohol synthesis reactors.

Table 68: Total Capital Investment (TCI) estimation methodology

Total Purchased Equipment Cost(TPEC)		100%	
Total Installed Cost (TIC)		TPEC·(Installation Factor)	
Installation factor when not given by reference	Purchased Equipment	100%	
	Purchased Equipment Installation	39%	
	Instrumentation and controls	26%	
	Piping	31%	
	Electrical Systems	10%	
	Buildings(including services)	29%	
	Yard Improvements	12%	
		Total: 247% of TPEC	
Indirect Costs (IC)	Engineering and Supervision	32%	
	Construction Expenses	34%	
	Legal Expenses	4%	
	Contractor's Fee	19%	
		Total: 89% of TPEC	
Total Direct and Indirect Costs (TDIC)		TIC+IC	
Contingency		20% of TDIC	
Fixed Capital Investment (FCI)		TDIC+Contingency	
Working Capital (WC)		15% of FCI	
Total Capital Investment (TCI)		FCI+WC	

Thus, the cost methodology for these reactors is the same to a MAS reactor [298]. Furthermore, having the Total Purchased Equipment Cost (TPEC) estimated, the next step is the Total Installed Cost (TIC) calculation. This is accomplished by multiplying each equipment cost with an installation factor, specified for each component (see **Annex**). The methodology followed for the estimation of TCI is summarized in **Table 68**.

Table 69: Fixed & Variable Operating Costs

Fixed Operating Costs		Reference
Maintenance	2% of FCI	[129]
Insurance and Taxes	2% of FCI	
General Overhead	60% of salaries	
Variable Operating Costs		
Component	Price	Reference
Biomass Feedstock (wood chips)	60 €/dry t	assumption
Waste treatment and disposal	0.4 €/t	[129]
Process water	0.4 €/t	[129]
Cooling water	0.06 €/t	[129]
Hydrocracking	3.02 €/barrel produced HC	[307]
PSA	1.7 €/kg	[307]
Rectisol solvent cost	0.32 €/l	[308]
WGS catalyst cost (applied every 3 years)	13.2 €/kg	[307]
ATR catalyst cost (applied every 3 years)	7.7 €/kg	[307]
Tar Reformer Catalyst Cost (applied every 3 years)	29.5 €/kg	[309]
LO-CAT chemicals	132.9 €/t sulphur	[307]
Sulphur disposal	13.6 €/t	[310]
FT Reactor Catalyst (applied every 3 years)	24.9 €/kg	[307]
MAS Catalyst Mod-FT (applied every 2 years)	49.4 €/kg	[309]
Ethanol Condensation Catalyst (applied every 2 years)	0.2 €/kg	[307]
Dehydration Mod-FT Case Catalyst (applied every 2 years)	377 €/kg	[269]
Oligomerization Mod-FT Case Catalyst (applied every 3 years)	231.5 €/kg	[269]
Hydrogenation Mod-FT Case Catalyst (applied every 3 years)	224.9 €/kg	[269]
MAS Catalyst Mod-MeOH (applied every 2 years)	66.1 €/kg	[311]
Methanol-Propanol Condensation Catalyst (applied every 2 years)	0.2 €/kg	[269]
Dehydration Mod-MeOH Case Catalyst (applied every 2 years)	0.9 €/kg	[269]
Oligomerization Mod-MeOH Case Catalyst (applied every 3 years)	537.9 €/kg	[129]
Hydrogenation Mod-MeOH Case Catalyst (applied every 3 years)	224.9 €/kg	[269]

Apart from the TCI calculation of each case, the estimation of the respective Operating Costs is also performed. The Operating Costs consist of Fixed and Variable Operating Costs. Fixed Costs include Maintenance Costs, Insurance and Taxes, as well as General Overhead Costs. The parameters that are used for the calculation of these costs are shown in **Table 69**. Regarding the Variable Operating Costs, the majority of them are determined according to the stream flows derived from process simulations. Variable Operating Costs include salaries, feedstock costs, main catalyst and solvents costs and waste disposal costs, calculated in an annual basis. Both fixed operational costs and salaries are divided by the number of

areas and are distributed depending on the number of process steps of each area. The salaries are calculated based on the number of process steps in each case, by estimating the amount of employee hours needed according to Peters & Timmerhaus [129] and multiplying them with the average employee hour cost found in Eurostat [312]. Feedstock price is considered as 60 €/dry metric ton. Catalysts replacement is assumed to take place every 2 or 3 years, depending on the catalyst type. The Variable Operating Costs Assumptions are described in **Table 69**.

Having the Total Capital Investment, the Fixed and Variable Operating Costs for each case determined, the Discounted Cash Flow Rate of Return (DCFROR) analysis is performed. Through this analysis, the economical viability of each case is examined for a 25-years operational plant life. According to this, the Present Value per unit volume of aviation fuel at a net present value of zero and a 10% internal rate of return is calculated. This value reflects the Minimum Fuel Selling Price (MFSP) that sets the boundaries for the investment feasibility.

The main economic assumptions are described in **Table 70**. The depreciation model used on the current paper is Modified Accelerated Cost Recovery System (MACRS) method through a Double-Declining-Balance (DDB) with a recovery time of 7 years with zero salvage value for the plant at the end of its lifetime. The plant is considered to be electrically independent, thus, there is no purchasing or selling electricity.

Table 70: Economic Assumptions

Biomass Input	864 dry tonne Wood Chips/day (10 kg/s)
Operational Days of Plant	310 days/year (85% capacity factor)
Life Plant	25 years
Plant Depreciation	7 years 200% DDB as per MACRS guidelines
Internal Rate of return	10%
currency	euro (€)
year cost	2011
Exchange Rate €/€	0.755
Biomass Purchased	60 €/dry tonne
Contrsuction Period	3 years with TCI spent at 8%, 60% and 32% per year
Land Purchase	6% of Total Purchased Equipment Cost
Financing	100% Equity
Electricity purchased/sold	0/0

7.5 Results and Discussion

In this section, the results of the current paper are presented. They are separated in two main parts. The results derived from the process modeling of the cases (stream tables, energy and mass balances etc.) and the results extracted from the economic evaluation of such concepts (Capex, Opex, MJFSP etc.).

The comparison of the produced aviation fuel with the typical jet A1 in terms of properties is illustrated in **Table 71**. It is clear that in both thermochemical cases the properties produced aviation fuels are very close to the typical characteristics.

Table 71. Main properties of the produced aviation fuel from the ATJ routes and comparison with the typical values [237]

property	units	mod-FT	mod-MeOH	Jet-A1 typical values
energy content	MJ/kg	43.9	43.6	42.8-43.2
viscosity at -20°C	cST	5.8	9.8	8.0
density at 15°C	kg/m ³	752.6	792.0	775-840
molecular weight	kg/kmol	181.3	194.1	170.0
bubble point	°C	163.9	181.0	176.0
dew point	°C	266.9	280.0	300.0

7.5.1 Mass and Energy Balance calculations

The basic results from the process analysis are summarized in **Table 72**. Apart from the specific productivity, another index for the plant performance determination is that of thermal efficiency. It evaluates the amount of the initial biomass feedstock heat input that remains at the final fuel product and is defined as in (**Eq. 40**):

$$\eta_{th} = \frac{m_{Jet\ Fuel} \cdot LHV_{Jet\ Fuel}}{m_{wood} \cdot LHV_{wood}} \quad (\text{Eq. 40})$$

The main results reveal a quite good biomass-to-aviation fuel conversion through the thermochemical route. Case 2, which is based on modMeOH for MAS, has a slightly better performance than case 1. This is mainly attributed to the higher MAS operation pressure in case 1 that leads to higher power consumptions for gas compression and better utilization of the produced alcohols mixture in case 2. It is pointed out that it should not be generalized that the methodology based on the modMeOH catalyst always leads to higher efficiency, compared to the modFT approach. The corresponding results from the FT case are discussed in following section.

Table 72. Main process results from the thermochemical routes

case	1	2	3
fuel synthesis route	MAS with modFT	MAS with modMeOH	FT
specific Jet Fuel production, kg _{JF} /kg _{wood}	0.112	0.138	0.097
specific Gasoline production, kg _G /kg _{wood}	0.042	0.034	0.076
specific Total Aviation Fuel production, kg _F /kg _{wood}	0.154	0.172	0.173
thermal efficiency, % LHV based	37.2 %	40.5 %	24.2/16.2 ¹
ASU power consumptions, kJ _e /kg _{wood}	677.8	653.7	534.1
acid gas removal power consumptions, kJ _e /kg _{wood}	215.2	300.8	237.0
gases compression power consumptions, kJ _e /kg _{wood}	836.9	405.8	16.5
total power consumptions, kJ _e /kg _{wood}	1730.0	1360.3	787.6
total carbon utilization, % C _{feedstock}	28.2 %	31.5 %	30.4%

¹ the first term refers to jet fuel and the second to the gasoline. The LPG is 20 times less than jet fuel and thus is practically neglected.

The thermodynamic characteristics of the most important streams of the biorefinery, for both thermochemical routes, are summarized in **Table 73a** and **b**.

Table 73a. Stream results of the ATJ biorefinery with modFT

a/a	<i>m</i> kg/s)	<i>T</i> (°C)	<i>p</i> (bar)	molar composition (% vol)												
				H ₂ O	CO ₂	H ₂	CO	CH ₄	H ₂ S	Ar	N ₂	methanol	ethanol	C3OH	C4OH	C5OH
1	10.00	15.0	27.0	see biomass composition in <i>Table 65</i>												
2	3.79	50.0	27.0	99.7% O ₂ , 0.3% Ar												
3	13.67	350.0	27.0	12.80%	10.04%	32.67%	42.89%	1.42%	0.1%	0.05%	0.02%					
4	11.49	110.0	26.0	0.00%	9.67%	38.31%	50.27%	1.66%	1 ppm	0.06%	0.03%					
5	2.32	277.0	30.0	100%												
6	13.81	300.0	26.0	1.18%	24.64%	48.16%	24.59%	1.36%	0.00%	0.05%	0.02%					
7	8.94	-15.6	0.2	0.03%	99.95%							0.02%				
8	17.12	-20.0	24.9	0.00%	0.14%	65.48%	32.46%	0.84%	0.00%	0.96%	0.09%	0.03%				
9	2.51	114.2	3.10									0.25%	80.06%	13.00%	4.69%	2.00%
10	2.13	15.0	1.1										1.0%	22.2%	68.2%	3.4%
11	1.52	30.0	1.0	olefins: 21.9% C3, 70.2% C4, 7.0% C6												
12	1.52	117.4	30.0	olefins: 39.8% C8, 25.6% C12, 34.6% C16												
13	1.00	58.8	136.4	0.11%	5.66%	64.63%	24.56%	3.03%	0.00%	1.24%	0.12%	0.24%	0.27%	0.02%		
14	0.02	57.6	136.4			100%										
15	12.86	57.8	26.0	0.11%	5.76%	64.51%	24.55%	3.03%	0.00%	1.26%	0.12%	0.25%	0.28%	0.02%		
16	0.13	250.0	26.0	100%												
17	1.71	15.0	26.0	99.7% O ₂ , 0.3% Ar												
18	1.12	249.6	1.2	paraffins: 0.7% C8, 41.5% C12, 57.9% C16												
19	0.43	139.8	1.2	paraffins: 98.2% C8, 1.8% C12, 0.0% C16												

Table 73b. Stream results of the ATJ biorefinery with modMeOH

a/a	<i>m</i> kg/s	<i>T</i> (°C)	<i>p</i> (bar)	molar composition (% vol)											
				H ₂ O	CO ₂	H ₂	CO	CH ₄	H ₂ S	Ar	N ₂	methanol	ethanol	C3OH	C4OH
1	10.00	15.0	27.0	see biomass composition in Table 65											
2	3.79	50.0	27.0	99.7% O ₂ , 0.3% Ar											
3	13.67	350.0	27.0	12.80%	10.04%	32.67%	42.89%	1.42%	0.10%	0.05%	0.02%				
4	11.49	110.0	26.0	0.00%	9.67%	38.31%	50.27%	1.66%	1 ppm	0.06%	0.03%				
5	2.31	277.0	30.0	100%											
6	13.80	300.0	26.0	1.17%	24.61%	48.14%	24.64%	1.36%	0.00%	0.05%	0.02%				
7	8.71	-15.6	0.2	0.03%	99.95%							0.02%			
8	19.18	-20.0	24.9	0.00%	0.12%	65.57%	32.54%	0.90%	0.00%	0.76%	0.09%	0.03%			
9	3.81	225.8	26.5	0.0%	1.4%	0.0%	0.0%	0.0%	0.0%	0.0%	0.0%	68.9%	22.1%	7.6%	0.0%
10	2.23	15.0	1.1	0.00%	0.00%	0.00%	0.00%	0.00%	0.00%	0.00%	0.00%	0.40%	0.00%	0.72%	98.88%
11	1.70	30.0	1.0	1.41%								0.40%		0.71%	97.5%
12	1.70	100.0	1.1					olefins: 27.6% C8, 69.0% C12, 3.4% C16							
13	0.87	14.5	88.5	0.00%	2.65%	66.17%	28.83%	1.14%	0.00%	0.00%	0.94%	0.11%	0.12%	0.02%	
14	0.02	13.2	88.5			100%									
15	14.77	27.8	25.0	0.00%	2.73%	65.15%	28.40%	1.13%	0.00%	0.00%	0.93%	0.11%	1.52%	0.03%	
16	0.09	250.0	26.0	100%											
17	1.52	15.0	27.0					99.7% O ₂ , 0.3% Ar							
18	1.72	120.0	30.0					paraffins: 0.0% C8, 95.2% C12, 4.8% C16							
19	0.35	180.0	30.0					paraffins: 99.7% C8, 0.3% C12, 0.0% C16							

Figure 93a-b shows the energy flow along the process via the Sankey diagram. Three forms of energy are observed: chemical, heat and work power.

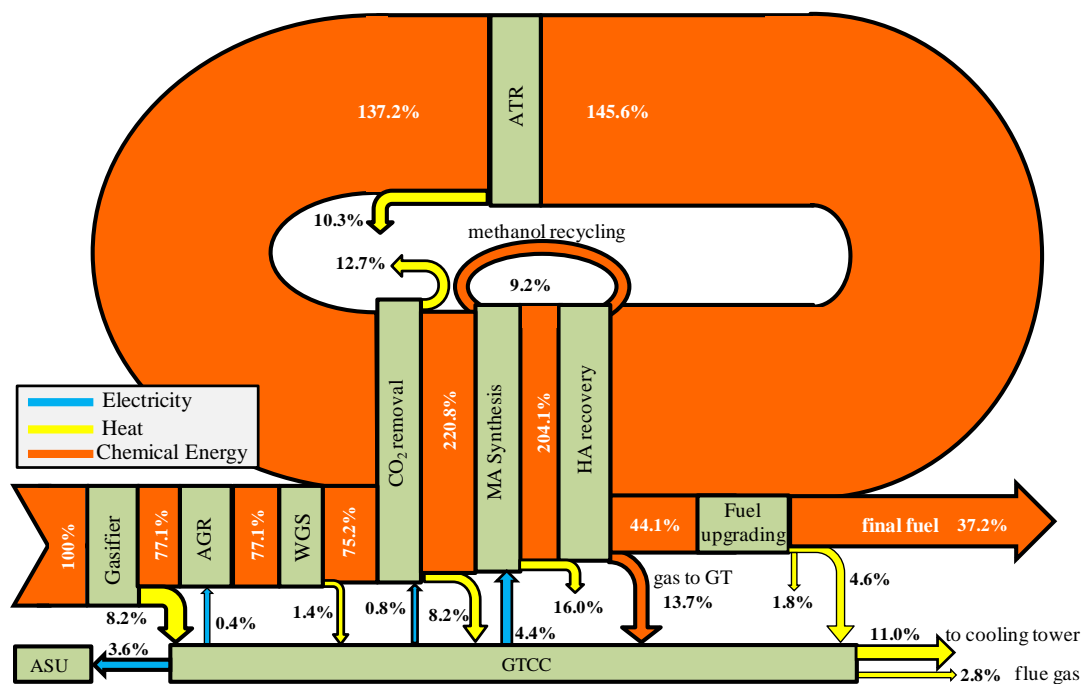


Figure 93a. Sankey diagram of the system (case 1 / MAS-mod FT)

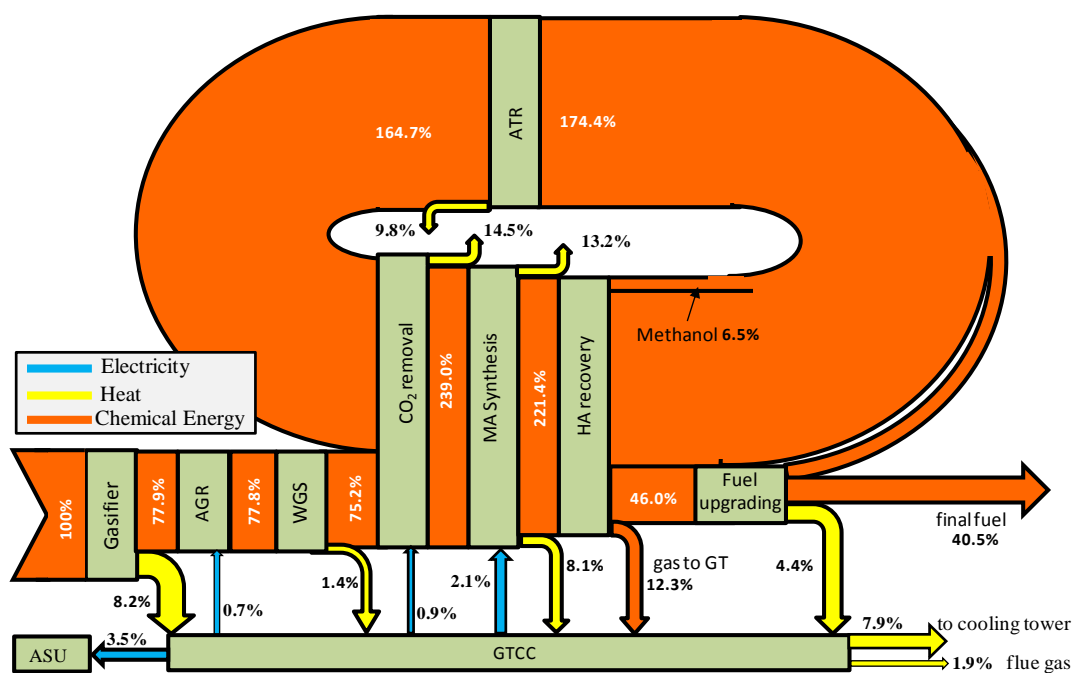


Figure 93b. Sankey diagram of the system (case 2 / MAS-mod MeOH)

The significance of MAS specifications (CO conversion and selectivity to alcohols) is illustrated by the large amount of recycling gas that is almost 1 and a half times greater than the total fuel heat input. Also, one fourth of the total energy content of the biomass feedstock is transformed into heat

during gasification and syngas conditioning, before the mixed alcohol synthesis. At it is seen, only a part of this heat can be recovered and utilized for steam generation in the GTCC unit.

In both cases, up to 50% of the fuel heating value is transformed into heat and rejected to the environment from various processes. A large amount of low enthalpy heat is released from the system in the cooling tower due to steam condensation and during syngas inter-cooling after the ATR. Part of the dissipated heat throughout the process, especially in the MAS Unit, is utilized for steam integration within the power plant. The very low quality segments of the rest of the dissipated heat are not usable and only represent cooling loads.

Several interesting conclusions can be extracted from the carbon balance analysis for each case. The fuel yields are strongly correlated with the fate of C atoms along the process; unlike H and O atoms that are partially derived from water, the C for fuel synthesis is exclusively derived from the feedstock biomass. Another aspect is that since CO_2 is of the most stable compounds, any carbon formation to carbon dioxide cannot longer be utilized. Through the thermochemical options, as it is seen in **Figure 94a-b**, around 50% of the total carbon is transformed into CO_2 along the syngas production and conditioning steps. The gasification process contributes by 20% to this, whereas the syngas conditioning (WGS reactor) by 20% and the rest of it comes from the fuel synthesis and from the reforming of the recycling light gases. Also, a part of carbon in the form of CO or other light organic gases is led for combustion to the GT, due to the heat and power requirements coverage. Consequently, about one third of C content is finally utilized for the advanced fuel synthesis through thermochemical routes (see **Table 72**).

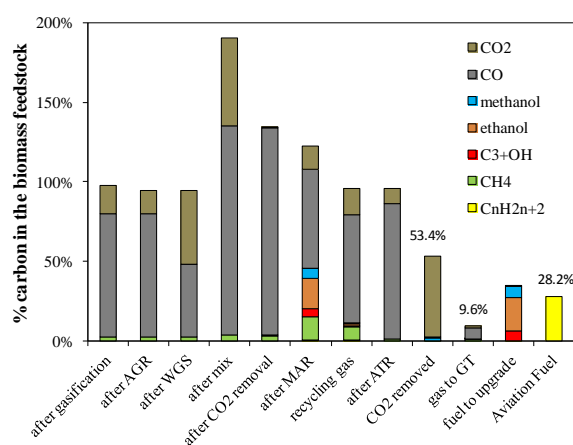


Figure 94a Carbon balance along the process (case 1, modFT)

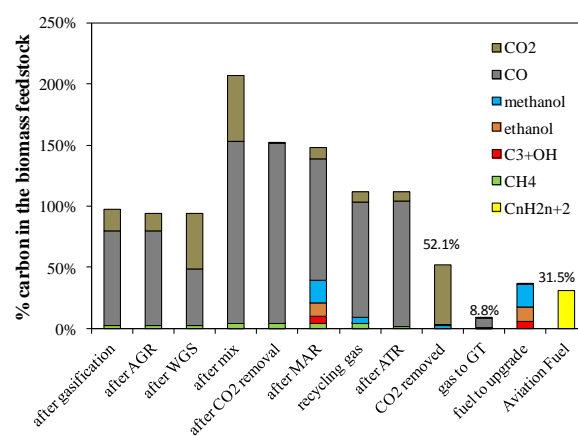


Figure 94b. Carbon balance along the process (case 2, modMeOH)

The water management in such energy systems is of high importance, since a large amount of water is needed or extracted from various points along the process. It is seen in **Figure 95** that the water treatment unit handles a total water flow equal to 29.1 kg/s for water cleaning. The water flow rates for cooling purposes, especially in the Fuel Synthesis Unit and the Fuel Upgrading Unit can be reduced with a more efficient heat recovery from the steam cycle. Since a part of water is released to the atmosphere from the flue gas stack and the cooling tower, 23.7 kg/s should be pumped from a natural deposit in order to meet the water balance of the system. In other words, the annual demands for fresh water of this plant with heat capacity $\sim 190\text{MW}_{\text{th}}$ are approximately 641000 m^3 . This fact should be taken into consideration in terms of the biorefinery impact on the environment in future studies.

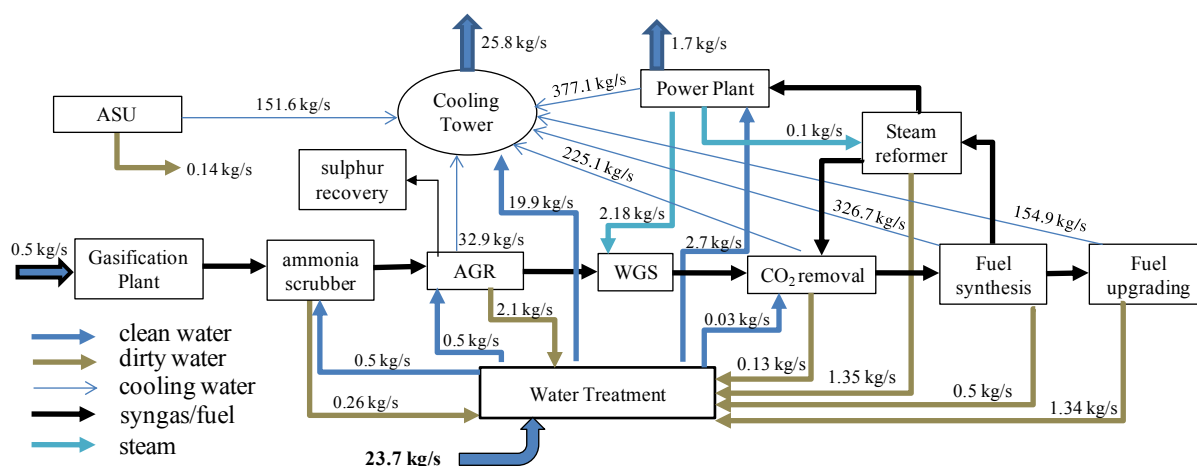


Figure 95. Water flow rates in the bio-refinery system (case 2- MAS with modMeOH catalyst)

7.5.2 Effect of self-power production for the coverage of the electrical demands

In the present study, the biorefinery system is considered as energetically autonomous. In other words, part of the fuel heat input is used for the coverage of the heat and power demands of the whole process. In this section, the potential connection of the plant with the electricity grid for the coverage part of the required electrical power is investigated. In any case, an amount of the produced syngas is sent for burning, the heat of the combustion is utilized for steam production, which has several uses, such as heating medium at steam reformers reactors and for power production in steam turbines.

In **Figure 96** two cases are examined, the autonomous system (base case) and the case that 60% of the required electricity from power consumptions coverage is provided from an external grid. In order to make the comparison on equal terms, the term of exergy efficiency is used, which is defined as:

$$\eta_{ex} = \frac{m_{Jet\ Fuel} \cdot E_{Jet\ Fuel}}{m_{wood} \cdot E_{wood} + P_{el, externally}} \quad (\text{Eq. 41})$$

The chemical exergy of jet fuel is set as $E_{Jet\ Fuel} = 45,897$ kJ/kg [313], whereas the corresponding chemical exergy of the wood feedstock is calculated from the equation (Eq. 42) [106]:

$$E_{wood} = LHV_{wood} \left(1.0438 + 0.0013 \frac{\gamma_H}{\gamma_C} + 0.1083 \frac{\gamma_O}{\gamma_C} + 0.0549 \frac{\gamma_N}{\gamma_C} \right) + 6740 \gamma_s \quad (\gamma_i \text{ in dry basis}) \quad (\text{Eq. 42})$$

It is clear from **Figure 96** that the electricity provision from grid has beneficial impact on the plant performance, from a thermodynamic point of view. An equivalent conclusion is expected to be drawn from the effect of this parameter on the economic feasibility of the system: the cost of electricity that is produced from syngas in the biorefinery is higher than if it is obtained from the grid. On the other hand, the in-house power production offers energy independence and sustainability, irrespective of the location of the plant. Furthermore, the energy mix of the external electricity probably contains conventional sources and thus this concept has no zero contribution to the Greenhouse Gas emissions.

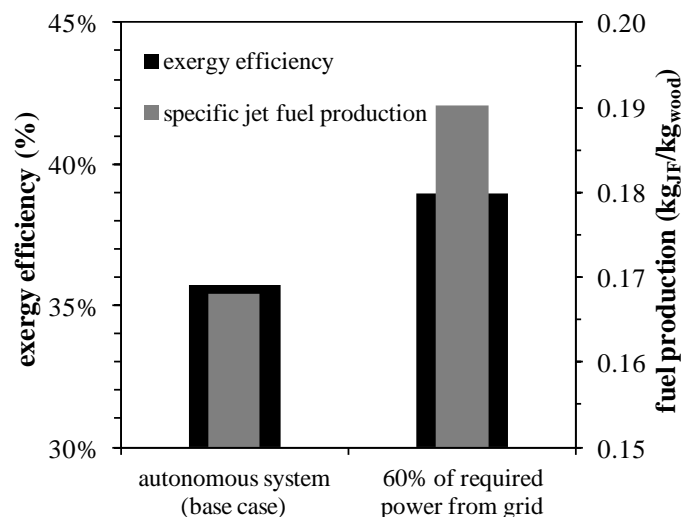


Figure 96. Influence of providing electricity from an external power grid on plant performance (case 2- MAS with modMeOH catalyst)

7.5.3 Investigation of the recycling gas returning route & the effect of gasification temperature

The alternative option of returning the recycling gases back to the gasifier instead of sending to an ATR reactor is also investigated. The main advantage of this concept is the avoidance of the catalytic autothermal reactor, the specific cost of which is rather high. The simulation study is performed for the case 2 and the recovered light gases are busted to the gasifier. In order to have the same syngas quality, the same gasification temperature with the case 2 (1000 °C) is assumed. Simulation results reveal that this recycling option is not beneficial for the plant performance enhancement. The produced syngas from the gasifier is more than two times greater than this in case 2, implying considerably higher equipment cost for the gasifier and the whole gas cleaning and conditioning system, too. **Table 74** summarizes the main results from this test case. Due to the greater syngas flow rate, the power duties in the AGR Unit are by 36% more. It is seen that the oxygen requirement in the case where light gases return back to the gasifier is greater and consequently, the ASU power consumptions are greater. Thus, the elevated power consumptions negatively effect on the Jet Fuel productivity and the thermal efficiency is by 7.5% lower.

Table 74. Recycling gas to the gasifier: main simulations results (case 2- MAS with modMeOH catalyst)

light gases return	to ATR	to gasifier
specific Aviation Fuel production, kg _{JF} /kg _{wood}	0.138	0.141
thermal efficiency, % <i>LHV</i> based	40.5 %	33.0%
total O ₂ used, kg _{O2} /kg _{wood}	0.546	0.652
ASU power consumptions, MJ _e /kg _{wood}	0.654	0.779
gas cleaning power consumptions, MJ _e /kg _{wood}	0.301	0.471
gases compression power consumptions, MJ _e /kg _{wood}	0.406	0.600
total power consumptions, MJ _e /kg _{wood}	1.360	1.850
total carbon utilization, % C _{feedstock}	31.50%	29.52%

7.5.4 Investigation of potential CO₂ utilization

It is clear from the carbon balance analysis that a considerable amount of carbon content of the biomass feedstock is not utilized for fuel synthesis and upgrading but is released to the atmosphere in the form of carbon dioxide. This fact is the motivation for the investigation of the CO₂ capture and utilization (CCU) aspect. According to this, carbon dioxide from the CO₂ separation and recovery unit reacts with H₂ in the presence of catalyst at high pressures and is converted into CO, methanol and other higher alcohols. The key process assumptions for the CCU modeling are based on the experimental study of Nieskens et al. [164] and are presented in **Table 75**.

Table 75. Process specifications for CO₂ utilization

pressure/ temperature	104 bar/ 340 °C
H ₂ /CO ₂ (mol/mol)	3.0
CO ₂ conversion	32.0
products selectivity	57.5% CO, 20.0% methanol, 5.5% ethanol, 0.5% propanol, 16% CH ₄ , 0.5% C ₂ H ₆

The results from the investigation of the CO₂ utilization are summarized in **Figure 97** illustrating the carbon balance for cases with different rate of carbon capture and utilization. As CO₂ conversion to CO or other organic compounds is conducted in high pressure, a significant amount of electrical power is required for CO₂/H₂ mixture compression. In this case, it is inevitable that a larger fraction of the recovered light gases to be sent to the power island (“gas to GT”). Hence, the portion of carbon that results to the final desired product (“final fuel”) is slightly greater in the case of no CCU. This is also illustrated to the corresponding thermal efficiency – 32.5% for 0% CCU, 29.4% for 50% CCU and 27.0% for 100% CCU. Taking also in consideration the fact of additional equipment cost of the CCU (mainly composed of the CO₂ compressor and the catalytic reactor), the CO₂ utilization with this concept is not adopted. Alternative concepts with different source of hydrogen (e.g. from water electrolysis) or power source (e.g. from RES or the electrical grid) may lead to different conclusions about carbon utilization.

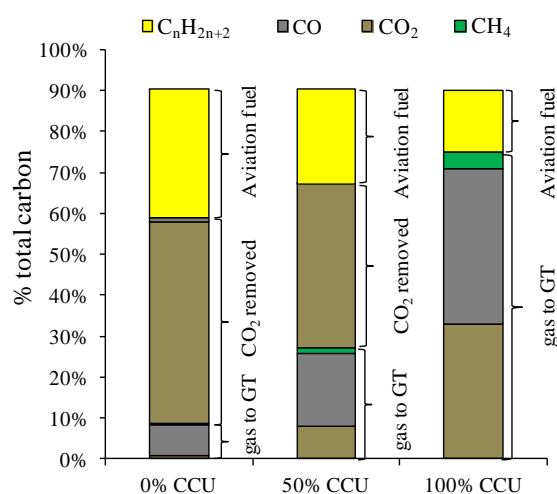


Figure 97. Effect of CCU rate on carbon distribution at the three outlet streams for case 2- MAS with modMeOH catalyst (the rest carbon consists the released CO₂ at the AGR unit)

7.5.5 Comparison with Fischer-Tropsch Synthesis process

In this section, the comparison with the conventional Fischer-Tropsch Synthesis process in thermodynamic point of view is performed and discussed. A general scheme of the fuel synthesis through the Fischer-Tropsch synthesis combined with fuel upgrading and separation is shown in **Figure 98**. The syngas stream that comes from the gas cleaning and conditioning unit is mixed with the recirculating unconverted syngas and enters the CO₂ removal unit for the last step of syngas conditioning. Until the Fischer-Tropsch synthesis, the processes are the same with the MAS cases.

The Fischer-Tropsch synthesis is conducted in 250°C and in the same pressure level with the gasification (25 bar), hence no syngas boosting is required after the Gas Conditioning Unit. The process specifications for FT synthesis, which is based on Anderson-Schulz-Flory (ASF) distribution [314, 315] is adopted from the study of Spyarakis et al.[223]. In order to maximize the yield of higher alkanes, the H₂/CO ratio should be as low as it can. On the other hand, lower H₂/CO ratio favors carbon deposition, which shortens the catalyst (Cu-based) lifetime. So the H₂/CO ratio is set equal to 1.0.

The recovered waxes from the 1st separation stage undergo hydrocracking in order to convert them into lower hydrocarbons. The hydrocracking modeling is simplified in the framework of this work. A typical composition of the products after the hydrocracking process is adopted from the study of Shah et al. [316] and is assumed 3.46% CH₄ (Fuel gas), 8.77% C₃ (LPG), 26.10% C₈ (Gasoline), 61.67% C₁₆ (Diesel). Each hydrocarbon represents a certain fuel product. The hydrogen from the hydrocracking process is recovered from the unconverted syngas by means of the Pressure Adsorption Process (PSA). The required flow rate of hydrogen is based on the mass ratio (=0.0103 kg/kg) of wax to hydrogen that is calculated in the study of Sudiro and Bertucco [317].

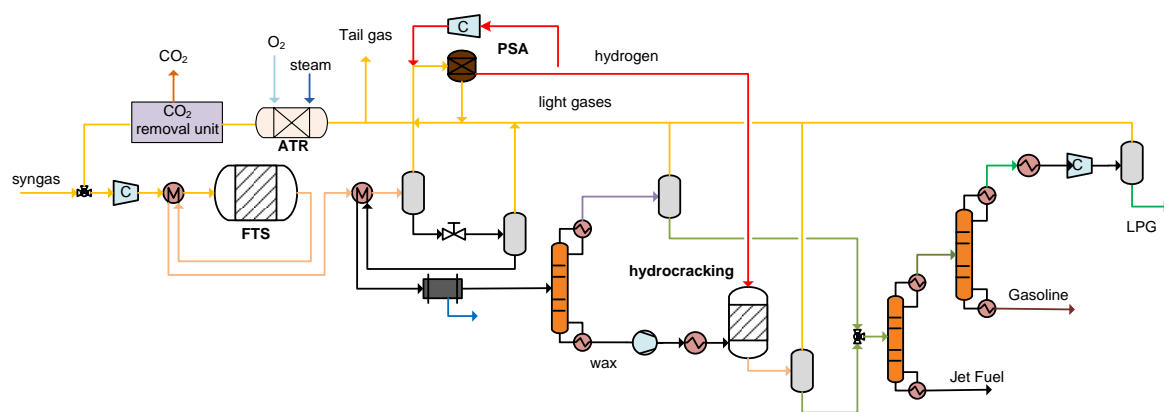


Figure 98. Process flowsheet for FT synthesis and products separation

Comparing the main data yielded for the FTS case with the corresponding data from the MAS routes in **Table 72** it is revealed that the MAS pathways have higher jet fuel productivity, since they are designed to have jet fuel as the main biofuel product. The overall thermal efficiency is calculated at 40.4% and the total carbon utilization at 30.4%, slightly lower than the corresponding values in modMeOH case. It is worth mentioning the considerably low power consumptions in this case: This is attributed both to the lower FT reactor operation pressure and to the high CO conversion rate that is assumed, which enables lower recirculating gas flows, contrary to the MAS cases.

7.6 Economic Evaluation

7.6.1 Thermochemical Cases 10kg/s biomass input (or 864 t/day)

According to the previous methodology and the mentioned economic data that is adopted, the DCFROR analysis resulted to the Minimum Jet Fuel Selling Prices for each case studied: 1.24, 1.49 and 1.28 €/l for each of the thermochemical cases: FT, MAS-ModFT and MAS-ModMeOH respectively, with a capacity of 864 ton of dry biomass per day. For the FT case, due to the great range of hydrocarbons produced, apart from jet fuel (end-product), other fuel types produced (LPG, Gasoline) are considered as by-products. It is assumed that they are available to buy with the 2011 year conventional price: LPG is considered to be sold at 0.29 €/l [318] whereas gasoline at 0.56 €/l [319]. Similarly, gasoline is considered as by-product for the other two thermochemical cases.

Figure 99 shows the contribution of CAPEX, OPEX, Biomass Feedstock Cost and By-product Credits (gasoline in all cases whereas LPG only for FT case) to the Production cost of jet fuel in €/l. The costs are also expressed in €/GJ of jet fuel's Higher Heating Value $-HHV$ (46.2 MJ/kg) for a plant's Capacity of 190 MW_{th}. For the calculations, it was assumed a jet fuel density equal to 0.81kg/l.

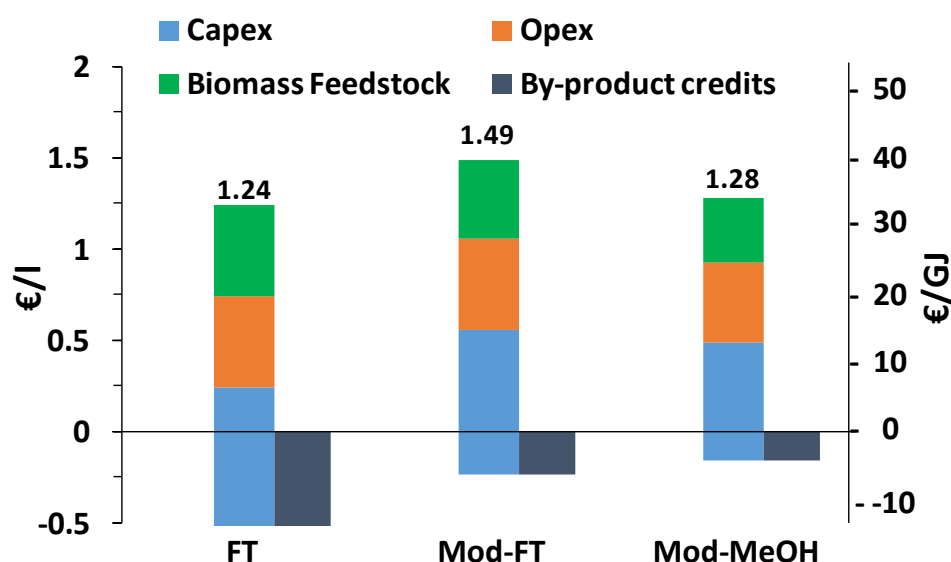


Figure 99. Contribution To Production Cost, MJFSP in €/l and €/GJ

The considerable effect of Capex on the Jet fuel production cost is illustrated in **Figure 99**, since it has the largest share to the product cost for all thermochemical cases. In addition, the cost of biomass feedstock participates in a significant portion to the cost of final product. FT Synthesis case seems to be a more economically feasible scenario. This is attributed to two main reasons: firstly, the capital investment cost of the alcohol based routes is higher, due to the complexity of fuel upgrading unit. Secondly, more by-products than the other two cases are produced in the FT case, which are considered to be sold according to current's market prices.

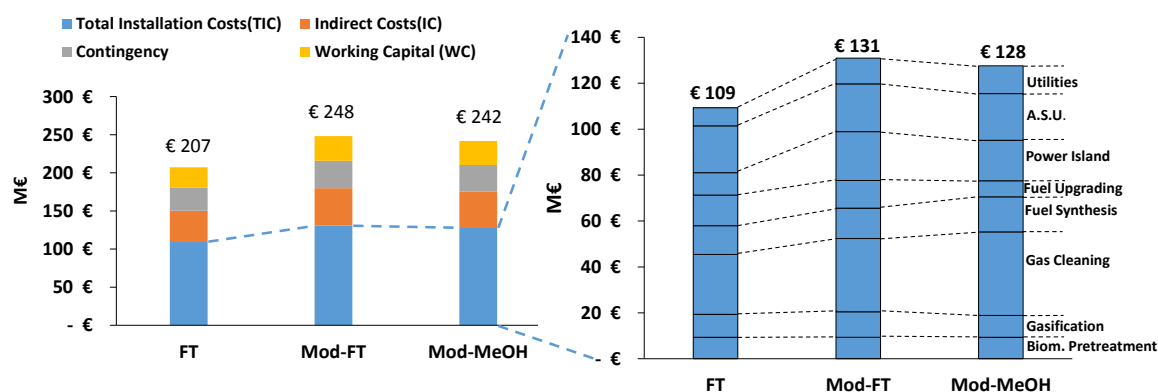


Figure 100. Breakdown of Total Capital Investment (left) and Total Installation Costs (right) in M€

Moreover, the total capital investment cost for each thermochemical case is described in **Figure 100**. The Mod-FT case has the highest TCI with 248 M€ whereas the lowest one is observed at the FT case with 207 M€. **Figure 100** also illustrates the breakdown of the installation cost of each case, showing the installed cost of each area of processes, too. Thus, a conclusion on the share that holds each area of processes in each case can be derived. The most expensive process unit is the Syngas Cleaning and Conditioning Area for all three cases. For FT case, this area has the highest share to the Total Installation cost with 23.85% of the TIC of the plant. Respectively, for the Mod-FT and Mod-MeOH cases, the values are 24.34% and 28.52%. Moreover, the Air Separation Unit and Power plant contribute greatly to the TIC of each case. In summary, Mod-FT case has the highest Installation Costs of equipment with 131 M€, with Mod-MeOH case having 128 M€ and FT case having the lowest Installation costs, near 109 M€. The fact that Mod-FT case has greater equipment/installation cost than the Mod-MeOH is attributed to the higher power consumption in the former case, as it is illustrated by the greater share of power island on total equipment cost. The other components of TCI are calculated as mentioned previously and depend on Installation and Purchased Equipment costs.

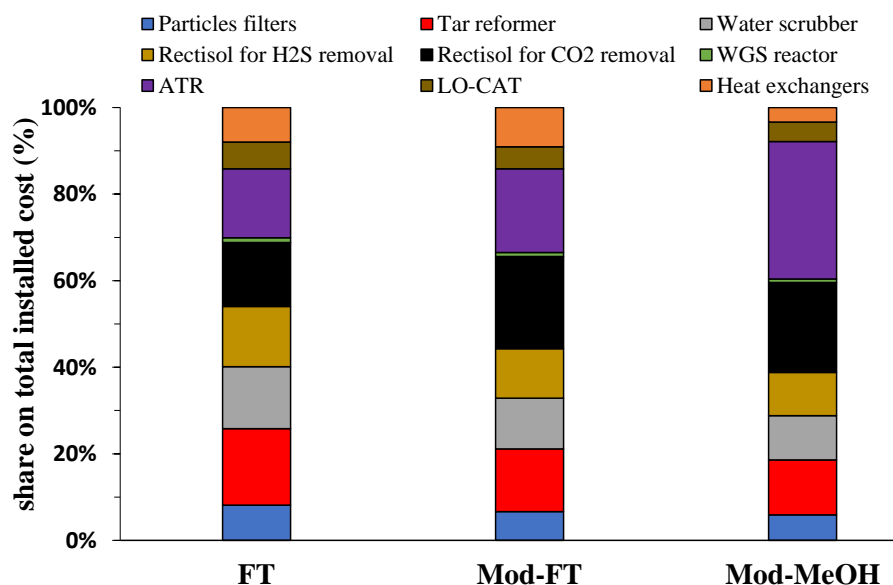


Figure 101. Installed cost distribution of the Units that consist the Syngas Cleaning & Conditioning Area

As Syngas Cleaning and Conditioning area has the most expensive processes, in **Figure 101**, a breakdown to its equipment is shown along with the share they have in the total installation cost of the area. Both in FT and Mod-MeOH cases, the most expensive equipment belong to ATR with a contribution of 16% and 32% in each case whereas in Mod-FT case it is the second most expensive process with 19%. This is due to the fact that large streams are sent to the ATR to be reformed. In Mod-FT case, the most expensive process is the Rectisol unit used for CO₂ removal with 21%, whereas in FT and Mod-MeOH cases, the contribution of Rectisol units is 15% and 21% respectively. Another costly process is that of tar reformer that contributes 18%, 14% and 13% of the total installation cost of cleaning and conditioning area in FT, Mod-FT and Mod-MeOH cases respectively.

In addition, the breakdown of OPEX for each case is described in **Figure 102**. The feedstock cost has the greatest contribution to the total amount of OPEX being nearly 45% of the total OPEX in each case. Mod-FT and Mod-MeOH cases have about the same OPEX, with Mod-MeOH case having higher catalyst costs, needed for the upgrading of higher alcohols to aviation fuels.

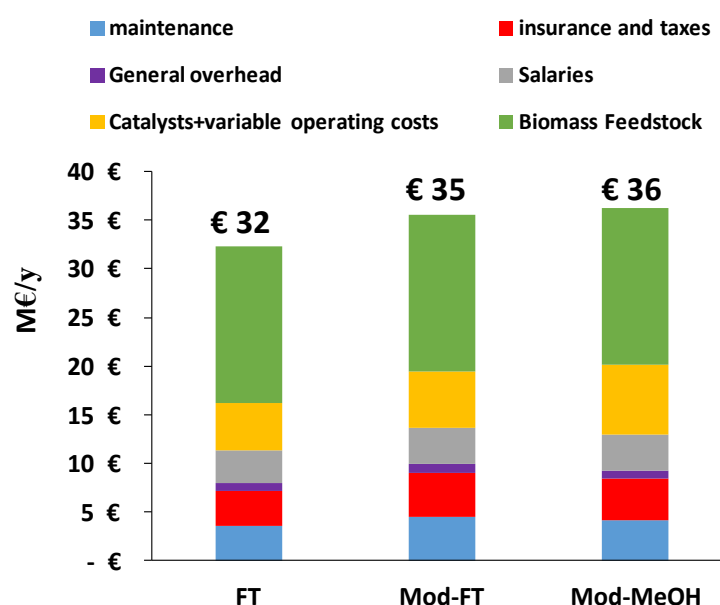


Figure 102. Breakdown of OPEX in M€/y

Figure 103 presents the breakdown of CAPEX and OPEX (without biomass feedstock) to the process areas, expressed in € per litre Jet Fuel. Fixed Operational Costs include General Overhead, Insurance and Taxes and Maintenance Costs. In the FT pathway, the most expensive units, concerning both CAPEX and OPEX, are the Syngas Cleaning and Conditioning, ASU, Fuel Upgrading and Utilities. Utilities part includes the Waste Water Treatment Unit and Cooling System of the biorefinery along with the variable costs of treating and disposing the wastes and process water. In the Mod-FT case, the most expensive areas are Syngas Cleaning and Conditioning, Power Plant, ASU, Fuel Upgrading and the Utilities section. In Mod-MeOH case, similarly with Mod-FT case, the most expensive areas are Syngas Cleaning and Conditioning, ASU, Power Plant, Fuel Upgrading, Utilities whereas Fuel Synthesis has a significant impact on the production cost of jet fuel. In comparison with the Mod-FT case, the OpeX of fuel upgrading is higher. This is due to the fact that in Mod-MeOH case, the catalyst used is more expensive and the amount of catalysts needed is higher. In addition, the CAPEX of Power Plant is significantly lower (from 21M€ down to 18M€), due to lower power consumptions in this case.

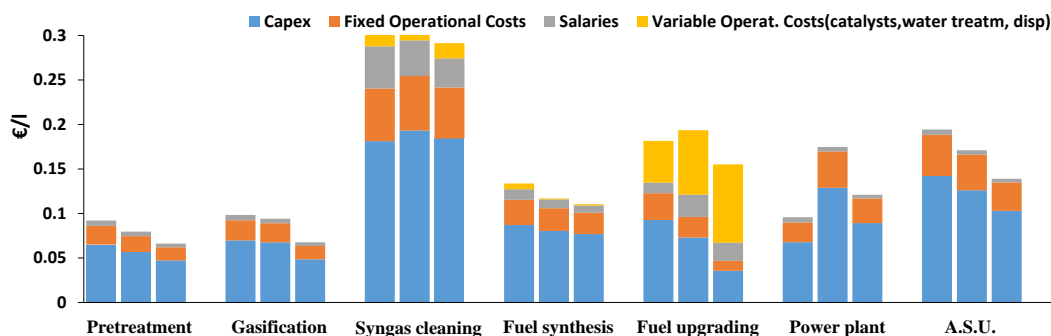


Figure 103. Breakdown of CAPEX & OPEX (excluding biomass cost) to Areas in €/l of Jet Fuel. 1st column: FT pathway, 2nd column: Mod-FT pathway and 3rd column: Mod-MeOH pathway

7.6.2 Effect of Plant capacity

Apart from the thermochemical pathways of converting biomass to biofuels, another important route is that of biochemical. Due to the fact that the three thermochemical Pathways described on the current paper have a capacity of 864 t/day biomass feedstock, a direct comparison with the biochemical Pathways with capacity of 2000 t/day is not convenient. Thus, via ASPEN Plus [320], the thermochemical case Mod-MeOH was modeled for 2000 t/day biomass feedstock. The economical analysis was conducted as described previously in order to calculate the Minimum Jet Fuel Selling Price. The calculation methods for equipment costs, CAPEX, OPEX are the same with the lower capacity model. The selection of Mod-MeOH was made because it is more economically desirable than Mod-FT case and with more novel technology than Fischer Tropsch Synthesis case.

In **Table 76**, the effect of plant capacity on different economical and thermodynamic parameters is shown as it is illustrated by the main results of each case. The two Capacities compared are 864 t/d and 2000 t/d of biomass feedstock in the thermochemical pathway of Mod-MeOH. For each parameter, the value is calculated and the percentage of the effect of plant capacity can be seen.

Table 76: Effect of Plant Capacity on Several Parameters

Parameter	Mod-MeOH 864 t/d	Mod-MeOH 2000 t/d	Relative difference in %
Biomass feed flow rate, kg/s	10.0	23.2	131
Fuel thermal input, MW _{th}	188.8	437	131
Jet Fuel production, kg/s	1.33	3.18	138
ASU Power Consumption, MWe	6.54	15.08	131
Gas Cleaning Power Consumption, MWe	3.01	6.98	132
Gas Compression Power Consumption, MWe	4.06	9.41	132
TCI (Total Capital Investment), M€	241.7	450.6	86
Operating Cost, M€/year	20.2	37.1	84
Biomass Cost, M€/year	16.1	37.2	131
By-product Credits, M€/year	7.0	16.6	137
MJFSP (Minimum Jet Fuel Selling Price), €/l jet fuel	1.28	1.02	-20

7.6.3 Comparison with Biochemical Pathways

The processes of the examined biochemical pathways are based on other reports [253, 321] along with their costs of equipment and operational costs. One biochemical pathway is based on Ethanol fermentation whereas the other is based on ABE (Acetone-Butanol-Ethanol) fermentation.

The ethanol fermentation process [253] starts with the biomass (corn stover) being milled and washed. The pretreated biomass is then processed with hydrolysis and catalyzed using dilute sulfuric acid and heat from steam. During this step, most of the hemicellulose is converted to soluble sugars however some inhibitors may be formed. Afterwards, the hydrolysate slurry is fed to a conditioning reactor where ammonia is added in order to raise its pH to 5-6 so enzymatic hydrolysis can be achieved. Enzymatic hydrolysis converts cellulose to glucose using cellulase enzymes in a continuous, high solids reactor. Cellulase Enzymes, can be purchased [322] or produced on-site [253] through an aerobic cultivation of microorganisms. After enzymatic hydrolysis, glucose and other sugars are sent to the batch fermentation vessels where a bacterium is added that can ferment glucose and xylose to ethanol (separate hydrolysis and fermentation). Lastly, the fermentation broth is introduced into the distillation columns where ethanol is separated from water, CO₂ and unconverted insoluble solids. In order to upgrade ethanol to aviation fuels, ethanol is fed to the upgrading area. The fermented ethanol follows the same processes mentioned before in Mod-FT scenario. Firstly n-butanol is produced through ethanol condensation, which via dehydration, oligomerization and hydrogenation is upgraded to aviation fuels.

For the economic evaluation of the ABE fermentation scenario, the processes and costs are based on Qureshi's report [321]. First of all, the biomass feedstock that is used is wheat straw. After being milled to 2-3mm particles, it is treated with dilute sulfuric acid and KOH/NaOH is added so the pH of the mixture can be readjusted. Continuously, enzymatic hydrolysis takes place and NaOH is added again to adjust the pH to 6.8. In addition, fermentation occurs with *C.beijerinckii* P260 for 42h producing ABE products. Finally, the recovery of products starts with a stripper that separates butanol with water from ethanol and acetone. Due to the fact that butanol and water form an azeotrope, they are separated by using a hydrophilic pervaporation membrane. As long as butanol is produced and separated, it is sent to the upgrading section along with ethanol. The butanol produced from fermentation is n-butanol, thus the processes following are the same described in Mod-FT scenario previously. Ethanol is condensed to form n-butanol and is added with the fermented butanol. Consequently, butanol via dehydration, oligomerization and hydrogenation is upgraded to aviation fuels.

The process analysis on the ethanol plant, having been conducted by Humbird et al. [253], revealed an overall thermal efficiency 44.0% and the carbon utilization factor is 29.4% of the total carbon that enters the system (both feedstock and glucose). This low carbon utilization factor is due to the fact that only 59.6% of the carbon content on the corn stover is carbohydrates and is able to be converted into ethanol through fermentation. Contrary to the thermochemical routes, the power requirements stand for only 3.5% of the total energy input. The majority of carbon that exits the plant is in the form of CO₂ that originates from the lignin combustion and from the fermentation process. Similarly, in the ABE case, the thermal efficiency of producing pure butanol is 40.4% and if take into account the heat content of the two other by-products (acetone and ethanol), the thermal efficiency is estimated at 65.8% [321]. The ethanol yield in the first biochemical route is 0.236 kg_{ethanol}/kg_{feedstock} whilst the corresponding yield of butanol in the ABE process is 0.197 kg_{butanol}/kg_{feedstock}. The production costs for ethanol and butanol are estimated 0.54€/kg and 0.78-1.01 €/kg, respectively. According to the corresponding reports on ethanol and butanol production from fermentation [253, 321], the corresponding alcohols are recovered

from the separation unit in high purity (>99.9%), and thus for the process analysis, they considered as completely pure.

For each biochemical case, the Capex and Opex costs of the upgrading section are added to the reference plant's costs (bioethanol and bioABE plant production), after being simulated in ASPEN Plus™ [320]. The only difference from the thermochemical cases in the upgrading section is the fact that the hydrogen, which is essential for the hydrogenation process, is purchased for 1.13 €/kg [323]. Thus, the PSA unit is removed and not considered in the costing of equipment. All costs are scaled for 310 operational days/year and 2000T/day feedstock input and in 2011 €.

In the ethanol fermentation case, the Total Capital Investment was estimated at 473.83 M€ with Operating Costs at 69.81 M€. The scaled Total Installation Cost of the equipment used for the production of ethanol, derived from NREL's paper [253], is at 195.26 M€, whereas the TIC of the upgrading equipment of ethanol to Jet Fuel is calculated at 23.445 M€. Regarding the ABE fermentation case, the TCI was estimated at 144.84 M€ with Operating Costs at 143.74 M€. The scaled TIC of the processes used for butanol production, derived from Qureshi's paper [321], is at 69.15 M€ with the TIC of the upgrading equipment of butanol to jet fuel at 11.87 M€. After calculating the TCI, Operating Costs, a DCFROR analysis is carried out as described in previous section, in order to determine the Minimum Jet Fuel Selling Price (MJFSP).

As mentioned above, the feedstock used for ethanol and ABE fermentation are the same from the corresponding papers, corn stover and wheat straw respectively. The feedstock prices and their compositions are described there. A cost figure of 48.69 €/dry t [253] was used for corn stover whereas for wheat straw a figure of 18.12 €/dry t was used [321].

Table 77. Analysis of the fuels used in the biochemical routes

Component	Corn Stover (dry wt%) [253]	Wheat Straw (dry wt%) [324]
Cellulose	35.05	48.57
Hemicellulose	23.94	27.7
Lignin	15.76	8.17
Ash	4.93	6.68
Carbohydrate Content	58.99	76.27
LHV (MJ/kg)	17.2	16.0

In **Figure 104**, a comparison can be made between the two biochemical and thermochemical case, according to the MJFSP of each case. Both Biochemical cases are economically more desirable than the thermochemical Mod-MeOH case though the latter is adequately competitive. It should be reminded that in each of these cases, different feedstock is used, bought with different price. Consequently, the purchased biomass feedstock contributes variously to the MJFSP for each case. The BioABE case has significantly lower Capital costs than the other two, but double the operating costs. Moreover, it has importantly more credits from the by-products, as it is considered that apart from the gasoline that is sold, acetone is sold too according to the market's price, 0.78 €/l [321].

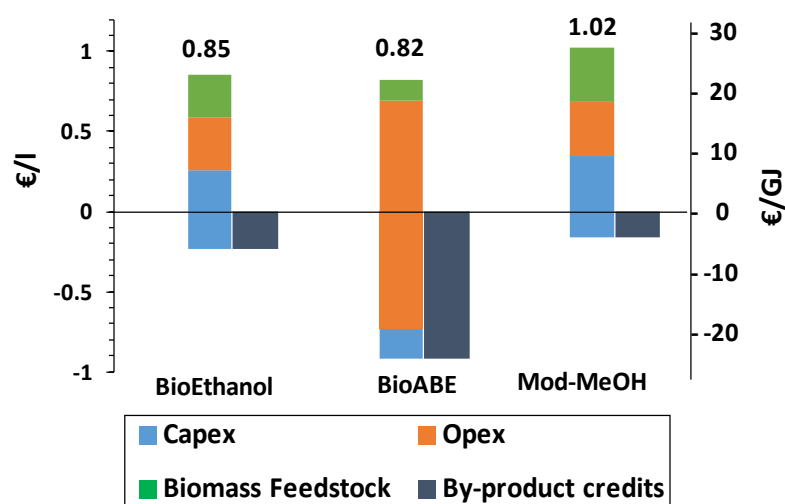


Figure 104. Contribution To Production Cost of Jet Fuel, MJFSP in €/l and €/GJ for biochemical routes compared to Mod-MeOH case

7.6.4 Sensitivity analysis

The effect of various parameters on the plant feasibility is discussed in this section. **Figure 105** demonstrates the influence of several parameters over the product value of jet fuel in each case. The parameter that has the greatest influence is the plant size as it decreases the MJFSP for 20% with an increase in plant capacity from 864 to 2000t/day. Another parameter with significant influence over the MJFSP is the biomass feedstock price that changes the MJFSP at $\pm 13\%$ for FT case and $\pm 10\%$ for Mod-FT and Mod-MeOH cases. Due to the fact that FT case produces a lot of by-products, it depends more on them than the other cases. Consequently, by changing the by-products selling price, the MJFSP of FT case is altered at $\pm 13\%$ whereas in the other cases for $\pm 4\%$ as the by-products that are produced in these cases are importantly fewer. The rest parameters have smaller influence over the MJFSP and can be seen in the figure below.

According to Peters and Timmerhaus [129], the method for calculating the total capital investment has $\pm 30\%$ accuracy. Consequently, it is examined how the minimum jet fuel selling price is affected by a 30% reduction or increase in CAPEX. This is shown in **Figure 105**, with indicating the range of TIC influence in the Selling price for each case. With a 30% reduction in TIC, the Minimum Jet Fuel Selling Prices are 1.03 €/l, 1.27 €/l and 1.10 €/l, for FT, Mod-FT and Mod-MeOH cases respectively, whereas with a 30% increase in TIC, the prices are 1.45 €/l, 1.71 €/l and 1.46 €/l, respectively. Concerning the corresponding biochemical routes, for a $\pm 30\%$ variation in TIC, the Minimum Jet Fuel Selling Price ranges from 0.73 to 0.97 €/l for the Bioethanol case, and from 0.78 to 0.86 €/l for the BioABE case. Hence, due to the uncertainty in predicting the investment cost with accuracy, a decisive conclusion about the most profitable route (thermochemical or biochemical) cannot be extracted.

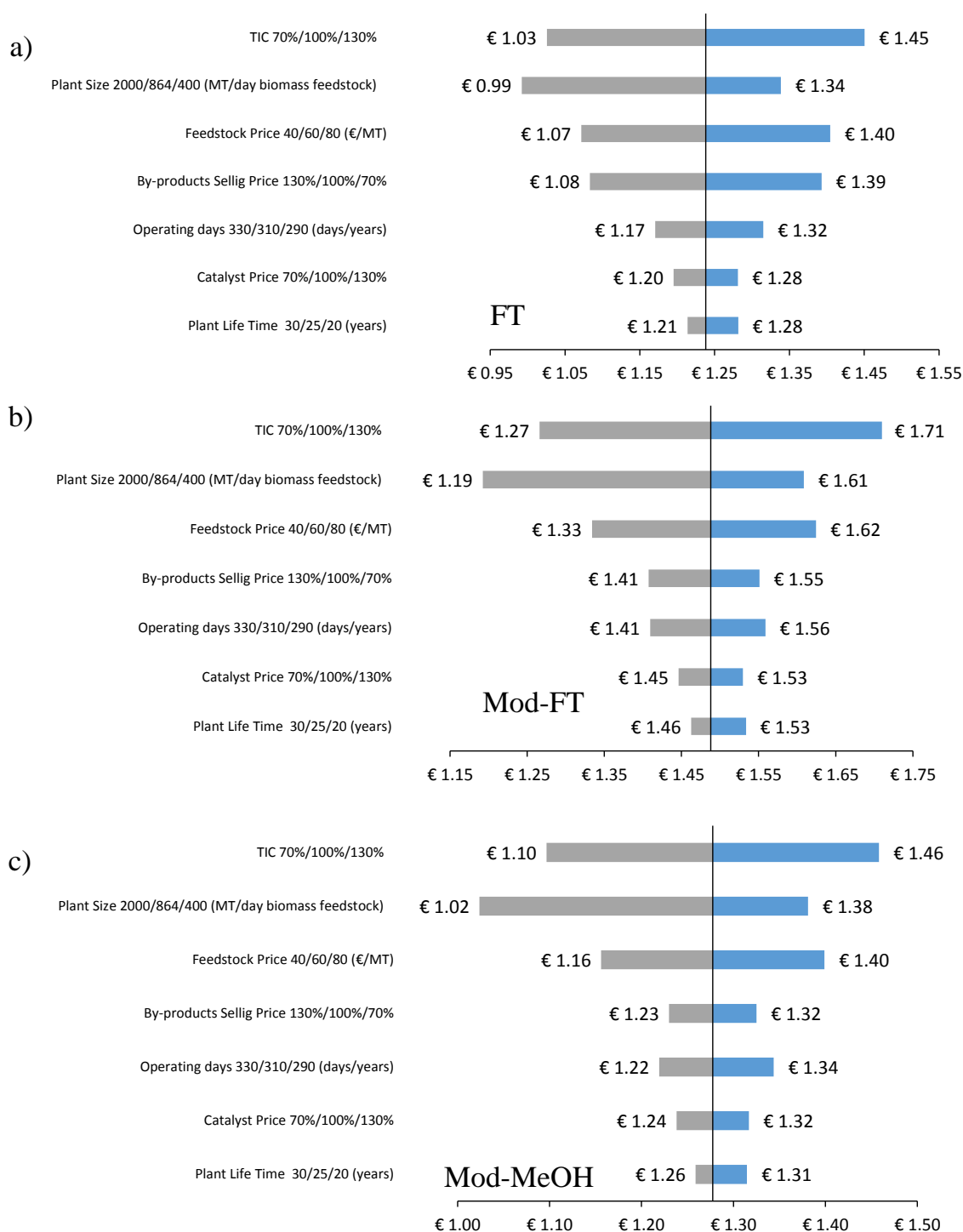


Figure 105. Sensitivity analysis of several parameters for the three thermochemical processes (864 Mt/d): a) FT, b) Mod-FT, c) Mod-MeOH

7.6.5 Investigation of setting the intermediate organic compounds as the final products

The proposed Alcohol to Jet Fuel routes that are investigated in this study, produce several valuable intermediate compounds (small and high olefins and higher alcohols) during the upgrading processes of alcohols to aviation fuels. Alternatively, these compounds can be retrieved, separated and considered as final products, making them available in the market. This potential is examined in this section.

In case where oligomers olefins are set as the final product, the hydrogenation unit, the PSA unit and the intermediate components (pumps, flash separators and distillation columns) are not considered for the costing. When the butene isomers are considered as the final products, the oligomerization reactor is not included in the costing method along with the above components. In case of considering the butanol isomers as final products, apart from the previously mentioned equipment, the dehydrating reactor is also excluded from the costing procedure. Moreover, the corresponding variable operational costs for each scenario are disregarded from the economic investigation. The purification step after each reactor is included. The only compound that should be removed from the product stream is water, which can be removed very effectively, since according to the experimental studies that the reactors modeling is based report 100% carbon selectivity on the desired products. The final products separation and purification (e.g. isobutene from n-butene separation or C12 olefins separation from C12 olefins etc.) is not taken into account in this analysis. However, a rough estimation of the expected increase in the final minimum selling price is presented, based on the study of Salgado-Gordon and Valbuena-Moreno [325]. In this report, a techno-economic study of a light olefins purification plant is performed. According to this assessment, for a ethylene purification plant with capacity 180 kt/year, the estimated CAPEX and OPEX was around 20M€ and 20M€/y, respectively. Taking into account that the annual production of the organic compounds in the fuel upgrading unit is of the order of 35 kt/year, the CAPEX and OPEX of the whole biorefinery are expected to rise by 4% and 11%, respectively. Hence, the increase in the minimum selling prices of the intermediate organic compounds that are presented in **Figure 106** is not expected to be more than 10%.

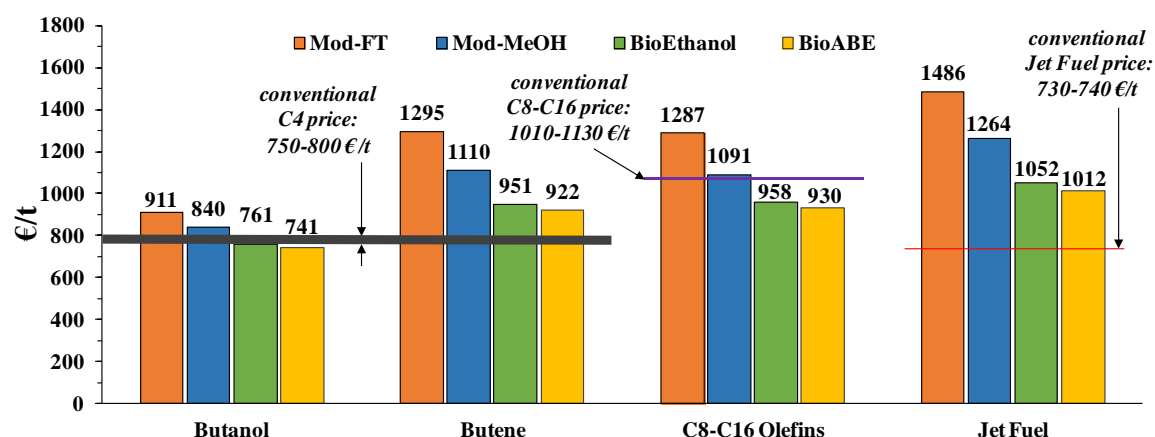


Figure 106. Specific prices (€/t) of the organic compound produced from the Alcohol-to-Jet fuel bio-based pathways (2000 t/d) and comparison with the corresponding conventional prices

As it is extracted from **Figure 106**, the concept of producing valuable organic chemicals is quite promising, since the resulting products prices are relative close to the corresponding current prices of the petrochemical derived chemicals. Especially, the biochemical routes can potentially compete with the petrochemical based organic compounds (lower and higher olefins and alcohols) industry. Furthermore, more motivation is gained for the improvement of thermochemical routes in the near future since they seem more competitive in case of producing valuable olefins and C4 isomers.

7.7 Further discussion and Conclusions

Figure 107 presents the product value of various biofuels products from selected studies in the literature, compared to the corresponding values resulted from the proposed pathways in this study. For

each study, the end product is expressed in €/GJ on HHV basis, so there can be a comparison between the biofuels on equal terms. With red and blue color markers the fuels produced by thermochemical and biochemical pathway respectively are presented. From the distribution of the prices, a clear conclusion can occur: The biofuel's price tend to increase as the years go by. The most recent studies shows a 200-300% increase in biofuel's price from the older ones. In other words, as the years pass, a more accurate estimation can be made, resulting in higher fuel prices, despite the fact that the technological developments have a beneficial contribution to the efficiency enhancement of each concept. Moreover, the value of the money changes due to inflation and the cost of equipment increases as new technologies arise. Finally, the price of feedstock continuously increases, having a great contribution to the product cost as it has been seen through the previous graphs.

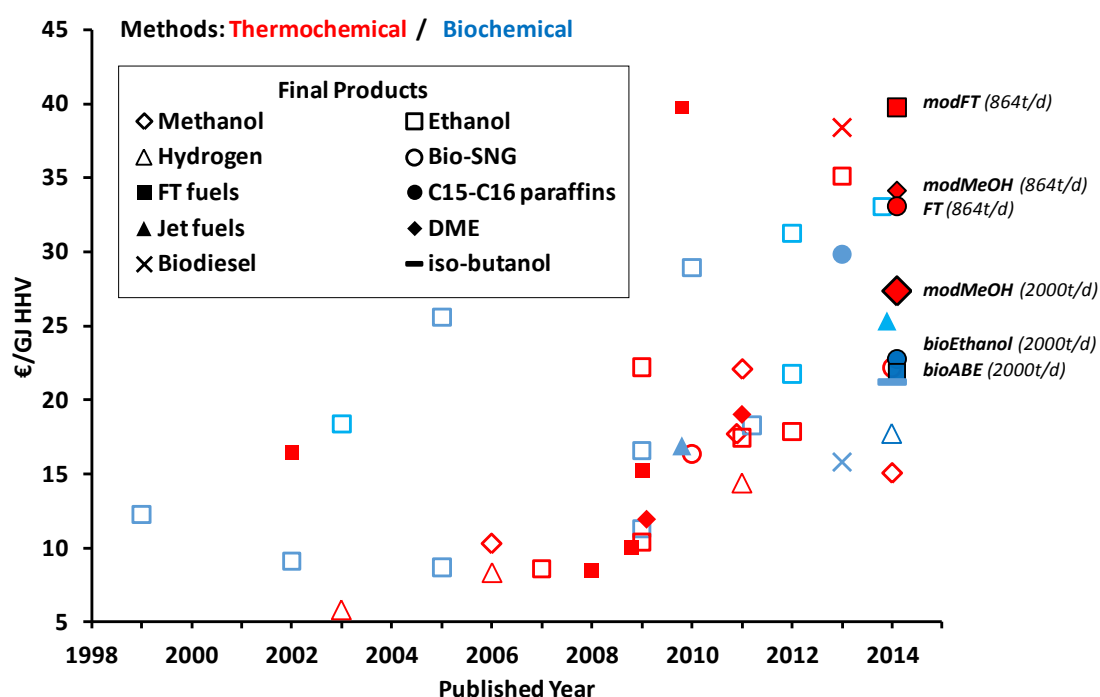


Figure 107. Specific product prices in €/GJ HHV from selected studies in the literature, in comparison with the corresponding values resulted from the proposed pathways in this study (with filled color and black marker line) [200, 250, 253, 266-272, 307, 309, 310, 322, 326-347]

In this study, a novel concept for biomass derived aviation fuel –mainly jet fuel- blends, produced via thermochemical route, is examined. Two main pathways based on mixed alcohols are modeled. Simulations results reveal quite high performance for both process configurations achieving a jet fuel production rate $0.138 \text{ kg}_{\text{JF}}/\text{kg}_{\text{feedstock}}$ in modMeOH case. The carbon balance along the process indicates that only 1/3 of the available carbon is found in the final product due to CO_2 production in several process steps such as the gasification, water gas shift, alcohol synthesis and tail gas combustion. Comparing to the conventional FTS case, it is shown that the mixed alcohols routes can achieve higher jet fuel productivity rates and better carbon utilization despite the higher power consumptions that are observed. The CO_2 valorization through hydrogenation and higher alcohols production does not results in improved plant performance due to high power requirements.

The water balance of the proposed bio refinery system shows that very large amounts of fresh water are required for the stable operation of such a large scale application. It was revealed that the demands for fresh water to compensate the released H_2O at the cooling tower and at the stack, for a plant with

190MW_{th} heat capacity are 23.7kg/s, emerging the water management as an important issue with considerable environmental impacts.

Additionally in this paper, the economic feasibility of a facility producing bio-based aviation fuels via alcohols derived either from biomass gasification or fermentation is also investigated. All the examined concepts are still far from global commercialization and market predominance over the “conventional” jet fuel, derived from fossil fuels, mainly due to the high biomass price and the high investment cost.

From the analysis on the thermochemical pathways, it is concluded that even though the Alcohol to Jet fuel concepts (ATJ) have better performance than the FTS route in terms of carbon utilization and thermal efficiency, the expected jet fuel price is higher. This is attributed to the higher CAPEX, especially in the Gas Cleaning Area and the Power Island. However, future developments on catalysts dedicated to mixed alcohol synthesis, regarding the enhancement of HA selectivity against light hydrocarbons, would contribute to the further improvement of the concept. Moreover, catalysts with improved selectivity would decrease recycling streams, resulting to a decrease in the size of equipment and bringing down the CAPEX. In addition, further attention should be given to the acid gas removal equipment that contributes most to the CAPEX. Apart from the method used on the current paper (Rectisol), other methods, e.g. amines, should be examined in future works as they could decrease the product price of jet fuel.

Regarding the biochemical cases, a direct comparison with the thermochemical cases should be avoided as different feedstock is used in each case, purchased with different price. However, overlooking this fact, the Acetone-Butanol-Ethanol (ABE) fermentation based biochemical process is considered as the most economically preferable option in spite of its high operational cost, due to the required chemicals and enzymes as well as the high power demanding final product’s separation.

The economic investigation of these alcohol based concepts indicated that providing the organic compounds, that are produced intermediately (i.e. light and heavy olefins, C4 alcohol isomers), can be a promising option for the feasibility of such biorefineries plants.

8. Conclusions – Future work

8.1 Main Conclusions

This PhD thesis was focused on the development and investigation of advanced energy systems based on processes that enable their operation with minimized GHG emissions, contributing to the evolution of the Low Carbon Economy. As is quoted in the Introduction, three are the main areas where the under investigation systems lie on; the Carbon Capture and Storage strategy, the Carbon Capture and Utilization option and the bio-based economy. The most significant conclusions derived from the studies on these specific areas are:

I. Carbon Capture and Storage

In the field of CO₂ mitigation of the power plants that operate with natural gas, the employment of Palladium Membrane Technology for CO₂ capture and sequestration was thoroughly investigated. The excellent performance of Pd membranes in H₂/CO₂ separation in terms of selectivity and HRF enables the opportunity to achieve even 100% Carbon Capture Rate. The sensitivity analysis of various operation parameters and the fine tuning of the process configuration towards the best operation led the net efficiency to an optimum value (50.82%) or -7.48% energy penalty. Among the reactors, the Autothermal Reformer performance affects considerably both the plant efficiency, and the operation of the steam cycle and the H₂ production and purification scheme. From the assessments of the CO₂ purification schemes after the membrane separator, it was revealed that, an oxy-combustion system with high combustion efficiency in near- stoichiometric conditions is the best option in terms of efficiency and Cost of Electricity. However, cryogenic systems have very high CO₂ purification abilities and can be effectively applied in the H₂ plants with CO₂ capture. After the process simulations of various options for CO₂ capture in a NG fired power plant, it was concluded that the Pd membrane technology offers the highest performance in terms of net efficiency among the others (pre combustion, post combustion and oxyfuel). The high Carbon capture rates, in conjunction to low CO₂ compression duties contribute to the lowest SPECCA index for NG case (2.91 MJ/kgCO₂). The economic assessment revealed that the high current capital cost of membranes negatively affects the cost of CO₂ avoided. Membrane area reduction by increasing the pressure difference between the two membrane sides decreases considerably the *COE* and consequently the cost of CO₂ avoided. Cost reduction through future advances and high volume production of the Palladium membrane can render the technology an even more competitive market option.

As far as the application of CO₂ capture in coal fire power plants is concerned, a thermodynamic analysis was performed in order to evaluate and compare three of the most attractive CO₂ capture techniques from exergetic point of view: amine scrubbing, Ca looping process and oxy-fuel combustion (or O₂/CO₂ cycle). Calcium Looping (CaL) process was proven the best option for CO₂ capture among the others, in terms of overall energy and exergy efficiency. Although a considerable amount of exergy (22.3% of total E_{fuel}) is lost in the CaL unit, the carbonation/calcination process has the lowest exergy penalty (-9.0%). Almost half of the fuel input is not burnt in the boiler, where the specific exergy losses are higher. The fact that the oxy-calcliner is more efficient by exergy point of view than the boiler (air or oxy fired) is the main reason why the total plant has the lowest irreversibilities when the CaL

technology is employed for CO₂ capture. From the sensitivity analysis in the CaL case, low limestone make-up ratios have little beneficial contribution to the exergy losses reduction. Sulfur content in the supplementary fuel has negative impact on both the plant efficiency and the CaL performance. Low sulfur fuels for the sorbent regeneration in the calciner are suggested. In the amine scrubbing case, 7.7% of the exergy input is lost in the capture unit and 1.0% during CO₂ compression. High MEA/CO₂ ratios and high MEA concentrations in the lean solvent promote the effectiveness of the process. In the oxy-combustion case, the ASU is the main unit where the majority of exergy losses (647.8kJ/kgCO₂) for CO₂ capture are observed. A potential development of O₂ selective membranes or other technology with minimum or zero power consumptions would help to save more than 9% of the total exergy input. It should be pointed out that this exergy analysis was performed in a thermal plant for power production and the main conclusions about the conclusions above cannot be generalized for any carbon capture case.

II. Carbon Capture and Utilization

Regarding the alternative option for CO₂ management after separation and capture from fossil fuel derived processes (e.g. flue gas after combustion), the design aspects for a power to fuel concept was investigated. The parameters that mostly affect the feasibility of such a concept were identified: it was revealed that the use of cheap electricity in conjunction with adequate time coverage throughout the annum is of high importance for lowering the overall H₂ production costs. Each of the three main parameters for the determination of the H₂ cost (electrolyzer capital cost, electricity cost and storage cost) can play the key role in the feasibility of the plant depending on the concept each time. Furthermore, a Power-to-Fuel system integrated with a coal fired power plant can be an interesting option for excess power transformation when the electricity sell is not profitable. Since the production cost of methanol from CO₂ is about 2.5 times higher than the corresponding conventional prices, a considerable effort is needed in order the CO₂ derived fuels to reach a competitive level in the global market. the key parameters that strongly affect the viability of the PtF concept are the following:

- The cost due to electrical consumptions that are required in order to produce hydrogen from water and then to transform CO₂ into organic compounds with high energy content is the most significant factor that influences the power to fuel economic feasibility.
- Examining the role of the system configuration in the economy, it is revealed that the hydrogen production is preferable to be near to the methanol plant, avoiding high logistics costs for delivery and storage of H₂. On the other hand, the location of the CO₂ capture unit has small influence on the inlet gas production and delivery cost.
- The investment cost has a 30% share on the methanol production cost, 2/3 of this is the alkaline electrolyzer cost. So, a new electrolyzer design with lower cost would reduce considerably the minimum selling price of the produced alcohol in order the investment to be profitable.
- The oxygen that is produced in the H₂ plant is in high quality and can be used in numerous applications in industrial, medical and other sectors. Selling the produced O₂ with a very competitive price, the methanol production cost reduces at least 10%.

Regarding the investigation of various design aspects for the valorization of industrially captured CO₂ towards liquid fuels, two novel concepts are examined: one for methanol and another for ethanol production. In the methanol case, a new scheme of employing a membrane reactor with high selectivity either in methanol permeation (organophilic) or in water permeation (hydrophilic) is explored via

process simulation. The methanol extraction has a beneficial effect on the methanol yield and requires a more compact sized reactor. In ethanol case, the novel synthesis route via DME has a higher efficiency (total energy efficiency: 70.3% on LHV basis whereas the corresponding efficiency of the conventional scheme is 63.2%) because of lower heat and power demands for its effective operation. From the economic analysis, it is shown that the novel ethanol plant results to lower ethanol production cost than the conventional one through the rWGS by 18% but the high cost for H_2 production through water electrolysis keeps it far for competitive levels.

III. Biomass utilization for advanced fuels/chemicals production

In the framework of the biomass utilization concept for conventional fuel substitution, a biorefinery plant was designed in ASPEN Plus in order to investigate the various design and operational aspects that affect the performance of the system. The case that was examined was the production and purification of ethanol and other higher alcohols via thermochemical route (gasification) and catalytic synthesis from syngas. The selection of catalyst type for the mixed alcohol synthesis, i.e. modified FT (MoS_2), modified MeOH (CuZn), determines the plant configuration in terms of the pressure level that fuel synthesis takes place, the products separation and gases recirculation. In case that methanol is not considered as desired product, catalysts with high carbon selectivity in C_2+ alcohols such MoS_2 are more preferable in terms of productivity and energetic efficiency. If this MeOH is a useful product then system efficiencies could be slightly improved. From the energy balance calculation, the oxygen production for gasification and hydrocarbons reforming and syngas compression for fuel synthesis have the highest power consumptions. Co-produced hydrocarbons have a detrimental effect on efficiency since the energetic penalties of their separation, oxygen driven autothermal reforming and recycling are great. These penalties are mainly associated with the air separation unit and the compression power required for unreacted gas recycling. The last aspect (unreacted gas) is correlated with the CO conversion in the reactor; the lower the gas hourly space velocity (GHSV) is achieved the lower the unconverted CO exits the reactor. Additionally, a considerable amount of power and steam is consumed in the gas cleaning unit especially for acid gas removal (H_2S and CO_2). The development and implementation of hot-dry gas cleaning methods is expected to reduce considerably the heat/power demands of such a thermochemical process leading to a more efficient operation.

Following the previous study, an alcohol based thermochemical route or the production of branched paraffins with high carbon number for aviation use (avfuel and avgas) was thoroughly investigated. The conceptual process design was described accompanied with the presentation of the results from the process simulations the economic evaluation and the comparison with the Fischer-Tropsch (FT) process and biochemical pathways. Two novel process schemes for paraffins with high C number was developed and presented in detail: one based on mixed alcohols produced using modified Methanol catalyst (modMeOH) with high selectivity in methanol, and one using modified FT catalyst (modFT), with high selectivity in ethanol. The flow sheeting results reveal high performance for both process configurations, resulting in an aviation fuel yield $0.172 \text{ kg/kg}_{\text{feedstock}}$ and a thermal efficiency of 40.5% in the case of employing a modified Methanol catalyst for the mixed alcohols synthesis (MAS). Such alternative pathways offer higher efficiencies compared to FT synthesis because specific products such as $C_{12}+$ branched paraffins for jet fuel applications are achieved with higher selectivity in the conversion processes. The water balance at the whole process reveals that the annual demands for fresh water from a $190 \text{ MW}_{\text{th}}$ biorefinery plant are $641,000 \text{ m}^3$, emerging the water management as an important issue with considerable environmental impacts. Simulations of the overall process show a rather high biomass carbon to product utilization ratio (up to 30%) leading to relative low CO_2

emissions. The economic evaluation reveals that the Minimum Jet Fuel Selling Price in a FT plant (1.24 €/l jet fuel) is lower than the corresponding price in a MAS plant (1.49 €/l and 1.28 €/l for cases with different catalysts). The biochemical route based on Acetone - Butanol - Ethanol fermentation is considered as the most economically desirable option (0.82 €/l). Moreover, the option of selling organic compounds, which are produced intermediately (i.e. light and heavy olefins, C4 alcohol isomers) via the alcohols' upgrading processes was proved promising enough for the feasibility of such biorefineries plants.

8.2 Innovative aspects

The aspects that were examined and considered as innovative are summarized below:

- Process integration, design analysis and optimization of an NGCC plant employed with Pd Membranes for pre-combustion capture of CO₂.
- Development and investigation for the best scheme for effective CO₂ purification
- Process integration, system design and investigation of other capture techniques (CO₂ selective membranes, RectisolTM, SelexolTM, hot potassium) in NG-fired power plants.
- Exergy analysis and comparison of the three most advanced capture technologies (amine scrubbing, CaL process and oxy fuel) for coal-fired power plants, taking into account the quality of CO₂ stream in terms of transport and storage, including the appropriate CO₂ purification scheme before compression.
- Identification of the conditions in order a power to methanol concept to be viable.
- Development of novel process configuration for ethanol production from CO₂ via DME.
- Investigation of impact of catalyst type for MAS on process configuration and performance for both alcohols and added value chemical products
- Design, optimization and economic assessment of a novel scheme for biomass derived aviation fuel through alcohols synthesis. Comparison of catalyst type for mixed alcohols synthesis
- Thermodynamic analysis for total carbon utilization in a biorefinery (hydrogenation of the rejected CO₂)
- Comparison of thermochemical and biochemical pathways for added value products synthesis (paraffins, olefins, higher alcohols)

8.3 Future study

In this Thesis, various advanced energy systems and processes are investigated through process simulation and economic analysis. Several issues are addressed for future study and are listed below:

1. *Potential use of Pd membranes in other applications (e.g. biorefineries) feasibility study*

Beyond the pre-combustion capture scheme for the effective H₂/CO₂ separation, Pd membranes can be implemented in numerous applications in chemical process industry, like a biorefinery system. In **Figure 108** the processes where it is possible for palladium (Pd) membrane technology to be applied in a bio-refinery system are marked, according to relevant studies found in the literature. A biorefinery in its general form can be designed for a wide variety of products, from advanced fuels to inorganic or organic chemicals. Hence, a study is proposed that is dedicated to the potential improvement of the operation of a biorefinery after the exploitation of the Pd membranes features.

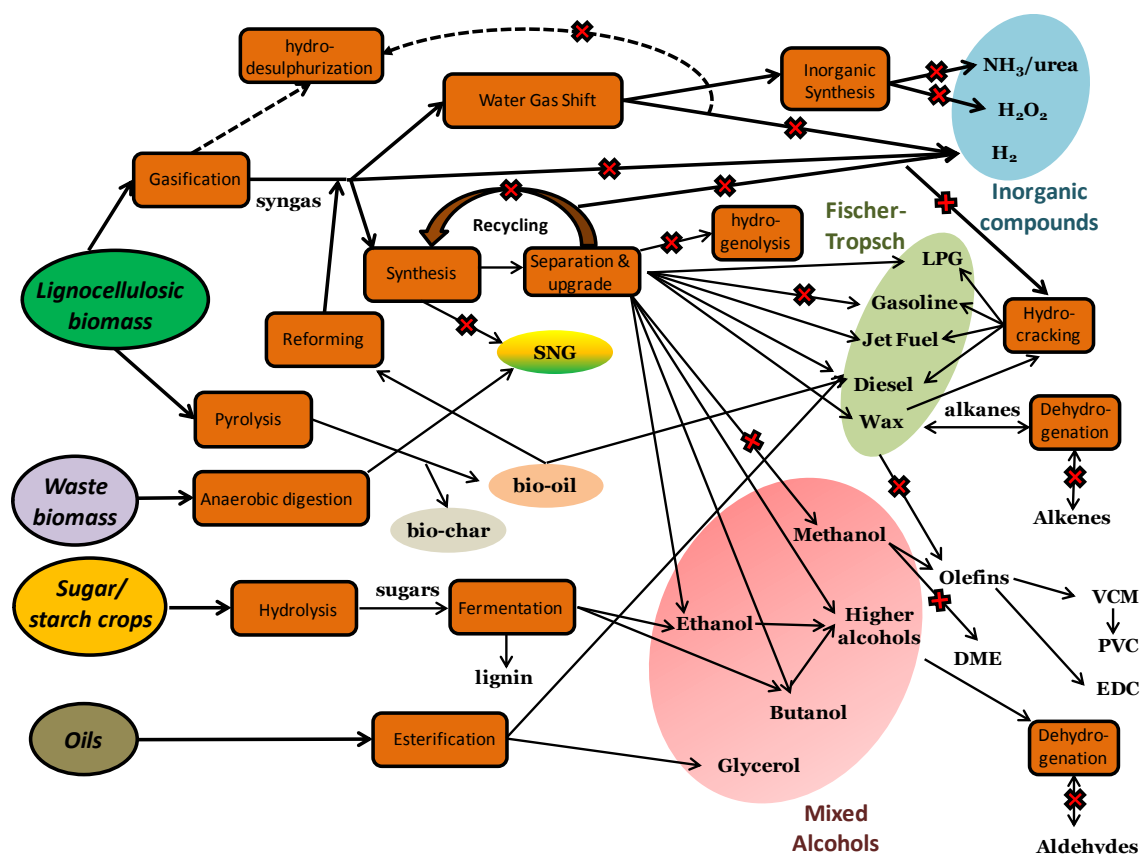


Figure 108. Biorefinery processes chart (with red X are the applications where Pd membrane can be potentially implemented)

2. Rigorous process modeling Pd membrane reactors

A study that is correlated with the previous one is the simulation and numerical investigation of Pd base membrane reactors where catalytic reactors that have not been investigated are conducted. As seen in **Figure 108**, there plenty of potential implementations of a catalytic reactor employed with Pd membrane, the detailed investigation of which is necessary for their up-scaling to industrial level.

3. New capture techniques (ionic liquids)

In this Thesis, it was concluded that the existing CO₂ capture options are still far for economic implementation and new concepts should be emerged and developed. Such a new concept that is under investigation in low Technology Readiness Level (TRL) but is very promising is the chemical absorption by mean of ionic liquids (ILs). The development of a thermodynamic model that predicts accurately the CO₂ absorption and desorption form the ILs incorporated in a process model is a challenge and is suggested as future work.

4. Dynamic simulations of advanced energy systems

All the process simulations in this Thesis were run in steady state conditions, assuming a stable operation. The dynamic behavior of such advanced systems under variable conditions (partial load, start and end of the plant operation, change in feedstock quality, etc.) and how their performance is influenced from them are suggested as a follow-up study.

5. Microbial electrosynthesis

Among the main conclusions in Chapter 4 was the large contribution of hydrogen production to the economic feasibility of a power-to-fuel concept. The development of microorganisms that use as

catalyst can directly convert the CO₂ and water into advanced fuels and chemicals under electrical current is a very promising concept. The development of the process simulation and economic evaluation of such systems in large scale will be a starting point for the comparison of the thermochemical routes based on CO₂ hydrogenation, that were investigated in Thesis.

6. *Hot & dry gas cleaning methods*

As it was revealed in Chapter 6, the gas cleaning and conditioning section has a considerable contribution to the investment and operational cost, in a thermochemical based biorefinery. Novel techniques based on hot and dry gas cleaning methods are expected to offer several benefits in the plant performance such the heat and power reduction, the size reduction and better by-products management. A techno-economic investigation on different gas cleaning methods would show the potential enhancement in the feasibility of a thermochemical plant, biomass or coal based.

7. *Syngas fermentation*

On the one hand, in biosyngas (thermochemical) pathways, total C is transformed into gaseous species (CO, CO₂, etc) but only CO practically takes part in the synthesis of the final product. On the other hand, in biochemical routes, only carbon in sugars (cellulosic biomass) is available for the final alcohol (ethanol/butanol) synthesis but with perfect selectivity. Syngas fermentation combines these two features in one: according to this microbial concept, specific microorganisms are used for syngas conversion into fuels and chemicals. The modeling of this concept using process simulation tools will determine the prospective for industrial implementation and will compare it with the bio-based routes that were investigated in this Thesis, in terms of economic feasibility.

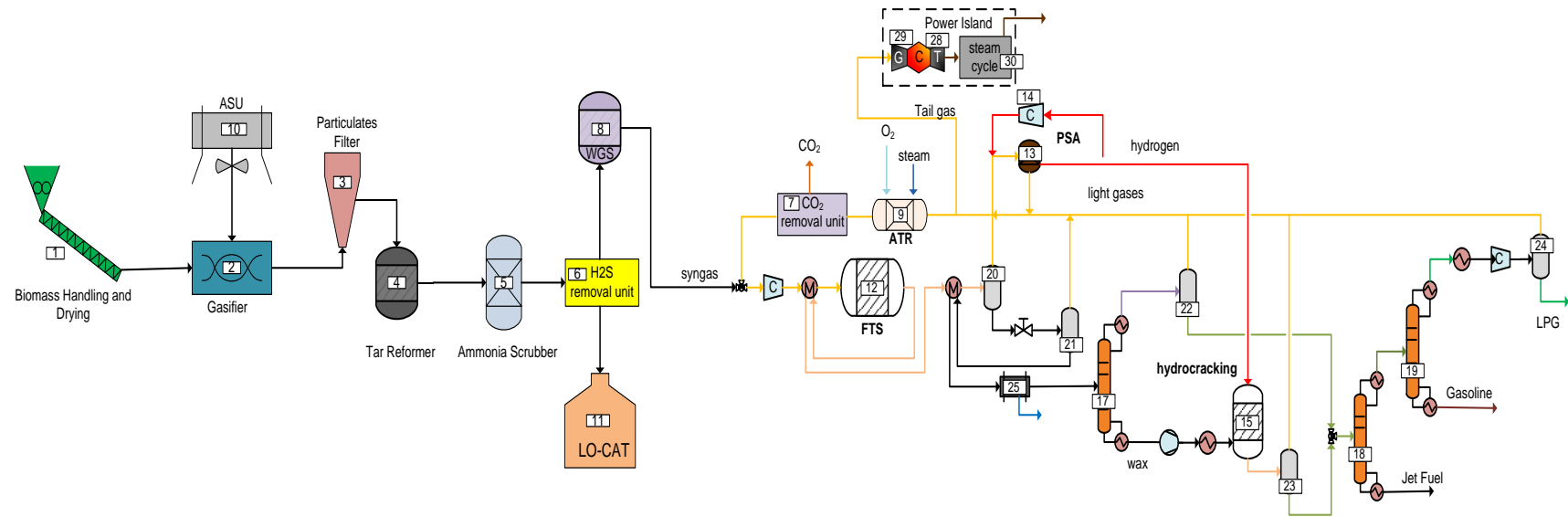
8. *Life Cycle Assessment (LCA)*

The environmental impact of the energy systems examined in this Thesis should be investigated performing the corresponding LCA. In these analyses the real CO₂ emissions that are avoided or indirectly produced will be estimated.

Annex

A. Supplementary Data related to cost equipment estimation in Chapter 7

Cost Equipment for Thermochemical FT 864 T/day Synthesis



#	Equipment name	Design Base	Units	New stream	Base Cost (€)	Year	Scaling factor	Purchased Cost/unit (€) ¹	Installation factor	Total installed Scaled Cost (€) ²	Ref.
1	Handling & Drying	65	biomass wet kg/s	10	14,244,130	2009	0.77	3,782,514	2.47	9,342,810	[348]
2	Gasifier	11.583	kg/s	2.5	2,419,775	2003	0.7	1,205,310	2	8,394,265	[349]
3	Particle filters	12.1	m ³ /s gas	2.69	1,900,000	2002	0.65	1,058,481	2	2,116,961	[350]
4	Tar reformer	33.8	Nm ³ /s	13.91	2,340,500	2001	0.7	1,867,501	2.47	4,612,727	[184]
5	water scrubber	0.056	m ³ /s	0.681	169,178	2010	0.6	809,086	2.47	3,729,227	[182]
6	Rectisol for H ₂ S removal							1,473,509	2.47	3,639,567	[129, 136]
7	Rectisol for CO ₂ removal							1,557,416	2.47	3,846,816	[129, 136]
8	Water–gas–shift reactor	58.33	kg/s	9.4	472,045	2010	0.8	116,486	2.47	287,720	[182]
9	Auto-thermal Reformer	119.6	standard m ³ /s output	7.64	9,481,822	2009	0.67	1,685,076	2.47	4,162,137	[351]

10	Air separation Unit	21.285	O ₂ produced (kg/s)	3.78	16,356,275	2006	0.5	8,081,068	2.47	19,960,239	[133]
11	LO-CAT	0.065	kg/s	0.03	755,000	2002	0.65	653,146	2.47	1,613,270	[330]
12	Slurry phase FT reactor	19.822	S m ³ /s	19.45	3,209,514	2003	0.72	4,612,472	2.47	11,392,807	[130]
13	PSA unit	0.294	kmol/s purge gas	0.01	1,668,947	2003	0.74	151,751	2.47	374,825	[130]
14	PSA purge gas compressor	10	MWe power	0.01	1,476,377	2003	0.67	13,364	2.47	33,008	[130]
15	Hydroprocessing unit	4.10E-03	m ³ /s	3.10E-04	22,650,000	2005	0.65	5,229,072	2.47	12,915,809	[258]
16	Waste Water Treatment	109.194	kg/s water input	5	15,366,543	2010	1.05	695,281	2.47	1,717,344	[135]
17	Distillation Column 1					2002		2,353	2.47	5,813	[129]
18	Distillation Column 2					2002		2,987	2.47	7,378	[129]
19	Distillation Column 3					2002		18,102	2.47	44,712	[129]
20	Flash tank/drum 1		kg/s	0.97		2000	0.8005	1,078	2.47	2,662	[136]
21	Flash tank/drum 2		kg/s	0.94		2000	0.8005	1,054	2.47	2,603	[136]
22	Flash tank/drum 3		kg/s	0.76		2000	0.8005	887	2.47	2,192	[136]
23	Flash tank/drum 4		kg/s	0.17		2000	0.8005	266	2.47	657	[136]
24	Flash tank/drum 5		kg/s	0.03		2000	0.8005	61	2.47	151	[136]
25	Decanter	44	kg/s	0.97	21,572	2002	0.6	3,240	2.47	8,003	[184]
26	Heat exchanger Network	355	MW	45.51	14,708,745	2009	1	2,116,048	2.47	5,226,639	[352]
27	Cooling System	470	MW	17.47	20,080,972	2009	0.67	2,482,580	2.47	6,131,974	[132]
28	Gas turbine	266	GT Mwe	3.27	17,117,409	2003	0.75	920,254	2.47	2,273,027	[130]
29	HRSg + heat exchangers	355	MWth heat duty	7.26	12,593,522	2003	1	375,345	2.47	927,102	[130]
30	Steam cycle ³	136	ST gross Mwe	6.54	13,907,895	2003	0.67	2,651,406	2.47	6,548,972	[130]
31	Pumps	0.0417	m ³ /s	0.001	46,170	2010	0.33	13,095	2.47	32,345	[352]

¹ scaled in 2011€

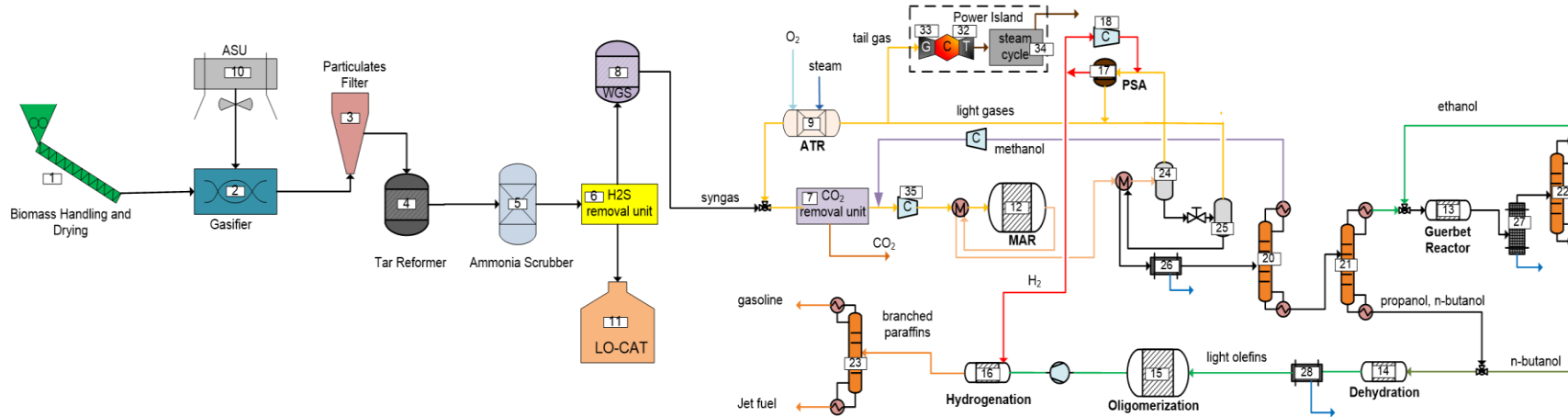
TPEC 46,005,305 €

² the number of pieces for each component is 1 except from Gasifier (4) and Water scrubber (2)

TIC 109,353,762 €

³ including condenser and steam turbine

Cost Equipment for Thermochemical MOD-FT 864 T/day Mixed Alcohol Synthesis



#	Equipment name	Design Base	Units	New stream	Base Cost (€)	Year	Scaling factor	Purchased Cost/unit (€) ¹	Installation factor	Total installed Scaled Cost (€) ²	Ref.
1	Handling and Drying	65	biomass wet kg/s	10	14,244,130	2009	0.77	3,782,514	2.47	9,342,810	[348]
2	Gasifier	11.58	kg/s	3	2,419,775	2003	0.7	1,205,310	2.00	8,394,265	[349]
3	Particle filters	12.1	m ³ /s gas	2.7	1,900,000	2002	0.65	1,061,001	2.00	2,122,002	[350]
4	Tar reformer	33.8	Nm ³ /s	13.91	2,340,500	2001	0.7	1,867,501	2.47	4,612,727	[184]
5	water scrubber	0.056	m ³ /s	0.68	169,178	2010	0.6	809,086	2.47	3,729,227	[182]
6	Rectisol for H ₂ S removal							1,473,509	2.47	3,639,567	[129, 136]
7	Rectisol for CO ₂ removal							2,755,451	2.47	6,805,963	[129, 136]
8	Water–gas-shift reactor	58.33	kg/s	9.4	472,045	2010	0.8	116,486	2.47	287,720	[182]
9	Autothermal reformer	119.6	standard m ³ /s output	13.71	9,481,822	2009	0.67	2,492,740	2.47	6,157,068	[351]
10	Air separation Unit	510.8333	O ₂ produced (kg/s)	90.73	16,356,275	2006	0.5	8,081,068	2.47	19,960,239	[133]
11	LO-CAT	0.065	kg/s	0.03	755,000	2002	0.65	662,421	2.47	1,636,179	[330]
12	Mixed Alcohol Reactor	92	kg/s	17.98	5,825,554	2005	0.65	2,523,993	2.47	6,234,263	[184]

13	Condensation ⁴	92	kg/s	6.02	5,825,554	2005	0.65	1,239,677	2.47	3,062,002	[184]
14	Dehydration ⁴	92	kg/s	2.13	5,825,554	2005	0.65	631,231	2.47	1,559,140	[184]
15	Oligomerisation							100,602	2.47	248,488	[129]
16	Hydrogenation							838,353	2.47	5,565,872	[129]
17	PSA unit	0.294	kmol/s purge gas	0.03	1,668,947	2003	0.74	416,233	2.47	1,028,095	[130]
18	PSA compressor	10	MWe power	0	1,476,377	2003	0.67	1,443	2.47	3,565	[130]
19	Waste Water Treatment	109.1944	kg/s water input	5	15,366,543	2010	1.05	695,281	2.47	1,717,344	[135]
20	Distillation Column 1					2002		266,037	2.47	657,113	[129]
21	Distillation Column 2					2002		250,388	2.47	618,459	[129]
22	Distillation Column 3					2002		328,635	2.47	811,727	[129]
23	Distillation Column 4					2002		187,791	2.47	463,844	[129]
24	Flash tank/drum 1		kg/s	17.98		2000	0.8005	11,144	2.47	27,526	[136]
25	Flash tank/drum 2		kg/s	3.95		2000	0.8005	3,316	2.47	8,191	[136]
26	Decanter 1	44	kg/s	3.85	21,572	2002	0.6	7,401	2.47	18,281	[184]
27	Decanter 2	44	kg/s	6.02	21,572	2002	0.6	9,682	2.47	23,916	[184]
28	Decanter 3	44	kg/s	1.95	21,572	2002	0.6	4,928	2.47	12,173	[184]
30	Heat exchanger Network	355	MW	66.03	14,708,745	2009	1	3,070,457	2.47	7,584,029	[352]
31	Cooling System	470	MW	33.38	20,080,972	2009	0.67	3,831,173	2.47	9,462,997	[132]
32	Gas turbine	266	GT MWe	25.1	17,117,409	2003	0.75	4,246,069	2.47	10,487,790	[130]
33	HRSG + heat exchangers	355	MWth heat duty	22.17	12,593,522	2003	1	1,145,969	2.47	2,830,544	[130]
34	Steam cycle ³	136	ST gross MWe	8.71	13,907,895	2003	0.67	3,214,332	2.47	7,939,400	[130]
35	MAS Feed Compressor	10	MWe	7.21	1,723,968	2009	0.67	1,554,554	2.47	3,839,749	[352]
36	Pumps	0.042	m3/s gas	0.01	46,170	2010	0.33	24,737	2.47	61,101	[352]

¹ scaled in 2011€

² the number of pieces for each component is 1 except from Gasifier (4) and Water scrubber (2), Hydrogenation (3)

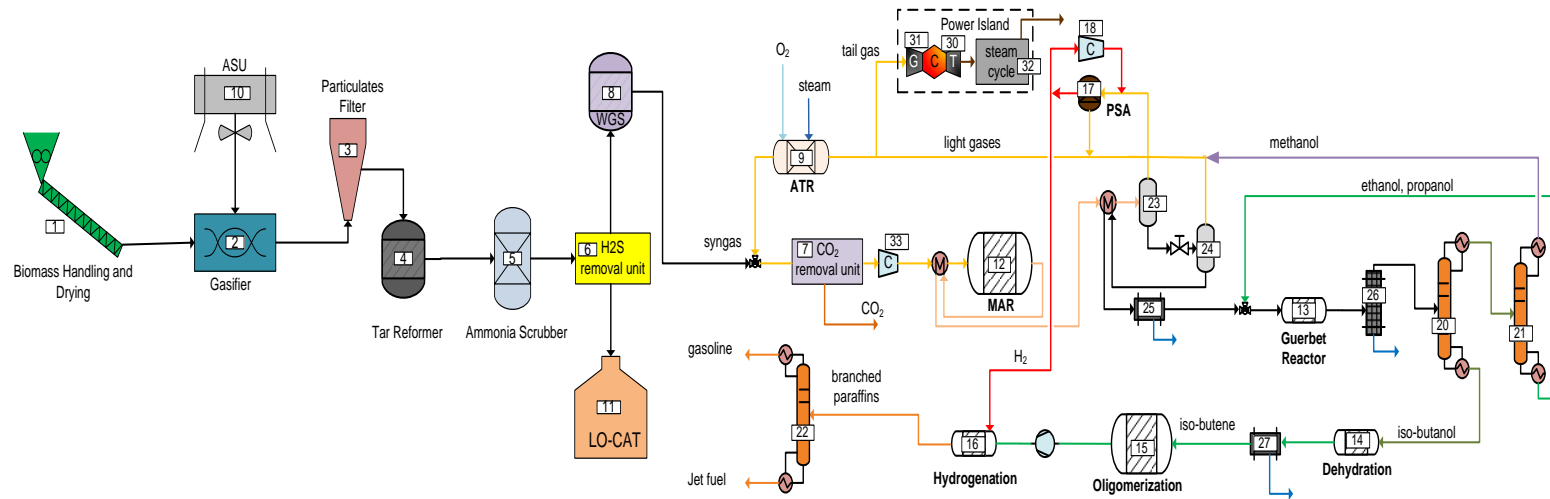
³ including condenser and steam turbine

⁴ the equipment cost of this reactor is estimated assuming its similarity with the MAS reactor (predominantly because of the high pressure operation, plug flow regime and type of reactants used).

TPEC 55,012,238 €

TIC 130,953,375 €

Cost Equipment for Thermochemical Mod-MeOH 864 T/day Mixed Alcohol Synthesis



#	Equipment name	Design Base	Units	New stream	Base Cost (€)	Year	Scaling factor	Purchased Cost/unit (€) ¹	Installation factor	Total installed Scaled Cost (€) ²	Ref.
1	Biomass Handling and Drying	65	biomass wet kg/s	10	14,244,130	2009	0.77	3,782,514	2.47	9,342,810	[348]
2	Gasifier	1000.8	Metric t/day	216	2,419,775	2003	0.7	1,205,310	2.00	8,394,265	[349]
3	Particle filters	12.1	m3/s gas	2.74	1,900,000	2002	0.65	1,070,219	2.00	2,140,437	[350]
4	Tar reformer	33.8	Nm3/s	13.91	2,340,500	2001	0.7	1,867,501	2.47	4,612,727	[184]
5	water scrubber	0.056	m3/s gas	0.68	169,178	2010	0.6	809,086	2.47	3,729,227	[182]
6	Rectisol for H2S removal							1,473,509	2.47	3,639,567	[129, 136]
7	Rectisol for CO2 removal							3,058,059	2.47	7,553,406	[129, 136]
8	Water–gas–shift reactor	58.33	kg/s	9.4	472,045	2010	0.8	116,486	2.47	287,720	[182]
9	Auto-thermal reformer	119.6	STD m ³ /s output	35.1	9,481,822	2009	0.67	4,680,255	2.47	11,560,230	[351]
10	Air separation Unit	21.28472	O ₂ prod. (kg/s)	3.78	16,356,275	2006	0.5	8,081,068	2.47	19,960,239	[133]
11	LO-CAT	5.983796	lb/h	2.68	755,000	2002	0.65	662,421	2.47	1,636,179	[330]

12	Mixed Alcohol Reactor	8,439	kg/s	1,902	5,825,554	2005	0.65	2,767,014	2.47	6,834,525	[184]
13	Condensation ⁴	8,439	kg/s	425.76	5,825,554	2005	0.65	1,045,841	2.47	2,583,228	[184]
14	Dehydration ⁴	8,439	kg/s	204.93	5,825,554	2005	0.65	650,205	2.47	1,606,006	[184]
15	Oligomerisation							78,246	2.47	360,652	[129]
16	Hydrogenation							290,629	2.47	1,929,502	[129]
17	PSA unit	0.294	kmol/s purge gas	0.01	1,668,947	2003	0.74	125,962	2.47	311,125	[130]
18	PSA compressor	10	MWe compressor	0	1,476,377	2003	0.67	1,137	2.47	2,809	[130]
19	Waste Water Treatment	109.2	kg/s water input	5	15,366,543	2010	1.05	695,281	2.47	1,717,344	[135]
20	Distillation Column 1					2002		297,336	2.47	734,420	[129]
21	Distillation Column 2					2002		234,739	2.47	579,805	[129]
22	Distillation Column 3					2002		179,967	2.47	444,517	[129]
23	Flash tank/drum 1		kg/s	19.18		2000	0.8	11,737	2.47	28,990	[136]
24	Flash tank/drum 2		kg/s	3.91		2000	0.8	3,288	2.47	8,122	[136]
25	Decanter 1	4,042	kg/s	357.34	21,572	2002	0.6	7,450	2.47	18,402	[184]
26	Decanter 2	4,042	kg/s	425.76	21,572	2002	0.6	8,276	2.47	20,442	[184]
27	Decanter 3	4,042	kg/s	204.93	21,572	2002	0.6	5,337	2.47	13,182	[184]
28	Heat exchanger Network	355	MW	28.03	14,708,745	2009	1	1,303,533	2.47	3,219,727	[352]
29	Cooling System	470	MW	38.41	20,080,972	2009	0.67	4,208,664	2.47	10,395,400	[132]
30	Gas turbine	266	GT Mwe	22.61	17,117,409	2003	0.75	3,926,180	2.47	9,697,663	[130]
31	HRSG + heat exchangers	355	MWth heat duty	14.24	12,593,522	2003	1	736,179	2.47	1,818,361	[130]
32	Steam cycle ³	136	ST gross Mwe	5.86	13,907,895	2003	0.67	2,465,707	2.47	6,090,297	[130]
33	MAS Feed Compressor	10	MW	15.18	1,723,968	2009	0.67	2,558,891	2.47	6,320,460	[352]
34	Pumps	0.0417	m3/s	4.20·10 ⁻⁴	46,170	2010	0.33	9,265	2.47	22,885	[352]

¹ scaled in 2011€

TPEC 53,501,811 €

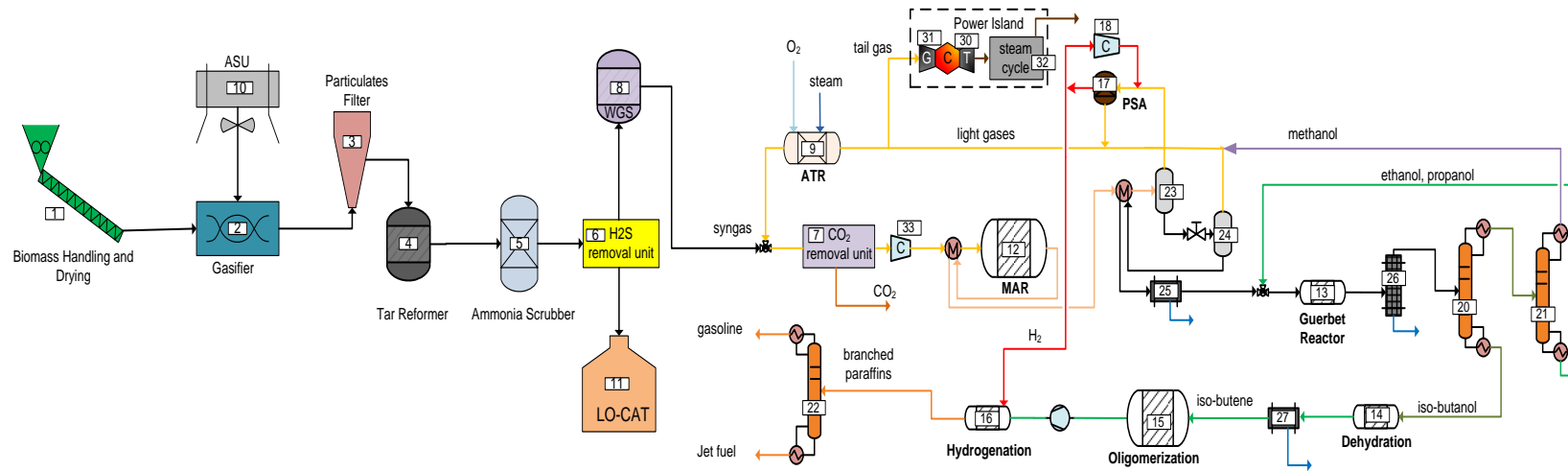
² the number of pieces for each component is 1 except from Gasifier (4), Water scrubber (2), Oligomerisation (2) and Hydrogenation (3)

TIC 127,614,671 €

³ including condenser and steam turbine

⁴ the equipment cost of this reactor is estimated assuming its similarity with the MAS reactor (predominantly because of the high pressure operation, plug flow regime and type of reactants used).

Cost Equipment for Thermochemical Mod-MeOH 2000t/Day Mixed Alcohol Synthesis



#	Equipment name	Design Base	Units	New stream	Base Cost (€)	Year	Scaling factor	Purchased Cost/unit (€) ¹	Installation factor	Total installed Scaled Cost (€) ²	Ref.
1	Handling and Drying	65	biomass wet kg/s	23	14,244,130	2009	0.77	7,218,685	2.47	17,830,151	[348]
2	Gasifier	11.58	MetricT/day	3	2,419,775	2003	0.7	1,335,178	2.00	17,352,020	[349]
3	Particle filters	12.1	m3/s gas	6.33	1,900,000	2002	0.65	1,846,656	2.00	3,693,312	[350]
4	Tar reformer	33.8	Nm3/s	34.74	2,340,500	2001	0.7	3,544,170	2.47	8,754,100	[184]
5	water scrubber	0.06	m3/s gas	0.62	169,178	2010	0.6	766,885	2.47	8,063,070	[182]
6	Rectisol for H2S removal							2,339,218	2.47	5,777,869	[129, 136]
7	Rectisol for CO2 removal							6,765,459	2.47	16,710,685	[129, 136]
8	Water–gas–shift reactor	58.33	kg/s	26.59	472,045	2010	0.8	267,745	2.47	661,330	[182]
9	Auto-thermal reformer	119.6	STD m ³ /s output	67.28	9,481,822	2009	0.67	7,237,264	2.47	17,876,041	[351]
10	Air separation Unit	21.28	O ₂ produced (kg/s)	12.14	16,356,275	2006	0.5	14,478,772	2.47	35,762,566	[133]
11	LO-CAT	0.07	lb/h	0.05	755,000	2002	0.65	966,266	2.47	2,386,677	[330]
12	Mixed Alcohol Reactor	92	kg/s	44.64	5,825,554	2005	0.65	4,558,692	2.47	11,259,970	[184]

13	Condensation ⁴	92	kg/s	10.7	5,825,554	2005	0.65	1,801,181	2.47	4,448,917	[184]
14	Dehydration ⁴	92	kg/s	5.15	5,825,554	2005	0.65	1,119,950	2.47	2,766,277	[184]
15	Oligomerisation							268,273	2.47	1,781,079	[129]
16	Hydrogenation							288,394	2.47	4,104,600	[129]
17	PSA unit	0.29	kmol/s purge gas	0.03	1,668,947	2003	0.74	501,068	2.47	1,237,638	[130]
18	PSA compressor	10	MWe compressor	0	1,476,377	2003	0.67	5,561	2.47	13,736	[130]
19	Waste Water Treatment	109.19	kg/s water input	11.88	15,366,543	2010	1.05	1,590,589	2.47	3,928,756	[135]
20	Distillation Column 1					2002		485,127	2.47	1,198,264	[129]
21	Distillation Column 2					2002		312,985	2.47	773,074	[129]
22	Distillation Column 3					2002		266,037	2.47	657,113	[129]
23	Flash tank/drum 1		kg/s	44.64		2000	0.8005	23,080	2.47	57,008	[136]
24	Flash tank/drum 2		kg/s	9.03		2000	0.8005	6,423	2.47	15,864	[136]
25	Decanter 1	44	kg/s	8.98	21,572	2002	0.6	12,305	2.47	30,393	[184]
26	Decanter 2	44	kg/s	10.7	21,572	2002	0.6	13,669	2.47	33,764	[184]
27	Decanter 3	44	kg/s	5.15	21,572	2002	0.6	8,816	2.47	21,775	[184]
28	Heat exchanger Network	355	MW	265.14	14,708,745	2009	1	12,328,298	2.47	30,450,895	[352]
29	Cooling System	470	MW	34.67	20,080,972	2009	0.67	3,929,363	2.47	9,705,526	[132]
30	Gas turbine	266	GT Mwe	17.97	17,117,409	2003	0.75	3,305,294	2.47	8,164,077	[130]
31	HRSG + heat exchangers	355	MWth heat duty	33.14	12,593,522	2003	1	1,713,069	2.47	4,231,280	[130]
32	Steam cycle ³	136	ST gross MWe	13.61	13,907,895	2003	0.67	4,335,155	2.47	10,707,832	[130]
33	MAS Feed Compressor	10	MW	14.94	1,723,968	2009	0.67	2,531,904	2.47	6,253,804	[352]
34	Pumps	0.042	m3/s	0.01	46,170	2010	0.33	25,661	2.47	63,382	[352]
										TPEC	100,877,886 €
										TIC	236,772,844 €

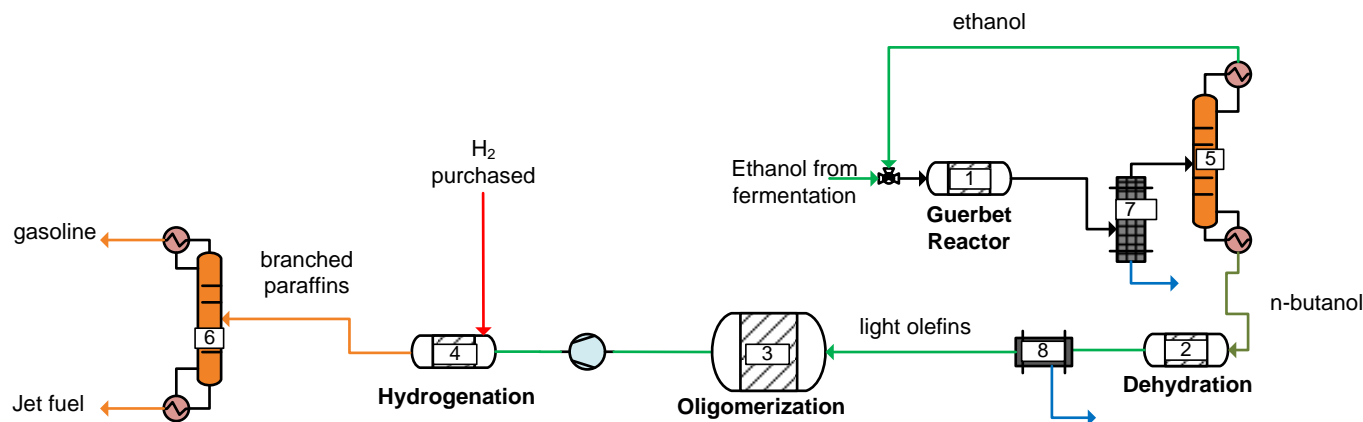
¹ scaled in 2011€

² the number of pieces for each component is 1 except from Gasifier (8), Water scrubber (5), Oligomerisation (3) and Hydrogenation (7)

³ including condenser and steam turbine

⁴ The equipment cost of this reactor is estimated assuming its similarity with the MAS reactor (predominantly because of the high pressure operation, plug flow regime and type of reactants used).

Cost Equipment for Biochemical - BioEthanol Fermentation 2000T/Day Upgrading Area



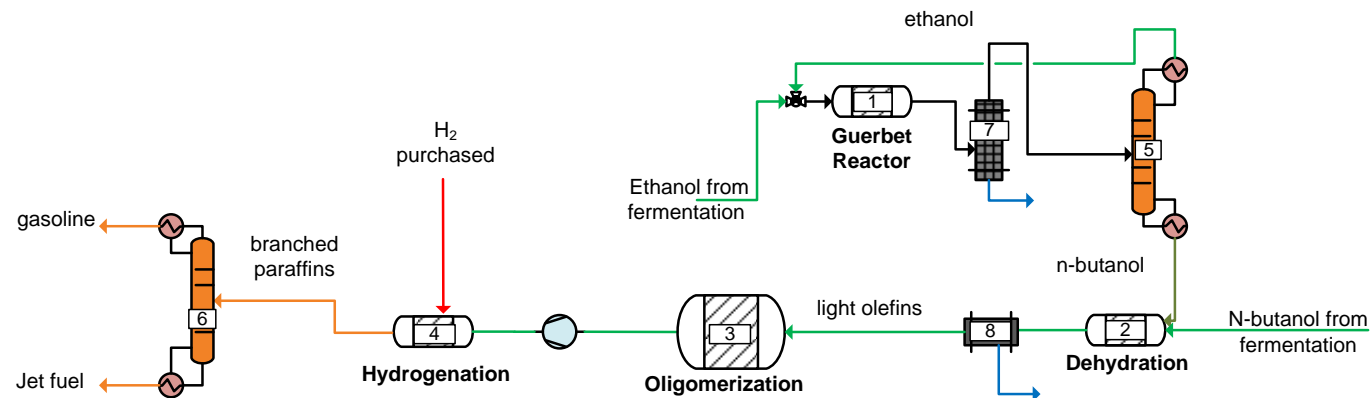
#	Equipment name	Design Base	Units	New stream	Scaling factor	Base Cost (€)	Year	Purchased Cost/unit (€) ¹	Installation factor	Total installed Scaled Cost (€) ²	Ref.
1	Condensation ³	92	kg/s	23.87	0.65	7,715,966	2005	3,416,453	2.47	6,371,172	[184]
2	Dehydration ³	92	kg/s	5.84	0.65	7,715,966	2005	1,367,614	2.47	2,550,396	[184]
3	Oligomerisation							279,451	2.47	1,855,291	[129]
4	Hydrogenation							301,807	2.47	4,844,039	[129]
5	Distillation Column 1						2002	1,450,925	2.47	2,705,758	[129]
6	Distillation Column 2						2002	352,368	2.47	657,113	[129]
7	Decanter 1	44	kg/s	23.87	0.6	21,572	2002	22,124	2.47	54,645	[184]
8	Decanter 2	44	kg/s	5.81	0.6	21,572	2002	7,055	2.47	17,425	[184]
9	Heat exchanger Network	355	MW	37.63	1.0	19,481,781	2009	2,317,622	2.47	4,322,018	[352]
10	Pumps	0.042	m ³ /s	0.01	0.33	46,170	2010	27,166	2.47	67,101	[352]
									TPEC	10,032,417€	
									TIC	23,444,956€	

¹ scaled in 2011€

² the number of pieces for each component is 1 except from Oligomerisation (3) and Hydrogenation (8)

³ the equipment cost of this reactor is estimated assuming its similarity with the MAS reactor (predominantly because of the high pressure operation, plug flow regime and type of reactants used).

Cost Equipment for Biochemical bio-ABE Fermentation 2000T/Day Upgrading Area



#	Equipment name	Design Base	Units	New stream	Scaling factor	Base Cost (€)	Year	Scaled Cost /unit (€) ¹	Installation factor	Total installed Scaled Cost (€) ²	Ref.
1	Condensation ³	92	kg/s	2.56	0.65	5,825,554	2005	710,439	2.47	1,754,785	[184]
2	Dehydration ³	92	kg/s	4.68	0.65	5,825,554	2005	1,052,254	2.47	2,599,068	[184]
3	Oligomerisation							245,917	2.47	1,632,656	[129]
4	Hydrogenation							281,687	2.47	4,009,144	[129]
5	Distillation Column 1						2002	281,687	2.47	695,766	[129]
6	Distillation Column 2						2002	250,388	2.47	618,459	[129]
7	Decanter 1	44	kg/s	2.56	0.6	21,572	2002	5,792	2.47	14,305	[184]
8	Decanter 2	44	kg/s	4.68	0.6	21,572	2002	8,323	2.47	20,557	[184]
9	Heat exchanger Network	355	MW	4.00	1.0	14,708,745	2009	185,869	2.47	459,095	[352]
10	Pumps	150	m3/h	20.11	0.33	46,170	2010	25,297	2.47	62,484	[352]
									TPEC	5,229,607 €	
									TIC	11,866,320 €	

¹ scaled in 2011€

² the number of pieces for each component is 1 except from Oligomerisation (3) and Hydrogenation (7)

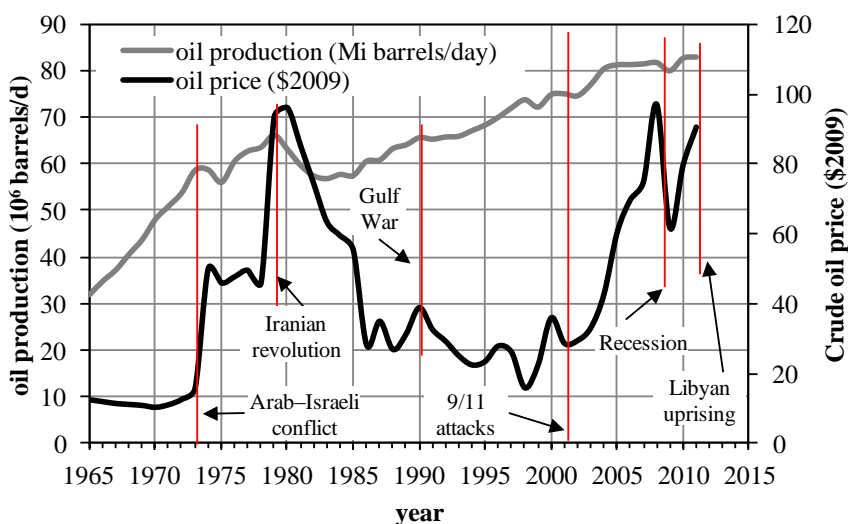
³ the equipment cost of this reactor is estimated assuming its similarity with the MAS reactor (predominantly because of the high pressure operation, plug flow regime and type of reactants used).

**Εκτεταμένη Περίληψη της Διδακτορικής
Διατριβής στην Ελληνική Γλώσσα**

1. Εισαγωγή

1.1 Η αναγκαιότητα για μετακίνηση προς ένα ενεργειακό σύστημα με χαμηλές εκπομπές άνθρακα

Από την αυγή της Βιομηχανικής Επανάστασης, η Ενέργεια θεωρείται ως ένα από τα σημαντικότερα αγαθά για την επιβίωση και εξέλιξη των ανθρώπινων κοινωνιών, τόσο στον Αναπτυγμένο όσο και στον Αναπτυσσόμενο Κόσμο. Ο σύγχρονος ανθρώπινος πολιτισμός οφείλει πολλά στην ύπαρξη των ορυκτών καυσίμων (άνθρακας, πετρέλαιο και φυσικό αέριο). Ειδικά τα τελευταία χρόνια, η τιμή του πετρελαίου συνδέεται άρρηκτα με τις εκάστοτε γεωπολιτικές εξελίξεις, κυρίως γύρω από την περιοχή της Μέσης Ανατολής (Εικόνα 109).

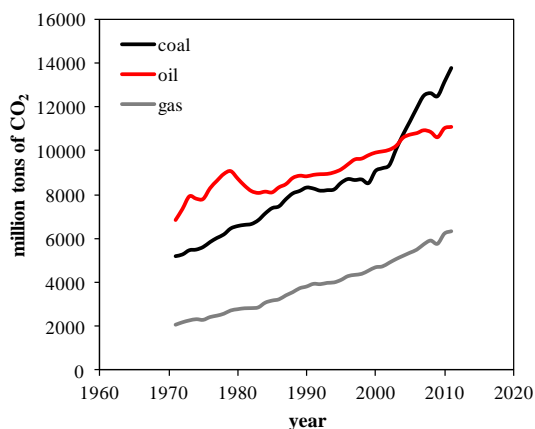


Εικόνα 109. Χρονική διακύμανση της τιμής του αργού πετρελαίου και η παγκόσμια παραγωγή τα τελευταία 50 χρόνια [1, 2]

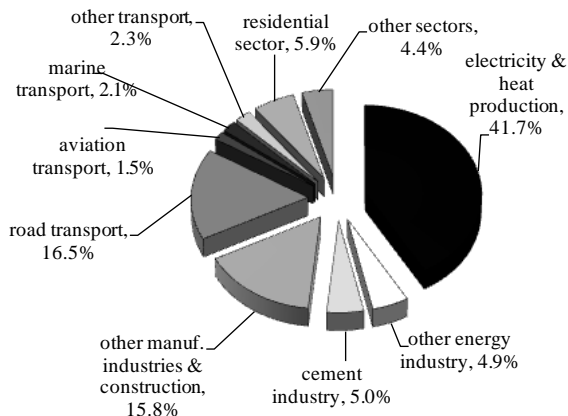
Οι διαρκώς αυξανόμενες ενεργειακές απαιτήσεις σε παγκόσμια κλίμακα θεωρούνται ένα από τα σημαντικότερα ζητήματα που πρέπει να διευθετηθούν σε σύντομο χρονικό διάστημα προτού η κατάσταση γίνει μη αναστρέψιμη. Σύμφωνα με τις προβλέψεις της Αμερικανικής Υπηρεσίας Ενέργειας (EIA), όλοι οι τύποι ορυκτών καυσίμων αναμένεται να αυξηθούν κατά 10% το 2040 [4] ενώ, επειδή οι ποσότητες αυτών δεν είναι απεριόριστες, από το 2042 και έως το 2112 μόνο άνθρακας θα έχει απομείνει προς διάθεση και χρήση [3].

Ένα άλλο ζήτημα που σχετίζεται με τα ορυκτά καύσιμα και απασχολεί την ανθρωπότητα είναι οι περιβαλλοντικές επιπτώσεις από την καύση αυτών. Οι εκπομπές διοξειδίου του άνθρακα (CO₂) έχουν αυξηθεί κατά 3.9% τα τελευταία 200 χρόνια σε σχέση με τον φυσικό κύκλο του άνθρακα, εξαιτίας της ανθρώπινης δραστηριότητας [5]. Μια τεράστια συζήτηση έχει ξεσπάσει τα τελευταία χρόνια για το κατά πόσο αυτές οι ανθρωπογενείς εκπομπές συμβάλλουν στο λεγόμενο «Φαινόμενο του Θερμοκηπίου» [6].

Σύμφωνα με το Διεθνές Πάνελ Κλιματικής Αλλαγής (IPCC), αν δεν παρθούν μέτρα για τη δραστική μείωση αυτών, η συγκέντρωση του CO₂ στην ατμόσφαιρα θα ανέλθει στα 570 ppm έως το 2100, προκαλώντας την αύξηση της μέσης θερμοκρασίας της ατμόσφαιρας κατά 1.9 °C με καταστροφικές συνέπειες για τους ζωντανούς οργανισμούς του Πλανήτη μας. [7].



Εικόνα 110. Παγκόσμιες εκπομπές διοξειδίου του άνθρακα από την χρήση των κυριότερων ορυκτών καυσίμων από το 1970 [8]



Εικόνα 111. Εκπομπές διοξειδίου του άνθρακα ανά τομέα το 2011 [8]

1.2 Στρατηγικές για ένα ενεργειακό σύστημα με χαμηλές εκπομπές άνθρακα

Υπό αυτό το πρίσμα, η ΕΕ έχει θέσει σε υψηλή προτεραιότητα την ανάπτυξη τεχνολογικών λύσεων που να είναι βιώσιμες οικονομικά και τεχνικά εφικτές για την «αποδέσμευση» των ενεργειακών συστημάτων του μέλλοντος από τον άνθρακα. Παράλληλα, η ΕΕ προσβλέπει στην διασφάλιση της ενεργειακής ασφάλειας της ηπείρου, σε συνδυασμό με την πραγματοποίηση των στόχων του Strategic Energy Technology Plan (SET-Plan) και της σχετικής ενεργειακής νομοθεσίας (οδηγίες για ΑΠΕ και δέσμευση CO₂).

Αν και η υιοθέτηση και ανάπτυξη των Ανανεώσιμων Πηγών Ενέργειας (ΑΠΕ) δείχνει να είναι μια βιώσιμη επιλογή προς αυτή την κατεύθυνση, υπάρχουν μερικά μειονεκτήματα που εμποδίζουν την υλοποίηση αυτής της προοπτικής. Ένα από αυτά είναι η αυξημένη τιμή κόστους της ηλεκτρικής κιλοβατώρας γεγονός που τις κάνουν λιγότερο ανταγωνιστικές από τους θερμικούς σταθμούς άνθρακα και πυρηνικούς. Δεύτερον, ένα ηλεκτρικό δίκτυο δεν μπορεί να εξαρτηθεί αποκλειστικά από τις ΑΠΕ λόγω της στοχαστικής και μη προβλεπόμενης παραγωγής ενέργειας από αυτά και οι απότομες αυξομειώσεις του φορτίου απαιτούν ένα σύστημα με μεγάλη ευελιξία. Για να διασφαλιστεί, λοιπόν, η σταθερότητα στην παροχή της ηλεκτρικής ενέργειας στο δίκτυο και λαμβάνοντας υπόψη ότι για την ώρα οι τεχνολογίες αποθήκευσης ενέργειας δεν είναι οικονομικά ελκυστικές, οι θερμικοί σταθμοί θα εξακολουθούν να έχουν τη μερίδα του λέοντος στην παγκόσμια ηλεκτροπαραγωγή. Επιπλέον, η διεθνής κοινότητα δεν είναι προετοιμασμένη για μια εποχή «χωρίς άνθρακα». Εκτός από την κατανάλωση ενέργειας, ο άνθρακας είναι ένα αναντικατάστατο συστατικό από το οποίο προκύπτει μια τεράστια γκάμα υλικών με αναρίθμητες χρήσεις και εφαρμογές (πλαστικά, ρούχα, χρώματα, χάλυβας, κτλ). Από τη μια μεριά, δηλαδή, η χρήση άνθρακα από ορυκτά καύσιμα θα πρέπει να μειωθεί δραστικά αλλά, από την άλλη η καθημερινότητα δεν μπορεί να απεξηγηθεί από αυτόν σε μικρό χρονικό διάστημα.

Ανάμεσα στις Καθαρές Τεχνολογίες Άνθρακα που σχετίζονται με τη μείωση των Αερίων του Θερμοκηπίου είναι η ανάπτυξη τεχνικών που αυξάνουν την απόδοση των σταθμών και η χρήση προξηραμένου λιγνίτη στις περιπτώσεις με χαμηλής ποιότητας καύσιμο, οδηγώντας σε μια αύξηση του βαθμού απόδοσης από 4 έως 6% [13-15]. Αν και αυτές οι επιλογές είναι διαθέσιμες, σε βιομηχανική κλίμακα έχουν περιορισμένη επίδραση στη δραστική μείωση των εκπομπών CO₂.

Οι τρεις βασικές στρατηγικές για τη δραστική μείωση των Αερίων του Θερμοκηπίου από ανθρωπογενείς πηγές είναι η Δέσμευση και Αποθήκευση CO₂ (CCS), η Δέσμευση και Επαναξιοποίηση

του CO₂ (CCU) και τα συστήματα που βασίζονται στη χρήση βιομάζας προς αντικατάσταση των στερεών καυσίμων.

1.2.1 Δέσμευση και Αποθήκευση CO₂

Σύμφωνα με το Σενάριο της Μπλε Χάρτας (Blue Map Scenario) του Διεθνούς Οργανισμού Ενέργειας (IEA), η Δέσμευση και Αποθήκευση CO₂ αναμένεται να παίζει καθοριστικό ρόλο για την επίτευξη του στόχου των 2°C συνεισφέροντας με 8.2 Gt δεσμευόμενου CO₂ [16]. Οι βασικές επιλογές για την αποθήκευση του CO₂ είναι είτε η απόθεσή του κάτω από τους ωκεανούς, είτε σε γεωλογικά διαμορφωμένες δεξαμενές ή στην ανάκτηση πετρελαίου και φυσικού αερίου (EOR and EGR) για την αύξηση της επίδοσης εξόρυξης. Το μεγαλύτερο έργο δέσμευσης CO₂ στον κόσμο αναμένεται να ξεκινήσει στα τέλη του 2016 στο Τέξας, όπου 4766 τόνοι θα διαχωρίζονται από καυσαέρια και θα αποθηκεύονται ημερησίως [18]. Επειδή ο διαχωρισμός CO₂ δεν αφορά μόνο την περίπτωση της αποθήκευσης αλλά βρίσκει χρήση και σε άλλες βιομηχανικές εφαρμογές, η εξέταση έχει πολλαπλό ενδιαφέρον τόσο για την προστασία του περιβάλλοντος όσο και για τη βελτίωση βιομηχανικών διεργασιών.

1.2.1.1 Δέσμευση CO₂ από σταθμό Φυσικού Αερίου

Οι πιο αντιπροσωπευτικές τεχνολογίες γι' αυτή την περίπτωση είναι η χημική απορρόφηση μέσω αμινών τύπου MEA για μετά-καύση δέσμευση και MDEA για προ-καύση δέσμευση [19]. Αν και η μετά-καύσης δέσμευση οδηγεί σε χαμηλότερο κόστος ηλεκτρισμού (COE), η προ-καύσης δέσμευση προσφέρει τη μοναδική δυνατότητα της συμπαραγωγής H₂ και ισχύος. Σε μια μελλοντική οικονομία που θα βασίζεται στην περιορισμένη χρήση άνθρακα, το υδρογόνο θα είναι από τους σημαντικότερους ενεργειακούς δείκτες με πολλαπλές εφαρμογές, είτε ως καύσιμο ως έχει, είτε ως συστατικό για την παραγωγή άλλων προϊόντων/καυσίμων. Γι' αυτό το λόγο αξίζει η περεταίρω διερεύνηση τέτοιων συστημάτων.

Ανάμεσα στις τεχνολογίες προ καύσης, οι μεμβράνες παλλαδίου (Pd) ή κράματα με βάση αυτό θεωρούνται μια πολλά υποσχόμενη επιλογή. Το βασικό τους προτέρημα είναι η δυνατότητα παραγωγής ενός υψηλής περιεκτικότητας ρεύματος υδρογόνου σε ένα μεγάλο εύρος θερμοκρασιών. Οι μεμβράνες αυτές είναι γνωστές και εφαρμόζονται είτε ως διαχωριστές υδρογόνου από ρεύμα που περιέχει αυτό ή σε αντιδραστήρες με μεμβράνες παλλαδίου. Η εφαρμογή αυτής της τεχνολογίας σε συνδυασμένο κύκλο φυσικού αερίου δεν έχει εξεταστεί έως τώρα.

1.2.1.2 Δέσμευση CO₂ από λιθανθρακικό σταθμό

Το ζήτημα της δέσμευσης CO₂ από θερμικούς σταθμούς στερεών ορυκτών καυσίμων έχει μελετηθεί διεξοδικά τα τελευταία χρόνια. Συγκεκριμένα τρεις διδακτορικές διατριβές έχουν εκπονηθεί έως σήμερα στο Εργαστήριο Ατμοπαραγωγών και Λεβήτων του Εθνικού Μετσόβιου Πολυτεχνείου πάνω στην εξέταση τεχνικών δέσμευσης CO₂ είτε για μετά-καύσης δέσμευση, καύση με καθαρό οξυγόνο [21, 22] και προ δέσμευσης [23]. Σύμφωνα με την IEA [24] και το Ερευνητικό Πρόγραμμα CAL-MOD [25], η τεχνολογία του κύκλου ασβεστίου παρουσιάζει καλύτερα χαρακτηριστικά από αυτές της καύσης με οξυγόνο και αυτή των αμινών όσον αφορά στον καθαρό βαθμό απόδοσης και το κόστος αποφυγής CO₂.

1.2.2 Δέσμευση CO₂ και επαναχρησιμοποίηση

Το εναλλακτικό σχέδιο για τη διαχείριση του δεσμευόμενου CO₂ είναι η μετατροπή του σε κάποιο ανώτερης ποιότητας καύσιμο. Η υδρογόνωση του CO₂ προς σχηματισμό μεθανίου εξετάζεται από τις

αρχές του 20^{ου} αιώνα. Τα κυριότερα πλεονεκτήματα της ιδέας του Power to Gas (PtG) είναι η υψηλή αποθηκευτική ικανότητα σε σχέση με το υδρογόνο, η υψηλή ενεργειακή πυκνότητα (~40 MJ/m³) και η υφιστάμενη υποδομή δικτύου για τη διανομή του παραγόμενου μεθανίου. Όμως, το κόστος παραγωγής είναι αρκετά υψηλό (5-6 φορές σε σχέση με το Φ.Α.) λόγω του υψηλού κόστους παραγωγής υδρογόνου με έναν βιώσιμο και «εναλλακτικό» τρόπο (απαλλαγμένο από ορυκτά καύσιμα όπως παράγεται αυτή τη στιγμή το 90% του υδρογόνου παγκοσμίως). Γι' αυτό και το ερευνητικό ενδιαφέρον έχει στραφεί τα τελευταία χρόνια στην παραγωγή άλλων καυσίμων, όπως η μεθανόλη, που απαιτεί λιγότερα μόρια υδρογόνου ανά mol παραγόμενου καυσίμου. Ιδιαίτερη έμφαση δίνεται στο να προορίζεται η παραγόμενη μεθανόλη για χρήση σε μεταφορικά οχήματα.

1.2.3 Χρήση βιομάζας προς αντικατάσταση των ορυκτών καυσίμων

Όπως αναφέρθηκε και παραπάνω, η εξάρτηση του σύγχρονου «αναπτυγμένου» πολιτισμού στα προϊόντα και στη χρήση των ορυκτών καυσίμων είναι πολύ μεγάλη. Η ενέργεια που βασίζεται στη χρήση βιομάζας (βιοενέργεια) αναμένεται να παίξει σημαντικό ρόλο στην επίτευξη των στόχων για τη μείωση των αερίων του θερμοκηπίου, καλύπτοντας περίπου το 11% των συνολικών ενεργειακών καταναλώσεων στην Ευρώπη. Παρόλα αυτά, αρκετά βήματα θα πρέπει να γίνουν ακόμα για την προώθηση των εναλλακτικών καυσίμων και προηγμένων βιοκαυσίμων ώστε αυτά να φτάσουν σε μια εμπορική κλίμακα [11].

Ο όρος «βιοδιυλιστήριο» αναφέρεται σε εκείνο το ενεργειακό σύστημα το οποίο χρησιμοποιεί βιομάζα σαν πρώτη ύλη βιομάζας για τη μετατροπή της σε πολύτιμα καύσιμα, θερμότητα και ηλεκτρισμό ή χημικά προϊόντα. Τα τέσσερα κριτήρια για την κατηγοριοποίηση ενός τέτοιου συστήματος είναι: α) το είδος της πρώτης ύλης, β) η πλατφόρμα μετατροπής, γ) το είδος της διεργασίας για τη διαμόρφωση του τελικού επιθυμητού προϊόντος και δ) το τελικό προϊόν και η μορφή του. Μερικές από τις χημικές ενώσεις που παράγονται κατά κόρον στα περισσότερα βιοδιυλιστήρια σήμερα είναι οι ανώτερες αλκοόλες. Με τον όρο αυτό εννοούμε τις αλκοόλες με αριθμό ατόμων άνθρακα μεγαλύτερο του 2 (C2+) με χαρακτηριστικότερη την αιθανόλη, με 23430 εκατομμύρια gal το 2013 παγκοσμίως [28]. Μόνο το 5% της παγκόσμιας παραγωγής προέρχεται από επεξεργασία πετρελαίου (συνθετικό) [27, 29]. Η Βραζιλία και οι ΗΠΑ είναι οι κορυφαίες χώρες στην παραγωγή βιοαιθανόλης, έχοντας ως πρώτη ύλη τα ζαχαρότευτλα και το καλαμπόκι, αντίστοιχα [30]. Η βασική τεχνολογία παραγωγής της βιοαιθανόλης είναι η αλκοολική ζύμωση, μετατρέποντας το κυτταρινικό μέρος της στερεάς βιομάζας σε αιθανόλη. Η εναλλακτική μέθοδος που προτείνεται σε αυτή τη διατριβή γίνεται μέσω θερμοχημικών μεθόδων και συγκεκριμένα μέσω της σύνθεσης αλκοολών από αέριο σύνθεσης (syngas) προερχόμενο από αεριοποίηση βιομάζας. Πολύ λίγες μελέτες επικεντρώνονται στην βελτίωση αυτής της διεργασίας όσον αφορά στην αύξηση της επιλεκτικότητας σε αλκοόλες με μεγάλο αριθμό ατόμων C.

1.3 Σκοπός της Διδακτορικής Διατριβής

Επιγραμματικά, ο σκοπός της παρούσας διατριβής είναι η ανάπτυξη και ο σχεδιασμός προηγμένων ενεργειακών συστημάτων με προσανατολισμό την σημαντική μείωση των εκπομπών διοξειδίου του άνθρακα. Κι ενώ στην πρώτη ενότητα εξηγήθηκε γιατί πρέπει να γίνει η μετάβαση σε μια ενεργειακή εποχή που θα έχει ελάχιστες εκπομπές, στη δεύτερη ενότητα τέθηκε το πλαίσιο στο οποίο κινούνται οι έρευνες για την υλοποίηση αυτού. Έτσι, καθορίζονται τρεις πλατφόρμες/μέρη διερεύνησης τέτοιων συστημάτων και διεργασιών, η Δέσμευση και Αποθήκευση CO₂, η Δέσμευση και Επαναχρησιμοποίηση CO₂ και η παραγωγή προηγμένων καυσίμων αξιοποιώντας βιομάζα.

Στο πρώτο μέρος, εξετάζεται η δυνατότητα εφαρμογής της τεχνολογίας των μεμβρανών παλλαδίου σε συνδυασμένο κύκλο φυσικού αερίου και η εξεργειακή ανάλυση των τριών πιο διαδομένων τεχνολογιών

δέσμευσης σε λιθανθρακικό σταθμό. Αφενός στην πρώτη εφαρμογή, μη έχοντας διερευνηθεί η ιδέα αυτή στο παρελθόν, επιχειρείται να προσδιοριστούν οι συνθήκες και ο κατάλληλος σχεδιασμός για βέλτιστη λειτουργία από πλευράς απόδοσης αλλά και κόστους ηλεκτροπαραγωγής. Αφετέρου, στη δεύτερη ανάλυση του πρώτου μέρους επιχειρείται να δοθεί απάντηση στο εξής ερώτημα: «ποιο είδος ενέργειας είναι προτιμότερο να καταναλωθεί για τη δέσμευση CO₂ από λιθανθρακικό σταθμό; χαμηλής ενθαλπίας θερμότητα όπως στη χημική απορρόφηση μέσω αμινών, υψηλής ποιότητας χημική ενέργεια όπως στην περίπτωση του κύκλου ασβεστίου ή ηλεκτρική ενέργεια/έργο όπως στην περίπτωση της καύσης με καθαρό οξυγόνο;». Ιδιαίτερη έμφαση δίνεται στην ποιότητα του τελικού ρεύματος CO₂ που προορίζεται για συμπίεση, μεταφορά και αποθήκευση από πλευράς της συγκέντρωσης των όποιων συστατικών περιέχονται σε αυτό.

Το δεύτερο μέρος σχετίζεται με την ανάπτυξη της δεύτερης στρατηγικής για τη διαχείριση του δεσμευμένου CO₂, αυτή της επαναξιοποίησής του μέσω της παραγωγής προηγμένων καυσίμων που προορίζονται κυρίως για τον τομέα των μέσων μεταφοράς. Πιο συγκεκριμένα, στην περίπτωση της παραγωγής μεθανόλης από CO₂ και την ανάγκη για περαιτέρω βελτίωση ώστε η ιδέα να γίνει οικονομικά πιο ανταγωνιστική, αναλύονται διάφορα τεchnοοικονομικά σενάρια και παραμετρικές διερευνήσεις ώστε να καθοριστούν οι προϋποθέσεις που τη θέτουν σαν μια οικονομικά ελκυστική επιλογή. Στο δεύτερο κεφάλαιο αυτού του μέρους, παρουσιάζονται δυο νέα συστήματα διεργασιών υδρογόνωσης του CO₂ προς παραγωγή μεθανόλης και αιθανόλης με βελτιωμένα χαρακτηριστικά σε σχέση με τα «συμβατικά».

Το τρίτο μέρος σχετίζεται με την ανάπτυξη, σχεδιασμό, μοντελοποίηση και οικονομοτεχνική ανάλυση ενός θερμοχημικού βιοδιωλιστηρίου που έχει ως «ένωση-βάση» (chemical block) τις ανώτερες αλκοόλες. Στο πρώτο κεφάλαιο γίνεται μια αναλυτική παρουσίαση του συστήματος παραγωγής ανώτερων αλκοολών και πώς μοντελοποιείται κάθε διεργασία. Επίσης, εξετάζεται η επίδραση διαφόρων παραμέτρων στη λειτουργία της μονάδας όσον αφορά στην μεγιστοποίηση του παραγόμενου προϊόντος και την ελαχιστοποίηση των θερμικών και ηλεκτρικών καταναλώσεων. Στο δεύτερο κεφάλαιο, γίνεται περαιτέρω εμβάθυνση αυτού του προηγμένου συστήματος προς την κατεύθυνση της παραγωγής αναβαθμισμένων καυσίμων για χρήση σε αεροπορικούς κινητήρες έχοντας ως βάση σύνθεσής τους ανώτερες αλκοόλες. Πιο συγκεκριμένα, παρουσιάζονται δυο πρωτότυπα σχήματα για την παραγωγή παραφινών με βάση την αιθανόλη και τη βουτανόλη, αντίστοιχα, κάνοντας χρήση διαφορετικών τύπων καταλυτών. Τα συστήματα αυτά εξετάζονται από ενεργειακή σκοπιά αλλά και από οικονομική και συγκρίνονται με τα αντίστοιχα βιοχημικά.

Η παρούσα διατριβή επικεντρώνεται σε κάποια προηγμένα και πρωτότυπα ενεργειακά συστήματα και οι βασικοί στόχοι που θέτονται επικεντρώνονται στα παρακάτω:

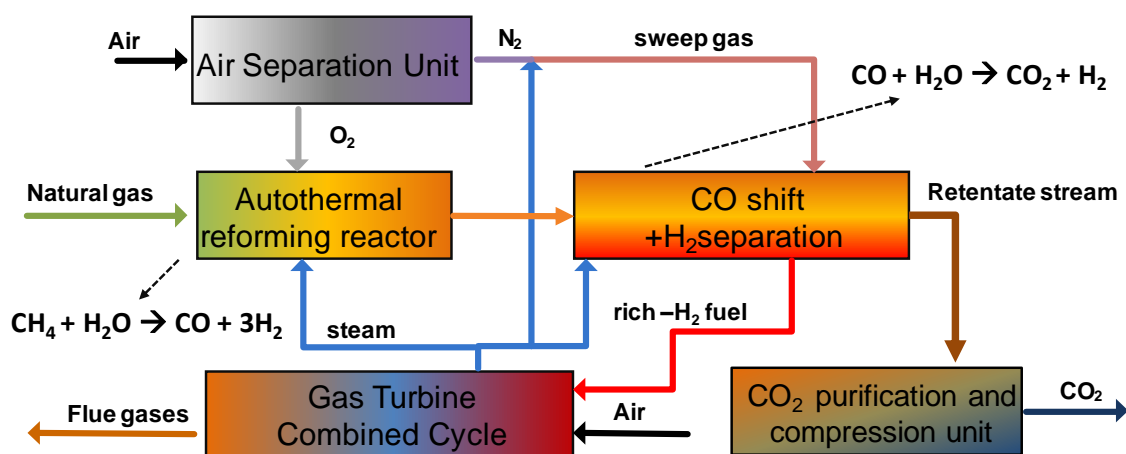
- Σχεδιασμό νέων και πρωτότυπων συστημάτων και καθορισμό των παραμέτρων για βέλτιστη λειτουργία
- Κατανόηση της λειτουργίας των διαφόρων διεργασιών και μονάδων των εν λόγω συστημάτων και πώς το κάθε ένα από αυτά επιδρά στη συνολική απόδοση της εγκατάστασης
- Εκτίμηση κόστους και προσδιορισμό των προϋποθέσεων για να γίνουν τα συστήματα αυτά οικονομικά πιο ελκυστικά
- Συγκριτική ανάλυση με αντίστοιχες τεχνολογίες και καθορισμό των πιο υποσχόμενων τεχνικών για περαιτέρω ανάλυση σε μεγαλύτερη κλίμακα.
- Καθορισμό των κατευθύνσεων που θα πρέπει να πάρει η μελλοντική έρευνα για περαιτέρω βελτίωση των ενεργειακών αυτών συστημάτων.

Το βασικό εργαλείο για τις υπολογιστικές προσομοιώσεις είναι το εμπορικό λογισμικό του ASPEN PlusTM.

2. Εφαρμογή μεμβρανών παλλαδίου για δέσμευση και αποθήκευση CO₂ σε σταθμό συνδυασμένου κύκλου: Ολοκληρωμένος σχεδιασμός και τεχνοοικονομική ανάλυση

2.1 Εισαγωγή

Στο δεύτερο κεφάλαιο εξετάζεται η εφαρμογή της τεχνολογίας μεμβρανών παλλαδίου για δέσμευση διοξειδίου του άνθρακα σε σταθμό που χρησιμοποιεί ως καύσιμο το φυσικό αέριο, τόσο σε τεχνικό μέσω θερμοδυναμικών υπολογισμών όσο και σε οικονομικό επίπεδο. Οι μεμβράνες παλλαδίου έχουν το ανταγωνιστικό πλεονέκτημα να είναι διαπερατές από υδρογόνο, όταν εμφανίζεται διαφορά στη μερική πίεση αυτού μεταξύ των δυο περιοχών εκατέρωθεν της μεμβράνης. Οι βασικές διεργασίες που διέπονται το εν λόγω σύστημα με δέσμευση CO₂ προ καύσης εικονίζονται στην παρακάτω **Εικόνα 112**:



Εικόνα 112. Διάγραμμα ροής διεργασιών του υπό εξέταση ενεργειακού συστήματος

Το φυσικό αέριο εισέρχεται στο σύστημα και αναμορφώνεται σε αυτόθερμο καταλυτικό αντιδραστήρα παρουσία ατμού και καθαρού οξυγόνου. Στη συνέχεια, το παραχθέν αέριο εισέρχεται σε αντιδραστήρα μετατόπισης για μεγιστοποίηση του H₂ και μετατροπής του μονοξειδίου του άνθρακα σε διοξείδιο. Παράλληλα, γίνεται ο διαχωρισμός του παραχθέντος υδρογόνου σε μεμβράνες παλλαδίου, το οποίο αποτελεί και το τελικό καύσιμο που οδηγείται στον αεριοστρόβιλο για καύση. Το απαιτούμενο οξυγόνο για τον αντιδραστήρα της αναμόρφωσης παράγεται σε μονάδα διαχωρισμού αέρα, ενώ το παραχθέν άζωτο χρησιμοποιείται ως αέριο σάρωσης του ανακτηθέντος υδρογόνου. Τα απαέρια από τον αεριοστρόβιλο οδηγούνται στο λέβητα ανάκτησης θερμότητας για περαιτέρω ηλεκτροπαραγωγή μέσω της παραγωγής και εκτόνωσης υπέρθερμου ατμού. Το υπόλοιπο αέριο που δεν διαπερνά τις μεμβράνες αποτελείται κυρίως από διοξείδιο του άνθρακα και οδηγείται σε καθαρισμό, συμπίεση και αποθήκευση CO₂.

Η θερμοδυναμική ανάλυση περιλαμβάνει τη βελτιστοποίηση τόσο του σχεδιασμού όσο και τον καθορισμό των παραμέτρων για βέλτιστη λειτουργία. Στο δεύτερο μέρος (οικονομική ανάλυση) γίνεται ο υπολογισμός του κόστους της ηλεκτροπαραγωγής και του κόστους αποφυγής του εκπεμπόμενου CO₂ για έξι επιλεγμένα σενάρια.

2.2 Σταθμός αναφοράς

Πριν την εξέταση του πρωτότυπου και προηγμένου ενεργειακού συστήματος προηγείται η παρουσίαση του σταθμού αναφοράς, του συνδυασμένου κύκλου, δηλαδή χωρίς σύστημα δέσμευσης CO₂. Οι παράμετροι λειτουργίας και οι επιδόσεις είναι σύμφωνα με τα χαρακτηριστικά του «Σημείου Αναφοράς» που καθιέρωσε η Ευρωπαϊκή Ομάδα Εργασίας (EBTF) [19], ενώ η μοντελοποίηση τόσο του Αεριοστροβίλου (GT) όσο και του κύκλου νερού ατμού (ST) γίνεται λεπτομερώς σε περιβάλλον ASPEN PlusTM. Το συνολικό σύστημα αναφοράς έχει συνολική καθαρή ηλεκτροπαραγωγή 830.7 MWe με αντίστοιχο καθαρό βαθμό απόδοσης 58.3%.

2.3 Σχεδιασμός της διάταξης του συστήματος για βέλτιστη λειτουργία

Σχετικά με τον καθορισμό της βέλτιστης διάταξης, αυτός αναπτύχθηκε σε όλα τα επιμέρους υποσυστήματα του σταθμού. Πιο συγκεκριμένα:

Μονάδα Διαχωρισμού του Αέρα: Η διάταξη της μονάδας καθορίστηκε αρκετά από το γεγονός ότι η μονάδα παραγωγής υδρογόνου και συγκεκριμένα ο αντιδραστήρας αναμόρφωσης απαιτεί καθαρό οξυγόνο σε υψηλή πίεση (52 bar). Δεδομένου ότι το ενεργειακό κόστος συμπίεσης αερίου οξυγόνου από ατμοσφαιρική πίεση είναι υψηλό, το προτεινόμενο σύστημα περιλαμβάνει την εξαγωγή του οξυγόνου από τη μονάδα σε υψηλή πίεση, η οποία θα έχει επιτευχθεί όταν αυτό είναι σε υγρή μορφή μέσω αντλίας και προτού εισέλθει στον κεντρικό εναλλάκτη και ατμοποιηθεί.

Αντιδραστήρας Αναμόρφωσης: Είναι ο σημαντικότερος αντιδραστήρας του συστήματος καθώς εκεί μετατρέπονται οι υδρογονάνθρακες του φυσικού αερίου σε CO, CO₂ και H₂ και είναι αναγκαίο η μετατροπή αυτή να είναι όσο το δυνατόν πιο πλήρης και αποδοτική. Αυτό εξαρτάται κυρίως από την ποσότητα οξυγόνου και ατμού που καθορίζουν τη θερμοκρασία, το βαθμό μετατροπής και την σύσταση του παραγόμενου αερίου.

Διάταξη αντιδραστήρων μετατόπισης και διαχωριστών (μεμβράνες): Ο διαχωρισμός του υδρογόνου σε δυο στάδια με ενδιάμεση χρήση αντιδραστήρων μετατόπισης δείχθηκε πως είναι η καλύτερη διάταξη όχι μόνο από άποψης απόδοσης της μονάδας αλλά και για λόγους μειωμένων απαιτήσεων σε επιφάνεια μεμβράνης και κόστους εξοπλισμού. Οι δυο αντιδραστήρες μετατόπισης λειτουργούν σε διαφορετική θερμοκρασία, ο πρώτος στους 400°C και ο δεύτερος στους 260°C για αποτελεσματική μετατροπή όλου του CO σε CO₂ και H₂.

Καθαρισμός ρεύματος CO₂, συμπίεση: Τρία σχήματα καθαρισμού του παρακρατηθέντος ρεύματος που μένει μετά το διαχωρισμό των μεμβρανών προτείνονται: μια με κρυογονικό διαχωρισμό μέσω flash διαχωριστών και αυτόψυκτη λειτουργία, κρυογονικό διαχωρισμό μέσω αποστακτικής στήλης και πρόσδοση απαιτούμενης ψύξης από εξωτερικό σύστημα ψύξης και μια με καύση των καύσιμων στοιχείων (CO, H₂ και CH₄) με καθαρό οξυγόνο. Η θερμοδυναμική ανάλυση έδειξε ότι η τρίτη επιλογή (καύση στο ίδιο επίπεδο πίεσης λειτουργίας με τις μεμβράνες) αποφέρει την υψηλότερη απόδοση στο σύστημα συνολικότερα. Βασική προϋπόθεση, τα υπολείμματα οξυγόνου που παραμένουν μετά την σχεδόν στοιχειομετρική καύση να μην αποτελούν πρόβλημα στη συμπίεση, μεταφορά και αποθήκευση του καθαρού CO₂.

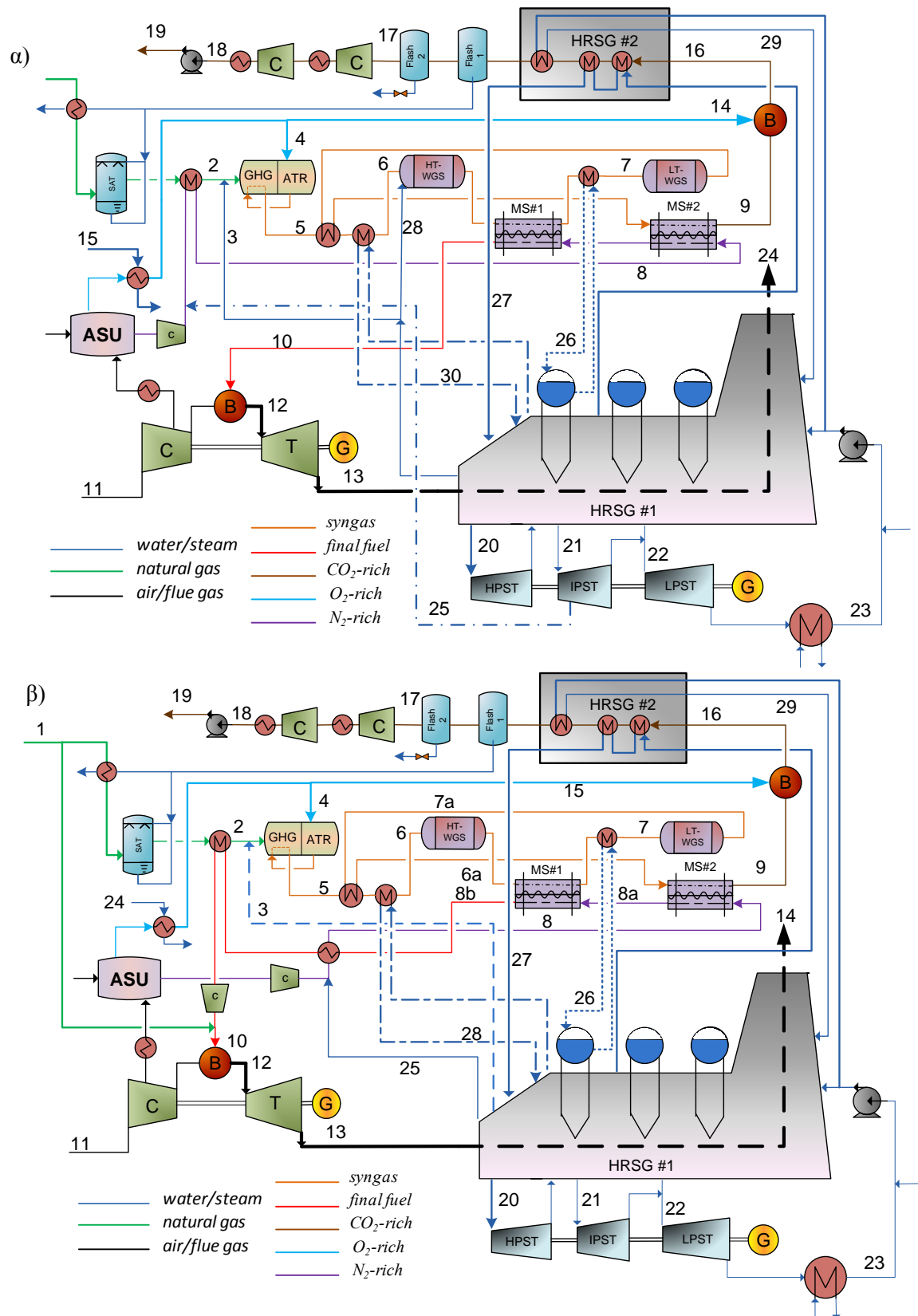
2.4 Καθορισμός των λειτουργικών παραμέτρων για βέλτιστη απόδοση

Έχοντας καθορίσει τη βέλτιστη διάταξη του ενεργειακού συστήματος, οι παράμετροι λειτουργίας που εξετάζονται μέσω ανάλυσης ευαισθησίας ώστε το σύστημα να λειτουργεί κατά το βέλτιστο τρόπο είναι: ο λόγος ατμού/άνθρακα στον αντιδραστήρα αναμόρφωσης (S/C), ο συντελεστής ανάκτησης υδρογόνου στις μεμβράνες (HRF), η θερμοκρασία στον αντιδραστήρα αναμόρφωσης, το ποσοστό δέσμευσης (δεδομένου ότι οι μεμβράνες δεν είναι διαπερατές στο CO₂, το ποσοστό δέσμευσης

καθορίζεται από το ποσοστό του εισερχόμενου φυσικού αερίου που υπόκεινται σε αναμόρφωση και δεν οδηγείται απευθείας στην αεριοστροβιλική μονάδα), η πίεση στις δυο πλευρές των μεμβρανών (τροφοδοσίας και διείσδυσης). Έτσι, προκύπτουν δυο σενάρια, το ένα (I) με μέγιστο καθαρό βαθμό απόδοσης και το άλλο με ελάχιστη απαιτούμενη επιφάνεια μεμβρανών (VI). Τα βασικά χαρακτηριστικά φαίνονται στον παρακάτω πίνακα.

Πίνακας 78. Παράμετροι λειτουργία και βασικά αποτελέσματα για τις περιπτώσεις I και VII (90% δέσμευση)

ΠΕΡΙΠΤΩΣΗ		I	VII
σχήμα καθαρισμού	καύση με καθαρό οξυγόνο		
λόγος ατμού/άνθρακα στον αναμορφωτή	mole/mole		1.7
θερμοκρασία Φ.Α. πριν τον αναμορφωτή	°C		360
Θερμοκρασία προ αναμόρφωσης	°C		700
Θερμοκρασία αναμόρφωσης	°C		1050
HRF στην πρώτη μεμβράνη	%		37.2
HRF στη δεύτερη μεμβράνη	%		89.2
HRF συνολικά	%		95.0
Θερμοκρασία στον υψηλής θερμοκρασίας αντιδραστήρα μετατόπισης	°C		400
Θερμοκρασία στο χαμηλής θερμοκρασίας αντιδραστήρα μετατόπισης	°C		360
Θερμοκρασία εισόδου στο αέριο σάρωσης στις μεμβράνες	°C		303
Καθαρότητα οξυγόνου	%		95.0
Δp_{H_2} στην έξοδο της πρώτης μεμβράνης	bar		9.0
πίεση στην πλευρά της τροφοδοσίας	bar	45	55
πίεση στην πλευρά της διείσδυσης	bar	25	10
συνολική απαιτούμενη επιφάνεια μεμβρανών	m ²	28,588	9,412
καθαρή ισχύς Αεριοστροβίλου	MWe	667.9	661.7
καθαρή ισχύς Ατμοστροβίλου	MWe	342.5	353.9
κατανάλωση στη Μονάδα Διαχωρισμού Αέρα	MWe	-33.97	-34.25
συμπίεση N ₂	MWe	-61.32	-96.56
καθαρισμός και συμπίεση CO ₂	MWe	-4.69	-3.27
Καθαρή ηλεκτρική ισχύς	MWe	910.50	881.5
Κ.Θ.Ι. καυσίμου	MWth	1791.7	1762.8
Καθαρή ηλεκτρική απόδοση σε βάση ΚΘΙ	%	50.82%	50.01%
Διαφορά στην απόδοση σε σχέση με το σταθμό αναφοράς	%	7.5%	8.3%
ειδικές εκπομπές CO ₂	g/kWh	42.16	42.16
δείκτης SPECCA	MJ _{LHV} /kgCO ₂	2.91	3.28



Εικόνα 113. Διάγραμμα ροής για τις Περιπτώσεις α) I και β) VII

2.5 Σύγκριση με άλλες τεχνικές δέσμευσης CO₂

Η ανάλυση περιλαμβάνει σύγκριση και με άλλες τεχνικές δέσμευσης, πάντα για την περίπτωση του σταθμού που έχει ως καύσιμο το φυσικό αέριο. Η σύγκριση περιλαμβάνει τεχνικές χημικής και φυσικής απορρόφησης, κρυογονικές μεθόδους, μεμβράνες διαπερατές από CO₂ και καύση με καθαρό οξυγόνο ή αλλιώς κύκλος O₂/CO₂.

Ο Πίνακας 79 συνοψίζει τα βασικά αποτελέσματα από τις υπολογιστικές προσομοιώσεις των διεργασιών. Σε κάθε τεχνική αναγράφεται σε παρένθεση σε ποια κατηγορία ανήκει ανάλογα με το αν αναφέρεται σε προ καύσης ή μετά καύσης δέσμευση. Είναι φανερό, ότι η τεχνολογία που μελετήθηκε εκτενώς σε αυτό το κεφάλαιο (μεμβράνες παλλαδίου) παρουσιάζει την καλύτερη επίδοση από πλευράς απόδοσης και δείκτη SPECCA. Σε αυτή την περίπτωση οι μεγαλύτερες ενεργειακές απώλειες λόγω καταναλώσεων παρουσιάζονται για την παραγωγή του οξυγόνου και τη συμπίεση του αζώτου. Από την άλλη μεριά, στην περίπτωση των αμινών, η απομάστευση ατμού για την πρόσδοση της απαιτούμενης θερμότητας για την αναγέννηση του διαλύτη ρίχνει κατά πολύ το βαθμό απόδοσης στον κύκλο νερού-ατμού. Η υψηλές καταναλώσεις για τη συμπίεση του CO₂ στην περίπτωση των φυσικών διαλυτών οφείλεται στη χαμηλή πίεση διαχωρισμού του CO₂ από το διαλύτη. Συγκρίνοντας την περίπτωση της αμίνης MDEA με τις δυο περιπτώσεις φυσικής απορρόφησης, φαίνεται ότι η χημική απορρόφηση έχει μεγαλύτερη δεσμευτική ικανότητα σε χαμηλές μερικές πιέσεις από ότι οι διαλύτες SelexolTM/RectisolTM. Αξίζει να σημειωθεί, ότι η συγκέντρωση CO₂ στο αέριο που προκύπτει από αναμόρφωση φυσικού αερίου είναι δυο με τρεις φορές μικρότερο από το αντίστοιχο αέριο σύνθεσης που προκύπτει από αεριοποίηση στερεού καυσίμου (άνθρακας ή βιομάζα). Η χρήση κρυογονικών τεχνικών για μετά-καύση δέσμευση έχει χειρότερο βαθμό απόδοσης από το αντίστοιχο προ-καύσης σενάριο. Τέλος, η καύση με καθαρό οξυγόνο είναι λιγότερο ανταγωνιστική επιλογή για την περίπτωση του φυσικού αερίου, λόγω των υψηλών ενεργειακών καταναλώσεων στη μονάδα διαχωρισμού αέρα και στη μονάδα καθαρισμού και συμπίεσης του CO₂.

Πίνακας 79. Δέσμευση CO₂ (CCR=90%) σε σταθμό Φ.Α. με διάφορες τεχνικές

τεχνική δέσμευσης CO ₂	Καθαρή ισχύς, % MWe/LHV	Διαφορά ισχύος %	αποφευχθέν CO ₂ , %	εκπομπές CO ₂ , g/kWh	SPECCA, MJ _{LHV} /kgCO ₂
χωρίς δέσμευση CO ₂	58.3	-	-	354.3	-
αμίνες MEA (μετά καύσης)	49.71	8.6	88.3	41.6	3.41
κρυογονικές (μετά καύσης)	36.78	21.52	83.3	56	12.11
αμίνες MDEA (προ καύσης)	50.37	7.93	88.4	41	3.1
Selexol TM (προ καύσης)	47.93	10.37	90	42.6	4.29
Rectisol TM (προ καύσης)	49.38	8.92	89.8	42.51	3.58
K ₂ CO ₃ (προ καύσης)	46.79	11.51	60.73	179.77	8.7
κρυογονικές (προ καύσης)	50.02	8.28	89.47	43.38	3.29
μεμβράνες CO ₂ (προ καύσης)	49.39	8.91	92.16	32.74	3.46
μεμβράνες Pd (προ καύσης)	50.82	7.48	89.5	42.16	2.91
καύση με καθαρό οξυγόνο	49.88	8.42	90.6	25.38	3.17

2.6 Οικονομική αξιολόγηση

Η οικονομική ανάλυση αποσκοπεί στο να υποδείξει μια εκτίμηση για την οικονομική βιωσιμότητα που έχει το υπό εξέταση ενεργειακό σύστημα και να προκύψουν κάποια συμπεράσματα όσον αφορά

το κόστος της επένδυσης, τα λειτουργικά κόστη, Το κόστος ηλεκτροπαραγωγής και το κόστος αποφυγής εκπομπών CO₂. Οι υποθέσεις και η μεθοδολογία που ακολουθήθηκε συνάδει με τις κατευθυντήριες γραμμές που δίνει το EBTF. Τα υπό εξέταση σενάρια συγκρίνονται με αυτό της καύσης δέσμευσης με αμίνες (MDEA). Τα υπό εξέταση σενάρια είναι:

- καύση με οξυγόνο των υπόλοιπων καυσίμων στοιχείων στο ρεύμα CO₂ (πίεση στην πλευρά τροφοδοσίας: 55 bar, πίεση στην πλευρά διείσδυσης: 10 bar) – Σενάριο VII
- καύση με οξυγόνο των υπόλοιπων καυσίμων στοιχείων στο ρεύμα CO₂ (πίεση στην πλευρά τροφοδοσίας: 46 bar, πίεση στην πλευρά διείσδυσης: 25 bar) – Σενάρια I και II
- καύση με οξυγόνο και εκτόνωση (πίεση στην πλευρά τροφοδοσίας: 46 bar, πίεση στην πλευρά διείσδυσης: 25 bar) – Σενάρια III και IV
- διαχωρισμός των καυσίμων με αποστακτική στήλη (πίεση στην πλευρά τροφοδοσίας: 46 bar, πίεση στην πλευρά διείσδυσης: 25 bar) – Σενάριο V
- διαχωρισμός των καυσίμων με flash διαχωρισμό (πίεση στην πλευρά τροφοδοσίας: 46 bar, πίεση στην πλευρά διείσδυσης: 25 bar) – Σενάριο VI

Πίνακας 80. Κόστη σταθμού και ειδικά κόστη επένδυσης για διαφορετικά σενάρια

Σενάριο	VII	II	I	IV	III	V	VI
ποσοστό δέσμευσης (%)	90%	100%	90%	100%	90%	90%	90%
Κόστος μεμβράνης (Μ€)	35.8	132.0	108.6	129.5	116.2	120.7	147.6
Συνολικό Κόστος Εξοπλισμού (Μ€)	482.8	607.7	563.2	625.8	584.8	589.4	591.4
Συνολικό Κόστος Σταθμού (Μ€)	924.7	1163.8	1078.6	1198.5	1120.1	1128.9	1132.7
Ειδικό κόστος (€/kW _{net})	1206.4	1456.8	1362.3	1524.9	1436.5	1492.5	1489.3

Πίνακας 81. Συνολικό κόστος σταθμού (Μ€) και ειδικό κόστος επένδυσης για τα διαφορετικά σενάρια

Σενάριο	VII	II	I	IV	III	V	VI
ποσοστό δέσμευσης (%)	90	90	100	90	100	90	90
Συνολικό κόστος εξοπλισμού	482.84	563.18	607.65	584.83	625.77	589.41	591.42
Συνολικό κόστος εγκατάστασης	328.33	382.96	413.20	397.69	425.52	400.80	402.17
Συνολικό άμεσο κόστος	811.17	946.14	1020.86	982.52	1051.29	990.22	993.59
Έμμεσα κόστη	113.56	132.46	142.92	137.55	147.18	138.63	139.10
Κόστος Σταθμού	924.73	1078.60	1163.78	1120.08	1198.47	1128.85	1132.69
Απρόβλεπτα έξοδα	92.47	107.86	116.38	112.01	119.85	112.88	113.27
Κόστος ιδιοκτησίας	46.24	53.93	58.19	56.00	59.92	56.44	56.63
Συνολικό απαιτούμενο κεφάλαιο	1063.44	1240.39	1338.34	1288.09	1378.24	1298.17	1302.60
Καθαρή παραγόμενη ισχύς (MW)	881.52	910.50	918.71	896.71	903.83	869.81	874.63
Ειδικό κόστος (€/kW)	1206.37	1362.32	1456.76	1436.45	1524.89	1492.49	1489.32

Από τον Πίνακα 80 προκύπτει ότι το ειδικό κόστος επένδυσης για καύση με καθαρό οξυγόνο είναι το χαμηλότερο. Επιβεβαιώνεται ότι οι μεμβράνες παρουσιάζουν ένα σημαντικό ποσοστό στο συνολικό κόστος επένδυσης μεταξύ 108.6 και 147.6 Μ€, με το συνολικό κόστος εξοπλισμού να κυμαίνεται μεταξύ 563.2–625.8 Μ€. Τα περισσότερα από τα κόστη της διάταξης αυτής (μεμβράνες) σχετίζονται με την κατασκευή τους και την απόθεση του υποστρώματος. Όμως, όταν η πίεση τροφοδοσίας στη μεμβράνη είναι πάνω από 55 bar και η πίεση διείσδυσης είναι κάτω από 10 bar, το κόστος εξοπλισμού μειώνεται σημαντικά. Ο συντελεστής δέσμευσης επηρεάζει επίσης το κόστος των

μεμβρανών καθώς, όσο μεγαλύτερο είναι το ποσοστό δέσμευσης τόσο μεγαλύτερη είναι και η απαιτούμενη επιφάνεια των μεμβρανών. Το δεύτερο πιο ακριβό στοιχείο του συστήματος είναι ο αεριοστρόβιλος (GT) (Πίνακας 81).

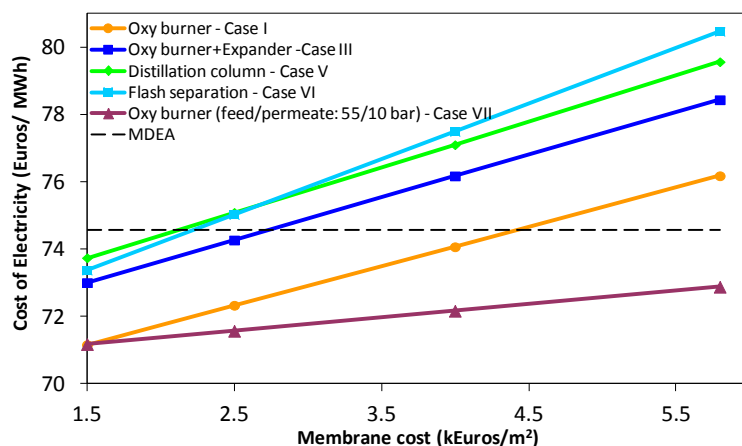
2.6.1 Κόστος ηλεκτροπαραγωγής και κόστος αποφυγής εκπομπών CO₂

Η ανάλυση κόστους των υπό εξέταση περιπτώσεων σε ετήσια βάση και ανά παραγόμενη μεγαβατώρα παρουσιάζεται στον παρακάτω πίνακα, μαζί με το κόστος ηλεκτροπαραγωγής και το κόστος αποφυγής εκπομπών CO₂. Η οικονομική βιωσιμότητα της εφαρμογής των μεμβρανών σε σταθμό φυσικού αερίου εξετάζεται με βάση το κριτήριο της καθαρής παρούσας αξίας. Το σημείο στο οποίο μηδενίζεται η καθαρή παρούσα αξία (ΚΠΑ) μεταβάλλοντας την τιμή της ηλεκτρικής ενέργειας, προσδιορίζει την ελάχιστη τιμή πώλησης, ώστε η επένδυση να είναι κερδοφόρα. Η σύγκριση των σεναρίων μεταξύ τους δείχνει ότι το κόστος ηλεκτροπαραγωγής εξαρτάται αρκετά από το κόστος των μεμβρανών. Το κόστος καυσίμου και το κόστος επένδυσης αποτελούν τα πιο σημαντικά μέρη του συνολικού κόστους ανά MWh. Δεδομένου ότι οι μεμβράνες πρέπει να αντικαθίσταται κάθε πέντε χρόνια, η μείωση του κόστους μεμβρανών είναι απαραίτητη για τη μείωση του κόστους αναλωσίμων και να γίνει η τεχνολογία πιο ανταγωνιστική. Η περίπτωση της 100% δέσμευσης οδηγεί σε μειωμένες αποδόσεις και ως εκ τούτου, αυξημένο κόστος ηλεκτροπαραγωγής. Όμως, το κόστος αποφυγής CO₂ είναι μικρότερο.

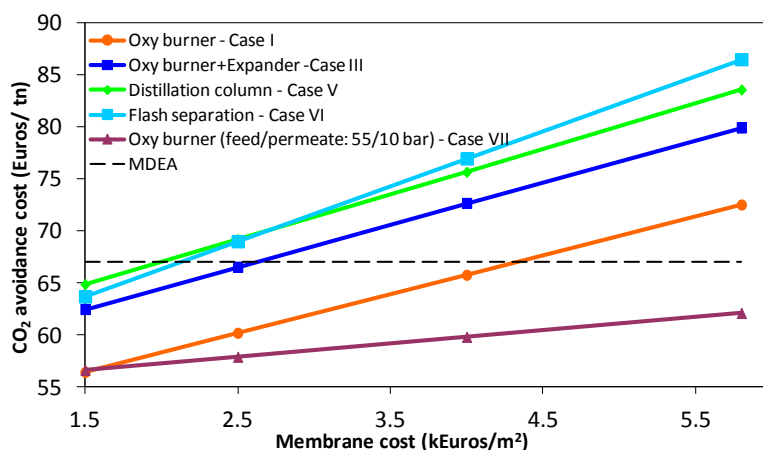
Πίνακας 82. Ανάλυση κόστους σε ετήσια βάση και ανά MWh_{el}

Σενάριο	VII	V	VI	I	II	III	IV
Καθαρή ηλεκτρική ισχύς (MW)	50.01	50.04	49.52	50.82	49.97	50.06	49.17
Ηλεκτρική απόδοση (%)	50.01	50.04	49.52	50.82	47.97	50.06	49.17
Κόστος καυσίμου (M€/y)	309.36	305.06	309.94	314.45	322.64	314.39	322.59
PAI (M€/y)	32.12	37.22	37.32	35.97	38.09	37.00	38.96
Συντήρηση (M€/y)	18.49	22.58	22.65	21.57	23.28	22.40	23.97
Αναλώσιμα, (M€/y)	9.73	17.24	20.32	17.25	19.87	17.78	19.40
Κόστος επένδυσης, (€/MWh)	16.78	20.76	20.72	18.95	20.27	19.98	21.21
Μόνιμα Σ&Λ κόστη, (€/MWh)	7.82	9.36	9.34	8.61	9.1	9.02	9.48
Συντήρηση, (€/MWh)	1.48	2.68	3.15	2.56	2.93	2.68	2.90
Κόστος καυσίμου, (€/MWh)	46.79	46.76	47.25	46.05	46.82	46.75	47.59
Κόστος ηλεκτροπαραγωγής, (€/MWh)	72.87	79.56	80.46	76.17	79.12	78.43	81.18
Κόστος αποφυγής CO₂, (€/tCO₂)	62.05	83.57	86.48	72.49	72.55	79.91	78.41

Το κόστος ηλεκτροπαραγωγής συναρτήσει του κόστους μεμβρανών για τα υπό εξέταση σενάρια φαίνονται στην **Εικόνα 114**, ενώ η **Εικόνα 115** δείχνει το κόστος αποφυγής εκπομπών CO₂ avoided. Φαίνεται ότι η περίπτωση με καύση οξυγόνου των υπολειμμάτων καυσίμων μετά το διαχωρισμό του H₂ στις μεμβράνες μπορεί να πετύχει μειωμένο κόστος αποφυγής CO₂, δεδομένου ότι το κόστος των μεμβρανών δεν ξεπερνά το όριο των περίπου 4.5 k€ m⁻², το οποίο μπορεί να θεωρηθεί σαν στόχος για πρώιμου σταδίου εφαρμογή. Είναι επίσης προφανές ότι όταν η πίεση στην πλευρά τροφοδοσίας ανέβει πάνω από 55 bar και η πίεση στην πλευρά διείσδυσης πέσει κάτω από 10 bar, το κόστος ηλεκτροπαραγωγής και διαφυγής CO₂ είναι σημαντικά χαμηλότερο από αυτό της περίπτωσης της αμίνης με MDEA ακόμα και για υψηλό ειδικό κόστος μεμβρανών.



Εικόνα 114. Κόστος ηλεκτροπαραγωγής και κόστος μεμβράνης



Εικόνα 115. Κόστος αποφυγής CO₂ και κόστος μεμβράνης

2.6.2 Επίδραση της μείωσης της επιφάνειας μεμβρανών στο κόστος ηλεκτροπαραγωγής και στο κόστος αποφυγής εκπομπών CO₂

Το κόστος ηλεκτροπαραγωγής και το κόστος αποφυγής εκπομπών CO₂ μπορούν να μειωθούν περαιτέρω, όταν διάφορα χαρακτηριστικά των μεμβρανών μεταβληθούν/βελτιωθούν. (Πίνακας 83). Στις δυο περιπτώσεις που εξετάζονται, η επιφάνεια των μεμβρανών μειώνεται κατά 14% και 26% αντίστοιχα σε σχέση με το αρχικό σενάριο.

Πίνακας 83. Κόστη για διαφορετικά χαρακτηριστικά των μεμβρανών

Ποσοστό δέσμμευσης (%)	Αρχικό σενάριο	Διπλάσια διεισδυτικότητα	Υποδιπλασιασμός του πάχους του υποστηρικτικού επιπέδου
Μεμβράνη (Μ€)	108.6	93.1	80.7
Συνολικό κόστος εξοπλισμού (Μ€)	563.2	547.7	535.3
Συνολικό κόστος σταθμού (Μ€)	1078.6	1048.9	1025.1
Ειδικό κόστος (€/kW _{net})	1362.3	1324.8	1294.7

Όπως αναμενόταν από τα αποτελέσματα από τη θερμοδυναμική ανάλυση και την ανάλυση κόστους, το χαμηλότερο κόστος ηλεκτροπαραγωγής επιτυγχάνεται όταν ελαχιστοποιείται η επιφάνεια των μεμβρανών.

2.7 Συμπεράσματα

Μέσω αναλυτικών προσομοιώσεων διεργασιών και αναλύσεων ευαισθησίας, εξάγεται το συμπέρασμα ότι εφαρμόζοντας την τεχνολογία των μεμβρανών παλλαδίου για δέσμευση διοξειδίου του άνθρακα σε συνδυασμένο κύκλο φυσικού αερίου, μπορεί να επιτευχθεί καθαρός βαθμός απόδοσης μεγαλύτερος από 50% με ταυτόχρονη 100% δέσμευση (51.1% για 90% δέσμευση). Η οικονομική αξιολόγηση έδειξε ότι το βέλτιστο σενάριο μπορεί να πετύχει κόστος αποφυγής CO₂ 7.4% χαμηλότερο από την περίπτωση της αμίνης με MDEA. Ο σημαντικότερος παράγοντας που διαμορφώνει το συνολικό κόστος είναι το κόστος επένδυσης, το οποίο συνδέεται άρρηκτα με την επιφάνεια των μεμβρανών και τα συναφή κόστη. Αυτό που προτείνεται, είναι ότι προκειμένου να καταστεί η τεχνολογία ανταγωνιστική, είναι απαραίτητο οι έρευνες να επικεντρωθούν στη μείωση αυτών των κοστών. Η μελλοντική ερευνητική δραστηριότητα πάνω στις μεμβράνες παλλαδίου θα πρέπει να αφιερώσει περισσότερη προσπάθεια στα εξαρτήματα των μεμβρανών και στο σχεδιασμό των υποστηρικτικών επιπέδων, για να μειωθεί η αντίσταση στη μεταφορά μάζας και να επέλθει μεγαλύτερη διείσδυση H₂ στις μεμβράνες.

3. Εξεργειακή ανάλυση και σύγκριση τεχνικών δέσμευσης CO₂ σε λιθανθρακικό θερμοηλεκτρικό σταθμό

3.1 Εισαγωγή

Στο παρόν κεφάλαιο παρουσιάζεται η ενεργειακή αλλά κυρίως η εξεργειακή ανάλυση τριών τεχνολογιών δέσμευσης CO₂ για εφαρμογή σε (υφιστάμενο) λιθανθρακικό σταθμό. Στον τομέα των τεχνικών μετά-καύσης δέσμευσης, η χημική απορρόφηση με διάλυμα αμινών αποτελεί την πιο ώριμη επιλογή. Μια άλλη υποσχόμενη τεχνολογία είναι αυτή του κύκλου ασβεστίου. Στη μεν πρώτη περίπτωση η κατανάλωση ενέργειας για τη λειτουργία της μονάδας έγκειται στην πρόσδοση θερμικής ενέργειας για την αναγέννηση του διαλύτη, ενώ στη δεύτερη περίπτωση στην πρόσδοση χημικής ενέργειας μέσω καυσίμου για την ασβεστοποίηση των προσροφητικών στερεών. Μια τρίτη επιλογή, είναι η καύση με τη χρήση καθαρού οξυγόνου ως οξειδωτικό μέσο. Σε αυτή την περίπτωση, και εφόσον ο διαχωρισμός του αέρα μέσω κρυογονικής μεθόδου είναι η πιο διαδεδομένη επιλογή για την παραγωγή καθαρού οξυγόνου, η απαιτούμενη ενέργεια δίνεται με τη μορφή έργου ή ηλεκτρικής ενέργειας.

Μέσω της εξεργειακής ανάλυσης επιχειρείται να υποδειχθεί ποιά από τις τεχνολογίες λειτουργεί με τον πιο αποδοτικό τρόπο. Καθορίζονται έτσι οι περιορισμοί για περαιτέρω βελτίωση σε σχέση με την τεχνολογία αιχμής. Έτσι, γίνεται η προσπάθεια να απαντηθεί το εξής ερώτημα: «τι είδους ενέργεια πρέπει να ξοδευτεί για τη δέσμευση CO₂, χαμηλής ενθαλπίας θερμότητα, υψηλής ενθαλπίας χημική ενέργεια ή ηλεκτρική ενέργεια;».

3.2 Περιγραφή μοντέλου

Οι προσομοιώσεις των μοντέλων έγιναν στο ASPEN Plus™. Τα βασικά χαρακτηριστικά του καυσίμου και σταθμού αναφοράς φαίνονται στους επόμενους πίνακες.

Πίνακας 84. Ιδιότητες καυσίμου

C	H	O	N	S	τέφρα	υγρασία	KΘI
(% d.b.)	(% d.b.)	(% d.b.)	(% d.b.)	(% d.b.)	(% d.b.)	(w/w %)	(kJ/kg ως έχει)
69.8	3.9	7.2	1.7	0.4	17.0	7.8	25460

Πίνακας 85. Χαρακτηριστικά σταθμού αναφοράς

Λόγος ισοδυναμίας αέρα καύσης	1.25	ισεντροπικός β.α. ατμοστροβίλου ΥΠ/ΜΠ/ΧΠ (%)	92/94/88
ΥΠ ατμός (°C/bar)	600/240	θερμοκρασία τροφοδοτικού νερού (ΥΠ/ΧΠ °C)	125/240
ψυχρός ανάθερμος (°C/bar)	370/65	θερμοκρασία καυσαερίων προ LUVΟ (°C)	325
θερμός ανάθερμος (°C/bar)	600/60	θερμοκρασία αέρα μετά LUVΟ (°C)	300
κενό ψυγείου (bar)	0.050		

Οι παράμετροι λειτουργίας των τριών διεργασιών δέσμευσης συνοψίζονται στον παρακάτω πίνακα.

Πίνακας 86. Μονάδες δέσμευσης CO₂ – προδιαγραφές λειτουργίας

χημική απορρόφηση με MEA	
βαθμίδες απορροφητή / αναγεννητή	8 / 4
φτωχό διάλυμα – περιεκτικότητα σε MEA w/w	40 %
φτωχό διάλυμα – θερμοκρασία	40°C
συμπλήρωμα MEA	1.2·10 ⁻⁴ kg/kg _{lean solvent}
ειδική κατανάλωση θερμότητας στον αναγεννητή	3.58 MJ _{th} /kg _{CO2}
διεργασία κύκλου ασβεστίου	
θερμοκρασία ενανθράκωσης/ασβεστοποίησης	650 / 900 °C
λόγος ανακυκλοφορίας, F_R	8.2 (mol/mol)
λόγος φρέσκου ασβεστολίθου, F_0	0.05 (mol/mol)
μέγιστη δεσμευτική ικανότητα, X_{max}	0.1624
ποσότητα στερεών στην κλίνη του ενανθρακωτή	415,000 kg
πτώση πίεσης στον ενανθρακωτή	150 mbar
όγκος ενανθρακωτή	4685 m ³
θερμαντήρας στερεών προ ασβεστοποιητή - θερμοκρασία	700 °C
ειδική ενεργειακή κατανάλωση για την παραγωγή O ₂	220 kWh/ton O ₂
συγκέντρωση O ₂ στο καθαρό ρεύμα οξυγόνου	95.0%
συγκέντρωση O ₂ στο οξειδωτικό μέσο	40.0%
συγκέντρωση O ₂ στην έξοδο του ασβεστοποιητή	6% v/v
καθαρή καύση με οξυγόνο (ή κύκλος O₂/CO₂)	
συγκέντρωση O ₂ στο καθαρό ρεύμα οξυγόνου	95.0%
συγκέντρωση O ₂ στο οξειδωτικό μέσο	21.0%
ειδική ενεργειακή κατανάλωση για την παραγωγή O ₂	211.9 kWh/tnO ₂
λόγος πίεσης στο συμπιεστή	4.8

3.2.1 Έκπλυση με αμίνες (MEA) Scrubbing

Στη δέσμευση του διοξειδίου του άνθρακα με χημική απορρόφηση, ο διαχωρισμός από τα καυσαέρια γίνεται φέρνοντας το εισερχόμενο αέριο σε επαφή με υδατικό διάλυμα αμίνης σε ατμοσφαιρικής πίεσης στήλη απορρόφησης. Η απαιτούμενη θερμότητα για την αναγέννηση του διαλύτη γίνεται με συμπύκνωση ατμού που απομαστεύεται από το στρόβιλο χαμηλής πίεσης. Το μοντέλο βασίστηκε στην υπάρχουσα βιβλιοθήκη θερμοφυσικών ιδιοτήτων που διαθέτει το ASPEN PlusTM και πιο συγκεκριμένα στην μεθοδολογία του NRTL με ηλεκτρολύτες [91].

3.2.2 Διεργασία Κύκλου Ασβεστίου

Η μεθοδολογία για την προσομοίωση της διεργασίας της ενανθράκωσης βασίστηκε στο μοντέλο που πρώτος εισήγαγε οι Χαρίτος et al. [93], ελαφρώς διαφοροποιημένο, έτσι ώστε να λαμβάνεται υπόψη η παρουσία του εκθειωμένου προσροφητή. Η εκτίμηση της μέγιστης δεσμευτικής ικανότητας των στερεών (X_{max}) συναρτήσει του λόγου ανακυκλοφορίας (F_R) και του λόγου εισαγωγής φρέσκου ασβεστόλιθου (F_0) έγινε με βάση την προσέγγιση των Hawthorne et al. [94]. Για τον υπολογισμό του ρυθμού της αντίδρασης ενανθράκωσης αναπτύχθηκε αλγόριθμος σε περιβάλλον FORTRAN ο οποίος έρχεται σε επικοινωνία με το υπόλοιπο μοντέλο της διεργασίας στο ASPEN PlusTM. Ο αναγεννητής (ασβεστοποιητής) μοντελοποιήθηκε βάσει της υπόθεσης της χημικής ισορροπίας, η οποία στις συγκεκριμένες συνθήκες λειτουργίας προβλέπει πλήρη μετατροπή του ασβεστόλιθου σε οξείδιο του ασβεστίου.

3.2.3 Καύση με καθαρό οξυγόνο

Η παραγωγή του καθαρού οξυγόνου πραγματοποιείται με κρυγονική μέθοδο σε Μονάδα Διαχωρισμού Αέρα. Οι παράμετροι λειτουργίας της μονάδας ρυθμίζονται έτσι ώστε να επιτυγχάνεται ρεύμα οξυγόνου καθαρότητας 95% και ρεύμα αζώτου >99%. Γίνεται λεπτομερής μοντελοποίηση της όλης μονάδας λαμβάνοντας υπόψη όλες τις βασικές διατάξεις, όπως ο συμπιεστής, το σύστημα ψύξης του αέρα, ο κεντρικός εναλλάκτης θερμότητας και οι δυο στήλες απόσταξης.

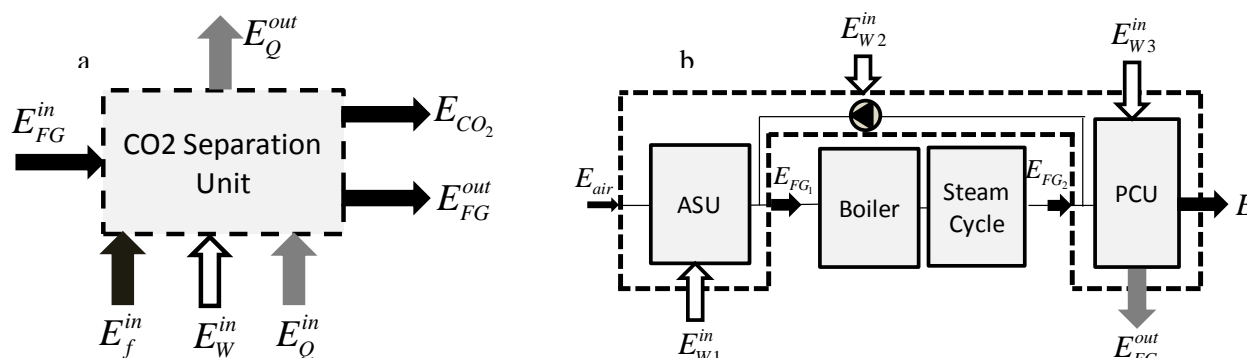
3.2.4 Καθαρισμός CO₂ και συμπίεση

Στην περίπτωση των δυο τελευταίων διεργασιών, λόγω του γεγονότος ότι η καύση γίνεται με περίσσεια οξυγόνου, τα υπολείμματα καύσης και οξυγόνου θα πρέπει να αφαιρεθούν σε κατάλληλη μονάδα καθαρισμού, προτού το αέριο ρεύμα CO₂ οδηγηθεί σε αποθήκευση για λόγους ασφάλειας αλλά και για τεχνικούς λόγους (διάβρωση κυρίως) [26-28]. Έτσι, σχεδιάζεται και μοντελοποιείται λεπτομερώς ένα σύστημα καθαρισμού και απομάκρυνσης των αερίων υπολειμμάτων κυρίως O₂ και H₂O, όπου οι σχετικές νόρμες για τις συγκεντρώσεις των λοιπών στοιχείων είναι πιο αυστηρές γι' αυτά τα δυο. Ο διαχωρισμός O₂/CO₂ βασίζεται στο φαινόμενο Joule-Thomson και γίνεται σε κρυογονικές συνθήκες. Από την άλλη μεριά, η απομάκρυνση H₂O γίνεται με τη βοήθεια διαλύματος triethylene-glycol (TEG)

3.3 Εξεργειακή ανάλυση

Η εξέργεια κάθε υλικού ρεύματος είναι το άθροισμα της φυσικής και της χημικής. Η χημική εξέργεια του εισερχόμενου καυσίμου βασίζεται σε εμπειρική σχέση [106], ενώ για τον υπολογισμό της εξέργειας της αμίνης ακολουθείται η μεθοδολογία που παρουσιάζεται στο [107]. Για τον υπολογισμό των εξεργειακών απωλειών I_{total} σε κάθε διεργασία, απαιτείται το εξεργειακό ισοζύγιο γύρω από το σύστημα δέσμευσης και συμπίεσης του CO₂:

$$E_{FG}^{in} + E_{air}^{in} + E_f^{in} + E_w^{in} + E_Q^{in} = E_{FG}^{out} + E_{CO_2}^{out} + E_Q^{out} + I_{total}$$



Εικόνα 116. Εξεργειακό ισοζύγιο για α) τις τεχνολογίες μετά-καύσης δέσμευσης και β) τεχνολογία καθαρού O₂

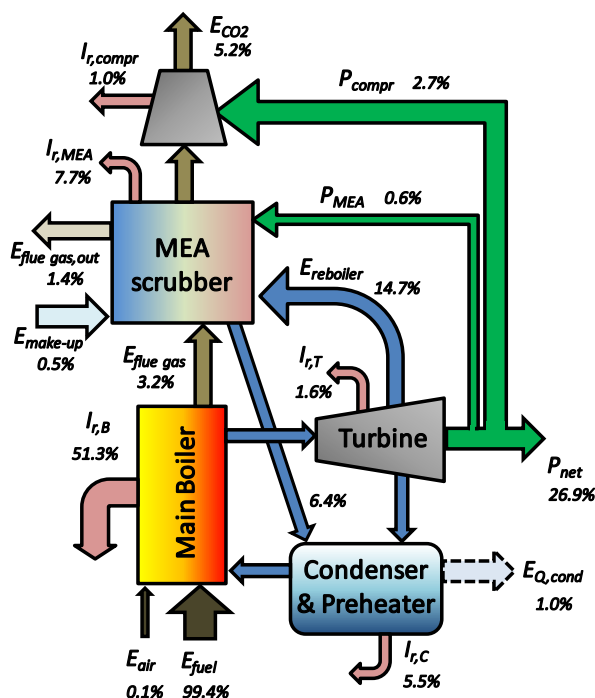
3.4 Αποτελέσματα

Από τους υπολογισμούς στο σταθμό αναφοράς προέκυψε ο καθαρός βαθμός απόδοσης 39.2% στη βάση του Κ.Θ.Ι και ο αντίστοιχος εξεργειακός 36.9%. Η μισή εξέργεια που εισέρχεται στο σύστημα χάνεται στο θάλαμο καύσης κατά τη μετατροπή της χημικής εξέργειας του καυσίμου σε θερμότητα για την ατμοπαραγωγή.

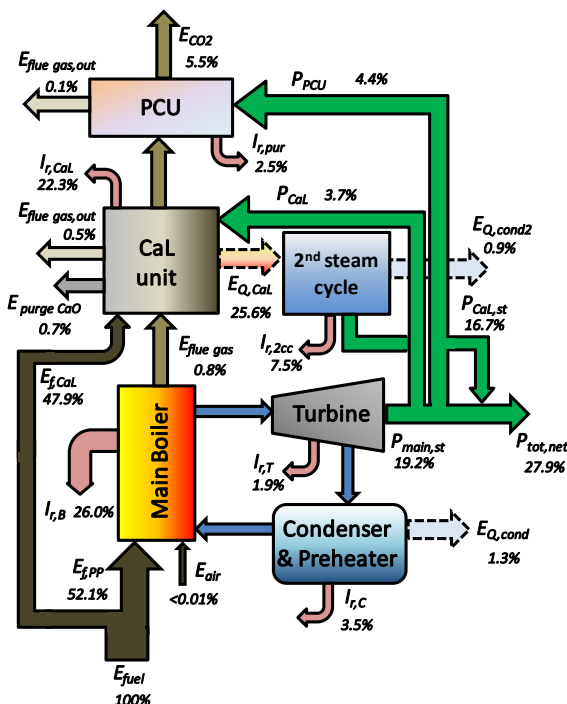
Στην περίπτωση της χημικής απορρόφησης με διάλυμα αμινών, παρατηρήθηκε ότι απαιτείται ένα σημαντικό ποσό εξέργειας σε μορφή χαμηλής ενθαλπίας ατμού για την αναγέννηση του διαλύτη. 11%

της συνολικής μικτής παραγόμενης ηλεκτρικής ενέργειας χρησιμοποιείται για την κάλυψη των ενεργειακών απαιτήσεων (8,8% της συνολικής εξέργειας).

Η περίπτωση του κύκλου ασβεστίου είναι διαφορετική: Περίπου η μισή (47.9%) εισερχόμενη εξέργεια μπαίνει υπό τη μορφή του συμπληρωματικού καυσίμου στον ασβεστοποιητή. Από τις συνολικές εξεργειακές απώλειες στη μονάδα δέσμευσης (22.3%), το 16.3% χάνονται στον ασβεστοποιητή, το 2.1% στον αντιδραστήρα ενανθράκωσης και 2.7% στη Μονάδα Διαχωρισμού του Αέρα. 25.6% της συνολικής εξέργειας ανακτάται σε μορφή θερμότητας υψηλής ποιότητας και αξιοποιείται για την έξτρα ατμοπαραγωγή και, κατά συνέπεια, για την επιπλέον ηλεκτροπαραγωγή. Το εισερχόμενο ρεύμα φρέσκου ασβεστόλιθου έχει αμελητέο εξεργειακό περιεχόμενο, ενώ το εξερχόμενο ρεύμα CaO περιέχει το 0.7% της συνολικής εισερχόμενης εξέργειας.



Εικόνα 117. Ροή εξέργειας στην περίπτωση της μετα-καύσης δέσμευσης με MEA



Εικόνα 118. Ροή εξέργειας στην περίπτωση της μετα-καύσης δέσμευσης με κύκλο ασβεστίου

Η διερεύνηση της επίδρασης της περιεκτικότητας σε θείο στο συμπληρωματικό καύσιμο έδειξε, ότι καύσιμα με υψηλά ποσοστά θείου δυσχεραίνουν σημαντικά τη λειτουργία της διεργασίας λόγω συσσώρευσης $CaSO_4$ στο σύστημα ανακυκλοφορίας. Έτσι, ο βαθμός απόδοσης του συστήματος πέφτει, ενώ και το προκύπτον ρεύμα ασβεστίου που εξέρχεται δεν είναι κατάλληλο για χρήση στην τσιμεντοβιομηχανία ως υποκατάσταση των πρώτων υλών προς παραγωγή κλίνκερ.

Στην περίπτωση της καύσης με καθαρό οξυγόνο, μεγάλα ποσά ενέργειας καταναλώνονται στους συμπιεστές για την παραγωγή του καθαρού οξυγόνου και τον καθαρισμό και συμπίεση του CO_2 . Αν και 70% των καυσασερίων ανακυκλοφορούν ώστε να μειωθεί η περιεκτικότητα του οξυγόνου στο οξειδωτικό μέσο, οι ενεργειακές ανάγκες στον ανεμιστήρα είναι 0.6% της συνολικής εισερχόμενης ΚΘΙ και 0.2% των εξεργειακών απωλειών. Με άλλα λόγια, ακόμα και αν ο λέβητας μπορεί τεχνικά να λειτουργεί χωρίς ανακυκλοφορία, αυτό θα έχει θετική επίπτωση στην εξοικονόμηση εξέργειας μόνο κατά 0.6%.

Είναι αξιοσημείωτο, ότι το 5.5% της συνολικής εισερχόμενης εξέργειας παραμένει στο «τελικό προϊόν», δηλαδή το ρεύμα CO_2 που οδηγείται προς αποθήκευση ή κάποια άλλη χρήση. Είναι επίσης

φανερό, ότι μια εξεργειακή ποινή της τάξης των 8.7% (συμπεριλαμβανομένου και τις ενεργειακές καταναλώσεις) είναι αναπόφευκτη για τον καθαρισμό και συμπίεση του τελικού ρεύματος CO₂.

Πίνακας 87. Ενεργειακό και εξεργειακό ισοζύγιο

	Σταθμός αναφοράς χωρίς δέσμευση	απορρόφηση με αμίνες	κύκλος ασβεστίου	κύκλος καθαρού οξυγόνου
συνολική δεσμευτική ικανότητα (%)	-	90.0%	90.0%	90.0%
καθαρός ηλεκτρικός β.α. (%)	39.2%	28.8%	29.4%	29.1%
καθαρός εξεργειακός β.α. (%)	36.9%	26.9%	27.9%	27.4%
ποινή ενέργειας (%)	-	-10.4%	-9.8%	-10.1%
ποινή εξέργειας (%)	-	-10.0%	-9.0%	-9.5%
ειδικές εκπομπές CO ₂ (kgCO ₂ /MWh)	851.7	116.2	119.8	115.3
δείκτης SPECCA (MJ _{LHV} /kgCO ₂) ¹	-	4.54	4.05	4.36
$\eta_{ex, required}$ (kJ/kgCO ₂) ²	-	2366.6	6892.8	1345.1
$\eta_{ex, spent}$ (kJ/kgCO ₂) ³	-	1113.5	3073.5	1565.7
$\eta_{ex, ut}$ (%) ⁴	-	59.8%	56.7%	48.6%

$$^1 SPECCA = 3600 \cdot \frac{1/\eta - 1/\eta_{ref}}{E_{ref} - E} (MJ_{LHV} / kg_{CO_2})$$

$$^2 \eta_{ex, required} = \frac{E_f^{in} + E_W^{in} + E_Q^{in}}{CO_2 \text{ captured}} [kJ / kg], ^3 \eta_{ex, spent} = \frac{I_{total}}{CO_2 \text{ captured}} [kJ/kg], ^4 \eta_{ex, ut} = 1 - \frac{I_{total}}{E_{FG}^{in} + E_{air}^{in} + E_f^{in} + E_W^{in} + E_Q^{in}}$$

Ο **Πίνακας 87** δείχνει τα βασικά αποτελέσματα από το ισοζύγιο ενέργειας και εξέργειας των τριών υπό εξέταση διεργασιών. Οι ειδικές εξεργειακές απαιτήσεις για την σωστή λειτουργία της διεργασίας του κύκλου ασβεστίου είναι κατά πολύ οι περισσότερες. Περίπου 86% αυτής είναι χημική ενέργεια υπό τη μορφή καυσίμου στον ασβεστοποιητή και το υπόλοιπο 14% έργο για τη λειτουργία της Μονάδας Διαχωρισμού του Αέρα και των λοιπών συμπιεστών του όλου συστήματος. Παρομοίως, οι συνολικές εξεργειακές απώλειες λόγω μη αναστρεψιμότητας σε αυτή την τεχνολογία είναι περίπου τρεις φορές μεγαλύτερες από τις άλλες δυο. Επίσης, ο βαθμός αξιοποίησης της διαθέσιμης εξέργειας είναι μικρότερος από την περίπτωση των αμινών, αλλά μεγαλύτερος από αυτόν στην περίπτωση της καθαρής καύσης με οξυγόνο.

Πίνακας 88. Συνεισφορά κάθε διεργασίας στη συνολική εξεργειακή ποινή για τις τρεις τεχνολογίες δέσμευσης

I_i (kJ/kgCO ₂) για κάθε διεργασία	τεχνολογία δέσμευσης		
	απορρόφηση με αμίνες	κύκλος ασβεστίου	κύκλος καθαρού οξυγόνου
κύριος θερμικός σταθμός	7424.0	3151.0	7110.0
διαχωρισμός CO ₂ από τα καυσαέρια	315.9	235.4	179.1
αναγέννηση διαλύτη/προσροφητή	661.3	1977.8	-
καθαρισμός και συμπίεση CO ₂	135.2	303.5	453.6
παραγωγή O ₂	-	322.5	647.8
συνολικές εξεργειακές απώλειες	8523.8	7711.3	8236.9

Ο **Πίνακας 88** εξηγεί γιατί η τεχνολογία κύκλου ασβεστίου έχει τον υψηλότερο βαθμό απόδοσης, αν και έχει και τις υψηλότερες ειδικές εξεργειακές απώλειες στη μονάδα δέσμευσης. Στην περίπτωση της τεχνολογίας αυτής, οι αντιδραστήρες για δέσμευση και απελευθέρωσή του έχουν κατά πολύ τις υψηλότερες απώλειες. Από την άλλη μεριά, η συνεισφορά της Μονάδας Διαχωρισμού του Αέρα είναι δυο φορές μικρότερη σε σχέση με την τρίτη περίπτωση. Επιπροσθέτως, λόγω της φύσης της διεργασίας, το μισό περίπου καύσιμο δεν καίγεται στο θάλαμο καύσης, οπότε οι ειδικές εξεργειακές απώλειες είναι

υψηλές. Το γεγονός ότι ο αυτόθερμος ασβεστοποιητής είναι πιο αποδοτικός από σκοπιάς εξέργειας από τον θάλαμο καύσης (είτε με αέρα ή με καθαρό οξυγόνο), είναι ο βασικός λόγος για τον οποίο το συνολικό ενεργειακό σύστημα στην περίπτωση του κύκλου ασβεστίου έχει τις λιγότερες απώλειες λόγω μη αναστρεψιμότητας.

Η διαφορά μεταξύ του κύκλου ασβεστίου και της καύσης με οξυγόνο στον καθαρισμό και συμπίεση του διοξειδίου του άνθρακα οφείλεται στη διαφορετική συγκέντρωση οξυγόνου στο πλούσιο σε CO_2 ρεύμα που εξέρχεται του ατμοπαραγωγού και οδηγείται για καθαρισμό.

3.5 Συμπεράσματα

Σε αυτό το κεφάλαιο παρουσιάζεται η ενεργειακή και εξεργειακή ανάλυση των τριών πιο διαδεδομένων τεχνολογιών δέσμευσης CO_2 σε υφιστάμενη λιθανθρακική μονάδα. Η διεργασία κύκλου του ασβεστίου αποδείχθηκε η καλύτερη επιλογή από πλευράς ενεργειακής και εξεργειακής απόδοσης. Στην περίπτωση των αμινών, 7.7% της εισερχόμενης εξέργειας στο σύστημα χάνεται στη μονάδα δέσμευσης και 1% κατά τη συμπίεση του ρεύματος CO_2 . Μεγάλοι λόγοι ΜΕΑ/ CO_2 και μεγάλες συγκεντρώσεις ΜΕΑ στο φτωχό σε CO_2 διάλυμα ευνοεί την αποδοτικότητα της διεργασίας. Αν και ένα σημαντικό ποσό εξέργειας (22.3% της συνολικής E_{fuel}) χάνεται στη μονάδα κύκλου του ασβεστίου, η διεργασία αυτή είναι πιο αποδοτική με τη μικρότερη εξεργειακή ποιινή (-9%). Επίσης, για την εν λόγω διεργασία συμπεραίνεται ότι χαμηλοί λόγοι εισαγωγής φρέσκου ασβεστόλιθου έχουν πολύ μικρή επίδραση στη μείωση των εξεργειακών απωλειών. Η περιεκτικότητα σε θείο στο δευτερεύον καύσιμο του ασβεστοποιητή έχει αρνητικές επιπτώσεις τόσο στον καθαρό ηλεκτρικό βαθμό απόδοσης του σταθμού αλλά όσο και στην λειτουργία του κύκλου ασβεστίου. Μόνο εάν το επίπεδο θερμοκρασίας των δυο αντιδραστήρων πέσει, θα μπορεί η εν λόγω διεργασία να έχει σημαντικά λιγότερες εξεργειακές απώλειες, κάτι το οποίο δεν είναι τεχνικά εύκολο και εφικτό σήμερα, με τους δεδομένους προσροφητές ασβεστίου. Στην περίπτωση της καύσης με καθαρό οξυγόνο, η πλειονότητα των εξεργειακών απωλειών παρατηρούνται στη Μονάδα Διαχωρισμού του Αέρα (647.8kJ/kg CO_2). Μια ενδεχόμενη ανάπτυξη μεμβρανών που είναι διαπερατές στο O_2 και που θα συνοδεύονται από ελαχιστοποιημένες ενεργειακές καταναλώσεις θα βοηθούσαν στην εξοικονόμηση παραπάνω από το 9% της συνολικής εισερχόμενης εξέργειας.

4. Οικονομοτεχνική διερεύνηση για την παραγωγή μεθανόλης μέσω υδρογόνωσης CO₂

4.1 Εισαγωγή

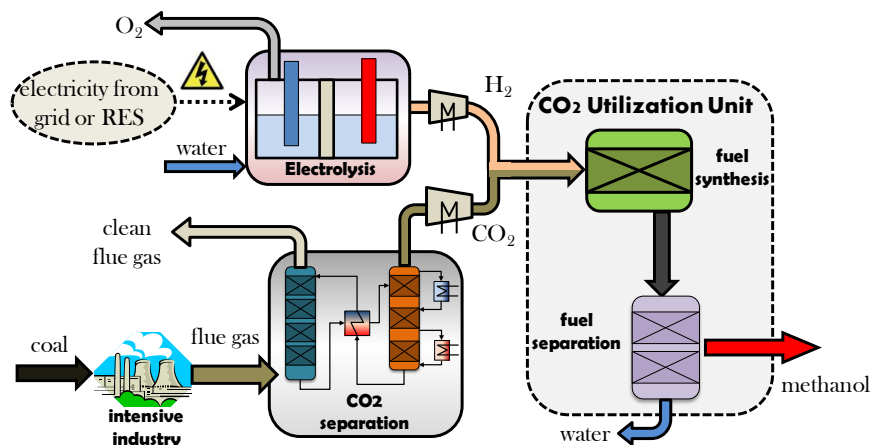
Το κεφάλαιο αυτό είναι το πρώτο από τα δυο που αναφέρονται στην εναλλακτική διαχείριση του δεσμευόμενου διοξειδίου του άνθρακα προερχόμενου από την καύση ορυκτών καυσίμων, αυτή της επαναχρησιμοποίησης του άνθρακα μέσω μετατροπής σε ανώτερης ποιότητας καύσιμα ή άλλα χημικά. Κι ενώ αυτό γίνεται στη φύση μέσω της φωτοσύνθεσης των φυτών, η πιο ώριμη τεχνολογία για να γίνει αυτό σε μεγάλη κλίμακα, είναι αυτή της καταλυτικής υδρογόνωσης. Η οργανική ένωση που επιλέγεται ως τελικό προϊόν στην παρούσα εργασία είναι η μεθανόλη, μιας και θεωρείται ως ένα από τα πιο αξιολόγητα εναλλακτικά υγρά καύσιμα με πολυάριθμες εφαρμογές (χρήση σαν καύσιμο στον τομέα της μεταφοράς, στοιχείο-βάση για τη σύνθεση άλλων χημικών ενώσεων κτλ.).

Το παρόν κεφάλαιο επικεντρώνεται σε αυτή, στην οποία πέρα από το διοξείδιο του άνθρακα, το έτερο αέριο που αποτελεί την πρώτη ύλη για την πραγματοποίηση της αντίδρασης είναι το υδρογόνο. Η παραγωγή του υδρογόνου είναι μια εν γένει ενεργοβόρα και κοστοβόρα διεργασία και απαιτεί ιδιαίτερη προσοχή στη μελέτη της εν λόγω ιδέας. Στην παρούσα εργασία, το απαιτούμενο υδρογόνο θεωρείται ότι προέρχεται από ηλεκτρόλυση νερού, καθώς είναι η πιο ώριμη και δοκιμασμένη τεχνολογία ακόμα και σε βιομηχανική κλίμακα [116] και η διεργασία του δε βασίζεται σε πρώτη ύλη που περιέχει άνθρακα όπως πχ. η παραγωγή H₂ μέσω αεριοποίησης βιομάζας. Η εύρεση φτηνής και δει ανανεώσιμης ηλεκτρικής ενέργειας αποτελεί βασικό ζητούμενο.

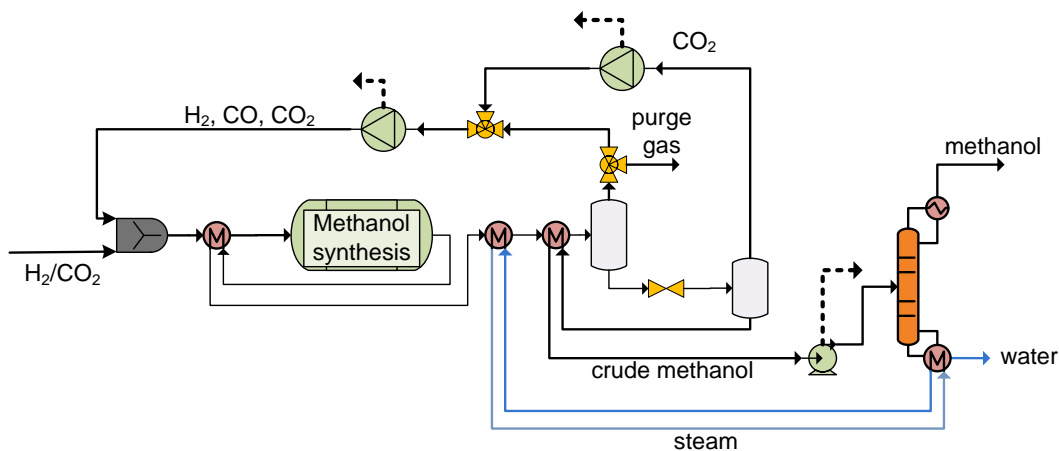
Ο σκοπός αυτού του κεφαλαίου είναι η διερεύνηση διαφόρων στοιχείων και παραμέτρων για την επαναξιοποίηση του δεσμευόμενου CO₂ για την παραγωγή μεθανόλης σε μεγάλης κλίμακας εφαρμογές. Τα στοιχεία αυτά σχετίζονται με την πηγή παραγωγής ενέργειας που απαιτείται κυρίως για την παραγωγή υδρογόνου, την τεχνολογία δέσμευσης διοξειδίου του άνθρακα και τη διαχείριση (μεταφορά και αποθήκευση) των αέριων αντιδρώντων (H₂ και CO₂). Η οικονομική αξιολόγηση γίνεται με γνώμονα την ελαχιστοποίηση του κόστους παραγωγής της μεθανόλης, καθορίζοντας τις οριακές συνθήκες και τα βελτιωτικά μέτρα που πρέπει να παρθούν, ώστε το προτεινόμενο ενεργειακό σύστημα να μπορέσει να γίνει οικονομικά βιώσιμο.

4.2 Περιγραφή της συνολικής διεργασίας παραγωγής μεθανόλης από CO₂

Η διάταξη της παραγωγής μεθανόλης μέσω υδρογόνωσης CO₂ φαίνεται στην **Εικόνα 119**. Το διάγραμμα ροής της σύνθεσης μεθανόλης φαίνεται στην **Εικόνα 120**. Το σύστημα περιλαμβάνει τη σύνθεση, το διαχωρισμό των αέριων στοιχείων που δεν αντέδρασαν με την ανακυκλοφορία τους και τον καθαρισμό της μεθανόλης από το παραχθέν νερό. Η μοντελοποίηση της όλης διεργασίας της εν λόγω μονάδας έγινε σε περιβάλλον ASPEN PlusTM του αντιδραστήρα σύνθεσης και βασίζεται στο κινητικό μοντέλο που παρουσιάζεται στο [128]. Τα βασικά αποτελέσματα της προσομοίωσης χρησιμοποιούνται στον υπολογισμό του κόστους εγκατάστασης και λειτουργίας της μονάδας. Η ανάλυση κόστους έγινε σύμφωνα με τη μεθοδολογία των Peters & Timmerhaus methodology [129].



Εικόνα 119. Η προτεινόμενη διάταξη παραγωγής μεθανόλης από CO₂



Εικόνα 120. Διάγραμμα ροής της σύνθεσης μεθανόλης από CO₂ και H₂

4.3 Καθαρό ρεύμα CO₂ από καυσαέρια που προέρχονται από ορυκτά καύσιμα

Η τεχνολογία δέσμευσης διοξειδίου του άνθρακα που επιλέγεται στην εν λόγω μελέτη είναι αυτή της χημικής απορρόφησης μέσω αμινών, μιας και είναι η πιο ώριμη με αρκετές εφαρμογές της σε βιομηχανική κλίμακα [137]. Το κόστος δέσμευσης ορίζεται στα 43.8 €/tnCO₂. Οι ειδικές θερμικές απαιτήσεις για την αναγέννηση του διαλύτη είναι 4.17 MJ_{th}/kgCO₂ και οι συνολικές ηλεκτρικές καταναλώσεις είναι 0.021 kWh/kgCO₂ [138]. Το συνολικό κόστος για την μεταφορά CO₂ (αν αυτή κρίνεται απαραίτητη) θεωρείται σταθερό και ίσο με 20 €/tnCO₂, ακολουθώντας την υπόθεση που γίνεται στο [127].

4.4 Παραγωγή υδρογόνου

Η αλκαλική ηλεκτρόλυση με διάλυμα KOH είναι η καλύτερη διαθέσιμη τεχνολογία για μεγάλης κλίμακας παραγωγή υδρογόνου από ηλεκτρόλυση νερού [142], η οποία και επιλέγεται στην ανάλυση που γίνεται σε αυτό το κεφάλαιο. Επίσης, έχει εξακριβωθεί η αποτελεσματική λειτουργία αυτών των τύπων ηλεκτρολυτών σε ασυνεχή λειτουργία και εκτός σημείου σχεδιασμού [121]. Τα τελικά αέρια προϊόντα (H₂ και O₂) εξέρχονται από τη μονάδα ηλεκτρόλυσης με πολύ υψηλή καθαρότητα (>99.9%). Οι συνθήκες λειτουργίας της ηλεκτρόλυσης είναι 80 °C/30 bar [121, 143, 144] με ειδική ηλεκτρική κατανάλωση στον ηλεκτρολύτη 4.34 kWh/Nm³ [121], ενώ οι συνολικές ενεργειακές απαιτήσεις είναι

55.56 kWh/kg_{H₂} [143]. Δεδομένου ότι πρόκειται για μια ενεργοβόρα διεργασία, ιδιαίτερη προσπάθεια καταβάλλεται ώστε να καθοριστεί η καλύτερη διάταξη με το μικρότερο κόστος παραγωγής υδρογόνου.

Μεγάλης κλίμακας ηλεκτρολύτης με ηλεκτρικό ρεύμα από το δίκτυο

Το πρώτο σενάριο βασίζεται στην παραγωγή υδρογόνου κεντρικά σε μεγάλης κλίμακας μονάδα (140 MW_e ή ισοδύναμα 60.5 t_{H₂}/day), όπου τροφοδοτείται με ρεύμα από το δίκτυο διανομής της ηλεκτρικής ενέργειας. Το σχήμα αυτό έχει το πλεονέκτημα της λειτουργίας της μονάδας με μεγάλους συντελεστές λειτουργίας (έως 90.0%), αλλά εφόσον θεωρούμε ότι η μονάδα μεθανόλης έχει συντελεστή λειτουργίας 85%, η συνολική ανάλυση γίνεται με ενιαίο συντελεστή για όλο το ενεργειακό σύστημα, το δεύτερο. Για την κοστολόγηση της μονάδας παραγωγής υδρογόνου υιοθετείται η μεθοδολογία που αναπτύχθηκε από το Τμήμα Ενέργειας H2A Analysis των ΗΠΑ όπως αυτή δημοσιεύτηκε στο [12]. Σύμφωνα με την ανάλυση αυτή, το συνολικό κόστος κεφαλαίου εκτιμάται στα 784.0 €/kg/ημέρα.

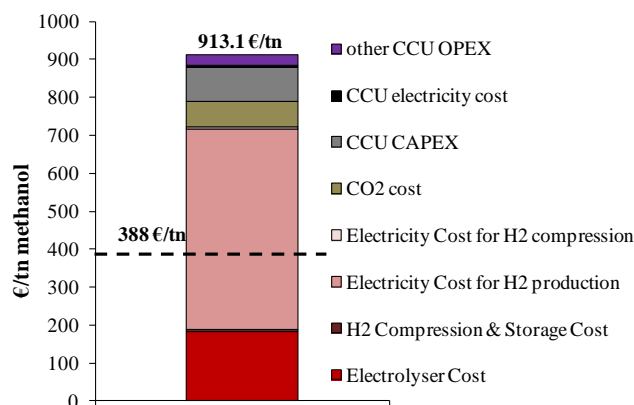
Σε αυτό το σενάριο, βασικό ρόλο παίζει η τιμή αγοράς της ηλεκτρικής ενέργειας. Η τιμολόγηση της κιλοβατώρας διαφέρει από χώρα σε χώρα και μάλιστα κατά πολύ, σε βαθμό που επιδρά σημαντικά και στον καθορισμό του συνολικού κόστους παραγωγής του υδρογόνου. Ένας άλλος σημαντικός παράγοντας, είναι η όλη αρχιτεκτονική του συστήματος συνολικά και η τοποθεσία των υπομονάδων μεταξύ τους. Το ειδικό κόστος για τη μεταφορά του υδρογόνου από το σημείο παραγωγής στο σημείο χρησιμοποίησης αλλάζει ανάλογα με το σενάριο διαχείρισης [144, 152-154].

Πίνακας 89. Σύγκριση διαφόρων επιλογών μεταφοράς H₂ [153]

a/a	μέγεθος μονάδας		απόσταση		προτιμητέα επιλογή μεταφοράς	εκτιμώμενο κόστος μεταφοράς (€/kg)
	μικρό	μεγάλο	μικρή	μεγάλη		
1	X		X		βυτιοφόρο αερίου H ₂	0.60
2	X			X	βυτιοφόρο υγρού H ₂	1.36
3		X	X		σύνδεση με σωλήνα	0.23
4		X		X	σύνδεση με σωλήνα	0.53

Από τον Πίνακα 89 συμπεραίνεται ότι για μεγάλης κλίμακας παραγωγή υδρογόνου ο καλύτερος τρόπος μεταφοράς είναι με σωληνώσεις, ανεξαρτήτου απόστασης. Το δίκτυο σωληνώσεων για τη μεταφορά και διανομή H₂ αναμένεται να αναπτυχθεί στο μέλλον [152]. Το ιδανικό σενάριο, το οποίο και επιλέγεται γι' αυτή την περίπτωση είναι η παραγωγή και η κατανάλωση του υδρογόνου να γίνεται στο ίδιο σημείο, κάτι που η επιλογή της πηγής παροχής ηλεκτρικής ενέργειας (δίκτυο) επιτρέπει μια τέτοια θεώρηση. Όπως προκύπτει από την Εικόνα 121, η παραγωγή υδρογόνου έχει τη μερίδα του λέοντος στην παραγωγή της μεθανόλης από CO₂.

Στην ανάλυση που προηγήθηκε δεν περιλαμβάνεται η οικονομική εκμετάλλευση του παραγόμενου υδρογόνου. Μια ενδεχόμενη εισαγωγή συστήματος υγροποίησης οξυγόνου το συνολικό ειδικό κόστος κεφαλαίου θα αυξηθεί κατά 14.9%, ενώ το λειτουργικό κόστος πέφτει κατά 1.3% λαμβάνοντας υπόψη ότι το οξυγόνο έχει τιμή πώλησης 87.4 €/tn [156]. Κατά συνέπεια, το κόστος παραγωγής πέφτει στα 859.2 €/tn (πτώση 10.1%).

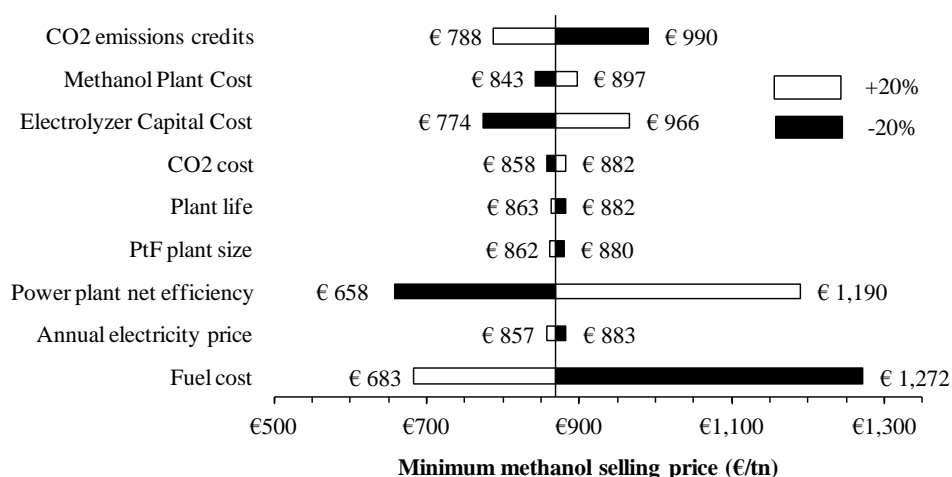


Εικόνα 121. Ανάλυση κόστους για το 1^ο σενάριο

Μεγάλης κλίμακας ηλεκτρολύτης με ηλεκτρικό ρεύμα από θερμικό σταθμό

Αναζητώντας για τη φτηνή ηλεκτρική ενέργεια, ένα σενάριο σε σ' αυτή την κατεύθυνση είναι η λειτουργία του ενεργειακού αυτού συστήματος σαν αποθήκη ενέργειας για τη σταθεροποίηση του ηλεκτρικού δικτύου. Με άλλα λόγια, σε χώρες όπου οι ΑΠΕ έχουν μεγάλο μερίδιο συνεισφοράς στην ηλεκτροπαραγωγή υπάρχει η ανάγκη για ευέλικτη λειτουργία των θερμοηλεκτρικών σταθμών εξαιτίας της στοχαστικής φύσης λειτουργίας και των μεγάλων διακυμάνσεων στην παραγωγή ηλεκτρικής ενέργειας από τις ΑΠΕ. Εδώ εξετάζονται οι συνθήκες με τις οποίες η χρήση της πλεονάζουσας ενέργειας από θερμικό σταθμό για παραγωγή μεθανόλης από CO₂ μπορεί να γίνει οικονομικά βιώσιμη σε αυτή την υποενοότητα.

Η ανάλυση βασίζεται σε δεδομένα από την European Energy Exchange με στοιχεία του 2014 για τη Γερμανία [157]. Η μέση τιμή της μεγαβατώρας προκύπτει στα 32.2 €/MWh. Θεωρώντας ένα τυπικό γερμανικό λιγνιτικό σταθμό 300 MWe [158] με μια τυπική τιμή καυσίμου 2.0 €/GJ_{th} και κόστος εκπομπών CO₂ 7.2 €/tnCO₂ το Κόστος Ηλεκτροπαραγωγής υπολογίζεται στα 29.0 €/MWh, το οποίο σημαίνει ότι 27% του χρόνου η πώληση της ηλεκτρικής ενέργειας στο δίκτυο δεν είναι κερδοφόρα επιλογή.



Εικόνα 122. Ανάλυση ευαισθησίας (με άσπρο όταν αυξάνει κατά 20% η κάθε παράμετρος και με μαύρο όταν μειώνεται)

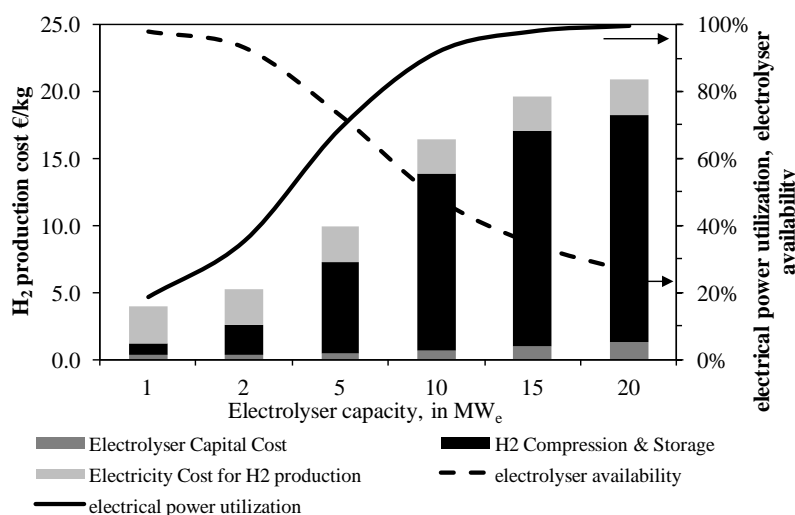
Η δυναμική της μονάδας παραγωγής υδρογόνου είναι η ίδια με τον σταθμό ηλεκτροπαραγωγής και λειτουργεί 2203 ώρες το χρόνο. Το ειδικό κόστος κεφαλαίου προκύπτει στα 582.92 k€/MW_{th}.

Αντίστοιχα, η μονάδα παραγωγής της μεθανόλης έχει ειδικό κόστος κεφαλαίου και λειτουργίας στα 42.05€/tn και 38.02 €/tn μεθανόλης, αντίστοιχα. Σε αντίθεση με το προηγούμενο σενάριο, ο σημαντικότερος παράγοντας που καθορίζει την οικονομικότητα είναι το κόστος κεφαλαίου του ηλεκτρολύτη, λόγω του χαμηλού συντελεστή λειτουργίας του όλου συστήματος (περίπου 25%). Μια ανάλυση ευαισθησίας διαφόρων παραμέτρων με τη μεταβολή τους κατά $\pm 20\%$ φαίνεται στην **Εικόνα 122**.

Φαίνεται ότι το κόστος καυσίμου και ο βαθμός απόδοσης έχουν τη μεγαλύτερη επίδραση στην τιμολόγηση της μεθανόλης. Ακόμα, η μείωση του κόστους του ηλεκτρολύτη και η αύξηση στη φορολόγηση των εκπομπών CO₂ ευνοούν τη μείωση του κόστους παραγωγής της μεθανόλης.

Αποκεντρωμένη παραγωγή H₂ σε μικρής κλίμακας μονάδες διασυνδεδεμένες με ΑΠΕ (πχ. αιολικό πάρκο)

Σε αυτή την περίπτωση όπου η ηλεκτρική ενέργεια είναι διαθέσιμη σε διακοπτόμενα διαστήματα και σε μεταβαλλόμενη ισχύ, ένας ενδιάμεσος αποθηκευτικός χώρος απαιτείται για το παραγόμενο υδρογόνο, ώστε να διασφαλίζεται η συνεχής ροή προς τη μονάδα σύνθεσης της μεθανόλης. Το ειδικό κόστος αποθήκευσης ορίζεται στα 400 €/kg [144]. Κι εδώ τα δεδομένα για την διακύμανση του φορτίου και της τιμής της παραγόμενης ηλεκτρικής ενέργειας από ένα αιολικό πάρκο με εγκατεστημένη ισχύ 25MW_e παίρνονται από το European Energy Exchange [146].



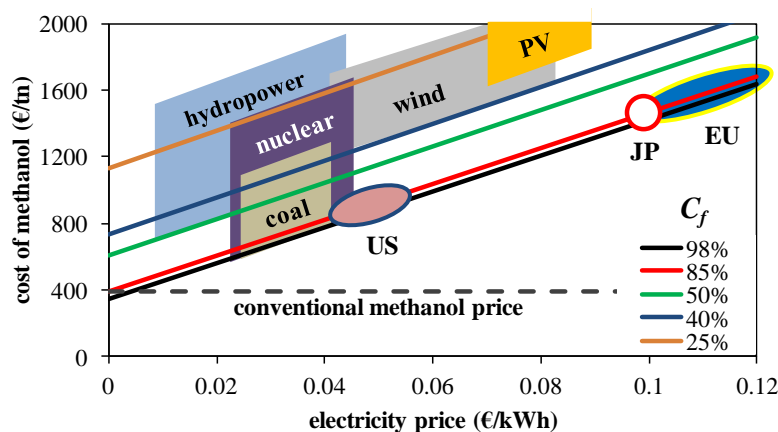
Εικόνα 123. Ανάλυση ευαισθησίας στο μέγεθος της μονάδας

Είναι φανερό από την **Εικόνα 123** ότι το κόστος αποθήκευσης του παραγόμενου υδρογόνου ενδέχεται να παίζει καθοριστικό ρόλο στη διαμόρφωση του συνολικού κόστους παραγωγής και διάθεσης, εφόσον η απαίτηση για σταθερή παροχή και σταθερή λειτουργία της μονάδας σύνθεσης μεθανόλης είναι απαραίτητη προϋπόθεση. Επίσης, η επιδίωξη για μεγιστοποίηση του συντελεστή λειτουργίας της μονάδας είναι πιο σημαντική σημαντική από τη μεγιστοποίηση του συντελεστή αξιοποίησης της διαθέσιμης ηλεκτρικής ενέργειας.

4.5 Συμπεράσματα - παρατηρήσεις

Ανακεφαλαιώνοντας την ανάλυση πάνω στο σχήμα παραγωγής και διάθεσης του απαιτούμενου υδρογόνου, κάθε μια καθεμιά από τις τρεις βασικές παραμέτρους για τον καθορισμό του κόστους του υδρογόνου (κόστος κεφαλαίου του ηλεκτρολύτη, κόστος ηλεκτρισμού και κόστος αποθήκευσης)

μπορεί να παίζει ρόλο-κλειδί για τη βιωσιμότητα του ενεργειακού συστήματος. Όταν ο συντελεστής λειτουργίας της μονάδας υδρογόνου μεγιστοποιείται (πχ. παροχή ρεύματος από το δίκτυο), το κόστος ηλεκτρισμού επικρατεί στον καθορισμό της ελάχιστης τιμής παραγωγής της μεθανόλης. Όταν φτηνή ηλεκτρική ενέργεια χρησιμοποιείται σε μεγάλης κλίμακας εφαρμογές αλλά με λίγες ώρες λειτουργίας, το κόστος κεφαλαίου του ηλεκτρολύτη είναι η πιο σημαντική παράμετρος. Τέλος, όταν η μονάδα υδρογόνου τροφοδοτείται με ανανεώσιμη ηλεκτρική ενέργεια ο κυριότερος παράγοντας είναι η διαχείριση και η αποθήκευση του παραγόμενου H_2 . Η ιδανικότερη αρχιτεκτονική για την ελαχιστοποίηση του κόστους παραγωγής της μεθανόλης είναι αυτή, όπου όλα τα υποσυστήματα βρίσκονται στο ίδιο σημείο.



Εικόνα 124. Επίδραση της τιμής ηλεκτρισμού και συντελεστή λειτουργίας στο κόστος παραγωγής μεθανόλης από CO_2 (US, JP, EU: τιμή δικτύου ηλεκτρισμού στις ΗΠΑ, Ιαπωνία και ΕΕ των 28, αντίστοιχα)

Η **Εικόνα 124** παρουσιάζει την επίδραση στην τιμή της ηλεκτρικής ενέργειας και τον συντελεστή λειτουργίας (C_f) στην προοπτική μιας βιώσιμης λειτουργίας του υπό εξέταση ενεργειακού συστήματος. Επιπροσθέτως αποτυπώνεται και η επίδραση του προμηθευτή ηλεκτρικής ενέργειας στη μονάδα υδρογόνου [12, 159].

Η τρέχουσα κατάσταση για τέτοιου τύπου ενεργειακά συστήματα που μετατρέπουν ηλεκτρική ενέργεια σε καύσιμα υψηλής ποιότητας δεν είναι οικονομικά ελκυστικά ελκυστική μιας και το κόστος παραγωγής πχ της μεθανόλης από CO_2 είναι 2.5 φορές υψηλότερο από την τρέχουσα συμβατική τιμή. Συνεπώς, πρέπει να καταβληθεί μεγάλη προσπάθεια ώστε το προτεινόμενο σύστημα να γίνει πιο ανταγωνιστικό. Αυτή η μελέτη αποσκοπούσε στο να ορίσει τα εμπόδια τα οποία πρέπει να ξεπεραστούν για να κινηθεί προς αυτή την κατεύθυνση. Πιο ειδικότερα, Ειδικότερα, οι παράμετροι κλειδιά που επηρεάζουν τη βιωσιμότητα του συστήματος είναι οι κάτωθι:

- Κόστος ηλεκτρισμού
- Διάταξη του ενεργειακού συστήματος στο σύνολό του
- Εκμετάλλευση του παραγόμενου οξυγόνου είτε σε κάποια άλλη εφαρμογή ή πουλώντας το
- Μείωση του κόστους επένδυσης

5. Αναβαθμισμένες διεργασίες σε ενεργειακά συστήματα βασισμένα στην καταλυτική υδρογόνωση CO₂ προς παραγωγή μεθανόλης και αιθανόλης

5.1 Εισαγωγή

Σε συνέχεια της προηγούμενης μελέτης, το παρόν κεφάλαιο επικεντρώνεται στην παρουσίαση δυο πρωτότυπων διεργασιών για την καλύτερη και αποδοτικότερη μετατροπή του CO₂ σε χρήσιμες ενώσεις, όπως η μεθανόλη και η αιθανόλη, οι οποίες μπορούν να χρησιμοποιηθούν και ως καύσιμα στο τομέα των μεταφορών. Η καταλυτική υδρογόνωση θεωρείται η πιο ώριμη τεχνική για μετατροπή του διοξειδίου του άνθρακα σε κάποια άλλη αναβαθμισμένη ένωση.

Από τη μια, η μεθανόλη θεωρείται ως ένα μια από τις πιο πολύτιμες χημικές ενώσεις με πολυποίκιλες χρήσεις σε διάφορους τομείς, είτε ως καύσιμο, είτε ως ένωση-βάση για τη σύνθεση άλλων πολυπλοκότερων ενώσεων. Επίσης, είναι το πιο αντιπροσωπευτικό υγρό καύσιμο της ιδέας «Ενέργεια για (υγρά) Καύσιμα» καθώς μεγάλα έργα παραγωγής μεθανόλης από CO₂ είναι υπό κατασκευή σε Ισλανδία και Καναδά [42],[43]. Από την άλλη πλευρά, η αιθανόλη είναι ένα εξίσου πολύτιμο καύσιμο/ένωση [160, 161] που αποτελεί τη βάση για την σύνθεση πολλών προϊόντων [39] και θεωρείται ως καταλληλότερη από τη μεθανόλη για υποκατάσταση συμβατικών καυσίμων MEK [80, 162]. Επίσης, ελάχιστες εργασίες έχουν αφιερωθεί στην παραγωγή αιθανόλης από CO₂ [117, 163, 164], καθώς η συντριπτική πλειοψηφία των μελετών πάνω στην εναλλακτική αιθανόλη επικεντρώνονται στην τεχνολογία της αλκοολικής ζύμωσης (βιοχημική διεργασία).

Η μελέτη και παρουσίαση των νέων σχημάτων παραγωγής των εν λόγω αλκοολών βασίζεται στην μοντελοποίηση των διεργασιών σε περιβάλλον ASPEN PlusTM και η στην οικονομική αξιολόγηση και σύγκριση με τις «παραδοσιακές» τεχνικές σύνθεσης από CO₂.

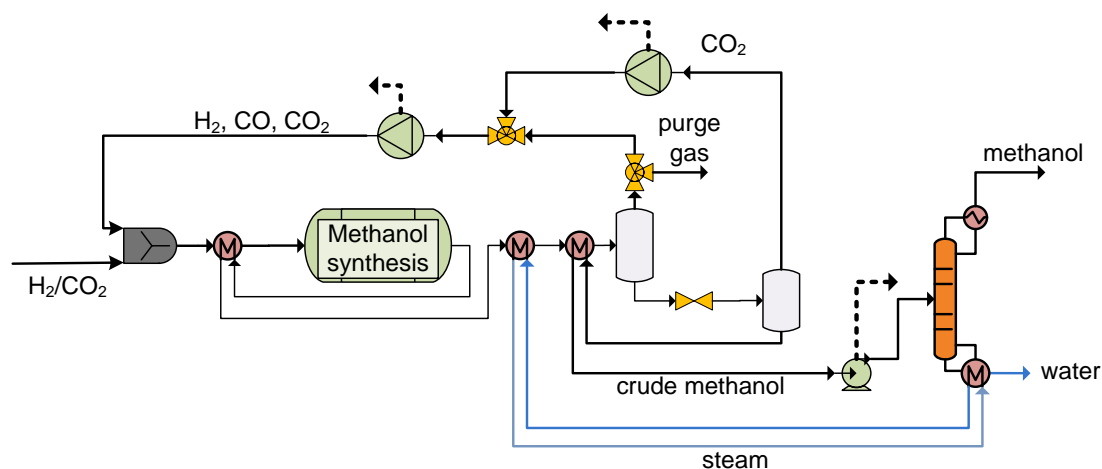
5.2 Περιγραφή των εξεταζόμενων διεργασιών

Τα βασικά στοιχεία των υπό εξέταση ενεργειακών συστημάτων παρουσιάστηκαν στο προηγούμενο κεφάλαιο: Το απαιτούμενο διοξείδιο του άνθρακα διαχωρίζεται και καθαρίζεται από καυσαέρια προερχόμενα από ενεργοβόρα βιομηχανία, ενώ το υδρογόνο προέρχεται από ηλεκτρόλυση νερού. Τα δυο αέρια ρεύματα οδηγούνται στη μονάδα αξιοποίησης του άνθρακα για την σύνθεση και καθαρισμό του/ων επιθυμητού/ων προϊόντος/ων. Οι ειδικές θερμικές καταναλώσεις για το διαχωρισμό του CO₂ με αμίνες θέτονται 4.17 MJ_{th}/kg_{CO2}, ενώ οι αντίστοιχες ενεργειακές 0.021 kWh/kg_{CO2} [138]. Αντίστοιχα, οι συνολικές ηλεκτρικές καταναλώσεις στον ηλεκτρολύτη είναι 55.56 kWh/kg_{H2} [121],[143].

5.2.1 Σύνθεση μεθανόλης από CO₂

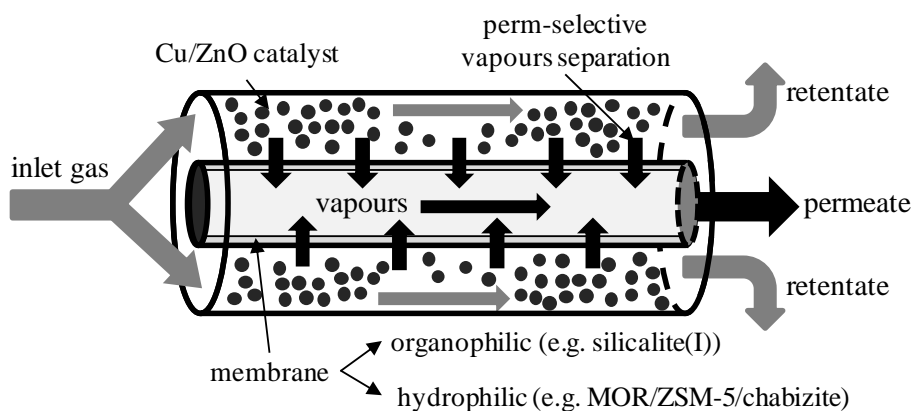
Σε μια τυπική μονάδα παραγωγής μεθανόλης, ο καταλυτικός αντιδραστήρας είναι σωληνοειδής, μόνιμης κλίνης, που λειτουργεί σε υψηλή πίεση και διαρρέεται από ψυκτικό νερό για να διατηρείται σταθερή η θερμοκρασία, καθ' όλο το μήκος του αντιδραστήρα. Το διάγραμμα ροής φαίνεται στην **Εικόνα 125**. Μετά τη σύνθεση, ακολουθεί ο διαχωρισμός των αερίων που δεν αντέδρασαν και η επιστροφή τους στην είσοδο του αντιδραστήρα, καθώς και ο καθαρισμός του τελικού προϊόντος. Οι αντιδράσεις σύνθεσης και ο προσδιορισμός του ποσοστού μετατροπής καθώς και τις οι συγκεντρώσεις

στα προϊόντα καθορίζονται από τους ρυθμούς των αντιδράσεων, όπως αυτοί προκύπτουν από τις εκφράσεις που δίνονται στο [128].



Εικόνα 125. Διάγραμμα ροής για το συμβατικό σενάριο παραγωγής μεθανόλης

Στην εναλλακτική περίπτωση, η χρήση αντιδραστήρα με μεμβράνη για την παραγωγή μεθανόλης εξετάζεται και συγκρίνεται με το συμβατικό αντιδραστήρα. Η πρωτοτυπία στη μελέτη έγκειται στο πώς σχεδιάζεται και λειτουργεί το ολοκληρωμένο σύστημα με αυτόν αυτό το είδος αντιδραστήρα (που έχει ήδη μελετηθεί [168-173]), λαμβάνοντας υπόψη την ανακυκλοφορία των αερίων αντιδρώντων και την οιαδήποτε τροποποίηση στο σχεδιασμό.



Εικόνα 126. Διάταξη του αντιδραστήρα σύνθεσης της μεθανόλης με μεμβράνη

Η Εικόνα 126 απεικονίζει ένα σχέδιο του εν λόγω αντιδραστήρα. Για τη μοντελοποίησή του στο ASPEN Plus™, θεωρήθηκε μια σειρά από αντιδραστήρες ισορροπίας με ενδιάμεσο διαχωρισμό της εκάστοτε ουσίας που διαπερνάει τη μεμβράνη: μεθανόλη για την οργανόφιλη μεμβράνη και νερό για την υδρόφιλη. Ο συντελεστής διαχωρισμού του στοιχείου i ορίζεται ως:

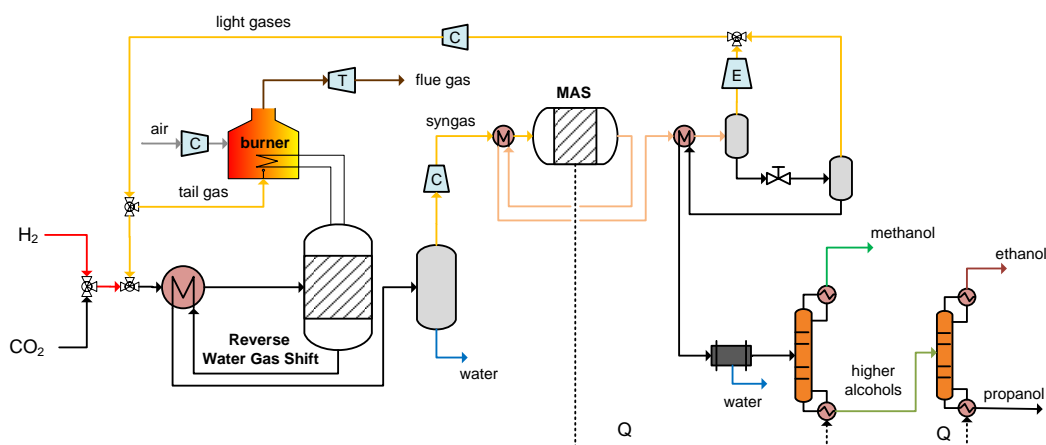
$$SF_i = \frac{F_i^{permeate}}{F_i^{permeate} + F_i^{retentate}}$$

5.2.2 Σύνθεση αιθανόλης από CO₂

Η συμβατική μέθοδος παραγωγής αιθανόλης βασίζεται στην αντίστροφη αντίδραση μετατόπισης rWGS για την παραγωγή μονοξειδίου του άνθρακα και σε δεύτερη φάση, στη σύνθεση της αιθανόλης σε υψηλή πίεση:

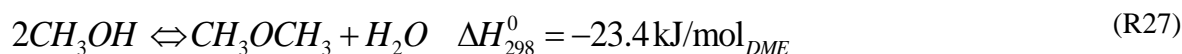
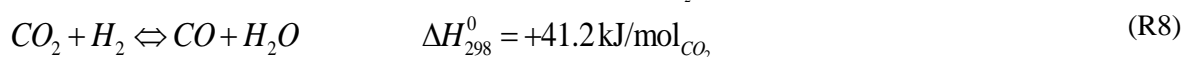
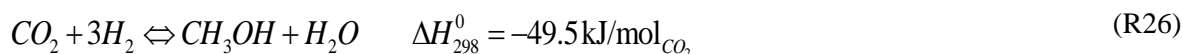


Η διάταξη του εν λόγω συστήματος φαίνεται στην παρακάτω εικόνα:



Εικόνα 127. Διάγραμμα ροής για την παραγωγή αιθανόλης με βάση την αντίστροφη αντίδραση μετατόπισης

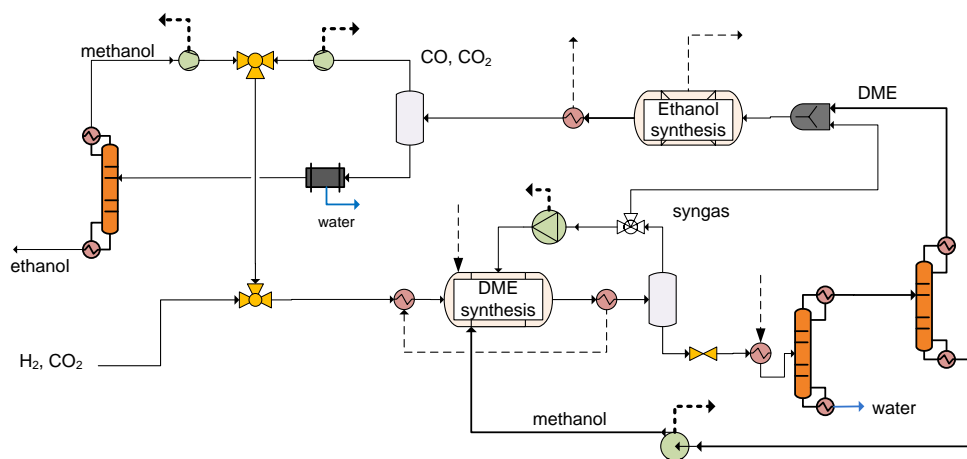
Το καινοτόμο θερμοχημικό σχήμα που προτείνεται, βασίζεται στην σύνθεση διμεθυλαιθέρα (DME) ως ενδιάμεσο προϊόν και αποτελείται από δυο στάδια. Το πρώτο στάδιο είναι η σύνθεση του DME από CO₂ και H₂. Οι κινητικοί παράμετροι βασίζονται στην εργασία των Lu et al. [179]. Η διεργασία λαμβάνει χώρα σε θερμοκρασία 220–300 °C και πίεση 30–60 bar.



Το δεύτερο στάδιο αφορά στην μετατροπή του DME σε αιθανόλη σε δυο βήματα [40, 180, 181]. Το πρώτο είναι η καρβονυλίωση του DME, ενώ το δεύτερο η υδρογόνωση του παραγόμενου εστέρα:



Το δεύτερο στάδιο πραγματοποιείται σε διπλό αντιδραστήρα σειριακά σε πίεση 15 bar και θερμοκρασία 220 °C [40, 180]. Η διάταξη του σχήματος φαίνεται στην παρακάτω εικόνα.



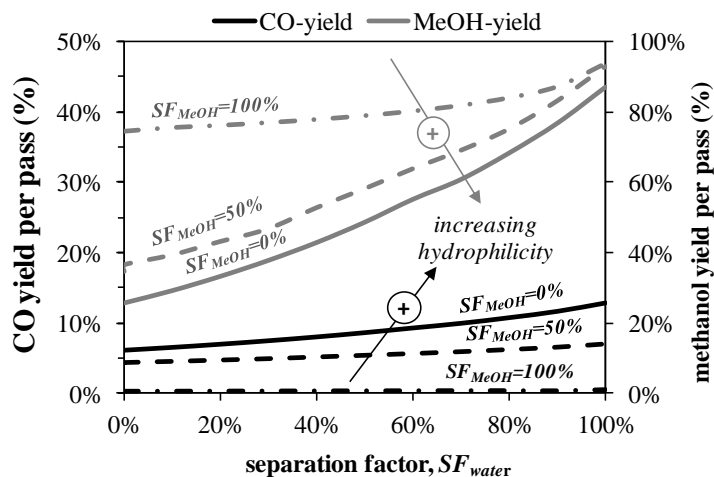
Εικόνα 128. Διάταξη της πρωτότυπης διεργασίας για μετατροπή του CO₂ σε αιθανόλη μέσω DME

5.3 Αποτελέσματα

5.3.1 Αποτελέσματα προσομοιώσεων

Σύστημα παραγωγής Μεθανόλης

Για την αξιολόγηση του ρυθμού παραγωγής κάθε συστατικού, εισάγεται ο όρος της απόδοσης (yield) το οποίο ορίζεται ως το γινόμενο της μετατροπής του CO₂ με την επιλεκτικότητα του κάθε συστατικού. Η ευεργετική επίδραση του συγκεκριμένου τύπου αντιδραστήρα με την αύξηση του SF_{MeOH} φαίνεται στη μείωση της ογκομετρικής παροχής του αερίου ρεύματος που μπαίνει στον αντιδραστήρα. Η ογκομετρική παροχή καθορίζει το μέγεθος του αντιδραστήρα και συνεπώς, το κόστος του. Αν και είναι πιο πολύπλοκη διάταξη, οι βασικές διαστάσεις του αναμένονται να είναι έως και 50% μικρότερες.



Εικόνα 129. Παραγωγή CO και CH₃OH συναρτήσει των συντελεστών διαχωρισμού SF_{water} και SF_{MeOH}

Κάτω υπό, είτε υδρόφιλες ή οργανόφιλες συνθήκες, παρατηρείται η αύξηση του ποσοστού μετατροπής του CO₂. Η αφαίρεση του νερού, όμως, έχει αμελητέα επίδραση στην ογκομετρική παροχή του εισερχόμενου αερίου, κάτι που αποδίδεται στην αύξηση της παραγωγής CO με την αύξηση του SF_{water} , όπως φαίνεται στην Εικόνα 129. Σε αυτή την περίπτωση, η απομάκρυνση νερού ευνοεί την αύξηση της παραγωγή μονοξειδίου του άνθρακα λόγω της αντίδρασης μετατόπισης. Από την άλλη μεριά, η παραγωγή μεθανόλης ευνοείται από την απομάκρυνση τόσο νερού όσο και μεθανόλης μέσω της μεμβράνης.

Για την αξιολόγηση της λειτουργίας κάθε μονάδας αξιοποίησης και μετατροπής του CO₂, εισάγεται ο παρακάτω βαθμός απόδοσης:

$$\eta_{CUV} = \frac{\dot{m}_{CH_3OH} \cdot LHV_{CH_3OH}}{\dot{m}_{H_2inlet} \cdot LHV_{H_2} + \sum P_{cons}}$$

Η παραγωγικότητα της μεθανόλης αυξάνεται κατά 26% με τη χρήση μεμβρανών σαν συνδυασμός της αύξησης του CO₂ και της επιλεκτικότητας σε μεθανόλη. Από τους ενεργειακούς υπολογισμούς σε όλο το σύστημα προκύπτει ότι το θερμικό περιεχόμενο των ανακυκλοφορούντων αερίων είναι 3.6 φορές μεγαλύτερες μεγαλύτερο από αυτό του ρεύματος τροφοδοσίας. Πάνω από το 97% των συνολικών ηλεκτρικών καταναλώσεων απαιτούνται στον ηλεκτρολύτη. Ο συνολικός εξεργειακός βαθμός απόδοσης στο συμβατικό σύστημα είναι 52.7% ενώ στο πρωτότυπο 53.7%.

Σύστημα παραγωγής Αιθανόλης

Τα βασικά αποτελέσματα από τις προσομοιώσεις των δυο διεργασιών παραγωγής αιθανόλης φαίνονται στον επόμενο πίνακα **Table 52**. Το σύστημα που βασίζεται στην παραγωγή αιθανόλης μέσω DME έχει μεγαλύτερη απόδοση. Αυτό αποδίδεται στις ηπιότερες αντιδράσεις που λαμβάνουν χώρα στη συνολική διεργασία, γεγονός που οδηγούν οδηγεί σε λιγότερες θερμικές απαιτήσεις, παρά τις υψηλότερες ενεργειακές καταναλώσεις. Ο συνολικός εξεργειακός βαθμός απόδοσης στο μεν πρώτο σύστημα είναι 41.9%, στο δε δεύτερο 49.3%.

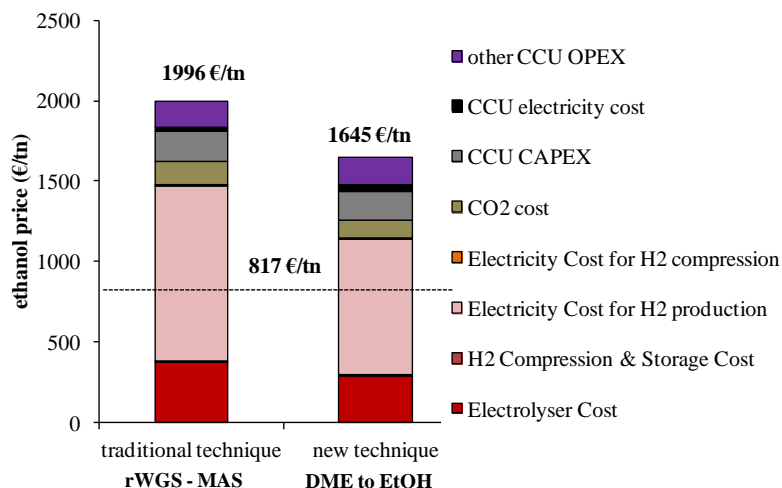
Πίνακας 90. Βασικά αποτελέσματα προσομοιώσεων για την περίπτωση της σύνθεσης αιθανόλης

	EtOH από rWGS	EtOH από DME
ετήσια παραγωγή DME	-	72036
ετήσια παραγωγή αιθανόλης (t/y)	32777	61983
ετήσια παραγωγή μεθανόλης (t/y)	12357	-
ετήσια παραγωγή προπανόλης (t/y)	10079	-
μετατροπή CO ₂ (%)	49.5	56.5
ποσοστό αξιοποίησης CO ₂ (%)	68.7 (81.1) ¹	98.0
συνολικές θερμικές καταναλώσεις (MW _{th})	13.78	13.18
θερμική ισχύς απαερίων (MW _{th})	14.03	1.82
απορριπτόμενη θερμότητα (MW _{th})	27.38	21.81
συνολικές ενεργειακές καταναλώσεις (MW _e)	2.05	4.18
θερμικός βαθμός απόδοσης (% KΘΙ)	63.2	70.3

¹ η τιμή στην παρένθεση αναφέρεται στον άνθρακα στη μεθανόλη και τις ανώτερες αλκοόλες μαζί

5.3.2 Οικονομική ανάλυση

Όσον αφορά στην οικονομική ανάλυση για την περίπτωση της αιθανόλης, η κατανομή κόστους του όλου συστήματος παρουσιάζεται στην **Εικόνα 130** και για τις δυο διεργασίες. Η εμπορική αξιοποίηση του οξυγόνου δε λαμβάνεται υπόψη. Συγκρίνοντας τα δυο σχήματα διεργασιών, το προτεινόμενο (πρωτότυπο) σχήμα οδηγεί σε μικρότερο κόστος παραγωγής αιθανόλης. Το εκτιμώμενο αυτό κόστος είναι 2.01 φορές μεγαλύτερο από την τρέχουσα εμπορική αξία της αιθανόλης.



Εικόνα 130. Παραγωγή Αιθανόλης από CO₂ - Κατανομή κόστους

Στην περίπτωση της εμπορικής αξιοποίησης του οξυγόνου σαν παραπροϊόν, η ελάχιστη τιμή πώλησης της αιθανόλης στην πρώτη περίπτωση πέφτει στα 1.27 €/l, ενώ στη δεύτερη στα 1.11 €/l. Λαμβάνοντας, επίσης, υπόψη ότι το κόστος της κυτταρινικής αιθανόλης (αυτής που προέρχεται από βιοχημικές διεργασίες- αλκοολική ζύμωση) είναι 0.70 €/l, περισσότερη προσπάθεια πρέπει να καταβληθεί, ώστε η εναλλακτική αιθανόλη από CO₂ να καταστεί ανταγωνιστική.

5.4 Συμπεράσματα

Αυτό το κεφάλαιο επικεντρώνεται στην βελτίωση των διεργασιών μετατροπής του CO₂ σε ανώτερης ποιότητας καύσιμα. Δυο κεντρικές ιδέες εξετάζονται, μια για παραγωγή μεθανόλης και μια για αιθανόλη, συγκρινόμενες με τις αντίστοιχες συμβατικές διεργασίες. Στην περίπτωση της μεθανόλης, η υιοθέτηση του αντιδραστήρα μεμβρανών δεν επιφέρει κάποιο ουσιαστικό όφελος στην αποδοση του συνολικού συστήματος, αλλά αυξάνει την παραγωγικότητα σε μεθανόλη, οδηγώντας σε έναν αντιδραστήρα με μικρότερες διαστάσεις. Στην περίπτωση της αιθανόλης, το πρωτότυπο σχήμα, που προτείνεται και εξετάζεται σε αυτή την εργασία, έχει υψηλότερη απόδοση λόγω των χαμηλών θερμικών απαιτήσεων και το κόστος παραγωγής είναι 18% χαμηλότερο. Παρόλα αυτά, αρκετή προσπάθεια θα πρέπει να καταβληθεί ακόμα, ώστε τα προερχόμενα από CO₂ καύσιμα να είναι ανταγωνιστικά στην αγορά προκειμένου τα αντίστοιχα συστήματα να εφαρμοστούν σε εμπορικό επίπεδο.

6. Σχεδιασμός και μοντελοποίηση βιοδιυλιστηρίου για τη καταλυτική μετατροπή αερίου σύνθεσης σε ανώτερες αλκοόλες

6.1 Εισαγωγή

Είναι γνωστό ότι η βιομάζα αποτελεί τη μοναδική ανανεώσιμη πηγή ενέργειας που μπορεί να χρησιμοποιηθεί για την ανάπτυξη και παραγωγή καυσίμων και προϊόντων που ως τώρα προέρχονται από τα ορυκτά καύσιμα και κυρίως το πετρέλαιο. Το έκτο κεφάλαιο της διατριβής έχει να κάνει με το λεπτομερή σχεδιασμό και τη μοντελοποίηση ενός βιοδιυλιστηρίου παραγωγής ανώτερων αλκοολών (αιθανόλη, προπανόλη κτλ) μέσω θερμοχημικών διεργασιών.

Στη συγκεκριμένη περίπτωση, η κύρια θερμοχημική μετατροπή της βιομάζας είναι η αεριοποίηση, όπου η στερεά βιομάζα μετατρέπεται σε ένα αέριο (αέριο σύνθεσης) που αποτελείται κυρίως από H_2 , CO και CO_2 , το οποίο αποτελεί τη βάση για τη σύνθεση μιας πληθώρας χημικών ενώσεων, κάποιες από τις οποίες είναι και οι αλκοόλες. Οι μοντελοποιούμενες περιοχές είναι η αεριοποίηση (μέλαν υγρό –black liquor-, ξύλο), η παραγωγή οξυγόνου, ο καθαρισμός του παραγόμενου αερίου και τέλος, η παραγωγή και η απομόνωση των ανώτερων αλκοολών που αποτελούν και το επιθυμητό προϊόν.

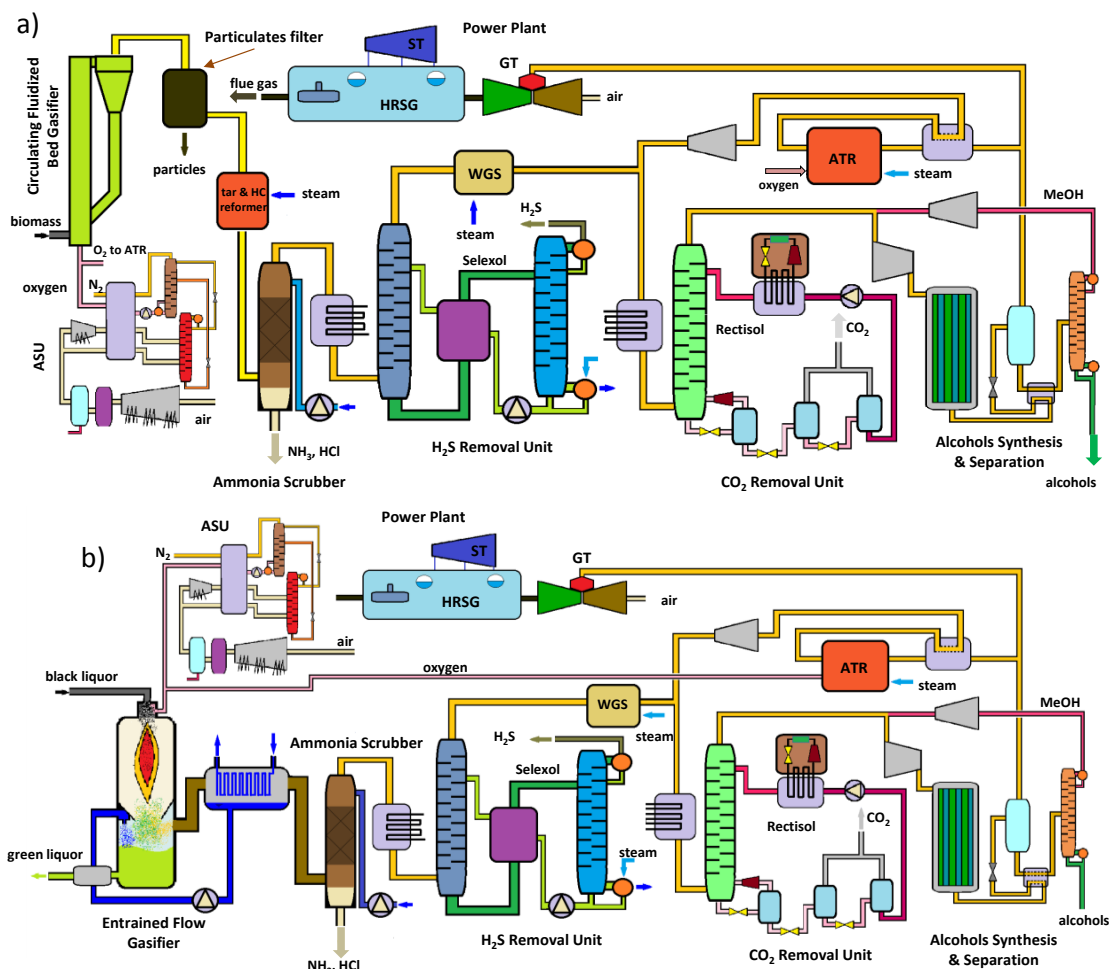
6.2 Περιγραφή του βιοδιυλιστηρίου

Τα δυο υπό εξέταση συστήματα φαίνονται στην **Εικόνα 131**. Η παραγωγή του οξυγόνου γίνεται σε Μονάδα Διαχωρισμού Αέρα μέσω κρυογονικών μεθόδων όπως και στο 2^ο Κεφάλαιο της διατριβής. Το παραγόμενο οξυγόνο είναι πολύ υψηλής καθαρότητας (98%), ώστε να ελαχιστοποιηθούν τα αδρανή αέρια (N_2 , Ar) κατά μήκος της συνολικής διεργασίας. Η τεχνολογία αεριοποίησης που επιλέγεται είναι παρασυρόμενης ροής για την περίπτωση του μέλανος υγρού και ρευστοποιημένη κλίνη ανακυκλοφορίας για την περίπτωση της ξυλώδους βιομάζας. Και οι δυο λαμβάνουν χώρα υπό πίεση (>27 bar), ενώ η θερμοκρασία στον παρασυρόμενης ροής είναι πάνω από 1200 °C, και στην κλίνη η θερμοκρασία δεν ξεπερνά τους 1000 °C.

Ο καθαρισμός του παραγόμενου αερίου σύνθεσης περιλαμβάνει την απομάκρυνση των στερεών σωματιδίων και πρισμών (μόνο στην περίπτωση της ξυλώδους βιομάζας), την απομάκρυνση NH_3 και HCl , και την απομάκρυνση των όξινων αερίων H_2S και CO_2 . Ιδιαίτερη έμφαση δίνεται για την μοντελοποίηση των μονάδων απομάκρυνσης των δυο τελευταίων αερίων. Για το μεν υδρόθειο, η τεχνολογία δέσμευσης που επιλέχθηκε είναι η φυσική απορρόφηση με διαλύτη SelexolTM, ενώ για την απομάκρυνση του διοξειδίου του άνθρακα αυτή με διαλύτη RectisolTM. Η καταλυτική σύνθεση των αλκοολών λαμβάνει χώρα σε σωληνοειδούς τύπου καταλυτικό αντιδραστήρα υπό πίεση. Δυο τύποι καταλυτών με διαφορετικές επιδόσεις και λειτουργία εξετάζονται: ο πρώτος, ένας τροποποιημένος καταλύτης που χρησιμοποιείται κατά βάση για διεργασία Fischer-Tropsch (MoS_2) και ο δεύτερος, ένας τροποποιημένος καταλύτης σύνθεσης μεθανόλης ($Cu-Zn$).

Εκτός από τα επιθυμητά οργανικά προϊόντα (ανώτερες αλκοόλες), στα προϊόντα συγκαταλέγονται και CO_2 με υδρογονάνθρακες που στην περίπτωση που εξετάζεται θεωρούνται ανεπιθύμητα και πρέπει να απομακρυνθούν. Το μεν διοξείδιο του άνθρακα απομακρύνεται στη μονάδα διαχωρισμού CO_2 , όταν το ανακυκλοφορούν αέριο ενωθεί με το αέριο σύνθεσης που έρχεται από την αεριοποίηση. Προηγουμένως, οι ανεπιθύμητοι υδρογονάνθρακες υπόκεινται σε αναμόρφωση σε αυτόθερμο αντιδραστήρα αναμόρφωσης. Το αέριο αυτό που αποτελείται από τα μη αντιδρώντα αέρια και τις

προαναφερθείσες ουσίες διαχωρίζεται από τα επιθυμητά προϊόντα στη μονάδα διαχωρισμού και καθαρισμού των αλκοολών, μετά τον αντιδραστήρα σύνθεσης. Ο διαχωρισμός των αλκοολών μεταξύ τους λαμβάνει χώρα σε αποστακτικές στήλες. Για να καλυφθούν οι όποιες θερμικές και ηλεκτρικές ανάγκες που απαιτούνται σε κάθε υποσύστημα του βιοδιυλιστηρίου, θεωρείται ότι υπάρχει και ένας σταθμός συμπαραγωγής που λειτουργεί με μέρος από τα ανακυκλοφορούντα αέρια (CO και H_2) στη μονάδα σύνθεσης. Ο σταθμός συμπαραγωγής είναι συνδυασμένος κύκλος για υψηλό βαθμό απόδοσης λειτουργίας και αξιοποίησης του αέριου καυσίμου που έρχεται στη μονάδα αυτή υπό πίεση.



Εικόνα 131. Διαγράμματα ροής για τα δυο διαφορετικά συστήματα έχοντας ως πρώτη ύλη α) ξυλώδη βιομάζα και β) μέλαν υγρό

6.3 Μεθοδολογία μοντελοποίησης και περιγραφή του μοντέλου

Η μοντελοποίηση της αεριοποίησης βασίστηκε στην υπόθεση της χημικής ισορροπίας μέσω της ελαχιστοποίηση της ενέργειας Gibbs. Στην περίπτωση της ξυλώδους βιομάζας στο μοντέλο ισορροπίας διορθώθηκε η συγκέντρωση του μεθανίου με βάση τη βιβλιογραφία [207]. Ιδιαίτερη έμφαση, λόγω δυσκολίας, δόθηκε για την αποτελεσματική μοντελοποίηση της αεριοποίησης του μέλανος υγρού, λόγω της ιδιαιτερότητας των ανόργανων συστατικών του να συμμετέχουν ενεργά στη διαμόρφωση των προϊόντων της διεργασίας, με το σχηματισμό του «πράσινου υγρού» (green liquor).

Η μοντελοποίηση του καθαρισμού του αερίου κυρίως επικεντρώθηκε στην απομάκρυνση του H_2S και CO_2 . Ιδιαίτερη έμφαση δόθηκε στην επιλογή των κατάλληλων θερμοφυσικών ιδιοτήτων και καταστατικών εξισώσεων. Η μοντελοποίηση του αντιδραστήρα σύνθεσης βασίστηκε σε αντιδραστήρα

εμβολικής ροής συνοδευόμενος με τις κινητικές εκφράσεις των αντιδράσεων που λαμβάνουν χώρα σε κάθε μια περίπτωση καταλύτη. Οι παράμετροι για το κινητικό μοντέλο της σύνθεσης αλκοολών κάνοντας χρήση MoS_2 πάρθηκαν από το [224], ενώ για την περίπτωση με καταλύτη Cu-Zn από το [214].

6.4 Αποτελέσματα

6.4.1 Σύγκριση της αποδοτικότητας των δυο διαφορετικών καταλυτών

Και οι δυο περιπτώσεις έχουν παρόμοια προφίλ θερμοκρασίας και πίεσης. Ο καταλύτης Cu-Zn έχει πολύ περισσότερες απαιτήσεις σε ανακυκλοφορία μεθανόλης και αερίου σύνθεσης που δεν αντέδρασε. Οι αντίστοιχες παροχές μάζας είναι μεγαλύτερες γι' αυτή την περίπτωση.

Στην περίπτωση του καταλύτη MoS_2 που εφαρμόζεται στο σενάριο της ξυλόδου βιομάζας (“περίπτωση A_1 ”), η μετατροπή CO και H_2 υπολογίζεται στα 32.8% και 17.2%, αντίστοιχα. Από την άλλη μεριά, χρησιμοποιώντας τον άλλο καταλύτη για την ίδια πρώτη ύλη (“περίπτωση B_1 ”) τα αντίστοιχα ποσοστά μετατροπής είναι 7.7% και 5.2%. Αυτό δείχνει ότι ο καταλύτης με βάση MoS_2 είναι κατά πολύ καλύτερος στο να επιτυγχάνει μεγαλύτερη παραγωγικότητα αιθανόλης και προπανόλης (Πίνακας 91). Ο Cu-Zn καταλύτης διατηρεί τα χαρακτηριστικά πιο πολύ για σύνθεση μεθανόλης και όχι τόσο για ανώτερες αλκοόλες, γεγονός που αυξάνει δραστικά τις απαιτήσεις για ανακυκλοφορία αερίων. Το μέγεθος του αντιδραστήρα είναι τουλάχιστον τριπλάσιο σε σχέση με την ιδανική περίπτωση ενός μονής διέλευσης αντιδραστήρα. Οι απαιτήσεις για ατμό και ηλεκτρική ενέργεια καθορίζει και την παροχή του αερίου το οποίο χρησιμοποιείται στη μονάδα συμπαραγωγής. Στην περίπτωση A_1 , αυτό το ποσοστό είναι 16.2% ενώ στην περίπτωση B_1 32.2%.

Πίνακας 91. Ειδικές παροχές μάζας προϊόντων και άλλων κύριων ρευμάτων του βιοδιωλιστηρίου.

τύπος καταλύτη	MoS_2	Cu-Zn
γραμμάρια προϊόντων ανά κιλό πρώτης ύλης		
αιθανόλη	89.45	39.64
προπανόλη	39.02	20.30
κιλά απαιτούμενου ατμού ανά κιλό πρώτης ύλης		
αντίδραση μετατόπισης	0.023	0.027
αντίδραση αναμόρφωσης	0.274	0.602
στήλη αναγέννησης στη μονάδα H_2S	0.005	0.019
κιλά απαιτούμενου οξυγόνου ανά κιλό πρώτης ύλης		
αεριοποίηση	0.653	0.653
αναμόρφωση	0.254	0.251

Ο Πίνακας 92 δείχνει τις ειδικές καταναλώσεις για τις δυο αυτές περιπτώσεις. Η περισσότερη από την απαιτούμενη ηλεκτρική ενέργεια καταναλώνεται στη Μονάδα Διαχωρισμού του Αέρα και για την συμπίεση των ανακυκλοφορούντων αερίων προ του αντιδραστήρα σύνθεσης. Η μονάδα αποθείωσης έχει και υψηλές ενεργειακές και θερμικές απαιτήσεις για την άντληση του διαλύτη και την αναγέννησή του, στον αναγεννητή αντίστοιχα.

Πίνακας 92. Ειδικές ενεργειακές καταναλώσεις σε κάθε μονάδα του βιοδιωλιστηρίου.

	καταλύτης MoS ₂		καταλύτης Cu-Zn	
		% ΑΘΙ		% ΑΘΙ
	kJ/g _{HA}	πρώτης ύλης	kJ/g _{HA}	πρώτης ύλης
Μονάδα Διαχωρισμού Αέρα (ΜΔΑ)	5.6	3.62	18.5	5.88
συμπίεση αερίου σύνθεσης	7.4	4.85	27.6	8.75
συμπίεση ανακυκλοφορούντων αερίων	0.6	0.37	3.0	0.94
απομάκρυνση H ₂ S	0.1	0.52	1.6	0.52
απομάκρυνση CO ₂	1.9	1.29	5.9	1.86
Σύνολο	15.6	10.17	56.6	17.96

Τα βασικά ενεργειακά μεγέθη του βιοδιωλιστηρίου, όταν αυτό λειτουργεί με τις δυο υπό εξέταση πρώτες ύλες, παρουσιάζεται παρουσιάζονται στον **Πίνακας 93**.

Πίνακας 93. Ενεργειακό ισοζύγιο των περιπτώσεων αεριοποίησης με μέλαν υγρό και ξυλόδη βιομάζα

πρώτη ύλη	ξύλο	μέλαν υγρό
	% ΑΘΙ της εισερχόμενης α' ύλης	
ΑΘΙ μη επεξεργασμένου αερίου σύνθεσης	74.0	60.7
ΑΘΙ επεξεργασμένου αερίου σύνθεσης	63.6	52.6
(ΜΔΑ) ενεργειακές καταναλώσεις	3.62	4.76
Μονάδες απομάκρυνσης H ₂ S, CO ₂ - ενεργειακές καταναλώσεις	1.33	2.02
Συνολικές ενεργειακές καταναλώσεις	10.2	10.4
Ανώτερες αλκοόλες Α.Θ.Ι.	21.0	14.2

Κάνοντας την θεώρηση της μεθανόλης ως «επιθυμητό προϊόν», η λίστα των τελικών προϊόντων διευρύνεται. Σ' αυτή την περίπτωση μειώνονται οι συνολικές καταναλώσεις καθώς δεν απαιτείται η ανακυκλοφορία της μεθανόλης. Ο **Πίνακας 94** συνοψίζει τα βασικά αποτελέσματα από τις περιπτώσεις που θεωρείται η μεθανόλη ως τελικό προϊόν (η περίπτωση C και D είναι με καταλύτη MoS₂ and Cu-Zn, αντίστοιχα).

Πίνακας 94. Επίδραση της ανακυκλοφορίας της μεθανόλης στη λειτουργία του σταθμού (περίπτωση μέλανος υγρού-BL).

περίπτωση	τύπος καταλύτη	ανακυκλοφορία μεθανόλης	μετατροπή CO (%)	μετατροπή H ₂ (%)	παραγωγή ανώτερων. αλκοολών (g/kg _{BL})	παραγωγή μεθανόλης (g/kg _{BL})
A ₂	MoS ₂	yes	21.89	11.50	27.03	-
B ₂	Cu-Zn	yes	5.3	3.6	13.84	-
C	MoS ₂	no	21.51	11.71	24.78	7.32
D	Cu-Zn	no	5.4	3.6	7.75	4.21

6.4.2 Ανάλυση ευαισθησίας

Χαμηλότερες τιμές της ωριαίας χωρικής ταχύτητας του εισερχόμενου αερίου ρεύματος (Gas Hourly Space Velocity, GHSV) οδηγεί οδηγούν σε μεγαλύτερη παραγωγή και επιλεκτικότητα των

επιθυμητών στοιχείων (ανώτερες αλκοόλες). Η αυξημένη πίεση επιδρά θετικά στην απόδοση του συστήματος, αν και αυτό σημαίνει και μεγαλύτερο κόστος εξοπλισμού. Χαμηλές τιμές στο λόγο H_2/CO υπό συγκεκριμένες πιέσεις και θερμοκρασίες έδειξαν την εμφάνιση στερεού άνθρακα, η επικάλυψη του οποίου στον καταλύτη επιφέρει σημαντική μείωση στο χρόνο ζωής του καταλύτη.

6.5 Συμπεράσματα

Το παρόν κεφάλαιο επικεντρώνεται στη λεπτομερή μοντελοποίηση ενός ολοκληρωμένου βιοδιωλιστηρίου περιλαμβάνοντας όλες τις διεργασίες που λαμβάνουν χώρα για την παραγωγή ανώτερων αλκοολών από βιομάζα (ξυλώδης ή μέλαν υγρό). Η μοντελοποίηση έγινε σε περιβάλλον ASPEN Plus™. Τα υπό εξέταση συστήματα αναλύθηκαν και συγκρίθηκαν για το βαθμό απόδοσης που έχουν και τις απώλειες και καταναλώσεις που παρατηρούνται καθ' όλη τη διεργασία συνολικά. Τα αποτελέσματα έδειξαν ότι το σύστημα που σχεδιάστηκε και λειτούργησε με βάση τον MoS_2 καταλύτη είναι κατά πολύ καλύτερο, όσον αφορά την απόδοση και την παραγωγικότητά του σε ανώτερες αλκοόλες από το αντίστοιχο με Cu-Zn καταλύτη. Στη δεύτερη περίπτωση, παρατηρείται αυξημένη παραγωγικότητα σε μεθανόλη, ο καθαρισμός και η ανακυκλοφορία της οποίας απαιτεί αρκετές καταναλώσεις. Η υψηλή πίεση λειτουργίας έχει θετική επίδραση στην παραγωγικότητα των αλκοολών. Τεχνικά,, η αεριοποίηση μπορεί να πραγματοποιηθεί σε υψηλότερες πιέσεις, αλλά αυτό θα οδηγήσει σε αυξημένες συγκεντρώσεις υδρογονανθράκων –κυρίως CH_4 – οι οποίοι θα πρέπει να αναμορφωθούν. Η σύνθεση υδρογονανθράκων σε αυτό το σχήμα βιοδιωλιστηρίου έχουν αρνητική επίπτωση στην επίδοση του συστήματος, καθώς είναι μεγάλες οι ενεργειακές απώλειες για το διαχωρισμό των προϊόντων, την παραγωγή του απαιτούμενου οξυγόνου για τη λειτουργία του αναμορφωτή και την ανακυκλοφορία των αερίων.

7. Εναλλακτικές θερμοχημικές τεχνικές για τη σύνθεση αεροπορικών βιοκαυσίμων μέσω αλκοολών: μοντελοποίηση και σχεδιασμός διεργασιών, οικονομοτεχνική αξιολόγηση και σύγκριση

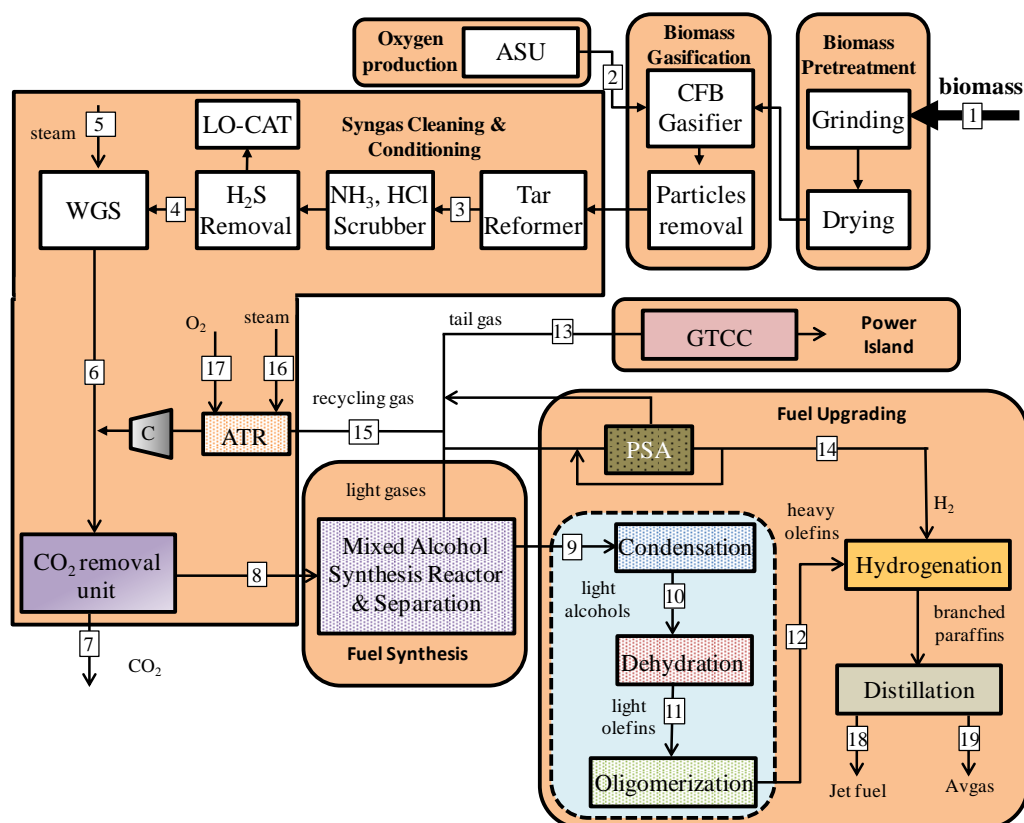
7.1 Εισαγωγή

Το 12% των εκπομπών CO₂ στις μεταφορές οφείλεται στη χρήση των αεροπορικών καυσίμων με 698 εκατομμύρια τόνους εκπομπών το 2012 [229]. Η ανάπτυξη καυσίμων προερχόμενα προερχομένων από βιομάζα όχι μόνο θα συμβάλλει στη μείωση των εκπομπών CO₂, αλλά και στη σταδιακή απαγκίστρωση από τα ορυκτά καύσιμα και τις απρόβλεπτες διακυμάνσεις στη τιμή του πετρελαίου και των παραγώγων του. Η βασική συμβατική μέθοδος παραγωγής αεροπορικών καυσίμων είναι μέσω κλασματικής απόσταξης του πετρελαίου. Μια άλλη μέθοδος είναι μέσω της διεργασίας σύνθεσης Fischer-Tropsch, όπου η πρώτη ύλη (άνθρακας, φυσικό αέριο ή βιομάζα) πρώτα μετατρέπεται σε αέριο μίγμα H₂ και CO το οποίο υπόκειται σε καταλυτική σύνθεση για την παραγωγή υδρογονανθράκων, κυρίως παραφινών.

Σε αυτό το κεφάλαιο παρουσιάζονται και γίνεται η οικονομοτεχνική μελέτη διαφόρων θερμοφυσικών διαδρομών διεργασιών για την παραγωγή διακλαδισμένων παραφινών από βιομάζα. Μεγαλύτερη έμφαση δίνεται στο τμήμα της αναβάθμισης του καυσίμου, όπου εκεί η όλη διεργασία καταλήγει στο τελικό επιθυμητό προϊόν. Μαζί με τις δυο πρωτότυπες διεργασίες μέσω σύνθεσης ανώτερων αλκοολών, παρουσιάζεται επίσης και η συμβατική μέθοδος μέσω της Fischer-Tropsch σύνθεσης. Για συγκριτικούς λόγους στην ενότητα της οικονομικής αξιολόγησης των σεναρίων, εξετάζονται επίσης και δυο σενάρια που βασίζονται σε βιοχημικές διεργασίες.

7.2 Περιγραφή των πρωτότυπων θερμοχημικών διεργασιών

Οι πολύπλοκες οργανικές δομές της λιγνοκυταρινικής βιομάζας μετατρέπονται θερμικά σε απλούστερες ενώσεις μέσω της αεριοποίησης. Μετά από μια διαδικασία που αποτελείται από διάφορα στάδια διεργασιών, το αέριο σύνθεσης που αποτελείται από CO και H₂ χρησιμοποιείται για τη σύνθεση ελαφρών αλκοολών [175, 265]. Όσες οργανικές ενώσεις δε, συμμετέχουν στην αναβάθμιση των αλκοολών προς παραγωγή αλκανίων με μεγάλο αριθμό ατόμων άνθρακα, οδηγούνται σε αντιδραστήρα αναμόρφωσης, ώστε ο C που βρίσκεται υπό τη μορφή CO να είναι σε θέση να χρησιμοποιηθεί ξανά. Το υπό εξέταση βιοδιυλιστήριο καλύπτει τις θερμικές και ενεργειακές του ανάγκες μέσω της χρησιμοποίησης μέρους από το ανακυκλοφορούν αέριο (απαέρια) σε μονάδα συμπαραγωγής ηλεκτρικής και θερμικής ενέργειας. Η δυναμική του ενεργειακού συστήματος θεωρείται 190 MW_{th} για να μπορεί να συγκριθεί εύκολα με παρόμοιες μελέτες βιοδιυλιστηρίων στη βιβλιογραφία. Ο τύπος βιομάζας που θεωρείται ως πρώτη ύλη είναι ξύλο. Το κομμάτι της αεριοποίησης ξυλόδους βιομάζας περιγράφεται αναλυτικά στο προηγούμενο κεφάλαιο της διατριβής.



Εικόνα 132. Σχηματική απεικόνιση της παραγωγής αεροπορικών βιοκαυσίμων από αλκοόλες

Στην παραπάνω **Εικόνα 132** παρουσιάζονται όλες οι διεργασίες από την παραγωγή του αερίου σύνθεσης σε αεριοποιητή υπό πίεσης και με οξειδωτικό μέσο καθαρό οξυγόνο, τον καθαρισμό του αερίου αυτού που περιλαμβάνει την απομάκρυνση ουσιών όπως NH_3 , HCl , H_2S και CO_2 και τη ρύθμιση της σύστασή του στον αντιδραστήρια μετατόπισης. Το κομμάτι αυτό μέχρι τον αντιδραστήρα σύνθεσης είναι κοινό για όλες τις υπό εξέταση περιπτώσεις.

7.2.1 Σύνθεση αλκοολών και αναβάθμιση καυσίμου

Όπως φαίνεται στην **Εικόνα 132**, από τη μονάδα σύνθεσης αλκοολών (MAS) και το διαχωρισμό των εξερχόμενων ρευμάτων από τον αντιδραστήρα προκύπτουν δυο βασικά ρεύματα: οι ανώτερες αλκοόλες (9) και ένα αέριο ρεύμα που περιέχει το αέριο σύνθεσης που δεν αντέδρασε, ελαφρούς υδρογονάνθρακες και διοξείδιο του άνθρακα. Μέρος από το δεύτερο ρεύμα χρησιμοποιείται στη μονάδα συμπαραγωγής, μέρος από το υδρογόνο που περιέχεται διαχωρίζεται στη μονάδα PSA για την υδρογόνωση στο τελευταίο στάδιο της αναβάθμισης και το υπόλοιπο οδηγείται στον αντιδραστήρα αναμόρφωσης. Οι παραγόμενες αλκοόλες υπόκεινται σε αντίδραση συμπύκνωσης για να αυξηθούν οι αλκοόλες με C₄₊ και στη συνέχεια σε αντίδραση αφύγρανσης για να μετατραπούν στις αντίστοιχες ολεφίνες (αλκένια. 11). Η αύξηση των ατόμων άνθρακα στις οργανικές ενώσεις επιτελείται στο επόμενο βήμα διεργασιών όπου λαμβάνει χώρα η σύνθεση C₄⁼ ολιγομερών (12). Τέλος, μέσω της αντίδρασης υδρογόνωσης παράγονται διακλαδισμένες παραφίνες (αλκάνια), που είναι οι απαραίτητες ενώσεις για ανάμιξη με αεροπορικά καύσιμα τύπου τζετ (18) και βενζίνη (19).

7.2.1.1 Σύνθεση Αλκοολών

Η σύνθεση αλκοολών πραγματοποιείται υπό υψηλή πίεση (>40 bar) και θερμοκρασία μεταξύ 250-320 °C παρουσία καταλύτη:



Σε αυτή τη μελέτη, εξετάζονται δυο καταλύτες ένας τροποποιημένος για σύνθεση Fischer–Tropsch (modFT) και ένας τροποποιημένος καταλύτης για σύνθεση μεθανόλης (modMeOH). Η διαδικασία για την παραγωγή των διακλαδισμένων παραφινών, που είναι και το επιθυμητό προϊόν, καθορίζεται κατά πολύ από τη λειτουργία και την απόδοση των εν λόγω καταλυτών.

7.2.1.2 Συμπύκνωση αλκοολών (αντιδράσεις Guerbet)

Στην περίπτωση που γίνεται χρήση του καταλύτη με τροποποιημένο καταλύτη για FT, το κύριο προϊόν είναι αιθανόλη. Σε αυτή την περίπτωση, η αντίδραση που συντελείται για να παραχθεί η N-βουτανόλη [186] είναι η:



Στην περίπτωση του τροποποιημένου καταλύτη που χρησιμοποιείται για σύνθεση μεθανόλης οι παρακάτω αντιδράσεις λαμβάνουν χώρα διαδοχικά για την παραγωγή ισοβουτανόλης [279]:



7.2.1.3 Αφύγρανση αλκοολών προς παραγωγή των ομόλογων αλκενίων

Στις αντιδράσεις αφύγρανσης γίνεται η απομάκρυνση του οξυγόνου από την οργανική ένωση (αλκοόλη) με τη μορφή νερού [281]:



7.2.1.4 Ολιγομερισμός αλκενίων

Η αντίδραση αυτή μπορεί να πραγματοποιηθεί με οποιοδήποτε ισομερές ολεφίνης με C₄. Η αντίδραση που περιγράφει αυτή τη διεργασία είναι η παρακάτω:



7.2.1.5 Υδρογόνωση ολιγομερών

Τέλος, για να μπορεί το παραγόμενο οργανικό προϊόν να χρησιμοποιηθεί σαν καύσιμο μεταφορών απαιτείται η μετατροπή των αλκενίων σε αλκάνια με H₂. Αυτό επιτυγχάνεται παρουσία καταλύτη Pd [294, 295] σε υψηλές πιέσεις (>20 bar) και θερμοκρασία μεταξύ 200 - 350 °C [296]:

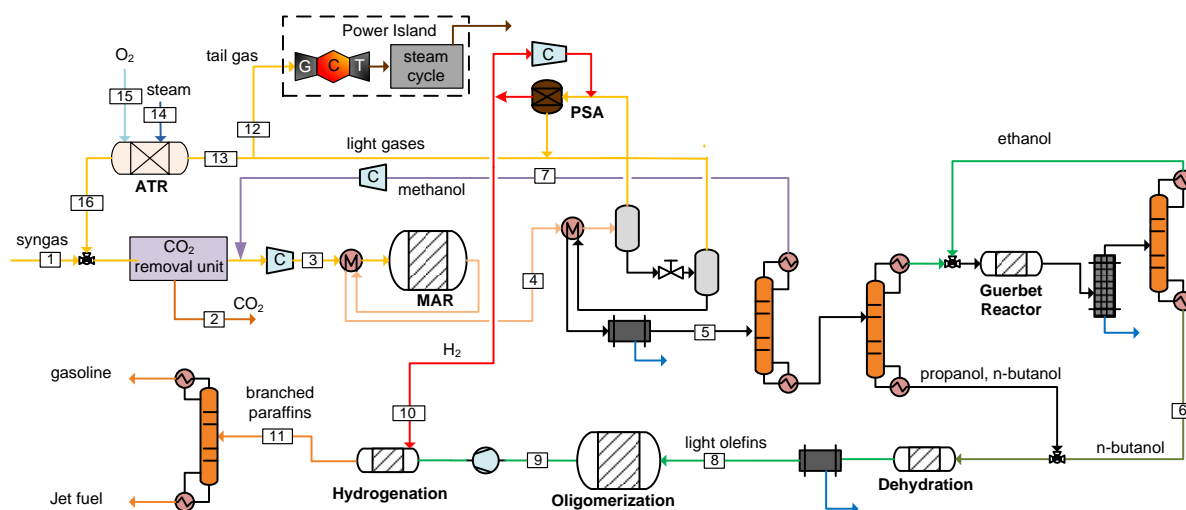


7.3 Περιγραφή της μοντελοποίησης των υπό εξέταση διεργασιών

Οι μοντελοποιήσεις και οι προσομοιώσεις των διεργασιών που εξετάστηκαν πραγματοποιήθηκαν με ASPEN Plus™. Το μοντέλο του βιοδιωλιστηρίου δυναμικότητας 190MW_{th} που αναπτύσσεται βασίζεται σε γενικά αποδεκτές μεθοδολογίες στην επιστήμη της μοντελοποίησης διεργασιών και σε δεδομένα που προκύπτουν από μικρής κλίμακας πειραματικές μελέτες ή πατέντες. Η επιλογή του κατάλληλου πακέτου θερμοφυσικών ιδιοτήτων είναι πολύ σημαντικό σημαντική: για το κομμάτι της παραγωγής και επεξεργασίας του αερίου σύνθεση επιλέγεται η RK-SOAVE, ενώ για την σύνθεση και αναβάθμιση των αλκοολών η NRTL [175]. Δυο κύρια σενάρια εξετάζονται με λεπτομέρεια. Στο πρώτο (περίπτωση 1), η σύνθεση των αλκοολών γίνεται με τροποποιημένο καταλύτη για FT σύνθεση (MAS modFT) [297], ενώ στο δεύτερο σενάριο (περίπτωση 2) ο καταλύτης που χρησιμοποιείται είναι τροποποιημένος για σύνθεση μεθανόλης (MAS modMeOH) [214].

7.3.1 Παραφίνες από μίγμα αλκοολών με τροποποιημένο FT καταλύτη (περίπτωση 1)

Το διάγραμμα ροής αυτού του σεναρίου φαίνεται στην **Εικόνα 133**. Η παραγόμενη αιθανόλη απομονώνεται και οδηγείται για συμπύκνωση παράγοντας N-βουτανόλη, ενώ η παραγόμενη μεθανόλη επιστρέφει στον αντιδραστήρα σύνθεσης αλκοολών. Για τη διεργασία της αφύγρανσης, γίνεται η αυθαίρετη αλλά ασφαλής υπόθεση ότι όλες οι αλκοόλες μετατρέπονται πλήρως στις αντίστοιχες ολεφίνες [301, 302]. Οι δυο πρώτοι αντιδραστήρες αναβάθμισης θεωρούνται ότι είναι εμβολικής ροής γεμισμένο με καταλύτη, ενώ ο ολιγομερισμός και η υδρογόνωση θεωρούνται ότι πραγματοποιούνται σε αντιδραστήρες με ανάμιξη, όπου ο καταλύτης είναι διαλυμένος στην υγρή φάση.



Εικόνα 133. Διάγραμμα ροής της παραγωγής παραφινών από μίγμα αλκοολών που παρήχθησαν με τη χρήση τροποποιημένου καταλύτη FT

7.3.2 Παραφίνες από μίγμα αλκοολών με τροποποιημένο καταλύτη μεθανόλης (περίπτωση 2)

Η λογική αυτής της διεργασίας έχει πολλές ομοιότητες με τη διεργασία της Genovese για παραγωγή τζετ καυσίμου [306] με βάση την ισοβουτανόλη [305]. Το διάγραμμα ροής φαίνεται στην Figure 92. Το μίγμα αλκοολών υπόκειται σε συμπύκνωση για την παραγωγή ισοβουτανόλης. Στη συνέχεια το ρεύμα εισέρχεται σε δυο στήλες διαδοχικά για το διαχωρισμό μεθανόλης/ισοβουτανόλης/ $C_{2-3}OH$. Οι C_{2-3} αλκοόλες που δεν αντέδρασαν επιστρέφουν στον αντιδραστήρα, ενώ η μεθανόλη οδηγείται προς αναμόρφωση και μετατροπή της σε H_2 και CO . Στη συνέχεια, η ισοβουτανόλη υπόκειται σε αφύγρανση για την παραγωγή ισοβουτενίου. Η αύξηση της ανθρακικής αλυσίδας πραγματοποιείται στον επόμενο αντιδραστήρα με την παραγωγή των διμερών, τριμερών και τετραμερών ολιγομερών, τα οποία στη συνέχεια υδρογονώνονται για την παραγωγή του τελικού επιθυμητού προϊόντος.

μεταβαλλόμενο). Για την εκτίμηση των εσόδων από την πώληση των παραγόμενων καυσίμων και των χρηματικών ροών ανά έτος, χρησιμοποιείται το κριτήριο της καθαρής παρούσας αξίας. Το σημείο στο οποίο μηδενίζεται η ΚΠΑ μεταβάλλοντας την τιμή των αεροπορικών καυσίμων, προσδιορίζει την Ελάχιστη Τιμή Πώλησης Καυσίμου Τζετ (ΕΤΠΚΤ), ώστε η επένδυση να είναι κερδοφόρα.

7.5 Αποτελέσματα

7.5.1 Ισοζύγιο μάζας και ενέργειας

Τα βασικά αποτελέσματα των πρωτότυπων διεργασιών συνοψίζονται στον **Πίνακα 96**. Ο θερμικός βαθμός απόδοσης ορίζεται από την παρακάτω σχέση (**Eq. 40**):

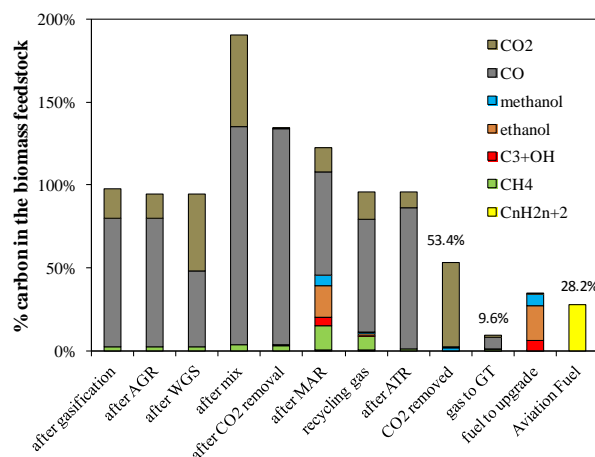
$$\eta_{th} = \frac{m_{Jet\ Fuel} \cdot LHV_{Jet\ Fuel}}{m_{wood} \cdot LHV_{wood}} \quad (\text{Eq. 33})$$

Πίνακας 96. Βασικά αποτελέσματα των θερμοχημικών διεργασιών

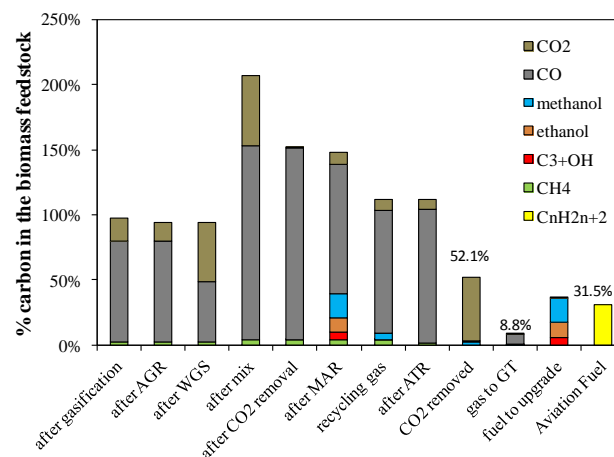
σενάριο	1	2	3
μέθοδος σύνθεσης καυσίμου	ΣΜΑ με modFT	ΣΜΑ με modMeOH	FT
ειδική παραγωγή καυσίμου τζετ, kg _{JF} /kg _{wood}	0.112	0.138	0.097
ειδική παραγωγή αεροπορικής βενζίνης, kg _G /kg _{wood}	0.042	0.034	0.076
συνολική ειδική παραγωγή καυσίμων, kg _F /kg _{wood}	0.154	0.172	0.173
θερμικός βαθμός απόδοσης, % LHV	37.2 %	40.5 %	24.2/16.2 ¹
ενεργειακές καταναλώσεις στη ΜΔΑ, kJ _e /kg _{wood}	677.8	653.7	534.1
ενεργειακές καταναλώσεις για απομάκρυνση H ₂ S/CO ₂ , kJ _e /kg _{wood}	215.2	300.8	237.0
ενεργειακές καταναλώσεις για συμπίεση αερίων, kJ _e /kg _{wood}	836.9	405.8	16.5
συνολικές ενεργειακές καταναλώσεις, kJ _e /kg _{wood}	1730.0	1360.3	787.6
συνολική αξιοποίηση άνθρακα, % C _{feedstock}	28.2 %	31.5 %	30.4%

¹ ο πρώτος όρος αναφέρεται στο καύσιμο τζετ και το δεύτερο στη βενζίνη. Το πετρογκάζ είναι 20 φορές μικρότερο από το καύσιμο τζετ και γι αυτό αμελείται.

Τα κύρια αποτελέσματα από τη θερμοδυναμική ανάλυση αναδεικνύουν μια αρκετά αποδοτική μετατροπή της εισερχόμενης στερεάς βιομάζας σε αεροπορικά καύσιμα μέσω θερμοχημικών διεργασιών. Το 2^ο σενάριο (modMeOH) για σύνθεση μίγματος αλκοολών (ΣΜΑ) έχει ελαφρώς καλύτερη απόδοση από το 1^ο σενάριο. Αυτό κυρίως αποδίδεται α) στην υψηλότερη πίεση λειτουργίας κατά τη ΣΜΑ, η οποία οδηγεί σε υψηλότερες ενεργειακές καταναλώσεις κατά τη συμπίεση και β) στην καλύτερη αξιοποίηση των παραγόμενων αλκοολών στο 2^ο σενάριο. Τα συμπεράσματα αυτά αφορούν τους συγκεκριμένους καταλύτες ΣΜΑ και τις διεργασίες που δομούνται με βάση αυτούς και δε θα πρέπει τα συμπεράσματα αυτά να γενικεύονται για την κατηγορία καταλυτών που αντιπροσωπεύουν.

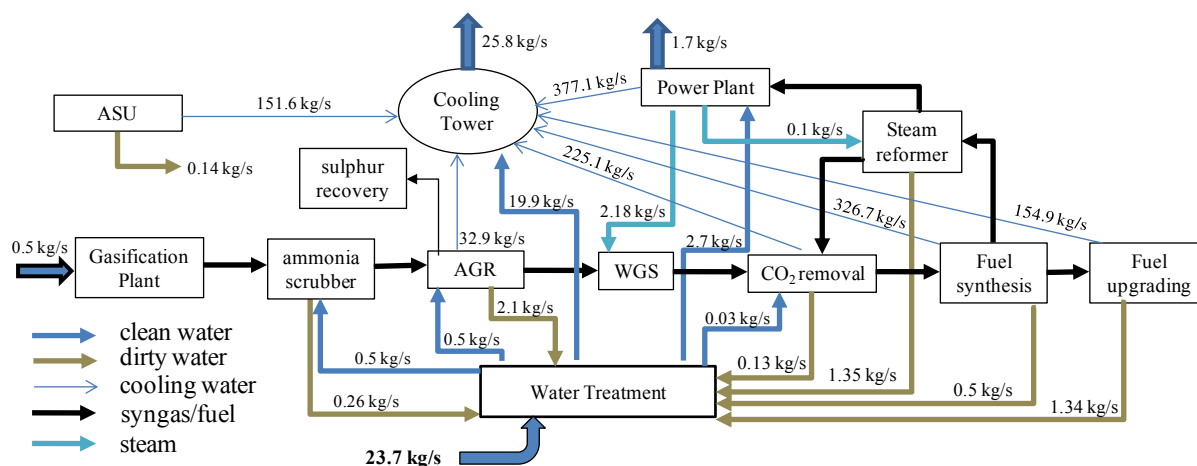


Εικόνα 135a. Ισοζύγιο άνθρακα κατά μήκους της όλης διεργασίας (1^ο σενάριο, modFT)



Εικόνα 27b. Ισοζύγιο άνθρακα κατά μήκους της όλης διεργασίας (1^ο σενάριο, modMeOH)

Αρκετά ενδιαφέροντα συμπεράσματα εξάγονται από την ισορροπία άνθρακα για κάθε σενάριο (**Εικόνα 135a-b**). Η παραγωγικότητα των καυσίμων είναι στενά συνδεδεμένη με την πορεία των ατόμων C κατά μήκος της διεργασίας, σε αντίθεση με τα άτομα H και O, κάποια από τα οποία προέρχονται από το νερό, ο άνθρακας προέρχεται αποκλειστικά από την εισερχόμενη βιομάζα. Περίπου 50% του συνολικού άνθρακα μετατρέπεται σε CO₂. Περίπου το 1/3 του συνολικού άνθρακα εμπεριέχεται στα τελικά προϊόντα της διεργασίας μέσω των θερμοχημικών διαδρομών (**Πίνακας 96**).



Εικόνα 136. Παροχές νερού στο σύστημα (2^ο σενάριο- MAS με modMeOH καταλύτη)

Το ισοζύγιο του νερού με τις βασικές ροές εισόδου και εξόδου στο σύστημα φαίνονται στην **Εικόνα 136**. Οι παροχές νερού για ψυκτικούς λόγους ειδικά στη μονάδα σύνθεσης και αναβάθμισης καυσίμου μπορούν να μειωθούν με τον σχεδιασμό ενός πιο αποδοτικού συστήματος για την ανάκτηση της απορριπτόμενης θερμότητας. Μεγάλα ποσά νερού σε ετήσια βάση απαιτούνται για την ομαλή λειτουργία του βιοδιυλιστηρίου.

7.5.2 Επίδραση της κάλυψης των ηλεκτρικών απαιτήσεων από αυτόνομη παραγωγή

Σε αυτή την παράγραφο, εξετάζεται η πιθανή σύνδεση του συστήματος με το δίκτυο ηλεκτρικής ενέργειας για την κάλυψη μέρους των απαιτούμενων ηλεκτρικών καταναλώσεων. Δυο περιπτώσεις εξετάζονται, το αυτόνομο σύστημα (βασικό σενάριο) και η περίπτωση όπου 60% της απαιτούμενης

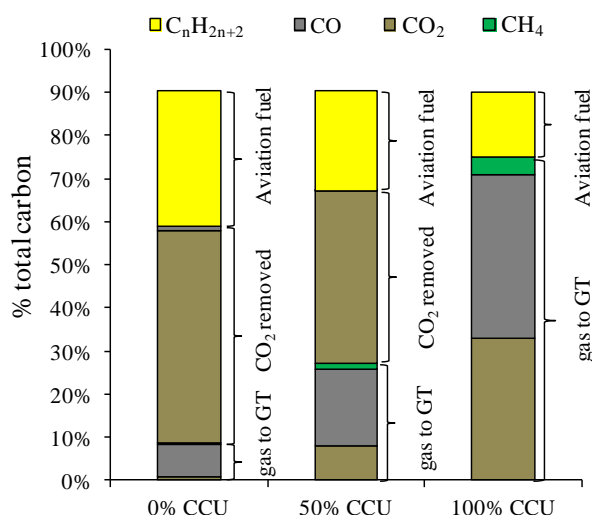
ηλεκτρικής ενέργειας δίδεται από το δίκτυο. Η παροχή ηλεκτρικής ενέργειας έχει θετική επίπτωση στη λειτουργία του όλου συστήματος από θερμοδυναμικής σκοπιάς. Από την άλλη μεριά, η αυτόνομη παραγωγή προσφέρει ανεξαρτησία και βιωσιμότητα, ανεξαρτήτου της τοποθεσίας του βιοδιυλιστηρίου.

7.5.3 Ανακυκλοφορία αερίων στον αεριοποιητή αντί για αναμόρφωση

Μελετήθηκε η εναλλακτική επιλογή της επιστροφής των ανακυκλοφορούντων αερίων στον αεριοποιητή, αντί να υποβληθούν σε αεριοποίηση. Το παραγόμενο αέριο σύνθεσης είναι πάνω από δυο φορές μεγαλύτερο από το 2^ο σενάριο, υπονοώντας σημαντικά υψηλότερο κόστος εξοπλισμού τόσο για τον αεριοποιητή όσο και για τη μονάδα καθαρισμού του αερίου.

7.5.4 Διερεύνηση της πιθανής αξιοποίησης του CO₂

Οι κύριες προδιαγραφές για τη μοντελοποίηση της μονάδας αξιοποίησης του CO₂ (CCU) βασίστηκαν στην πειραματική εργασία των Nieskens et al [164] και τα αποτελέσματα του ισοζυγίου άνθρακα από αυτή τη διερεύνηση συνοψίζονται στην **Εικόνα 137**.



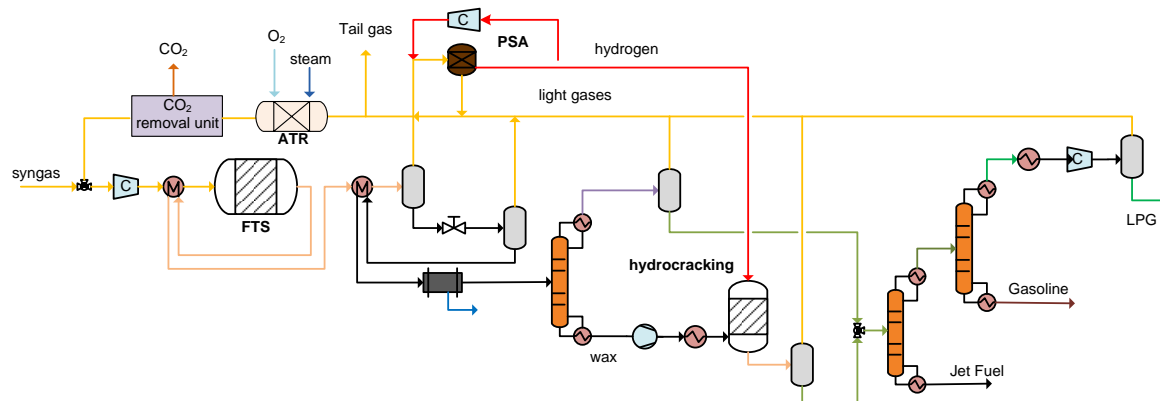
Εικόνα 137. Επίδραση του ποσοστού αξιοποίησης CO₂ στα τρία ρεύματα εξόδου για το 2^ο σενάριο- MAS με modMeOH καταλύτη (το υπόλοιπο CO₂ απελευθερώνεται στη μονάδα καθαρισμού του H₂S)

Ένα μεγάλο ποσό ηλεκτρικής ενέργειας απαιτείται για τη συμπίεση του ρεύματος CO₂/H₂. Έτσι, είναι αναπόφευκτο να οδηγηθεί μεγαλύτερο ποσοστό αερίου στη μονάδα συνδυασμένου κύκλου (“gas to GT”). Έτσι το ποσοστό του άνθρακα που καταλήγει στο τελικό προϊόν (“final fuel”) είναι ελαφρώς μεγαλύτερο στην περίπτωση της μη αξιοποίησης του CO₂. Το ίδιο επίσης φαίνεται και από την αντίστοιχη θερμική απόδοση: 32.5% για 0% CCU, 29.4% για 50% CCU για 27.0% για 100% CCU. Λαμβάνοντας υπόψη ότι επιπλέον εξοπλισμός απαιτείται, η αξιοποίηση CO₂ σε αυτό το ενεργειακό σύστημα δεν εγκρίνεται.

7.5.5 Σύγκριση με τη διεργασία σύνθεσης κατά Fischer-Tropsch

Ένα γενικό σχήμα της σύνθεσης καυσίμου μέσω Fischer-Tropsch σε συνδυασμό με το κατάλληλο σχήμα για την αναβάθμιση του καυσίμου εικονίζεται στην **Εικόνα 138**. Η σύνθεση γίνεται στους 250°C στα 25 bar και με λόγο H₂/CO=1.0. Τα βασικά χαρακτηριστικά της διεργασίας, η μοντελοποίηση της οποίας βασίζεται στην κατανομή Anderson-Schulz-Flory (ASF) [314, 315] υιοθετήθηκαν από την εργασία των Spyraakis et al.[223]. Η σύσταση των προϊόντων που βγαίνουν από τη μονάδα υδρογονοδιάσπασης

λήφθηκε από τη μελέτη των Shah et al. [316], ενώ η απαιτούμενη ποσότητα υδρογόνου καθορίζεται από την εργασία των Sudiro και Bertuccio [317].



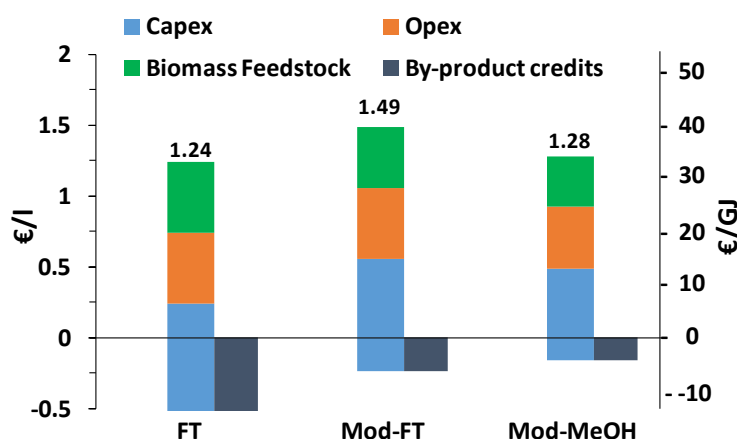
Εικόνα 138. Διάγραμμα ρής για σύνθεση FT και διαχωρισμός των προϊόντων

Συγκρίνοντας τα βασικά εξαγόμενα αποτελέσματα για το σενάριο «FT» με τα άλλα δυο πρωτότυπα θερμοχημικά στον **Πίνακας 96** φαίνεται ότι οι διαδρομές μέσω αλκοολών έχουν μεγαλύτερη παραγωγικότητα σε καύσιμο τζετ, μιας και αυτά σχεδιάστηκαν ώστε να αποτελούν το βασικό τελικό προϊόν. Αξίζει να σημειωθεί όμως ότι οι σημαντικά χαμηλές ενεργειακές καταναλώσεις στο FT σενάριο, το οποίο οφείλεται στη χαμηλή πίεση στην οποία γίνεται η σύνθεση καυσίμου αλλά και στα μεγάλα ποσοστά μετατροπής CO, γεγονός που επιτρέπει μικρότερα ποσά αερίου να ανακυκλοφορούν στις μονάδες σύνθεσης και αναβάθμισης καυσίμου.

7.6 Οικονομική Αξιολόγηση

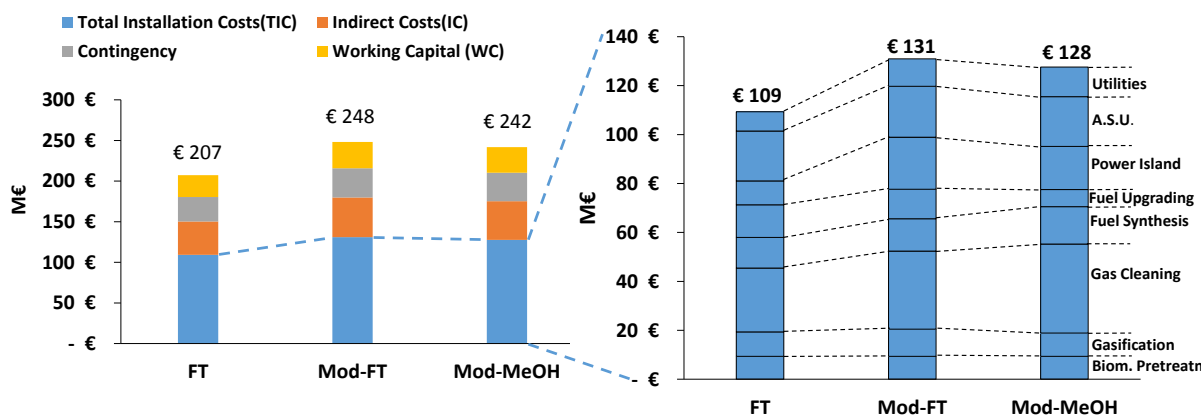
7.6.1 Θερμοχημικά σενάρια με εισαγωγή βιομάζας 10kg/s (ή 864 t/ημέρα)

Η Ελάχιστη Τιμή Πώλησης Καυσίμου Τζετ (ΕΤΠΚΤ) για τα τρία βασικά θερμοχημικά σενάρια (FT, MAS-ModFT and MAS-ModMeOH) είναι 1.24, 1.49 και 1.28 €/l, αντίστοιχα. Στην πρώτη περίπτωση, τα «παραπροϊόντα» όπως το πετρογκάζ (LPG) και η βενζίνη (Gasoline) θεωρούνται ότι διατίθενται προς πώληση με τιμές 2011 0.29 €/l [318] και 0.56 €/l [319], αντίστοιχα. Η τελευταία τιμή χρησιμοποιείται και στις άλλες δυο θερμοχημικές περιπτώσεις.



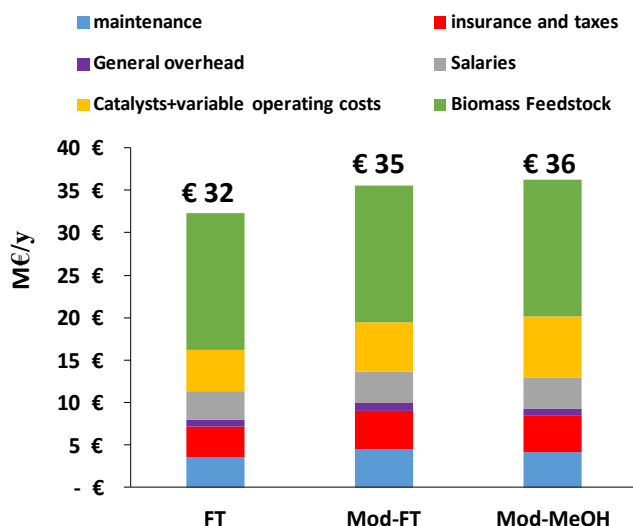
Εικόνα 139. Συνεισφορά στο κόστος παραγωγής καυσίμου τζετ, ΕΤΠΚΤ σε €/l και €/GJ

Η σημαντική επίδραση του κόστους κεφαλαίου (Capex) στο κόστος παραγωγής του καυσίμου τζετ φαίνεται στην **Εικόνα 139** καθώς έχει τη μεγαλύτερη συνεισφορά για όλα τα θερμοχημικά σενάρια. Επιπλέον, το κόστος βιομάζας συμμετέχει σημαντικά στη διαμόρφωση της ΕΤΠΚΤ. Η περίπτωση με την FT σύνθεση δείχνει να είναι το οικονομικά πιο βιώσιμο σενάριο. Αυτό οφείλεται σε δυο λόγους: πρώτον, στο κόστος επένδυσης και δεύτερον, στην παραγωγή μεγάλων ποσοτήτων «παραπροϊόντων» που διατίθενται προς πώληση.



Εικόνα 140. Ανάλυση κόστους του κεφαλαίου επένδυσης (αριστερά) και του κόστους εγκατάστασης (δεξιά)

Το συνολικό κόστος επένδυσης (ΣΚΕ) για κάθε θερμοχημική περίπτωση περιγράφεται στην **Εικόνα 140**. Το σενάριο «Mod-FT» έχει το υψηλότερο ΣΚΕ με 248 Μ€, ενώ το μικρότερο συναντάται στο σενάριο «FT» με 207 Μ€. Η **Εικόνα 140**, επίσης, δείχνει την ανάλυση του κόστους εγκατάστασης για κάθε σενάριο και για κάθε διεργασία/μονάδα. Η πιο κοστοβόρα διεργασία/μονάδα είναι αυτή του καθαρισμού και διαμόρφωσης του αερίου σύνθεσης και στα τρία θερμοχημικά σενάρια. Ακολουθούν η Μονάδα Διαχωρισμού του Αέρα και η Μονάδα Συμπαράγωγής ηλεκτρισμού και θερμότητας. Το γεγονός ότι το «Mod-FT» σενάριο έχει μεγαλύτερο κόστος εξοπλισμού και εγκατάστασης από το σενάριο «Mod-MeOH» αποδίδεται στις υψηλότερες ενεργειακές απαιτήσεις στο πρώτο, το οποίο αποκρυσταλλώνεται στη μεγαλύτερη μονάδα του συνδυασμένου κύκλου.



Εικόνα 141. Ανάλυση Λειτουργικού Κόστους σε Μ€/y

Η ανάλυση του λειτουργικού κόστους (OPEX) για κάθε περίπτωση φαίνεται στην **Εικόνα 141**. Το κόστος πρώτης ύλης (βιομάζα) έχει τη μεγαλύτερη συνεισφορά καθώς αυτή είναι στο 45% του συνολικού λειτουργικού κόστους.

7.6.2 Επίδραση της δυναμικότητας της μονάδας

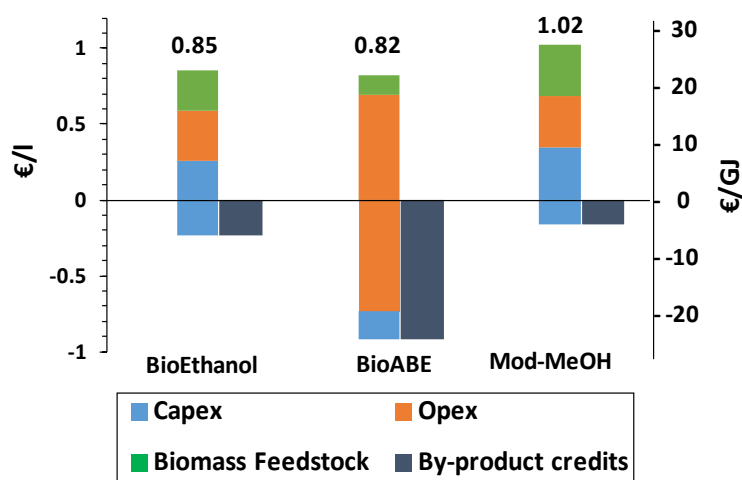
Στον Πίνακα 97 παρουσιάζεται η επίδραση της δυναμικότητας της μονάδας σε διάφορους βασικούς παραμέτρους για ημερήσια εισαγωγή πρώτης ύλης 864 t/d και 2000 t/d.

Πίνακας 97. Επίδραση της δυναμικότητας της μονάδας σε διάφορες παραμέτρους

Παράμετροι	Mod-MeOH 864 t/d	Mod-MeOH 2000 t/d	Σχετική διαφορά, %
Θερμική ισχύς εισερχόμενου καυσίμου, MW_{th}	188.8	437	131
παραγωγή καυσίμου τζετ, kg/s	1.33	3.18	138
Συνολική Επένδυση Κεφαλαίου, Μ€	241.7	450.6	86
Λειτουργικά Κόστη, Μ€/έτος	20.2	37.1	84
Κόστος βιομάζας, Μ€/ έτος	16.1	37.2	131
Κέρδη από πώληση παραπροϊόντων, Μ€/ έτος	7.0	16.6	137
Ελάχιστη Τιμή Πώλησης Καυσίμου Τζετ (ΕΤΠΚΤ), €/l jet fuel	1.28	1.02	-20

7.6.3 Σύγκριση με τις αντίστοιχες Βιοχημικές διαδρομές

Οι υπό εξέταση διεργασίες που βασίζονται σε βιοχημικές διαδρομές βασίστηκαν σε εργασίες από τη βιβλιογραφία [253, 321]. Το ένα σενάριο βασίζεται στην αλκοολική ζύμωση προς παραγωγή αιθανόλης, ενώ η άλλη βασίζεται στην αλκοολική ζύμωση προς παραγωγή Ακετόνης-Βουτανόλης-Αιθανόλης (ABE). Η ανάλυση της περίπτωσης της βιοαιθανόλης που έγινε από τους Humbird et al. [253] έδειξε έναν συνολικό βαθμό απόδοσης 44.0%, με συντελεστή αξιοποίησης άνθρακα 29.4%. Παρόμοια, στην ABE διεργασία, η συνολική απόδοση και 65.8% κάνοντας τη θεώρηση ότι και τα τρία προϊόντα είναι «επιθυμητά» [321]. Η παραγωγή αιθανόλης στην πρώτη διεργασία είναι 0.236 kg_{ethanol}/kg_{feedstock}, ενώ η αντίστοιχη της βουτανόλης στη δεύτερη περίπτωση είναι 0.197 kg_{butanol}/kg_{feedstock}. Το κόστος παραγωγής για την αιθανόλη και την βουτανόλη εκτιμάται στα 0.54 €/kg και 0.78-1.01 €/kg, αντίστοιχα. Για την περίπτωση της βιοαιθανόλης, η συνολική επένδυση κεφαλαίου (ΣΕΚ) εκτιμήθηκε στα 473.83 Μ€ με Λειτουργικά Κόστη στα 69.81 Μ€, ενώ η ΣΕΚ για τη μονάδα αναβάθμισης καυσίμου από αιθανόλη σε καύσιμο τζετ υπολογίστηκε στα 23.445 Μ€. Σχετικά με την ABE ζύμωση, η ΣΕΚ εκτιμήθηκε στα 144.84 Μ€ με Λειτουργικά Κόστη στα 143.74 Μ€, ενώ η ΣΕΚ της μονάδας αναβάθμισης βουτανόλης σε καύσιμο τζετ στα 11.87 Μ€.



Εικόνα 142. ΕΤΠΚΤ σε €/l και €/GJ για βιοχημικές διαδρομές, σε σύγκριση με το σενάριο Mod-MeOH

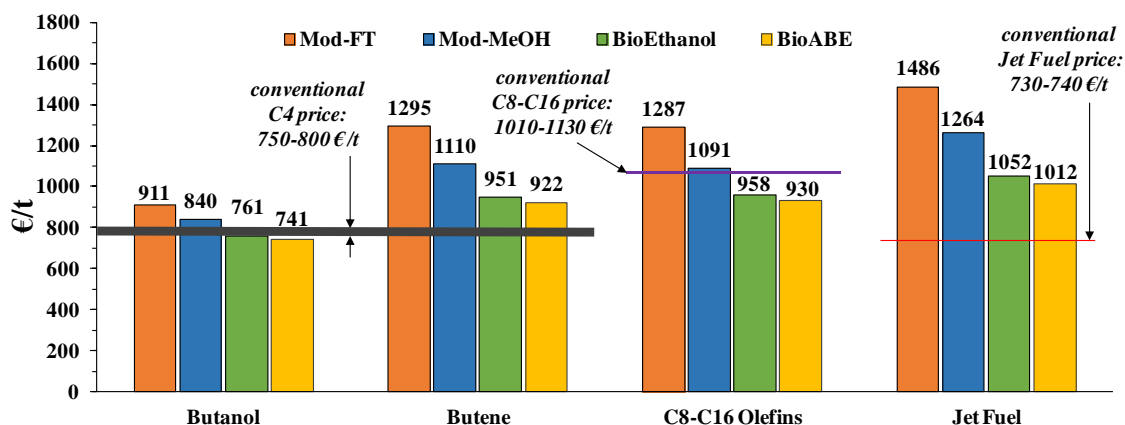
Στην **Εικόνα 142**, δείχνεται η σύγκριση μεταξύ των 2 βιοχημικών με μία θερμοχημική τεχνική (Mod-MeOH). Και οι δυο βιοχημικές είναι οικονομικά πιο προτιμητέες από τη θερμοχημική. Η ABE διεργασία έχει σημαντικά χαμηλότερο κόστος κεφαλαίου από τα άλλα δυο σενάρια, αλλά διπλάσιο λειτουργικό κόστος. Επίσης, έχει αρκετά παραπροϊόντα τα οποία θεωρούνται ότι διατίθενται στην αγορά, καθώς εκτός από την αεροπορική βενζίνη διατίθεται και η ακετόνη σε τιμή 0.78 €/l [321].

7.6.4 Ανάλυση ευαισθησίας

Η επίδραση διαφόρων παραμέτρων στη διαμόρφωση της Ελάχιστης Τιμής Πώλησης Καυσίμου Τζέτ (ΕΤΠΚΤ) διερευνάται σε αυτή την παράγραφο. Η παράμετρος που έχει τη μεγαλύτερη επίδραση είναι το μέγεθος του βιοδιυλιστηρίου καθώς η ΕΤΠΚΤ μειώνεται κατά 20%, όταν η δυναμικότητα του συστήματος αυξάνεται από 864 σε 2000 t/day. Μια άλλη με μεγάλη επιρροή στη βιωσιμότητα της επένδυσης είναι το κόστος βιομάζας. Σύμφωνα με τους Peters and Timmerhaus [129], η μέθοδος που εφαρμόζεται για τον υπολογισμό του συνολικού κόστους επένδυσης (ΣΚΕ) έχει $\pm 30\%$ ακρίβεια. Με 30% μείωση του ΣΚΕ, η ΕΤΠΚΤ διαμορφώνεται στα 1.03 €/l, 1.27 €/l and 1.10 €/l, για την περίπτωση του FT, Mod-FT και Mod-MeOH, αντίστοιχα, ενώ με αύξηση κατά 30% του ΣΚΕ οι ΕΤΠΚΤ είναι 1.45 €/l, 1.71 €/l και 1.46 €/l. Η μεταβολή της ΕΤΠΚΤ στα βιοχημικά σενάρια είναι μεταξύ 0.73 - 0.97 €/l για την περίπτωση της Βιοαιθανόλης και 0.78 - 0.86 €/l για την περίπτωση της Βιοβουτανόλης.

7.6.5 Ορίζοντας τις ενδιάμεσες οργανικές ενώσεις ως τελικά προϊόντα

Το προτεινόμενο σχήμα παραγωγής καυσίμου τζετ από αλκοόλες περιλαμβάνει την παραγωγή διάφορων ενδιάμεσων πολύτιμων οργανικών ενώσεων, όπως ολεφίνες και ανώτερες αλκοόλες. Στην υποενότητα αυτή διερευνάται η περίπτωση της απομόνωσης των ενδιάμεσων αυτών ενώσεων και η θεώρησή τους ως τελικά «επιθυμητά» προϊόντα. Για την κάθε μια περίπτωση, λαμβάνονται υπόψη διάφορες τροποποιήσεις στη διεργασία (προσθαφαίρεση εξοπλισμού, και λοιπές τροποποιήσεις στη λειτουργία του όλου συστήματος), έτσι ώστε να λειτουργεί κατά το βέλτιστο τρόπο.



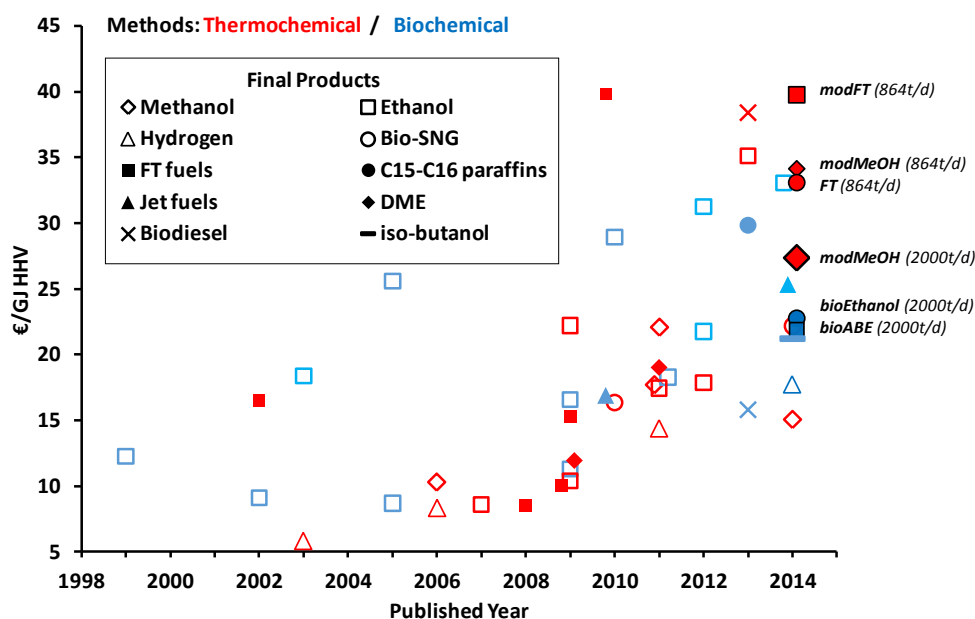
Εικόνα 143. Ειδικές τιμές (€/t) των ενδιάμεσων οργανικών ενώσεων που παράγονται από αλκοόλες (2000 t/d) και σύγκριση με τις αντίστοιχες συμβατικές τιμές

Όπως προκύπτει από την **Εικόνα 143**, η παραγωγή υψηλής αξίας οργανικών ενώσεων με το προτεινόμενο σχήμα διεργασιών είναι μια πολλά υποσχόμενη επιλογή, καθώς οι τιμές των προϊόντων που προκύπτουν είναι αρκετά κοντά στις αντίστοιχες συμβατικές τιμές των προϊόντων που προέρχονται από το πετρέλαιο. Ειδικότερα, οι βιοχημικές διαδρομές είναι εν δυνάμει ανταγωνιστικές με τις συμβατικές τιμές. Επιπλέον περισσότερο κίνητρο απαιτείται για τη βελτίωση των θερμοχημικών διαδρομών στο εγγύς μέλλον, μιας και δείχνουν αρκετά ανταγωνιστικές στην περίπτωση της παραγωγής ολεφινών και C4 ισομερών.

7.7 Συμπεράσματα

Η **Εικόνα 144** παρουσιάζει την αξία διαφόρων βιοκαυσίμων από επιλεγμένες μελέτες, εκφρασμένη σε €/GJ, ώστε η σύγκριση να γίνεται επί ίσοις όροις. Είναι χαρακτηριστική η αύξηση της εκτιμώμενης τιμής όσο περνάνε τα χρόνια, επειδή γίνονται πιο ακριβείς εκτιμήσεις που οδηγούν σε υψηλότερες τιμές καυσίμων, παρά τις τεχνολογικές εξελίξεις που εμφανίζονται αποδοτικότερες τεχνικές παραγωγής για κάθε περίπτωση. Επίσης, η τιμή της πρώτης ύλης της βιομάζας συνεχώς αυξάνεται, μεγαλώνοντας τη συνεισφορά της στο κόστος προϊόντος.

Σε αυτό το κεφάλαιο παρουσιάζεται και εξετάζεται ένα πρωτότυπο σχέδιο για την παραγωγή αεροπορικών βιοκαυσίμων – κυρίως καύσιμο τζετ – μέσω θερμοχημικών διεργασιών. Τα αποτελέσματα των προσομοιώσεων έδειξαν αρκετά υψηλή απόδοση και στις δυο προτεινόμενες θερμοχημικές διαδρομές, επιτυγχάνοντας παραγωγικότητα έως και $0.138 \text{ kg}_F/\text{kg}_{\text{πρώτη ύλη}}$. Μόνο το 1/3 του συνολικού άνθρακα της εισερχόμενης βιομάζας συναντάται στο τελικό προϊόν εξαιτίας της παραγωγής CO_2 σε διάφορες επιμέρους διεργασίες, όπως στην αεριοποίηση, στην αντίδραση μετατόπισης για τη ρύθμιση του λόγου H_2/CO , στη σύνθεση των αλκοολών και στην καύση των απαερίων. Συγκρίνοντάς τες με την τεχνολογία Fischer-Tropsch, αποδεικνύεται ότι οι προτεινόμενες διεργασίες μπορούν να πετύχουν μεγαλύτερη ειδική παραγωγή σε καύσιμο τζετ και καλύτερη αξιοποίηση του άνθρακα, παρά τις υψηλότερες ενεργειακές απαιτήσεις. Η αξιοποίηση και επαναχρησιμοποίηση του διοξειδίου του άνθρακα μέσω καταλυτικής υδρογόνωσης δεν βελτιώνει την απόδοση του συστήματος λόγω των πολύ υψηλών ενεργειακών απαιτήσεων.



Εικόνα 144. Ειδικές τιμές προϊόντων σε €/GJ ΑΘΙ από επιλεγμένες εργασίες/μελέτες στη βιβλιογραφία (με γεμιστό χρώμα και μαύρο περίγραμμα οι τιμές των αντίστοιχων προϊόντων που προέκυψαν από αυτή τη μελέτη) [200, 250, 253, 266-272, 307, 309, 310, 322, 326-347]

Το ισοζύγιο νερού στο προτεινόμενο βιοδιωλιστήριο δείχνει ότι μεγάλες ποσότητες φρέσκου νερού απαιτούνται για την ομαλή λειτουργία του. Χαρακτηριστικά, για ένα σύστημα με δυναμικότητα $190 \text{ MW}_{\text{th}}$, 23.7 kg/s παροχή νερού απαιτείται για να αναπληρωθεί το νερό που απελευθερώνεται στον πύργο ψύξης και στην καμινάδα, αναδεικνύοντας τη διαχείριση του νερού ως ένα σημαντικό ζήτημα με περιβαλλοντικές προεκτάσεις.

Η οικονομική αξιολόγηση έδειξε ότι όλα τα υπό εξέταση σενάρια είναι μακριά από την εμπορική τους εκμετάλλευση και την επικράτησή τους έναντι του συμβατικού καυσίμου τζετ, κυρίως λόγω του

υψηλού κόστους βιομάζας και του υψηλού κόστους επένδυσης. Μελλοντικές βελτιώσεις στην απόδοση των καταλυτών, κυρίως στην επιλεκτικότητα των ανώτερων αλκοολών έναντι των ελαφρών υδρογονανθράκων, θα συμβάλλει στη μείωση του ρεύματος που ανακυκλοφορεί, οδηγώντας σε μειωμένο μέγεθος και κόστος εξοπλισμού. Επίσης, προτείνεται να δοθεί έμφαση στην ανάπτυξη νέων τεχνικών απομάκρυνσης των ανεπιθύμητων συστατικών, καθώς οι πιο ώριμες τεχνολογίες καθιστούν το σύστημα καθαρισμού του αερίου σύνθεσης το πιο ακριβό υποσύστημα του βιοδιωλιστηρίου.

Η βιοχημική διεργασία που βασίζεται στην αλκοολική ζύμωση προς παραγωγή Ακετόνης, Βουτανόλης και αιθανόλης αποδεικνύεται η πιο προτιμητέα επιλογή, παρά το υψηλό λειτουργικό της κόστος. Η αξιοποίηση των ενδιαμέσων οργανικών προϊόντων που παράγονται (ολεφίνες, ανώτερες αλκοόλες κτλ) στις διεργασίες, που έχουν ως βάση τις αλκοόλες, μπορεί να αποτελέσει μια υποσχόμενη επιλογή για την βιωσιμότητα τέτοιων ενεργειακών συστημάτων.

8. Συμπεράσματα – προτάσεις για μελλοντική εργασία

8.1 Καινοτόμα στοιχεία

Τα στοιχεία πρωτοτυπίας που έχει η εν λόγω διατριβή που εξετάστηκαν και αποτελούν συνοψίζονται παρακάτω:

- Ολοκληρωμένος σχεδιασμός, μοντελοποίηση και βελτιστοποίηση ενός συνδυασμένου κύκλου φυσικού αερίου όπου γίνεται χρήση μεμβρανών παλλαδίου για προ-καύσης δέσμευση CO₂.
- Ανάπτυξη και εξέταση διαφόρων πρωτότυπων σχημάτων για αποδοτικό καθαρισμό του τελικού ρεύματος CO₂ του προηγούμενου ενεργειακού συστήματος.
- Ολοκληρωμένος σχεδιασμός και διερεύνηση άλλων τεχνικών δέσμευσης CO₂ που δεν έχουν εφαρμοστεί ξανά σε σταθμούς ηλεκτροπαραγωγής που έχουν ως καύσιμο το φυσικό αέριο (CO₂ selective membranes, RectisolTM, SelexolTM, hot potassium).
- Εξεργειακή ανάλυση και σύγκριση των τριών πιο διαδεδομένων τεχνικών δέσμευσης από λιθανθρακική μονάδα ηλεκτροπαραγωγής, λαμβάνοντας υπόψη την ποιότητα του τελικού ρεύματος CO₂ όσον αφορά την καταλληλότητά του για μεταφορά και αποθήκευση, περιλαμβάνοντας το κατάλληλο σύστημα καθαρισμού.
- Προσδιορισμό των προϋποθέσεων και προοπτικών για τη βιώσιμη και εμπορική λειτουργία της ιδέας του “Power to Fuel” στο μέλλον
- Ανάπτυξη πρωτότυπης διάταξης για την παραγωγή αιθανόλης με πρώτη ύλη CO₂ και H₂ μέσω διμεθυλαιθέρα (DME).
- Σχεδιασμός, βελτιστοποίηση και οικονομική αξιολόγηση πρωτότυπου συστήματος για την παραγωγή αεροπορικών βιοκαυσίμων μέσω σύνθεσης ανώτερων αλκοολών. Σύγκριση του τύπου καταλύτη για τη σύνθεση μίγματος αλκοολών.
- Θερμοδυναμική ανάλυση για την πλήρη αξιοποίηση του άνθρακα σε ένα βιοδιυλιστήριο
- Σύγκριση θερμοχημικών και βιοχημικών διεργασιών για αναβαθμισμένης ποιότητας βιοκαύσιμα.

8.2 Βασικά συμπεράσματα

Αυτή η διδακτορική διατριβή επικεντρώθηκε στην ανάπτυξη και διερεύνηση προηγμένων ενεργειακών συστημάτων η λειτουργία των οποίων έχει ελαχιστοποιημένες έως μηδαμινές εκπομπές αερίων του Θερμοκηπίου. Τα συστήματα αυτά φιλοδοξούν να συμβάλλουν στην ανάπτυξη ενός συνολικού ενεργειακού συστήματος με μειωμένες εκπομπές άνθρακα. Όπως αναφέρθηκε και στην Εισαγωγή, οι βασικές περιοχές στις οποίες εδράζεται αυτή η ανάλυση είναι τρεις: η Δέσμευση και Αποθήκευση Διοξειδίου του Άνθρακα, Δέσμευση και Επαναχρησιμοποίηση Διοξειδίου του Άνθρακα και η Αξιοποίηση της Βιομάζας για την παραγωγή αναβαθμισμένης ποιότητας προϊόντων και καυσίμων.

1. Δέσμευση και Αποθήκευση Διοξειδίου του Άνθρακα

Στον τομέα της μείωσης των εκπομπών CO₂ από θερμικούς σταθμούς που λειτουργούν με φυσικό αέριο, εξετάστηκε διεξοδικά η εφαρμογή της τεχνολογίας των μεμβρανών παλλαδίου. Οι άριστες επιδόσεις τους στο διαχωρισμό H₂ και CO₂ δίνει τη δυνατότητα για επίτευξη έως και 100% δέσμευση CO₂. Η ανάλυση ευαισθησίας διαφόρων παραμέτρων λειτουργίας και η διαμόρφωση της βέλτιστης διάταξης, ώστε η συνολική μονάδα να λειτουργεί αποδοτικά, συνετέλεσαν στη βελτιστοποίηση του όλου συστήματος, επιτυγχάνοντας καθαρό βαθμό απόδοσης 50.82% ή 7.48% μειωμένη απόδοση σε σχέση με την περίπτωση αναφοράς (χωρίς δέσμευση CO₂). Από την αξιολόγηση των υπό εξέταση σχημάτων καθαρισμού CO₂ προέκυψε ότι η καλύτερη επιλογή είναι η καύση των υπολειμμάτων

καυσίμων στοιχείων με καθαρό οξυγόνο υπό στοιχειομετρικές συνθήκες, τόσο από πλευράς απόδοσης όσο και από οικονομικής σκοπιάς. Όμως τα κρυογονικά σχήματα επιτυγχάνουν πολύ καλό καθαρισμό και μπορούν κάλλιστα να εφαρμοστούν στην περίπτωση που το καθαρό υδρογόνο αποτελεί το τελικό προϊόν. Από τη σύγκριση των αποτελεσμάτων προσομοίωσης διαφόρων τεχνολογιών δέσμευσης διαπιστώθηκε ότι οι μεμβράνες παλλαδίου προσφέρουν την υψηλότερη απόδοση. Τα υψηλά επίπεδα δέσμευσης CO₂ σε συνδυασμό με τις χαμηλές καταναλώσεις για τη συμπίεση CO₂ συνεισφέρουν στο χαμηλότερο δείκτη SPECCA για περιπτώσεις με Φ.Α. (2.91 MJ/kg_{CO2}). Η οικονομική ανάλυση έδειξε ότι το υψηλό τρέχον κόστος των μεμβρανών επιδρά αρνητικά στο κόστος του αποφυγόντος CO₂. Η μείωσης της απαιτούμενης επιφάνειας μεμβρανών μέσω της αύξησης της διαφοράς πίεσης μεταξύ των δυο πλευρών μειώνει σημαντικά το κόστος ηλεκτρισμού και συνεπώς το κόστος του αποφυγόντος CO₂. Μελλοντικές βελτιώσεις στη λειτουργία και στο κόστος των μεμβρανών εκτιμάται πως θα συμβάλλουν θετικά στο να γίνουν οι μεμβράνες οικονομικά πιο ανταγωνιστικές στην αγορά στο μέλλον.

Όσον αφορά στην εφαρμογή συστήματος δέσμευσης CO₂ σε λιθανθρακικές μονάδες, έγινε η θερμοδυναμική ανάλυση και σύγκριση από εξεργειακής σκοπιάς τριών από τις πιο διαδεδομένες τεχνικές δέσμευσης: έκπλυση με αμίνες, κύκλος ασβεστίου και καύση με καθαρό οξυγόνο. Η δεύτερη τεχνολογία (κύκλος ασβεστίου) αποδείχθηκε η καλύτερη επιλογή σε σχέση με τις άλλες καθώς παρουσίασε τον υψηλότερο ενεργειακό και εξεργειακό βαθμό απόδοσης. Αν και ένα σημαντικό ποσό εξέργειας (22.3% της συνολικής E_{fuel}) χάνεται στη μονάδα του κύκλου ασβεστοποίησης-ενανθράκωσης, ο συνολικός σταθμός έχει τις λιγότερες εξεργειακές απώλειες (-9.0%). Σχεδόν το μισό εισερχόμενο καύσιμο δεν καίγεται στο θάλαμο καύσης όπου οι ειδικές εξεργειακές απώλειες είναι περισσότερες. Το γεγονός ότι η αναγέννηση των στερεών CaO στον ασβεστοποιητή με παράλληλη καύση με καθαρό οξυγόνο είναι πιο αποδοτική από εξεργειακής σκοπιάς από ότι ο λέβητας, είναι ο κύριος λόγος που εξηγεί, γιατί συμβαίνει και έχουμε λιγότερες συνολικές εξεργειακές απώλειες στην εν λόγω περίπτωση. Από την ανάλυση ευαισθησίας, συμπεραίνεται ότι μικροί ρυθμοί εισαγωγής φρέσκου ασβεστόλιθου έχουν μικρή θετική συνεισφορά στο β.α. του σταθμού, αλλά και στη λειτουργία της μονάδας δέσμευσης. Καύσιμα χαμηλής περιεκτικότητας σε θείο προτείνονται για χρήση στον ασβεστοποιητή κατά την αναγέννηση των στερεών ασβεστίου. Στην περίπτωση των αμινών (MEA), 7.7% της εξέργειας χάνεται στη μονάδα δέσμευσης και 1% κατά τη συμπίεση του διοξειδίου του άνθρακα. Μεγάλοι λόγοι MEA/CO₂ και υψηλές συγκεντρώσεις MEA στο φτωχό σε CO₂ ρεύμα διαλύματος ευνοούν την αποδοτικότητα της διεργασίας. Στην περίπτωση της καύσης με καθαρό οξυγόνο, η Μονάδα Διαχωρισμού Αέρα είναι η κύρια μονάδα στην οποία παρατηρείται η πλειοψηφία των εξεργειακών απωλειών (647.8 kJ/kg_{CO2}). Μια πιθανή ανάπτυξη της τεχνολογίας μεμβρανών που είναι επιλεκτικές στο οξυγόνο, με ελάχιστες ή μηδενικές ενεργειακές καταναλώσεις θα συνεισέφερε στην εξοικονόμηση πάνω από 9% της συνολικής εξέργειας που εισέρχεται στο σύστημα.

II. Δέσμευση CO₂ και επαναχρησιμοποίηση

Σχετικά με την εναλλακτική επιλογή της διαχείρισης και χρήσης του δεσμευόμενου διοξειδίου του άνθρακα προερχόμενο από ορυκτά καύσιμα, διερευνήθηκαν οι σχεδιαστικές και λειτουργικές παράμετροι ενός συστήματος παραγωγής καυσίμου από CO₂ και H₂ και καθορίστηκαν αυτοί που επηρεάζουν κυρίως τη βιωσιμότητα ενός τέτοιου συστήματος. Προέκυψε ότι η χρήση φτηνής ηλεκτρικής ενέργειας σε συνδυασμό με έναν υψηλό συντελεστή λειτουργίας πρέπει να επιδιώκονται για την ελαχιστοποίηση του κόστους παραγωγής του υδρογόνου. Καθένας από τους τρεις βασικούς παράγοντες για τον καθορισμό του κόστους του H₂ (κόστος κεφαλαίου ηλεκτρολύτη, κόστος απαιτούμενης ηλεκτρικής ενέργειας και κόστος αποθήκευσης) μπορεί να παίζει ρυθμιστικό ρόλο στη βιωσιμότητα του έργου, ανάλογα με το εκάστοτε σχήμα-πλαίσιο λειτουργίας. Επιπλέον, ένα τέτοιο σύστημα συνδεδεμένο με ένα θερμικό σταθμό κρίνεται ως μια ενδιαφέρουσα επιλογή για την διαχείριση και εκμετάλλευση της παραγόμενης ηλεκτρικής ενέργειας, όταν δεν είναι οικονομικά

επικερδές να πωληθεί στο δίκτυο. Μιας και το κόστος παραγωγής της μεθανόλης από CO₂ είναι περίπου 2μιας φορές υψηλότερο από τη συμβατική τιμή, διαπιστώνεται ότι πρέπει να καταβληθεί σημαντική προσπάθεια για να φτάσει σε ένα ανταγωνιστικό επίπεδο στην αγορά. Παράμετροι-κλειδιά για να γίνει αυτό είναι:

- η ελαχιστοποίηση των ενεργειακών καταναλώσεων ειδικά για την παραγωγή του απαιτούμενου υδρογόνου
- η θέση που έχουν τα επιμέρους υποσυστήματα μεταξύ τους και το κόστος διάθεσης και μεταφοράς των πρώτων υλών στη μονάδα παραγωγής της μεθανόλης
- η μείωση του κόστους επένδυσης του ηλεκτρολύτη μιας και καταλαμβάνει τα 2/3 του συνολικού κόστους επένδυσης
- η εμπορική αξιοποίηση του παραγόμενου οξυγόνου (έως και 10% μείωση στο κόστος παραγωγής της μεθανόλης)

Όσον αφορά τη βελτίωση των συστημάτων μετατροπής CO₂ και H₂ σε ανώτερα καύσιμα, εξετάστηκαν δυο πρωτότυπα σχήματα/διεργασίες: ένα για παραγωγή μεθανόλης και ένα για παραγωγή αιθανόλης. Στην πρώτη περίπτωση εξετάστηκε και προσομοιώθηκε ένα νέο σχήμα βασισμένο σε αντιδραστήρα σύνθεσης της μεθανόλης με μεμβράνες με υψηλή διαπερατότητα είτε στη μεθανόλη (οργανοφιλικές) ή στο νερό (υδροφιλικές). Οι υπολογισμοί έδειξαν ότι η απομάκρυνση της μεθανόλης από την περιοχή σύνθεσής της συμβάλλει θετικά στην αύξηση της παραγωγής αυτής, ενώ έχει μικρές απαιτήσεις όσον αφορά στο μέγεθος του αντιδραστήρα. Στη δεύτερη περίπτωση, το πρωτότυπο σχήμα παραγωγής αιθανόλης μέσω DME έχει μεγαλύτερη απόδοση (70.3% στη βάση ΚΘΙ τη στιγμή που η αντίστοιχη απόδοση του «συμβατικού» σχήματος είναι 63.2%), επειδή έχει λιγότερες θερμικές και ενεργειακές καταναλώσεις. Από την οικονομική ανάλυσηδείχθηκε ότι το πρωτότυπο σχήμα που προτείνεται οδηγεί σε μείωση του κόστους παραγωγής της αιθανόλης κατά 18%.

III. Αξιοποίηση βιομάζας για την παραγωγή αναβαθμισμένων καυσίμων/χημικών

Στο μέρος που εξετάζεται η αξιοποίηση της βιομάζας για την υποκατάσταση των συμβατικών καυσίμων, η όλη ανάλυση βασίζεται σε ένα βιοδιυλιστήριο το οποίο μοντελοποιείται και μελετάται λεπτομερώς για να διερευνηθούν όλες οι σχεδιαστικές και λειτουργικές παράμετροι, οι οποίες επηρεάζουν τις επιδόσεις του εργοστασίου. Η περίπτωση που μελετήθηκε ήταν αυτή της παραγωγής ανώτερων αλκοολών μέσω θερμοχημικών διεργασιών. Από τη μεθοδολογία που ακολουθήθηκε για το σχεδιασμό του όλου συστήματος, φάνηκε ότι ο τύπος του καταλύτη καθορίζει την όλη διάταξη τόσο στο κομμάτι του καθαρισμού και της απομόνωσης των τελικών προϊόντων όσο και της ανακυκλοφορίας των αερίων που δεν αντέδρασαν. Παράλληλα, επειδή το σημείο βέλτιστης λειτουργίας του καταλύτη καθορίζει τα βασικά λειτουργικά χαρακτηριστικά του συστήματος, η συνολική απόδοση εξαρτάται άμεσα από αυτόν. Στην περίπτωση που η μεθανόλη δεν θεωρείται ως τελικό/επιθυμητό προϊόν, οι καταλύτες με υψηλή επιλεκτικότητα ατόμων άνθρακα σε C₂+ αλκοόλες όπως MoS₂ είναι περισσότερο επιθυμητοί, από άποψη απόδοσης. Το ενεργειακό ισοζύγιο στο σύστημα έδειξε ότι η παραγωγή οξυγόνου και η συμπίεση του αερίου σύνθεσης πριν τον αντιδραστήρα σύνθεσης έχουν τις υψηλότερες καταναλώσεις. Σημαντικό μερίδιο στις καταναλώσεις έχει και το ανακυκλοφορούν αέριο, που είναι άρρηκτα συνδεδεμένο με τον συντελεστή μετατροπής του CO στον αντιδραστήρα σύνθεσης. Τέλος, ένα σημαντικό ποσό ενέργειας σε μορφή έργου ή ατμού απαιτείται για τον καθαρισμό του αερίου σύνθεσης πριν τον αντιδραστήρα σύνθεσης.

Έχοντας ως βάση το βιοδιυλιστήριο που αναπτύχθηκε και μελετήθηκε στο προηγούμενο κεφάλαιο, στο δεύτερο κεφάλαιο της τρίτης ενότητας παρουσιάζεται ένα πρωτότυπο θερμοχημικό σχήμα παραγωγής διακλαδισμένων παραφινών με βάση τις παραγόμενες αλκοόλες για χρήση σε αεροπορικούς κινητήρες. Μαζί με τον αναλυτικό σχεδιασμό του συστήματος αναβάθμισης των αλκοολών σε παραφίνες με

μεγάλο αριθμό ατόμων άνθρακα για δυο διαφορετικούς τύπους καταλυτών παραγωγής μίγματος αλκοολών, παρουσιάζεται και η μεθοδολογία της οικονομικής ανάλυσης και σύγκρισης με ένα σύστημα Fischer-Tropsch (FT) και με δυο συστήματα βασισμένα σε βιοχημικές διεργασίες. Δυο πρωτότυπα σχήματα παρουσιάζονται με διαφορετική αφετηρία μίγματος αλκοολών λόγω διαφορετικού τύπου καταλύτη, αλλά και διαφορετική πορεία έως τη σύνθεση των ανώτερων παραφινών, το ένα με βάση την αιθανόλη, και το άλλο με βάση μίγματος μεθανόλης, αιθανόλης και προπανόλης. Τα αποτελέσματα των προσομοιώσεων έδειξαν υψηλές επιδόσεις και στις δυο διεργασίες, καταλήγοντας σε θερμικό βαθμό απόδοσης έως και 40.5%, αρκετά υψηλότερο από τον αντίστοιχο του συστήματος FT. Το ισοζύγιο νερού έδειξε πως οι ετήσιες ανάγκες για φρέσκο νερό για μια μονάδα με δυναμικό 190 MW_{th} ισοδυναμούν με 641,000 m³, αναδεικνύοντας την ανάγκη για χρηστή διαχείριση του νερού για περιβαλλοντικούς λόγους. Επίσης, οι υπολογισμοί έδειξαν ένα υψηλό βαθμό αξιοποίησης του συνολικού άνθρακα που εμπεριέχεται στην αρχική βιομάζα (έως 30%), κάτι που μεταφράζεται σε περιορισμένες εκπομπές CO₂. Η οικονομική ανάλυση έδειξε ότι η Ελάχιστη Επιτρεπτή Τιμή Πώλησης του καυσίμου Jet σε ένα εργοστάσιο FT είναι μικρότερη (1.24 €/l καυσίμου jet) από αυτή των προτεινόμενων σχημάτων (1.49 €/l και 1.28 €/l). Όμως, η δυνατότητα πώλησης των ενδιάμεσων οργανικών προϊόντων, όπως ελαφρές και βαριές ολεφίνες, ισομερή της βουτανόλης προβάλλεται ως μια πολλά υποσχόμενη επιλογή για την οικονομική βιωσιμότητα της εν λόγω ιδέας. Τέλος, η βιοχημική διεργασία που βασίζεται στην αλκοολική ζύμωση προς παραγωγή Ακετόνη-Βουτανόλη-Αιθανόλη είναι η οικονομικά πιο επιθυμητή επιλογή (0.82 €/l).

8.3 Μελλοντική εργασία

Σε αυτή τη Διατριβή μελετήθηκαν διάφορα προηγμένα ενεργειακά συστήματα και διεργασίες με βάση το εργαλείο της μοντελοποίησης διεργασιών. Αρκετά ζητήματα εγείρονται για περαιτέρω διερεύνηση:

1. Πιθανή χρήση των μεμβρανών παλλαδίου σε άλλες εφαρμογές (πχ βιοδιυλιστήρια)
2. Λεπτομερής μοντελοποίηση αντιδραστηρίων με μεμβράνες παλλαδίου σε διάφορες περιπτώσεις
3. Μοντελοποίηση νέων τεχνικών δέσμευσης όπως *ionic liquids*
4. Δυναμική προσομοίωση ολοκληρωμένων προηγμένων ενεργειακών συστημάτων
5. Μικροβιακή ηλεκτροσύνθεση και σύγκριση με την καταλυτική υδρογόνωση CO₂
6. Ζεστές & ξηρές μέθοδοι καθαρισμού αερίων και η σύνδεσή τους με το υπόλοιπο ενεργειακό σύστημα
7. Ζύμωση με πρώτη ύλη αέριο σύνθεσης και σύγκριση με τα συστήματα που μελετήθηκαν στην διατριβή
8. Ανάλυση Κύκλου Ζωής των ενεργειακών συστημάτων που εξετάστηκαν στην εν λόγω διατριβή

References

- [1] OPEC - World proven crude oil reserves by country.
<http://www.opec.org/library/Annual%20Statistical%20Bulletin/interactive/current/FileZ/XL/T31.HTM>.
- [2] Analysis WE-OpHa. <http://www.wtrg.com/prices.htm>.
- [3] Shafiee S, Topal E. When will fossil fuel reserves be diminished? *Energy Policy*. 2009;37:181-9.
- [4] US Energy Information Administration. International energy outlook, With Projections to 2040. In: Administration USEI, editor. 2013
- [5] Aresta M, Dibenedetto A. Utilisation of CO₂ as a chemical feedstock: opportunities and challenges. *Dalton Transactions*. 2007:2975-92.
- [6] Robinson AB, Robinson NE, Soon W. Environmental Effects of Increased Atmospheric Carbon Dioxide. *The Journal of American Physicians and Surgeons*. 2007;12:79-90.
- [7] Yang H, Xu Z, Fan M, Gupta R, Slimane RB, Bland AE, et al. Progress in carbon dioxide separation and capture: A review. *Journal of Environmental Sciences*. 2008;20:14-27.
- [8] IEA. <http://www.iea.org/statistics/topics/CO2emissions/>.
- [9] European Commission. A Roadmap for moving to a competitive low carbon economy in 2050. 2011. p. 15.
- [10] European Commission. Europe 2020 Targets: climate change and energy.
http://ec.europa.eu/europe2020/europe-2020-in-a-nutshell/targets/index_en.htm
- [11] European Commission. Horizon 2020 Work Programme 2014 – 2015. Secure, clean and efficient energy. 2014. p. 136.
- [12] Kost C, Mayer JN, Thomsen J, Hartmann N, Senkpiel C, Philipps S, et al. Levelized cost of electricity renewable energy technologies. Fraunhofer Institute for Solar Energy Systems; 2013. p. 50.
- [13] Agraniotis M, Koumanakos A, Doukelis A, Karellas S, Kakaras E. Investigation of technical and economic aspects of pre-dried lignite utilisation in a modern lignite power plant towards zero CO₂ emissions. *Energy*. 2012;45:134-41.
- [14] Atsonios K, Panopoulos KD, Doukelis A, Koumanakos AK, Kakaras E, Peters TA, et al. 1 - Introduction to palladium membrane technology. In: Doukelis A, Panopoulos K, Koumanakos A, Kakaras E, editors. *Palladium Membrane Technology for Hydrogen Production, Carbon Capture and Other Applications*: Woodhead Publishing; 2015. p. 1-21.
- [15] Agraniotis M. Substitution of coal by alternative and supporting fuels in pulverised fuel boilers towards reduction of CO₂ emissions [PhD]. Athens: NTUA; 2011.
- [16] IEA. Carbon Capture and Storage roadmap,
https://www.iea.org/publications/freepublications/publication/CCS_roadmap_foldout.pdf. Paris 2010.
- [17] Global CCS Institute. Large Scale CCS Projects.
<http://www.globalccsinstitute.com/projects/large-scale-ccs-projects>
- [18] Hirata T, Nagayasu H, Yonekawa T, Inui M, Kamijo T, Kubota Y, et al. Current Status of MHI CO₂ Capture Plant technology, 500 TPD CCS Demonstration of Test Results and Reliable Technologies Applied to Coal Fired Flue Gas. *Energy Procedia*. 2014;63:6120-8.

References

- [19] Franco F, Anantharaman R, Bolland O, Booth N, van Dorst E, Ekstrom C, et al. D 4.9 European best practice guidelines for assessment of CO₂ capture technologies. Collaborative large-scale integrating project 2011.
- [20] Atsonios K, Panopoulos KD, Doukelis A, Kakaras E. 16 - Review of palladium membrane use in biorefinery operations. In: Doukelis A, Panopoulos K, Koumanakos A, Kakaras E, editors. *Palladium Membrane Technology for Hydrogen Production, Carbon Capture and Other Applications*: Woodhead Publishing; 2015. p. 345-68.
- [21] Koumanakos A. Thermal cycles for fossil fuel fired power plants with integrated CO₂ capture technologies. Athens: National Technical University of Athens; 2009.
- [22] Vorrias I. Advanced CO₂ capture systems. Athens: National Technical University of Athens; 2014.
- [23] Perdikaris N. Development of advanced electricity production systems with biomass. Athens: National Technical University of Athens; 2009.
- [24] Finkenrath M. Cost and Performance of Carbon Dioxide Capture from Power Generation. France: International Energy Agency 2011. p. 51.
- [25] Schaupp D. Economic analysis of the Calcium Looping Process. CALMOD Workshop. Stuttgart 2014.
- [26] European best practice guidelines for assessment of CO₂ capture technologies. CAESAR D 4.9 Report. 2009. http://www.gecos.polimi.it/research/EBTF_best_practice_guide.pdf
- [27] Abbas Z, Mezher T, Abu-Zahra MRM. Evaluation of CO₂ Purification Requirements and the Selection of Processes for Impurities Deep Removal from the CO₂ Product Stream. *Energy Procedia*. 2013;37:2389-96.
- [28] de Visser E, Hendriks C, Barrio M, Mølnvik MJ, de Koeijer G, Liljemark S, et al. Dynamis CO₂ quality recommendations. *International Journal of Greenhouse Gas Control*. 2008;2:478-84.
- [29] Wang J, Ryan D, Anthony EJ, Wigston A, Basava-Reddi L, Wildgust N. The effect of impurities in oxyfuel flue gas on CO₂ storage capacity. *International Journal of Greenhouse Gas Control*. 2012;11:158-62.
- [30] Mikkelsen M, Jorgensen M, Krebs FC. The teraton challenge. A review of fixation and transformation of carbon dioxide. *Energy & Environmental Science*. 2010;3:43-81.
- [31] Markewitz P, Kuckshinrichs W, Leitner W, Linssen J, Zapp P, Bongartz R, et al. Worldwide innovations in the development of carbon capture technologies and the utilization of CO₂. *Energy & Environmental Science*. 2012;5:7281-305.
- [32] Kuuskraa VA, Godec ML, Dipietro P. CO₂ Utilization from “Next Generation” CO₂ Enhanced Oil Recovery Technology. *Energy Procedia*. 2013;37:6854-66.
- [33] Vorrias I, Atsonios K, Nikolopoulos A, Nikolopoulos N, Grammelis P, Kakaras E. Calcium looping for CO₂ capture from a lignite fired power plant. *Fuel*. 2013;113:826-36.
- [34] Yu KMK, Curcic I, Gabriel J, Tsang SCE. Recent Advances in CO₂ Capture and Utilization. *ChemSusChem*. 2008;1:893-9.
- [35] Whipple DT, Kenis PJA. Prospects of CO₂ Utilization via Direct Heterogeneous Electrochemical Reduction. *The Journal of Physical Chemistry Letters*. 2010;1:3451-8.
- [36] Stewart C, Hessami M-A. A study of methods of carbon dioxide capture and sequestration—the sustainability of a photosynthetic bioreactor approach. *Energy Conversion and Management*. 2005;46:403-20.
- [37] Jessop PG, Ikariya T, Noyori R. Homogeneous Hydrogenation of Carbon Dioxide. *Chemical Reviews*. 1995;95:259-72.

- [38] Metz B, Davidson O, De Coninck HC, Loos M, Meyer LA. Intergovernmental Panel on climate change Special report on Carbon Dioxide Capture and Storage. Cambridge, UK and New York, USA2005.
- [39] Sun J, Wang Y. Recent Advances in Catalytic Conversion of Ethanol to Chemicals. *ACS Catalysis*. 2014;4:1078-90.
- [40] Lunde PJ, Kester FL. Carbon Dioxide Methanation on a Ruthenium Catalyst. *Industrial & Engineering Chemistry Process Design and Development*. 1974;13:27-33.
- [41] Buchholz OS, van der Ham AGJ, Veneman R, Brilman DWF, Kersten SRA. Power-to-Gas: Storing Surplus Electrical Energy. A Design Study. *Energy Procedia*. 2014;63:7993-8009.
- [42] Carbon Recycling International. <http://www.cri.is/>.
- [43] Blue Fuel Energy. <http://bluefuelenergy.com/>.
- [44] IEA. Energy Technology Perspectives – Scenarios & Strategies to 2050. Paris: OECD/IEA; 2010.
- [45] Lemonidou A. Biobased Aviation Fuels. Creation of a new value chain from lignocellulosic materials. Tomorrow's biorefineries in Europe. Brussels, Belgium2014.
- [46] Thiruvenkatachari R, Su S, An H, Yu XX. Post combustion CO₂ capture by carbon fibre monolithic adsorbents. *Progress in Energy and Combustion Science*. 2009;35:438-55.
- [47] Olajire AA. CO₂ capture and separation technologies for end-of-pipe applications : A review. *Energy*. 2010;35:2610-28.
- [48] Kanniche M, Gros-Bonnivard R, Jaud P, Valle-Marcos J, Amann J-M, Bouallou C. Pre-combustion, post-combustion and oxy-combustion in thermal power plant for CO₂ capture. *Applied Thermal Engineering*. 2010;30:53-62.
- [49] Nikolopoulos N, Nikolopoulos A, Karampinis E, Grammelis P, Kakaras E. Numerical investigation of the oxy-fuel combustion in large scale boilers adopting the ECO-Scrub technology. *Fuel*. 2011;90:198-214.
- [50] Amann J-MG, Bouallou C. CO₂ capture from power stations running with natural gas (NGCC) and pulverized coal (PC): Assessment of a new chemical solvent based on aqueous solutions of N-methyldiethanolamine + triethylene tetramine. *Energy Procedia*. 2009;1:909-16.
- [51] Ertesvåg IS, Kvamsdal HM, Bolland O. Exergy analysis of a gas-turbine combined-cycle power plant with precombustion CO₂ capture. *Energy*. 2005;30:5-39.
- [52] Manzolini G, Macchi E, Binotti M, Gazzani M. Integration of SEWGS for carbon capture in Natural Gas Combined Cycle. Part B: Reference case comparison. *International Journal of Greenhouse Gas Control*. 2011;5:214-25.
- [53] Nord LO, Anantharaman R, Bolland O. Design and off-design analyses of a pre-combustion CO₂ capture process in a natural gas combined cycle power plant. *International Journal of Greenhouse Gas Control*. 2009;3:385-92.
- [54] Romano MC, Chiesa P, Lozza G. Pre-combustion CO₂ capture from natural gas power plants, with ATR and MDEA processes. *International Journal of Greenhouse Gas Control*. 2010;4:785-97.
- [55] Amann J-M, Kanniche M, Bouallou C. Reforming natural gas for CO₂ pre-combustion capture in combined cycle power plant. *Clean Technologies and Environmental Policy*. 2009;11:67-76.
- [56] Najmi B, Soltanieh M. Process integration of membrane reactor for steam methane reforming for hydrogen separation with CO₂ capture in power production by natural gas combined cycle. *Energy Procedia*. 2009;1:279-86.
- [57] Manzolini G, Vigano F. Co-production of hydrogen and electricity from autothermal reforming of natural gas by means of Pd-Ag membranes. *Energy Procedia*. 2009;1:319-26.

References

- [58] Scholes CA, Smith KH, Kentish SE, Stevens GW. CO₂ capture from pre-combustion processes: Strategies for membrane gas separation. *International Journal of Greenhouse Gas Control*. 2010;4:739-55.
- [59] Kaggerud K, Gjerset M, Mejdell T, Kumakiri I, Bolland O, Bredeesen R. Power production with CO₂ management-integration of high temperature CO₂ selective membranes in power cycles. *Greenhouse Gas Control Technologies 7*. Oxford: Elsevier Science Ltd; 2005. p. 1857-60.
- [60] Phair JW, Donelson R. Developments and Design of Novel (Non-Palladium-Based) Metal Membranes for Hydrogen Separation. *Industrial & Engineering Chemistry Research*. 2006;45:5657-74.
- [61] Brinker CJ, Ward TL, Sehgal R, Raman NK, Hietala SL, Smith DM, et al. Ultramicroporous silica-based supported inorganic membranes. *Journal of Membrane Science*. 1993;77:165-79.
- [62] Jansen KC, Coker EN. Zeolitic membranes. *Current Opinion in Solid State and Materials Science*. 1996;1:65-8.
- [63] Uhlhorn RJR, Zaspalis VT, Keizer K, AJ B. Synthesis of ceramic membranes. Part II: Modification of alumina thin film: reservoir method. *Journal of materials science*. 1992;27:538-52.
- [64] Lu GQ, Diniz da Costa JC, Duke M, Giessler S, Socolow R, Williams RH, et al. Inorganic membranes for hydrogen production and purification: A critical review and perspective. *Journal of Colloid and Interface Science*. 2007;314:589-603.
- [65] Petropoulos J, Paul D, Yampolskii Y. Mechanisms and Theories for Sorption and Diffusion of Gases in Polymers. In: Paul DR, YR Y, editors. *Polymeric Gas Separation Membranes*. Boca Raton, FL, USA: CRC Press; 1994. p. 17-81.
- [66] Ravanchi TM, Kaghazchi T, Kargari A. Application of membrane separation processes in petrochemical industry: a review. *Desalination*. 2009;235:199-244.
- [67] Rezvani S, Huang Y, McIlveen-Wright D, Hewitt N, Mondol JD. Comparative assessment of coal fired IGCC systems with CO₂ capture using physical absorption, membrane reactors and chemical looping. *Fuel*. 2009;88:2463-72.
- [68] Dias JAC, Assaf JM. Autothermal reforming of methane over Ni/ γ -Al₂O₃ catalysts: the enhancement effect of small quantities of noble metals. *Journal of Power Sources*. 2004;130:106-10.
- [69] Ding OL, Chan SH. Autothermal reforming of methane gas: Modelling and experimental validation. *International Journal of Hydrogen Energy*. 2008;33:633-43.
- [70] Pina J, Borio DO. Modeling an simulation of an autothermal reformer. *Latin American applied research*. 2006;36:289-94.
- [71] Chan SH, Wang HM. Thermodynamic analysis of natural-gas fuel processing for fuel cell applications. *International Journal of Hydrogen Energy*. 2000;25:441-9.
- [72] Morud JC. 9 - Simulation of palladium membrane reactors: a simulator developed in the CACHET-II project. In: Doukelis A, Panopoulos K, Koumanakos A, Kakaras E, editors. *Palladium Membrane Technology for Hydrogen Production, Carbon Capture and Other Applications*: Woodhead Publishing; 2015. p. 193-211.
- [73] Sipöcz N, Tobiesen A, Assadi M. Integrated modelling and simulation of a 400 MW NGCC power plant with CO₂ capture. *Energy Procedia*. 2011;4:1941-8.
- [74] Zhang Y, Chen C-C. Thermodynamic Modeling for CO₂ Absorption in Aqueous MDEA Solution with Electrolyte NRTL Model. *Industrial & Engineering Chemistry Research*. 2010;50:163-75.
- [75] Kothandaraman A. Carbon Dioxide Capture by Chemical Absorption: A Solvent Comparison Study [PhD Thesis]2010.

- [76] Rochelle GT, Chen E, Cullinane JT, Hilliard M, Lu J, Oyekan B, et al. CO₂ Capture by Absorption with Potassium Carbonate. Other Information: PBD: 29 Jul 20042004. p. Medium: ED; Size: 52 pages.
- [77] Sun L, Smith R. Rectisol wash process simulation and analysis. *Journal of Cleaner Production*. 2013;39:321-8.
- [78] Larson E, Consonni S, Katofsky R. A Cost-Benefit Assessment of Biomass Gasification Power Generation in the Pulp and Paper Industry. In: Report F, editor.: Princeton University 2003.
- [79] Huang J, Zou J, Ho WSW. Carbon Dioxide Capture Using a CO₂-Selective Facilitated Transport Membrane. *Industrial & Engineering Chemistry Research*. 2008;47:1261-7.
- [80] Dinca C, Badea A. The parameters optimization for a CFBC pilot plant experimental study of post-combustion CO₂ capture by reactive absorption with MEA. *International Journal of Greenhouse Gas Control*. 2013;12:269-79.
- [81] Shimizu T, Hiramata T, Hosoda H, Kitano K, Inagaki M, Tejima K. A Twin Fluid-Bed Reactor for Removal of CO₂ from Combustion Processes. *Chemical Engineering Research and Design*. 1999;77:62-8.
- [82] Hanak DP, Biliyok C, Anthony EJ, Manovic V. Modelling and comparison of calcium looping and chemical solvent scrubbing retrofits for CO₂ capture from coal-fired power plant. *International Journal of Greenhouse Gas Control*. 2015;42:226-36.
- [83] Amrollahi Z, Ertesvåg IS, Bolland O. Thermodynamic analysis on post-combustion CO₂ capture of natural-gas-fired power plant. *International Journal of Greenhouse Gas Control*. 2011;5:422-6.
- [84] Romeo LM, Usón S, Valero A, Escosa JM. Exergy analysis as a tool for the integration of very complex energy systems: The case of carbonation/calcination CO₂ systems in existing coal power plants. *International Journal of Greenhouse Gas Control*. 2010;4:647-54.
- [85] Wang D, Chen S, Xu C, Xiang W. Energy and exergy analysis of a new hydrogen-fueled power plant based on calcium looping process. *International Journal of Hydrogen Energy*. 2013;38:5389-400.
- [86] Fu C, Gundersen T. Techno-economic analysis of CO₂ conditioning processes in a coal based oxy-combustion power plant. *International Journal of Greenhouse Gas Control*. 2012;9:419-27.
- [87] Hagi H, Nemer M, Le Moullec Y, Bouallou C. Pathway for Advanced Architectures of Oxy-pulverized Coal Power Plants: Minimization of the Global System Exergy Losses. *Energy Procedia*. 2013;37:1331-40.
- [88] Xiong J, Zhao H, Zheng C. Exergy Analysis of a 600 MWe Oxy-combustion Pulverized-Coal-Fired Power Plant. *Energy & Fuels*. 2011;25:3854-64.
- [89] Atsonios K, Panopoulos KD, Doukelis A, Koumanakos A, Kakaras E. Exergy analysis of a hydrogen fired combined cycle with natural gas reforming and membrane assisted shift reactors for CO₂ capture. *Energy Conversion and Management*. 2012;60:196-203.
- [90] Nikolopoulos N, Isemin R, Atsonios K, Kourkoumpas D, Kuzmin S, Mikhalev A, et al. Modeling of Wheat Straw Torrefaction as a Preliminary Tool for Process Design. *Waste Biomass Valor*. 2013;4:409-20.
- [91] Aspen Technology I. Aspen Plus User Guide2009.
- [92] Strube R, Manfrida G. CO₂ capture in coal-fired power plants—Impact on plant performance. *International Journal of Greenhouse Gas Control*. 2011;5:710-26.
- [93] Charitos A, Rodríguez N, Hawthorne C, Alonso Mn, Zieba M, Arias B, et al. Experimental Validation of the Calcium Looping CO₂ Capture Process with Two Circulating Fluidized Bed Carbonator Reactors. *Industrial & Engineering Chemistry Research*. 2011;50:9685-95.

References

- [94] Hawthorne C, Trossmann M, Galindo Cifre P, Schuster A, Scheffknecht G. Simulation of the carbonate looping power cycle. *Energy Procedia*. 2009;1:1387-94.
- [95] Kakaras E, Koumanakos A, Doukelis A, Giannakopoulos D, Vorrias I. Oxyfuel boiler design in a lignite-fired power plant. *Fuel*. 2007;86:2144-50.
- [96] Hofbauer G, Beisheim T, Dieter H, Scheffknecht G. Experiences from Oxy-fuel Combustion of Bituminous Coal in a 150 kWth Circulating Fluidized Bed Pilot Facility. *Energy Procedia*. 2014;51:24-30.
- [97] Duan L, Zhao C, Zhou W, Qu C, Chen X. O₂/CO₂ coal combustion characteristics in a 50kWth circulating fluidized bed. *International Journal of Greenhouse Gas Control*. 2011;5:770-6.
- [98] Duan L, Sun H, Zhao C, Zhou W, Chen X. Coal combustion characteristics on an oxy-fuel circulating fluidized bed combustor with warm flue gas recycle. *Fuel*. 2014;127:47-51.
- [99] Jia L, Tan Y, Anthony EJ. Emissions of SO₂ and NO_x during Oxy-Fuel CFB Combustion Tests in a Mini-Circulating Fluidized Bed Combustion Reactor. *Energy & Fuels*. 2009;24:910-5.
- [100] Arias B, Diego ME, Abanades JC, Lorenzo M, Diaz L, Martínez D, et al. Demonstration of steady state CO₂ capture in a 1.7 MWth calcium looping pilot. *International Journal of Greenhouse Gas Control*. 2013;18:237-45.
- [101] Ylätaalo J, Ritvanen J, Tynjälä T, Hyppänen T. Model based scale-up study of the calcium looping process. *Fuel*. 2014;115:329-37.
- [102] Perrin N, Dubettier R, Lockwood F, Tranier J-P, Bourhy-Weber C, Terrien P. Oxycombustion for coal power plants: Advantages, solutions and projects. *Applied Thermal Engineering*. 2015;74:75-82.
- [103] Li H, Hu Y, Ditaranto M, Willson D, Yan J. Optimization of Cryogenic CO₂ Purification for Oxy-coal Combustion. *Energy Procedia*. 2013;37:1341-7.
- [104] Posch S, Haider M. Optimization of CO₂ compression and purification units (CO₂CPU) for CCS power plants. *Fuel*. 2012;101:254-63.
- [105] Hofbauer G, Beisheim T, Zieba M. Oxyfuel combustion of bituminous coal in a 150 kWth CFB test facility. 2nd International Workshop on Oxyfuel FBC Technology 2012.
- [106] Zaleta-Aguilar A, Correas-Uson L, Kubiak-Szyszk J, Sierra-Espinosa FZ. Concept on thermoeconomic evaluation of steam turbines. *Applied Thermal Engineering*. 2007;27:457-66.
- [107] Szargut J, Morris DR, Steward FR. Exergy Analysis of Thermal Chemical and Metallurgical Processes. New York: Hemisphere Publishing; 1988.
- [108] Amrollahi Z, Ertesvåg IS, Bolland O. Optimized process configurations of post-combustion CO₂ capture for natural-gas-fired power plant—Exergy analysis. *International Journal of Greenhouse Gas Control*. 2011;5:1393-405.
- [109] Atsonios K, Grammelis P, Antiohos SK, Nikolopoulos N, Kakaras E. Integration of calcium looping technology in existing cement plant for CO₂ capture: Process modeling and technical considerations. *Fuel*. 2015;153:210-23.
- [110] Anthony EJ. Ca looping technology: current status, developments and future directions. *Greenhouse Gases: Science and Technology*. 2011;1:36-47.
- [111] Gandía LM, Arzamendi G, Diéguez PM. Chapter 1 - Renewable Hydrogen Energy: An Overview. In: Gandía LM, Arzamendi G, Diéguez PM, editors. *Renewable Hydrogen Technologies*. Amsterdam: Elsevier; 2013. p. 1-17.
- [112] Li Z, Luo W, Zhang M, Feng J, Zou Z. Photoelectrochemical cells for solar hydrogen production: current state of promising photoelectrodes, methods to improve their properties, and outlook. *Energy & Environmental Science*. 2013;6:347-70.

- [113] Bak T, Nowotny J, Rekas M, Sorrell CC. Photo-electrochemical hydrogen generation from water using solar energy. Materials-related aspects. *International Journal of Hydrogen Energy*. 2002;27:991-1022.
- [114] Oasmaa A, Czernik S. Fuel Oil Quality of Biomass Pyrolysis Oils-State of the Art for the End Users. *Energy & Fuels*. 1999;13:914-21.
- [115] Goteti AC. Experimental investigation and systems modeling of fractional catalytic pyrolysis of pine: School of Chemical and Biomolecular Engineering; 2010.
- [116] Holladay JD, Hu J, King DL, Wang Y. An overview of hydrogen production technologies. *Catalysis Today*. 2009;139:244-60.
- [117] Mignard D, Sahibzada M, Duthie JM, Whittington HW. Methanol synthesis from flue-gas CO₂ and renewable electricity: a feasibility study. *International Journal of Hydrogen Energy*. 2003;28:455-64.
- [118] Yumurtaci Z, Bilgen E. Hydrogen production from excess power in small hydroelectric installations. *International Journal of Hydrogen Energy*. 2004;29:687-93.
- [119] Varone A, Ferrari M. Power to liquid and power to gas: An option for the German Energiewende. *Renewable and Sustainable Energy Reviews*. 2015;45:207-18.
- [120] Sarrias-Mena R, Fernández-Ramírez LM, García-Vázquez CA, Jurado F. Electrolyzer models for hydrogen production from wind energy systems. *International Journal of Hydrogen Energy*. 2015;40:2927-38.
- [121] Mansilla C, Dautremont S, Shoai Tehrani B, Cotin G, Avril S, Burkhalter E. Reducing the hydrogen production cost by operating alkaline electrolysis as a discontinuous process in the French market context. *International Journal of Hydrogen Energy*. 2011;36:6407-13.
- [122] Van-Dal ÉS, Bouallou C. Design and simulation of a methanol production plant from CO₂ hydrogenation. *Journal of Cleaner Production*. 2013;57:38-45.
- [123] Anicic B, Trop P, Goricanec D. Comparison between two methods of methanol production from carbon dioxide. *Energy*. 2014;77:279-89.
- [124] Pontzen F, Liebner W, Gronemann V, Rothaemel M, Ahlers B. CO₂-based methanol and DME – Efficient technologies for industrial scale production. *Catalysis Today*. 2011;171:242-50.
- [125] Specht M, Bandi A, Baumgart F, Murray CN, Gretz J. Synthesis of methanol from biomass/CO₂ resources. In: Eliasson B, Riemer PWF, Wokaun A, editors. *Greenhouse Gas Control Technologies*. Amsterdam Pergamon; 1999. p. 723.
- [126] Cardenas Barranon DC. Methanol and Hydrogen Production - Energy and Cost Analysis [Master Thesis]. Lulea - Sweden: Lulea University of Technology; 2006.
- [127] Barbato L, Iaquaniello G, Mangiapane A. Reuse of CO₂ to Make Methanol Using Renewable Hydrogen. In: Falco MD, Iaquaniello G, Centi G, editors. *CO₂: A Valuable Source of Carbon*: Springer London; 2013. p. 67-79.
- [128] Graaf GH, Winkelman JGM, Stamhuis EJ, Beenackers AACM. Kinetics of the three phase methanol synthesis. *Chemical Engineering Science*. 1988;43:2161-8.
- [129] Peters MS, Timmerhaus K, D., West RE. *Plant Design and Economics for Chemical Engineers*. 5th ed 2003.
- [130] Eric D. Larson HJ, Fuat E. Celik. *Gasification-Based Fuels and Electricity Production from Biomass, without and with Carbon Capture and Storage*. 2005.
- [131] Kreutz T, Larson E, Liu G, Williams R. *Fischer-Tropsch fuels from coal and biomass*. New Jersey: Princeton Environmental Institute, Princeton University; 2008.
- [132] DOE-NETL. *Cost and performance baselines for fossil energy plants, Volume 1*. DOE; 2007.

References

- [133] Manzolini G, Dijkstra J, Macchi E, Jansen D. Technical Economic Evaluation of a system for electricity production with CO₂ capture using membrane reformer with permeate side combustion. GT2006 ASME Turbo Expo 2006: Power for Land, Sea and Air Barcelona, Spain 2006.
- [134] Atsonios K, Koumanakos A, Panopoulos KD, Doukelis A, Kakaras E. Techno-economic comparison of CO₂ capture technologies employed with natural gas derived GTCC. 2013.
- [135] D. Humbird RD, L. Tao, C. Kinchin, D. Hsu, A. Aden, P. Schoen, J. Lukas, B. Olthof, M. Worley, , D. Sexton aDD. Process Design and Economics for Biochemical Conversion of Lignocellulosic Biomass to Ethanol: Dilute-Acid Pretreatment and Enzymatic Hydrolysis of Corn Stover. NREL. 2011.
- [136] Chen C. A Technical and Economic Assessment of CO₂ Capture Technology for IGCC Power Plants. Carnegie Mellon University 2005.
- [137] Rubin E. S. CO₂ Capture and Transport. Elements 2008;4:311–317
- [138] Atsonios K, Panopoulos KD, Grammelis P, Kakaras E. Exergetic comparison of CO₂ capture techniques from solid fossil fuel power plants ECOS 2014. Turku, Finland 2014.
- [139] Grant T, Morgan D, Gerdes K. Carbon Dioxide Transport and Storage Costs in NETL Studies. Quality Guidelines for Energy System Studies: National Energy Technology Laboratory; 2013. p. 22.
- [140] Shoko E, McLellan B, Dicks AL, da Costa JCD. Hydrogen from coal: Production and utilisation technologies. International Journal of Coal Geology. 2006;65:213-22.
- [141] Arnaud E. Hydrogen Systems Modeling, Analysis and Optimization. Glasgow: University Strathclyde; 2009.
- [142] Zoulias E, Varkaraki E, Lymberopoulos N, Christodoulou CN, Karagiorgis GN. A Review on Water Electrolysis. TCJST. 2004;4: 41-71.
- [143] Independent Review Panel. Current (2009) State-of-the-Art Hydrogen Production Cost Estimate Using Water Electrolysis. Independent Review Panel Summary Report. National Renewable Energy Laboratory; 2009.
- [144] Simbeck D, Chang E. Hydrogen Supply: Cost Estimate for Hydrogen Pathways □ Scoping Analysis. National Renewable Energy Laboratory; 2002. p. 69.
- [145] Soyachak T, Pitayagulsarn P, Paik K, Riter J. Technoeconomic Evaluation of Large-Scale Electrolytic Hydrogen Production Technologies. Stone & Webster Engineering corporation; 1985. p. 106.
- [146] Ketterer JC. The impact of wind power generation on the electricity price in Germany. 12th IAAE European Energy Conference. Venice, Italy 2012.
- [147] Prince-Richard S. A Techno-Economic Analysis of Decentralized Electrolytic Hydrogen Production for Fuel Cell Vehicles: University of Victoria; 2004.
- [148] James B, Colella W, Moton J. PEM Electrolysis H₂A Production Case Study - Documentation. Strategic Analysis; 2013. p. 27.
- [149] Saur G, Ramsden T. Wind Electrolysis: Hydrogen Cost Optimization. National Renewable Energy Laboratory; 2011.
- [150] Mason J, Zweibel K. Centralized Production of Hydrogen using a Coupled Water Electrolyzer-Solar Photovoltaic System. In: Rajeshwar K, McConnell R, Licht S, editors. Solar Hydrogen Generation: Springer New York; 2008. p. 273-313.
- [151] DOE H₂A Production Analysis Archive. http://www.hydrogen.energy.gov/h2a_production_archive.html. 2015.
- [152] Tzimas E, Castello P, Peteves S. The evolution of size and cost of a hydrogen delivery infrastructure in Europe in the medium and long term. International Journal of Hydrogen Energy. 2007;32:1369-80.

- [153] Yang C, Ogden J. Determining the lowest-cost hydrogen delivery mode. *International Journal of Hydrogen Energy*. 2007;32:268-86.
- [154] Amos WA. Costs of Storing and Transporting Hydrogen. *National Renewable Energy Laboratory*; 1998. p. 216.
- [155] Kato T, Kubota M, Kobayashi N, Suzuoki Y. Effective utilization of by-product oxygen from electrolysis hydrogen production. *Energy*. 2005;30:2580-95.
- [156] Frank D, Howell D, Reed T, Harwood S. Feasibility Study for In-situ Oxygen Separation for Hospitals: Technical Report and Market Analysis O2n-Site Inc. . Capstone Design Project 2006.
- [157] EEX. European Energy Exchange.
- [158] RWE. Facts and Figures. 2008.
- [159] Idaho National Laboratory. http://hydropower.inel.gov/hydrofacts/plant_costs.shtml.
- [160] Surisetty VR, Dalai AK, Kozinski J. Alcohols as alternative fuels: An overview. *Applied Catalysis A: General*. 2011;404:1-11.
- [161] Zhang W. Automotive fuels from biomass via gasification. *Fuel Processing Technology*. 2010;91:866-76.
- [162] European Parliament and of the Council. Fuel Quality Directive (2009/30/EC). 23 April 2009 ed 2009.
- [163] Kusama H, Okabe K, Sayama K, Arakawa H. CO₂ hydrogenation to ethanol over promoted Rh/SiO₂ catalysts. *Catalysis Today*. 1996;28:261-6.
- [164] Nieskens DLS, Ferrari D, Liu Y, Kolonko Jr R. The conversion of carbon dioxide and hydrogen into methanol and higher alcohols. *Catalysis Communications*. 2011;14:111-3.
- [165] Global CCS Institute. Large Scale CCS Projects. 2015.
- [166] Koytsoumpa EI, Atsonios K, Panopoulos KD, Karellas S, Kakaras E, Karl J. Modelling and assessment of acid gas removal processes in coal-derived SNG production. *Applied Thermal Engineering*. 2015;74:128-35.
- [167] Carbon Recycling International. World's Largest CO₂ Methanol Plant. http://www.carbonrecycling.is/index.php?option=com_content&view=article&id=14&Itemid=8&lang=en
- [168] van der Ham L, van den Berga H, Bennekera A, Simmelinka G, Timmera J, van Weerdena S. Hydrogenation of Carbon Dioxide for Methanol Production. *Chemical Engineering Transactions*. 2012;29:181-6.
- [169] Struis RPWJ, Stucki S, Wiedorn M. A membrane reactor for methanol synthesis. *Journal of Membrane Science*. 1996;113:93-100.
- [170] Gallucci F, Basile A. A theoretical analysis of methanol synthesis from CO₂ and H₂ in a ceramic membrane reactor. *International Journal of Hydrogen Energy*. 2007;32:5050-8.
- [171] Gallucci F, Paturzo L, Basile A. An experimental study of CO₂ hydrogenation into methanol involving a zeolite membrane reactor. *Chemical Engineering and Processing: Process Intensification*. 2004;43:1029-36.
- [172] Barbieri G, Marigliano G, Golemme G, Drioli E. Simulation of CO₂ hydrogenation with CH₃OH removal in a zeolite membrane reactor. *Chemical Engineering Journal*. 2002;85:53-9.
- [173] Struis RPWJ, Stucki S. Verification of the membrane reactor concept for the methanol synthesis. *Applied Catalysis A: General*. 2001;216:117-29.
- [174] Nagata H, Yamada K, Kishida M, Wada Y, Wakabayashi K. Catalytic hydrogenation of carbon dioxide into C₂+ alcohols with Ir-Mo/SiO₂. *Energy Conversion and Management*. 1995;36:657-60.

References

- [175] Atsonios K, Christodoulou C, Koytsoumpa EI, Panopoulos KD, Kakaras E. Plant design aspects of catalytic biosyngas conversion to higher alcohols. *Biomass and Bioenergy*. 2013;53:54-64.
- [176] Atsonios K, Kouglioumtzis M-A, D. Panopoulos K, Kakaras E. Alternative thermochemical routes for aviation biofuels via alcohols synthesis: Process modeling, techno-economic assessment and comparison. *Applied Energy*. 2015;138:346-66.
- [177] Qi G-X, Fei J-H, Zheng X-M, Hou Z-Y. DME synthesis from carbon dioxide and hydrogen over Cu–Mo/HZSM-5. *Catalysis Letters*. 2001;72:121-4.
- [178] Ng KL, Chadwick D, Toseland BA. Kinetics and modelling of dimethyl ether synthesis from synthesis gas. *Chemical Engineering Science*. 1999;54:3587-92.
- [179] Lu W-Z, Teng L-H, Xiao W-D. Simulation and experiment study of dimethyl ether synthesis from syngas in a fluidized-bed reactor. *Chemical Engineering Science*. 2004;59:5455-64.
- [180] Yang G, San X, Jiang N, Tanaka Y, Li X, Jin Q, et al. A new method of ethanol synthesis from dimethyl ether and syngas in a sequential dual bed reactor with the modified zeolite and Cu/ZnO catalysts. *Catalysis Today*. 2011;164:425-8.
- [181] Wang D, Yang G, Ma Q, Yoneyama Y, Tan Y, Han Y, et al. Facile solid-state synthesis of Cu–Zn–O catalysts for novel ethanol synthesis from dimethyl ether (DME) and syngas (CO+H₂). *Fuel*. 2013;109:54-60.
- [182] Trippe F, Fröhling M, Schultmann F, Stahl R, Henrich E. Techno-economic assessment of gasification as a process step within biomass-to-liquid (BtL) fuel and chemicals production. *Fuel Processing Technology*. 2011;92:2169-84.
- [183] Larson ED, Jin H, Celik FE. Large-scale gasification-based coproduction of fuels and electricity from switchgrass. *Biofuels, Bioproducts and Biorefining*. 2009;3:174-94.
- [184] Zhu Y, Gerber M, Jones S, Stevens D. Analysis of the Effects of Compositional and Configurational Assumptions on Product Costs for the Thermochemical Conversion of Lignocellulosic Biomass to Mixed Alcohols – FY 2007 Progress Report 2008.
- [185] Phillips S, Aden A, Jechura J, Dayton D, Eggeman T. Thermochemical Ethanol via Indirect Gasification and Mixed Alcohol Synthesis of Lignocellulosic Biomass. Springfield: NREL; 2007. p. 132.
- [186] Ndou AS, Plint N, Coville NJ. Dimerisation of ethanol to butanol over solid-base catalysts. *Applied Catalysis A: General*. 2003;251:337-45.
- [187] Cherubini F. The biorefinery concept: Using biomass instead of oil for producing energy and chemicals. *Energy Conversion and Management*. 2010;51:1412-21.
- [188] Bangala DN, Abatzoglou N, Martin J-P, Chornet E. Catalytic Gas Conditioning: Application to Biomass and Waste Gasification. *Industrial & Engineering Chemistry Research*. 1997;36:4184-92.
- [189] Corella J, Orío A, Toledo J-M. Biomass Gasification with Air in a Fluidized Bed: Exhaustive Tar Elimination with Commercial Steam Reforming Catalysts. *Energy & Fuels*. 1999;13:702-9.
- [190] Kavalov B, Peteves S. Status and Perspectives of Biomass-to-Liquid Fuels in the European Union. Petten NL: European Commission, Directorate General Joint Research Centre (DGJRC); 2005. p. 162.
- [191] Narayan R. Rationale, drivers, standards and technology for biobased materials. In: Graziana M, Fornaserio P, editors. *Renewable resources and renewable energy: a global challenge*. Boca Raton, Florida: CRC Press-Taylor and Francis Group; 2007.
- [192] Speight J. *Synthetic Fuels Handbook: Properties, Process, and Performance* 1st ed 2008.
- [193] Brown TR, Zhang Y, Hu G, Brown RC. Techno-economic analysis of biobased chemicals production via integrated catalytic processing. *Biofuels, Bioproducts and Biorefining*. 2012;6:73-87.

- [194] Dutta A, Bain RL, Biddy MJ. Techno-economics of the production of mixed alcohols from lignocellulosic biomass via high-temperature gasification. *Environmental Progress & Sustainable Energy*. 2010;29:163-74.
- [195] NREL Biorefinery Analysis Process Models (Last updated: November 2012) http://www.nrel.gov/extranet/biorefinery/aspen_models/.
- [196] Zhu Y, Gerber M, Jones S, Stevens D. Analysis of the Effects of Compositional and Configurational Assumptions on Product Costs for the Thermochemical Conversion of Lignocellulosic Biomass to Mixed Alcohols. Progress Report. Springfield, US: PNNL; 2007. p. 120.
- [197] Mills GA. Status and future opportunities for conversion of synthesis gas to liquid fuels. *Fuel*. 1994;73:1243-79.
- [198] Carlini C, Girolamo MD, Marchionna M, NovIELLO M, Galletti AMR, Sbrana G. Selective synthesis of isobutanol by means of the Guerbet reaction: Part 1. Methanol/n-propanol condensation by using copper based catalytic systems. *Journal of Molecular Catalysis A: Chemical*. 2002;184:273-80.
- [199] Yang W. *Handbook of Fluidization and Fluid Particle Systems*. New York: Taylor & Francis Group LLC; 2003.
- [200] He J, Zhang W. Techno-economic evaluation of thermo-chemical biomass-to-ethanol. *Applied Energy*. 2011;88:1224-32.
- [201] Donat F, Florin NH, Anthony EJ, Fennell PS. Influence of High-Temperature Steam on the Reactivity of CaO Sorbent for CO₂ Capture. *Environmental Science & Technology*. 2011;46:1262-9.
- [202] van der Heijden H, Ptasiński KJ. Exergy analysis of thermochemical ethanol production via biomass gasification and catalytic synthesis. *Energy*. 2012;46:200-10.
- [203] Villanueva Perales AL, Reyes Valle C, Ollero P, Gómez-Barea A. Technoeconomic assessment of ethanol production via thermochemical conversion of biomass by entrained flow gasification. *Energy*. 2011;36:4097-108.
- [204] Ekblom T, Lindblom M, Berglin N, Ahlvik P. Technical and Commercial Feasibility Study of Black Liquor Gasification with Methanol/DME Production as Motor Fuels for Automotive Uses – BLGMF. European Commission: Nykomb Synergetics AB SWE; 2003. p. 293.
- [205] Smith AR, Klosek J. A review of air separation technologies and their integration with energy conversion processes. *Fuel Processing Technology*. 2001;70:115-34.
- [206] Higman C, van der Burgt M. *Gasification*. Burlington: Elsevier; 2003.
- [207] Panopoulos KD, Fryda LE, Karl J, Poulou S, Kakaras E. High temperature solid oxide fuel cell integrated with novel allothermal biomass gasification: Part I: Modelling and feasibility study. *Journal of Power Sources*. 2006;159:570-85.
- [208] Nexant Inc. Equipment Design and Cost Estimation for Small Modular Biomass Systems, Synthesis Gas Cleanup, and Oxygen Separation Equipment. Springfield: NREL; 2006.
- [209] Spath P, Dayton D. Preliminary Screening —Technical and Economic Assessment of Synthesis Gas to Fuels and Chemicals with Emphasis on the Potential for Biomass-Derived Syngas. Springfield: NREL; 2003.
- [210] Stevens D. Hot Gas Conditioning: Recent Progress With Larger-Scale Biomass Gasification, Systems Update and Summary of Recent Progress. Springfield: NREL; 2001.
- [211] Beretta A, Tronconi E, Forzatti P, Pasquon I, Micheli E, Tagliabue L, et al. Development of a Mechanistic Kinetic Model of the Higher Alcohol Synthesis over a Cs-Doped Zn/Cr/O Catalyst. 1. Model Derivation and Data Fitting. *Industrial & Engineering Chemistry Research*. 1996;35:2144-53.
- [212] Quaderer GJ, Cochran GA. Catalytic process for producing mixed alcohols from hydrogen and carbon monoxide. USA1984.

References

- [213] Gunturu AK, Kugler EL, Cropley JB, Dadyburjor DB. A Kinetic Model for the Synthesis of High-Molecular-Weight Alcohols over a Sulfided Co–K–Mo/C Catalyst. *Industrial & Engineering Chemistry Research*. 1998;37:2107-15.
- [214] Kulawska M, Skrzypek J. Kinetics of the synthesis of higher aliphatic alcohols from syngas over a modified methanol synthesis catalyst. *Chemical Engineering and Processing: Process Intensification*. 2001;40:33-40.
- [215] Carlsson P, Wiinikka H, Marklund M, Grönberg C, Pettersson E, Lidman M, et al. Experimental investigation of an industrial scale black liquor gasifier. 1. The effect of reactor operation parameters on product gas composition. *Fuel*. 2010;89:4025-34.
- [216] Forzatti P, Tronconi E, Pasquon I. Higher Alcohol Synthesis. *Catalysis Reviews*. 1991;33:109-68.
- [217] Wong S, Patel M, Storm D. Retrofitting Methanol Plants For Higher Alcohols. 78th American Institute of Chemical Engineers, National Meeting. Orleans, LA1986.
- [218] Naqvi M, Yan J, Fröling M. Bio-refinery system of DME or CH₄ production from black liquor gasification in pulp mills. *Bioresource Technology*. 2010;101:937-44.
- [219] Sricharoenchaikul V, Frederick Jr WJ, Agrawal P. Carbon distribution in char residue from gasification of kraft black liquor. *Biomass and Bioenergy*. 2003;25:209-20.
- [220] ASPEN Plus V7.1. Physical property methods. Burlington Aspen Technology Inc., 2009.
- [221] Doherty W, Reynolds A, Kennedy D. Computer simulation of a biomass gasification-solid oxide fuel cell power system using Aspen Plus. *Energy*. 2010;35:4545-55.
- [222] De Kam MJ, Vance Morey R, Tiffany DG. Biomass Integrated Gasification Combined Cycle for heat and power at ethanol plants. *Energy Conversion and Management*. 2009;50:1682-90.
- [223] Spyraakis S, Panopoulos KD, Kakaras E. Synthesis, Modeling and Exergy Analysis of Atmospheric Air Blown Biomass Gasification for Fischer-Tropsch Process. *International Journal of Thermodynamics*. 2009;12:187-92.
- [224] Larson E, Consonni S, Katofsky R, Iisa K, Frederick J. A Cost-Benefit Assessment of Gasification-Based Biorefining in the Kraft Pulp and Paper Industry, Volume 2, Detailed Biorefinery Design and Performance Simulation. Princeton University; 2006.
- [225] Crocker M. Thermochemical Conversion of Biomass to Liquid Fuels and Chemicals. In: Series REaE, editor. Cambridge: Royal Society of Chemistry; 2010.
- [226] Gerber M, White J, Stevens D. Mixed Alcohol Synthesis catalyst screening. Washington: PNNL; 2007.
- [227] Beretta A, Sun Q, Herman RG, Klier K. Higher alcohol synthesis over a Cs-Cu/ZnO/Cr₂O₃ catalyst: effect of the reaction temperature on product distribution and catalyst stability. *Abstracts of Papers of the American Chemical Society*. 1995;209:142-7.
- [228] Fang K, Li D, Lin M, Xiang M, Wei W, Sun Y. A short review of heterogeneous catalytic process for mixed alcohols synthesis via syngas. *Catalysis Today*. 2009;147:133-8.
- [229] Group ATA. <http://www.atag.org/facts-and-figures.html>.
- [230] Solutions CfCaE. http://www.c2es.org/technology/factsheet/Aviation#_edn4.
- [231] <http://www.indexmundi.com/energy.aspx?product=jet-fuel&graph=consumptionIndex>. Mundi, World Jet Fuel Consumption by Year.
- [232] European Commission. Reducing emissions from aviation. http://ec.europa.eu/clima/policies/transport/aviation/index_en.htm
- [233] Jin C, Yao M, Liu H, Lee C-fF, Ji J. Progress in the production and application of n-butanol as a biofuel. *Renewable and Sustainable Energy Reviews*. 2011;15:4080-106.

- [234] Vaillancourt K, Alcocer Y, Bahn O, Fertel C, Frenette E, Garbouj H, et al. A Canadian 2050 energy outlook: Analysis with the multi-regional model TIMES-Canada. *Applied Energy*. 2014;132:56-65.
- [235] Yan J, Lin T. Biofuels in Asia. *Applied Energy*. 2009;86, Supplement 1:S1-S10.
- [236] Tonini D, Astrup T. LCA of biomass-based energy systems: A case study for Denmark. *Applied Energy*. 2012;99:234-46.
- [237] Handbook of Aviation Fuel Properties. Coordinating Research Council. 1988.
- [238] services USDohah. Toxicological Profile for Jet Fuels JP-4 and JP-7. 1995.
- [239] Michael E. Wright, Benjamin G. Harvey, Quintana RL. Diesel and Jet Fuels based on the oligomerization of butene. 2013.
- [240] <http://www.rita.dot.gov/>. Research and Innovative Technology Administration - Bureau of Transportation Statistics.
- [241] Blakey S, Rye L, Wilson CW. Aviation gas turbine alternative fuels: A review. *Proceedings of the Combustion Institute*. 2011;33:2863-85.
- [242] Marsh G. Biofuels: aviation alternative? *Renewable Energy Focus*. 2008;9: 48–51.
- [243] Hammond GP, Seth SM. Carbon and environmental footprinting of global biofuel production. *Applied Energy*. 2013;112:547-59.
- [244] Chuck CJ, Donnelly J. The compatibility of potential bioderived fuels with Jet A-1 aviation kerosene. *Applied Energy*. 2014;118:83-91.
- [245] Sasol. <http://www.sasol.com/media-centre/media-releases/sasol-achieves-approval-100-synthetic-jet-fuel>.
- [246] Syntroleum. Synthetic fuels technology for a clean future.
- [247] Air-Force U. http://www.fischer-tropsch.org/DOD/USAF/Reports/Air_Force_Alternative_Fuels.pdf.
- [248] Gevo. <http://gevo.com/>.
- [249] Byogy Renewables Inc. <http://www.byogy.com/index.html>.
- [250] Reyes Valle C, Villanueva Perales AL, Vidal-Barrero F, Gómez-Barea A. Techno-economic assessment of biomass-to-ethanol by indirect fluidized bed gasification: Impact of reforming technologies and comparison with entrained flow gasification. *Applied Energy*. 2013;109:254-66.
- [251] Ahn J-H, Sang B-I, Um Y. Butanol production from thin stillage using *Clostridium pasteurianum*. *Bioresource Technology*. 2011;102:4934-7.
- [252] Ennis BM GN, Maddox. The acetone-butanol- ethanol fermentation: a current assessment. *Process Biochemistry*. 1986;21:131-47.
- [253] Humbird D, Davis R, Tao L, Kinchin C, Hsu D, Aden A, et al. Process Design and Economics for Biochemical Conversion of Lignocellulosic Biomass to Ethanol: Dilute-Acid Pretreatment and Enzymatic Hydrolysis of Corn Stover. NREL. 2011.
- [254] Kumar M, Goyal Y, Sarkar A, Gayen K. Comparative economic assessment of ABE fermentation based on cellulosic and non-cellulosic feedstocks. *Applied Energy*. 2012;93:193-204.
- [255] Matsuda M, Horio M. Process for preparation of Guerbet alcohols. Japan: Kao Corporation; 1985.
- [256] Kolombos AJ. Oligomerization Process. The British Petroleum Company; 1978.
- [257] Graça I, Lopes JM, Cerqueira HS, Ribeiro MF. Bio-oils Upgrading for Second Generation Biofuels. *Industrial & Engineering Chemistry Research*. 2012;52:275-87.

References

- [258] Jones SB, Holladay JE, Valkenburg C, Stevens DJ, Walton CW, Kinchin C, et al. Production of gasoline and diesel from biomass via fast pyrolysis; hydrotreating and hydrocracking: A design case. Pacific Northwest National Laboratory: Richland, WA; 2009.
- [259] Hileman JJ, Ortiz DS, Bartis JT, Wong HM, Donohoo PE, Weiss MA, et al. Near-Term Feasibility of Alternative Jet Fuels. Santa Monica, CA: PARTNER; 2009.
- [260] Chisti Y, Yan J. Energy from algae: Current status and future trends: Algal biofuels – A status report. *Applied Energy*. 2011;88:3277-9.
- [261] Fortier M-OP, Roberts GW, Stagg-Williams SM, Sturm BSM. Life cycle assessment of bio-jet fuel from hydrothermal liquefaction of microalgae. *Applied Energy*. 2014;122:73-82.
- [262] Fierro J, Gómez X, Murphy JD. What is the resource of second generation gaseous transport biofuels based on pig slurries in Spain? *Applied Energy*. 2014;114:783-9.
- [263] Kim J, Miller JE, Maravelias CT, Stechel EB. Comparative analysis of environmental impact of S2P (Sunshine to Petrol) system for transportation fuel production. *Applied Energy*. 2013;111:1089-98.
- [264] Rakopoulos DC, Rakopoulos CD, Giakoumis EG, Dimaratos AM, Kyritsis DC. Effects of butanol–diesel fuel blends on the performance and emissions of a high-speed DI diesel engine. *Energy Conversion and Management*. 2010;51:1989-97.
- [265] Heracleous E, Liakakou ET, Lappas AA, Lemonidou AA. Investigation of K-promoted Cu-Zn-Al, Cu-X-Al and Cu-Zn-X (X=Cr, Mn) catalysts for carbon monoxide hydrogenation to higher alcohols. *Applied Catalysis A: General*. 2013;455:145-54.
- [266] Tijmensen MJA, Faaij APC, Hamelinck CN, van Hardeveld MRM. Exploration of the possibilities for production of Fischer Tropsch liquids and power via biomass gasification. *Biomass and Bioenergy*. 2002;23:129-52.
- [267] Gassner M, Maréchal F. Thermo-economic process model for thermochemical production of Synthetic Natural Gas (SNG) from lignocellulosic biomass. *Biomass and Bioenergy*. 2009;33:1587-604.
- [268] Huisman GH, Van Rens GLMA, De Lathouder H, Cornelissen RL. Cost estimation of biomass-to-fuel plants producing methanol, dimethylether or hydrogen. *Biomass and Bioenergy*. 2011;35, Supplement 1:S155-S66.
- [269] Humbird D, Aden A. Biochemical Production of Ethanol from Corn Stover: 2008 State of Technology Model. 2009.
- [270] Aden A, Ruth M, Ibsen K, Jechura J, Neeves K, Sheehan J, et al. Lignocellulosic Biomass to Ethanol Process Design and Economics Utilizing Co-Current Dilute Acid Prehydrolysis and Enzymatic Hydrolysis for Corn Stover. National Renewable Energy Laboratory; 2002.
- [271] Davis R, Tao L, Tan ECD, Biddy MJ, Beckham GT, Scarlata C, et al. Process Design and Economics for the Conversion of Lignocellulosic Biomass to Hydrocarbons: Dilute-Acid and Enzymatic Deconstruction of Biomass to Sugars and Biological Conversion of Sugars to Hydrocarbons. MREL; 2013. p. 147.
- [272] Kabir Kazi F, Fortman J, Anex R, Kothandaraman G, Hsu D, Aden A, et al. Techno-Economic Analysis of Biochemical Scenarios for Production of Cellulosic Ethanol. NREL; 2010.
- [273] Lynd LR, Wyman C, Laser M, Johnson D, Landucci R. Strategic Biorefinery Analysis. Analysis of biorefineries. Colorado, US: National Renewable Energy Laboratory 2005.
- [274] Leboreiro J, Hilaly AK. Biomass transportation model and optimum plant size for the production of ethanol. *Bioresource Technology*. 2011;102:2712-23.
- [275] Spath P, Dayton D. Preliminary Screening —Technical and Economic Assessment of Synthesis Gas to Fuels and Chemicals with Emphasis on the Potential for Biomass-Derived Syngas. NREL Report, NREL/TP-510-34929. 2003.

- [276] Atsonios K, Panopoulos KD, Doukelis A, Koumanakos A, Kakaras E. Techno economic comparison of CO₂ capture technologies employed with natural gas derived GTCC. ASME Turbo Expo 2013 San Antonio, Texas, USA2013.
- [277] León M, Díaz E, Vega A, Ordóñez S, Auroux A. Consequences of the iron–aluminium exchange on the performance of hydrotalcite-derived mixed oxides for ethanol condensation. *Applied Catalysis B: Environmental*. 2011;102:590-9.
- [278] Dowson GRM, Haddow MF, Lee J, Wingad RL, Wass DF. Catalytic Conversion of Ethanol into an Advanced Biofuel: Unprecedented Selectivity for n-Butanol. *Angewandte Chemie International Edition*. 2013;52:9005-8.
- [279] Carlini C, Di Girolamo M, Macinai A, Marchionna M, Noviello M, Raspolli Galletti AM, et al. Selective synthesis of isobutanol by means of the Guerbet reaction: Part 2. Reaction of methanol/ethanol and methanol/ethanol/n-propanol mixtures over copper based/MeONa catalytic systems. *Journal of Molecular Catalysis A: Chemical*. 2003;200:137-46.
- [280] Carlini C, Girolamo MD, Macinai A, Marchionna M, Noviello M, Galletti AMR, et al. Synthesis of isobutanol by the Guerbet condensation of methanol with n-propanol in the presence of heterogeneous and homogeneous palladium-based catalytic systems. *Journal of Molecular Catalysis A: Chemical*. 2003;204–205:721-8.
- [281] Taylor J, Jenni M, Peters M. Dehydration of Fermented Isobutanol for the Production of Renewable Chemicals and Fuels. *Top Catal*. 2010;53:1224-30.
- [282] Makarova MA, Williams C, Thomas JM, Zamaraev KI. Dehydration of n-butanol on HNa-ZSM-5. *Catalysis Letters*. 1990;4:261-3.
- [283] Lee IC, St Clair JG, Gamson AS. Catalytic Oxidative Dehydration of Butanol Isomers: 1-Butanol, 2-Butanol, and Isobutanol. Adelphi, MD: Army Research Laboratory; 2011.
- [284] Heveling J, Nicolaides CP, Scurrall MS. Catalysts and conditions for the highly efficient, selective and stable heterogeneous oligomerisation of ethylene. *Applied Catalysis A: General*. 1998;173:1-9.
- [285] Malgas-Enus R, Mapolie SF. Nickel metallodendrimers as catalyst precursors in the tandem oligomerization of ethylene and Friedel–Crafts alkylation of its olefinic products. *Inorganica Chimica Acta*. 2014;409, Part A:96-105.
- [286] Lin S, Shi L, Zhang H, Zhang N, Yi X, Zheng A, et al. Tuning the pore structure of plug-containing Al-SBA-15 by post-treatment and its selectivity for C₁₆ olefin in ethylene oligomerization. *Microporous and Mesoporous Materials*. 2014;184:151-61.
- [287] Coelho A, Caeiro G, Lemos MANDA, Lemos F, Ribeiro FR. 1-Butene oligomerization over ZSM-5 zeolite: Part 1 – Effect of reaction conditions. *Fuel*. 2013;111:449-60.
- [288] Lavrenov AV, Duplyakin VK. Oligomerization of butenes on borate-containing alumina. *Kinet Catal*. 2009;50:235-40.
- [289] Alcántara R, Alcántara E, Canoira L, Franco MaJ, Herrera M, Navarro A. Trimerization of isobutene over Amberlyst-15 catalyst. *Reactive and Functional Polymers*. 2000;45:19-27.
- [290] Yoon JW, Chang J-S, Lee H-D, Kim T-J, Jung SH. Trimerization of isobutene over cation exchange resins: Effect of physical properties of the resins and reaction conditions. *Journal of Molecular Catalysis A: Chemical*. 2006;260:181-6.
- [291] Hauge K, Bergene E, Chen D, Fredriksen GR, Holmen A. Oligomerization of isobutene over solid acid catalysts. *Catalysis Today*. 2005;100:463-6.
- [292] Yoon JW, Lee JH, Chang J-S, Choo DH, Lee SJ, Jung SH. Trimerization of isobutene over zeolite catalysts: Remarkable performance over a ferrierite zeolite. *Catalysis Communications*. 2007;8:967-70.

References

- [293] Yoon JW, Jhung SH, Choo DH, Lee SJ, Lee K-Y, Chang J-S. Oligomerization of isobutene over dealuminated Y zeolite catalysts. *Applied Catalysis A: General*. 2008;337:73-7.
- [294] Kittisakmontree P, Pongthawornsakun B, Yoshida H, Fujita S-i, Arai M, Panpranot J. The liquid-phase hydrogenation of 1-heptyne over Pd–Au/TiO₂ catalysts prepared by the combination of incipient wetness impregnation and deposition–precipitation. *Journal of Catalysis*. 2013;297:155-64.
- [295] Mastalir Á, Notheisz F, Király Z, Bartók M, Dékány I. Novel clay intercalated metal catalysts: a study of the hydrogenation of styrene and 1-octene on clay intercalated Pd catalysts. In: H.U. Blaser AB, Prins R, editors. *Studies in Surface Science and Catalysis*: Elsevier; 1997. p. 477-84.
- [296] Clarence D. Chang, Stuart D. Hellring, Striebel RF. Process for hydrogenating alkenes in the presence of alkanes and a heterogeneous catalyst. 1993.
- [297] Aden A, Spath P, Atherton A. The Potential of Thermochemical Ethanol Via Mixed Alcohols Production. In: Report MC, editor. Golden, CO: National Renewable Energy Laboratory; 2005.
- [298] Zhu Y, Gerber M, Jones SB, Stevens DJ. Analysis of the Effects of Compositional and Configurational Assumptions on Product Costs for the Thermochemical Conversion of Lignocellulosic Biomass to Mixed Alcohols. Progress Report: Pacific Northwest National Laboratory; 2009.
- [299] Ding M, Qiu M, Liu J, Li Y, Wang T, Ma L, et al. Influence of manganese promoter on co-precipitated Fe–Cu based catalysts for higher alcohols synthesis. *Fuel*. 2013;109:21-7.
- [300] Xu R, Yang C, Wei W, Li W-h, Sun Y-h, Hu T-d. Fe-modified CuMnZrO₂ catalysts for higher alcohols synthesis from syngas. *Journal of Molecular Catalysis A: Chemical*. 2004;221:51-8.
- [301] Morávek V. Further evidence for the substitution mechanism of 2-propanol dehydration on alumina. *React Kinet Catal Lett*. 1986;30:71-5.
- [302] Wu Y, Marwil SJ. Dehydration of alcohols. Bartlesville, Okla 1980.
- [303] Koroneos C, Dompros A, Roumbas G. Hydrogen production via biomass gasification—A life cycle assessment approach. *Chemical Engineering and Processing: Process Intensification*. 2008;47:1261-8.
- [304] Sues A, Juraščík M, Ptasiński K. Exergetic evaluation of 5 biowastes-to-biofuels routes via gasification. *Energy*. 2010;35:996-1007.
- [305] Peters MW, Taylor JD. Renewable jet fuel blendstock from isobutanol. GEVO, INC.; 2011.
- [306] GEVO white paper. Isobutanol - A renewable solution for the transportation fuels value chain. <http://www.gevo.com/assets/pdfs/GEVO-wp-iso-fff.pdf>, May 2011.
- [307] Swanson RM, Satrio JA, Brown RC, Platon A, Hsu DD. Techno-Economic Analysis of Biofuels Production Based on Gasification. NREL2010.
- [308] Larson ED, Jin H, Celik F. Gasification-Based Fuels and Electricity Production from Biomass, without and with Carbon Capture and Storage. 2005.
- [309] Dutta A, Talmadge M, Hensley J, Worley M, Dudgeon D, Barton D, et al. Process Design and Economics for Conversion of Lignocellulosic Biomass to Ethanol Thermochemical Pathway by Indirect Gasification and Mixed Alcohol Synthesis. NREL. 2011.
- [310] Dutta A, Phillips SD. Thermochemical Ethanol via Direct Gasification and Mixed Alcohol Synthesis of Lignocellulosic Biomass. NREL: National Renewable Energy Laboratory; 2009.
- [311] Nexant. Equipment Design and Cost Estimation for Small Modular Biomass Systems, Synthesis Gas Cleanup, and Oxygen Separation Equipment, Task 9: Mixed Alcohols From Syngas —State of Technology National Renewable Energy Laboratory; 2006.
- [312] Eurostat. <http://epp.eurostat.ec.europa.eu/portal/page/portal/eurostat/home/>.

- [313] Dincer I, Rosen MA. Exergy: Energy, Environment and Sustainable Development: Elsevier Science; 2007.
- [314] Perry RH, Green D, Maloney JO. Chemical Engineers' Handbook. New York: McGraw-Hill; 1999.
- [315] Tavakoli A, Sohrabi M, Kargari A. Application of Anderson–Schulz–Flory (ASF) equation in the product distribution of slurry phase FT synthesis with nanosized iron catalysts. Chemical Engineering Journal. 2008;136:358-63.
- [316] Shah PP, Sturtevant GC, Gregor JH, Humbach MJ, Padrta FG, Steigleder KZ. Fischer-Tropsch wax characterization and upgrading: Final report. 1988.
- [317] Sudiro M, Bertuccio A. Production of synthetic gasoline and diesel fuel by alternative processes using natural gas and coal: Process simulation and optimization. Energy. 2009;34:2206-14.
- [318] <http://www.indexmundi.com/commodities/?commodity=propane&months=60>. Mundi, LPG Monthly Price.
- [319] <http://www.indexmundi.com/commodities/?commodity=gasoline&months=60&commodity=jet-fuel>. Mundi, Gasoline Monthly Price.
- [320] AspenTech. Aspen Plus v7.1. <http://www.aspentech.com/products/engineering/aspen-plus/>
- [321] Qureshi N, Saha BC, Cotta MA, Singh V. An economic evaluation of biological conversion of wheat straw to butanol: A biofuel. Energy Conversion and Management. 2013;65:456-62.
- [322] Wooley R, Ruth M, Sheehan J, Ibsen K, Majdeski H, Galvez A. Lignocellulosic Biomass to Ethanol Process Design and Economics Utilizing Co-Current Dilute Acid Prehydrolysis and Enzymatic Hydrolysis Current and Futuristic Scenarios. 1999.
- [323] Wright MM, Dugaard DE, Satrio JA, Brown RC. Techno-economic analysis of biomass fast pyrolysis to transportation fuels. Fuel. 2010;89, Supplement 1:S2-S10.
- [324] Saha BC, Iten LB, Cotta MA, Wu YV. Dilute acid pretreatment, enzymatic saccharification and fermentation of wheat straw to ethanol. Process Biochemistry. 2005;40:3693-700.
- [325] Salgado-Gordon H-J, Valbuena-Moreno G. Technical and economic evaluation of the separation of light olefins (ethylene and propylene) by using p-complexation with silver salts. Journal of Ciencia, Tecnologia y Futuro. 2011;4:73-87.
- [326] Foust T, Aden A, Dutta A, Phillips S. An economic and environmental comparison of a biochemical and a thermochemical lignocellulosic ethanol conversion processes. Cellulose. 2009;16:547-65.
- [327] Consonni S, Katofsky RE, Larson ED. A gasification-based biorefinery for the pulp and paper industry. Chemical Engineering Research and Design. 2009;87:1293-317.
- [328] Diana C, Cardenas B. Methanol and Hydrogen Production - Energy and Cost Analysis [Master]. Sweden: Lulea University of Technology; 2006.
- [329] Xing R, Subrahmanyam AV, Olcay H, Qi W, van Walsum GP, Pendse H, et al. Production of jet and diesel fuel range alkanes from waste hemicellulose-derived aqueous solutions. Green Chemistry. 2010;12:1933-46.
- [330] Phillips SD, Aden A, Jechura J, Dayton D, Eggeman T. Thermochemical Ethanol Via Indirect Gasification and Mixed Alcohol Synthesis of Lignocellulosic Biomass. NREL: National Renewable Energy Laboratory; 2007.
- [331] Tunå P, Hulteberg C. Woody biomass-based transportation fuels – A comparative techno-economic study. Fuel. 2014;117, Part B:1020-6.

References

- [332] Wingren A, Galbe M, Zacchi G. Techno-Economic Evaluation of Producing Ethanol from Softwood: Comparison of SSF and SHF and Identification of Bottlenecks. *Biotechnology Progress*. 2003;19:1109-17.
- [333] Macrelli S, Mogensen J, Zacchi G. Techno-economic evaluation of 2nd generation bioethanol production from sugar cane bagasse and leaves integrated with the sugar-based ethanol process. *Biotechnol Biofuels*. 2012;5:1-18.
- [334] Haro P, Ollero P, Villanueva Perales AL, Reyes Valle C. Technoeconomic assessment of lignocellulosic ethanol production via DME (dimethyl ether) hydrocarbonylation. *Energy*. 2012;44:891-901.
- [335] Taylor B, Xiao N, Sikorski J, Yong M, Harris T, Helme T, et al. Techno-economic assessment of carbon-negative algal biodiesel for transport solutions. *Applied Energy*. 2013;106:262-74.
- [336] Shabangu S, Woolf D, Fisher EM, Angenent LT, Lehmann J. Techno-economic assessment of biomass slow pyrolysis into different biochar and methanol concepts. *Fuel*. 2014;117, Part A:742-8.
- [337] Bowen D, Lau F, Zabransky R, Remick R, Slimane R, Doong S, et al. Techno-Economic Analysis of Hydrogen Production by Gasification of Biomass. In: Report FP, editor. *Hydrogen, Fuel Cells, and Infrastructure Technologies*: DOE; 2003.
- [338] Ou L, Brown TR, Thilakaratne R, Hu G, Brown RC. Techno-economic analysis of co-located corn grain and corn stover ethanol plants. *Biofuels, Bioproducts and Biorefining*. 2014;n/a-n/a.
- [339] Yusuf NNAN, Kamarudin SK. Techno-economic analysis of biodiesel production from *Jatropha curcas* via a supercritical methanol process. *Energy Conversion and Management*. 2013;75:710-7.
- [340] Tao L, Tan ECD, McCormick R, Zhang M, Aden A, He X, et al. Techno-economic analysis and life-cycle assessment of cellulosic isobutanol and comparison with cellulosic ethanol and n-butanol. *Biofuels, Bioproducts and Biorefining*. 2014;8:30-48.
- [341] Bond JQ, Upadhye AA, Olcay H, Tompsett GA, Jae J, Xing R, et al. Production of renewable jet fuel range alkanes and commodity chemicals from integrated catalytic processing of biomass. *Energy & Environmental Science*. 2014;7:1500-23.
- [342] Sanchez-Segado S, Lozano LJ, de Los Rios AP, Hernandez-Fernandez FJ, Godinez C, Juan D. Process design and economic analysis of a hypothetical bioethanol production plant using carob pod as feedstock. *Bioresour Technol*. 2012;104:324-8.
- [343] Murphy JD, McCarthy K. Ethanol production from energy crops and wastes for use as a transport fuel in Ireland. *Applied Energy*. 2005;82:148-66.
- [344] Hamelinck CN, Hooijdonk Gv, Faaij APC. Ethanol from lignocellulosic biomass: techno-economic performance in short-, middle- and long-term. *Biomass and Bioenergy*. 2005;28:384-410.
- [345] Wright MM, Brown RC, Boateng AA. Distributed processing of biomass to bio-oil for subsequent production of Fischer-Tropsch liquids. *Biofuels, Bioproducts and Biorefining*. 2008;2:229-38.
- [346] Koutinas AA, Chatzifragkou A, Kopsahelis N, Papanikolaou S, Kookos IK. Design and techno-economic evaluation of microbial oil production as a renewable resource for biodiesel and oleochemical production. *Fuel*. 2014;116:566-77.
- [347] Zhang Y, Brown TR, Hu G, Brown RC. Comparative techno-economic analysis of biohydrogen production via bio-oil gasification and bio-oil reforming. *Biomass and Bioenergy*. 2013;51:99-108.
- [348] Eric D. Larson HJ, Fuat E. Celik. Large-scale gasification-based coproduction of fuels and electricity from switchgrass. *Biofuels, Bioproducts and Biorefining*. 2009;3.
- [349] Ryan M. Swanson, Justinus A. Satrio, Robert C. Brown, Alexandru Platon, Hsu DD. Techno-Economic Analysis of Biofuels Production Based on Gasification. NREL2010.

- [350] Hamelinck CN, Faaij APC, den Uil H, Boerrigter H. Production of FT transportation fuels from biomass; technical options, process analysis and optimisation, and development potential. *Energy*. 2004;29:1743-71.
- [351] Thomas G. Kreutz EDL, Guangjian Liu, Robert H. Williams Fischer-Tropsch Fuels from Coal and Biomass. 2008.
- [352] Elia JA, Baliban RC, Xiao X, Floudas CA. Optimal energy supply network determination and life cycle analysis for hybrid coal, biomass, and natural gas to liquid (CBGTL) plants using carbon-based hydrogen production. *Computers & Chemical Engineering*. 2011;35:1399-430.

References